Statistical Analysis of the Capacity of Mobile Radio Channels

Gulzaib Rafiq

Statistical Analysis of the Capacity of Mobile Radio Channels

Doctoral Dissertation for the Degree *Philosophiae Doctor (PhD)* in Information and Communication Technology

University of Agder
Faculty of Engineering and Science
2011

Doctoral Dissertation by the University of Agder 29
ISBN: 978-82-7117-686-0
ISSN: 1504-9272

Printed in the Printing Office, University of Agder
Kristiansand

To my wife, Saira and to
my parents, Rafiq and Rehmat

Preface and Acknowledgements

The research work in this dissertation was carried out at the Department of Information and Communication Technology (ICT), Mobile Communications Group of the University of Agder (UiA) in Grimstad, Norway. The research was funded by the Research Council of Norway (Norges Forskningsråd, NFR) through the project 176773/S10 entitled “Optimized Heterogeneous Multiuser MIMO Networks - OptiMO”.

The gigantic task of the completion of this dissertation would have not been possible without the help and support of many individuals to whom I want to express my gratitude.

Firstly, I want to express my heartiest gratitude to Almighty Allah, the most gracious and the most merciful. His endless blessings and guidance gave me the vision and the strength to stay on the right course leading to the completion this task.

I am very grateful to my supervisor Prof. Matthias Pätzold. His careful supervision, encouragement, visionary ideas, and constant support helped me a lot in moulding my efforts into favorable outcomes. I am thankful to the members of the evaluation committee, Prof. Ramón Parra Michel (CINVESTAV-IPN, Mexico), Prof. Yuming Jiang (NTNU, Norway), and Prof. Andreas Prinz (UiA, Norway) for their useful suggestions regarding the improvement of the manuscript. I would also like to thank Secretary of the MCG, Mrs. Katharina Pätzold, for her extensive support regarding administrative and personal matters. I am also thankful to the Coordinator of the PhD program in the ICT department of UiA, Mrs. Trine Tønnessen, for her timely advices.

I am grateful to Prof. Valeri Kontorovich (CINVESTAV-IPN, Mexico) for giving me the opportunity to work with him on a summer internship at CINVESTAV-IPN, Mexico. It was a great learning experience and I would like to acknowledge all the discussions I had with Prof. Valeri Kontorovich since then.

My sincere gratitude goes to the Doctoral Fellows from the ICT Department, especially to Adrian Gutiérrez, Ahmed Aboughonim, Akmal Fayziyev, Ali Chelli, Anis Yazidi, Batool Talha, Bjørn Olav Hogstad, Dmitry Umansky, Nurilla Avazov, Ram Kumar, Yuanyuan Ma, and Ziaul Haq Abbas. They made my stay in Grimstad very pleasant and I was immensely benefited from their knowledge and expertise. Specifically, I can not forget the friendly support of Batool Talha and Yuanyuan Ma at numerous occasions during my stay in Grimstad.

Last, but certainly not the least, I would like to acknowledge the commitment,

sacrifice and support of my parents, Rafiq and Rehmat; my brothers Jahan Zaib and Zohaib; and my sister Saima . Their prayers and affection always kept me going through thick and thin. Finally, I would like to express my deepest gratitude to my wife, Saira who was a continuous source of encouragement and determination for me. Without the love and support of my wife it was not possible for me to accomplish this task.

Gulzaib Rafiq
January 2011
Grimstad, Norway

Contents

Summary

Evolving wireless technologies such as multi-antenna systems, state of the art coding techniques, diversity combining schemes, etc., constantly strive to achieve the capacity limits of wireless communication systems. On the other hand, it is a well-known fact that information theory holds the secret of describing the fundamental limits for reliable communication over the wireless medium. Information-theoretic analysis of mobile fading channels not only provides an insight into the potential and limitations of fading channels, but also provides a yardstick to design efficient wireless communication systems. The capacity is considered to be one of the most important information-theoretic measures of fading channels. The channel capacity evolves in time as a random process and can be described using appropriate stochastic models. Hence, studies pertaining to unveil the dynamics of the channel capacity can be very helpful to achieve higher data rates while keeping the probability of errors as low as possible. Statistical properties, such as mean, variance, probability density function (PDF), and cumulative distribution function (CDF) adequately characterize the channel capacity. However, these statistical quantities do not provide an insight into the temporal behavior of the channel capacity, which is imperative for the efficient design of future mobile communication systems. It is therefore, absolutely necessary to study, in addition to the first order statistical properties of the channel capacity, also the second order statistical properties, such as the level-crossing rate (LCR) and the average duration of fades (ADF).

In wireless communication systems, the random amplitude fluctuations of the received signal can be described with the help of proper statistical channel models. For single-input single-output (SISO) systems, modeling and capacity analysis of mobile fading channels are extensively studied topics. However, there still exist a few unsolved problems in this domain. Specifically, the literature lacks information regarding the influence of important phenomena, such as the severity of fading, shadowing, number of multipath components, and the amplitude of LOS components on the statistical properties of the channel capacity. This dissertation aims to address these problems by studying the capacity of specific SISO channels, namely multipath fading channels, Rice-m channels, and land mobile terrestrial channels.

A fruitful method to obtain increased spectral efficiency and improved link quality by utilizing the existing resources of the wireless network is known as cooperative communications. In relay-based cooperative networks, single-antenna mobile stations assist each other to relay the transmitted signal from the source mobile station (SMS) to the destination mobile station (DMS). Such systems are also re-

ferred to as multihop communication systems. This kind of communication scheme promises an increased network coverage, enhanced mobility, and improved system performance. It has applications in wireless local area networks (WLANs), cellular networks, ad-hoc networks, and hybrid networks. This dissertation studies the capacity of multihop communication systems employing amplify-and-forward-based blind relays under various propagation scenarios.

The performance of wireless communication systems is greatly affected by the multipath fading phenomenon. The received signal impairments, caused by multipath fading, can be reduced by diversity combining methods, such as maximal ratio combining (MRC) and equal gain combining (EGC). In diversity combining schemes, the received signals in different diversity branches are combined in a way that results in an increased signal-to-noise ratio (SNR). Hence, such methods increase the system throughput and therefore enhance the overall system performance. Motivated by the advantages of using diversity combining schemes, this dissertation also includes the analysis pertaining to the statistical properties of the capacity of fading channels in systems employing MRC and EGC. In addition, the case when diversity branches are spatially correlated, is also investigated.

Designing very high-speed wireless links that offer good quality-of-service (QoS) constitutes a significant research and engineering challenge. To perform this task, particularly in power and bandwidth limited systems, multiple-input multiple-output (MIMO) technology was proposed in the literature. By employing multiple antennas at the transmitter and the receiver, MIMO systems can provide remarkable gain in the spectral efficiency of wireless communication systems. The enormous spectral efficiency originally attributed to MIMO systems was based on the premise of a rich scattering environment, providing independent transmission paths between the transmitter and receiver antennas. Under such ideal conditions, a linear increase in the channel capacity w.r.t. the increase in the minimum of the number of transmitter and receiver antennas was observed. However, such idealized propagation conditions are rarely met in real life. Due to the spatial correlation between subchannels, realistic MIMO channels show a reduced channel capacity. It is therefore of great practical and theoretical interest to study the capacity of MIMO systems when the elements of the channel matrix are correlated. Hence, in this dissertation, a special emphasis has been put on the statistical analysis of the capacity of spatially correlated MIMO channels. To achieve the desired capacity in MIMO channels, space-time coding techniques, such as orthogonal space-time block codes (OSTBC) are considered to be an effective method. Therefore, in this PhD thesis, the capacity analysis of both correlated and uncorrelated OSTBC MIMO channels

is presented.

In summary, this dissertation deals with the derivation and analysis of the first order as well as the second order statistical properties of the capacity of mobile fading channels in various wireless communication systems. The topics studied in depth include the capacity of specific SISO channels, amplify-and-forward channels in cooperative networks, fading channels in spatial diversity combining systems, and MIMO channels.

List of Figures

List of Tables

Abbreviations

3G	third generation
3GPP	third generation partnership project
4G	fourth generation
ACF	autocorrelation function
ADF	average duration of fades
AWGN	additive white Gaussian noise
CDF	cumulative distribution function
CSI	channel state information
DMS	destination mobile station
DPSD	Doppler power spectral density
EGC	equal gain combining
EMEDS	extended method of exact Doppler spread
EUTRA	evolved universal terrestrial radio access
FSMM	finite-state Markov modeling
GMEDS	generalized method of exact Doppler spread
HD	high-definition
HDTV	high-definition television
HSDPA	high speed downlink packet access
IEEE	Institute of Electrical and Electronics Engineers
LCR	level-crossing rate
LDPC	low density parity check
LOS	line-of-sight
LTE	long term evolution
LTE-A	long term evolution-Advanced
M2M	mobile-to-mobile
MIMO	multiple-input multiple-output
MISO	multiple-input single-output
MLSS	multiple-line-of-sight second-order scattering
MMEA	modified method of equal areas

MR	mobile relay
MRC	maximal ratio combining
NLN	Nakagami-lognormal
NLOS	non-line-of-sight
NLSS	non-line-of-sight second-order scattering
OSTBC	orthogonal space-time block codes
PDF	probability density function
PSD	power spectral density
QoS	quality-of-service
SIMO	single-input multiple-output
SISO	single-input single-output
SLDS	single-line-of-sight double-scattering
SLSS	single-line-of-sight second-order scattering
SMS	source mobile station
SNR	signal-to-noise ratio
SOC	sum-of-cisoids
SOS	sum-of-sinusoids
STBC	space-time block codes
STTC	space-time trellis codes
UIU	unitary-independent-unitary
WiMAX	worldwide interoperability for microwave access
WLAN	wireless local area network
WSS	wide-sense stationary

Chapter 1

Introduction

To provide high data rate communication with higher spectral efficiency, both in cellular mobile networks and wireless local area networks (WLANs), is one of the epic challenges faced by the next generation (4G[1]) wireless communication systems. One of the motivations behind this strive is to cope with the rapidly growing desire of replacing cables with high-speed wireless connectors. Moreover, the availability of recently popular high-definition (HD) audio/video [1] over the internet as well as the presence of high-definition television (HDTV) networks [2, 3] are among the other reasons which have triggered an enormous hike in the consumers' demands for higher data rates. The modern technological advancements in electronic platforms enable users to transfer/share rich media content (e.g., high-quality audio/video) in wired networks. However, performing this task over the wireless medium requires high-speed wireless links, which are not provided by the prevailing 3G[2] cellular networks (e.g., HSDPA[3] by 3GPP[4] [4], which support up to 10 Mb/s [5, 6]) and WLANs (offering up to 50 Mb/s [7, 8]). Hence, in order to accommodate a large amount of data traffic in wireless networks with seamless connectivity, future mobile communication systems are expected to provide data rates much higher than 100 Mb/s and spectral efficiencies far greater than 10 b/s/Hz [8].

In the following, those peculiar aspects of wireless communications will be reviewed, which provide a basis for the analysis and improvement of the system performance.

[1] 4G stands for fourth generation
[2] 3G stands for third generation
[3] HSDPA corresponds to high speed downlink packet access
[4] 3GPP is an abbreviation of third-generation partnership project

1.1 Channel Capacity: Overview, Definition, Importance, and Statistical Properties

One of the reasons behind the limited success of 3G technology in achieving high data rates is mainly a lack in the understanding of the underlying fading channel characteristics, leading to the unavailability of realistic channel models [9, 10, 11]. Moreover, the unavailability of information-theoretic tools for the analysis and cross-layer optimization of wireless communication systems has also been a bottle neck in maximizing the transmission rates. Since its advent by Shannon in 1948 [12, 13], information theory has found diverse applications in the fields of communications [14], economics [15], biology [16, 17], etc. In wireless communications, information theory has widely been used in the past to study fading phenomena [18]. However, it is relatively recently that the information-theoretic analysis of complex (but realistic) fading channel models is attracting the researchers' interest [19]. Harnessing information-theoretic tools for the investigation of mobile fading channels not only provides an insight into the potential and limitations of fading channels, but also provides a yardstick to design efficient wireless communication systems [18, 20, 21].

The framework of information theory, established by Shannon for wireless communications, describes the fundamental limits for reliable communication over the wireless medium [12, 13]. This theory is based on the notion of channel capacity, which sets an upper bound on the maximum amount of information that can be reliably transmitted over a channel with a negligible probability of error. Specifically, the channel capacity determines the maximum transmission rate that a wireless channel can sustain with a negligible error probability in terms of bits per second per unit bandwidth. For the case of an ideal channel, where the only impairment in the wireless channel is the introduction of additive white Gaussian noise (AWGN), the channel capacity is given by Shannon's well-known formula [12, 13]

$$C = \log_2(1+\gamma) \text{ (bits/s/Hz)} \tag{1}$$

where γ is the ratio of the received signal power to the AWGN power, also known as the received signal-to-noise ratio (SNR). The consequence of Shannon's mathematical construct was the Shannon coding theorem and its converse. The Shannon coding theorem proves that there exists a code, which if utilized, allows to transmit data without errors at a rate r (bits/s/Hz) as long as $r < C$. While, the converse theorem showed that the error probability is always larger than zero if the transmission rate r is higher than the capacity C. In addition, Shannon demonstrated that

the channel capacity can be achieved with a negligible error probability by coding the transmitted data with infinitely long random codes. However, there exists no specification for designing such codes. In addition, infinitely long random codes are practically not realizable due to the enormous effort required for their decoding. Moreover, utilization of such lengthy codes also introduces intolerable delays in communication. For decades, the efforts of coding theorists were mainly focused to find practical codes. Finally, this problem was solved by the emergence of very effective coding techniques, such as turbo codes [22] and low density parity check (LDPC) codes [23, 24], which approach the Shannon's capacity limit very closely.

The channel capacity formula in (1) considers a simple scenario, by assuming an ideal AWGN channel. However, a realistic description of wireless propagation environment is far more complex. Mobile fading channels, particularly in urban environments, are generally classified as time-variant multipath fading channels, which can well be characterized with the help of proper statistical channel models. The dynamic behavior of mobile fading channels in turn results in a time-varying channel capacity [25], which evolves in time as a random process. For such channels, the channel capacity is described not only in terms of the received SNR γ, but it also incorporates the information regarding the statistics of the received signal envelope (see, e.g., (2)–(7), in the subsequent sections). It is demonstrated via various examples in [26, Section 4.2.6] that the actual capacity of mobile fading channels is much less than the one predicted in (1). Therefore, to get the knowledge of maximum achievable transmission rates in practical systems, it is important to study the channel capacity by considering realistic propagation conditions. Since future mobile communication systems aim to maximize the transmission rate, much consideration has been put on the analysis of the channel capacity in recent years. A large number of articles can be found in the literature that highlight the significance of using the channel capacity and its statistics as a tool for the analysis and optimization of mobile communication systems (e.g., [27, 28, 19]). Hence, in addition to the knowledge of underlying fading channel characteristics, a profound understanding of the channel capacity and its statistics is equally important.

The well-known statistical quantities describing the random behavior of the channel capacity include the mean channel capacity (or the ergodic capacity), the outage capacity, the probability density function (PDF), and the cumulative distribution function (CDF) of the channel capacity [29, 25, 28]. Among these statistical quantities, the ergodic capacity and the outage capacity are very widely explored by researchers in the literature due to their importance from the performance analysis point of view. The ergodic capacity provides the information regarding the average

data rate offered by a wireless link (where the average is taken over all the realizations of the channel capacity) [21, 29]. On the other hand, the outage capacity quantifies the capacity (or the data rate) that is guaranteed with a certain level of reliability [21, 29]. However, these two aforementioned statistical measures describe the capacity behavior on the average sense, e.g., the outage capacity gives an idea regarding the probability of a specific percentage of capacity outage, but it does not give any indication of the spread of the outage intervals or the rate at which these outage durations occur over the time scale. Whereas, the information regarding the temporal behavior of the channel capacity is very useful for the improvement of the system performance [28].

A decrease in the channel capacity below a certain desired level results in a capacity outage, which in turn causes burst errors. In the past, the level-crossing and outage duration analysis have been carried out merely for the received signal envelope to study hand-off algorithms in cellular networks as well as to design channel coding schemes to minimize burst errors [30, 31]. However, for systems employing multiple antennas (specifically at the receiver), the authors in [28] provide sufficient evidence to choose the channel capacity as a more pragmatic performance merit than the received signal envelope. Therein, the significance of studies pertaining to the analysis of the level-crossing rate (LCR) of the channel capacity can easily be witnessed for the cross-layer optimization of overall network performance. In a similar fashion, for multi-antenna systems, the importance of investigating the average duration of fades (ADF) of the channel capacity for the burst error analysis can be argued. The LCR of the channel capacity is a measure of the expected number of up-crossings (or down-crossings) of the channel capacity through a certain threshold level in a time interval of one second. While, the ADF of the channel capacity describes the average duration of the time interval over which the channel capacity is below a given level [32, 33]. It is here noteworthy that the LCR and ADF of the channel capacity are the important statistical quantities that describe the dynamic nature of the channel capacity. Hence, studies pertaining to unveil the dynamics of the channel capacity are cardinal to meet the data rate requirements of future mobile communication systems.

In the subsequent sections, some of the key technologies of wireless communications will be introduced that carry a fundamental importance in the literature and have been thoroughly investigated in this dissertation.

1.1.1 Single-Input Single-Output Systems

Single-input single-output (SISO) systems are the conventional means for wireless communications, employing single antennas at the transmitter and the receiver. The random amplitude fluctuations of the received signal in such systems can be modeled by using an appropriate stochastic process. If the channel is unknown to the transmitter but the receiver has perfect channel state information (CSI), the capacity of SISO systems, assuming flat fading[5], can be expressed as [34]

$$C(t) = \log_2\left(1+\gamma|h(t)|^2\right) \text{ (bits/s/Hz)}. \tag{2}$$

Throughout this dissertation, we have considered flat fading channels, assuming perfect CSI at the receiver. In accordance with the definition given in [34, 35, 36, 37], in this dissertation, we refer to $C(t)$ as the channel capacity. However, in the literature, it is also known to as the instantaneous channel capacity [38, 39] or the mutual information [40, 41, 42, 43]. In (2), γ denotes the average received SNR, $h(t)$ is a stochastic process, which describes the fading behavior in SISO channels, and $|h(t)|$ denotes the envelope of the process $h(t)$. For $h(t)$, a large number of models have been proposed in the literature. The widely used SISO channel models include the Nakagami-*m* [44], Rice [45], and Rayleigh [46, 47, 48] processes. The Rice and Rayleigh models have applications in line-of-sight (LOS) and non-line-of-sight (NLOS) propagation environments, respectively. While, the Nakagami-*m* process represents a more general channel model, which can be utilized to study scenarios where the fading is more (or less) severe compared to Rayleigh fading. Moreover, the Nakagami-*m* model reduces to the Rayleigh and one-sided Gaussian models in special cases. Another class of channel models, which provide a deep insight into the fundamental multipath propagation characteristics are known as multipath channel models. Such models (e.g., the sum-of-cisoids (SOC) model [49, 50, 51]), are not only accurate in modeling SISO fading channels, but also provide a clearer physical interpretation in terms of the wave propagation phenomena.

The aforementioned models however, do not incorporate the shadowing effect in land mobile terrestrial channels. For overcoming this problem, a Suzuki process is considered to be a more suitable statistical channel model [52]. The shadowing effect can be adequately modeled by a lognormal process, which can be incorporated in the channel model as a multiplicative process. Thus, the Suzuki process is generated by taking the product of a Rayleigh and a lognormal process [53]. However, by employing a Nakagami-*m* process instead of the Rayleigh process in a Suzuki pro-

[5] In flat fading, the coherence bandwidth of the channel is larger than the bandwidth of the signal, therefore all frequency components of the signal will experience the same magnitude of fading.

cess, a more general channel model referred to as the Nakagami-lognormal (NLN) model [54, 55] is obtained, which contains the Suzuki process as a special case. Hence, by using the NLN process as a channel model, the impact of shadowing on the channel capacity can be studied under different fading conditions. Moreover, the effects of severity of fading on the channel capacity can also be studied.

Although, modeling and capacity analysis of SISO channels are widely explored topics, without leaving much room for further research, there exist a few unsolved problems in this domain. Specifically, the literature lacks information regarding the influence of important phenomena, such as the severity of fading, shadowing, the number of multipath components, and the amplitude of LOS components on the statistical properties of the channel capacity. This dissertation aims to address these problems by studying the capacity of specific SISO channels, namely multipath fading channels, Rice-*m* channels, and land mobile terrestrial channels.

1.1.2 Cooperative Communication Systems

A fruitful method to obtain increased spectral efficiency and improved link quality by utilizing the existing resources of the wireless network is known as cooperative communications [56, 57, 58]. In cooperative networks, a diversity gain is attained when single-antenna mobile stations collaborate together and share their antennas to form a so-called virtual multiple-input multiple-output (MIMO) system [59]. In such scenarios, mobile stations not only transmit their own data, but also act as a relay node for other mobile stations. Hence, the transmitted signal from the source mobile station (SMS) is received at the destination mobile station (DMS) via multiple relays. This cooperation between mobile stations results in an increased network coverage with enhanced mobility support.

The simplest configuration of such relay-based cooperative networks is shown in Fig. 1.1, employing single mobile relay (MR). In the scenario depicted here, it is assumed that the direct transmission link between the SMS and DMS is not available. The MR receives the transmitted signal and forwards it to the DMS. For such systems, the channel capacity can be written similarly to (2) as

$$C(t) = \frac{1}{2}\log_2\left(1+\gamma\left|h_{eq}(t)\right|^2\right) \text{ (bits/s/Hz).} \tag{3}$$

Here, γ denotes the average received SNR at the DMS, while $h_{eq}(t)$ describes the overall SMS-DMS channel. The factor $1/2$ in (3) is due to the fact that the MR in Fig. 1.1 is assumed to be operating in a half-duplex mode, and hence the signal transmitted from the SMS is received at the DMS in two time slots. Such channels

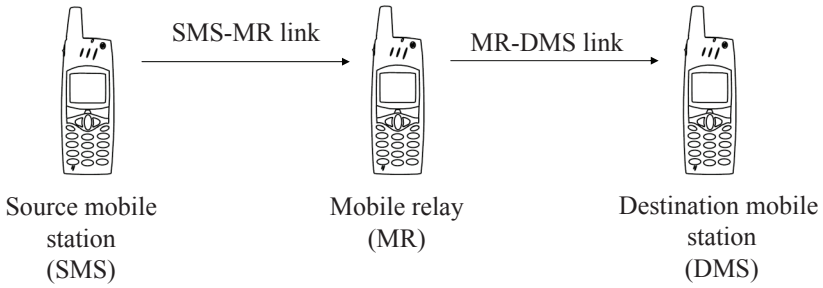

Figure 1.1: The propagation scenario describing a relay-based cooperative communication system.

are usually modeled with the help of cascaded channel models and will be discussed in detail in Chapter 3.

Figure 1.1 merely depicts a simple propagation scenario, while in practice, multiple relays exist in a relay-based cooperative network. Such systems are usually referred to as multihop communication systems. Multihop communication systems have applications in WLANs [60], cellular networks [61], ad-hoc networks [62, 63], and hybrid networks [64]. Based on the amount of signal processing used for relaying the received signal, the relays can generally be classified into two types, namely amplify-and-forward (or non-regenerative) relays [65, 66] and decode-and-forward (or regenerative) relays [67]. The relay nodes in multihop communication systems can further be categorized into channel state information (CSI) assisted relays [68], which employ the CSI to calculate the relay gains and blind relays with fixed relay gains [69]. This dissertation studies the capacity of multihop communication systems employing amplify-and-forward-based blind relays under various propagation scenarios.

1.1.3 Spatial Diversity Combining Systems

The performance of wireless communication systems is greatly affected by the multipath fading phenomenon. The aim of spatial diversity combining techniques is to combat multipath fading in contrast to modern MIMO systems which benefit from it [70, 71]. Due to this reason, spatial diversity combining provides a logarithmic increase in the spectral efficiency as compared to a linear gain (w.r.t. the number of antennas) expected from future MIMO wireless communication systems. Despite providing a limited gain in the spectral efficiency, spatial diversity combining is widely accepted to be an effective method to mitigate the effects of fading [70, 71] and has been explored quite thoroughly by researchers (see, e.g., [72, 73, 74, 75]).

Figure 1.2 shows a block diagram representation of the L-branch spatial diver-

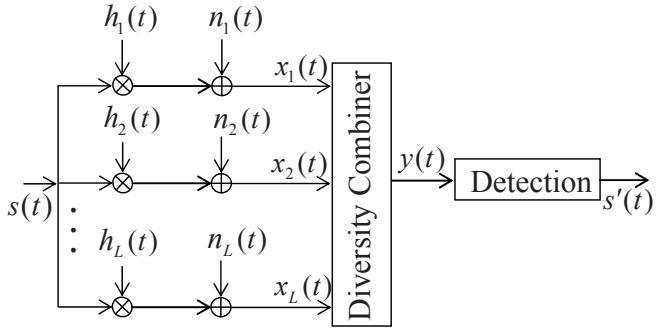

Figure 1.2: The block diagram representation of a diversity combining system.

sity combining system. Here, $s(t)$ denotes the transmitted signal, the received signals at the combiner input are represented by $x_l(t)$ $(l = 1,2,\ldots,L)$, $y(t)$ is the output of the diversity combiner and $s'(t)$ is the detected signal. The complex random channel gains, characterizing the fading behavior in the lth diversity branch, are denoted by $h_l(t)$ $(l = 1,2,\ldots,L)$, and $n_l(t)$ $(l = 1,2,\ldots,L)$ designates the corresponding AWGN. In spatial diversity combining, such as maximal ratio combining (MRC) and equal gain combining (EGC), the received signals $x_l(t)$ $(l = 1,2,\ldots,L)$ in different diversity branches are combined in such a way that results in an increased overall received SNR [70]. Hence, the system throughput increases and therefore the performance of the mobile communication system improves. The channel capacity of systems with MRC is given by [70, 34]

$$C(t) = \log_2\left(1+\gamma\sum_{l=1}^{L}|h_l(t)|^2\right) \text{ (bits/s/Hz).} \tag{4}$$

On the other hand, when EGC is employed, the channel capacity is expressed as [70, 34]

$$C(t) = \log_2\left[1+\gamma\left(\sum_{l=1}^{L}|h_l(t)|\right)^2\right] \text{ (bits/s/Hz).} \tag{5}$$

In (4) and (5), γ denotes the average received SNR of each branch. This dissertation includes the analysis pertaining to the statistical properties of the channel capacity of diversity combining systems, for both MRC and EGC. The formulas in (4) and (5) assume spatially uncorrelated diversity branches. However, studies show that the spatial correlation has a significant influence on the capacity of diversity combining systems. Therefore, in this dissertation, the case when diversity branches are spatially correlated is also considered. To keep the simplicity in presentation, the

expressions for the capacity of systems with spatially correlated diversity branches are not presented here. However, they can be found in Paper X included in Appendix J.

1.1.4 Multiple-Input Multiple-Output Systems

Designing high-speed wireless links that offer good quality-of-service (QoS), specifically in NLOS environments constitutes a significant research and engineering challenge. This task is particularly more complicated in systems with limited power and bandwidth. The scarcity of available recourses has in turn led the wireless communication system designers to explore new realms in the wireless domain, in order to satiate the ever growing consumers' demands for high data rates. One of the significant breakthroughs in this regard was the emergence of the MIMO technology, which employs multiple antennas at the transmitter and the receiver. MIMO systems provide remarkable gain in the spectral efficiency of wireless communication systems [34, 40]. This discovery resulted in a significant upsurge of interest towards MIMO systems, and since then, a large number of articles have been published in the literature dealing with MIMO channel modeling and performance analysis (see, e.g., [76, 77, 78, 36], and the references therein).

A typical block diagram representation of MIMO systems is shown in Fig. 1.3. Here, T_X represents the transmitter with N_T antennas and R_X denotes the receiver with N_R antennas. A MIMO channel is usually described by an $N_R \times N_T$ MIMO channel matrix $\mathbf{H}(t)$ with complex random entries $h_{i,j}(t)$, which model the fading behavior in the channel between the ith receiver and jth transmitter antenna. In the literature, $h_{i,j}(t)$ are also referred to as MIMO channel coefficients, channel gains, or MIMO sub-channels. In general, the capacity of MIMO channels is given by

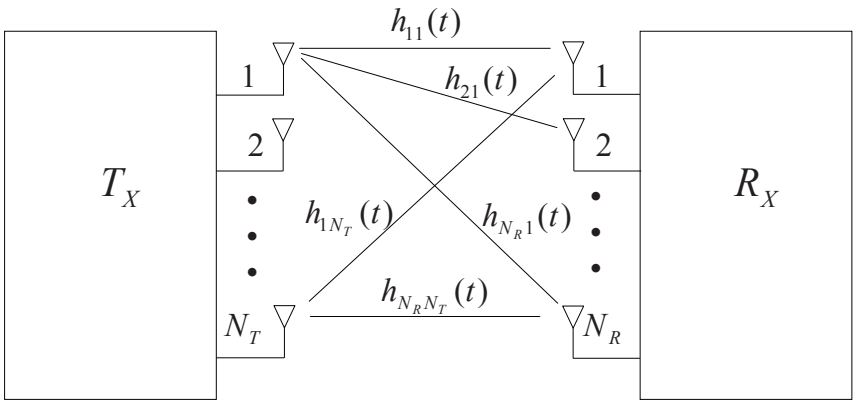

Figure 1.3: The block diagram representation of MIMO systems.

[34]

$$C(t) = \log_2 \left[\det \left(\mathbf{I}_{N_R} + \frac{\gamma}{N_T} \mathbf{H}(t) \mathbf{H}^H(t) \right) \right] \text{ (bits/s/Hz)} \tag{6}$$

where $\mathbf{I}_{N_R}$ is an $N_R \times N_R$ identity matrix, γ represents the average received SNR, and $(\cdot)^H$ denotes the Hermitian operator. The enormous spectral efficiency attributed to MIMO systems by the pioneering works of Foschini [34] and Telatar [40] is based on the premise of a rich scattering environment, providing independent transmission paths between the transmitter and receiver antennas. Hence, it results in a full-ranked channel matrix $\mathbf{H}(t)$ with independent and identically distributed (i.i.d.) entries $h_{i,j}(t)$. Under such ideal conditions, a linear increase in the channel capacity w.r.t. the increase in the minimum of the number of transmitter and receiver antennas was observed [40, 34]. However, such idealized propagation conditions can rarely be found in practice. It is shown in [79] and multiple references therein that due to the spatial correlation between the MIMO channel coefficients, realistic MIMO channels show a reduced channel capacity as compared to the results found under ideal conditions assumed in [40] and [34]. It is therefore of great practical and theoretical interest to study the capacity of MIMO systems when the elements of the channel matrix are correlated. Hence, this dissertation puts a special emphasis on the statistical analysis of the capacity of spatially correlated MIMO channels. In order to address the problem of correlated fading in MIMO channels, one of the most commonly used channel models known as the Kronecker model [80, 81, 82, 36, 42] is employed. This model, though restrictive to some cases, provides an adequate framework for the capacity analysis of MIMO channels.

Due to the exceptional spectral efficiency, employment of the MIMO architecture in the system design constitutes one of the major distinctions between 3G and 4G wireless communication systems [83]. There are many efforts underway to design high-speed wireless links in cellular networks and WLANs using MIMO technology. To name a few standards, the IEEE[6] 802.11n for WLANs [84, 7, 85] and IEEE 802.16e (also known as WiMAX: worldwide interoperability for microwave access) for broadband cellular networks [86, 87, 83] are under investigation. In addition, the 3GPP EUTRA[7] standard LTE[8]-Advanced (LTE-A) also aims to employ the MIMO architecture in order to achieve higher data rates over large distances [88, 89]. For NLOS environments, the IEEE 802.16 based systems have already been deployed, offering a peak spectral efficiency of 12 b/s/Hz [87, 8].

To increase the capacity in MIMO channels, space-time coding techniques, such

[6] IEEE corresponds to Institute of Electrical and Electronics Engineers
[7] Evolved universal terrestrial radio access is abbreviated as EUTRA
[8] LTE stands for long term evolution

as space-time trellis codes (STTC) [90] or space-time block codes (STBC) [91, 92] are considered to be an effective method. Among different space-time coding techniques, orthogonal-STBC (OSTBC) has gained much attention in recent years due to its orthogonal structure, which allows to use maximum likelihood decoding at the receiver [92]. Hence, it results in a decrease in the complexity of the receiver structure. Another advantage of using OSTBC is that it transforms MIMO fading channels into equivalent SISO channels, which significantly simplifies the mathematical formulation of MIMO channels [93]. When using OSTBC, the capacity of MIMO channels in (6) reduces to [29]

$$C(t) = \log_2 \left(1 + \frac{\gamma}{N_T} \mathbf{h}^H(t)\mathbf{h}(t) \right) \text{ (bits/s/Hz)} \tag{7}$$

where $\mathbf{h}(t)$ represents the $N_R N_T \times 1$ vector formed by stacking the columns of the $N_R \times N_T$ matrix $\mathbf{H}(t)$ one below the other. Due to the aforementioned advantages of using OSTBC in MIMO channels, it is of utmost importance to perform the capacity analysis of OSTBC MIMO channels. The analysis in this dissertation covers the capacity studies of both correlated and uncorrelated OSTBC MIMO channels.

1.2 Organization of the Dissertation

The exposition in this dissertation deals with the derivation and analysis of the first order as well as the second order statistical properties of the capacity of mobile fading channels. The topics studied in depth include the capacity of specific SISO channels, amplify-and-forward channels in cooperative networks, fading channels in spatial diversity combining systems, and MIMO channels.

The dissertation is organized as an assortment of fourteen technical papers. These technical papers are included at the end of this dissertation as Appendices A–N. Those papers which focus on similar topics are collected together to form chapters. The concordance between different papers is highlighted in the chapters. The dissertation is organized as follows:

- **Chapter 2** presents a brief discussion regarding the statistical analysis of the capacity of some specific SISO channels. The considered channels include multipath fading channels, Rice-*m* channels, and land mobile terrestrial channels. Therein, the peculiar characteristics as well as advantages of employing the corresponding SISO channel models are also highlighted. An overview of the Papers I–IV (Appendices A–D) is presented in this chapter dealing with the analysis of the influence of real-world phenomena, such as the severity of

fading, shadowing, number of multipath components, and the amplitude of LOS components on the statistical properties of the channel capacity.

- **Chapter 3** sheds light on the major contributions of the Papers V–VII (Appendices E–G). These papers deal with the capacity studies of amplify-and-forward relay-based multihop communication systems under various propagation scenarios. Chapter 3 is an effort to highlight the key factors (e.g., the severity of fading, number of hops, and LOS components) influencing the statistical properties of the capacity of multihop communication systems.

- **Chapter 4** is a compendium of the capacity analysis of fading channels in spatial diversity combining systems. Spatial diversity combining is widely accepted to be an effective method to mitigate the effects of fading and has been explored thoroughly in the literature. The Papers VIII–X (Appendices H–J) deal with a comprehensive statistical analysis of the capacity of fading channels for two different diversity combining methods, namely MRC and EGC. In addition, the influence of the LOS components as well as the spatial correlation on the channel capacity is also studied. This chapter is dedicated to review the main findings of these papers.

- **Chapter 5** is devoted to summarize important results of the Papers XI – XIV (Appendices K–N), which deal with the derivation and analysis of the statistical properties of the capacity of MIMO channels. This chapter puts a special emphasis on the statistical analysis of the capacity of spatially correlated MIMO channels. In addition, it also presents a brief discussion pertaining to the capacity analysis of both correlated and uncorrelated OSTBC MIMO channels.

- **Chapter 6** recapitulates the major contributions of this dissertation. It also highlights various important but unaddressed issues that need further research work.

Each chapter comprises various sections that discuss the sub-topics addressed in the chapter. The layout for each chapter has the following structure.

- **Introduction** provides an overview and state of the art of the main topic of the chapter.

- **Section** *N* presents a joint discussion of those papers which address a similar sub-topic under the umbrella of the main topic of the chapter. Specifically,

  - Each section begins with a short introduction of the sub-topic.
  - It then presents the problem description followed by a brief discussion on the motivation behind the problem(s) of interest. Additionally, the significance of the expected outcome(s) is elucidated.
  - Afterwards, the main results of the paper(s) are reviewed. The discussion includes advantages and disadvantages of the proposed method. Moreover, the connection between different papers addressing a sub-topic is also elaborated.

- **Chapter Summary and Conclusion** highlights the peculiar findings of the chapter.

Chapter 2

Capacity Studies of Specific SISO Channels

2.1 Introduction

The statistical analysis of the capacity of mobile fading channels has been a very active area of research in recent years. It is an established fact that for the development of future mobile communication systems a thorough understanding of underlying multipath fading channel characteristics is essential. In addition, it is also gaining recognition that a profound knowledge of channel capacity and its statistics are equally important to improve the system performance and to increase the spectral efficiency. Keeping in view the importance of capacity studies of mobile fading channels, this chapter is dedicated to the statistical analysis of the capacity of some specific SISO channels. In the following, we will articulate some of the salient features of specific SISO fading channels of interest and their respective channel models. Thereafter, in the subsequent sections, an extensive statistical analysis of the capacity of the considered fading channels will be presented.

2.1.1 Multipath Fading Channels

In wireless communications, typically in urban environments, the transmitted signal propagates to the receiver through a multitude of paths. So, the received signal is in general a superposition of a large number of multipath components. Mobile fading channels which are statistically characterized in terms of these multipath components are usually referred to as multipath fading channels. Multipath fading channel models not only describe the propagation environment accurately, but also give a deep insight into the fundamental multipath propagation characteristics. The

development of accurate and efficient channel models for the analysis of multipath fading channels has gained considerable attention in past years. Different methods have been proposed in the literature over the last few decades that deal with the design and analysis of channel models for different radio environments. One of the very promising techniques employs the sum-of-sinusoids (SOS) method to model colored Gaussian processes [94, 95]. The SOS method, originally proposed by Rice [94, 95], has been widely used by researchers ever since due to its simplicity in implementation, accuracy, and flexibility to model nearly all kinds of fading channels [96]. The versatility of this model also derives from the fact that many well-known channels, namely the Nakagami-*m* [97], Rice [98], Rayleigh [70], log-normal [99], and Suzuki [53] channels can be derived with the help of Gaussian processes. Hence, the SOS method provides the basis for the design of efficient mobile fading channel models.

The SOS-based channel models are generally designed with the assumption of symmetrical Doppler power spectral density (DPSD), for isotropic scattering environments. However, it has been shown in [100, 101, 102, 103] that the real-world channels have asymmetrical DPSDs due to non-isotropic scattering conditions. Therefore, in order to model such real-world channels, a new class of channel models known as the SOC model has been introduced in the literature [49, 50, 51]. Such SOC-based multipath channel models provide the flexibility of having correlated in-phase and quadrature phase components of the received signal, which is a main requirement for the synthesis of channels characterized by asymmetrical DPSD. Apart from the accuracy in modeling non-isotropic scattering environments, the SOC model also provides a clearer physical interpretation in terms of wave propagation phenomena when viewed in line with the plane wave propagation model [104]. The SOC model has its basis in the central limit theorem [99, p. 278] and the Clarke's scattering propagation model [49], which allows to express the channel's diffuse part in terms of a sum of scattered azimuthal plane waves [105]. The performance of the SOC model heavily relies on a careful selection of model parameters. By choosing the model parameters appropriately, it is shown in [105] that the SOC model with a small number of multipath components performs equally well as its reference model, which employs an infinite number of multipath components. The first and second order statistical properties of the SOC model are thoroughly investigated in [51] and [106]. Moreover, a detailed note on the state of the art regarding the design and analysis of the SOC model can be found in [105].

As mentioned in Chapter 1, the statistical analysis of the channel capacity is very important for the improvement in the system performance. However, to the

best of the author's knowledge, the statistical analysis of the capacity of multipath fading channels represented by an SOC model, under LOS conditions, is still an open problem. Motivated by the work presented in [105], we have adopted the SOC model as an appropriate stochastic model for multipath fading channels. Section 2.2 provides a brief account of our work pertaining to the analysis of the statistical properties of the capacity of multipath fading channels. The statistical properties of interest include the PDF, CDF, LCR, and the ADF of the channel capacity.

2.1.2 Rice-*m* Channels

Even after decades of research, the researchers of future mobile communication systems are still aiming to provide solutions to attain the maximum possible information transfer rate in communication links. The goal is to provide a better and more general description of the wireless propagation environment compared to the existing channel models, e.g., the Rice and Rayleigh channel models. The Rice and Rayleigh distributions are widely accepted as suitable frequency-nonselective channel models for modeling the fading behavior in dispersive urban environments. However, it has been reported in the literature that it is very common to come across scenarios where the fading is more (or less severe) as compared to the Rayleigh fading [107, 108]. Thus, in order to study more realistic fading scenarios, a more general channel model compared to the Rayleigh model is required. For this reason, the Nakagami-*m* process has gained much attention in recent years due to its flexibility of modeling different fading conditions, mathematical ease, and good fitness with experimental data [107, 108, 97]. The generality of this model also derives from the fact that it incorporates Rayleigh and one-sided Gaussian models as special cases. The second order statistical properties of Nakagami-*m* channels are investigated in [97]. Moreover, a large number of articles can be found in the literature dealing with the analysis of the capacity of Rice and Rayleigh channels [36, 33, 43, 109]. Furthermore, the statistical analysis of the channel capacity of Nakagami-*m* channels can be found in [110, 111]. Although there exist a large number of channel models, there is still a need for a better description of the mobile radio environment.

Propelled by the advantages of using a general model for describing the channel statistics, the work summarized in Section 2.3 proposes a channel model referred to as the Rice-*m* channel model. In the literature, the presented Rice-*m* model is also termed as the Rice model of order 2*m* [112] or the non-central chi model [113]. It is worth mentioning here that for the integer values of 2*m*, the Nakagami-*m* process can be represented as a square root of a sum of 2*m* squared zero-mean i.i.d. Gaussian processes [97]. As the novelty of the Rice-*m* channel model comes from

the assumption that the underlying random processes in the Nakagami-*m* channel model are i.i.d. Gaussian processes, each with non-zero mean. Hence, the received signal envelope in Rice-*m* channels is modeled as the square root of a sum of $2m$ squared non-zero mean i.i.d. Gaussian processes. The proposed channel model includes the Nakagami-*m*, Rice, Rayleigh and one-sided Gaussian fading channel models as special cases.

2.1.3 Land Mobile Terrestrial Channels

As mentioned earlier, the random amplitude fluctuations of the received signal can be modeled using an appropriate stochastic process. Moreover, it is also an established fact that for urban and suburban areas, where the LOS signal component is blocked by obstacles, the Rayleigh process is a suitable stochastic process to model the channel [46, 47, 48]. Furthermore, in rural regions, the LOS component is often a part of the received signal, so that the Rice process is an appropriate choice for modeling such channels. However, the validity of Rice and Rayleigh channel models is limited to small areas having dimensions in the order of a few tens of wavelengths. It is also assumed that the local mean of the received signal envelope remains approximately constant in these areas [70]. On the other hand, in land mobile terrestrial channels, the local mean fluctuates in large areas due to shadowing effects. It has widely been reported in the literature that shadowing can adequately be modeled by a lognormal process [114, 115, 116, 117]. Therefore, for the case of land mobile terrestrial channels, a Suzuki process is considered to be a more suitable statistical channel model [52].

The Suzuki process is generated by taking the product of a Rayleigh and a lognormal process [53]. Therefore, modeling the channel by a Suzuki process enables us to study the combined effects of shadowing and fast fading on the statistics of the received signal envelope [52]. In the preceding section, it was pointed out that there exist scenarios where the fading is more (or less) severe than Rayleigh fading. In addition, the previous section also convincingly argued on the generality of the Nakagami-*m* model, since it contains the Rayleigh and one-sided Gaussian processes as special cases (i.e., for $m = 1$ and $m = 0.5$, respectively). Therefore, it is more appropriate to use a Nakagami-*m* process instead of the Rayleigh process to model fast fading [44, 107, 97, 118]. Hence, by employing a Nakagami-*m* process instead of the Rayleigh process in a Suzuki process, we obtain a more general channel model referred to as the NLN channel model [54, 55], which contains the Suzuki process as a special case when $m = 1$. By using the NLN process as a channel model, the impact of shadowing and severity of fading on the received signal

envelope can be studied.

The analysis of the PDF, CDF, LCR, and ADF of the channel capacity of fast fading channels, like Rayleigh channels can easily be found in the literature, e.g., in [33, 36, 32, 35, 119]. However, there is a lack of information regarding the combined effects of shadowing and fast fading on the channel capacity. Section 2.4 aims to fill this gap by studying the statistical properties of the capacity of Suzuki channels. Moreover, to go a step further, the analysis is extended to the case of NLN channels to study the influence of severity of fading on the channel capacity in land mobile terrestrial channels.

2.2 Statistical Analysis of the Capacity of Multipath Fading Channels

In Section 2.1.1, the distinctive features of multipath fading channel models were explicated. Therein, the advantages of using the SOC-based channel modeling approach were highlighted. Motivated by these advantages, Paper I employs an SOC model for the characterization of multipath fading channels under LOS conditions. Thereafter, the statistical properties of the channel capacity are investigated. This section aims to summarize the discussion presented in Paper I that can be found in full in Appendix A [120]. Therein, the scattered component of the received signal in a multipath fading channel is modeled as a weighted sum of N complex exponentials, also known as cisoids. As mentioned in Section 2.1.1, this model is based on the Clarke's scattering propagation model [49], which represents the channel's diffuse part in terms of a sum of scattered azimuthal plane waves [105]. So, each cisoid in the SOC model characterizes a plane wave with the help of the model parameters, namely the gains, phases and Doppler frequencies. Based on the nature (i.e., either deterministic or random) of these model parameters, the SOC model can be classified into different categories (consult [105, Table 3.1] for details). In Paper I, we have assumed constant gains, constant Doppler frequencies, but random phases uniformly distributed over the interval $(0, 2\pi]$. Under LOS conditions with $N \to \infty$, it follows from the central limit theorem that the received signal envelope described by an SOC model using specific values of gains follows the classical Rice PDF [51]. In our work, this constitutes the reference model for the SOC model. The reference model (which arises when $N \to \infty$ in the SOC model) serves as a benchmark for the performance evaluation of the SOC model. Specifically, the aim is to choose the model parameters in such a way that the SOC model with least possible number of cisoids N produces similar results as the reference model.

The values of the gains and Doppler frequencies can be found with the help of an appropriate parameter computation method. Depending on the propagation conditions, there exist numerous methods in the literature for the computation of the SOC model parameters (see, e.g., [105, Chapter 4] and [51, 106, 121]). Although the SOC model can efficiently be used to characterize channels having asymmetrical DPSDs, we have restricted our analysis in Paper I to the case of isotropic scattering conditions to keep the simplicity in presentation. However, it is noteworthy that the presented results in Paper I do not alter for non-isotropic scattering scenarios. Instead, for such cases, it is only needed to use a suitable parameter computation method to find the respective values of the underlying model parameters. To find the gains and Doppler frequencies, the extended method of exact Doppler spread (EMEDS) [106, 105] is employed. It is due to the reason that the EMEDS, introduced in [122], is considered to be a very efficient method to reproduce the Doppler spreads of isotropic scattering channels [105].

Paper I is aimed at the derivation and analysis of the statistical properties of the capacity of multipath fading channels represented by an SOC model, under LOS conditions. The statistical properties studied in depth include the PDF, CDF, LCR, and ADF of the channel capacity. The mean channel capacity and spread of the channel capacity can be studied with the help of the PDF and CDF of the channel capacity. While, the LCR and ADF of the channel capacity are important statistical quantities that give an insight into the temporal behavior of the channel capacity [36, 33]. As stated in Chapter 1, the LCR is a measure of the average rate of the up-crossings (or down-crossing) of the capacity through a certain threshold level in one second. On the other hand, the ADF determines the average duration of time over which the channel capacity is below a certain threshold level [33]. In Paper I, exact analytical expressions for the PDF, CDF, LCR, and ADF of the channel capacity are derived. The mathematical developments can be found in the paper included in Appendix A. In this section, only the major contributions of the paper are highlighted. The results are studied for different values (N) of the number of multipath components (cisoids) in the SOC model. The results for the reference model are also presented, which can be obtained from the SOC model when $N \to \infty$. It has been observed that as the value of N increases, the results obtained using the SOC model approach to those of the reference model. Specifically, for $N \geq 10$, a very good fitting between the reference model and the SOC model is observed. It is also observed that the parameter N has more influence on the statistical properties of the capacity of the channels with a lower value of the amplitude of the LOS component ρ (e.g., $\rho = 0$) than the channels with higher values of ρ (e.g., $\rho = 2$). All the

results show that the presented SOC model with 10 cisoids can be very effectively used for the statistical analysis of the capacity of multipath fading channels.

2.3 Statistical Analysis of the Envelope and the Capacity of Rice-m Channels

In Section 2.1.2, the need for an efficient and general channel model was emphasized that can be applied to a variety of propagation scenarios as well as incorporates the well-known classical channel models, such as the Nakagami-m, Rice, and Rayleigh models as special cases. In order to fulfil this need, the Rice-m model is introduced in Paper II as a more general and appropriate channel model than the aforementioned classical channel models. This section aims to sum up the findings of Paper II included in Appendix B [123] of this dissertation. As stated previously, the received signal envelope in Rice-m channels is modeled as the square root of a sum of $2m$ squared non-zero mean i.i.d. Gaussian processes. It is important to mention here that the Rice-m model has two important parameters, namely m and ρ. From the model perspective, the parameter m sets the order of the Rice process [112], while in terms of physical phenomenon it controls the severity of fading in Rice-m channels. Specifically, as the value of m increases, the fading severity decreases and vice versa. On the other hand, the parameter ρ can be termed as the noncentrality parameter [112] and is dependent on the mean values of the underlying Gaussian processes. By increasing the mean values of the underlying Gaussian processes, the value of ρ increases and vice versa. For $m = 1$, it can be observed that the Rice-m channel reduces to the classical Rice channel. Moreover, it can be proved that for $\rho \to 0$, the Rice-m model tends to the Nakagami-m model presented in [97, Eqs. (7a,b)]. Furthermore, the Rice-m channel equals the Rayleigh channel if $m = 1$ and $\rho \to 0$.

Paper II presents a thorough statistical analysis of the capacity of channels described using the Rice-m model. Exact analytical closed-form expressions are derived for the statistical properties of the envelope and the capacity of Rice-m channels. The validity of the analytical results is verified with the help of simulations, whereby a very good fitting is observed. Mostly in this dissertation, for simulation purposes, the underlying uncorrelated Gaussian distributed waveforms are simulated by employing the SOS model [94, 95, 96], which was discussed briefly in Section 2.1.1. The motivation behind choosing an SOS-based channel simulator is that it is widely acknowledged for its simplicity in implementation, accuracy, and flexibility to simulate nearly all kinds of fading channels under isotropic scattering

conditions [96]. The SOS model is based on the superposition principle stating that a superposition of infinitely large number of weighted harmonic wave forms results in a stochastic Gaussian process. The harmonic waveforms are describe with the help of model parameters, namely the gains, frequencies and phases. Alike the SOC model considered in Section 2.1.1, the performance of the SOS model is strongly dependent on the parameters computation method. We have employed an SOS model with constant gains, constant frequencies and random phases uniformly distributed over the interval $(0, 2\pi]$. To calculate the suitable values for the gains and frequencies we have used the generalized method of exact Doppler spread (GMEDS_1) [121]. The GMEDS is considered to be an extremely efficient method for the generation of an unlimited number of uncorrelated Gaussian waveforms [121]. In addition, it also includes the EMEDS (introduced in the previous section) as a special case.

To present a complete picture, Paper II also illustrates the results of the aforementioned special cases of Rice-m channels, namely Nakagami-m channels ($\rho \to 0$), Rice channels ($m = 1$), and Rayleigh channels ($\rho \to 0$, $m = 1$). The study shows that the mean values of the underlying Gaussian processes and the severity of fading have a significant influence on the statistical properties of the channel capacity. Specifically, it is observed that an increase in the mean values of the underlying Gaussian processes or a decrease in the severity of fading increases the mean channel capacity. While, the spread of the channel capacity decreases. Moreover, at higher levels, the LCR of the capacity of Nakagami-m channels is lower as compared to that of Rice-m channels. The importance of the analysis in Paper II lies in merging the Nakagami-m and classical Rice channel characteristics into a new channel model, which has thus a higher flexibility than the two former ones.

2.4 Statistical Analysis of the Capacity of Land Mobile Terrestrial Channels

The works summarized in the preceding two sections only consider fast fading in mobile fading channels due to multipath propagation in dispersive urban environments. For fast fading channels, the Rice and Rayleigh distributions are widely accepted as suitable frequency-nonselective channel models for modeling the fading behavior. Moreover, for such channels, the previous section convincingly articulated the advantages of employing more general channel models such as the Nakagami-m or Rice-m models. However, the validity of the aforementioned channel models, specifically the Rice and Rayleigh channel models, is limited to small areas where the local mean of the received signal envelope remains approximately

constant [70]. As highlighted in Section 2.1.3, in land mobile terrestrial channels, the local mean fluctuates in large areas due to shadowing effects [124]. It is reported in the literature that shadowing can adequately be modeled by a lognormal process and can be incorporated in the channel model as a multiplicative process [124, 52, 54, 55]. Therefore, for land mobile terrestrial channels, the Suzuki process is considered to be a more appropriate channel model [52]. A Suzuki process can be expressed as a product of a Rayleigh process and a lognormal process. Due to the assumption of isotropic scattering, the underlying Gaussian processes in the Suzuki process possess a symmetric power spectral density (PSD) [49, 70]. For this reason, the widely used Jakes PSD is employed for the underlying Gaussian process in the Rayleigh process. Whereas, for the spectral shape of the Gaussian process in the lognormal process, various models have been proposed in the literature [125]. One of these models employs a Gaussian PSD, which is also used in our study in Paper III.

Paper III included in Appendix C [126] investigates the influence of shadowing on the statistical properties of the channel capacity. The problem is addressed by using a Suzuki process as an appropriate statistical channel model for land mobile terrestrial channels. Using this model, exact expressions for the PDF, CDF, LCR, and ADF of the channel capacity are derived. In a Suzuki process, the shadowing effect is controlled by the parameter σ_L, known as the shadow standard deviation. Previous studies show that the shadow standard deviation can have a wide range of values depending on the terrestrial environment [114]. Specifically, it has been shown in [114] that $\sigma_L = 4.3$ dB can be chosen as a suitable value for urban environments, whereas $\sigma_L = 7.5$ dB is an appropriate value for suburban areas. Therefore, it is important to study the statistical properties of the channel capacity for different values of the shadow standard deviation. Paper III takes into account different values of σ_L, ranging from 1 dB to 10 dB. Moreover, the results obtained for $\sigma_L = 4.3$ dB (urban environment [114]) and $\sigma_L = 7.5$ dB (suburban environment [114]) are also shown. In addition, some special cases, e.g., Rayleigh fading $(\sigma_L \to 0 \text{ dB})$ and lognormal fading $(\sigma_0^2 = 0)$ are also included, for comparison purposes. Here, the parameter σ_0^2 denotes the variance of the underlying Gaussian processes in the Rayleigh process.

The theoretical results have been verified by simulations, where the simulation results match the theoretical expectations very closely. In order to obtain simulation results, a high-performance stochastic channel simulator based on the SOS principle [94, 95, 96] was employed. The resulting structure of the simulation model for the analysis of the capacity of Suzuki channels is shown in Fig. C.1 in Appendix C. For the underlying Gaussian processes in the Rayleigh process, the model param-

eters (i.e., the gains and the frequencies) are calculated using the GMEDS_1 [121]. Whereas, for the case of lognormal processes, the SOS model employs the modified method of equal areas (MMEA) [127] to simulate the underlying Gaussian process. One of the reasons behind choosing the MMEA instead of the GMEDS for simulating Gaussian processes with a Gaussian PSD is that the GMEDS was developed especially for the commonly used Jakes PSD [96]. On the other hand, the developments in the MMEA do not assume any specific PSD as a starting point. However, it is worth mentioning that by doing slight modification in the GMEDS, similar results obtained using the MMEA can be found from the GMEDS. In other words, the GMEDS includes the MMEA as a special case.

The study in Paper III revealed that the variance as well as the maximum value of the PDF and LCR of the channel capacity, respectively, are highly influenced by the shadow standard deviation. Results show that as the value of the shadow standard deviation increases the variance of the channel capacity increases. However, this parameter has only a minor effect on the mean channel capacity. It is also observed that as the shadow standard deviation approaches 0 dB, the statistics of the channel capacity of Suzuki channels approaches to that of Rayleigh channels. Although the findings of Paper III are very helpful for analyzing the dynamic behavior of the channel capacity for land mobile terrestrial channels in different terrestrial environments, they do not provide an insight into the influence of severity of fading on the channel capacity. This shortcoming of the Suzuki channel model can be removed by employing a more general channel model, which is the topic of Paper IV included in Appendix D [128].

Paper IV employs a Nakagami-*m* process instead of the Rayleigh process in a Suzuki process to obtain a more general channel model referred to as the NLN channel model [54, 55]. The NLN channel model contains the Suzuki process as a special case, i.e., when $m = 1$. It was already emphasized in the previous section that it is more appropriate to use a Nakagami-*m* process instead of a Rayleigh process to model fast fading. In addition, the Nakagami-*m* process contains the Rayleigh process as special case. Hence, by using the NLN process as a channel model, the impact of shadowing on the channel capacity can be studied under different fading conditions. Moreover, the effects of severity of fading on the channel capacity can also be studied. Motivated by the advantages of using the NLN channel model, the work presented in Paper III is extended to the case of NLN channels in Paper IV. Specifically, analytical expressions for the PDF, CDF, LCR, and ADF of the capacity of NLN channels are derived, to investigate the influence of the shadowing effect and the severity of fading on the statistical properties of the channel

capacity. It has been observed that if the fading is less severe as compared to the Rayleigh fading, the spread of the PDF and the maximum value of the LCR of the channel capacity decrease, while the mean channel capacity increases. On the other hand, increasing the shadowing standard deviation increases the spread of the PDF, while it decreases the maximum value of the LCR of the channel capacity. However, the shadowing standard deviation has no effect on the mean channel capacity for any fading condition. The results presented in Paper IV provide a flexibility to the communication system designers to choose between different fading conditions, corresponding to different terrestrial environments, and are hence quite useful for the design and analysis of land mobile terrestrial channels. All analytical results obtained in Paper IV are verified by simulations where a very good fitting between theoretical and simulation results is found. Here, the simulation results are generated with the help of an SOS-based channel simulator [94, 95, 96], while the model parameters are calculated by using the GMEDS_1 [121].

2.5 Chapter Summary and Conclusion

Future wireless communication systems demand a comprehensive as well as generic description of real-world propagation environments, incorporating the most distinctive propagation characteristics. To achieve this goal, numerous statistical models have been published in the literature for the characterization of mobile fading channels. In addition, it is also gaining recognition that the studies pertaining to the statistical analysis of the channel capacity not only provide the information regarding the potential and limitations of the fading channels but also help to improve the system performance. For this reason, the current chapter was dedicated to the statistical analysis of the capacity of specific SISO channels that are of great theoretical and practical interest.

This chapter started by stressing the motivation behind the investigation of some specific SISO channels. Therein, the peculiar characteristics as well as advantages of employing the corresponding SISO channel models were also highlighted. Thereafter, the need for the analysis of multipath fading channels was emphasized. It was mentioned that multipath channel models, such as the SOC model, provide a deep insight into the fundamental multipath propagation characteristics. However, to know the potential limits in terms of the spectral efficiency of such fading channels, a solid understanding of the statistical properties of the channel capacity is cardinal. Hence, a thorough statistical analysis of the channel capacity of multipath fading channels described using an SOC model under LOS propagation conditions was carried out. This work illustrated the influence of the number of multipath com-

ponents and the amplitude of the LOS components on the channel capacity. It was observed that the number of multipath components has more influence on the statistical properties of the capacity of the channels with a lower value of the amplitude of the LOS component ρ (e.g., $\rho = 0$) than on the channels with higher values of ρ (e.g., $\rho = 2$). This study also revealed that the presented SOC model with 10 cisoids can be very effectively used for the statistical analysis of the capacity of multipath fading channels. This chapter merely summarized the important results of the work related to the capacity analysis of multipath fading channels; however, the details can be found in Paper I included in Appendix A.

The chapter then articulated the reasons behind using a more general channel model than the Rice and Rayleigh models. Propelled by those reasons, this chapter introduced the Rice-*m* model as a more general and appropriate channel model than the aforementioned classical channel models. Afterwards, the statistical properties of the capacity of Rice-*m* channels were briefly discussed. This chapter highlighted the important finding of Paper II (Appendix B), which deals with the derivation and analysis of the statistical properties of the envelope and the capacity of Rice-*m* channels. The statistical properties studied in depth include the PDF, CDF, LCR, and ADF of the channel capacity. The importance of the work presented in Paper II lies in merging the Nakagami-*m* and classical Rice channel characteristics into the Rice-*m* channel model, thus providing a higher flexibility than the two former ones.

The chapter ended by summing up the main findings of Papers III and IV (Appendices C and D), which deal with the capacity studies of land mobile terrestrial channels. It was pointed out that in land mobile terrestrial channels, the local mean of the received signal envelope fluctuates due to the shadowing effect. However, the well-known channel models, namely the Nakagami-*m*, Rice, and Rayleigh models, only consider fast fading. Hence, to study the influence of shadowing on the statistical properties of the channel capacity, Paper III employs the Suzuki process as an appropriate channel model for land mobile terrestrial channels. Our study revealed that the variance and the maximum value of the PDF and LCR of the channel capacity, respectively, are highly influenced by the shadow standard deviation. However, the flexibility of the results presented in Paper III is limited due to the fact that these results do not provide an insight into the influence of severity of fading on the channel capacity. This limitation of the Suzuki channel model was removed by employing a more general channel model referred to as the NLN model, which is the topic of Paper IV included in Appendix D. By using the NLN process as a channel model, the impact of shadowing and severity of fading on the statistical properties of the channel capacity was investigated.

Chapter 3

Capacity Studies of Amplify-and-Forward Channels in Cooperative Networks

3.1 Introduction

Increased network coverage, improved link quality, and provision of new applications with increased mobility support are the basic demands imposed on future mobile communication systems. One promising solution to fulfil these requirements by utilizing the existing resources of the wireless networks is the use of cooperative diversity techniques [56, 57, 58]. Single-antenna mobile stations in cooperative networks assist each other to relay the transmitted signal from the SMS to the DMS. Such a cooperation between mobile stations results in an increased network coverage with enhanced mobility support.

In relay-based cooperative networks, the transmitted signal from the SMS is received at the DMS via MRs. Based on the amount of signal processing used for relaying the received signal, the relays can generally be classified into two types, namely amplify-and-forward (or non-regenerative) relays [65, 66] and decode-and-forward (or regenerative) relays [67]. The relay nodes in such cooperative networks can further be categorized into CSI assisted relays [68], which employ the CSI to calculate the relay gains and blind relays with fixed relay gains [69]. This chapter is devoted to the capacity studies of cooperative communication systems employing amplify-and-forward-based blind relays under various propagation scenarios.

For the development and analysis of wireless communication systems that exploit cooperative diversity, a profound knowledge of the multipath fading channel characteristics is required. Recent studies illustrate that mobile-to-mobile (M2M)

fading channels associated with relay-based cooperative networks under NLOS propagation conditions in different propagation scenarios can be modeled either as a double Rayleigh process [129, 130, 131, 132] or an NLOS second-order scattering (NLSS) process [133]. On the other hand, different scenarios under LOS propagation conditions lead to modeling the overall M2M fading channel either by a double Rice process [134], a single-LOS double-scattering (SLDS) process [135], a single-LOS second-order scattering (SLSS) process [133], or a multiple-LOS second-order scattering (MLSS) process [136, 137]. These studies provide results for the statistical characterization of M2M fading channels in cooperative networks under different propagation conditions.

The previously mentioned channel models (e.g., the double Rice and double Rayleigh models) belong to the class of cascaded fading channel models. For the case of amplify-and-forward-based cooperative networks employing single relay, cascaded channel models represent the overall channel between the SMS and the DMS via an MR as a concatenation of the SMS-MR and MR-DMS channels. For such dualhop communication systems, the overall SMS-DMS channel under LOS (or NLOS) propagation conditions can be described using a double Rice (or double Rayleigh) process. The impact of double Rayleigh fading on the performance of a communication system is investigated in [138]. Moreover, studies pertaining to the analysis of the outage capacity of double Rayleigh channels can be found in [139, 140]. Even with all this research going on, the important question regarding the maximum possible information transfer rate in such fading channels is still unanswered. Specifically, to the best of the author's knowledge, the statistical properties of the capacity of double Rice channels have never been investigated. Thus, the purpose of the work summarized in Section 3.2 is to fill in this gap in information regarding the capacity of amplify-and-forward channels in dualhop cooperative networks. Therein, we have briefly discussed the influence of the amplitude of LOS components, corresponding to the two transmission links of double Rice fading channels, on the channel capacity.

As mentioned at multiple occasions in this dissertation, the Nakagami-*m* process is considered to be a more general channel model as compared to the Rayleigh process. Due to this reason, the double Rayleigh model has been extended to the double Nakagami-*m* channel model in [141]. Moreover, second order statistics for the double Nakagami-*m* process can be found in [142]. To generalize the discussion regarding the capacity of amplify-and-forward channels in dualhop cooperative networks, the statistical analysis of the capacity of double Nakagami-*m* channels is performed. Section 3.3 presents an overview of this work pertaining to the analy-

sis of the statistical properties of the capacity of double Nakagami-*m* channels. It is worth mentioning that cascaded channel models not only find application in dualhop communication systems [129, 143, 144, 134], but are also widely acknowledged for their use in keyhole channels [138, 142]. It is shown in [131, 145] that in the presence of a keyhole, the fading between each transmit and receive antenna pair in a MIMO system can be characterized using a double Rayleigh process. In [138], the authors have listed a few real-world scenarios which give rise to the keyhole effect. Two such scenarios include diffraction through the street edges in urban microcellular environments [131] and traversal of the propagation paths through a narrow space for the case when the distance between the rings of scatterers around the transmitter and receiver is large [140]. Hence, our work pertaining to the analysis of the capacity of double Nakagami-*m* channels can be adapted accordingly to the case of keyhole channels.

The dualhop scenario described above constitutes the simplest configuration of cooperative networks, comprising a transmitting terminal, a receiving terminal, and a relaying node. However, in practice, there can exist more than one relay in amplify-and-forward channels in cooperative networks. Such systems are commonly referred to as multihop communication systems. Multihop communication promises an increased network coverage and enhanced mobility. It has applications in WLANs [60], cellular networks [61], ad-hoc networks [62, 63], and hybrid networks [64]. To characterize the fading in the end-to-end link between the SMS and the DMS in a multihop communication system, the authors in [143] have proposed the $N*$Nakagami-*m* channel model, assuming that the fading in each link between the wireless nodes can be modeled by a Nakagami-*m* process. The second order statistical properties of multihop Rayleigh fading channels have been studied in [144]. Moreover, the performance analysis of multihop communication systems for different kinds of relaying can be found in [146, 69, 65, 66], and multiple references therein. Hence, to extend our work dealing with the capacity analysis of double Nakagami-*m* channels to the case of multihop communication systems, the statistical properties of the capacity of $N*$Nakagami-*m* channels are studied. This work is reviewed briefly in Section 3.4. In addition to provide a broader perspective of amplify-and-forward channels in cooperative networks, the $N*$Nakagami-*m* channel model includes the double Nakagami-*m* model as a special case.

The remainder of this chapter is organized as follows. Section 3.2 articulates important results related to the capacity studies of double Rice channels. Thereafter, statistical properties of the capacity of double Nakagami-*m* channels are studied in Section 3.3. An extension of this work is presented in Section 3.4, which deals with

the capacity analysis of $N*$Nakagami-m channels. Finally, the chapter summary is given in Section 3.5.

3.2 Statistical Analysis of the Capacity of Double Rice Channels

Amplify-and-forward channels in cooperative networks provide a promising improvement in the network coverage and system throughput. Figure 3.1 depicts an example of the transmission link from the SMS to the DMS via an MR in such amplify-and-forward relay-based cooperative networks. It is noteworthy that the considered scenario assumes the absence of a direct transmission link between the SMS and the DMS. As mentioned in the preceding section, such channels can be described using cascaded channel models, where the overall channel between the SMS and the DMS via an MR is represented as a concatenation of the SMS-MR and MR-DMS channels [134, 132]. Under LOS propagation conditions, the fading in the SMS-MR and MR-DMS links is characterized using statistically independent non-zero-mean complex Gaussian processes $\mu_\rho^{(1)}(t)$ and $\mu_\rho^{(2)}(t)$, respectively. Thus, the overall fading channel describing the SMS-DMS link is modeled as a product of two non-zero-mean complex Gaussian processes $\mu_\rho^{(i)}(t)$ $(i=1,2)$. The envelope of the product-process, describing the SMS-DMS fading channel, results in a double Rice process [134, 132].

This section presents an overview of the work dealing with the capacity analysis

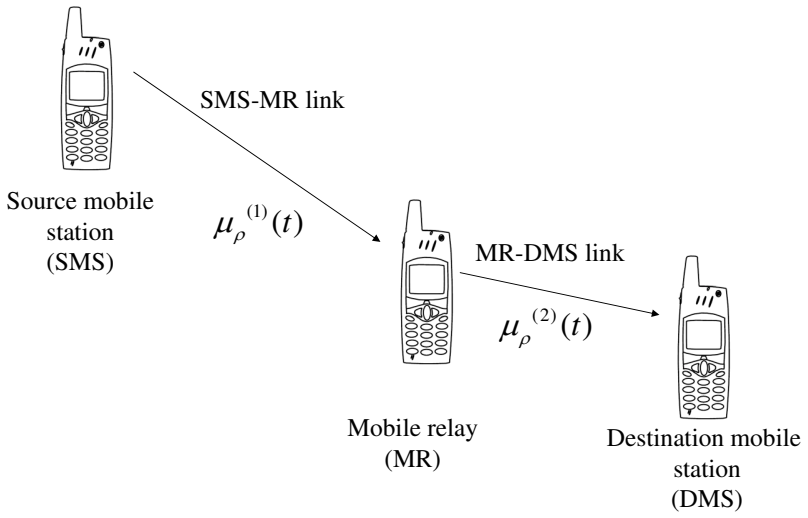

Figure 3.1: The propagation scenario describing dualhop fading channels.

of double Rice channels. The detailed discussion on this topic can be found in Paper V included in Appendix E [147]. Paper V presents the derivation of analytical expressions for the PDF, CDF, LCR, and ADF of the channel capacity. The obtained results are studied for different values of the amplitudes of the LOS components in the two transmission links of double Rice fading channels. The statistical properties of the capacity of double Rice channels reduce to those of double Rayleigh channels by setting the amplitude of the LOS components in the SMS-MR and MR-DMS links equal to zero. In this study, the results for double Rayleigh channels are included as a special case. Additionally, Paper V also presents the statistical properties of the capacity of classical Rice and classical Rayleigh channels for comparison purposes.

It has been observed that the statistics of the capacity of double Rice fading channels are quite different from those of double Rayleigh, classical Rice, and classical Rayleigh fading channels. Specifically, the presence of an LOS component in one or both of the links (i.e., the SMS-MR and MR-DMS links) increases the mean channel capacity. Hence, double Rayleigh channels have a lower mean channel capacity compared to double Rice channels. It is also observed that the capacity of classical Rice channels has a lower mean value and a lower capacity variance as compared to that of double Rice channels. This is because Paper V assumes that the MR operates in a full-duplex mode, which allows it to receive and transmit at the same time. On the other hand, when the MR operates in a half-duplex mode, the mean capacity of double Rice channels is expected to be lower than that of classical Rice channels. In practical systems, the full-duplex assumption is very difficult to fulfil. Therefore, to study realistic scenarios, half-duplex relaying should be considered. This drawback of Paper V is removed in Paper VI, which considers a half-duplex MR. The important findings of Paper VI will be reviewed in the next section.

Results in Paper V also reveal that for medium and high levels, the presence of LOS components in the two cascaded transmission links increases the LCR of the channel capacity. However, it results in a decrease in the ADF of the channel capacity. It is also observed that the LCR of the capacity of classical Rice channels is much lower compared to that of double Rice channels. Study in Paper V also revealed that the LCR and ADF of the capacity of double Rice channels are strongly dependent on the Doppler frequencies of the MR and the DMS. The correctness of the derived results is checked by simulations, whereby a very good fitting between the analytical and simulation results is found. A high-performance channel simulator is employed to obtain the simulation results. The channel simulator operates on

the SOS principle [94, 95, 96] to simulate the underlying Gaussian processes that make up the overall double Rice process. The parameters of the channel simulator are computed using the GMEDS_1 [121].

3.3 Statistical Analysis of the Capacity of Double Nakagami-*m* Channels

The previous section dealt with the capacity analysis of double Rice channels. The double Rice channel model allows to study the statistical properties of the channel capacity of amplify-and-forward channels under LOS propagation conditions. In addition, the results can easily be reduced to double Rayleigh channels in the absence of LOS components in both the transmission links of double Rice channels. Despite of having profound theoretical and practical importance, the results presented in the preceding section only consider similar fading conditions (e.g., Rayleigh fading) in both the links of the dualhop communication system. However, there exist studies in the literature reporting the possibility to come across scenarios where the fading is more (or less severe) as compared to the Rayleigh fading [107, 108]. For this reason, it is proposed in the literature to employ the Nakagami-*m* process as a more appropriate channel model. In a similar fashion, the possibility of having different fading conditions (e.g., due to dissimilar propagation environments) in the two transmission links of dualhop communication systems can be argued. Due to this reason, the double Nakagami-*m* channel model has been adopted as a more suitable model for amplify-and-forward channels than the one studied in the previous section. By employing the double Nakagami-*m* channel model, we can study the influence of severity fading, in the two transmission links of dualhop communication systems, on the channel capacity. Moreover, as mentioned earlier, double Nakagami-*m* channel model is also useful for modeling real-world scenarios such as keyhole channels [141, 142]. Though a lot of papers have been published in the literature employing the cascaded fading channel model, the statistical properties of the capacity of double Nakagami-*m* channels have not been investigated so far, which finds applications both in keyhole channels and dualhop communication systems [142]. To address this problem, a thorough statistical analysis of the capacity of double Nakagami-*m* channels is performed in Paper VI, which can be found in Appendix F [148] of this dissertation.

This section aims to present a brief overview of Paper VI (Appendix F). Therein, we have considered a similar dualhop communication system as shown in Fig. 3.1. However, in this case the fading in the ith $(i = 1, 2)$ transmission link is modeled

by Nakagami-*m* processes $\chi_i(t)$ $(i = 1,2)$, instead of the non-zero-mean complex Gaussian processes $\mu_\rho^{(i)}(t)$ $(i = 1,2)$. Hence, the overall fading channel describing the SMS-DMS link is characterized by a double Nakagami-*m* process. Moreover, in contrast to Paper V, Paper VI considers a more realistic scenario by assuming that the MR operates in a half-duplex mode. Paper VI deals with the derivation and analysis of the PDF, CDF, LCR, and ADF of the capacity of double Nakagami-*m* channels. Moreover, the influence of the severity of fading on the statistical properties of the channel capacity has been investigated. It is worth mentioning that in the Nakagami-*m* model, the parameter *m* controls the severity of fading. Specifically, as the value of *m* increases, the fading severity decreases and vice versa. It is observed that an increase in the severity of fading in one or both transmission links of double Nakagami-*m* channels decreases the mean channel capacity, while it results in an increase in the ADF of the channel capacity. Moreover, at lower levels, this effect increases the LCR of the channel capacity. Results also show that the mobility of the MR and DMS has a significant influence on the LCR and ADF of the channel capacity. Specifically, an increase in the maximum Doppler frequencies of the MR and DMS increases the LCR, while it has an opposite influence on the ADF of the channel capacity. The theoretical results are validated with the help of simulations. The underlying uncorrelated Gaussian processes that make up Nakagami-*m* processes are simulated by exploiting the SOS concept [94, 95, 96]. The parameters of the SOS-based simulator are calculated using the GMEDS_1 [121]. A very good fitting between the simulation and theoretical results confirm the correctness of derived expressions.

3.4 Statistical Analysis of the Capacity of $N*$Nakagami-*m* Channels

The dualhop scenario considered in the previous sections only takes into account one relaying node, however there can exist more than one relay in amplify-and-forward channels in cooperative networks. To address this problem, multihop communication in cooperative networks was introduced in Section 3.1, where several relays assist each other by relaying the transmitted signal from the SMS to the DMS in amplify-and-forward channels. This kind of communication scheme promises an increased network coverage, enhanced mobility, and improved system performance. It has applications in WLANs [60], cellular networks [61], ad-hoc networks [62, 63], and hybrid networks [64].

In order to characterize the fading in the end-to-end link between the SMS and

the DMS in a multihop communication system with N hops, the authors in [143] have proposed the $N*$Nakagami-m channel model, assuming that the fading in each link between the wireless nodes can be modeled by a Nakagami-m process. The propagation scenario describing $N*$Nakagami-m channels is illustrated in Fig. 3.2. The considered multihop communication system consists of an SMS, a DMS, and $N-1$ blind mobile relays MR_n $(n = 1,2,...,N-1)$, as shown in Fig. 3.2. Here, the fading in the transmission links between the intermediate wireless nodes is characterized by independent but not necessarily identical Nakagami-m processes $\chi_n(t)$ $(n = 1,2,...,N)$. Moreover, we have assumed an absence of the direct transmission link between the SMS and the DMS. The $N*$Nakagami-m model considers a general amplify-and-forward relay-based multihop scenario and can be reduced to the special case of double Nakagami-m channels. Thus, to extend our work related to the capacity analysis of double Nakagami-m channels, the statistical properties of the capacity of $N*$Nakagami-m channels are investigated. The derivation and analysis of the statistical properties of the capacity of such channels are presented in detail in Paper VII, which is included in Appendix G [149].

This section aims to summarize the findings of Paper VII. Therein, exact analytical expressions are derived for the PDF, CDF, LCR, and ADF of the capacity of $N*$Nakagami-m channels. The first order statistics, namely the PDF and the CDF of the capacity of $N*$Nakagami-m channels can be expressed in terms of the Meijer's G-function [150, Eq. (9.301)]. Despite being in closed-form, the obtained results

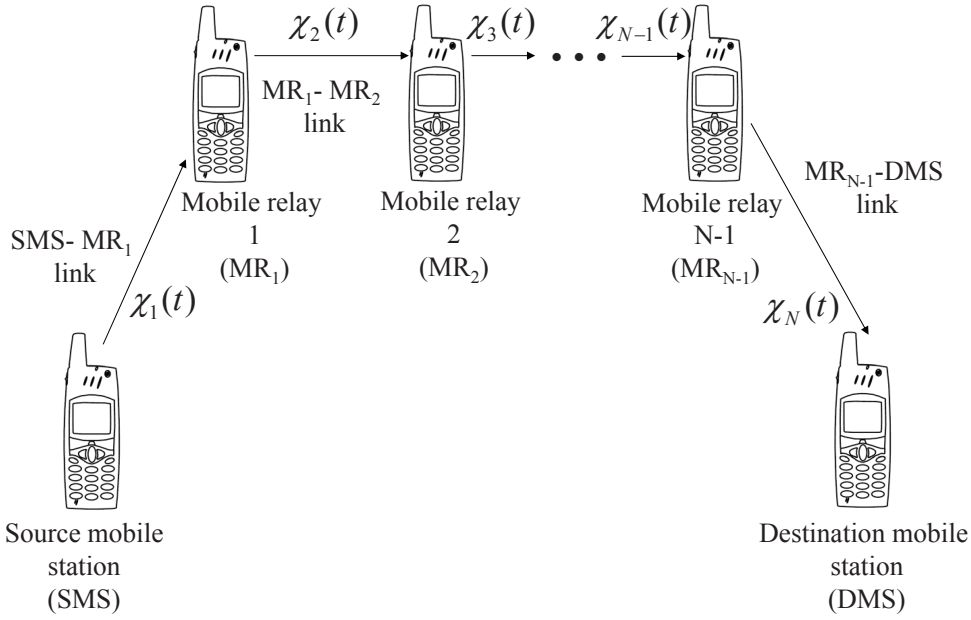

Figure 3.2: The propagation scenario describing $N*$Nakagami-m fading channels.

are mathematically intractable. In order to simplify the results, the central limit theorem of products [99] is applied, to obtain an accurate approximation for the PDF of $N*$Nakagami-m processes. The results revealed that the PDF of $N*$Nakagami-m processes gets very closely fitted to the lognormal distribution as the number of hops (N) increases. Thereafter, assuming that the fading amplitude of $N*$Nakagami-m channels can be modeled as a lognormal process, the first order statistics of the channel capacity are studied for a large number of hops. Alike first order statistics, the exact solution for the LCR of the channel capacity is also mathematically very complex, since it contains multifold integrals. Hence, to reduce the analytical complexity, an accurate closed-form approximation has been derived for the LCR of the channel capacity. The results are studied for different values of the number of hops as well as for different values of the Nakagami parameters, controlling the severity of fading in different transmission links of the multihop communication system. The results show that an increase in the number of hops or the severity of fading decreases the mean channel capacity, while the ADF of the channel capacity increases. Moreover, an increase in the severity of fading or the number of hops decreases the LCR of the capacity of Nakagami-m channels at higher levels. The converse statement is true for lower levels. The presented results provide an insight into the influence of the number of hops and the severity of fading on the channel capacity, and hence they are very useful for the design and performance analysis of the multihop communication systems.

3.5 Chapter Summary and Conclusion

By utilizing the existing resources of wireless networks, amplify-and-forward channels in cooperative networks promise an increased network coverage with enhanced mobility support. Single-antenna mobile stations in amplify-and-forward relay-based cooperative networks assist each other to relay the transmitted signal from the SMS to the DMS. This chapter dealt with the capacity analysis of such cooperative networks. The chapter began with the analysis of dualhop communication systems, comprising an SMS, a DMS, and an MR. Such channels can be described using cascaded channel models, where the overall channel between the SMS and the DMS via an MR was represented as a concatenation of the SMS-MR and MR-DMS channels. Therefore, under LOS propagation conditions, the overall fading channel describing the SMS-DMS link was modeled by a double Rice process. This chapter presented an insightful review regarding the influence of the LOS components, in the two transmission links of double Rice fading channels, on the channel capac-

ity. In addition, the results pertaining to the statistical properties of the capacity of double Rayleigh, classical Rice and classical Rayleigh channels were also discussed for comparison purposes. The obtained results illustrate that the statistics of the capacity of double Rice fading channels are quite different from those of double Rayleigh fading channels. Specifically, the presence of an LOS component in one or both of the links (i.e., the SMS-MR and MR-DMS links) increases the mean channel capacity, while the ADF of the channel capacity decreases. However, this effect increases the LCR of the channel capacity at only medium and high levels. The detailed analysis of these results can be found in Paper V (Appendix E).

Afterwards, the chapter highlighted the motivation and advantages behind extending the previously mentioned work to the case of double Nakagami-*m* channels. It was reported that by employing the double Nakagami-*m* channel model, we can study the influence of severity fading, in the two transmission links of dualhop communication systems, on the channel capacity. In addition, the double Nakagami-*m* channel model is also useful for modeling real-world scenarios such as keyhole channels. Paper VI (Appendix F) presents the derivation and analysis of the statistical properties of the capacity of double Nakagami-*m* channels. Whereas, this chapter merely articulated the important findings of Paper VI.

The chapter ended with a discussion regarding the capacity of multihop communication systems, which constitutes a more general scenario in amplify-and-forward-based cooperative networks. The considered multihop communication system consists of an SMS, a DMS, and $N-1$ blind mobile relays. In order to characterize the fading in the end-to-end link between the SMS and the DMS in such channels, the $N*$Nakagami-*m* model was employed. Thereafter, exact analytical expressions for the PDF, CDF, LCR, and ADF of the capacity of $N*$Nakagami-*m* channels were derived. In addition, accurate approximations for the PDF, CDF, and LCR of the channel capacity were also derived to reduce the complexity of the exact results. The statistical properties of the channel capacity were studied for different values of the number of hops as well as for different values of the Nakagami parameters controlling the severity of fading in different links of the multihop communication system. This chapter presents a summary of the obtained results, while this work can be found in full in Paper VII (Appendix G).

Chapter 4

Capacity Studies of Fading Channels in Spatial Diversity Combining Systems

4.1 Introduction

The performance of wireless communication systems is greatly affected by the multipath fading phenomenon. In order to mitigate the effects of fading, spatial diversity combining is widely accepted to be an effective method [70, 71]. In diversity combining schemes, the received signals of all diversity branches are combined in an intelligent way which results in an increase in the average received SNR [151, 70, 71, 72] and hence the system throughput increases. Two of such combining techniques include MRC and EGC [70, 71]. In MRC, originally proposed by Kahn [152], the co-phased received signals in the diversity branches are first weighted in accordance with the SNRs of the individual branches and then summed. Such a scheme results in an SNR at the combiner output which is equal to the sum of individual SNRs of the diversity branches. MRC constitutes the most optimal method of diversity combining [70] and has been thoroughly investigated in the literature (see, e.g., [153, 154, 155, 75, 72]). Other advantages of this method include the analytical tractability and the realizable implementation in practical receivers, such as the RAKE receiver [156]. On the other hand, EGC offers a simpler solution by summing the co-phased received signals in the diversity branches with a unit weighting factor, which significantly simplifies the practical implementation. In addition, the performance of EGC is also found to be quite close to the optimal MRC. However, the associated price for such ease in the system design is the intricacy of the analytical treatment. This complexity stems from the difficulty in finding the

PDF of a sum of received signal envelopes in the diversity branches. The exact solution to this problem is still unknown, since it contains multifold integrals due to the convolution of PDFs of the received signal envelopes. Nevertheless, there exist numerous papers that propose approximate solutions to this problem [157, 158, 159].

Spatial diversity combining techniques, specifically MRC and EGC, have gained considerable attention in the past few decades due to their potential to improve the overall system performance. The authors in [160] have accentuated the significance of such studies in Rice channels. Therein, some practical propagation scenarios are listed where the specular components cannot be neglected. Hence, for such cases, received signal envelopes in diversity branches are assumed to follow the Rice distribution [45, 160]. For Rice channels, the performance analysis of MRC and EGC is presented in [74, 161]. On the other hand, the performance analysis of EGC in Rayleigh channels can be found in [73, 162, 163]. Moreover, the capacity of Rice and Rayleigh channels with MRC is studied in [72, 75, 155]. However, no study has been conducted so far to investigate the statistical properties of the capacity of Rice (or Rayleigh) channels in systems employing MRC or EGC. The work summarized in Section 4.2 addresses this problem by presenting the derivation and analysis of the PDF, CDF, LCR, and ADF of the capacity Rice channels for both MRC and EGC schemes.

The widely acknowledged features of the Nakagami-*m* model, such as versatility, analytical tractability, and experimental validity have inspired the researchers to employ the Nakagami-*m* process as an appropriate channel model for a variety of propagation scenarios. For such reasons, a large number of papers have been published in the past decade, highlighting the importance of studies pertaining to the analysis of Nakagami-*m* channels in systems with spatial diversity combining [164, 151, 165, 161, 166]. In addition, as a special case, the results obtained using the Nakagami-*m* model reduce to those of Rayleigh channels in an exact manner. Hence, to extend the work related to the capacity analysis of Rice and Rayleigh channels, statistical properties of the capacity of Nakagami-*m* channels with MRC and EGC are studied. The peculiar findings of this work are discussed in Section 4.3. The importance of this study lies in the fact that it provides the flexibility to analyze the channel capacity in different fading conditions. In the literature, it is usually assumed that the received signals in diversity branches are spatially uncorrelated. Analogously, the analyses presented in Sections 4.3 and 4.2 also consider spatially uncorrelated diversity branches. This assumption is acceptable if the receiver antennas separation is far more than the carrier wavelength of the received signal [167]. However, due to the scarcity of space on small mobile devices, this

requirement cannot always be fulfilled. Thus, due to the spatial geometry of the receiver antenna array, the receiver antennas are spatially correlated. Moreover, it is an established fact that the spatial correlation has a significant influence on the performance of mobile communication systems employing diversity combining techniques [168, 169, 73]. Therefore, in order to study a more realistic scenario, it is necessary to consider spatially correlated diversity branches. To address this problem, the statistical analysis of the capacity of spatially correlated Nakagami-*m* channels is performed for both MRC and EGC. This is the topic of the work briefly discussed in Subsection 4.3.1.

The rest of the chapter is structured as follows. Section 4.2 studies the statistical properties of the capacity of Rice channels with MRC and EGC. In Section 4.3, an insightful review regarding the influence of severity of fading on the capacity of Nakagami-*m* channels is presented for both MRC and EGC schemes. Thereafter, Subsection 4.3.1 highlights the important findings of the work dealing with the capacity analysis of spatially correlated Nakagami-*m* channels with MRC and EGC. The chapter summary is given in Section 4.4.

4.2 Statistical Analysis of the Capacity of Rice Channels with MRC and EGC

The previous section highlighted the significance of the capacity analysis of Rice channels in systems with MRC and EGC. This section aims to summarize the work in Paper VIII, which is included in Appendix H [170] of this dissertation. Paper VIII deals with the analysis of the statistical properties of the capacity of Rice channels with MRC and EGC. Therein, an L-branch diversity system is considered, in which it is assumed that the received signals at the combiner input experience flat fading in all fading branches. Due to the assumption of LOS propagation conditions, the received signal envelopes in the fading branches are characterized by statistically independent Rice processes. Exact analytical expressions are derived for the PDF, CDF, LCR and ADF of the capacity of Rice channels for the case when MRC is employed. Whereas, when EGC is used, the analytical expressions for the PDF, CDF, LCR, and ADF of the channel capacity are derived using an approximation for the PDF of a sum of Rice processes. This is due to the reason that the exact solution for the PDF of a sum of Rice processes is still unknown. However, to overcome this problem, different approximations have been proposed in the literature [157, 158]. We have employed the approximation suggested in [157] for the PDF of a sum of Rice processes. This approximation makes use of nonlinear least squares fitting

with the exact PDF, based on the interior-reflective Newton method [171]. By using this method, appropriate values of three constant terms in the approximate expression for the PDF are calculated. The values of these constants are given in Table H.1 (Appendix H) for different values of the number of diversity branches (L) and the amplitude of the LOS components (ρ) in different Rice branches. The accuracy of the approximate analytical expressions is tested by exact simulation results. In addition, the correctness of exact analytical expressions is also confirmed via simulations. To obtain the simulation results, a high-performance SOS-based channel simulator is employed. Meaning thereby, the SOS principle [94, 95, 96] is exploited to simulate the underlying Gaussian processes making up the received signal envelopes in the fading branches. The model parameters of the channel simulator are calculated by utilizing the GMEDS_1 [121].

The results are studied for different values of L and ρ. For comparison purposes, the results for Rayleigh channels $(\rho \to 0)$ are shown for both MRC and EGC. Moreover, the results for the classical Rayleigh and Rice channels are also presented, which arise when $L = 1$. It is observed that the amplitude of the LOS components and the number of diversity branches have a significant effect on the statistics of the channel capacity. Specifically, an increase in the value of L or ρ increases the mean channel capacity for both MRC and EGC. However, it results in a decrease in the variance of the channel capacity. It is also observed that for any of the two aforementioned combining methods, the capacity of Rice channels with a lower value of L or ρ has a higher LCR at low and medium levels. The ADF of the channel capacity, on the other hand, decreases with an increase in the value of the parameters L or ρ. The findings of Paper VIII also show that the MRC diversity scheme outperforms the EGC diversity scheme w.r.t. the mean channel capacity.

4.3 Statistical Analysis of the Capacity of Nakagami-m Channels with MRC and EGC

In order to study a variety of fading conditions, a more general channel model compared to the Rice or the Rayleigh model is required. This requirement is acknowledged in numerous studies [107, 108]. For this reason, the Nakagami-m process has gained much attention in recent years due to its flexibility of modeling different fading conditions, mathematical ease, and good fitness with experimental data [107, 108, 97]. Such distinctive characteristics have propelled numerous researchers to study Nakagami-m channels with MRC and EGC [164, 151, 165, 161, 166]. However, the information regarding the statistical properties of the capacity of

Nakagami-*m* channels with MRC and EGC is not available in the literature, which calls for further research. Therefore, the aim of the work in Paper IX (Appendix I [172]) is to fill in this gap of information. This section presents an overview of Paper IX included in Appendix I of this dissertation.

Analogously to the procedure followed in the previous section, the statistical properties of the capacity of Nakagami-*m* channels with EGC are derived in Paper IX with the help of the PDF of a sum of fading envelopes in the diversity branches. Alike the sum of Rice (or Rayleigh) processes, finding the exact solution for the PDF of a sum of Nakagami-*m* processes is an open problem. However, for overcoming this problem, there exist highly-accurate closed-form approximate solutions in the literature (e.g., [44, 173, 159]). In addition to produce accurate results, these methods refrain from using the cumbersome curve-fitting techniques used in the previous section for Rice processes. In Paper IX, a sum of Nakagami-*m* processes is approximated by another Nakagami-*m* process, as suggested in [159]. Thereafter, based on this accurate approximation, results for the statistical properties of the capacity of Nakagami-*m* channels with EGC are obtained. On the other hand, when MRC is employed, exact analytical expressions are derived for the PDF, CDF, LCR and ADF of the channel capacity. An excellent fitting between theoretical and simulation results verifies the correctness of derived expressions. An SOS-based channel simulator has been employed to simulate the underlying Gaussian processes in Nakagami-*m* processes [94, 95, 96]. In this work, the GMEDS$_1$ is used to compute the simulation model parameters [121].

The statistical properties of the channel capacity are studied for different values of the number of diversity branches L and for different values of the Nakagami parameter m, controlling the severity of fading in Nakagami-*m* channels. In this study, the results for Rayleigh channels (which arise for the case when $m = 1$) are also included for comparison purposes. It is observed that for both MRC and EGC, an increase in the number of diversity branches L increases the mean channel capacity, while the variance and the ADF of the channel capacity decrease. Moreover, an increase in the severity of fading results in a decrease in the mean channel capacity, however the variance and ADF of the channel capacity increase. It is also observed that at lower levels, the LCR is higher for channels with smaller values of L or higher severity levels of fading than for channels with higher values of L or lower severity levels of fading. This work constitutes a general framework, providing the flexibility to study the statistical properties of the capacity of fading channels in systems with diversity combining under a variety of fading conditions. However, it lacks information regarding the impact of spatial correlation, between diversity

branches, on the channel capacity. The next subsection summarizes the work that attempts to overcome this drawback.

4.3.1 The Influence of Spatial Correlation on the Statistical Properties of the Capacity of Nakagami-*m* Channels with MRC and EGC

The final remarks of Section 4.3 highlighted a limitation of the work summarized in the previous section. This limitation stems from the assumption of spatially uncorrelated fading branches. Alike the analyses presented in Sections 4.3 and 4.2, most of the published works also assume that the fading envelopes in diversity branches are spatially uncorrelated. However, due to the scarcity of space on the small mobile devices, the receiver antennas are generally spatially correlated. Therefore, in order to study a more realistic scenario, it is necessary to take into account spatially correlated fading branches. For this reason, the statistical properties of the capacity of spatially correlated Nakagami-*m* channels with MRC and EGC are studied in Paper X included in Appendix J. By considering spatially correlated fading branches, this work eliminates the previously mentioned drawback of Paper IX (Appendix I).

Paper X (Appendix J) presents a profound statistical analysis of the channel capacity for different values of the number of diversity branches as well as for different values of the receiver antennas separation. The receiver antennas separation controls the spatial correlation in diversity branches. Specifically, as the receiver antennas separation increases, the spatial correlation decreases and vice versa. The statistical properties of interest include the PDF, CDF, LCR, and ADF of the channel capacity. In order to study spatially correlated Nakagami-*m* channels, the problem formulation in Paper X makes use of the well-known Kronecker model [80, 81, 82, 36, 42], which is more comprehensively discussed in Section 5.2 of the next chapter. It is worth mentioning that the presented results are also useful to investigate the effect of severity of fading on the statistics of the channel capacity. Moreover, for comparison purposes, Paper X also presents the results for the mean and variance of the capacity of spatially correlated Rayleigh channels with MRC and EGC (which arise when $m = 1$). The results show that an increase in the spatial correlation in the diversity branches of an MRC system increases the variance as well as the LCR of the channel capacity, while the ADF of the channel capacity decreases. On the other hand, for the case of EGC, increasing the receiver antennas separation increases the mean channel capacity, whereas the ADF of the channel capacity decreases. Moreover, an increase in the spatial correlation increases the LCR of the channel capacity

only at lower levels.

An excellent fitting between theoretical and simulation results proves the correctness of analytical expressions. The simulation results are obtained by utilizing an SOS-based channel simulator [94, 95, 96]. The model parameters of the channel simulator are obtained using the GMEDS_1 [121]. The importance of the presented results is reflected from the fact that they provide a deep insight into the influence of spatial correlation and the severity of fading on the capacity of Nakagami-*m* channels in systems with diversity combining. Moreover, in special cases, the results can be reduced to those obtained for spatially uncorrelated Nakagami-*m* channels in Section 4.3 as well as for Rayleigh channels.

4.4 Chapter Summary and Conclusion

Diversity combining is an effective method to mitigate the effects of fading in wireless propagation environments. If, for example, spatial diversity techniques are used, the received signals of all diversity branches are combined in an intelligent way which results in an increase in the average received SNR and hence the system throughput increases. Spatial diversity combining techniques, such as MRC and EGC, have been thoroughly investigated by researchers in past few decades due to their potential to improve the overall system performance. To get a deep insight into the potential and capacity limits of wireless communication systems employing spatial diversity combining, a solid knowledge of the statistical properties of channel capacity is of vital importance. In addition, capacity studies of such systems are very helpful to optimize the overall system performance. Therefore, this chapter was devoted to analyze the statistical properties of the channel capacity of wireless communication systems for both cases, namely MRC and EGC.

The chapter began with an overview regarding the capacity analysis of Rice channels with MRC and EGC. It was elucidated that in many propagation scenarios specular components cannot be neglected. Hence, for such cases, the Rice process is considered to be an appropriate model to describe the fading behavior. Thereafter, important observations regarding the influence of LOS components on the PDF, CDF, LCR, and ADF of the channel capacity are articulated. The discussion included a brief analysis of obtained results, for both MRC and EGC. It was illustrated that the LOS components significantly influence the statistics of the channel capacity. The detailed discussion on this topic can be found in Paper VIII, which is included in Appendix H.

Afterwards, the chapter presented the statistical analysis of the capacity of Naka-

gami-*m* channels with MRC and EGC. By offering the flexibility to study different fading conditions, this work provides a general framework for the capacity analysis of wireless communication systems with MRC and EGC. The statistical properties of the channel capacity are studied for different values of the number of diversity branches L and for different values of the Nakagami parameter m, controlling the severity of fading in Nakagami-*m* channels. The important findings are highlighted in this chapter, while a comprehensive analysis of these results is reported in Paper IX (Appendix I). Papers VIII and IX only consider spatially uncorrelated fading branches. However, this not an acceptable assumption in many practical systems. This problem is addressed in Paper X (Appendix J), which is summarized in the last section of this chapter. Paper X eliminates the limitations of Papers VIII and IX by considering spatially correlated fading branches.

Chapter 5

Capacity Studies of MIMO channels

5.1 Introduction

Future mobile communication systems are expected to provide higher data rates with higher spectral efficiency. However, designing wireless links that offer good QoS as well as high data rates, especially in NLOS environments, constitutes a significant research and engineering challenge. This task is particularly more complicated for power and bandwidth limited systems. The conventional communication means, employing single-antenna terminals at the transmitter and the receiver, do not provide the desired spectral efficiency envisioned for the next generation mobile communication systems. Due to the scarcity of available resources, researchers came up with an innovative idea of exploiting the spatial diversity by employing multiple antennas at both the transmitter and the receiver [34, 40]. Such a technological breakthrough showed great improvement in the link reliability, increased the overall system capacity, and provided remarkable gain in the spectral efficiency [34, 40]. Utilization of multiple antennas at the transmitter and receiver facilitated the design of MIMO systems in order to increase the spectral efficiency and to acquire a diversity gain [174]. This discovery resulted in a significant upsurge of interest towards MIMO systems, and since then, a large number of articles have been published in the literature dealing with MIMO channel modeling and performance analysis (see, e.g., [76, 77, 78, 36], and the references therein). Due to the provision of exceptional gain in the capacity, the employment of the MIMO architecture in the system design constitutes one of the major distinctions between 3G and 4G wireless communication systems [83].

The enormous spectral efficiency ascribed to MIMO systems in the seminal works of Foschini [34] and Telatar [40] is based on the premise of a rich scattering environment, providing independent transmission paths between the transmitter

and receiver antennas. Hence, it results in a full-ranked channel matrix with i.i.d. entries. Under such ideal conditions, a linear increase in the channel capacity w.r.t. the increase in the minimum of the number of transmitter and receiver antennas was observed [40, 34]. However, such idealized propagation conditions are rarely met in real practice. It is shown in [175, 176, 79] and multiple references therein that due to the spatial correlation between MIMO channel coefficients, realistic MIMO channels show a reduced channel capacity. It is therefore of great practical and theoretical interest to study MIMO systems when the elements of the channel matrix are spatially correlated.

In recent years, it is increasingly gaining recognition that the studies pertaining to unveil the dynamics of the capacity of MIMO channels can be very helpful to achieve higher data rates while keeping the probability of errors as low as possible. Statistical properties, such as mean, variance, PDF, and CDF adequately characterize the channel capacity. However, these statistical quantities do not provide an insight into the temporal behavior of the channel capacity, which is imperative for the efficient design of future mobile communication systems. An evidence supporting this fact can be found in [28], where the authors have utilized the LCR of the channel capacity for the cross-layer optimization of the overall network performance. In addition to the LCR, the ADF of the channel capacity is another important statistical quantity that gives an insight into the temporal behavior of the channel capacity [32, 33]. Therefore, a major portion of this chapter deals with the analysis of the PDF, CDF, LCR, and ADF of the capacity of spatially correlated MIMO channels. In order to address the problem of correlated fading in MIMO channels, we have employed one of the most commonly used channel models known as the Kronecker model [80, 81, 82, 36, 42]. The underlying principle behind this modeling approach is elaborated in Section 5.2. This model, though restrictive to some cases, provides an adequate framework for the capacity analysis of MIMO channels.

One promising method to increase the capacity in MIMO channels is to use space-time coding techniques, such as STTC [90] or STBC [91, 92]. Among different space-time coding techniques, OSTBC has gained much attention in recent years. One of the advantages of using OSTBC is that it transforms MIMO channels into equivalent SISO channels, which significantly simplifies the mathematical formulation of MIMO systems [93]. Moreover, being orthogonal in structure, maximum likelihood decoding can be applied at the receiver that results in a significant decrease in the complexity of the receiver structure, compared to the prevailing coding techniques (e.g., STTC) [92]. Due to the aforementioned advantages of using OSTBC in MIMO channels, it is of utmost importance to perform the capac-

ity analysis of OSTBC MIMO channels. Studies pertaining to the analysis of the capacity of OSTBC MIMO channels can be found in [177, 178]. Moreover, the outage performance and the error probability analysis of OSTBC MIMO systems have been studied in [179, 180, 181]. However, the absence of treatises dealing with the statistical properties of the capacity of OSTBC MIMO Nakagami-*m* channels demands further research work in this domain. This is the topic of our work summarized in Section 5.4. Therein, the capacity studies of both correlated and uncorrelated OSTBC MIMO channels are included.

The remaining part of this chapter is organized as follows. Section 5.2 presents a brief discussion on the influence of spatial correlation on the capacity of MIMO Rice channels. In Section 5.3, the statistical properties of the capacity of spatially correlated MIMO Nakagami-*m* channels are studied. Section 5.4 deals with the statistical analysis of the capacity of OSTBC MIMO channels. In Section 5.4, both spatially correlated as well as uncorrelated channels are analyzed. In addition, the impact of shadowing on the statistical properties of the capacity of OSTBC MIMO Nakagami-*m* channels is investigated. In Section 5.5, the chapter summary is given.

5.2 Statistical Analysis of the Capacity of Spatially Correlated MIMO Rice Channels

Since the pioneering works in [40, 34], there has been a tremendous amount of research activity dealing with modeling and capacity analysis of MIMO channels. However, most of the research work shares a common ground, assuming i.i.d. Rayleigh MIMO channel coefficients. As mentioned in the preceding section, measurements have shown that the i.i.d. assumption is not valid in many realistic situations, e.g., when the separation between the antennas is small [80, 182, 167]. For such cases, spatially correlated MIMO Rayleigh channels have been thoroughly investigated [183, 184, 37]. In addition to the spatial correlation, another factor influencing the capacity of MIMO channels is the presence of the LOS component. Such scenarios are usually studied with the help of the Rice channel model [45, 160]. The Rice channel model not only provides a better description of the fading environment, it also includes the Rayleigh model as special case. In past few years, many researchers have devoted their efforts to study the capacity of MIMO Rice channels [43, 185, 186]. However, these results are very intricate and they do not provide insight into the statistical properties of the channel capacity. Although various bounds and approximations of the channel capacity have also been proposed in the literature to reduce the mathematical complexity (see e.g., [187, 188, 189]), there exists no

study in the literature that deals with the analysis of the PDF, CDF, LCR, and ADF of the capacity of spatially correlated MIMO Rice channels. Paper XI, included in the Appendix K [190] of this dissertation, addresses this problem by studying the statistical properties of the capacity of spatially correlated MIMO Rice channels. This section presents a summary of the work in Paper XI.

In Paper XI, an exact closed-form expression for the PDF and an exact expression for the CDF of the channel capacity is derived for single-input multiple-output (SIMO[1]) and multiple-input single-output (MISO[2]) systems. Furthermore, an accurate closed-form expression has been derived for the LCR and an accurate expression has been obtained for the ADF of the SIMO and MISO channel capacities. For the MIMO case, the PDF, CDF, LCR, and ADF are investigated based on a lower bound on the channel capacity. This is due the mathematical intricacy involved in finding the exact solution for the statistical properties of the capacity of spatially correlated MIMO Rice channels. This lower bound was originally proposed in Paper XII [110] and therefore will be discussed in detail in the next section. The results are studied for different number of transmit and receive antennas. However, the proposed method can also be used to investigate the influence of some key parameters on the channel capacity, such as the antenna spacings of the transmitter and the receiver antenna arrays, as well as the amplitude of the LOS component. It is noteworthy that as the antennas separation increases, the spatial correlation decreases and vice versa.

In the literature, different MIMO channel models have been proposed, which take the correlations between the subchannels into account. An overview of the most commonly used MIMO channel models can be found in [76]. In Paper XI, a popular separable correlation model known as the Kronecker model [191, 82, 80] is employed. The Kronecker model assumes that the transmitter has no influence on the spatial properties of the received signal. Therefore, it allows to express the full[3] channel correlation matrix as a Kronecker product of the transmitter and receiver correlation matrices [80]. Hence, the resulting MIMO channel model incorporates the correlation properties at the transmitter and receiver side separately, which significantly simplifies the mathematical formulation of spatially correlated MIMO channels. Although it has been observed that the Kronecker model underestimates the channel capacity in some environments [192], it remains a cornerstone of a large number of analyses [42]. The obtained results reveal that to increase the channel

[1] SIMO systems employ single transmitter antenna and multiple receiver antennas.

[2] In MISO systems, multiple transmitter antennas and single receiver antenna are used.

[3] The full channel correlation matrix describes the correlation between all the possible pairs of MIMO channel coefficients [79, 80].

capacity, it is more important to have a high number of receive antennas rather than a high number of transmit antennas. It is also observed that an increase in the spatial correlation increases the spread of the channel capacity. The correctness of the derived expressions is confirmed by simulation results, obtained by utilizing a high-performance channel simulator. The channel simulator exploits the SOS principle [94, 95, 96] to simulate the underlying Gaussian processes in the Rice processes. The model parameters of the resulting SOS-based channel simulator are calculated by using the GMEDS_1 [121].

5.3 Statistical Analysis of the Capacity of Spatially Correlated MIMO Nakagami-*m* Channels

Despite the popularity of the Rayleigh and Rice models for the characterization of the fading behavior in MIMO systems, a more general channel model, namely the Nakagami-*m* model has drawn much attention in recent years. Although Nakagami-*m* model was originally proposed long ago in [44], it has received much acknowledgement relatively recently due to its applications in a variety of propagation environments, tractable analytical form, and having good fitness with experimental results [107, 108, 97, 118, 53, 193]. Additionally, the Nakagami-*m* model reduces to the Rayleigh and one-sided Gaussian models in special cases. Propelled by the advantages of using the Nakagami-*m* model, in the past few years, various articles have been published in the literature aiming to explore the capacity limits of MIMO Nakagami-*m* channels [78, 194, 177, 38, 195]. However, the statistical properties of the capacity of spatially correlated MIMO Nakagami-*m* channels, such as the PDF, CDF, LCR, and ADF have not been reported so far in the literature. To fill this gap of information, a profound statistical analysis of the capacity of spatially correlated MIMO Nakagami-*m* channels is performed in Paper XII. This section aims to summarize the discussion presented in Paper XII, which can be found in full in Appendix L [110].

In Paper XII, the impact of the spatial correlation on the capacity of MIMO Nakagami-*m* channels is studied. The exact solution for the PDF, CDF, LCR, and ADF of the capacity of spatially correlated MIMO Nakagami-*m* channels is mathematically very complex to obtain. Hence, for overcoming this problem, Paper XII proposes a tight lower bound on the capacity of MIMO Nakagami-*m* channels. Recently, the authors in [78] have also suggested a lower bound on the MIMO Nakagami-*m* channel capacity, obtained by utilizing various tools within the majorization theory framework [196]. A comparative study elucidates that our pro-

posed lower bound is in exact accordance with the one presented in [78]. Moreover, the authors in [78] have shown that this lower bound is very tight in the low SNR regime. Based on this lower bound, closed-form analytical expressions for the PDF, CDF, LCR, and ADF of the capacity of spatially correlated MIMO Nakagami-*m* channels are derived. The Kronecker model is used to address the problem of correlated fading in MIMO channels [80]. In order to study the influence of the spatial correlation on the channel capacity, the analysis of the statistical properties of the channel capacity is carried out for different receiver antenna spacings. It is observed that the antenna spacing has a significant influence on the spread and maximum value of the PDF and LCR. Specifically, an increase in the separation between receiver antennas results in a decrease in the capacity variance, while the maximum value of the LCR increases. Moreover, increasing the receiver antenna spacing increases the ADF of the channel capacity only at higher levels. Paper XII also studies the channel capacity for different number of transmitter and receiver antennas. The obtained results reveal that as the number of antennas increases, the capacity of the system increases, whereas the spread of the PDF of the capacity decreases. On the other hand, with an increase in the number of antennas, a decrease in the maximum value of the LCR was observed. Analogously, the converse statement is true for the ADF of the channel capacity. The proposed method can also be employed to study the statistical properties of the capacity of MIMO channels in different fading environments. A good correspondence between the simulation and analytical results proves the correctness of derived expressions. To obtain the simulation results a high-performance channel simulator is employed. The channel simulator operates on the SOS-principle [94, 95, 96] to generate the underlying Gaussian processes, which make up the Nakagami-*m* processes. To ensure the desired characteristics of the simulated Gaussian processes, the model parameters of the channel simulator are computed using the GMEDS_1 [121].

5.4 Statistical Analysis of the Capacity of OSTBC MIMO Channels

Section 5.1 highlighted that the performance of mobile communication systems can be improved by exploiting the spatial diversity offered by the MIMO technology. Without the expense of additional bandwidth, an OSTBC MIMO system fulfils this task [91, 92]. Moreover, a lower implementation complexity (attained by, e.g., using maximum likelihood decoding at the receiver) makes it more attractive compared to other potential MIMO solutions. It is due to this reason, OSTBC MIMO systems

have been thoroughly investigated in the literature. A few recent studies exploring the capacity limits of OSTBC MIMO systems can be found in [197, 198, 177, 199, 200, 201]. Despite a widely explored topic, the statistical properties of the capacity of OSTBC MIMO Nakagami-*m* channels have not been investigated so far. This section highlights the main contributions of the papers pertaining to the statistical analysis of the capacity of OSTBC MIMO Nakagami-*m* channels.

5.4.1 The Impact of Spatial Correlation on the Statistical Properties of the Capacity of OSTBC MIMO Nakagami-*m* Channels

This section articulates important findings of the work presented in Paper XIII, which can be found in Appendix M [111]. Paper XIII extends the analysis of the statistical properties of the capacity of uncorrelated OSTBC MIMO Rayleigh channels, presented in [197], to uncorrelated OSTBC MIMO Nakagami-*m* channels. A widely documented reason behind this extension is the ability of the Nakagami-*m* model to describe a wide range of fading conditions. Moreover, the Rayleigh and one-sided Gaussian processes are inherently included in the Nakagami-*m* process as special cases. In Paper XIII, analytical expressions for the PDF, CDF, LCR, and ADF of the capacity of uncorrelated OSTBC MIMO Nakagami-*m* channels are derived. Additionally, in Paper XIII, the capacity of spatially correlated OSTBC MIMO Nakagami-*m* channels is also investigated. For correlated channels, firstly, an approximate expression for the channel capacity is derived. Thereafter, the expressions for the PDF, CDF, LCR, and ADF of the channel capacity are found. This approximation was originally proposed in [29, Eq. (4.40)] and is valid for spatially correlated MIMO channels at high SNR. However, in Paper XIII, it is adapted accordingly for spatially correlated OSTBC MIMO channels.

The mean value and variance of the channel capacity has been analyzed with the help of the PDF of the channel capacity. The aforementioned statistical quantities are studied for different MIMO dimensions[4] as well as for different values of the Nakagami parameter *m*, controlling the severity of fading in Nakagami-*m* channels. In addition, the influence of spatial correlation on the statistical properties of the channel capacity is investigated. It is worth mentioning that the results for the PDF, CDF, LCR, and ADF of the capacity of OSTBC MIMO Rayleigh channels, reported in [197], can be readily obtained as special cases from the results in Paper XIII by

[4] In this dissertation, the MIMO dimension corresponds to $N_R \times N_T$, where N_R is the number of receive antennas and N_T denotes the number of transmit antennas.

setting $m = 1$. It is observed that an increase in the MIMO dimension or a decrease in the severity of fading results in an increase in the mean channel capacity. The obtained results show that the spatial correlation significantly reduces the mean channel capacity, while it increases the ADF of the channel capacity. Moreover, at lower levels, the LCR of the capacity of spatially correlated MIMO channels is higher compared to uncorrelated channels. Theoretical results are verified by simulations, whereby a very good fitting is observed. The simulation results were generated with the help of an SOS-based channel simulator [94, 95, 96], whereas the model parameters of the channel simulator were obtained using the GMEDS_1 [121].

5.4.2 The Influence of Shadowing on the Statistical Properties of the Capacity of OSTBC MIMO Nakagami-*m* Channels

The analysis presented in the previous section only considers fast fading in MIMO channels, where the local mean of the received signal envelope is assumed to be constant [70]. While for land mobile terrestrial channels, the local mean fluctuates due to shadowing effects [124]. To study such channels, Chapter 2 convincingly introduced the Suzuki as well as the NLN channel models in Section 2.1.3, by highlighting the need and significance of using such channel models. However, the capacity analysis of the Suzuki and NLN channels presented in Chapter 2 was limited to only SISO channels. In order to eliminate this limitation, a MIMO channel model is utilized in Paper XIV [202], which takes into account the joint effects of shadowing and fast fading in MIMO channels. The employed channel model is based on the one proposed in [203], which was also used later in [204] to study the outage performance in OSTBC MIMO channels. However, the analyses in [203] and [204] is restricted to only MIMO Rayleigh channels. While in Paper XIV, a more general channel model referred to as MIMO NLN channel model is considered, where the fast fading in MIMO channels is modeled by Nakagami-*m* processes in contrast to Rayleigh processes used in [203]. To the best of the author's knowledge, the statistical properties of the capacity of OSTBC MIMO NLN channels have not been investigated so far. Therefore, in Paper XIV, the statistical properties of the capacity of MIMO NLN channels are analyzed for the case when OSTBC is employed. The MIMO NLN channel model provides the flexibility to study the impact of shadowing on the channel capacity under different fading conditions. Moreover, the effects of severity of fading on the channel capacity can also be studied. The details of this work can be found in Paper XIV included in Appendix N [202] of this dissertation. This section aims to highlight the important findings of this paper.

Paper XIV analyzes the statistical properties of the capacity of OSTBC MIMO NLN channels for various levels of shadowing and for different MIMO dimensions. Exact analytical expressions are derived for the PDF, CDF, LCR, and ADF of the capacity of MIMO NLN channels. The mean value and variance of the channel capacity has been analyzed with the help of the PDF of the channel capacity. On the other hand, the analysis of the LCR and ADF of the channel capacity is very helpful to study the temporal behavior of the channel capacity. The obtained results illustrate that an increase in the MIMO dimension or a decrease in the severity of fading results in an increase in the mean channel capacity, while the variance of the channel capacity decreases. Moreover, the shadowing effect has no influence on the mean channel capacity, whereas an increase in the shadowing standard deviation increases the spread of the channel capacity. It is also observed that an increase in either the shadow standard deviation or the MIMO dimension decreases the maximum value of the LCR of the channel capacity. However, this effect decreases the ADF of the channel capacity at only higher levels. Paper XIV also presents approximation results for the statistical properties of the channel capacity obtained using the Gauss-Hermite integration method [205]. It is observed that the approximation results not only reduce the intricacy, but also have a very good fitting with the exact results. Here simulation results are considered as the true results. This allows us to check the correctness of the derived expressions as well as to study the accuracy of the approximation results. The simulation results are obtained using an SOS-based channel simulator [94, 95, 96], which generates the underlying Gaussian processes making up the Nakagami-*m* and lognormal processes. The model parameters of the simulator are computed using the GMEDS_1 [121]. All the presented results show a very good fitting with the simulation results.

5.5 Chapter Summary and Conclusion

MIMO systems exploit spatial diversity by utilizing multiple antennas at the transmitter and receiver in order to increase the spectral efficiency and to acquire a diversity gain. To transmit close to the capacity limit of MIMO systems, a profound knowledge of the channel capacity and its statistics is imperative. Studies pertaining to unveil the dynamics of the capacity of MIMO channels can be very helpful to achieve higher data rates while keeping the probability of errors as low as possible. Under ideal propagation conditions, i.e., when the channel matrix has i.i.d. entries, the MIMO channel capacity increases linearly with the minimum of the number of transmitter and receiver antennas. However, it is also well known that the gains in the MIMO channel capacity are sensitive to the presence of spatial cor-

relation between MIMO sub-channels. Therefore, it is of great importance to study the MIMO channel capacity under non-idealized propagation conditions, i.e., when the elements of the channel matrix are correlated. Hence, a major portion of this chapter was dedicated to study the capacity of spatially correlated MIMO channels. One promising method to increase the capacity of MIMO systems is to use space-time coding techniques, such as OSTBC. In this chapter, capacity analysis of both correlated and uncorrelated OSTBC MIMO channels is presented.

The chapter began by highlighting the need for the capacity analysis of spatially correlated MIMO Rice channels. Thereafter, the important findings of the work related to the analysis of the statistical properties of the capacity of spatially correlated MIMO Rice channels were briefly reviewed. The detailed analysis on this topic is presented in Paper XI (Appendix K). Therein, the results are studied for different numbers of transmit and receive antennas. However, the proposed method can also be used to investigate the influence of some key parameters on the channel capacity, such as the antenna spacings of the transmitter and the receiver antenna arrays, and the amplitude of the LOS component.

The chapter then summarized the work presented in Paper XII (Appendix L), which deals with the statistical analysis of the capacity of spatially correlated MIMO Nakagami-*m* channels. The results are based on a lower bound on the channel capacity, which is very tight in the low SNR regime. In order to study the effect of the spatial correlation on the channel capacity, the analysis of the statistical properties of the channel capacity was carried out for different receiver antenna spacings. Results showed that the antenna spacing has a significant influence on the statistics of the channel capacity.

The chapter ended with a discussion on the statistical properties of the capacity of OSTBC MIMO channels. Firstly, the main findings of Paper XIII (Appendix M) were summarized. Paper XIII is aimed at the derivation and analysis of the PDF, CDF, LCR, and ADF of the capacity of spatially uncorrelated OSTBC MIMO Nakagami-*m* channels. In addition, the capacity of spatially correlated OSTBC MIMO Nakagami-*m* channels was also investigated, by making use of an approximate expression for the channel capacity. Thereafter, important results of Paper XIV (Appendix N) were discussed, which gave an insight into the impact of shadowing on the statistical properties of the capacity of spatially uncorrelated OSTBC MIMO Nakagami-*m* channels. The findings of Paper XIII and Paper XIV elucidated that real-world phenomena, such as the severity of fading, spatial correlation, and shadowing substantially influence the statistical properties of the capacity of OSTBC MIMO Nakagami-*m* channels.

Chapter 6

Summary of Contributions and Outlook

6.1 Major Contributions

This dissertation dealt with the capacity analysis of mobile fading channels. Specifically, the first order as well as the second order statistical properties of the channel capacity were derived and thoroughly investigated. The topics studied in depth include the capacity analysis of specific SISO channels, amplify-and-forward channels in cooperative networks, fading channels in spatial diversity combining systems, and MIMO channels. In this regard, the most peculiar developments made in this dissertation are summarized as follows:

- It is well known that frequency-nonselective multipath fading channels can be modeled using an SOC-based channel model, which not only is very accurate in modeling the non-isotropic scattering environments but also provides a clearer physical interpretation in terms of the wave propagation phenomena when viewed in line with the plane wave propagation model. This dissertation presented a thorough statistical analysis of the capacity of multipath fading channels represented by an SOC model, under LOS conditions.

- Statistical properties of the capacity of Rice-*m* channels were extensively studied. The importance of this study lies in merging the Nakagami-*m* and classical Rice channel characteristics into a new channel model, which has thus a higher flexibility than the two former ones. In addition, the Rice-*m* model includes the Nakagami-*m*, classical Rice, and classical Rayleigh models as special cases.

- In order to study the capacity of land mobile terrestrial channels, statistical anlysis of the capacity of Suzuki channels was performed. The key objective of this study was to investigate the influence of shadowing on the statistical properties of the channel capacity.

- The results obtained for Suzuki channels were extended to a more general case of NLN channels. The NLN channel model allows to study the combined effects of severity of fading and shadowing on the capacity of land mobile terrestrial channels. Moreover, it includes the Suzuki model as a special case.

- To optimize the performance of amplify-and-forward channels in cooperative networks under LOS propagation conditions, an extensive capacity analysis of double Rice channels is required. To fill this gap of knowledge, the derivation and analysis of the first and second order statistical properties of the capacity of double Rice channels was presented.

- As an extension to the capacity analysis of double Rice model, the statistical properties of the capacity of double Nakagami-*m* channels were analyzed. Here, the main emphasis was on the investigation of the impact of severity of fading on the statistics of the channel capacity. The double Nakagami-*m* channel model has applications in amplify-and-forward relay-based dualhop cooperative networks. Moreover, it is also useful for modeling real-world scenarios, such as keyhole channels.

- In practice, there can exist more than one relay in amplify-and-forward channels in cooperative networks. Such systems are commonly referred to as multihop communication systems. To generalize the aforementioned works in amplify-and-forward relay-based cooperative networks, a thorough statistical analysis of the capacity of $N*$Nakagami-*m* channels was performed.

- Diversity combining is a well known method to mitigate the effects of fading in wireless propagation environments. Due to its importance and extensive use in wireless communications, the statistical properties of the capacity of Rice channels with MRC and EGC were analyzed. This work was then extended to the case of Nakagami-*m* channels for both MRC and EGC. It is widely reported in the literature that the spatial correlation has a significant influence on the performance of mobile communication systems employing diversity combining techniques. Hence, a further extension was made to study the statistical properties of the capacity of Nakagami-*m* channels with MRC and EGC when diversity branches were spatially correlated.

- For MIMO systems, a tight lower bound on the capacity of spatially correlated MIMO Rice as well as Nakagami-*m* channels was presented. Based on this lower bound, the derivation and analysis of the statistical properties of the channel capacity was carried out.

- OSTBC is considered to be an effective method to increase the capacity in MIMO channels. Due to numerous advantages of using OSTBC in MIMO channels, it is of great theoretical and practical interest to study the statistical properties of the capacity of OSTBC MIMO channels. In this dissertation, a detailed statistical analysis of the capacity of OSTBC MIMO Nakagami-*m* channels was presented. Moreover, the influence of spatial correlation on the statistical properties of the channel capacity was also explored. As mentioned previously, the NLN process is a suitable channel model for land mobile terrestrial channels. In order to study the capacity of MIMO systems in land mobile terrestrial channels, the statistical properties of the capacity of OSTBC NLN MIMO channels were analyzed. It allowed to investigate the influence of shadowing, severity of fading, and MIMO dimension on the statistics of the channel capacity.

6.2 Outlook

This dissertation was primarily aimed at the statistical analysis of the capacity of various mobile fading channels under a variety of propagation scenarios. Although the discussion covered various peculiar aspects of mobile communication systems, there are still numerous problems that remain unaddressed. In the following, some of these problems are highlighted.

- This dissertation only considers narrowband wide-sense stationary (WSS) mobile fading channels. However, in practice, it is common to come across scenarios where either the stationary property is not valid or channels can only be assumed stationary for very short time intervals. Moreover, real-world channels also exhibit frequency selectivity. Therefore, efforts are required to extend the analysis in this dissertation for the case of frequency selective non-stationary mobile fading channels.

- For the case of cooperative networks, only amplify-and-forward-based blind relays were considered. However, to achieve better performance advanced relaying mechanisms such as CSI-assisted relays should be employed. In addition, this dissertation assumes an arbitrary noise power at the DMS in

such cooperative networks. Whereas, by employing an exact figure for the noise power at the DMS, the influence of the number of relays and the relay gains on the channel capacity can be studied in an accurate manner.

- The entire dissertation was devoted for the analysis of the statistical properties of the channel capacity in a variety of propagation scenarios. Various studies in the literature suggest that the statistics of the channel capacity can be used for the performance analysis and cross-layer optimization of wireless communication systems. However, this problem was out of the scope of this dissertation, therefore it was not addressed in this work.

- Multihop communication systems addressed in this dissertation assume that relays are connected in a cascade. This topology gives rise to an exceptional increase in the network coverage with the mobility support. However, in practical cooperative communication systems, multiple relays can transmit in parallel and the receiver can make use of diversity combining techniques by employing multiple antennas to obtain a diversity gain. Such kind of relaying mechanism was not studied in this dissertation, hence this topic needs further investigation.

- In the literature, numerous real-world scenarios are reported which give rise to the keyhole effect. For MIMO channels, the key hole effect reduces the rank of the MIMO channel matrix, that degrades the system performance. Therefore, studies pertaining to the analysis of the capacity of MIMO keyhole channels are of great importance. In addition to the amplify-and-forward channels, the double Nakagami-m channel model explored in this dissertation is also useful for modeling SISO keyhole channels. However, it requires further research to study the capacity of MIMO keyhole channels.

- The results for the statistical properties of the capacity of spatially correlated MIMO channels were based on a tight lower bound on the channel capacity. More efforts are required to find the exact results for the statistics of the channel capacity for such MIMO channels.

REFERENCES

[1] A. Kashyap and B. Bing, "Efficient HD video streaming over the internet," in *Proc. IEEE SoutheastCon, SoutheastCon 2010*, pp. 272–275, Mar. 2010. DOI 10.1109/SECON.2010.5453873.

[2] Y. Wu, S. Hirakawa, U. H. Reimers, and J. Whitaker, "Overview of digital television development worldwide," *Proceedings of the IEEE*, vol. 94, pp. 8–21, Jan. 2006. DOI 10.1109/JPROC.2005.861000.

[3] M. Macedonia, "The future arrives ... finally," *Computer*, vol. 40, pp. 101–103, Feb. 2007. DOI 10.1109/MC.2007.75.

[4] 3rd Generation Partnership Project, "3GPP TS 25.308 High Speed Downlink Packet Access (HSDPA); overall description; stage 2 (R5)," V5.2.0 (2002-03).

[5] K. Miyoshi, O. Kato, A. Matsumoto, M. Uesugi, and H. Suzuki, "Enhanced multi-antenna technologies on OFDM for future mobile communication systems," *Wireless Personal Communications (WPC)*, vol. 26, pp. 237–248, Sept. 2003.

[6] M. Assaad and D. Zeghlache, "Effect of circuit switched services on the capacity of HSDPA," *IEEE Trans. Wireless Commun.*, vol. 5, pp. 1044–1054, May 2006.

[7] S. Ortiz Jr., "IEEE 802.11n: The road ahead," *Computer*, vol. 42, pp. 13–15, July 2009. DOI 10.1109/MC.2009.224.

[8] A. J. Paulraj, D. A. Gore, R. U. Nabar, and H. Bolcskei, "An overview of MIMO communications - A key to gigabit wireless," *Proceedings of the IEEE*, vol. 92, pp. 198–218, Feb. 2004.

[9] R. R. Müller, "Random matrix methods for design of multiuser communication systems," *Acta Physica Polonica B*, vol. 36, pp. 2733–2745, Sept. 2005.

[10] T. Miki, T. Ohya, H. Yoshino, and N. Umeda, "The overview of the 4th generation mobile communication system," in *Proc. 5th Int. Conf. Commun. and Signal Processing, ICICS 2005*, pp. 1600–1604, Bangkok, Thailand, Dec. 2005. DOI 10.1109/ICICS.2005.1689329.

[11] J. Govil, "4G mobile communication systems: Turns, trends and transition," in *Proc. Int. Conf. Convergence Information Technology 2007, ICCIT 2007*, pp. 13–18, Nov. 2007. DOI 10.1109/ICCIT.2007.305.

[12] C. E. Shannon, "A mathematical theory of communication," *Bell Syst. Tech. J.*, vol. 27, pp. 379–423, July 1948.

[13] C. E. Shannon, "A mathematical theory of communication," *Bell Syst. Tech. J.*, vol. 27, pp. 623–656, Oct. 1948.

[14] T. M. Cover and J. A. Thomas, *Elements of Information Theory*. New York: John Wiley & Sons, 2nd edition ed., 2006.

[15] H. Theil, *Economics and Information Theory*. Amsterdam: North-Holland, 1967.

[16] F. Rieke, D. Warland, R. Ruyter, and W. Bialek, *Spikes: Exploring the Neural Code*. The MIT Press, 1997.

[17] J. P. Huelsenbeck, F. Ronquist, R. Nielsen, and J. P. Bollback, "Bayesian inference of phylogeny and its impact on evolutionary biology," *Science*, vol. 294, pp. 2310–2314, Dec. 2001. DOI 10.1126/science.1065889.

[18] E. Biglieri, J. Proakis, and S. Shamai, "Fading channels: Information-theoretic and communications aspects," *IEEE Trans. Inform. Theory*, vol. 44, pp. 2619–2692, Oct. 1998.

[19] M. D. Renzo, F. Graziosi, and F. Santucci, "Channel capacity over generalized fading channels: A novel MGF-Based approach for performance analysis and design of wireless communication systems," *IEEE Trans. Veh. Technol.*, vol. 59, pp. 127–149, Jan. 2010.

[20] G. E. Oien, "Information theory: The foundation of modern communications," *Telenors J.: Telektronikk: Information Theory and its Applications*, vol. 1.2002, pp. 3–19, 2002.

[21] D. Gesbert and J. Akhtar, "Breaking the barriers of Shannons capacity: An overview of MIMO wireless systems," *Telenors J.: Telektronikk: Information Theory and its Applications*, vol. 1.2002, pp. 53–64, 2002.

[22] C. Berrou, A. Glavieux, and P. Thitimajshima, "Near Shannon limit error-correcting coding and decoding: Turbo-codes (1)," in *Proc. IEEE International Conference on Communications, ICC 1993*, vol. 2, Geneva, Switzerland, May 1993.

[23] R. G. Gallager, *Low Density Parity Check Codes*. PhD dissertation, Massachusetts Institute of Technology, 1963.

[24] D. J. C. MacKay and R. M. Neal, "Near Shannon limit performance of low density parity check codes," vol. 33, pp. 457–458, Mar. 1997.

[25] B. O. Hogstad, *Multiple-Iinput Multiple-Output Fading Channel Models and their Capacity*. PhD dissertation, Department of Communication Technology, Faculty of Engineering and Science, Aalborg University, Aalborg, Denmark, 2008.

[26] A. Goldsmith, *Wireless Communications*. Cambridge University Press, New York, NY, USA, 2005.

[27] M. Luccini, S. Primak, and A. Shami, "On the capacity of MIMO channels and its effect on network performance," in *Proc. 5th Int. Conf. Information and Communication Technologies: From Theory to Applications, ICTTA 2008*, pp. 1–6, Apr. 2008.

[28] M. Luccini, A. Shami, and S. Primak, "Cross-layer optimization of network performance over multiple-input multiple-output wireless mobile channels," *IET Communications*, vol. 4, pp. 683–696, Apr. 2010.

[29] A. J. Paulraj, R. U. Nabar, and D. A. Gore, *Introduction to Space-Time Wireless Communications*. Cambridge, UK: Cambridge University Press, 2003.

[30] K. Otani, K. Daikoku, and H. Omori, "Burst error performance encountered in digital land mobile radio channel," *IEEE Trans. Veh. Technol.*, vol. 30, pp. 156–160, Nov. 1981.

[31] R. Vijayan and J. M. Holtzman, "Foundations for level crossing analysis of handoff algorithms," in *Proc. IEEE Int. Conf. on Communications, ICC 1993*, pp. 935–939, Geneva ,Switzerland, May 1993.

[32] B. O. Hogstad and M. Pätzold, "Capacity studies of MIMO models based on the geometrical one-ring scattering model," in *Proc. 15th IEEE Int. Symp. on Personal, Indoor and Mobile Radio Communications, PIMRC 2004*, vol. 3, pp. 1613–1617, Barcelona, Spain, Sept. 2004.

[33] B. O. Hogstad and M. Pätzold, "Exact closed-form expressions for the distribution, level-crossing rate, and average duration of fades of the capacity of MIMO channels," in *Proc. 65th Semiannual Vehicular Technology Conference, IEEE VTC 2007-Spring*, pp. 455–460, Dublin, Ireland, Apr. 2007.

[34] G. J. Foschini and M. J. Gans, "On limits of wireless communications in a fading environment when using multiple antennas," *Wireless Pers. Commun.*, vol. 6, pp. 311–335, Mar. 1998.

[35] P. J. Smith, L. M. Garth, and S. Loyka, "Exact capacity distributions for MIMO systems with small numbers of antennas," *IEEE Commun. Letter*, vol. 7, pp. 481–483, Oct. 2003.

[36] A. Giorgetti, P. J. Smith, M. Shafi, and M. Chiani, "MIMO capacity, level crossing rates and fades: The impact of spatial/temporal channel correlation," *J. Commun. Net.*, vol. 5, pp. 104–115, June 2003.

[37] M. Chiani, M. Z. Win, and A. Zanella, "On the capacity of spatially correlated MIMO Rayleigh-fading channels," *IEEE Trans. Inform. Theory*, vol. 49, pp. 2363–2371, Oct. 2003.

[38] G. Fraidenraich, O. Leveque, and J. M. Cioffi, "On the MIMO channel capacity for the Nakagami-*m* channel," *IEEE Trans. Inform. Theory*, vol. 54, pp. 3752–3757, Aug. 2008.

[39] N. Costa and S. Haykin, *Multiple-Input, Multiple-Output Channel Models: Theory and Practice*. New Jersey: John Wiley & Sons, 2010.

[40] I. E. Telatar, "Capacity of multi-antenna Gaussian channels," *European Trans. Telecommun. Related Technol.*, vol. 10, pp. 585–595, Nov./Dec. 1999.

[41] O. Oyman, R. U. Nabar, H. Bolcskei, and A. J. Paulraj, "Characterizing the statistical properties of mutual information in MIMO channels," *IEEE Trans. Signal Processing*, vol. 51, Nov. 2003.

[42] A. Tulino, A. Lozano, and S. Verdu, "Impact of antenna correlation on the capacity of multiantenna channels," *IEEE Trans. Inform. Theory*, vol. 51, pp. 2491–2509, July 2005.

[43] M. Kang and S. M. Alouini, "Capacity of MIMO Rician channels," *IEEE Trans. Wireless Commun.*, vol. 5, pp. 112–122, Jan. 2006.

[44] M. Nakagami, "The *m*-distribution: A general formula of intensity distribution of rapid fading," in *Statistical Methods in Radio Wave Propagation* (W. G. Hoffman, ed.), Oxford, UK: Pergamon Press, 1960.

[45] R. J. C. Bultitude and G. K. Bedal, "Propagation characteristics on microcellular urban mobile radio channels at 910 MHz," *IEEE J. Select. Areas Commun.*, vol. 7, pp. 31–39, Jan. 1989.

[46] W. R. Young, "Comparison of mobile radio transmission at 150, 450, 900, and 3700 MHz," vol. 31, pp. 1068–1085, Nov. 1952.

[47] H. W. Nylund, "Characteristics of small-area signal fading on mobile circuits in the 150 MHz band," *IEEE Trans. Veh. Technol.*, vol. 17, pp. 24–30, Oct. 1968.

[48] Y. Okumura, E. Ohmori, T. Kawano, and K. Fukuda, "Field strength and its variability in VHF and UHF land mobile radio services," *Rev. Elec. Commun. Lab.*, vol. 16, pp. 825–873, Sept./Oct. 1968.

[49] R. H. Clarke, "A statistical theory of mobile-radio reception," *Bell Syst. Tech. Journal*, vol. 47, pp. 957–1000, July/Aug. 1968.

[50] M. Pätzold, U. Killat, Y. Li, and F. Laue, "Modelling, analysis, and simulation of nonfrequency-selective mobile radio channels with asymmetrical Doppler power spectral density shapes," *IEEE Trans. Veh. Technol.*, vol. 46, pp. 494–507, May 1997.

[51] M. Pätzold and B. Talha, "On the statistical properties of sum-of-cisoids-based mobile radio channel simulators," in *Proc. 10th International Symposium on Wireless Personal Multimedia Communications, WPMC 2007*, pp. 394–400, Jaipur, India, Dec. 2007.

[52] M. Pätzold, U. Killat, and F. Laue, "An extended Suzuki model for land mobile satellite channels and its statistical properties," *IEEE Trans. Veh. Technol.*, vol. 47, pp. 617–630, May 1998.

[53] H. Suzuki, "A statistical model for urban radio propagation," *IEEE Trans. Commun.*, vol. 25, pp. 673–680, July 1977.

[54] T. T. Tjhung and C. C. Chai, "Fade statistics in Nakagami-lognormal channels," *IEEE Trans. on Communications*, vol. 47, pp. 1769–1772, Dec. 1999.

[55] F. Ramos, V. Y. Kontorovitch, and M. Lara, "Generalization of Suzuki model for analog communication channels," in *Proc. IEEE Antennas and Propagation for Wireless Communication, IEEE APS 2000*, pp. 107–110, Nov. 2000.

[56] A. Sendonaris, E. Erkip, and B. Aazhang, "User cooperation diversity—Part I: System description," *IEEE Trans. Commun.*, vol. 51, pp. 1927–1938, Nov. 2003.

[57] A. Sendonaris, E. Erkip, and B. Aazhang, "User cooperation diversity—Part II: Implementation aspects and performance analysis," *IEEE Trans. Commun.*, vol. 51, pp. 1939–1948, Nov. 2003.

[58] J. N. Laneman, D. N. C. Tse, and G. W. Wornell, "Cooperative diversity in wireless networks: Efficient protocols and outage behavior," *IEEE Trans. Inform. Theory*, vol. 50, pp. 3062–3080, Dec. 2004.

[59] M. Dohler, *Virtual Antenna Arrays*. Ph.D. dissertation, King's College, London, United Kingdom, 2003.

[60] T. J. Harrold and A. R. Nix, "Intelligent relaying for future personal communication systems," in *Proc. IEE Colloq. Capacity and Range Enhancement Techniques for the Third Generation Mobile Communications and Beyond*, pp. 9/1–9/5, London, UK, Feb. 2000.

[61] V. Sreng, H. Yanikomeroglu, and D. Falconer, "Coverage enhancement through two-hop relaying in cellular radio systems," in *Proc. IEEE Wireless Communications and Networking Conference, WCNC 1999*, vol. 2, pp. 881–885, Mar. 2002.

[62] *IEEE J. Select. Areas Commun.: Issue on Wireless ad hoc Networks*, vol. 17, Aug. 1999.

[63] *IEEE Pers. Commun. Mag.: Special Issue on Advances in Mobile ad hoc Networking*, vol. 8, Jan. 2001.

[64] O. Dousse, P. Thiran, and M. Hasler, "Connectivity in ad-hoc and hybrid networks," in *Proc. 21st Annual Joint Conf. of the IEEE Computer and Communications Societies, INFOCOM 2002*, vol. 2, pp. 1079–1088, June 2002.

[65] M. O. Hasna and M. S. Alouini, "End-to-end performance of transmission systems with relays over Rayleigh-fading channels," *IEEE Trans. Wireless Commun.*, vol. 2, pp. 1126–1131, Nov. 2003.

[66] M. O. Hasna and M. S. Alouini, "Outage probability of multihop transmission over Nakagami fading channels," *IEEE Commun. Letters*, vol. 7, pp. 216–218, May 2003.

[67] G. Farhadi and N. C. Beaulieu, "On the ergodic capacity of multi-hop wireless relaying systems," *IEEE Trans. Wireless Commun.*, vol. 8, pp. 2286–2291, May 2009.

[68] P. A. Anghel and M. Kaveh, "Exact symbol error probability of a cooperative network in a Rayleigh-fading environment," *IEEE Trans. Wireless Commun.*, vol. 3, pp. 1416–1421, Sept. 2004.

[69] G. K. Karagiannidis, "Performance bounds of mltihop wireless communications with blind relays over generalized fading channels," *IEEE Trans. Wireless Commun.*, vol. 5, pp. 498–502, Mar. 2006.

[70] W. C. Jakes, ed., *Microwave Mobile Communications*. Piscataway, NJ: IEEE Press, 1994.

[71] W. C. Y. Lee, *Mobile Communications Engineering*. New York: McGraw-Hill, 2nd ed., 1998.

[72] M. S. Alouini and A. J. Goldsmith, "Capacity of Rayleigh fading channels under different adaptive transmission and diversity-combining techniques," *IEEE Trans. Veh. Technol.*, vol. 48, pp. 1165–1181, July 1999.

[73] Y. Chen and C. Tellambura, "Performance analysis of L-branch equal gain combiners in equally correlated Rayleigh fading channels," *IEEE Communications Letters*, vol. 8, pp. 150–152, Mar. 2004.

[74] A. A. Abu-Dayya and N. C. Beaulieu, "Microdiversity on Rician fading channels," *IEEE Trans. Commun.*, vol. 42, pp. 2258–2267, June 1994.

[75] S. Khatalin and J. P. Fonseka, "On the channel capacity in Rician and Hoyt fading environments with MRC diversity," *IEEE Trans. Veh. Technol.*, vol. 55, pp. 137–141, Jan. 2006.

[76] P. Almers, E. Bonek, A. Burr, N. Czink, M. Debbah, V. Degli-Esposti, H. Hofstetter, P. Kyösti, D. Laurenson, G. Matz, A. F. Molisch, C. Oestges, and H. Özcelik, "Survey of channel and radio propagation models for wireless MIMO systems," *EURASIP J. Wirel. Commun. Netw.*, vol. 2007, pp. 56–56, Jan. 2007. DOI 10.1155/2007/19070.

[77] A. Goldsmith, S. A. Jafar, N. Jindal, and S. Vishwanath, "Capacity limits of MIMO channels," *IEEE J. Select. Areas Commun.*, vol. 21, pp. 684–702, June 2003.

[78] C. Zhong, K. Wong, and S. Jin, "Capacity bounds for MIMO Nakagami-m fading channels," *IEEE Trans. Signal Processing*, vol. 57, pp. 3613–3623, Sept. 2009.

[79] W. Weichselberger, M. Herdin, H. Özcelik, and E. Bonek, "A stochastic MIMO channel model with joint correlation of both link ends," *IEEE Trans. Wireless Commun.*, vol. 5, pp. 90–100, Jan. 2006.

[80] J. P. Kermoal, L. Schumacher, K. I. Pedersen, P. E. Mogensen, and F. Fredriksen, "A stochastic MIMO radio channel model with experimental validation," *IEEE Journal on Selected Areas in Communications*, vol. 20, pp. 1211–1226, Aug. 2002.

[81] N. Costa and S. Haykin, "A novel wideband MIMO channel model and experimental validation," *IEEE Trans. Antennas Propagat.*, vol. 56, pp. 550–562, Feb. 2008.

[82] C. N. Chuah, J. M. Kahn, and D. Tse, "Capacity of multiantenna array systems in indoor wireless environment," in *Proc. 50th IEEE Global Telecommunications Conference, GLOBECOM 2007*, vol. 4, pp. 1894–1899, Sydney, Australia, Nov. 1998.

[83] Q. Li, G. Li, W. Lee, M. Lee, D. Mazzarese, B. Clerckx, and Z. Li, "MIMO techniques in WiMAX and LTE: A feature overview," *IEEE Communications Magazine*, vol. 48, pp. 86–92, May 2010.

[84] "IEEE Std. 802.11n - 2009, IEEE standard for information technology–Telecommunications and information exchange between systems–Local and metropolitan area networks–Specific requirements Part 11: Wireless LAN medium access control (MAC) and physical layer (PHY) specifications amendment 5: Enhancements for higher throughput," pp. c1–502, Oct. 2009.

[85] E. Perahia, "IEEE 802.11n development: History, process, and technology," *IEEE Communications Magazine*, vol. 46, pp. 48–55, July 2008.

[86] "IEEE Std. 802.16 - 2009 (Revision of IEEE Std. 802.16 - 2004), IEEE standard for local and metropolitan area networks Part 16: Air interface for broadband wireless access systems," pp. c1–2004, May 2009.

[87] J. B. Bruyne, W. Joseph, L. Verloock, C. Olivier, W. D. Ketelaere, and L. Martens, "Field measurements and performance analysis of an 802.16 system in a suburban environment," *IEEE Trans. Wireless Commun.*, vol. 8, pp. 1424–1434, Mar. 2009.

[88] 3rd Generation Partnership Project, "3GPP TS 36.913 requirements for further advancements for evolved universal terrestrial radio access (EUTRA)," v.8.0.1 (2009-03).

[89] A. Ghosh, R. Ratasuk, B. Mondal, N. Mangalvedhe, and T. Thomas, "LTE-advanced: Next-generation wireless broadband technology [invited paper]," *IEEE Wireless Communications Magazine*, vol. 17, pp. 10–22, June 2010.

[90] V. Tarokh, N. Seshadri, and A. R. Calderbank, "Space-time codes for high data rate wireless communication: performance criterion and code construction," *IEEE Trans. Inform. Theory*, vol. 44, pp. 744–765, Mar. 1998.

[91] S. M. Alamouti, "A simple transmit diversity technique for wireless communications," *IEEE J. Select. Areas Commun.*, vol. 16, pp. 1451–1458, Oct. 1998.

[92] V. Tarokh, H. Jafarkhani, and A. R. Calderbank, "Space-time block codes from orthogonal designs," *IEEE Trans. on Inform. Theory*, vol. 45, pp. 1456–1467, July 1999.

[93] E. G. Larsson and P. Stoica, *Space-Time Block Coding for Wireless Communications*. Cambridge Univ. Press, 1st ed., 2003.

[94] S. O. Rice, "Mathematical analysis of random noise," *Bell Syst. Tech. J.*, vol. 23, pp. 282–332, July 1944.

[95] S. O. Rice, "Mathematical analysis of random noise," *Bell Syst. Tech. J.*, vol. 24, pp. 46–156, Jan. 1945.

[96] M. Pätzold, *Mobile Fading Channels*. Chichester: John Wiley & Sons, 2002.

[97] M. D. Yacoub, J. E. V. Bautista, and L. G. de Rezende Guedes, "On higher order statistics of the Nakagami-*m* distribution," *IEEE Trans. Veh. Technol.*, vol. 48, pp. 790–794, May 1999.

[98] S. O. Rice, "Statistical properties of a sine wave plus random noise," *Bell Syst. Tech. J.*, vol. 27, pp. 109–157, Jan. 1948.

[99] A. Papoulis and S. U. Pillai, *Probability, Random Variables and Stochastic Processes*. New York: McGraw-Hill, 4th ed., 2002.

[100] W. A. T. Kotterman, G. F. Pedersen, and K. Olsen, "Diversity properties of multiantenna small handheld terminals," *EURASIP Journal on Applied Signal Processing*, vol. 2004, pp. 1340–1353, Jan. 2004.

[101] A. Abdi, J. A. Barger, and M. Kaveh, "A parametric model for the distribution of the angle of arrival and the associated correlation function and power spectrum at the mobile station," *IEEE Trans. Veh. Technol.*, vol. 51, pp. 425–434, May 2002.

[102] X. Zhao, J. Kivinen, P. Vainikainen, and K. Skog, "Characterization of Doppler spectra for mobile communications at 5.3 GHz," vol. 52, pp. 14–23, Jan. 2003.

[103] N. Blaunstein and Y. Ben-Shimol, "Spectral properties of signal fading and Doppler spectra distribution in urban mobile links," *Wirel. Commun. Mob. Comput.*, vol. 6, pp. 113–126, Feb. 2006.

[104] S. R. Saunders and A. Aragón-Savala, *Antennas and Propagation for Wireless Communication Systems*. Chichester: John Wiley & Sons, second ed., 2007.

[105] C. A. Gutiérrez, *Channel Simulation Models for Mobile Broadband Communication Systems*. PhD dissertation, Department of Information and Communication Technology, Faculty of Engineering and Science, University of Agder, Grimstad, Norway, 2009.

[106] M. Pätzold and C. A. Gutiérrez, "Level-crossing rate and average duration of fades of the envelope of a sum-of-cisoids," in *Proc. IEEE 67th Vehicular Technology Conference, IEEE VTC 2008-Spring*, pp. 488–494, Marina Bay, Singapore, May 2008.

[107] S. H. Choi, P. J. Smith, B. Allen, W. Q. Malik, and M. Shafi, "Severely fading MIMO channels: Models and mutual information," in *Proc. IEEE International Conference on Communications, ICC 2007*, pp. 4628–4633, Glasgow, UK, June 2007.

[108] S. Elnoubi, S. A. Chahine, and H. Abdallah, "BER performance of GMSK in Nakagami fading channels," in *Proc. 21st National Radio Science Conference, NRSC 2004*, pp. C13–1–8, Mar. 2004.

[109] G. Lebrun, M. Faulkner, M. Shafi, and P. J. Smith, "MIMO Ricean channel capacity," in *Proc. IEEE Int. Conf. Commun., ICC 2004*, vol. 5, pp. 2939–2943, June 2004.

[110] G. Rafiq, V. Kontorovich, and M. Pätzold, "On the statistical properties of the capacity of the spatially correlated Nakagami-*m* MIMO channels," in *Proc. IEEE 67th Vehicular Technology Conference, IEEE VTC 2008-Spring*, pp. 500–506, Marina Bay, Singapore, May 2008.

[111] G. Rafiq, M. Pätzold, and V. Kontorovich, "The influence of spatial correlation and severity of fading on the statistical properties of the capacity of OSTBC Nakagami-*m* MIMO channels," in *Proc. IEEE 69th Vehicular Technology Conference, IEEE VTC 2009-Spring*, pp. 1–5, Barcelona, Spain, Apr. 2009.

[112] M. K. Simon, *Probability Distributions Involving Gaussian Random Variables: A Handbook for Engineers and Scientists*. Dordrecht: Kluwer Academic Publishers, 2002.

[113] S. M. Moser, "Some expectations of a non-central chi-square distribution with an even number of degrees of freedom," in *Proc. 2007 IEEE Region 10 Conference, TENCON 2007*, pp. 1–4, Oct. 2007.

[114] M. Gudmundson, "Correlation model for shadow fading in mobile radio systems," *Electron. Lett.*, vol. 27, pp. 2145–2146, Nov. 1991.

[115] D. M. Black and D. O. Reudink, "Some characteristics of mobile radio propagation at 836 MHz in the Philadelphia area," *IEEE Trans. Veh. Technol.*, vol. 21, pp. 45–51, Feb. 1972.

[116] D. O. Reudink, "Comparison of radio transmission at X-band frequencies in suburban and urban areas," *IEEE Trans. Ant. Prop.*, vol. 20, pp. 470–473, July 1972.

[117] M. F. Ibrahim and J. D. Parsons, "Signal strength prediction in built-up areas," *Proc. IEE*, vol. 130F, pp. 377–384, Aug. 1983.

[118] M.-S. Alouini, A. Abdi, and M. Kaveh, "Sum of gamma variates and performance of wireless communication systems over Nakagami-fading channels," *IEEE Trans. Veh. Technol.*, vol. 50, pp. 1471–1480, Nov. 2001.

[119] H. Ge, K. D. Wong, M. Barton, and J. C. Liberti, "Statistical characterization of multiple-input multiple-output (MIMO) channel capacity," in *Proc. IEEE Wireless Communications and Networking Conference, WCNC 2002*, vol. 2, pp. 789–793, Mar. 2002.

[120] G. Rafiq and M. Pätzold, "Statistical properties of the capacity of multipath fading channels," in *Proc. 20th IEEE Int. Symp. on Personal, Indoor and Mobile Radio Communications, PIMRC 2009*, pp. 1103–1107, Tokyo, Japan, Sept. 2009.

[121] M. Pätzold, C. X. Wang, and B. O. Hogstad, "Two new sum-of-sinusoids-based methods for the efficient generation of multiple uncorrelated Rayleigh fading waveforms," *IEEE Trans. Wireless Commun.*, vol. 8, pp. 3122–3131, June 2009.

[122] B. O. Hogstad, M. Pätzold, N. Youssef, and K. Dongwoo, "A MIMO mobile-to-mobile channel model: Part II - the simulation model," in *Proc. 16th IEEE Int. Symp. on Personal, Indoor and Mobile Radio Communications, PIMRC 2005*, vol. 1, pp. 562–567, Sept. 2005.

[123] G. Rafiq and M. Pätzold, "A study of the statistical properties of the envelope and the capacity of Rice-*m* channels," in *Proc. 12th International Symposium on Wireless Personal Multimedia Communications, WPMC 2009*, Sendai, Japan, Sept. 2009. ISSN 1883-1192.

[124] G. L. Stüber, *Principles of Mobile Communications*. Boston, MA: Kluwer Academic Publishers, 2nd ed., 2001.

[125] M. Pätzold and K. Yang, "An exact solution for the level-crossing rate of shadow fading processes modelled by using the sum-of-sinusoids principle," *Wireless Personal Communications (WPC)*, vol. 52, pp. 57–68, Jan. 2010.

[126] G. Rafiq and M. Pätzold, "A study of the influence of shadowing on the statistical properties of the capacity of mobile radio channels," *Wireless Personal Communications (WPC)*, vol. 50, pp. 5–18, July 2009.

[127] M. Pätzold and K. Yang, "An exact solution for the level-crossing rate of shadow fading processes modelled by using the sum-of-sinusoids principle," in *Proc. 9th International Symposium on Wireless Personal Multimedia Communications, WPMC 2006*, pp. 188–193, San Diego, USA, Sept. 2006.

[128] G. Rafiq and M. Pätzold, "The influence of the severity of fading and shadowing on the statistical properties of the capacity of Nakagami-lognormal channels," in *Proc. IEEE Global Telecommunications Conference IEEE GLOBECOM 2008*, pp. 1–6, Nov. 2008. DOI 10.1109/GLOCOM.2008.ECP.824.

[129] J. B. Andersen, "Statistical distributions in mobile communications using multiple scattering," in *Proc. 27th URSI General Assembly*, Maastricht, Netherlands, Aug. 2002.

[130] I. Z. Kovacs, P. C. F. Eggers, K. Olesen, and L. G. Petersen, "Investigations of outdoor-to-indoor mobile-to-mobile radio communication channels," in *Proc. IEEE 56th Veh. Technol. Conf., VTC'02-Fall*, pp. 430–434, Vancouver BC, Canada, Sept. 2002.

[131] V. Ercerg, S. J. Fortune, J. Ling, A. J. Rustako Jr., and R. A. Valenzuela, "Comparison of a computer-based propagation prediction tool with experimental data collected in urban microcellular environment," *IEEE J. Select. Areas Commun.*, vol. 15, pp. 677–684, May 1997.

[132] C. S. Patel, G. L. Stüber, and T. G. Pratt, "Statistical properties of amplify and forward relay fading channels," *IEEE Trans. Veh. Technol.*, vol. 55, pp. 1–9, Jan. 2006.

[133] J. Salo, H. M. El-Sallabi, and P. Vainikainen, "Statistical analysis of the multiple scattering radio channel," *IEEE Trans. Antennas Propagat.*, vol. 54, pp. 3114–3124, Nov. 2006.

[134] B. Talha and M. Pätzold, "On the statistical properties of double Rice channels," in *Proc. 10th International Symposium on Wireless Personal Multimedia Communications, WPMC 2007*, pp. 517–522, Jaipur, India, Dec. 2007.

[135] B. Talha and M. Pätzold, "On the statistical properties of mobile-to-mobile fading channels in cooperative networks under line-of-sight conditions," in *Proc. 10th International Symposium on Wireless Personal Multimedia Communications, WPMC 2007*, pp. 388–393, Jaipur, India, Dec. 2007.

[136] B. Talha and M. Pätzold, "A novel amplify-and-forward relay channel model for mobile-to-mobile fading channels under line-of-sight conditions," in *Proc. 19th IEEE Int. Symp. on Personal, Indoor and Mobile Radio Communications, PIMRC 2008*, pp. 1–6, Cannes, France, Sept. 2008.

[137] B. Talha and M. Pätzold, "Level-crossing rate and average duration of fades of the envelope of mobile-to-mobile fading channels in cooperative networks under line-of-sight conditions," in *Proc. 51st IEEE Global Telecommunications Conference, GLOBECOM 2008*, pp. 1–6, New Orleans, US, Nov. 2008.

[138] J. Salo, H. M. El-Sallabi, and P. Vainikainen, "Impact of double-Rayleigh fading on system performance," in *Proc. 1st IEEE Int. Symp. on Wireless Pervasive Computing, ISWPC 2006*, Phuket, Thailand, Jan. 2006.

[139] P. Almers, F. Tufvesson, and A. F. Molisch, "Keyhole effect in MIMO wireless channels: Measurements and theory," *IEEE Trans. Wireless Commun.*, vol. 5, pp. 3596–3604, Dec. 2006.

[140] D. Gesbert, H. Bölcskei, D. A. Gore, and A. J. Paulraj, "Outdoor MIMO wireless channels: Models and performance prediction," *IEEE Trans. Wireless Commun.*, vol. 50, pp. 1926–1934, Dec. 2002.

[141] H. Shin and J. H. Lee, "Performance analysis of space-time block codes over keyhole Nakagami-*m* fading channels," *IEEE Trans. Veh. Technol.*, vol. 53, pp. 351–362, Mar. 2004.

[142] N. Zlatanov, Z. H. Velkov, and G. K. Karagiannidis, "Level crossing rate and average fade duration of the double Nakagami-*m* random process and application in MIMO keyhole fading channels," *IEEE Communications Letters*, vol. 12, pp. 822–824, Nov. 2008.

[143] G. K. Karagiannidis, N. C. Sagias, and P. T. Mathiopoulos, "$N*$Nakagami: A novel stochastic model for cascaded fading channels," *IEEE Trans. Commun.*, vol. 55, pp. 1453–1458, Aug. 2007.

[144] Z. H. Velkov, N. Zlatanov, and G. K. Karagiannidis, "On the second order statistics of the multihop Rayleigh fading channel," *IEEE Trans. Commun.*, vol. 57, pp. 1815–1823, June 2009.

[145] D. Chizhik, G. J. Foschini, M. J. Gans, and R. A. Valenzuela, "Keyholes, correlations, and capacities of multielement transmit and receive antennas," *IEEE Trans. Wireless Commun.*, vol. 1, pp. 361–368, Apr. 2002.

[146] J. Boyer, D. D. Falconer, and H. Yanikomeröglu, "Multihop diversity in wireless relaying channels," *IEEE Trans. Commun.*, vol. 52, pp. 1820–1830, Oct. 2004.

[147] G. Rafiq and M. Pätzold, "The influence of LOS components on the statistical properties of the capacity of amplify-and-forward channels," *Wireless Sensor Networks (WSN)*, vol. 1, pp. 7–14, Apr. 2009.

[148] G. Rafiq, B. O. Hogstad, and M. Pätzold, "Statistical properties of the capacity of double Nakagami-*m* channels," in *Proc. IEEE 5th Int. Symposium on Wireless Pervasive Computing, IEEE ISWPC 2010*, pp. 39–44, Modena, Italy, Apr. 2010. DOI 10.1109/ISWPC.2010.5483776.

[149] G. Rafiq, B. O. Hogstad, and M. Pätzold, "On the first and second order statistics of the capacity of $N*$Nakagami-*m* channels," 2010. to be submitted for publication.

[150] I. S. Gradshteyn and I. M. Ryzhik, *Table of Integrals, Series, and Products*. New York: Academic Press, 6th ed., 2000.

[151] D. A. Zogas, G. K. Karagiannidis, and S. A. Kotsopoulos, "Equal gain combining over Nakagami-*n* (Rice) and Nakagami-*q* (Hoyt) generalized fading channels," *IEEE Trans. Wireless Commun.*, vol. 4, pp. 374–379, Mar. 2005.

[152] L. R. Kahn, "Ratio squarer," *Proc. IRE (Corresp.)*, vol. 42, pp. 1698–1704, Nov. 1954.

[153] M. Z. Win and J. H. Winters, "On maximal ratio combining in correlated Nakagami channels with unequal fading parameters and SNRs among branches: an analytical framework," in *Proc. IEEE Wireless Communications and Networking Conference, WCNC 1999*, vol. 3, pp. 1058–1064, Sept. 1999.

[154] N. C. Beaulieu and X. Dong, "Level crossing rate and average fade duration of MRC and EGC diversity in Ricean fading," vol. 51, pp. 722–726, May 2003.

[155] K. A. Hamdi, "Capacity of MRC on correlated Rician fading channels," *IEEE Trans. Commun.*, vol. 56, pp. 708–711, May 2008.

[156] T. S. Rappaport, *Wireless Communications: Principles and Practice*. 2001.

[157] J. A. López-Salcedo, "Simple closed-form approximation to Ricean sum distributions," *IEEE Signal Processing Letters*, vol. 16, pp. 153–155, June 2009.

[158] N. C. Beaulieu, "An infinite series for the computation of the complementary probability distribution function of a sum of independent random variables and its application to the sum of Rayleigh random variables," *IEEE Trans. Commun.*, vol. 38, pp. 1463–1474, Sept. 1990.

[159] D. B. da Costa, M. D. Yacoub, and J. C. S. Santos Filho, "An improved closed-form approximation to the sum of arbitrary Nakagami-*m* variates," *IEEE Trans. Veh. Technol.*, vol. 57, pp. 3854–3858, Nov. 2008.

[160] C. Chayawan and V. A. Aalo, "On the outage probability of optimum combining and maximal ratio combining schemes in an interference-limited Rice fading channel," *IEEE Trans. Commun.*, vol. 50, pp. 532–535, Apr. 2002.

[161] H. Samimi and P. Azmi, "An approximate analytical framework for performance analysis of equal gain combining technique over independent Nakagami, Rician and Weibull fading channels," *Wireless Personal Communications (WPC)*, vol. 43, pp. 1399–1408, Dec. 2007. DOI 10.1007/s11277-007-9314-z.

[162] A. Annamalai, C. Tellambura, and V. K. Bhargava, "Equal-gain diversity receiver performance in wireless channels," *IEEE Trans. Commun.*, vol. 48, pp. 1732–1745, Oct. 2000.

[163] Q. T. Zhang, "Probability of error for equal-gain combiners over Rayleigh channels: Some closed-form solutions," *IEEE Trans. Commun.*, vol. 45, pp. 270–273, Mar. 1997.

[164] M. D. Yacoub, C. R. C. M. da Silva, and J. E. B. Vargas, "Second-order statistics for diversity-combining techniques in Nakagami-fading channels," *IEEE Trans. Veh. Technol.*, vol. 50, pp. 1464–1470, Nov. 2001.

[165] D. A. Zogas, G. K. Karagiannidis, and S. A. Kotsopoulos, "Equal-gain and maximal-ratio combining over nonidentical Weibull fading channels," *IEEE Trans. Wireless Commun.*, vol. 4, pp. 841–846, May 2005.

[166] P. Dharmawansa, N. Rajatheva, and K. Ahmed, "On the distribution of the sum of Nakagami-*m* random variables," *IEEE Trans. Commun.*, vol. 55, pp. 1407–1416, July 2007.

[167] J. Salz and J. H. Winters, "Effect of fading correlation on adaptive arrays in digital mobile radio," *IEEE Trans. Veh. Technol.*, vol. 43, pp. 1049–1057, Nov. 1994.

[168] E. A. Jorswieck, T. J. Oechtering, and H. Boche, "Performance analysis of combining techniques with correlated diversity," in *Proc. IEEE Wireless Communications and Networking Conference, WCNC 2005*, vol. 2, pp. 849–854, Mar. 2005.

[169] P. Lombardo, G. Fedele, and M. M. Rao, "MRC performance for binary signals in Nakagami fading with general branch correlation," *IEEE Trans. Commun.*, vol. 47, pp. 44–52, Jan. 1999.

[170] G. Rafiq and M. Patzold, "Statistical properties of the capacity of Rice channels with MRC and EGC," in *Proc. Int. Conf. on Wireless Communications and Signal Processing, WCSP 2009*, pp. 1–5, Nov. 2009.

[171] T. F. Coleman and Y. Li, "An interior trust region approach for nonlinear minimization subject to bounds," *SIAM J. Optimization,*, vol. 6, pp. 418–445, May 1996.

[172] G. Rafiq, V. Kontorovich, and M. Pätzold, "The influence of severity of fading on the statistical properties of the capacity of Nakagami-*m* channels with MRC and EGC," in *Proc. 2010 European Wireless Conference, EW 2010*, pp. 406–410, Apr. 2010.

[173] J. C. S. Santos Filho and M. D. Yacoub, "Nakagami-*m* approximation to the sum of M non-identical independent Nakagami-*m* variates," *IEEE Electronics Letters*, vol. 40, pp. 951–952, July 2004.

[174] L. Zheng and D. N. C. Tse, "Diversity and multiplexing: A fundamental tradeoff in multiple antenna channels," *IEEE Trans. Inform. Theory*, vol. 49, pp. 1073–1096, May 2003.

[175] M. Kiessling and J. Speidel, "Mutual information of MIMO channels in correlated Rayleigh fading environments - A general solution," in *Proc. IEEE Int. Conf. Commun., ICC 2004*, vol. 2, pp. 814–818, June 2004.

[176] M. Kiessling, "Unifying analysis of ergodic MIMO capacity in correlated rayleigh fading environments," *European Trans. Telecommun.*, vol. 16, pp. 17–35, Jan. 2005.

[177] J. Chen, Z. Du, and X. Gao, "Approximate capacity of OSTBC-OFDM in spatially correlated MIMO Nakagami-*m* fading channels," *IEEE Electronics Letters*, vol. 44, pp. 534–535, Apr. 2008.

[178] L. Musavian, M. Dohler, M. R. Nakhai, and M. H. Aghvami, "Closed-form capacity expressions of orthogonalized correlated MIMO channels," *IEEE Commun. Letter*, vol. 8, pp. 365–367, June 2004.

[179] L. Yang, "Outage performance of OSTBC in double scattering MIMO channels," *Wireless Personal Communications (WPC)*, vol. 45, pp. 225–230, Apr. 2008.

[180] H. Zhang and T. A. Gulliver, "Capacity and error probability analysis for orthogonal space-time block codes over fading channels," *IEEE Trans. Wireless Commun.*, vol. 4, pp. 808–819, Mar. 2005.

[181] A. Maaref and S. Aïssa, "Performance analysis of orthogonal space-time block codes in spatially correlated MIMO Nakagami fading channels," *IEEE Trans. Wireless Commun.*, vol. 5, pp. 807–817, Apr. 2006.

[182] K. Yu, M. Bengtsson, B. Ottersten, D. McNamara, P. Karlsson, and M. Beach, "Second order statistics of NLOS indoor MIMO channels based on 5.2 GHz measurements," in *Proc. IEEE Global Telecommunications Conference, GLOBECOM 2001*, vol. 1, pp. 156–160, Nov. 2001.

[183] T. Ratnarajah, "Spatially correlated multiple-antenna channel capacity distributions," *IEE Proc. Commun.*, vol. 153, pp. 263–271, Apr. 2006.

[184] P. J. Smith, S. Roy, and M. Shafi, "Capacity of MIMO systems with semicorrelated flat fading," *IEEE Trans. Inform. Theory*, vol. 49, pp. 2781–2788, Oct. 2003.

[185] T. Ratnarajah, "Spatially correlated MIMO Rician channel capacity," in *Proc. 38th Asilomar Conf. on Signals, Systems and Computers 2004*, vol. 1, pp. 1188–1192, Nov. 2004.

[186] E. Riegler and G. Taricco, "Asymptotic statistics of the mutual information for spatially correlated Rician fading MIMO channels with interference," *IEEE Trans. Inform. Theory*, vol. 56, pp. 1542–1559, Apr. 2010.

[187] J. Dumont, W. Hachem, S. Lasaulce, P. Loubaton, and J. Najim, "High SNR approximations of the capacity of MIMO correlated Rician channels: A large system approach," in *Proc. IEEE Int. Sym. Inf. Theo., ISIT 2007*, pp. 536–540, June 2007.

[188] J. Salo, F. Mikas, and P. Vainikainen, "An upper bound on the ergodic mutual information in Rician fading MIMO channels," vol. 5, pp. 1415–1421, June 2006.

[189] M. R. McKay and I. B. Collings, "General capacity bounds for spatially correlated Rician MIMO channels," *IEEE Trans. Inform. Theory*, vol. 51, pp. 3121–3145, Sept. 2005.

[190] B. O. Hogstad, G. Rafiq, V. Kontorovitch, and M. Pätzold, "Capacity studies of spatially correlated MIMO Rice channels," in *Proc. IEEE 5th Int. Symposium on Wireless Pervasive Computing, IEEE ISWPC 2010*, pp. 45–50, May 2010.

[191] D.-S. Shiu, G. J. Foschini, M. J. Gans, and J. M. Kahn, "Fading correlation and its effect on the capacity of multielement antenna systems," *IEEE Trans. Commun.*, vol. 48, pp. 502–513, Mar. 2000.

[192] H. Özcelik, M. Herdin, W. Weichselberger, J. Wallace, and E. Bonek, "Deficiencies of 'Kronecker' MIMO radio channel model," *IEEE Electronics Letters*, vol. 39, pp. 1209–1210, Aug. 2003.

[193] T. Aulin, "Characteristics of a digital mobile radio channel," *IEEE Trans. Veh. Technol.*, vol. 30, pp. 45–53, May 1981.

[194] C. Zhong, S. Jin, T. Ratnarajah, and K. Wong, "On the capacity of non-uniform phase MIMO Nakagami-*m* fading channels," *IEEE Communications Letters*, vol. 14, pp. 536–538, June 2010.

[195] D. B. da Costa and M. D. Yacoub, "Average channel capacity for generalized fading scenarios," *IEEE Communications Letters*, vol. 11, pp. 949–951, Dec. 2007.

[196] D. P. Palomar and Y. Jiang, "MIMO transceiver design via majorization theory," *Found. Trends Commun. Inf. Theory*, vol. 3, pp. 331–551, Nov. 2006.

[197] B. O. Hogstad, M. Pätzold, N. Youssef, and V. Kontorovitch, "Exact closed-form expressions for the distribution, level-crossing rate, and average duration of fades of the capacity of OSTBC-MIMO channels," *IEEE Trans. Veh. Technol.*, vol. 58, pp. 1011–1016, Feb. 2009.

[198] R. C. Palat, A. Annamalai, and J. H. Reed, "An efficient method for evaluating information outage probability and ergodic capacity of OSTBC system," *IEEE Communications Letters*, vol. 12, pp. 191–193, Mar. 2008.

[199] A. Sezgin and O. Henkel, "Stacked OSTBC: Error performance and rate analysis," *IEEE Trans. Signal Processing*, vol. 55, pp. 4599–4611, Sept. 2007.

[200] G. A. Ropokis, A. A. Rontogiannis, P. T. Mathiopoulos, and K. Berberidis, "An exact performance analysis of MRC/OSTBC over generalized fading channels," *IEEE Trans. Commun.*, vol. 58, pp. 2486–2492, Sept. 2010.

[201] K. T. Phan and C. Tellambura, "Capacity analysis for transmit antenna selection using orthogonal space-time block codes," *IEEE Communications Letters*, vol. 11, pp. 423–425, May 2007.

[202] G. Rafiq and M. Pätzold, "The impact of shadowing and the severity of fading on the first and second order statistics of the capacity of OSTBC Nakagami-Lognormal MIMO channels," *Wireless Personal Communications (WPC)*, 2010. Submitted for publication.

[203] Z. Shen, R. W. Heath Jr., J. G. Andrews, and B. L. Evans, "Space-time water-filling for composite MIMO fading channels," *EURASIP J. Wirel. Commun. Netw.*, vol. 2006, no. 2, pp. 48–48, 2006.

[204] L. Yang, "Outage performance of OSTBC in MIMO channels with shadowing," *Wireless Personal Communications (WPC)*, vol. 43, pp. 1751–1754, Dec. 2007.

[205] H. E. Salzer, R. Zucker, and R. Capuano, "Table of the zeros and weight factors of the first twenty hermite polynomials," *J. Res. Nat. Bu. Standards*, vol. 48, pp. 111–116, Feb. 1952.

Appendices A–N

List of Publications

The purpose of this preface to Appendices A–N is to record all the articles that are an outcome of the research work carried out by the author of this dissertation. The list of publications consists of submitted, accepted, and already published papers. Firstly, the next section lists those articles which are briefly discussed in Chapters 2–5 of this dissertation and are replicated in Appendices A–N. Thereafter, the subsequent section details those papers which are published within the framework of this doctoral thesis, however they are not included in this dissertation.

Articles Included in this Dissertation

Those articles which are included in Appendices A–N of this dissertation are tabulated as follows:

Paper I G. Rafiq and M. Pätzold, Statistical properties of the capacity of multipath fading channels, *Proc. IEEE International Symposium on Personal, Indoor and Mobile Radio Communications, PIMRC 2009*, Tokyo, Japan, Sept. 2009, pp. 1103 – 1107.

Paper II G. Rafiq and M. Pätzold, A study of the statistical properties of the envelope and the capacity of Rice-*m* channels, *Proc. 12th International Symposium on Wireless Personal Multimedia Communications, WPMC 2009*, Sendai, Japan, Sept. 2009, ISSN 1883-1192.

Paper III G. Rafiq and M. Pätzold, A study of the influence of shadowing on the statistical properties of the capacity of mobile radio channels, *Wireless Personal Communications, Special Issue on "Wireless Future"*,

vol. 50, no. 1, Jul. 2009, pp. 5 – 18.

Paper IV G. Rafiq and M. Pätzold, The influence of the severity of fading and shadowing on the statistical properties of the capacity of Nakagami-Lognormal channels, *Proc. IEEE Global Communications Conference, GLOBECOM 2008*, New Orleans, LA, USA, Nov. /Dec. 2008, pp. 1 – 6.

Paper V G. Rafiq and M. Pätzold, The influence of LOS components on the statistical properties of the capacity of amplify-and-forward channels, *Wireless Sensor Networks (WSN), Invited Paper*, vol. 1, no. 1, Apr. 2009, pp. 7 – 14.

Paper VI G. Rafiq, B. O. Hogstad, and M. Pätzold, Statistical properties of the capacity of double Nakagami-*m* channels, *Proc. 5th International Symposium on Wireless Pervasive Computing, ISWPC 2010*, Modena, Italy, May 2010, pp. 39 – 44.

Paper VII G. Rafiq, B. O. Hogstad, and M. Pätzold, On the first and second order statistics of the capacity of $N*$Nakagami-*m* channels, to be submitted for publication.

Paper VIII G. Rafiq and M. Pätzold, Statistical properties of the capacity of Rice channels with MRC and EGC, *Proc. International Conference on Wireless Communications and Signal Processing, WCSP 2009*, Nanjing, China, Nov. 2009, pp. 1 – 5.

Paper IX G. Rafiq, V. Kontorovich, and M. Pätzold, The influence of severity of fading on the statistical properties of the capacity of Nakagami-*m* channels with MRC and EGC, *Proc. 16th European Wireless Conference, EW 2010*, Lucca, Italy, Apr. 2010, pp. 406 – 410.

Paper X G. Rafiq, V. Kontorovich, and M. Pätzold, The impact of spatial correlation on the statistical properties of the capacity of Nakagami-*m* channels with MRC and EGC, to be submitted for publication.

Paper XI B. O. Hogstad, G. Rafiq, V. Kontorovich, and M. Pätzold, Capacity studies of spatially correlated MIMO Rice channels, *Proc. 5th International Symposium on Wireless Pervasive Computing, ISWPC 2010*, Modena, Italy, May 2010, pp. 45 – 50.

Paper XII G. Rafiq, V. Kontorovich, and M. Pätzold, On the statistical properties of the capacity of spatially correlated Nakagami-*m* MIMO channels, *Proc. 67th IEEE Vehicular Technology Conference, VTC2008-Spring*, Singapore, May. 2008, pp. 500 – 506.

Paper XIII G. Rafiq, M. Pätzold, and V. Kontorovich, The influence of spatial correlation and severity of fading on the statistical properties of the capacity of OSTBC Nakagami-*m* MIMO channels, *Proc. 69th IEEE Vehicular Technology Conference, VTC2009-Spring*, Barcelona, Spain, Apr. 2009, pp. 1 – 5.

Paper XIV G. Rafiq and M. Pätzold, The impact of shadowing and the severity of fading on the first and second order statistics of the capacity of OSTBC Nakagami-lognormal MIMO channels, *Wireless Personal Communications*, 2010, submitted for publication.

In the next section, those papers are listed which have not been reproduced in this paper collection.

Articles Not Included in this Dissertation

The articles pointed out in the following are also published during this PhD study and carry equal importance as the ones mentioned in previous section. However, to reduce the overlap between the articles making up the final manuscript, they are not included in this dissertation.

Paper XV [1]G. Rafiq and M. Pätzold, The impact of shadowing on the capacity of mobile fading channels, *Proc. 4th IEEE International Symposium on Wireless Communication Systems, ISWCS 2007*, Trondheim, Norway, Oct. 2007, pp. 209 – 214.

Paper XVI G. Rafiq and M. Pätzold, On the statistical properties of the capacity of amplify-and-forward channels under LOS conditions, *Proc. 11th IEEE International Conference on Communications Systems, ICCS 2008*, Guangzhou, China, Nov. 2008, pp. 1614 – 1619.

Paper XVII G. Rafiq, B. O. Hogstad, and M. Pätzold, Statistical properties of the capacity of double Nakagami-*m* channels for applications in V2V

[1]This article received the Best Student Paper Award at the 4th IEEE International Symposium on Wireless Communication Systems, ISWCS 2007

dualhop communication systems, *Vehicular Technologies, IN-TECH Education and Publishing*, Vienna, Austria, 2010, accepted for publication.

Paper XVIII G. Rafiq and M. Pätzold, On the statistical properties of the capacity of OSTBC Nakagami-Lognormal MIMO channels, *Proc. 4th International Conference on Signal Processing and Communication Systems, ICSPCS 2010*, Gold Coast, Australia, Dec. 2010, accepted for publication.

Appendix A

Paper I

Title:	Statistical Properties of the Capacity of Multipath Fading Channels
Authors:	**Gulzaib Rafiq** and Matthias Pätzold
Affiliation:	University of Agder, Faculty of Engineering and Science, P. O. Box 509, NO-4898 Grimstad, Norway.
Conference:	*IEEE International Symposium on Personal, Indoor and Mobile Radio Communications, PIMRC 2009*, Tokyo, Japan, Sept. 2009, pp. 1103 – 1107.

Statistical Properties of the Capacity of Multipath Fading Channels

Gulzaib Rafiq and Matthias Pätzold
Department of Information and Communication Technology
Faculty of Engineering and Science, University of Agder
Servicebox 509, NO-4898 Grimstad, Norway
E-mails: {gulzaib.rafiq, matthias.paetzold}@uia.no

***Abstract* — It is well known that a frequency-nonselective multipath fading channel can be modeled by a sum of complex sinusoids, also called sum-of-cisoids (SOC). By using the SOC, we can efficiently model the scattered component of the received signal in non-isotropic scattering environments. Such SOC-based multipath channel models provide the flexibility of having correlated in-phase and quadrature phase components of the received signal. This paper presents the derivation and analysis of the statistical properties of the capacity of multipath fading channels under LOS conditions. As an appropriate stochastic model for the multipath fading channel, we have adopted the SOC model. We have derived the exact analytical expressions for the probability density function (PDF), cumulative distribution function (CDF), level-crossing rate (LCR), and average duration of fades (ADF) of the channel capacity. The statistical behavior of the channel capacity is studied for different values of the number of multipaths (cisoids) in the SOC model and the results are compared with the reference model which can be obtained by using an infinite number of cisoids. It is shown that the SOC model with ten cisoids produces results very close to the reference model. The validity of all the theoretical expressions is tested with the help of simulations.**

I. Introduction

Development of accurate and efficient channel models for the analysis of mobile fading channels has gained considerable attention in recent years. Different methods have been proposed in the literature over the last few decades that deal with the design and analysis of channel models for different radio environments. One of the very promising techniques employs the sum-of-sinusoids (SOS) method to model colored Gaussian processes. The SOS method, originally proposed by Rice [16, 17],

has been widely used by researchers ever since due to its simplicity in implementation, accuracy, and flexibility to model nearly all kinds of fading channels [10]. The versatility of this model also derives from the fact that many well-known channels, namely Rayleigh [7], Rice [18], lognormal [9], Suzuki [20], and Nakagami-m [21] channels can be derived with the help of Gaussian processes. Hence, SOS method provides the basis for the design of efficient mobile fading channel models. However, SOS-based channel models are generally designed with the assumption of symmetrical Doppler power spectral density (DPSD), for isotropic scattering environments. While, it has been shown in [8, 1, 22, 2] that the real-world channels have asymmetrical DPSDs due to non-isotropic scattering conditions. Therefore, in order to model such real-world channels a new class of channel models known as sum-of-cisoids (SOC) has been introduced in the literature [3, 12, 13]. Apart from the accuracy in modeling the non-isotropic scattering environments, the SOC model also provides a clearer physical interpretation in terms of the wave propagation phenomena when viewed in line with the plane wave propagation model [19]. The first and second order statistical properties of the SOC model are thoroughly investigated in [13] and [11].

In this article, we have studied the statistical properties of the capacity of multipath fading channels represented by an SOC model, under line-of-sight (LOS) conditions. We have derived the exact analytical expressions for the PDF, CDF, LCR, and ADF of the channel capacity. The mean channel capacity and spread of the channel capacity can be studied with the help of the PDF and CDF of the channel capacity. While, the LCR and ADF of the channel capacity are important statistical quantities that give an insight into the temporal behavior of the channel capacity [4, 6]. The LCR is a measure of the average rate of the up-crossings (or down-crossing) of the capacity through a certain threshold level in one second. The ADF on the other hand determines the average duration of time over which the channel capacity is below a certain threshold level [6]. We have studied the results for different values (N) of the number of multipath components (cisoids) in the SOC model. We have also presented the results for the reference model, which can be obtained from the SOC model when $N \to \infty$. It has been observed that as the value of N increases, the results obtained using the SOC model approach to those of the reference model. Specifically for $N \geq 10$, a very good fitting between the reference model and SOC model is observed. The correctness of the presented results is verified using simulations.

The remainder of this paper is organized as follows. In Section II, we will briefly describe the SOC model. We will present some of the statistical properties

of the SOC model which are used thereafter in Section III to derive the statistical properties of the capacity of multipath fading channels represented by an SOC model. Section IV presents the reference model for the capacity of multipath fading channels. In Section V, we will discuss and compare the analytical and simulation results. Finally, the conclusions are drawn in Section VI.

II. The SOC-based Multipath Fading Channel Model

Consider a process $\hat{\mu}(t)$ for modeling the scattered component of the received signal in a mobile fading channel in the complex baseband. The process $\hat{\mu}(t)$ can be expressed as [13, 11]

$$\hat{\mu}(t) = \sum_{n=1}^{N} c_n e^{j(2\pi f_n t + \theta_n)} \tag{1}$$

where c_n, f_n, and θ_n represent the gains, Doppler frequencies, and phases of the nth propagation path, respectively. Here, c_n and f_n are assumed to be constants. However, θ_n are considered to be independent and identically distributed (i.i.d.) random variables, uniformly distributed over the interval $(0, 2\pi]$. By applying the central limit theorem, the process $\hat{\mu}(t) = \hat{\mu}_1(t) + j\hat{\mu}_2(t)$ tends to a zero-mean complex Gaussian process with variance $2\sigma_0^2$ as $N \to \infty$. The autocorrelation function of the process $\hat{\mu}(t)$ is given by [13]

$$r_{\hat{\mu}\hat{\mu}}(\tau) = \sum_{n=1}^{N} c_n^2 e^{j2\pi f_n \tau}. \tag{2}$$

Moreover, the autocorrelation function and cross-correlation function of the inphase and quadrature components of the process $\hat{\mu}(t)$ is given by [13]

$$r_{\hat{\mu}_i\hat{\mu}_i}(\tau) = \frac{1}{2}\mathrm{Re}\left\{r_{\hat{\mu}\hat{\mu}}(\tau)\right\} = \sum_{n=1}^{N} \frac{c_n^2}{2}\cos(2\pi f_n \tau) \tag{3}$$

for $i = 1, 2$, and

$$r_{\hat{\mu}_1\hat{\mu}_2}(\tau) = \frac{1}{2}\mathrm{Im}\left\{r_{\hat{\mu}\hat{\mu}}(\tau)\right\} = \sum_{n=1}^{N} \frac{c_n^2}{2}\sin(2\pi f_n \tau) \tag{4}$$

respectively. Under LOS conditions, the envelope $\hat{\xi}(t)$ of the received signal can be expressed as

$$\hat{\xi}(t) = \left|\hat{\mu}_\rho(t)\right| = |\hat{\mu}(t) + m| \tag{5}$$

where $m = \rho e^{j\theta_\rho}$ represents the line-of-sight (LOS) component. Here, ρ and θ_ρ denote the amplitude and phase of the LOS component, respectively. In order to

derive the statistical properties of the capacity of multipath channels, provided that the received signal envelope $\hat{\xi}(t)$ is given by (5), we need to find the joint PDF $p_{\hat{\xi}^2\dot{\hat{\xi}}^2}(z,\dot{z})$ of the process $\hat{\xi}^2(t)$ and its time derivative $\dot{\hat{\xi}}^2(t)$ as well as the PDF $p_{\hat{\xi}^2}(z)$ of the process $\hat{\xi}^2(t)$. In this article, we represent the time derivative of a process by a raised dot. The joint PDF $p_{\hat{\xi}^2\dot{\hat{\xi}}^2}(z,\dot{z})$ can be obtained by employing the concept of transformation of random variables [9] and by using the expression for the joint PDF $p_{\hat{\xi}\dot{\hat{\xi}}}(z,\dot{z})$ presented in [11, Eq. (20)] as follows

$$\begin{aligned} p_{\hat{\xi}^2\dot{\hat{\xi}}^2}(z,\dot{z}) &= \frac{1}{4z} p_{\hat{\xi}\dot{\hat{\xi}}}(\sqrt{z}, \frac{\dot{z}}{2\sqrt{z}}) \\ &= \frac{\pi}{2\sqrt{z}} \int_0^{\infty} \int_{-\infty}^{\infty} w \left[\prod_{n=1}^{N} J_0\left(4\pi^2 |c_n f_n| w\right) \right] J_0\left(2\pi w \sqrt{\frac{\dot{z}^2}{4z} + \dot{\theta}^2 z} \right) d\dot{\theta} dw \\ &\quad \times p_{\hat{\xi}}(z), \;\; z \geq 0, |\dot{z}| < \infty. \end{aligned} \tag{6}$$

Moreover, the PDF $p_{\hat{\xi}^2}(z)$ can be found using the PDF $p_{\hat{\xi}}(z)$ given in [13, Eq. (26)] as

$$\begin{aligned} p_{\hat{\xi}^2}(z) &= \frac{1}{2\sqrt{z}} p_{\hat{\xi}}(\sqrt{z}) \\ &= (2\pi)^2 \int_0^{\infty} \left[\prod_{n=1}^{N} J_0\left(2\pi |c_n| x\right) \right] J_0\left(2\pi\sqrt{z}x\right) J_0\left(2\pi\rho x\right) x dx, \;\; z \geq 0 \end{aligned} \tag{7}$$

where $J_0(\cdot)$ represents the Bessel function of the first kind of order zero [5]. In the next section, we will first define the capacity of multipath fading channels described using the SOC model given in (5). Thereafter, the statistical properties of the channel capacity will be derived.

III. Statistical Properties of the Capacity of Multipath Fading Channels

The instantaneous capacity $\hat{C}(t)$ of the multipath fading channels with the received signal envelope $\hat{\xi}(t)$ can be expressed as

$$\hat{C}(t) = \log_2\left(1 + \gamma_s \hat{\xi}^2(t)\right) \text{ (bits/s/Hz)} \tag{8}$$

where γ_s denotes the signal-to-noise ratio (SNR). In order to derive the PDF $p_{\hat{C}}(r)$ of the channel capacity $\hat{C}(t)$, we will make use of the expression (7) and will apply the concept of transformation of random variables [9] according to the mapping of

random variables in (8) as follows

$$\begin{aligned} p_{\hat{C}}(r) &= \frac{2^r \ln(2)}{\gamma_s} p_{\hat{\xi}^2}\left(\frac{2^r-1}{\gamma_s}\right) \\ &= \frac{2^{r+1}\ln(2)\pi^2}{\gamma_s}\int_0^\infty \left[\prod_{n=1}^{N} J_0\left(2\pi|c_n|x\right)\right] J_0\left(2\pi\rho x\right) J_0\left(2\pi\sqrt{\frac{(2^r-1)}{\gamma_s}}x\right) x dx \end{aligned} \tag{9}$$

for $r \geq 0$. The CDF $F_{\hat{C}}(r)$ of the channel capacity $\hat{C}(t)$ can be obtained using the PDF $p_{\hat{C}}(r)$ as [9]

$$F_{\hat{C}}(r) = \int_0^r p_{\hat{C}}(z)dz. \tag{10}$$

After substituting (9) in (10), the resulting simplified expression for the CDF $F_{\hat{C}}(r)$ of the channel capacity is given by

$$F_{\hat{C}}(r) = 2\pi\sqrt{\frac{(2^r-1)}{\gamma_s}}\int_0^\infty \left[\prod_{n=1}^{N} J_0\left(2\pi|c_n|x\right)\right] J_0\left(2\pi\rho x\right) J_1\left(2\pi\sqrt{\frac{(2^r-1)}{\gamma_s}}x\right) dx, \quad r \geq 0 \tag{11}$$

where $J_1(\cdot)$ represents the Bessel function of the first kind of order one [5]. The LCR $N_{\hat{C}}(r)$ of the channel capacity $\hat{C}(t)$ is defined as [6]

$$N_{\hat{C}}(r) = \int_0^\infty \dot{z}\, p_{\hat{C}\dot{\hat{C}}}(r,\dot{z})d\dot{z}, \;\; r \geq 0 \tag{12}$$

where $p_{C\dot{C}}(z,\dot{z})$ is the joint PDF of the channel capacity $\hat{C}(t)$ and its time derivative $\dot{\hat{C}}(t)$. The joint PDF $p_{\hat{C}\dot{\hat{C}}}(z,\dot{z})$ can be obtained by employing (6) and by applying the concept of transformation of random variables as

$$\begin{aligned} p_{\hat{C}\dot{\hat{C}}}(z,\dot{z}) = \frac{\left(2^z\ln(2)/\gamma_s\right)^2\pi}{2\sqrt{(2^z-1)/\gamma_s}} p_{\hat{\xi}}\left(\sqrt{\frac{(2^z-1)}{\gamma_s}}\right) \int_0^\infty\int_{-\infty}^\infty w\left[\prod_{n=1}^{N} J_0\left(4\pi^2|c_n f_n|w\right)\right] \\ \times J_0\left(2\pi w\sqrt{\frac{\left(2^z\ln(2)\dot{z}\right)^2}{4\gamma_s(2^z-1)} + \dot{\theta}^2\frac{(2^z-1)}{\gamma_s}}\right) d\dot{\theta}dw \end{aligned} \tag{13}$$

for $z \geq 0$ and $|\dot{z}| < \infty$. By inserting (13) in (12) and by employing the relationship presented in (A.3), the LCR $N_{\hat{C}}(r)$ can be expressed as

$$N_{\hat{C}}(r) = 2\pi p_{\hat{\xi}}\left(\sqrt{\frac{(2^z-1)}{\gamma_s}}\right)\int_0^\infty\int_0^\infty\left[\prod_{n=1}^{N}J_0\left(2\pi|c_n f_n|w\right)\right]J_0\left(2\pi wy\right)wy^2dydw, \quad r\geq 0. \tag{14}$$

The ADF $T_{\hat{C}}(r)$ of the channel capacity $\hat{C}(t)$ is finally obtained using

$$T_{\hat{C}}(r) = \frac{F_{\hat{C}}(r)}{N_{\hat{C}}(r)} \tag{15}$$

where $F_{\hat{C}}(r)$ and $N_{\hat{C}}(r)$ represent the CDF and LCR of the channel capacity given in (11) and (14), respectively.

IV. Reference Model for the SOC Model

In this section, we will present the reference model for the SOC model described in Section II. We will present the expressions for the statistical properties of the channel capacity of the reference model. These results will be studied in the next section along with the results obtained using the SOC model for comparison purposes. It is shown in [13] that the PDF $p_{\hat{\xi}}(z)$ of the envelope $\hat{\xi}(t)$ of the SOC model approaches to that of the classical Rice PDF for $c_n = \sigma_0\sqrt{2/N}$ and $N\to\infty$, which is considered as a reference model for (5). Hence, by setting $c_n = \sigma_0\sqrt{2/N}$ and $N\to\infty$ the PDF, CDF, and LCR of the channel capacity $\hat{C}(t)$ of multipath fading channels can be expressed as

$$p_{\hat{C}}(r)\,|_{N\to\infty} = \frac{2^r\ln(2)}{2\gamma_s\sigma_0^2}e^{-\frac{2^r-1+\gamma_s\rho^2}{2\sigma_0^2\gamma_s}}I_0\left(\sqrt{\frac{(2^r-1)\rho^2}{\sigma_0^4\gamma_s}}\right),\ r\geq 0 \tag{16}$$

$$F_{\hat{C}}(r)\,|_{N\to\infty} = 1-Q_1\left(\frac{\rho}{\sigma_0},\sqrt{\frac{(2^r-1)}{\sigma_0^2\gamma_s}}\right),\ r\geq 0 \tag{17}$$

and

$$N_{\hat{C}}(r)\,|_{N\to\infty} = \sqrt{\frac{(2^r-1)}{\sigma_0^4\gamma_s}}\frac{e^{-\frac{2^r-1+\gamma_s\rho^2}{2\sigma_0^2\gamma_s}}}{\sqrt{2\pi/\beta}}I_0\left(\sqrt{\frac{(2^r-1)}{\sigma_0^4\gamma_s/\rho^2}}\right),\ r\geq 0 \tag{18}$$

respectively. In (17), $Q_1(\cdot,\cdot)$ represents the Marcum Q-function [15, Eq. (2-1-122)]. In (18), $\beta = -\ddot{r}_{\mu_i\mu_i}(0)$, where $r_{\mu_i\mu_i}(\tau)$ denotes the autocorrelation function of the inphase component $(i=1)$ or the quadrature component $(i=2)$ of the underlying

complex Gaussian process $\mu(t) = \mu_1(t) + j\mu_2(t)$. For isotropic scattering conditions, one obtains $\beta = 2(\pi f_{\max}\sigma_0)^2$, where $f_{\max}$ denotes the maximum Doppler frequency. It can be proved that the expressions (16)–(18) represent the PDF, CDF, and LCR of the channel capacity of the reference model (i.e., classical Rice channels). Moreover, it can also easily be proved that the results for the PDF, CDF, and LCR of the channel capacity of the SOC model as well as reference model approach to that of the Rayleigh process for the case when $\rho \to 0$.

V. Numerical Results

This section aims at the verification and analysis of the findings of the previous sections with the help of an SOC-based channel simulator presented in [11, Fig. 1]. The model parameters c_n and f_n in (1) are calculated using the extended method of exact Doppler spread (EMEDS) [14] according to

$$c_n = \sigma_0\sqrt{\frac{2}{N}} \tag{19}$$

$$f_n = f_{\max}\cos\left[\frac{2\pi}{N}\left(n - \frac{1}{4}\right)\right] \tag{20}$$

respectively, for $n = 1, 2, ..., N$. The results are studied for different values of the amplitude of the LOS component ρ, especially the Rayleigh channel (i.e., $\rho = 0$) and the Rice channel (for $\rho = 1$ and 2). In order to generate the process $\hat{\mu}(t)$, three different values i.e., $N = 3, 5,$ and 10, were chosen as the number of cisoids in the SOC model for comparison purposes. The maximum Doppler frequency $f_{\max}$ was 91 Hz, the SNR $\gamma_s = 15$ dB, and the parameter σ_0 was chosen to be equal to unity. Finally, using the SOC-based channel simulator [11, Fig. 1] in conjunction with (8) the simulation results for the statistical properties of the channel capacity $\hat{C}(t)$ of multipath fading channels were obtained.

The PDFs $p_{\hat{\xi}}(t)$ of the envelope $\hat{\xi}(t)$ of the SOC model and the reference model are shown in Fig. A.1 for different values of the number of cisoids N and the amplitude of the LOS component ρ. We have also presented the simulation results obtained from the SOC-based channel simulator. It can be observed that the results from the reference model and the SOC model match quite closely as the value of the parameter N increases. Specifically for $N = 10$, a very good fitting between the PDF curves obtained from the reference model and SOC model is observed. Hence, the SOC model with $N = 10$ can be used quite effectively to model Rice channels.

Figures A.2 and A.3 present the PDF and CDF respectively, of the capacity of multipath fading channels for different values (N) of the number of multipaths

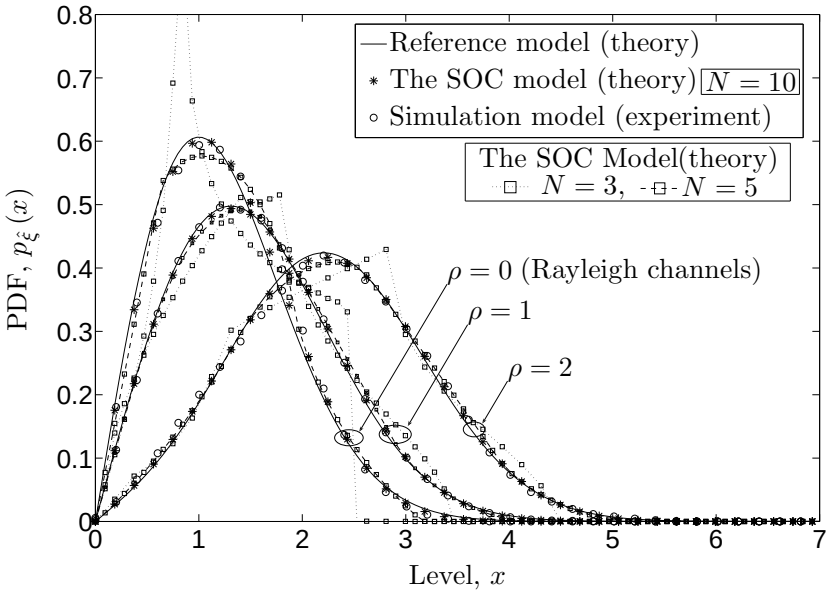

Figure A.1: The PDF $p_{\hat{\xi}}(z)$ of the envelope $\hat{\xi}(t)$ of the SOC model for different values of the number of cisoids N.

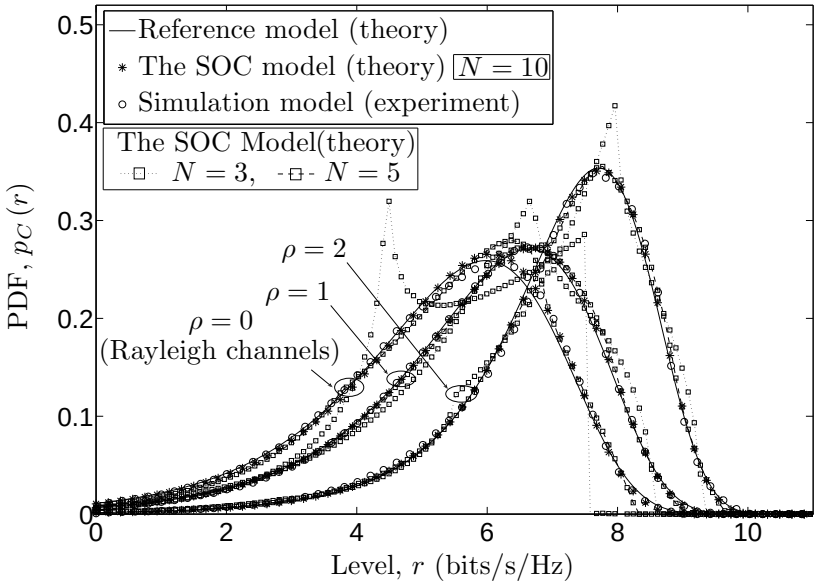

Figure A.2: The PDF $p_C(r)$ of the capacity of multipath fading channels.

(cisoids). It is observed that the number of cisoids N has a more significant effect on the capacity of channels with no LOS component (i.e., $\hat{\xi}(t)$ for $\rho = 0$) as compared to those with the LOS component (e.g., $\rho = 1$ and 2). It can also be seen that the PDF of the channel capacity is more sensitive to the parameter N than the CDF of the channel capacity. Moreover, the curves in both the figures support the fact that $N = 10$ is a suitable value for the SOC model for the analysis of the capacity of

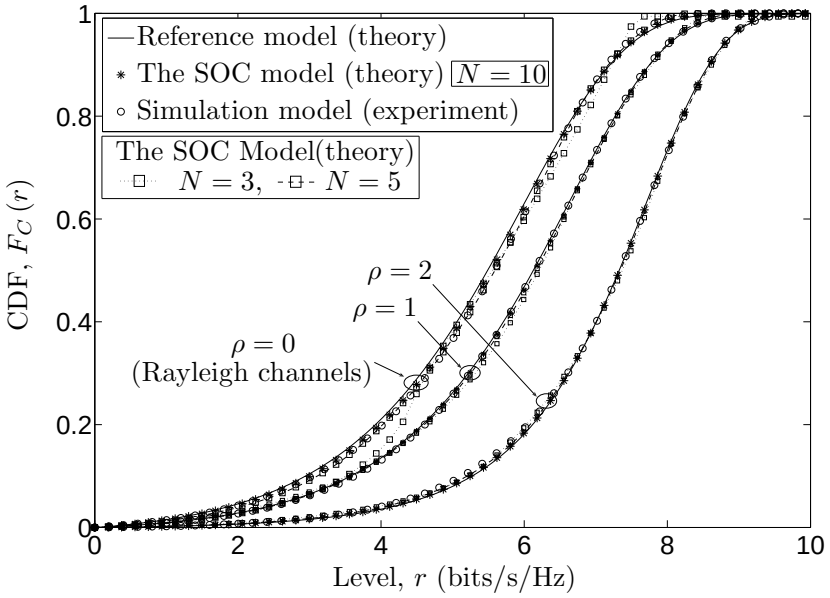

Figure A.3: The CDF $F_C(r)$ of the capacity of multipath fading channels.

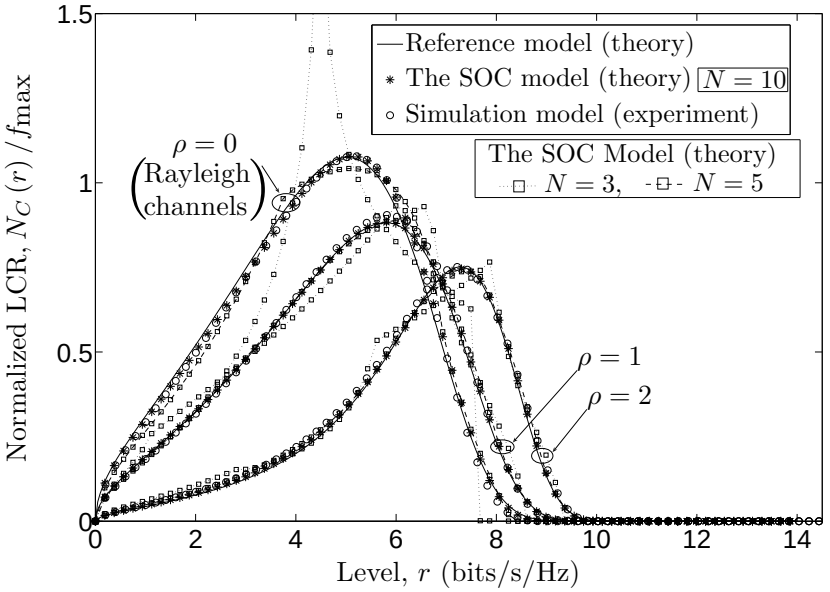

Figure A.4: The LCR $N_C(r)$ of the capacity of multipath fading channels.

multipath fading channels.

Figures A.4 and A.5 show the LCR and ADF respectively, of the channel capacity of the reference model and the SOC model. It can be concluded from these figures that the LCR and ADF of the channel capacity of the SOC model is quite close to that of the reference model for $N \geq 10$. However, it can be seen that the change in the value of the parameter N has more influence on the LCR than the ADF

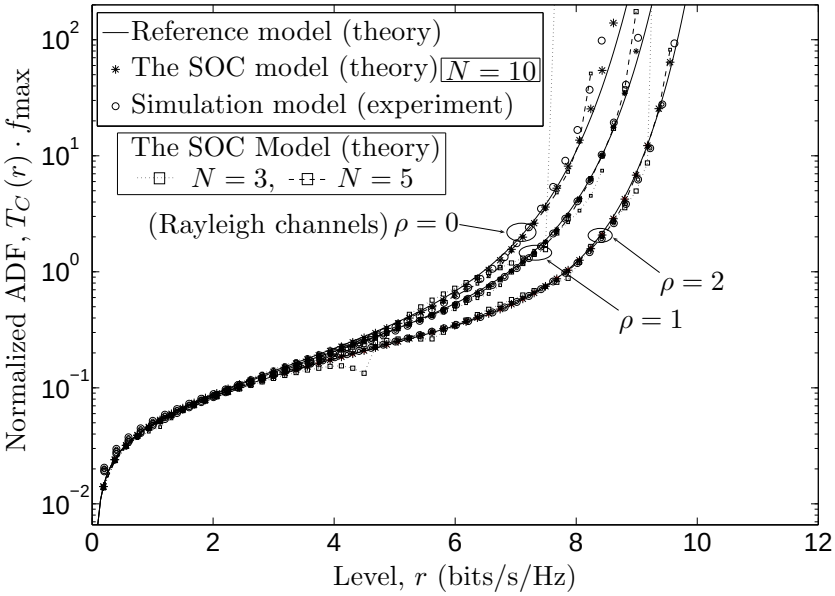

Figure A.5: The ADF $T_C(r)$ of the capacity of multipath fading channels.

of the channel capacity for low and medium signal levels r. The correctness of the theoretical results is verified using the simulations, whereby a very good fitting is observed.

VI. Conclusion

In this article, we have presented the statistical properties of the capacity of the multipath fading channels represented by an SOC model. We have derived the exact analytical expressions for the PDF, CDF, LCR, and the ADF of the capacity of multipath fading channels. We have also presented the theoretical expressions for the reference model for comparison purposes. All the theoretical results obtained for the statistical properties of the channel capacity are confirmed with the help of simulations. We have studied the results for different values of the LOS component as well as for the SOC model parameter N. We have shown that the results for the statistical properties of the channel capacity obtained using the SOC model match quite closely to those of the reference model if $N \geq 10$. It is also observed that the parameter N has more influence on the statistical properties of the capacity of the channels with a lower value of the amplitude of the LOS component ρ (e.g., $\rho = 0$) than the channels with higher values of ρ (e.g., $\rho = 2$). All the results show that the presented SOC model with 10 cisoids can be very effectively used for the statistical analysis of the capacity of multipath fading channels.

A. A Proof of (14)

Let

$$I = \int_0^{\infty} \int_{-\infty}^{\infty} \dot{z} J_0 \left(2\pi w \sqrt{\frac{\left(2^z \ln(2)\dot{z}\right)^2}{4\gamma_s \left(2^z - 1\right)} + \dot{\theta}^2 \frac{\left(2^z - 1\right)}{\gamma_s}} \right) d\dot{\theta} d\dot{z}. \tag{A.1}$$

By substituting $\dot{z}\, 2^z \ln(2) / \gamma_s = \dot{X}$ and $\left(2^z - 1/\gamma_s\right) 2\dot{\theta} = \dot{Y}$, we can write

$$I = \frac{\left(2^z \ln(2)/\gamma_s\right)^{-2}}{2\left(2^z - 1/\gamma_s\right)} \int_0^{\infty} \int_{-\infty}^{\infty} \dot{X} J_0 \left(\frac{2\pi w \sqrt{\dot{X}^2 + \dot{Y}^2}}{\sqrt{\left(2^z - 1/\gamma_s\right)}} \right) d\dot{Y} d\dot{X}. \tag{A.2}$$

Transforming the Cartesian coordinates $\left(\dot{Y}, \dot{X}\right)$ to polar coordinates (x, θ) using $\dot{Y} = x \sin\theta$ and $\dot{X} = x \cos\theta$ allows us to express the equation (A.2) as

$$I = \frac{\left(2^z \ln(2)/\gamma_s\right)^{-2}}{2\left(2^z - 1/\gamma_s\right)} \int_0^{\infty} x^2 J_0 \left(\frac{2\pi w x}{\sqrt{2^z - 1/\gamma_s}} \right) dx. \tag{A.3}$$

REFERENCES

[1] A. Abdi, J. A. Barger, and M. Kaveh. A parametric model for the distribution of the angle of arrival and the associated correlation function and power spectrum at the mobile station. *IEEE Trans. Veh. Technol.*, 51(3):425–434, May 2002.

[2] N. Blaunstein and Y. Ben-Shimol. Spectral properties of signal fading and Doppler spectra distribution in urban mobile links. *Wirel. Commun. Mob. Comput.*, 6(1):113–126, February 2006.

[3] R. H. Clarke. A statistical theory of mobile-radio reception. *Bell Syst. Tech. Journal*, 47:957–1000, July/August 1968.

[4] A. Giorgetti, P. J. Smith, M. Shafi, and M. Chiani. MIMO capacity, level crossing rates and fades: The impact of spatial/temporal channel correlation. *J. Commun. Net.*, 5(2):104–115, June 2003.

[5] I. S. Gradshteyn and I. M. Ryzhik. *Table of Integrals, Series, and Products*. New York: Academic Press, 6th edition, 2000.

[6] B. O. Hogstad and M. Pätzold. Exact closed-form expressions for the distribution, level-crossing rate, and average duration of fades of the capacity of

MIMO channels. In *Proc. 65th Semiannual Vehicular Technology Conference, IEEE VTC 2007-Spring*, pages 455–460. Dublin, Ireland, April 2007.

[7] W. C. Jakes, editor. *Microwave Mobile Communications*. Piscataway, NJ: IEEE Press, 1994.

[8] W. A. T. Kotterman, G. F. Pedersen, and K. Olsen. Diversity properties of multiantenna small handheld terminals. *EURASIP Journal on Applied Signal Processing*, 2004(9):1340–1353, January 2004.

[9] A. Papoulis and S. U. Pillai. *Probability, Random Variables and Stochastic Processes*. New York: McGraw-Hill, 4th edition, 2002.

[10] M. Pätzold. *Mobile Fading Channels*. Chichester: John Wiley & Sons, 2002.

[11] M. Pätzold and C. A. Gutiérrez. Level-crossing rate and average duration of fades of the envelope of a sum-of-cisoids. In *Proc. IEEE 67th Vehicular Technology Conference, IEEE VTC 2008-Spring*, pages 488–494. Marina Bay, Singapore, May 2008.

[12] M. Pätzold, U. Killat, Y. Li, and F. Laue. Modelling, analysis, and simulation of nonfrequency-selective mobile radio channels with asymmetrical Doppler power spectral density shapes. *IEEE Trans. Veh. Technol.*, 46(2):494–507, May 1997.

[13] M. Pätzold and B. Talha. On the statistical properties of sum-of-cisoids-based mobile radio channel simulators. In *Proc. 10th International Symposium on Wireless Personal Multimedia Communications, WPMC 2007*, pages 394–400. Jaipur, India, December 2007.

[14] M. Pätzold, C. X. Wang, and B. O. Hogstad. Two new sum-of-sinusoids-based methods for the efficient generation of multiple uncorrelated Rayleigh fading waveforms. *IEEE Trans. Wireless Commun.*, 8(6):3122–3131, June 2009.

[15] J. Proakis. *Digital Communications*. New York: McGraw-Hill, 4th edition, 2001.

[16] S. O. Rice. Mathematical analysis of random noise. *Bell Syst. Tech. J.*, 23:282–332, July 1944.

[17] S. O. Rice. Mathematical analysis of random noise. *Bell Syst. Tech. J.*, 24:46–156, January 1945.

[18] S. O. Rice. Statistical properties of a sine wave plus random noise. *Bell Syst. Tech. J.*, 27:109–157, January 1948.

[19] S. R. Saunders and A. Aragón-Savala. *Antennas and Propagation for Wireless Communication Systems*. Chichester: John Wiley & Sons, second edition, 2007.

[20] H. Suzuki. A statistical model for urban radio propagation. *IEEE Trans. Commun.*, 25(7):673–680, July 1977.

[21] M. D. Yacoub, J. E. V. Bautista, and L. G. de Rezende Guedes. On higher order statistics of the Nakagami-*m* distribution. *IEEE Trans. Veh. Technol.*, 48(3):790–794, May 1999.

[22] X. Zhao, J. Kivinen, P. Vainikainen, and K. Skog. Characterization of Doppler spectra for mobile communications at 5.3 GHz. 52(1):14–23, January 2003.

Appendix B

Paper II

Title:	A Study of the Statistical Properties of the Envelope and the Capacity of Rice-*m* Channels
Authors:	**Gulzaib Rafiq** and Matthias Pätzold
Affiliation:	University of Agder, Faculty of Engineering and Science, P. O. Box 509, NO-4898 Grimstad, Norway.
Conference:	*12th International Symposium on Wireless Personal Multimedia Communications, WPMC 2009*, Sendai, Japan, Sept. 2009, ISSN 1883-1192.

A Study of the Statistical Properties of the Envelope and the Capacity of Rice-*m* Channels

Gulzaib Rafiq and Matthias Pätzold
Department of Information and Communication Technology
Faculty of Engineering and Science, University of Agder
Servicebox 509, NO-4898 Grimstad, Norway
E-mails: {gulzaib.rafiq, matthias.paetzold}@uia.no

***Abstract* — In this paper, we have introduced a new channel model referred to as the Rice-*m* channel model for frequency non-selective fading channels. The Rice-*m* channel model is defined as the Euclidean norm of a vector process consisting of $2m$ real-valued non-zero mean Gaussian processes. The generality of this model comes from the fact that it inherently incorporates the classical Rice channel and the Nakagami-*m* channel as special cases. The proposed channel model is employed for the statistical analysis of the received signal envelope and the channel capacity. We present exact closed-form analytical expressions for the probability density function (PDF), cumulative distribution function (CDF), level-crossing rate (LCR), and average duration of fades (ADF) of both the signal envelope as well as the channel capacity of Rice-*m* channels. The results are analyzed for different values of the fading parameter m and the mean values of the underlying Gaussian processes. We will show that the statistical properties of the envelope and the capacity of Rice-*m* channels are quite different from those of Nakagami-*m* channels. Specifically, Rice-*m* channels have a higher mean channel capacity and a lower spread of the channel capacity. The correctness of the theoretical results is verified by simulations. The importance of this study lies in merging the classical Rice and Nakagami-*m* channel characteristics into a new channel model, which has thus a higher flexibility than the two former ones.**

I. Introduction

The statistical analysis of the channel capacity of mobile fading channels has been a very active area of research in the past decade. Especially, since the pioneering works of Foschini and Gans [5] as well as Telatar [22], numerous articles have been published dealing with the analysis of the channel capacity of Rayleigh and Ricean channels [6, 8, 10, 11]. The Rayleigh and Rice distributions are widely accepted as suitable frequency-nonselective channel models for modeling the fading behavior in

dispersive urban environments. However, it has been reported in the literature that it is very common to come across scenarios where the fading is more (or less severe) as compared to the Rayleigh fading [3, 4]. Thus, in order to study more realistic fading scenarios, a more general channel model compared to the Rayleigh model is required. For this reason, the Nakagami-*m* process has gained much attention in recent years due to its flexibility of modeling different fading conditions, mathematical ease, and good fitness with experimental data [3, 4, 23]. The statistical analysis of the channel capacity of Nakagami-*m* channels can be found in [16, 19]. Moreover, in land mobile terrestrial channels, the combined effects of severity of fading and shadowing on the channel capacity has been studied in [17] by employing the Nakagami-lognormal channel model. Even with all this research going on, the communication engineers are still striving to provide a better description of the wireless fading channel to provide the basis for a realistic study of the performance of wireless communication systems.

In this article, we have proposed a channel model referred to as the Rice-*m* channel model. The novelty in this channel model comes from the assumption that the underlying random processes in the Nakagami-*m* channel model are independent and identically distributed (i.i.d.) Gaussian processes, each with non-zero mean. Hence, the received signal envelope of the Rice-*m* channel is modeled as the square root of a sum of $2m$ squared non-zero mean i.i.d. Gaussian processes. The proposed channel model includes the Nakagami-*m*, Rice, and Rayleigh fading channel models as special cases. We have derived closed-form analytical expressions for the statistical properties of both the envelope and the capacity of Rice-*m* channels. The analysis of the received signal envelope and the channel capacity for different levels of the severity of fading as well as for different mean values of the underlying Gaussian processes is presented in this paper. It is observed that the statistics of the envelope and the channel capacity of Rice-*m* channels are quite different from those of the Nakagami-*m* channels. The obtained results show that the spread of the received signal envelope decreases with a decrease in the severity of fading. Moreover, the received signal envelope corresponding to Rice-*m* channels has a higher mean value as compared to that of Nakagami-*m* channels. It is also observed that the channel capacity of the Nakagami-*m* channels has a lower mean and broader spread as compared to that of Rice-*m* channels. Moreover, at medium and high signal levels, the ADF of the channel capacity of Nakagami-*m* channels is higher than the ADF corresponding to Rice-*m* channels. In order to check the correctness of the derived theoretical expressions, we have used a high performance channel simulator.

The rest of the paper is organized as follows. In Section II, we will briefly describe the Rice-*m* channel model. Here, we will also present the PDF and the CDF of the Rice-*m* process along with the LCR and the ADF. The statistical properties of the channel capacity of Rice-*m* channels are derived in Section III. In Section IV, some special cases of the Rice-*m* process are discussed. Section V deals with the analysis of the theoretical and simulation results. Finally, the conclusions are presented in Section VI.

II. The Rice-*m* Channel Model

Let us consider a vector process $\mathbf{X}(t) = [x_1(t)\, x_2(t) \cdots x_{2m}(t)]^T$, where $x_i(t)$ $(i = 1, 2, ..., 2m)$ are i.i.d. real-valued Gaussian processes with zero-mean and variance σ_0^2/m and a vector $\mathbf{m}_X = [m_{x_1}\, m_{x_2} \cdots m_{x_{2m}}]^T$ with real constant entries m_{x_i} $(i = 1, 2, ..., 2m)$. Here, $2m \geq 1$ is a positive integer and $(\cdot)^T$ represents the matrix transposition. The underlying Gaussian processes $x_i(t)$ have the same autocorrelation function (ACF) denoted by $r_{x_i x_i}(\tau)$ for $i = 1, 2, ..., 2m$. From [23] we know that the Euclidean norm $\|\mathbf{X}(t)\|$ of the process $\mathbf{X}(t)$ follows the Nakagami-*m* distribution. The Rice-*m* process is defined as

$$\begin{aligned} \chi(t) &= \|\mathbf{X}(t) + \mathbf{m}_X\| \\ &= \sqrt{\chi_1^2(t) + \chi_2^2(t) + \cdots + \chi_{2m}^2(t)} \end{aligned} \tag{1}$$

where $\chi_i(t) = x_i(t) + m_{x_i}$ $(i = 1, 2, ..., 2m)$. The process $\chi(t)$ can be interpreted as a Rice process of order $2m$ [21]. Here, the parameter m controls the severity of the fading. As the value of m increases, the fading severity decreases and vice versa. The PDF $p_\chi(z)$ of the Rice-*m* process $\chi(t)$ is given by [21, Eq. (2.21)]

$$p_\chi(z) = \frac{m z^m}{\sigma_0^2 \rho^{m-1}} e^{-\frac{z^2+\rho^2}{2\sigma_0^2}} I_{m-1}\left(\frac{z\rho\, m}{\sigma_0^2}\right), \; z \geq 0 \tag{2}$$

where $\rho = \|\mathbf{m}_X\|$ and $I_n(\cdot)$ is the modified Bessel function of the first kind of order n [7]. By using $m = 1$ in (2), it can be observed that the PDF $p_\chi(z)$ reduces to the classical Rice distribution given by [12, Eq. (6-74)]. Moreover, by using the small argument representation of the modified Bessel function [1, Eq. (9.6.7)], it can be proved that for $\rho \to 0$ the PDF $p_\chi(z)$ is equal to the Nakagami-*m* distribution presented in [12, Eq. (4-45)]. Similarly, for $m = 1$ and $\rho \to 0$ in (2), the Rayleigh distribution is obtained. It can be seen here that the mean values of the underlying Gaussian processes $x_i(t)$ $(i = 1, 2, ..., 2m)$ control the parameter ρ. Hence, by increasing the mean values of the underlying Gaussian processes, the value of ρ increases and vice versa. The CDF $F_\chi(r)$ of the Rice-*m* process $\chi(t)$ can be obtained

using $F_\chi(z) = \int_0^z p_\chi(x)dx$. The expression for the CDF $F_\chi(z)$ can be found in [21, Eq. (2.22)].

One of the most important characteristic statistical quantities of fading channels is the LCR, which provides an insight into the fading rate of the channel. The LCR is defined as the average number of up-crossings (or down crossings) of the received signal envelope through a certain threshold in a time duration of one second [13]. In order to find the LCR of the Rice-m channel, we need the joint PDF $p_{\chi\dot{\chi}}(z,\dot{z})$ of $\chi(t)$ and its time derivative $\dot{\chi}(t)$ at the same point in time. Throughout this paper, we will represent the time derivative of a process by a raised dot. The joint PDF $p_{\chi\dot{\chi}}(z,\dot{z})$ can be found using a similar procedure found in [2] as

$$\begin{aligned} p_{\chi\dot{\chi}}(z,\dot{z}) &= \frac{m z^m}{\sqrt{2\pi\beta}\sigma_0^2\rho^{m-1}} e^{-\frac{\dot{z}^2}{2\beta}} e^{-\frac{z^2+\rho^2}{2\sigma_0^2/m}} I_{m-1}\left(\frac{z\rho\, m}{\sigma_0^2}\right) \\ &= p_\chi(z)\sqrt{\frac{1}{2\pi\beta}} e^{-\frac{\dot{z}^2}{2\beta}},\ z \geq 0, |\dot{z}| < \infty \end{aligned} \tag{3}$$

where $\beta = -\ddot{r}_{x_i x_i}(0)$. Under the assumption of isotropic scattering, the quantity β is given by $2\left(\pi\sigma_0 f_{\max}\right)^2/m$ [13]. Here, $f_{\max}$ represents the maximum Doppler frequency. The LCR $N_\chi(r)$ of the Rice-m process $\chi(t)$ can be obtained by using [20]

$$N_\chi(r) = \int_0^\infty \dot{z}\, p_{\chi\dot{\chi}}(r,\dot{z})d\dot{z} \tag{4}$$

as follows

$$N_\chi(r) = \sqrt{\frac{\beta}{2\pi}}\, p_\chi(z),\ r \geq 0. \tag{5}$$

The ADF of the received signal envelope in a fading channel represents the average duration of time over which the signal is below a certain threshold level. It can be expressed as [9, Eq. (1.3-41)]

$$T_\chi(r) = \frac{F_\chi(r)}{N_\chi(r)} \tag{6}$$

where $F_\chi(r)$ and $N_\chi(r)$ are given by [21, Eq. (2.22)] and (5). In the next section, we will study the statistical properties of the capacity of Rice-m channels.

III. Statistical Properties of the Capacity of Rice-*m* Channels

The instantaneous capacity $C(t)$ of Rice-*m* channels can be expressed as [5]

$$C(t) = \log_2\left(1+\gamma_s\chi^2(t)\right) \text{ (bits/s/Hz)} \tag{7}$$

where γ_s denotes the signal-to-noise ratio (SNR). The above expression can be considered as a mapping of a random process $\chi(t)$ to another random process $C(t)$. Hence, the statistical properties of the channel capacity can be found with the help of the statistical properties of the process $\chi(t)$. In order to find the PDF of the channel capacity, we first need to find the PDF $p_{\chi^2}(z)$ of the process $\chi^2(t)$, which can be achieved by using the relation $p_{\chi^2}(z) = p_\chi(\sqrt{z})\,/2\sqrt{z}$. Thereafter, the PDF $p_C(r)$ of the channel capacity $C(t)$ is obtained using the concept of transformation of random variables [12] as

$$\begin{aligned} p_C(r) &= \frac{2^r\ln(2)}{\gamma_s}\,p_{\chi^2}\left(\frac{2^r-1}{\gamma_s}\right) \\ &= \frac{2^r\ln(2)(2^r-1)^{\frac{m-1}{2}}}{(\rho^2\gamma_s)^{\frac{m-1}{2}}\,2\,\gamma_s\sigma_0^2/m} I_{m-1}\left(\sqrt{\frac{(2^r-1)\,\rho^2}{\sigma_0^4\gamma_s\,/m^2}}\right) e^{-\frac{2^r-1+\gamma_s\rho^2}{2\sigma_0^2\gamma_s/m}},\ r\geq 0. \end{aligned} \tag{8}$$

The CDF $F_C(r)$ of the channel capacity $C(t)$ can now be obtained by solving the following integral [12]

$$F_C(r) = \int_0^r p_C(z)dz. \tag{9}$$

By inserting the expression of the PDF $p_C(r)$ from (8) in (9) allows us to express the CDF $F_C(r)$ as

$$F_C(r) = 1 - Q_m\left(\frac{\sqrt{m}\,\rho}{\sigma_0}, \sqrt{\frac{(2^r-1)}{\sigma_0^2\gamma_s/m}}\right),\ r\geq 0 \tag{10}$$

where $Q_m(\cdot,\cdot)$ represents the Marcum Q-function [15, Eq. (2-1-122)]. Analogously to (4), the LCR $N_C(r)$ of the channel capacity $C(t)$ is defined as

$$N_C(r) = \int_0^\infty \dot{z}\,p_{C\dot{C}}(r,\dot{z})d\dot{z},\ r\geq 0 \tag{11}$$

where $p_{C\dot{C}}(z,\dot{z})$ denotes the joint PDF of the channel capacity $C(t)$ and its time derivative $\dot{C}(t)$. Using (3) and by applying the concept of transformation of random variables, we can express the joint PDF $p_{C\dot{C}}(z,\dot{z})$ as

$$p_{C\dot{C}}(z,\dot{z}) = \left(\frac{2^z\ln(2)}{\gamma_s}\right)^2 p_{\chi^2\dot{\chi}^2}\left(\frac{2^z-1}{\gamma_s},\frac{2^z\dot{z}\ln(2)}{\gamma_s}\right)$$
$$= \left(\frac{2^z\ln(2)}{\gamma_s}\right)^2 \frac{m\left(2^r-1/\gamma_s\right)^{\frac{m}{2}-1}}{4\sigma_0^2\rho^{m-1}\sqrt{2\pi\beta}} e^{-\frac{2^z-1+\gamma_s\rho^2}{2\sigma_0^2\gamma_s/m}} e^{-\frac{(2^z\dot{z}\ln(2))^2}{8\beta(2^z-1)\gamma_s}} I_{m-1}\left(\sqrt{\frac{(2^z-1)\rho^2}{\sigma_0^4\gamma_s/m^2}}\right) \quad (12)$$

for $z \geq 0$ and $|\dot{z}| < \infty$. By substituting (12) in (11), the resulting expression of the LCR $N_C(r)$ can be presented in closed form as

$$N_C(r) = \sqrt{\frac{\beta}{2\pi}} \frac{m\left(2^r-1/\gamma_s\right)^{m/2}}{\sigma_0^2\rho^{m-1}} e^{-\frac{2^r-1+\gamma_s\rho^2}{2\sigma_0^2\gamma_s/m}} I_{m-1}\left(\sqrt{\frac{(2^r-1)\rho^2}{\sigma_0^4\gamma_s/m^2}}\right), \ r \geq 0. \quad (13)$$

Finally, the ADF $T_C(r)$ of the channel capacity $C(t)$ can be obtained using

$$T_C(r) = \frac{F_C(r)}{N_C(r)} \quad (14)$$

where $F_C(r)$ and $N_C(r)$ are given by (10) and (13), respectively.

IV. Special Cases of the Rice-*m* Channel Model

In this section, we will discuss some of the special cases of the Rice-*m* channel model. We will present the conditions in which the statistical properties of the capacity of Rice-*m* channels are equal to that of the Nakagami-*m*, Rice, and Rayleigh channels. To the best of our knowledge the analytical expressions for the PDF, CDF, and LCR of the channel capacity of classical Rice and Nakagami-*m* channels are not published in the literature.

A. The Rice Channel

The Rice-*m* channel model reduces to the classical Rice channel model for the special case when $m = 1$. Hence, by setting m to 1 in (8), (10), and (13), the PDF, CDF, and LCR of the capacity of the Rice-*m* channel can be expressed as

$$p_C(r)|_{m=1} = \frac{2^r\ln(2)}{2\gamma_s\sigma_0^2} e^{-\frac{2^r-1+\gamma_s\rho^2}{2\sigma_0^2\gamma_s}} I_0\left(\sqrt{\frac{(2^r-1)\rho^2}{\sigma_0^4\gamma_s}}\right), \ r \geq 0 \quad (15)$$

$$F_C(r)|_{m=1} = 1 - Q_1\left(\frac{\rho}{\sigma_0},\sqrt{\frac{(2^r-1)}{\sigma_0^2\gamma_s}}\right), \ r \geq 0 \quad (16)$$

and

$$N_C(r)\,|_{m=1} = \sqrt{\frac{(2^r-1)\,\beta}{\pi 2\sigma_0^4\gamma_s}}\, e^{-\frac{2^r-1+\gamma_s\rho^2}{2\sigma_0^2\gamma_s}}\, I_0\left(\sqrt{\frac{(2^r-1)}{\sigma_0^4\gamma_s/\rho^2}}\right),\ r\geq 0 \tag{17}$$

respectively. The expressions presented in (15)–(17) correspond to the statistical properties of the capacity of Rice channels.

B. The Nakagami-m Channel

Let $\rho \to 0$, then the Rice-*m* channel reduces to the Nakagami-*m* channel. In this case, the PDF, CDF, and LCR of the capacity of the Rice-*m* channel can be written as

$$p_C(r)\,\big|_{\rho\to 0} = \frac{2^r \ln(2) m^m}{\gamma_s \Gamma(m)\Omega^m}\left(\frac{2^r-1}{\gamma_s}\right)^{m-1} e^{-\frac{m(2^r-1)}{\Omega\gamma_s}},\ r\geq 0 \tag{18}$$

$$F_C(r)\,\big|_{\rho\to 0} = 1 - \frac{\Gamma\left(m, \frac{m(2^r-1)}{\Omega\gamma_s}\right)}{\Gamma(m)},\ r\geq 0 \tag{19}$$

and

$$N_C(r)\,\big|_{\rho\to 0} = \frac{2\sqrt{\beta}\left(2^r-1/\gamma_s\right)^{m-\frac{1}{2}}}{\sqrt{2\pi}\,\Gamma(m)\left(\Omega/m\right)^m} e^{-\frac{m(2^r-1)}{\Omega\gamma_s}},\ r\geq 0 \tag{20}$$

respectively. Starting from the Nakagami-*m* channel, it can be proved that (18), (19), and (20) indeed correspond to the PDF, CDF, and LCR, respectively, of the channel capacity of Nakagami-*m* channels. Hence, the statistical properties of the capacity of Rice-*m* channels approach to that of Nakagami-*m* channels as $\rho \to 0$.

C. The Rayleigh Channel

The Rice-*m* channel equals the Rayleigh channel if $m = 1$ and $\rho \to 0$. Hence, the expressions for the PDF, CDF, and LCR of the capacity of Rayleigh channels can be obtained as a special case of the previously derived expressions in (8), (10), and (13), respectively, by setting $m = 1$ and $\rho \to 0$. The expressions for the PDF, CDF, and LCR of the capacity of Rayleigh channels can be found in [18, Eqs. (23–25)], respectively.

V. Numerical Results

In this section, we will discuss the analytical results obtained in the previous sections. The validity of the analytical results will be verified with the help of simulations. For comparison purposes, we have also shown the results of some special cases, such as Nakagami-*m* channels ($\rho \to 0$), Rice channels ($m = 1$), and Rayleigh channels ($\rho \to 0, m = 1$). In order to generate the Gaussian distributed waveforms $x_i(t)$ $(i = 1, 2, ..., 2m)$, we have employed the sum-of-sinusoids model [13]. The

model parameters were calculated using the generalized method of exact Doppler spread (GMEDS$_1$) [14]. The number of sinusoids for the generation of Gaussian distributed waveforms $x_i(t)$ was chosen to be $N_i = 29 + i$ for $i = 1, 2, ..., 2m$. The maximum Doppler frequency $f_{\max}$ was 91 Hz, the SNR γ_s was equal to 15 dB, and the parameter σ_0 was set to unity. Finally, using (1) and (7) the simulation results for the statistical properties of the channel capacity $C(t)$ of Rice-*m* channels $\chi(t)$ were obtained.

The PDF $p_\chi(x)$ of the Rice-*m* processes $\chi(t)$ is shown in Fig. B.1 for different values of the fading parameter *m* and the parameter ρ. It can be seen that for any value of *m*, increasing the value of ρ increases the spread of the PDF of Rice-*m* processes $\chi(t)$. However, for any value of ρ, an increase in the severity of fading (i.e., decreasing the value of the parameter *m*) increases the spread of the PDF. The PDF $p_C(r)$ of the capacity $C(t)$ of Rice-*m* channels $\chi(t)$ is presented in Fig. B.2. It is observed that for any value of ρ, a decrease in the severity of fading (i.e., increasing the value of the parameter *m*) results in an increase in the mean channel capacity for small values of *m*, say $m \leq 4$. However, for large values of *m*, the severity of fading has no influence on the mean channel capacity. Figure B.3 illustrates the same effect, where the mean channel capacity is plotted in terms of the fading parameter *m* for two different values of ρ. It is also clear from Fig. B.3 that Nakagami-*m* channels have a lower mean channel capacity as compared to Rice-*m* channels. Figure B.2 is also helpful for understanding the relationship between the spread of the channel capacity and the severity of fading for different values of the

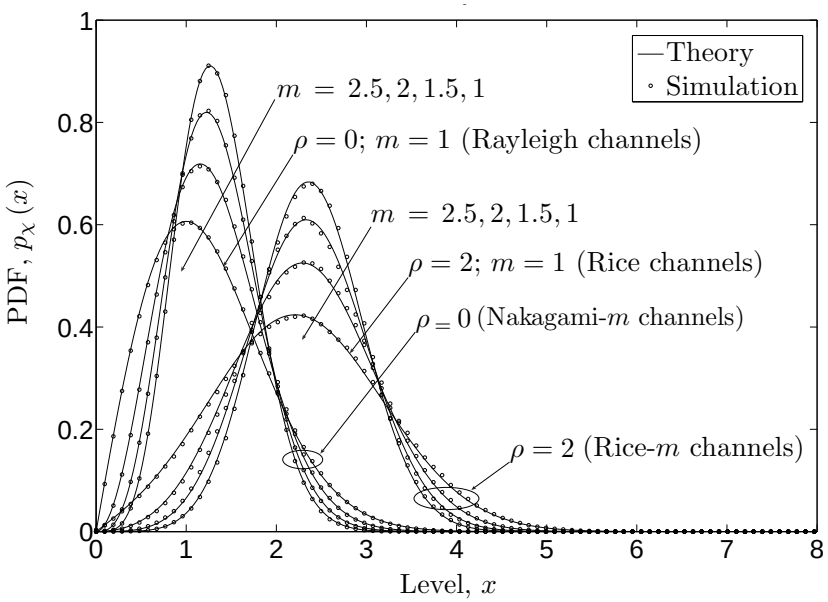

Figure B.1: The PDF $p_\chi(z)$ of Rice-*m* processes $\chi(t)$.

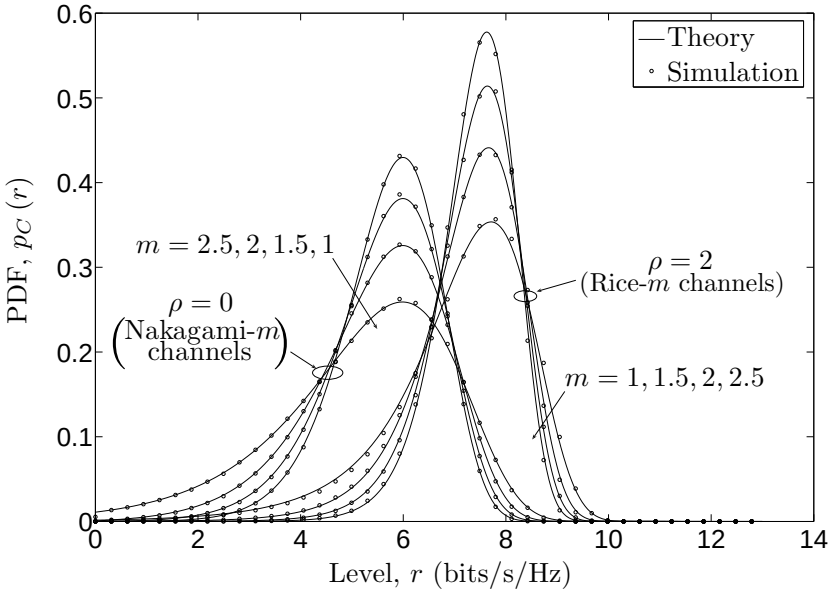

Figure B.2: The PDF $p_C(r)$ of the capacity of Rice-*m* channels.

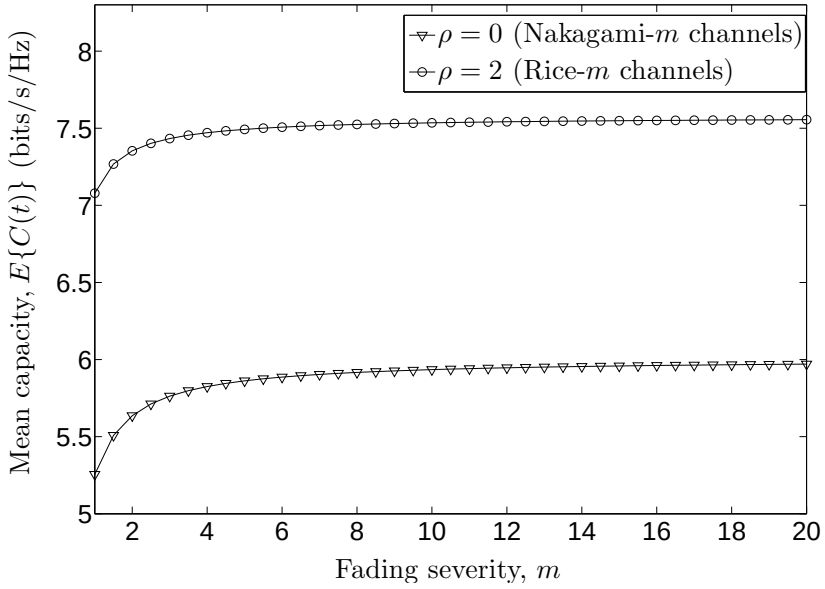

Figure B.3: The mean capacity E$\{C(t)\}$ of Rice-*m* channels.

parameter ρ. It can be noticed that increasing the value of *m* decreases the spread of the channel capacity. It is also observed that the capacity of Nakagami-*m* channels has a broader spread as compared to the Rice-*m* channels ($\rho = 2$). The LCR of the channel capacity is studied in Fig. B.4. It is observed that for any value of ρ, a decrease in the severity of fading decreases the LCR of the channel capacity. Moreover, at higher signal levels, we can observe that Rice-*m* channels have a higher LCR of the channel capacity as compared to that of Nakagami-*m* channels. Fur-

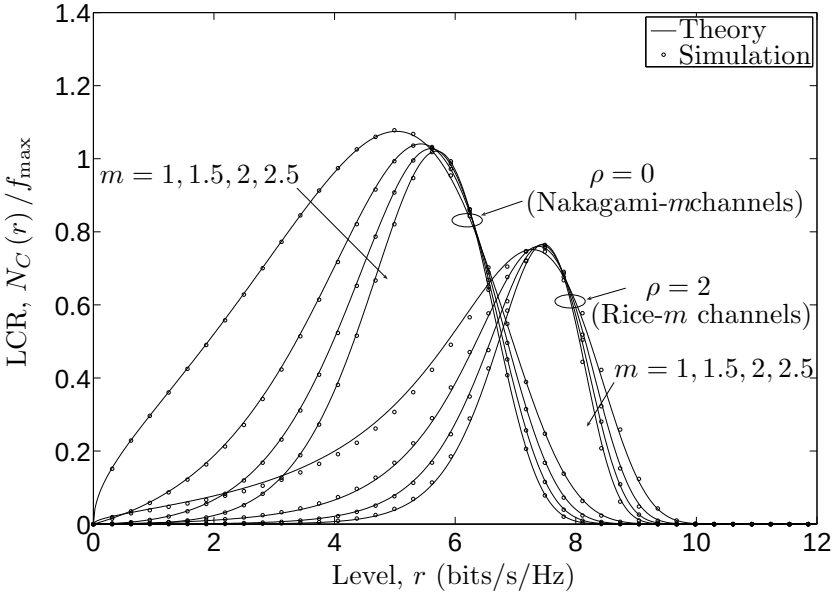

Figure B.4: The LCR $N_C(r)$ of the capacity of Rice-*m* channels.

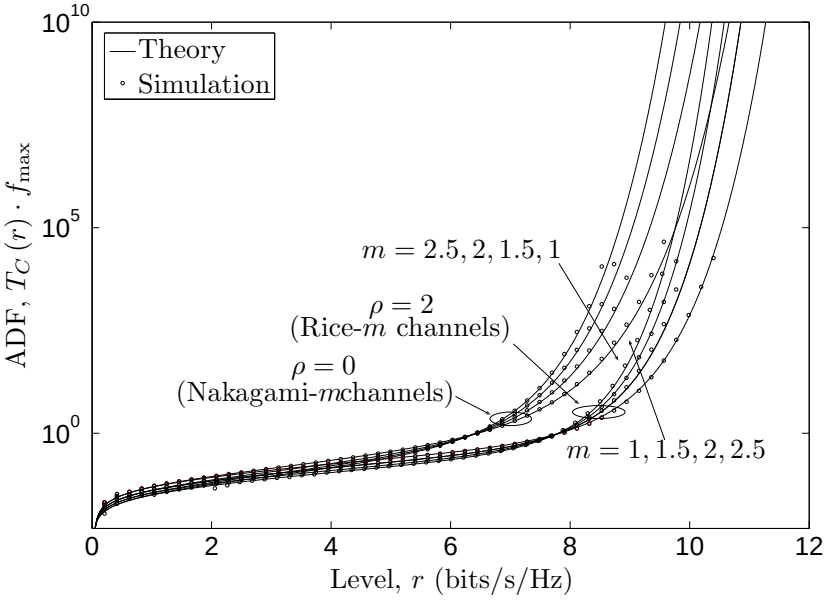

Figure B.5: The ADF $T_C(r)$ of the capacity of Rice-*m* channels.

thermore, the maximum value of the LCR of the capacity of Nakagami-*m* channels is higher as compared to that of Rice-*m* channels.

Finally, the ADF of the channel capacity is shown in Fig. B.5. It can be seen that for any value of ρ, the channels with high values of m have a higher ADF of the channel capacity and vice versa. It is also observed that for medium and higher signal levels r, channels with low values of ρ have a higher ADF of the channel capacity. However, at low signal levels, the value of the parameter ρ does not have

a significant influence on the ADF of the channel capacity. Similar observations have been made for the ADF of Rice and Rayleigh channels in [13, p. 45].

VI. Conclusion

In this article, we have proposed a general channel model referred to as the Rice-*m* channel model. The proposed channel model assumes that the underlying Gaussian processes in the Nakagami-*m* channel model have non-zero mean values. The received signal envelope in the Rice-*m* channel model is obtained as the square root of a sum of 2*m* squared non-zero mean i.i.d. Gaussian processes. The generality of the channel model comes from the fact that it contains Rice, Rayleigh, and Nakagami-*m* channels as special cases. We have derived exact analytical closed-form expressions for the statistical properties of the envelope and the channel capacity of Rice-*m* channels. Our study shows that the mean value of the underlying Gaussian processes and the severity of fading have a significant influence on the statistical properties of the channel capacity. Specifically, we have observed that increasing the mean values of the underlying Gaussian processes (or decreasing the severity of fading) increases the mean channel capacity. While, the spread of the channel capacity decreases. Moreover at higher signal levels, the LCR of the channel capacity of Nakagami-*m* channels is lower as compared to that of Rice-*m* channels. The ADF of the channel capacity of Nakagami-*m* channels on the other hand, is higher for medium and high signal levels as compared to that of Rice-*m* channels. However, the mean values of the underlying Gaussian processes have no influence on the ADF of the channel capacity at low signal levels. The correctness of the theoretical results is confirmed by simulations.

References

[1] M. Abramowitz and I. A. Stegun. *Handbook of Mathematical Functions with Formulas, Graphs, and Mathematical Tables*. Washington: National Bureau of Standards, 1984.

[2] N. C. Beaulieu and X. Dong. Level crossing rate and average fade duration of MRC and EGC diversity in Ricean fading. 51(5):722–726, May 2003.

[3] S. H. Choi, P. J. Smith, B. Allen, W. Q. Malik, and M. Shafi. Severely fading MIMO channels: Models and mutual information. In *Proc. IEEE International Conference on Communications, ICC 2007*, pages 4628–4633. Glasgow, UK, June 2007.

[4] S. Elnoubi, S. A. Chahine, and H. Abdallah. BER performance of GMSK in Nakagami fading channels. In *Proc. 21st National Radio Science Conference, NRSC 2004*, pages C13–1–8, March 2004.

[5] G. J. Foschini and M. J. Gans. On limits of wireless communications in a fading environment when using multiple antennas. *Wireless Pers. Commun.*, 6:311–335, March 1998.

[6] A. Giorgetti, P. J. Smith, M. Shafi, and M. Chiani. MIMO capacity, level crossing rates and fades: The impact of spatial/temporal channel correlation. *J. Commun. Net.*, 5(2):104–115, June 2003.

[7] I. S. Gradshteyn and I. M. Ryzhik. *Table of Integrals, Series, and Products*. New York: Academic Press, 6th edition, 2000.

[8] B. O. Hogstad and M. Pätzold. Exact closed-form expressions for the distribution, level-crossing rate, and average duration of fades of the capacity of MIMO channels. In *Proc. 65th Semiannual Vehicular Technology Conference, IEEE VTC 2007-Spring*, pages 455–460. Dublin, Ireland, April 2007.

[9] W. C. Jakes, editor. *Microwave Mobile Communications*. Piscataway, NJ: IEEE Press, 1994.

[10] M. Kang and S. M. Alouini. Capacity of MIMO Rician channels. *IEEE Trans. Wireless Commun.*, 5(1):112–122, January 2006.

[11] G. Lebrun, M. Faulkner, M. Shafi, and P. J. Smith. MIMO Ricean channel capacity. In *Proc. IEEE Int. Conf. Commun., ICC 2004*, volume 5, pages 2939–2943, June 2004.

[12] A. Papoulis and S. U. Pillai. *Probability, Random Variables and Stochastic Processes*. New York: McGraw-Hill, 4th edition, 2002.

[13] M. Pätzold. *Mobile Fading Channels*. Chichester: John Wiley & Sons, 2002.

[14] M. Pätzold, C. X. Wang, and B. O. Hogstad. Two new sum-of-sinusoids-based methods for the efficient generation of multiple uncorrelated Rayleigh fading waveforms. *IEEE Trans. Wireless Commun.*, 8(6):3122–3131, June 2009.

[15] J. Proakis. *Digital Communications*. New York: McGraw-Hill, 4th edition, 2001.

[16] G. Rafiq, V. Kontorovich, and M. Pätzold. On the statistical properties of the capacity of the spatially correlated Nakagami-*m* MIMO channels. In *Proc. IEEE 67th Vehicular Technology Conference, IEEE VTC 2008-Spring*, pages 500–506. Marina Bay, Singapore, May 2008.

[17] G. Rafiq and M. Pätzold. The influence of the severity of fading and shadowing on the statistical properties of the capacity of Nakagami-lognormal channels. In *Proc. IEEE Global Telecommunications Conference IEEE GLOBECOM 2008*, pages 1–6, November 2008. DOI 10.1109/GLOCOM.2008.ECP.824.

[18] G. Rafiq and M. Pätzold. A study of the influence of shadowing on the statistical properties of the capacity of mobile radio channels. *Wireless Personal Communications (WPC)*, 50(1):5–18, July 2009.

[19] G. Rafiq, M. Pätzold, and V. Kontorovich. The influence of spatial correlation and severity of fading on the statistical properties of the capacity of OSTBC Nakagami-*m* MIMO channels. In *Proc. IEEE 69th Vehicular Technology Conference, IEEE VTC 2009-Spring*, pages 1–5. Barcelona, Spain, April 2009.

[20] S. O. Rice. Mathematical analysis of random noise. *Bell Syst. Tech. J.*, 24:46–156, January 1945.

[21] M. K. Simon. *Probability Distributions Involving Gaussian Random Variables: A Handbook for Engineers and Scientists*. Dordrecht: Kluwer Academic Publishers, 2002.

[22] I. E. Telatar. Capacity of multi-antenna Gaussian channels. *European Trans. Telecommun. Related Technol.*, 10(6):585–595, November/December 1999.

[23] M. D. Yacoub, J. E. V. Bautista, and L. G. de Rezende Guedes. On higher order statistics of the Nakagami-*m* distribution. *IEEE Trans. Veh. Technol.*, 48(3):790–794, May 1999.

Appendix C

Paper III

Title:	A Study of the Influence of Shadowing on the Statistical Properties of the Capacity of Mobile Radio Channels
Authors:	**Gulzaib Rafiq** and Matthias Pätzold
Affiliation:	University of Agder, Faculty of Engineering and Science, P. O. Box 509, NO-4898 Grimstad, Norway.
Journal:	*Wireless Personal Communications, Special Issue on "Wireless Future"*, vol. 50, no. 1, Jul. 2009, pp. 5 – 18.

A Study of the Influence of Shadowing on the Statistical Properties of the Capacity of Mobile Radio Channels

Gulzaib Rafiq and Matthias Pätzold
Department of Information and Communication Technology
Faculty of Engineering and Science, University of Agder
Servicebox 509, NO-4898 Grimstad, Norway
E-mails: {gulzaib.rafiq, matthias.paetzold}@uia.no

***Abstract* — This paper[1] studies the influence of shadowing on the statistical properties of the channel capacity. The problem is addressed by using a Suzuki process as an appropriate statistical channel model for land mobile terrestrial channels. Using this model, exact solutions for the probability density function (PDF), cumulative distribution function (CDF), level-crossing rate (LCR), and average duration of fades (ADF) of the channel capacity are derived. The results are studied for different levels of shadowing, corresponding to different terrestrial environments. It is observed that the shadowing effect has a significant influence on the variance and the maximum value of the PDF and LCR of the channel capacity, but it has almost no impact on the mean capacity of the channel. The correctness of the theoretical results is confirmed by simulation using a stochastic channel simulator based on the sum-of-sinusoids principle.**

Keywords—Land mobile terrestrial channels, channel capacity, shadowing effects, lognormal process, Suzuki process, level-crossing rate, average duration of fades.

I. Introduction

The channel capacity can be considered as a measure of how much information can be transmitted over a channel with a negligible probability of error [8]. The precise knowledge of the statistical properties of the channel capacity is indispensable for the development of future mobile communication systems. While studying the

[1]The material in this paper is based on "The Impact of Shadowing on the Capacity of Mobile Fading Channels", by Gulzaib Rafiq and Matthias Pätzold which appeared in the proceedings of 4th IEEE International Symposium on Wireless Communication Systems, ISWCS 2007, Trondheim, Norway, October 2007.

capacity of mobile fading channels, the dynamic behavior of the channel is generally ignored. However, for the development of future optimized heterogeneous multiuser communication networks, it is important to know how fast the channel capacity changes with time. Therefore, studies pertaining to unveil the dynamics of the channel capacity can be very helpful to achieve higher data rates while keeping the probability of error as low as possible. In mobile communication systems, the LCR and ADF of the channel capacity are important characteristic quantities which provide insight into the dynamic behavior of the channel capacity [7], [4]. The LCR of the channel capacity describes the average number of up-crossings (or down-crossings) of the capacity through a fixed level within a time interval of one second. Analogously, the ADF of the channel capacity is the expected value of the length of the time intervals in which the capacity is below a given level [7, 4, 6].

The random amplitude fluctuations of the received signal can be modeled using an appropriate stochastic process. It has widely been accepted that for urban and suburban areas, where the line-of-sight (LOS) signal component is blocked by obstacles, the Rayleigh process is a suitable stochastic process to model the channel [21, 11, 12]. In rural regions, however, the LOS component is often a part of the received signal, so that the Rice process is an appropriate choice for modeling such channels. The validity of Rayleigh and Rice channel models is limited to small areas having dimensions in the order of a few tens of wavelengths. The local mean of the received signal envelope remains approximately constant in these areas [10]. The local mean, however, fluctuates in large areas due to shadowing effects. It has widely been reported in the literature that shadowing can adequately be modeled by a lognormal process [5, 1, 18, 9]. Therefore, for the case of land mobile terrestrial channels, a Suzuki process is considered to be a more suitable statistical channel model [15]. The Suzuki process is generated by taking the product of a Rayleigh and a lognormal process [20]. The analysis of the PDF, CDF, LCR, and ADF of the channel capacity of fast fading channels, like Rayleigh channels can be found, e.g., in [7, 4, 6], [19], [3]. However, there is a lack of information regarding the combined effects of shadowing and fast fading on the channel capacity. The purpose of this paper is to close this gap by using a Suzuki process as an appropriate channel model.

The paper studies the influence of shadowing on the channel capacity. In particular, we have derived analytical expressions for the PDF, CDF, LCR, and ADF of the capacity of Suzuki channels. Previous studies show that the shadow standard deviation can have a wide range of values depending on the terrestrial environment [5]. Therefore, it is important to study the statistical properties of the channel capac-

ity for different values of the shadow standard deviation. Our analysis has revealed that the variance and the maximum value of the PDF and LCR of the channel capacity, respectively, are highly influenced by the shadow standard deviation. However, this parameter has nearly no effect on the mean channel capacity.

The rest of the paper is organized as follows. In Section 2, we review briefly the Suzuki process. The statistical properties of the channel capacity for this model are analyzed in Section 3. Section 4 introduces some special cases of the presented channel model. The simulation model used to verify the theoretical results is introduced in Section 5. In Section 6, the theoretical and simulation results are discussed. Finally, the conclusions are given in Section 7.

II. The Suzuki Channel Model

In this section, we will describe the Suzuki process $\eta(t)$, which is considered as a proper statistical channel model for our problem. The Suzuki process is defined by [20]

$$\eta(t) = \zeta(t) \cdot \lambda(t) \tag{1}$$

where $\zeta(t)$ represents a Rayleigh process and $\lambda(t)$ denotes a lognormal process.

The Rayleigh process $\zeta(t)$ can be described as

$$\zeta(t) = |\mu(t)| \tag{2}$$

where $\mu(t)$ is a complex Gaussian process, i.e.,

$$\mu(t) = \mu_1(t) + j\mu_2(t). \tag{3}$$

In (3), $\mu_1(t)$ and $\mu_2(t)$ are uncorrelated zero-mean real-valued Gaussian processes with identical variances σ_0^2. Under the assumption of isotropic scattering, the autocorrelation function (ACF) $r_{\mu\mu}(\tau)$ of the complex Gaussian process $\mu(t)$ is given by [14]

$$r_{\mu\mu}(\tau) = r_{\mu_1\mu_1}(\tau) + r_{\mu_2\mu_2}(\tau) \tag{4}$$

where

$$r_{\mu_i\mu_i}(\tau) = \sigma_0^2 J_0(2\pi f_{\max}\tau), \;\; i = 1, 2. \tag{5}$$

In (5), $J_0(\cdot)$ denotes the 0th-order Bessel function of the first kind, $r_{\mu_i\mu_i}(\tau)$ is the ACF of the process $\mu_i(t)$, and $f_{\max}$ represents the maximum Doppler frequency.

The lognormal process $\lambda(t)$ in (1) can be expressed as

$$\lambda(t) = 10^{[\sigma_L v_3(t) + m_L]/20} \tag{6}$$

where $\nu_3(t)$ is a zero-mean real-valued Gaussian process with unit variance. The third Gaussian process $\nu_3(t)$ is statistically independent of the other two Gaussian processes $\mu_1(t)$ and $\mu_2(t)$. The parameters σ_L and m_L are called the shadow standard deviation and the area mean, respectively. It has been observed that the shadow standard deviation depends on the terrestrial environment [5]. Specifically, it has been shown in [5] that $\sigma_L = 4.3$ dB can be chosen as a suitable value for urban environments, whereas $\sigma_L = 7.5$ dB is an appropriate value for suburban areas. The PDF $p_\lambda(z)$ of the lognormal process $\lambda(t)$ is given by

$$p_\lambda(z) = \frac{20}{\sqrt{2\pi}\ln(10)\sigma_L z} e^{-\frac{(20\log(z)-m_L)^2}{2\sigma_L^2}}, \quad z \geq 0. \tag{7}$$

For the spectral shape of the process $\nu_3(t)$ in (6), we have assumed a Gaussian power spectral density (PSD) given by [15], [17]

$$S_{\nu_3\nu_3}(f) = \frac{1}{\sqrt{2\pi}\sigma_c} e^{-\frac{f^2}{2\sigma_c^2}} \tag{8}$$

where σ_c is related to the 3 dB cutoff frequency f_c by $f_c = \sigma_c\sqrt{2\ln(2)}$. It is assumed that f_c is much smaller than $f_{\max}$, i.e., $\kappa_c = f_{\max}/f_c \gg 1$. The inverse Fourier transform of $S_{\nu_3\nu_3}(f)$ in (8) results in the ACF $r_{\nu_3\nu_3}(\tau)$ of the process $\nu_3(t)$ as

$$r_{\nu_3\nu_3}(\tau) = e^{-2(\pi\sigma_c\tau)^2}. \tag{9}$$

The time derivative of the Suzuki process $\eta(t)$ is represented by $\dot{\eta}(t)$.[2] In order to analyze the statistical properties of the Suzuki channel capacity (see Section 3), it is necessary to find the joint PDF $p_{\eta^2\dot{\eta}^2}(z,\dot{z})$ of $\eta^2(t)$ and $\dot{\eta}^2(t)$. This problem can be solved by first finding the joint PDF $p_{\eta\dot{\eta}}(z,\dot{z})$ of $\eta(t)$ and $\dot{\eta}(t)$ at the same time t. Thereafter, using the obtained expression for $p_{\eta\dot{\eta}}(z,\dot{z})$, the joint PDF $p_{\eta^2\dot{\eta}^2}(z,\dot{z})$ can be found by applying the concept of transformation of random variables [13]. After some algebraic manipulations on the results found in [15], the PDF $p_\eta(z)$ of $\eta(t)$ can be written as

$$p_\eta(z) = \frac{20\cdot z}{\ln(10)\sqrt{2\pi}\sigma_0^2\sigma_L} \int_0^\infty \frac{1}{y^3}\cdot e^{-\left(\frac{z}{\sqrt{2}\sigma_0 y}\right)^2} e^{-\left(\frac{20\log(y)-m_L}{\sqrt{2}\sigma_L}\right)^2} dy, \; z \geq 0. \tag{10}$$

[2] Throughout this paper, we will represent the time derivative of a process by an overdot.

Similarly, the joint PDF $p_{\eta\dot{\eta}}(z,\dot{z})$ can be expressed as [15]

$$p_{\eta\dot{\eta}}(z,\dot{z}) = \frac{20\cdot z}{2\pi\ln(10)\sqrt{\beta}\sigma_0^2\sigma_L}\int_0^\infty \frac{e^{-\left(\frac{z}{\sqrt{2}\sigma_0 y}\right)^2} e^{-\left(\frac{20\log(y)-m_L}{\sqrt{2}\sigma_L}\right)^2}}{y^4 K(z,y)} e^{-\left(\frac{\dot{z}}{\sqrt{2\beta}yK(z,y)}\right)^2} dy, \quad z\geq 0, |\dot{z}|<\infty \tag{11a}$$

where

$$K(z,y) = \sqrt{1+\frac{\gamma}{\beta}\left(\frac{z\sigma_L\ln(10)}{20y}\right)^2} \tag{11b}$$

and

$$\beta = -\ddot{r}_{\mu_i\mu_i}(0) = 2\left(\pi f_{\max}\sigma_0\right)^2,\ i=1,2 \tag{11c}$$

$$\gamma = -\ddot{r}_{\nu_3\nu_3}(0) = (2\pi\sigma_c)^2. \tag{11d}$$

Here, β represents the negative curvature of the ACF $r_{\mu_i\mu_i}(\tau)$ of $\mu_i(t)$ at the origin [14], i.e.,

$$\beta = -\frac{d^2}{d\tau^2} r_{\mu_i\mu_i}(\tau)\Big|_{\tau=0} = -\ddot{r}_{\mu_i\mu_i}(0),\ i=1,2. \tag{12}$$

In accordance with (12), the parameter γ is defined.

In order to find the joint PDF $p_{\eta^2\dot{\eta}^2}(z,\dot{z})$, the concept of transform-ation of random variables [13] is applied. Hence, by using the relationship $p_{\eta^2\dot{\eta}^2}(z,\dot{z}) = (1/4z)\times p_{\eta\dot{\eta}}(\sqrt{z},\dot{z}/2\sqrt{z})$, we can write by using (11a)

$$p_{\eta^2\dot{\eta}^2}(z,\dot{z}) = \frac{5/\sqrt{\beta z}}{2\pi\ln(10)\sigma_0^2\sigma_L}\int_0^\infty \frac{e^{-\left(\frac{\sqrt{z}}{\sqrt{2}\sigma_0 y}\right)^2} e^{-\left(\frac{20\log(y)-m_L}{\sqrt{2}\sigma_L}\right)^2}}{y^4 K(\sqrt{z},y)} e^{-\left(\frac{\dot{z}}{\sqrt{8\beta z}yK(\sqrt{z},y)}\right)^2} dy \quad z\geq 0, |\dot{z}|<\infty. \tag{13}$$

The expression for $p_{\eta^2\dot{\eta}^2}(z,\dot{z})$ in (13) will be used in the next section for the calculation of the LCR of the channel capacity. From (13), it can be observed that $\eta^2(t)$ and $\dot{\eta}^2(t)$ are not statistically independent processes, since their joint PDF cannot be written as a product of the marginal PDFs $p_{\eta^2}(z)$ and $p_{\dot{\eta}^2}(\dot{z})$. By using (13) in $p_{\eta^2}(z) = \int_{-\infty}^{\infty} p_{\eta^2\dot{\eta}^2}(z,\dot{z})d\dot{z}$, the PDF $p_{\eta^2}(z)$ of $\eta^2(t)$ can be written as

$$p_{\eta^2}(z) = \frac{10}{\sqrt{2\pi}\ln(10)\sigma_0^2\sigma_L}\int_0^\infty \frac{e^{-\left(\frac{\sqrt{z}}{\sqrt{2}\sigma_0 y}\right)^2} e^{-\left(\frac{20\log(y)-m_L}{\sqrt{2}\sigma_L}\right)^2}}{y^3} dy,\ z\geq 0. \tag{14}$$

The formula presented above will be used in the next section to calculate the PDF of the channel capacity.

III. Statistical Properties of the Capacity of Suzuki Channels

In this section, we will first introduce the capacity of the channel described by Suzuki processes. Thereafter, the expressions for the statistical properties of the channel capacity will be derived using the results obtained in the previous section.

The expression for the channel capacity $C(t)$ of an additive white Gaussian noise (AWGN) channel can be written using the Shannon capacity formula [2] as

$$C(t) = \log_2\left(1+\gamma_s\left|H(t)\right|^2\right) \quad \text{(bits/sec/Hz)} \tag{15}$$

where the quantity γ_s is the signal-to-noise ratio (SNR). In (15), $H(t)$ represents the random complex channel gain described using any suitable stochastic channel model. In this article, we have represented the random channel $H(t)$ by a Suzuki process $\eta(t)$. From the fact that the Suzuki process $\eta(t)$ is a real-valued random process, the instantaneous capacity of the Suzuki channel in (15) can be expressed as

$$C(t) = \log_2\left(1+\gamma_s\eta^2(t)\right). \tag{16}$$

The expression presented in (16) can be considered as a mapping of the random process $\eta(t)$ to another random process $C(t)$. Therefore, by applying the concept of transformation of random variables [13], the PDF $p_{C,\eta}(r)$ of the channel capacity $C(t)$ can be written by substituting (14) in the expression $p_{C,\eta}(r) = (2^r\ln(2)/\gamma_s)\times p_{\eta^2}\left(2^r-1/\gamma_s\right)$ as

$$p_{C,\eta}(r) = \frac{2^r\ln(2)10}{\sqrt{2\pi}\ln(10)\gamma_s\sigma_0^2\sigma_L}\int_0^\infty \frac{e^{-\left(\frac{\sqrt{2^r-1}}{\sqrt{2\gamma_s}\sigma_0 y}\right)^2} e^{-\left(\frac{20\log(y)-m_L}{\sqrt{2}\sigma_L}\right)^2}}{y^3}dy,\ r\geq 0. \tag{17}$$

The CDF $F_{C,\eta}(r)$ of the channel capacity $C(t)$ can now be expressed by using $F_{C,\eta}(r) = \int_0^r p_{C,\eta}(x)dx$ as

$$F_{C,\eta}(r) = \frac{20}{\sqrt{2\pi}\ln(10)\sigma_L}\int_0^\infty \frac{1}{y}\cdot e^{-\left(\frac{20\log(y)-m_L}{\sqrt{2}\,\sigma_L}\right)^2}\left[1-e^{-\left(\frac{\sqrt{2^r-1}}{\sqrt{2\gamma_s}\sigma_0 y}\right)^2}\right]dy,\ r\geq 0. \tag{18}$$

The LCR $N_{C,\eta}(r)$ of the channel capacity $C(t)$ is defined as [7]

$$N_{C,\eta}(r) = \int_0^\infty \dot{z} p_{C\dot{C},\eta}(r,\dot{z}) d\dot{z}, \;\; r \geq 0. \tag{19}$$

Thus, in order to find the LCR $N_{C,\eta}(r)$, the joint PDF $p_{C\dot{C},\eta}(z,\dot{z})$ of $C(t)$ and $\dot{C}(t)$ is required. Applying the concept of transformation of random variables [13], $p_{C\dot{C},\eta}(z,\dot{z})$ can be expressed after substituting (13) in $p_{C\dot{C},\eta}(z,\dot{z}) = (2^z \ln(2)/\gamma_s)^2 \times p_{\eta^2\dot{\eta}^2}(2^z - 1/\gamma_s, 2^z \dot{z} \ln(2)/\gamma_s)$ as

$$\begin{aligned} p_{C\dot{C},\eta}(z,\dot{z}) &= \frac{5 \times (2^z \ln(2))^2}{2\pi\sqrt{2^z-1}\ln(10)\gamma_s^{\frac{3}{2}}\sqrt{\beta}\sigma_0^2\sigma_L} \int_0^\infty \frac{e^{-\left(\frac{\sqrt{2^z-1}}{\sqrt{2\gamma_s}\sigma_0 y}\right)^2}}{y^4 K\left(\sqrt{\frac{2^z-1}{\gamma_s}}, y\right)} e^{-\left(\frac{20\log(y)-m_L}{\sqrt{2}\sigma_L}\right)^2} \\ &\quad \times e^{-\left(\frac{\dot{z}(2^z\ln(2))}{y\sqrt{8\beta\gamma_s(2^z-1)}K\left(\sqrt{\frac{2^z-1}{\gamma_s}}, y\right)}\right)^2} dy, \;\; z \geq 0, |\dot{z}| < \infty \end{aligned} \tag{20}$$

where $K(\cdot,\cdot)$ is the function introduced in (11b).

After substituting (20) in (19) and carrying out some algebraic calculations, we obtain

$$\begin{aligned} N_{C,\eta}(r) &= \frac{20\sqrt{\beta(2^r-1)}}{2\pi\ln(10)\sqrt{\gamma_s}\sigma_0^2\sigma_L} \int_0^\infty \frac{e^{-\left(\frac{\sqrt{2^r-1}}{\sqrt{2\gamma_s}\sigma_0 y}\right)^2} e^{-\left(\frac{20\log(y)-m_L}{\sqrt{2}\sigma_L}\right)^2}}{y^2} K\left(\sqrt{\frac{2^r-1}{\gamma_s}}, y\right) dy, \\ &\quad r \geq 0. \end{aligned} \tag{21}$$

Due to the quantity β, appearing in the numerator of (21), it is observed that the LCR $N_{C,\eta}(r)$ of the channel capacity $C(t)$ is proportional to the maximum Doppler frequency $f_{\max}$. This can be seen by replacing β in (21) by the expression presented in (11c). Thus, by normalizing $N_{C,\eta}(r)$ on $f_{\max}$, the influence of the mobile speed on the LCR can be removed.

Finally, from (18) and (21), the ADF $T_{C,\eta}(r)$ of the channel capacity $C(t)$ can be obtained using [7]

$$T_{C,\eta}(r) = \frac{F_{C,\eta}(r)}{N_{C,\eta}(r)}. \tag{22}$$

IV. Special Cases of the Suzuki Channel Model

In this section, we will derive the statistical properties of the channel capacity of Rayleigh and lognormal processes. It will be shown that the corresponding statistical quantities like the PDF, CDF, LCR, and ADF of the channel capacity can be obtained as special cases of the respective results derived for Suzuki processes in

the previous section. The detailed discussion on the relationships between the statistical properties of channel capacity of Suzuki, Rayleigh, and lognormal processes can be found in Section 6.

A. The Channel Capacity of Rayleigh Processes

Let $\sigma_L \to 0$ and $m_L = 1$ (unit area mean), then the PDF, CDF, and LCR of the channel capacity of Suzuki channels can be written as

$$p_{C,\eta}(r)\Big|_{\substack{\sigma_L\to 0\\ m_L=1}} = \frac{2^r \ln(2)}{2\gamma_s\sigma_0^2} e^{-\left(\frac{2^r-1}{2\gamma_s\sigma_0^2}\right)},\ r \geq 0 \tag{23}$$

$$F_{C,\eta}(r)\Big|_{\substack{\sigma_L\to 0\\ m_L=1}} = 1 - e^{-\left(\frac{2^r-1}{2\gamma_s\sigma_0^2}\right)},\ r \geq 0 \tag{24}$$

and

$$N_{C,\eta}(r)\Big|_{\substack{\sigma_L\to 0\\ m_L=1}} = \frac{1}{\sigma_0^2}\sqrt{\frac{\beta\,(2^r-1)}{2\pi\gamma_s}} e^{-\left(\frac{2^r-1}{2\gamma_s\sigma_0^2}\right)},\ r \geq 0 \tag{25}$$

respectively. It can be observed that the expressions presented above correspond to those known for the channel capacity of Rayleigh channels [7]. Hence, the Rayleigh process is a special case of the Suzuki process when $\sigma_L \to 0$ and $m_L = 1$.

B. The Channel Capacity of Lognormal Processes

In order to derive the expressions for the statistical properties of the capacity of lognormal channels, a similar procedure can be applied as developed here for Suzuki channels. By using the result for the joint PDF $p_{\lambda\dot{\lambda}}(z,\dot{z})$ of $\lambda(t)$ and $\dot{\lambda}(t)$ in [15] and following similar steps from (13) to (21), the expressions for the PDF, CDF, and LCR of the capacity of lognormal channels can be expressed as

$$p_{C,\lambda}(r) = \frac{2^r \ln(2)10}{\sqrt{2\pi}\ln(10)\,(2^r-1)\,\sigma_L} e^{-\left(\frac{20\log\left(\sqrt{\frac{2^r-1}{\gamma_s}}\right)-m_L}{\sqrt{2}\sigma_L}\right)^2},\ r \geq 0 \tag{26}$$

$$F_{C,\lambda}(r) = \frac{\ln(2)10}{\sqrt{2\pi}\ln(10)\sigma_L}\int_0^r \frac{2^x}{(2^x-1)}\cdot e^{-\left(\frac{20\log\left(\sqrt{\frac{2^x-1}{\gamma_s}}\right)-m_L}{\sqrt{2}\sigma_L}\right)^2} dx,\ r \geq 0 \tag{27}$$

and

$$N_{C,\lambda}(r) = \frac{\sqrt{\gamma}}{2\pi} e^{-\left(\frac{20\log\left(\sqrt{\frac{2^r-1}{\gamma_s}}\right)-m_L}{\sqrt{2}\sigma_L}\right)^2},\ r \geq 0 \tag{28}$$

respectively. Furthermore, the ADF of the capacity of lognormal channels can be found using (22), (27), and (28). Alternatively, one can show that the expressions (26)–(28) can be obtained by setting $\sigma_0^2 = 0$ in (17)–(21).

V. The Simulation Model

In this section, the analytical results derived in the previous section will be verified by simulation. We have employed a stochastic channel simulator based on the sum-of-sinusoids principle [14]. The resulting structure of the simulation model for the analysis of the capacity of Suzuki channels is shown in Fig. C.1. Here, the hat $(\hat{})$ symbolizes the fact that the underlying stochastic processes are modeled by

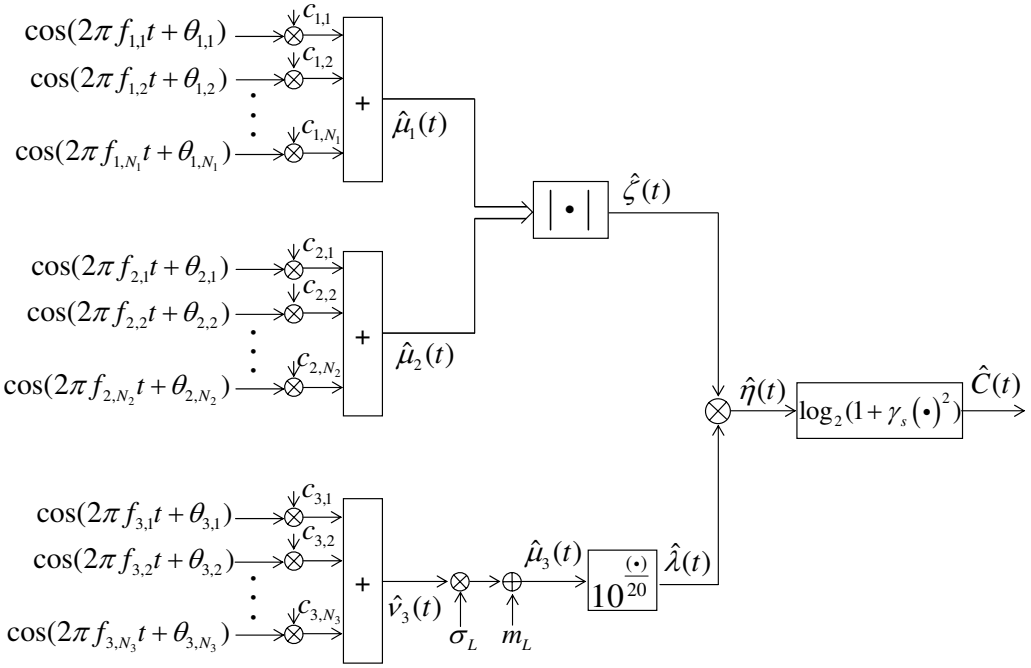

Figure C.1: The stochastic simulation model for the capacity analysis of Suzuki channels.

applying the sum-of-sinusoids method with constant gains $c_{i,n}$, constant frequencies $f_{i,n}$, and random phases $\theta_{i,n}$, respectively. The phases $\theta_{i,n}$ are independent and identically distributed (i.i.d.) random variables, each having a uniform distribution over the interval $(0, 2\pi]$. For the stochastic processes $\hat{\mu}_1(t)$ and $\hat{\mu}_2(t)$ in Fig. C.1, the parameters $f_{i,n}$ and $c_{i,n}$ are calculated using the generalized method of exact Doppler spread (GMEDS$_1$) [16]. Whereas, for the stochastic process $\hat{v}_3(t)$, these parameters are calculated by applying the modified method of equal areas (MMEA) [17]. In Fig. C.1, the mapping of the Suzuki process $\hat{\eta}(t)$ to the capacity $\hat{C}(t)$ is

also shown. Finally, by using this model, all simulation results presented in the next section are obtained by averaging over 15 sample functions of the capacity $\hat{C}(t)$.

VI. Numerical Results

In this section, we will discuss the analytical and simulation results for the statistical properties of the channel capacity. In order to illustrate the influence of the shadowing effect on the statistics of the channel capacity, we have taken into account different values of σ_L, ranging from 1 dB to 10 dB. We have also included some special cases, e.g., Rayleigh fading ($\sigma_L \to 0$ dB) and lognormal fading ($\sigma_0^2 = 0$), in our study for comparison purposes. Moreover, the results obtained for $\sigma_L = 4.3$ dB (urban environment [5]) and $\sigma_L = 7.5$ dB (suburban environment [5]) are also shown. For the simulation model presented in Fig. C.1, we have used $N_1 = 30$, $N_2 = 31$, and $N_3 = 32$. The maximum Doppler frequency $f_{\max}$ was chosen to be 91 Hz. The value for the parameter κ_c was taken as 5 and the value for σ_0^2 and area mean m_L was set to unity. Unless otherwise stated, the value of the SNR γ_s was set to 25 dB.

Firstly, the PDFs of the lognormal and Suzuki processes are shown in Figs. C.2 and C.3, respectively. These figures demonstrate that the shadow standard deviation σ_L has a dominant effect on the spread and the peak value of the PDFs of these processes. The PDF and CDF of the capacity of the Suzuki process are presented in Figs. C.4 and C.5, respectively. Results for the special cases, i.e., for $\sigma_L \to 0$ dB and $\sigma_0^2 = 0$, are also shown in these figures. From these results it can be observed that, as the value of σ_L approaches 0 dB, the statistics of the capacity of the Suzuki

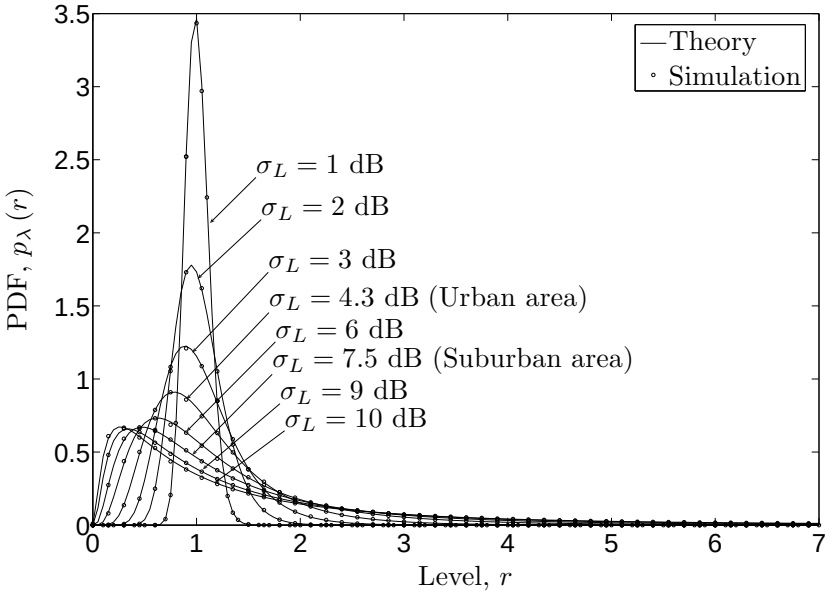

Figure C.2: The PDF of lognormal processes.

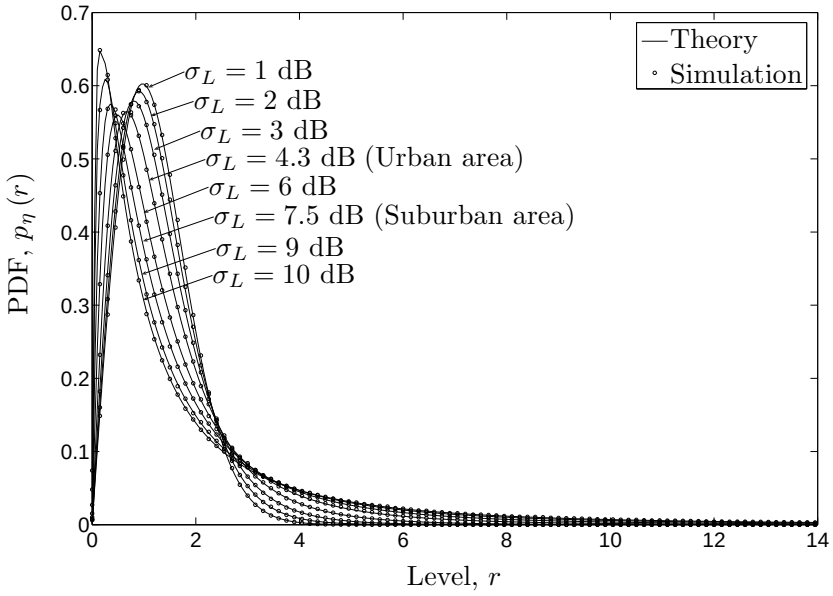

Figure C.3: The PDF of Suzuki processes.

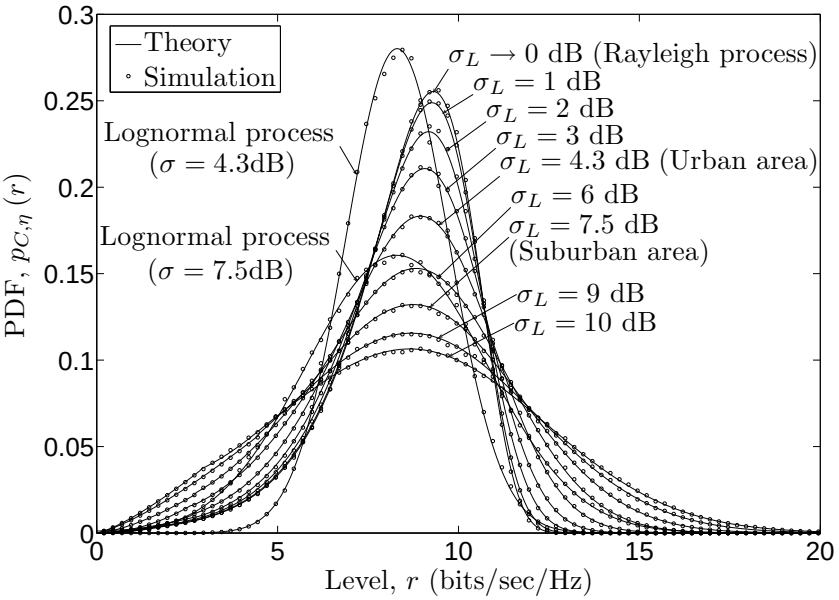

Figure C.4: The PDF of the capacity of Suzuki and lognormal channels.

process approaches the statistics of the capacity of the Rayleigh process.

The mean capacity $E[C(t)]$ of the Suzuki process is shown in Fig. C.6 for different values of the SNR γ_s. From Figs. C.4 and C.6, it can easily be seen that the shadow standard deviation σ_L has nearly no influence on the mean capacity of the Suzuki process. The variance of the channel capacity is presented in Fig. C.7. It is quite evident that an increase in the shadow standard deviation σ_L increases the variance of the channel capacity. This observation is in accordance with the results

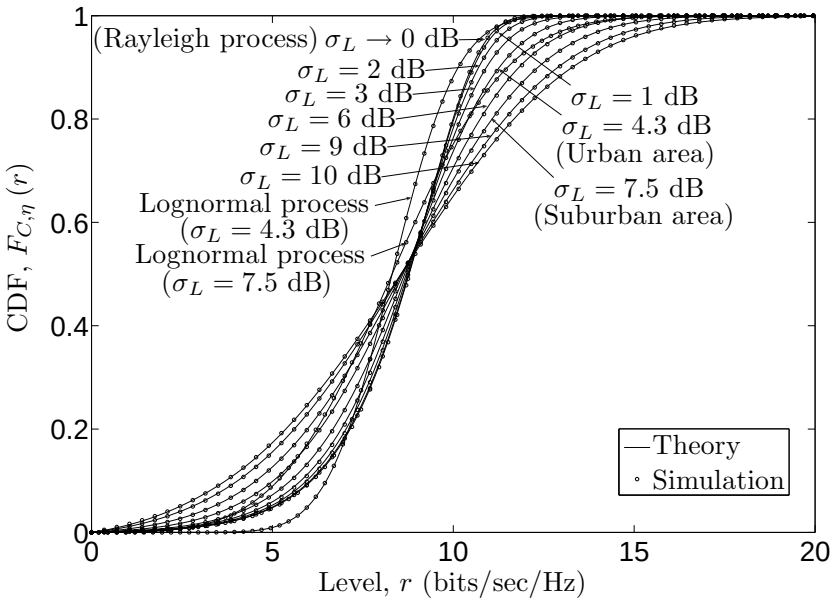

Figure C.5: The CDF of the capacity of Suzuki and lognormal channels.

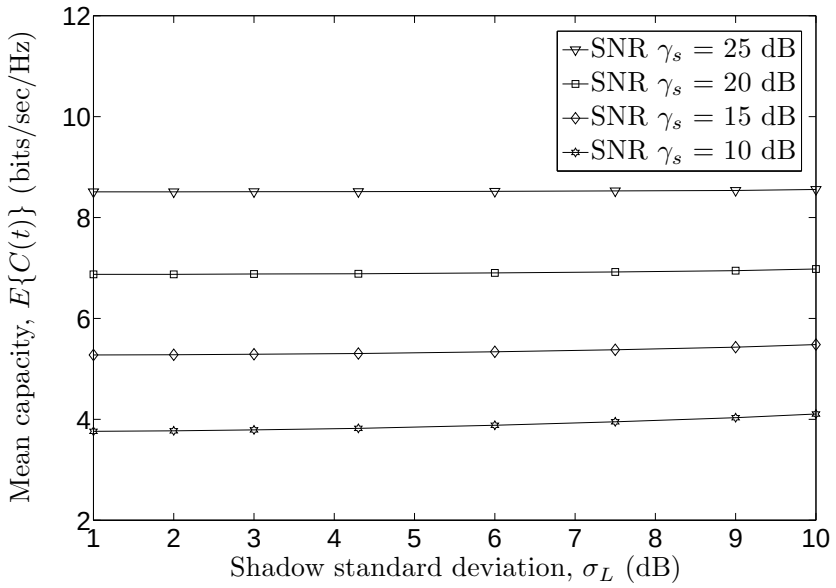

Figure C.6: The mean capacity of Suzuki channels.

presented in Fig. C.4. Similarly, the same effect can be observed by increasing the value of the SNR γ_s. In Figs. C.8 and C.9, the normalized LCR and ADF of the channel capacity are shown, respectively. It can be observed that the Rayleigh and lognormal processes set an upper and a lower bound, respectively, on the LCR of the capacity of the Suzuki process. For low and medium signal levels r, the LCR of the capacity of the lognormal process is lower than the LCR of the capacity of the Suzuki and Rayleigh processes. However, for high signal levels r, the LCR of

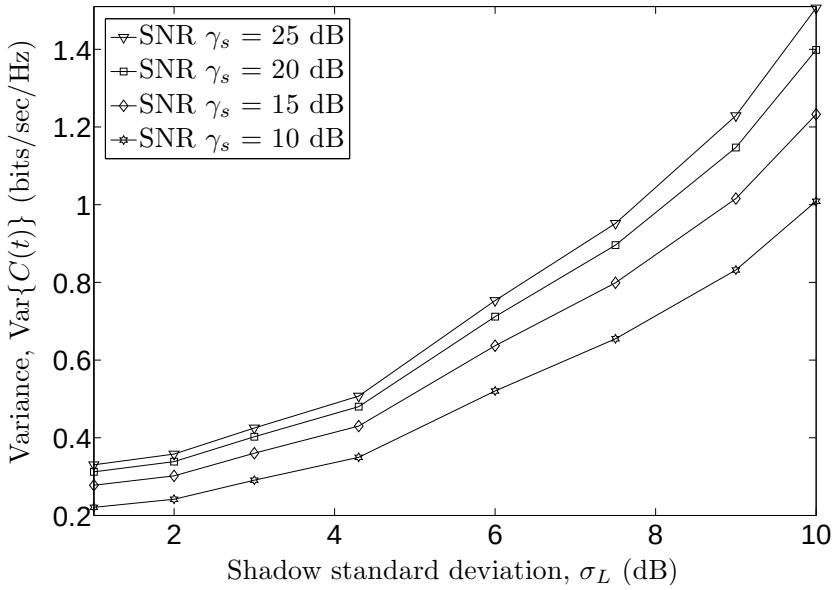

Figure C.7: The variance of the capacity of Suzuki channels.

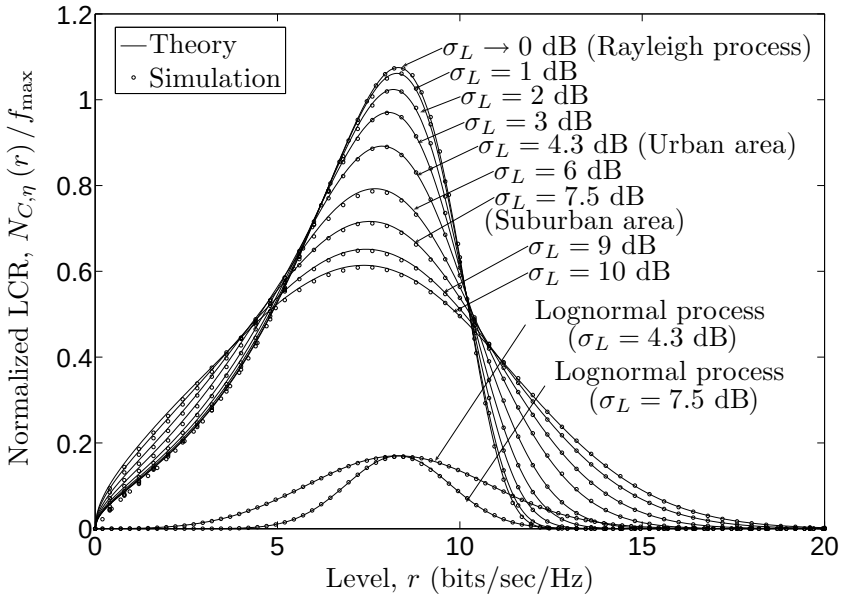

Figure C.8: The normalized LCR of the capacity of Suzuki and lognormal channels.

the capacity of the lognormal process is higher than that of the Suzuki and Rayleigh processes. Analogously, the converse statement is true for the ADF of the channel capacity. It is also observed from Figs. C.4 and C.8 that increasing the value of the shadow standard deviation σ_L results in an increase of the spread of the PDF and LCR of the channel capacity, where the peak value of these quantities decreases. From the results presented in Figs. C.4–C.9, we gain an insight into how the statistics of the Suzuki channel capacity approaches those of the Rayleigh and lognormal

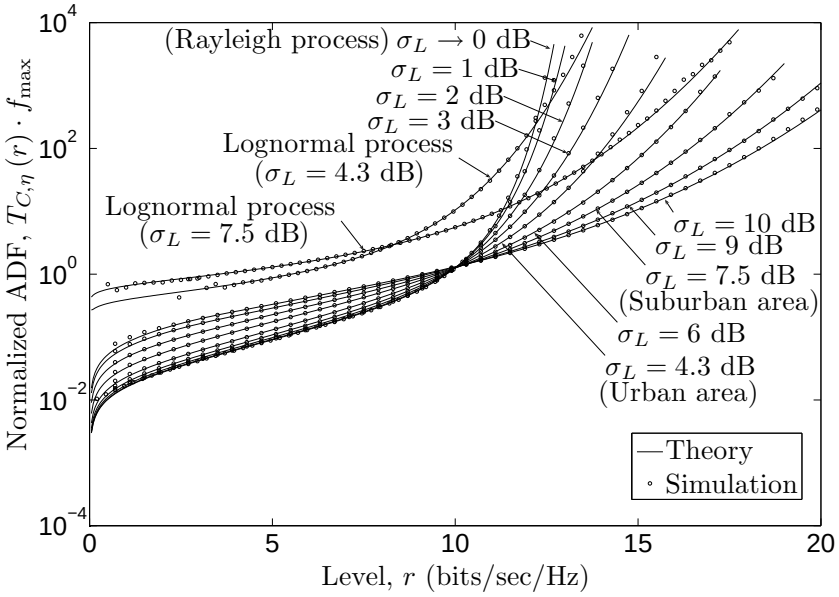

Figure C.9: The normalized ADF of the capacity of Suzuki and lognormal channels.

channels.

VII. Conclusion

In all results presented here, the simulation results are found to be in a very good correspondence with the analytical results. In this paper, we have studied the statistical properties of the capacity of Suzuki channels. We have derived exact analytical expressions for the PDF, CDF, LCR, and ADF of the channel capacity. Moreover, the influence of shadowing on the statistics of the channel capacity has been investigated. It has been observed that the variance and the maximum value of the PDF and LCR of the channel capacity, respectively, are highly influenced by the shadow standard deviation. It has been shown that as the value of shadow standard deviation increases the variance of the channel capacity increases. However, this parameter has only a minor effect on the mean channel capacity. It has also been observed that as the shadow standard deviation approaches 0 dB, the statistics of the channel capacity of Suzuki channels approaches to that of Rayleigh channels. Findings of this paper are helpful for analyzing the dynamic behavior of the channel capacity for land mobile terrestrial channels in different terrestrial environments. The theoretical results obtained have been verified by simulations, where the simulation results match the theoretical expectations very closely.

REFERENCES

[1] D. M. Black and D. O. Reudink. Some characteristics of mobile radio propagation at 836 MHz in the Philadelphia area. *IEEE Trans. Veh. Technol.*, 21:45–51, February 1972.

[2] G. J. Foschini and M. J. Gans. On limits of wireless communications in a fading environment when using multiple antennas. *Wireless Pers. Commun.*, 6:311–335, March 1998.

[3] H. Ge, K. D. Wong, M. Barton, and J. C. Liberti. Statistical characterization of multiple-input multiple-output (MIMO) channel capacity. In *Proc. IEEE Wireless Communications and Networking Conference, WCNC 2002*, volume 2, pages 789–793, March 2002.

[4] A. Giorgetti, P. J. Smith, M. Shafi, and M. Chiani. MIMO capacity, level crossing rates and fades: The impact of spatial/temporal channel correlation. *J. Commun. Net.*, 5(2):104–115, June 2003.

[5] M. Gudmundson. Correlation model for shadow fading in mobile radio systems. *Electron. Lett.*, 27(23):2145–2146, November 1991.

[6] B. O. Hogstad and M. Pätzold. Capacity studies of MIMO models based on the geometrical one-ring scattering model. In *Proc. 15th IEEE Int. Symp. on Personal, Indoor and Mobile Radio Communications, PIMRC 2004*, volume 3, pages 1613–1617. Barcelona, Spain, September 2004.

[7] B. O. Hogstad and M. Pätzold. Exact closed-form expressions for the distribution, level-crossing rate, and average duration of fades of the capacity of MIMO channels. In *Proc. 65th Semiannual Vehicular Technology Conference, IEEE VTC 2007-Spring*, pages 455–460. Dublin, Ireland, April 2007.

[8] B. Holter. On the capacity of the MIMO channel — a tutorial introduction. In *Proc. IEEE Norwegian Symposium on Signal Processing*, pages 167–172. Trondheim, Norway, October 2001.

[9] M. F. Ibrahim and J. D. Parsons. Signal strength prediction in built-up areas. *Proc. IEE*, 130F(5):377–384, August 1983.

[10] W. C. Jakes, editor. *Microwave Mobile Communications*. Piscataway, NJ: IEEE Press, 1994.

[11] H. W. Nylund. Characteristics of small-area signal fading on mobile circuits in the 150 MHz band. *IEEE Trans. Veh. Technol.*, 17:24–30, October 1968.

[12] Y. Okumura, E. Ohmori, T. Kawano, and K. Fukuda. Field strength and its variability in VHF and UHF land mobile radio services. *Rev. Elec. Commun. Lab.*, 16:825–873, September/October 1968.

[13] A. Papoulis and S. U. Pillai. *Probability, Random Variables and Stochastic Processes*. New York: McGraw-Hill, 4th edition, 2002.

[14] M. Pätzold. *Mobile Fading Channels*. Chichester: John Wiley & Sons, 2002.

[15] M. Pätzold, U. Killat, and F. Laue. An extended Suzuki model for land mobile satellite channels and its statistical properties. *IEEE Trans. Veh. Technol.*, 47(2):617–630, May 1998.

[16] M. Pätzold, C. X. Wang, and B. O. Hogstad. Two new sum-of-sinusoids-based methods for the efficient generation of multiple uncorrelated Rayleigh fading waveforms. *IEEE Trans. Wireless Commun.*, 8(6):3122–3131, June 2009.

[17] M. Pätzold and K. Yang. An exact solution for the level-crossing rate of shadow fading processes modelled by using the sum-of-sinusoids principle. In *Proc. 9th International Symposium on Wireless Personal Multimedia Communications, WPMC 2006*, pages 188–193. San Diego, USA, September 2006.

[18] D. O. Reudink. Comparison of radio transmission at X-band frequencies in suburban and urban areas. *IEEE Trans. Ant. Prop.*, 20:470–473, July 1972.

[19] P. J. Smith, L. M. Garth, and S. Loyka. Exact capacity distributions for MIMO systems with small numbers of antennas. *IEEE Commun. Letter*, 7(10):481–483, October 2003.

[20] H. Suzuki. A statistical model for urban radio propagation. *IEEE Trans. Commun.*, 25(7):673–680, July 1977.

[21] W. R. Young. Comparison of mobile radio transmission at 150, 450, 900, and 3700 MHz. 31:1068–1085, November 1952.

Appendix D

Paper IV

Title:	The Influence of the Severity of Fading and Shadowing on the Statistical Properties of the Capacity of Nakagami-Lognormal Channels
Authors:	**Gulzaib Rafiq** and Matthias Pätzold
Affiliation:	University of Agder, Faculty of Engineering and Science, P. O. Box 509, NO-4898 Grimstad, Norway
Conference:	*IEEE Global Communications Conference, GLOBECOM 2008*, New Orleans, LA, USA, Nov. /Dec. 2008, pp. 1 – 6.

The Influence of the Severity of Fading and Shadowing on the Statistical Properties of the Capacity of Nakagami-Lognormal Channels

Gulzaib Rafiq and Matthias Pätzold
Department of Information and Communication Technology
Faculty of Engineering and Science, University of Agder
Servicebox 509, NO-4898 Grimstad, Norway
E-mails: {gulzaib.rafiq, matthias.paetzold}@uia.no

***Abstract* — This paper deals with the study of the statistical properties of the capacity of Nakagami-lognormal (NLN) channels for various fading environments. Specifically, the impact of shadowing and the severity of fading on the channel capacity is investigated. We have derived analytical expressions for the probability density function (PDF), cumulative distribution function (CDF), level-crossing rate (LCR), and average duration of fades (ADF) of the channel capacity. These results are analyzed for different levels of shadowing and for various fading conditions, corresponding to different terrestrial environments. It is observed that the severity of fading and shadowing has a significant influence on the spread and the maximum value of the PDF and LCR of the channel capacity. Moreover, it is also observed that if the fading gets less severe as compared to the Rayleigh fading, the mean channel capacity increases. However, the shadowing effect has no impact on the mean channel capacity. The validity of all analytical results is confirmed by simulations.**

I. Introduction

Even after decades of research, the researchers of future mobile communication systems are still aiming to provide solutions to attain the maximum possible information transfer rate in communication links. Keeping the probability of error negligible, the maximum attainable information transfer rate over a channel is referred to as the channel capacity [9]. Due to the time-varying nature of mobile communication channels, the channel capacity is a random process. Thus, to cope with the high data rate requirements of new mobile communication systems, the analysis of the dynamic behavior of the channel capacity is inevitable. The statistical characterization of the channel capacity can be done with the help of the mean, variance, PDF, and CDF of the channel capacity [10]. However, these statistics do

not provide any insight into the temporal behavior of the channel capacity. In order to get the information pertaining to the fading behavior of the channel capacity, the LCR and the ADF of the channel capacity can be studied [8, 4]. The LCR of the channel capacity is a quantity that describes the average number of times the random capacity crosses a certain threshold level from up to down (or vice versa) per second. Whereas the ADF is defined as the expected value of the time period over which the channel capacity is below a certain threshold level [8, 7].

For land mobile terrestrial channels, the Suzuki process is considered to be a more appropriate channel model as the Rayleigh or Rice process [14]. A Suzuki process can be expressed as a product of a Rayleigh process and a lognormal process. Therefore, modeling the channel by a Suzuki process enables us to study the combined effects of shadowing and fast fading on the channel capacity. It is however, very common to find scenarios where the fading is more (or less) severe as Rayleigh fading. For such cases, it is more appropriate to use a Nakagami-m process instead of the Rayleigh process to model fast fading [11, 2, 19, 1]. The Nakagami-m process is considered to be a more general channel model since it contains the Rayleigh and Gaussian process as special cases (i.e., for $m = 1$ and $m = 0.5$, respectively). Moreover, the Nakagami-m process can be used for cases when the fading is less severe as Rayleigh fading (e.g., for $m > 1$) [19]. Therefore, by employing a Nakagami-m process instead of the Rayleigh process in a Suzuki process, we obtain a more general channel model referred to as the NLN channel model [18, 17], which contains the Suzuki process as a special case when $m = 1$. Hence, by using the NLN process as a channel model, the impact of shadowing on the channel capacity can be studied under different fading conditions. Moreover, the effects of severity of fading on the channel capacity can also be studied.

This paper is aimed at analyzing the statistical properties of the channel capacity for various levels of shadowing under different fading conditions. We have employed the NLN channel model, which allows us to pose more fading conditions on the channel capacity as compared to the amount of fading that can be achieved by using the classical Suzuki channel model. We have derived analytical expressions for the PDF, CDF, LCR, and ADF of the capacity of NLN channels. All these results are investigated for different levels of shadowing. Our results show that the severity of fading and the shadowing effect dominantly influence the spread and the maximum value of the PDF and LCR. It is also observed that, as the severity of fading increases, the mean channel capacity decreases, while the shadowing effect has no influence on the mean channel capacity.

The rest of the paper is organized as follows. In Section II, we present the NLN process and some of its statistical properties. The statistical properties of the capacity of the NLN channels are studied in Section III. Numerical results are discussed in Section IV. Finally, the concluding remarks are given in Section V.

II. The NLN Channel Model

In this section, we will review the NLN process, which is a product process of a Nakagami-*m* and a lognormal process [18, 17]. This process, in contradiction to the classical Suzuki process, represents a more general model, where the fading can be more (or less) severe as Rayleigh fading. The NLN process $\chi(t)$ is defined as [18, 17]

$$\chi(t) = X(t) \cdot \lambda(t) \tag{1}$$

where $X(t)$ denotes a Nakagami-*m* process and $\lambda(t)$ represents a lognormal process.

The PDF $p_X(z)$ of the Nakagami-*m* process $X(t)$ is given by

$$p_X(z) = \frac{2m^m z^{2m-1}}{\Gamma(m)\Omega^m} e^{-\frac{mz^2}{\Omega}}, \ z \geq 0 \tag{2}$$

where $\Omega = E\left\{z^2\right\}$, $m = \Omega^2 \big/ \mathrm{Var}\left\{z^2\right\}$, and $\Gamma(\cdot)$ represents the gamma function [5]. The normalized autocorrelation function (ACF) of the squared Nakagami-*m* process $X^2(t)$ under isotropic scattering conditions is given by [18]

$$\psi(\tau) = 1 + J_0^2(2\pi f_{\max}\tau) \tag{3}$$

where $J_0(\cdot)$ is the Bessel function of the first kind of order zero [5] and $f_{\max}$ denotes the maximum Doppler frequency. The joint PDF of the Nakagami-*m* process $X(t)$ and its time derivative $\dot{X}(t)$[1] is given by [20]

$$p_{X\dot{X}}(z,\dot{z}) = p_X(z) \cdot \sqrt{\frac{m}{\Omega\pi\beta_N}} e^{-\frac{m\dot{z}}{\Omega\beta_N}} \tag{4}$$

where β_N is given by [18]

$$\beta_N = -\frac{1}{2}\frac{d^2}{d\tau^2}\psi(\tau)\bigg|_{\tau=0} = 2(\pi f_{\max})^2. \tag{5}$$

In order to generate the lognormal process $\lambda(t)$ in (1), we have used the following expression

$$\lambda(t) = 10^{[\sigma_L v(t) + m_L]/20} \tag{6}$$

[1] Throughout this paper, we will represent the time derivative of a process by an overdot.

where σ_L represents the shadow standard deviation, m_L denotes the area mean, and $v(t)$ is a zero-mean real-valued Gaussian process with unit variance. The PDF $p_\lambda(z)$ of the lognormal process $\lambda(t)$ can be written as

$$p_\lambda(z) = \frac{20}{z\sigma_L\sqrt{2\pi}\ln(10)} e^{-\frac{(20\log(z)-m_L)^2}{2\sigma_L^2}}, \; z \geq 0. \tag{7}$$

In the literature, different models have been proposed for the spectral shape of the Gaussian process $v(t)$ in (6). In this article, we have assumed a Gaussian power spectral density (PSD) for the Gaussian process $v(t)$ given by [14], [16]

$$S_{vv}(f) = \frac{1}{\sqrt{2\pi}\sigma_c} e^{-\frac{f^2}{2\sigma_c^2}} \tag{8}$$

where the parameter σ_c controls the spread of the PSD $S_{vv}(f)$ and can be expressed in terms of the 3 dB cutoff frequency f_c as $\sigma_c = f_c/\sqrt{2\ln(2)}$. We have assumed that the value of f_c is much smaller than $f_{\max}$, i.e., $f_{\max}/f_c \gg 1$. By taking the inverse Fourier transform of $S_{vv}(f)$, the ACF $r_{vv}(\tau)$ of the process $v(t)$ can be expressed as

$$r_{vv}(\tau) = e^{-2(\pi\sigma_c\tau)^2}. \tag{9}$$

The PDF $p_\chi(z)$ of the NLN process $\chi(t)$ is given by [17]

$$p_\chi(z) = \frac{40 \cdot m^m z^{2m-1}}{\sigma_L\sqrt{2\pi}\ln(10)\Gamma(m)\Omega^m} \int_0^\infty \frac{1}{y^{2m+1}} \cdot e^{-\frac{mz^2}{\Omega y^2}} e^{-\left(\frac{20\log(y)-m_L}{\sqrt{2}\sigma_L}\right)^2} dy, \; z \geq 0. \tag{10}$$

In order to derive the expressions for the statistical properties of the NLN channel capacity, we require the expressions for the joint PDF $p_{\chi^2\dot{\chi}^2}(z,\dot{z})$ of $\chi^2(t)$ and $\dot{\chi}^2(t)$ and the PDF $p_{\chi^2}(z)$ of $\chi^2(t)$. The joint PDF $p_{\chi^2\dot{\chi}^2}(z,\dot{z})$ can be obtained from the joint PDF $p_{\chi\dot{\chi}}(z,\dot{z})$, presented in [11, Eq. (6)], and by applying the concept of transformation of random variables [12] as

$$\begin{aligned} p_{\chi^2\dot{\chi}^2}(z,\dot{z}) &= \frac{1}{4z} p_{\chi\dot{\chi}}(\sqrt{z},\dot{z}/2\sqrt{z}) \\ &= \frac{5 \cdot z^{m-3/2} m^m}{\pi\sigma_L\sqrt{\beta_N}\ln(10)\Gamma(m)\Omega^m} \int_0^\infty \frac{e^{-\frac{mz}{\Omega y^2}}}{y^{2m+2} K(\sqrt{z},y)} e^{-\left(\frac{20\log(y)-m_L}{\sqrt{2}\sigma_L}\right)^2} \\ &\qquad \times e^{-\left(\frac{\dot{z}}{\sqrt{8\beta_N zy}K(\sqrt{z},y)}\right)^2} dy, \; z \geq 0, \; |\dot{z}| < \infty \end{aligned} \tag{11}$$

where

$$\gamma = -\frac{d^2}{d\tau^2} r_{vv}(\tau)\bigg|_{\tau=0} = (2\pi\sigma_c)^2 \tag{12a}$$

and

$$K(z,y) = \sqrt{1+\frac{\gamma}{\beta_N}\left(\frac{z\sigma_L \ln(10)}{20y}\right)^2}. \tag{12b}$$

From (11) it can clearly be seen that the joint PDF $p_{\chi^2\dot{\chi}^2}(z,\dot{z})$ cannot be written as a product of the marginal PDFs $p_{\chi^2}(z)$ and $p_{\dot{\chi}^2}(\dot{z})$. Hence, the processes $\chi^2(t)$ and $\dot{\chi}^2(t)$ are not statistically independent processes. Now, the PDF $p_{\chi^2}(z)$ of $\chi^2(t)$ can be found as follows

$$\begin{aligned} p_{\chi^2}(z) &= \int_{-\infty}^{\infty} p_{\chi^2\dot{\chi}^2}(z,\dot{z})d\dot{z} \\ &= \frac{20\cdot z^{m-1}m^m}{\sqrt{2\pi}\ln(10)\Gamma(m)\Omega^m\sigma_L}\int_0^{\infty}\frac{e^{-\frac{mz}{\Omega y^2}}}{y^{2m+1}}e^{-\left(\frac{20\log(y)-m_L}{\sqrt{2}\sigma_L}\right)^2}dy,\ z\geq 0. \end{aligned} \tag{13}$$

The expressions presented in (11) and (13) will be used in the next section to calculate the PDF and LCR of the channel capacity.

III. Statistical Properties of the Capacity of NLN Channels

The instantaneous channel capacity $C(t)$ of the NLN channel $\chi(t)$ can be expressed as [3]

$$C(t) = \log_2\left(1+\gamma_s\chi^2(t)\right)\ \text{(bits/sec/Hz)}. \tag{14}$$

where γ_s denotes the signal-to-noise ratio (SNR). The above expression (14) represents the mapping of a random process $\chi(t)$ to another random process $C(t)$. Hence, using the concept of transformation of random variables [12], the PDF $p_C(r)$ of the channel capacity $C(t)$ can be found as

$$\begin{aligned} p_C(r) &= \frac{2^r\ln(2)}{\gamma_s}p_{\chi^2}\left(\frac{2^r-1}{\gamma_s}\right) \\ &= \frac{20\cdot 2^r(2^r-1)^{m-1}m^m\ln(2)}{\sigma_L\sqrt{2\pi}\ln(10)\Gamma(m)\gamma_s^m\Omega^m}\int_0^{\infty}\frac{e^{-\frac{m\cdot 2^r-1}{\Omega\gamma_s y^2}}}{y^{2m+1}}e^{-\left(\frac{20\log(y)-m_L}{\sqrt{2}\sigma_L}\right)^2}dy,\ r\geq 0. \end{aligned} \tag{15}$$

The CDF $F_C(r)$ of the channel capacity $C(t)$ can be derived using (15) as follows

$$F_C(r) = \int_0^r p_C(x)dx$$

$$= \frac{20/\ln(10)}{\sigma_L\sqrt{2\pi}\Gamma(m)} \int_0^\infty \frac{e^{-\left(\frac{20\log(y)-m_L}{\sqrt{2}\sigma_L}\right)^2}}{y} \left[\Gamma(m) - \Gamma\left(m, \frac{m\cdot 2^r-1}{\Omega\gamma_s y^2}\right)\right] dy, \;\; r \geq 0. \quad (16)$$

The LCR $N_C(r)$ of the channel capacity $C(t)$ is defined as [8]

$$N_C(r) = \int_0^\infty \dot{z} p_{C\dot{C}}(r,\dot{z}) d\dot{z}, \;\; r \geq 0. \quad (17)$$

The joint PDF $p_{C\dot{C}}(z,\dot{z})$ of $C(t)$ and $\dot{C}(t)$ in (17) can be obtained using (11) and by applying the concept of transformation of random variables [12], as follows

$$\begin{aligned} p_{C\dot{C}}(z,\dot{z}) &= \left(\frac{2^z\ln(2)}{\gamma_s}\right)^2 p_{\chi^2\dot{\chi}^2}\left(\frac{2^z-1}{\gamma_s}, \frac{2^z\dot{z}\ln(2)}{\gamma_s}\right) \\ &= \frac{5\left(2^z\ln(2)\right)^2 m^m \left(2^z-1\right)^{m-3/2}}{\pi\sigma_L\sqrt{\beta_N}\ln(10)\Gamma(m)\Omega^m\gamma_s^{m+1/2}} \int_0^\infty \frac{e^{-\frac{m\cdot 2^r-1}{\Omega\gamma_s y^2}}}{y^{2m+2}K\left(\sqrt{\frac{2^z-1}{\gamma_s}}, y\right)} e^{-\left(\frac{20\log(y)-m_L}{\sqrt{2}\sigma_L}\right)^2} \\ &\quad \times e^{-\left(\frac{\dot{z}(2^z\ln(2))}{\sqrt{8\beta_N\gamma_s(2^z-1)}yK\left(\sqrt{\frac{2^z-1}{\gamma_s}}, y\right)}\right)^2} dy, \;\; z \geq 0, |\dot{z}| < \infty \end{aligned} \quad (18)$$

where $K(\cdot,\cdot)$ is defined in (12b). After substituting (18) in (17), the resulting simplified expression of the LCR $N_C(r)$ of the channel capacity $C(t)$ can be written as

$$N_C(r) = \frac{5\sqrt{\beta_N} m^m \left(2^z-1\right)^{m-1/2}}{\pi\sigma_L\ln(10)\Gamma(m)\gamma_s^{m-1/2}\Omega^m} \int_0^\infty \frac{e^{-\frac{m\cdot 2^r-1}{\Omega\gamma_s y^2}}}{y^{2m}} e^{-\left(\frac{20\log(y)-m_L}{\sqrt{2}\sigma_L}\right)^2} K\left(\sqrt{\frac{2^r-1}{\gamma_s}}, y\right) dy, \quad (19)$$

for $r \geq 0$. Replacing β_N in (19) by (5), it can be observed that the LCR $N_C(r)$ of the channel capacity $C(t)$ is proportional to $f_{\max}$. However, the effect of the mobile speed on the LCR can be removed by normalizing $N_C(r)$ by $f_{\max}$.

Finally, the ADF $T_C(r)$ of the channel capacity $C(t)$ can be obtained as follows [8]

$$T_C(r) = \frac{F_C(r)}{N_C(r)} \quad (20)$$

where $F_C(r)$ and $N_C(r)$ are given by (16) and (19), respectively.

IV. Numerical Results

In this section, we will present the analytical and the simulation results for the statistical properties of the capacity of NLN channels. In order to investigate the impact

of shadowing on the capacity of NLN channels, we have studied the results obtained in the previous section for different values of the shadow standard deviation σ_L, ranging from 1 dB to 10 dB. Specifically, the results for $\sigma_L = 4.3$ dB (urban environment [6]) and $\sigma_L = 7.5$ dB (suburban environment [6]) are also shown. Moreover for comparison purposes, we have also included some special cases, such as the Nakagami-m channels ($\sigma_L \to 0$ dB) and the lognormal channels ($\Omega = 0$). Furthermore, the statistical behavior of the channel capacity is investigated under different fading conditions by using different values for the parameter m in the Nakagami-m distribution.

In order to generate different Nakagami-m fading waveforms $X(t)$, we have applied the following model [19]

$$X(t) = \sqrt{\sum_{i=1}^{2\times m} r_i^2(t)} \tag{21}$$

where $r_i(t)$ $(i = 1, 2, ..., 2m)$ are the Gaussian distributed random processes and m is the parameter of the Nakagami-m distribution. In order to generate these Gaussian distributed waveforms $r_i(t)$, we have employed the sum-of-sinusoids model [13]. For the computation of model parameters, we have used the generalized method of exact Doppler spread (GMEDS_1) [15]. The number of sinusoids for the generation of Gaussian distributed waveforms $r_i(t)$ was chosen to be $N_i = 29 + i$. The maximum Doppler frequency $f_{\max}$ was 91 Hz, the SNR $\gamma_s = 25$ dB, the parameter Ω for Nakagami-m distribution was set to be equal to $2 \times m$, and the value for the area mean m_L was set to unity.

The underlying Gaussian process $v(t)$ in the lognormal process $\lambda(t)$ was also generated by employing the sum-of-sinusoids model [13]. In this case, the model parameters were calculated by applying the modified method of equal areas (MMEA) [16]. The number of sinusoids for the Gaussian process $v(t)$ was equal to $N = 30 + 2m$. The NLN process was finally generated according to (1).

The PDF of the NLN processes for $m = 2$ is shown in Fig. D.1, for various values of the shadowing standard deviation σ_L. It can be seen that increasing the value of shadowing standard deviation σ_L results in a prominent increase in the spreads of the PDFs. The PDF and CDF of the capacity of the NLN process for $m = 2$ are presented in Figs. D.2 and D.3, respectively. It can be observed that as the value of σ_L approaches 0 dB, the statistics of the capacity of NLN channels approach to those of Nakagami-m channels. The results for the case when $\Omega = 0$ (i.e., lognormal process) are also shown in these figures. The mean channel capacity of the NLN

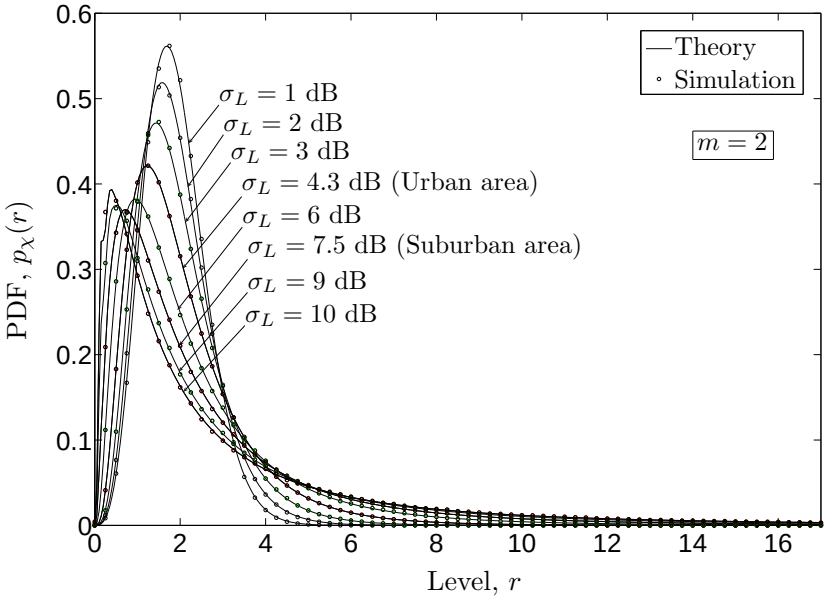

Figure D.1: The PDF of NLN processes.

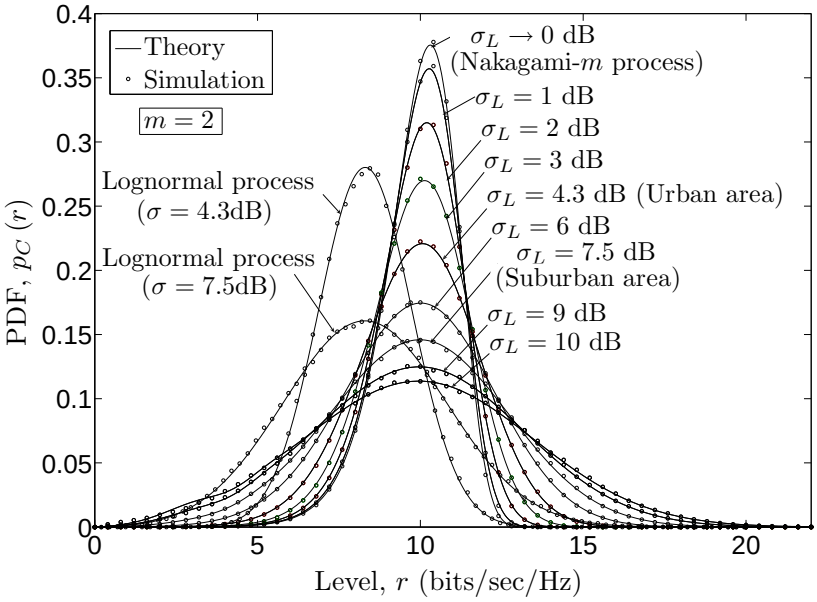

Figure D.2: The PDF of the capacity of NLN and lognormal channels.

process is shown in Fig. D.4 for different values of the SNR γ_s. It can be seen that for a given SNR γ_s the mean channel capacity remains constant for all the values of the shadowing standard deviation σ_L. This fact can also be observed from Fig. D.2.

The LCR and ADF of the channel capacity for $m = 2$ are shown in Figs. D.5 and D.6, respectively. It can be observed that increasing the value of the shadowing standard deviation σ_L increases the spread of the LCR of the channel capacity,

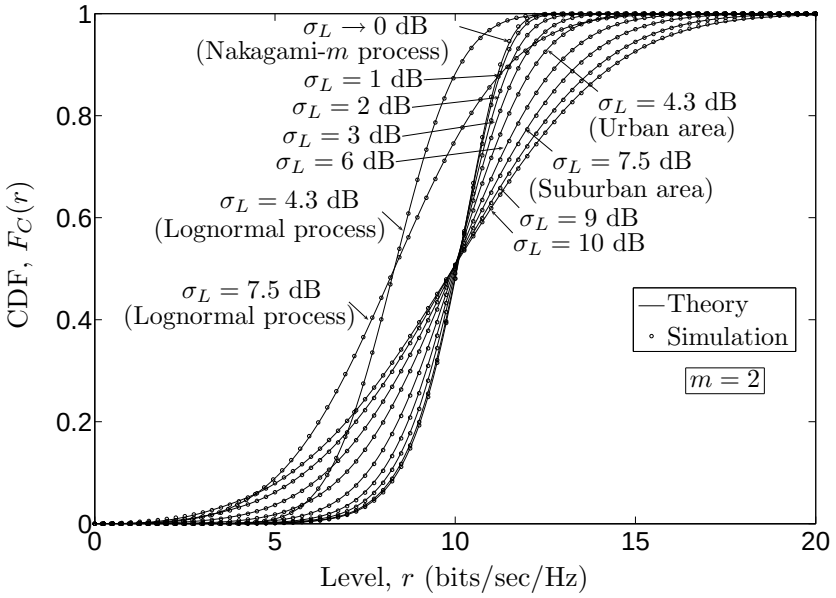

Figure D.3: The CDF of the capacity of NLN and lognormal channels.

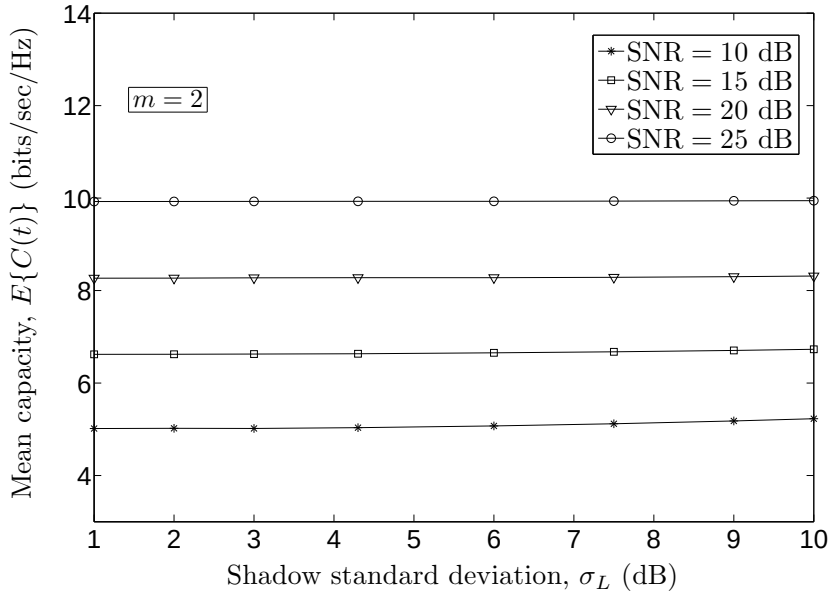

Figure D.4: The mean capacity of NLN channels for different values of SNR.

while it decreases the maximum value of LCR. Moreover, for medium signal levels, the Nakagami-*m* process and the lognormal process set an upper and lower bound, respectively, on the LCR of the channel capacity of the NLN channel. On the other hand, the converse statement is true for the ADF of the channel capacity.

The PDF, CDF, LCR, and ADF of the capacity of the NLN channel for different fading environments, (i.e., for different values of *m*) are presented in Figs. D.7–D.10, respectively. All these results are analyzed for urban ($\sigma_L = 4.3$ dB) and sub-

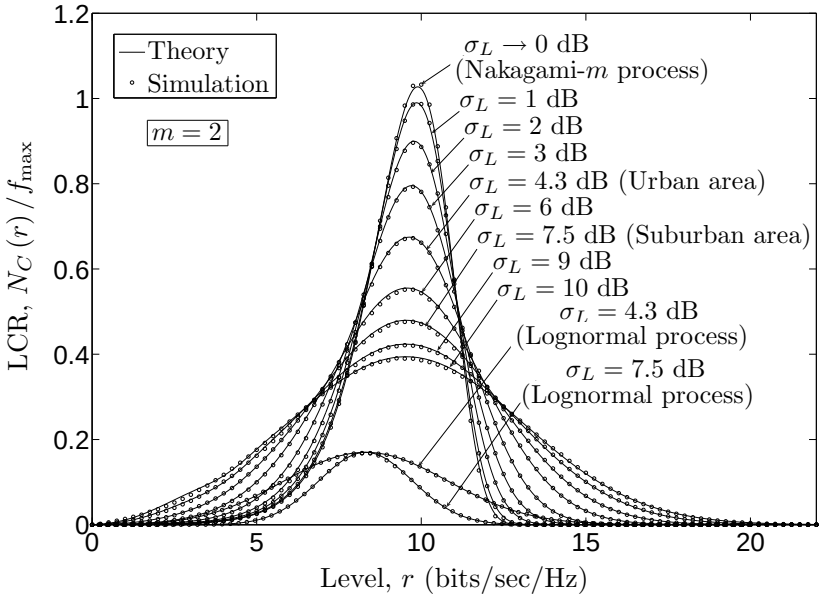

Figure D.5: The normalized LCR of the capacity of NLN and lognormal channels.

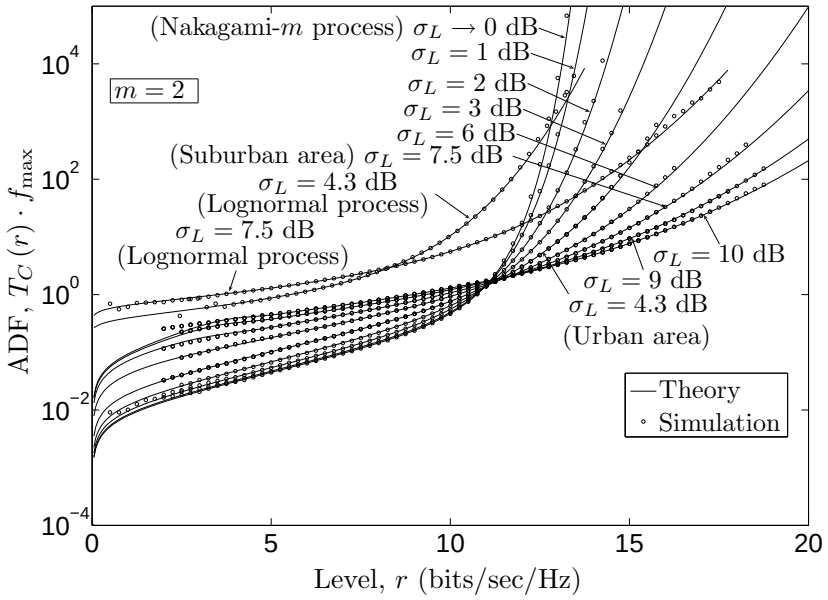

Figure D.6: The normalized ADF of the capacity of NLN and lognormal channels.

urban ($\sigma_L = 7.5$ dB) areas. It is quite obvious from these results that the parameter *m* has a prominent effect on the statistics of the channel capacity of the NLN channels. Increasing the value of *m* results in the increase of the mean channel capacity while the spread of the capacity decreases. For low signal levels *r*, the LCR of the channels with low values of *m* is higher as compared to that of the channels with higher values of *m*. While, for high signal levels *r*, the LCR of the channels with low values of *m* is lower as compared to the ones with higher values of *m*. Analogously,

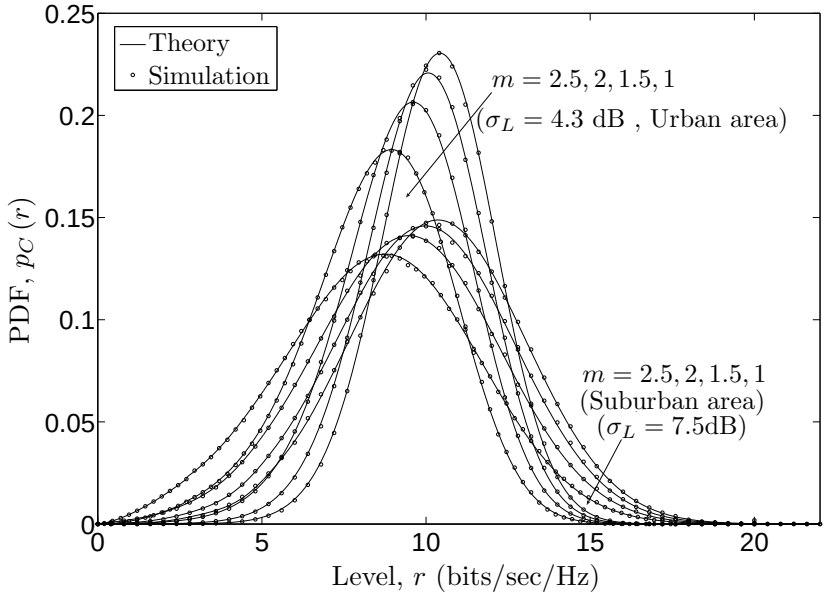

Figure D.7: The PDF of the capacity of NLN and lognormal channels for different values of *m*.

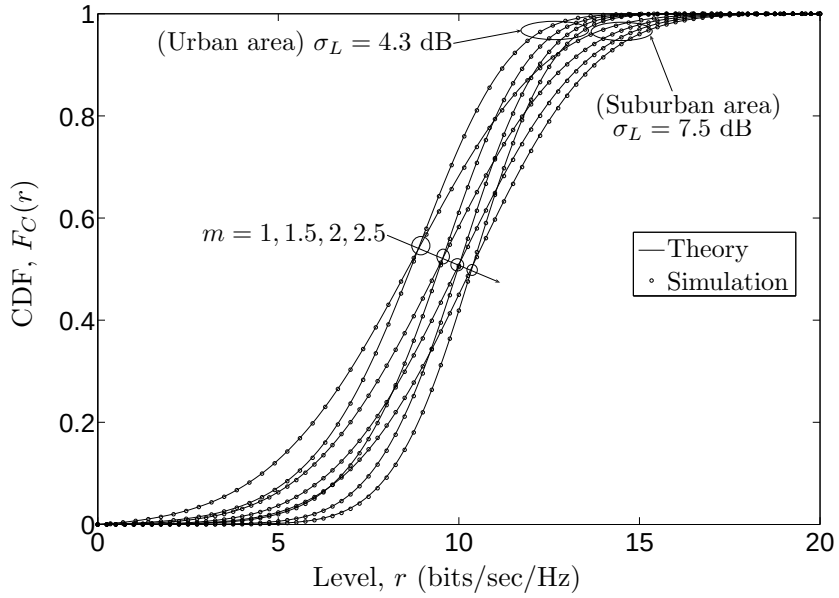

Figure D.8: The CDF of the capacity of NLN and lognormal channels for different values of *m*.

the converse statement is true for the ADF of the channel capacity. Moreover, it can also be seen that the maximum value of the LCR of the channel capacity decreases with the increase in the value of *m*. The mean channel capacity of the NLN channel for different values of *m* is shown in Fig. D.11. It is observed that the shadowing standard deviation σ_L has no influence on the mean channel capacity for any value

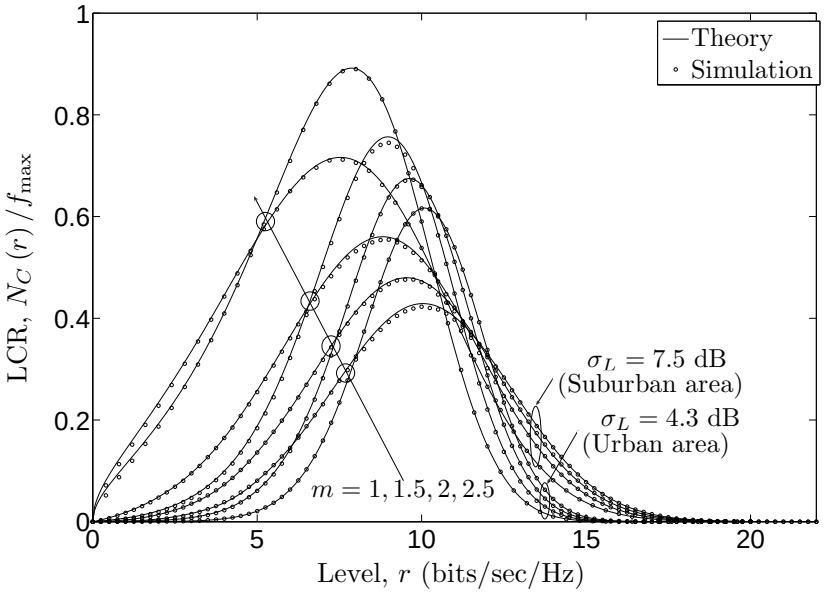

Figure D.9: The normalized LCR of the capacity of NLN and lognormal channels for different values of *m*.

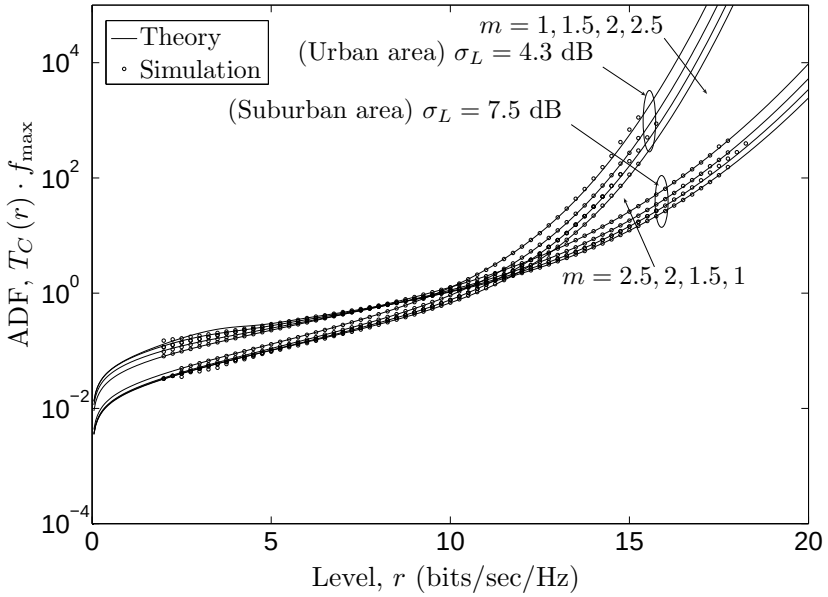

Figure D.10: The normalized ADF of the capacity of NLN and lognormal channels for different values of *m*.

of *m*. Moreover, it can also be noticed that increasing the value of *m* results in an increase of the mean channel capacity.

V. CONCLUSION

In this paper, we have studied the statistical properties of the capacity of NLN channels. We have derived analytical expressions for the PDF, CDF, LCR, and ADF of

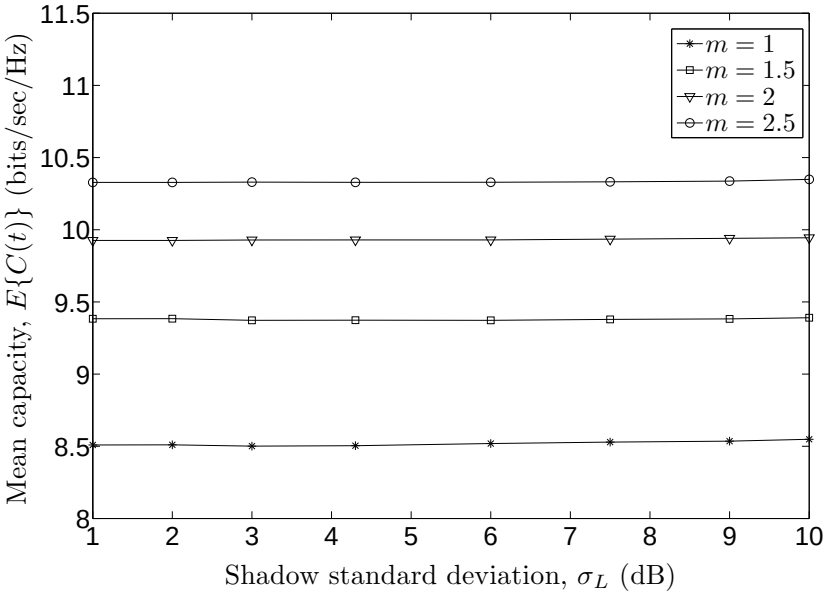

Figure D.11: The mean capacity of NLN channels for different values of *m*.

the capacity of the NLN channels. Moreover, the influence of the shadowing effect and the severity of fading on the statistical properties of the channel capacity has been investigated. It has been observed that if the fading is less severe as compared to the Rayleigh fading, the spread of the PDF and the maximum value of the LCR of channel capacity decrease, while the mean channel capacity increases. On the other hand, increasing the shadowing standard deviation increases the spread of the PDF, while it decreases the maximum value of the LCR of the channel capacity. However, the shadowing standard deviation has no effect on the mean channel capacity for any fading condition. The results presented in this article provide a flexibility to the communication system designers to choose between different fading conditions, corresponding to different terrestrial environments, and are hence quite useful for the design and analysis of land mobile terrestrial channels. All analytical results are verified by simulations where a very good fitting between theoretical and simulation results is found.

REFERENCES

[1] Mohamed-Slim. Alouini, A. Abdi, and M. Kaveh. Sum of gamma variates and performance of wireless communication systems over Nakagami-fading channels. *IEEE Trans. Veh. Technol.*, 50(6):1471–1480, November 2001.

[2] S. H. Choi, P. J. Smith, B. Allen, W. Q. Malik, and M. Shafi. Severely fading MIMO channels: Models and mutual information. In *Proc. IEEE Interna-*

tional Conference on Communications, ICC 2007, pages 4628–4633. Glasgow, UK, June 2007.

[3] G. J. Foschini and M. J. Gans. On limits of wireless communications in a fading environment when using multiple antennas. *Wireless Pers. Commun.*, 6:311–335, March 1998.

[4] A. Giorgetti, P. J. Smith, M. Shafi, and M. Chiani. MIMO capacity, level crossing rates and fades: The impact of spatial/temporal channel correlation. *J. Commun. Net.*, 5(2):104–115, June 2003.

[5] I. S. Gradshteyn and I. M. Ryzhik. *Table of Integrals, Series, and Products*. New York: Academic Press, 6th edition, 2000.

[6] M. Gudmundson. Correlation model for shadow fading in mobile radio systems. *Electron. Lett.*, 27(23):2145–2146, November 1991.

[7] B. O. Hogstad and M. Pätzold. Capacity studies of MIMO models based on the geometrical one-ring scattering model. In *Proc. 15th IEEE Int. Symp. on Personal, Indoor and Mobile Radio Communications, PIMRC 2004*, volume 3, pages 1613–1617. Barcelona, Spain, September 2004.

[8] B. O. Hogstad and M. Pätzold. Exact closed-form expressions for the distribution, level-crossing rate, and average duration of fades of the capacity of MIMO channels. In *Proc. 65th Semiannual Vehicular Technology Conference, IEEE VTC 2007-Spring*, pages 455–460. Dublin, Ireland, April 2007.

[9] B. Holter. On the capacity of the MIMO channel — a tutorial introduction. In *Proc. IEEE Norwegian Symposium on Signal Processing*, pages 167–172. Trondheim, Norway, October 2001.

[10] A. Müller and J. Speidel. Characterization of mutual information of spatially correlated MIMO channels with keyhole. In *Proc. IEEE Int. Conf. Commun., ICC 2007*, pages 750–755. Glasgow, UK, June 2007.

[11] M. Nakagami. The *m*-distribution: A general formula of intensity distribution of rapid fading. In W. G. Hoffman, editor, *Statistical Methods in Radio Wave Propagation*. Oxford, UK: Pergamon Press, 1960.

[12] A. Papoulis and S. U. Pillai. *Probability, Random Variables and Stochastic Processes*. New York: McGraw-Hill, 4th edition, 2002.

[13] M. Pätzold. *Mobile Fading Channels*. Chichester: John Wiley & Sons, 2002.

[14] M. Pätzold, U. Killat, and F. Laue. An extended Suzuki model for land mobile satellite channels and its statistical properties. *IEEE Trans. Veh. Technol.*, 47(2):617–630, May 1998.

[15] M. Pätzold, C. X. Wang, and B. O. Hogstad. Two new sum-of-sinusoids-based methods for the efficient generation of multiple uncorrelated Rayleigh fading waveforms. *IEEE Trans. Wireless Commun.*, 8(6):3122–3131, June 2009.

[16] M. Pätzold and K. Yang. An exact solution for the level-crossing rate of shadow fading processes modelled by using the sum-of-sinusoids principle. In *Proc. 9th International Symposium on Wireless Personal Multimedia Communications, WPMC 2006*, pages 188–193. San Diego, USA, September 2006.

[17] F. Ramos, V. Ya. Kontorovitch, and M. Lara. Generalization of Suzuki model for analog communication channels. In *Proc. IEEE Antennas and Propagation for Wireless Communication, IEEE APS 2000*, pages 107–110, November 2000.

[18] T. T. Tjhung and C. C. Chai. Fade statistics in Nakagami-lognormal channels. *IEEE Trans. on Communications*, 47(12):1769–1772, December 1999.

[19] M. D. Yacoub, J. E. V. Bautista, and L. G. de Rezende Guedes. On higher order statistics of the Nakagami-*m* distribution. *IEEE Trans. Veh. Technol.*, 48(3):790–794, May 1999.

[20] N. Youssef, T. Munakata, and M. Takeda. Fade statistics in Nakagami fading environments. In *Proc. IEEE 4th Int. Symp. on Spread Spectrum Techniques & Applications, ISSSTA'96*, pages 1244–1247. Mayence, Germany, September 1996.

Appendix E

Paper V

Title:	The Influence of LOS Components on the Statistical Properties of the Capacity of Amplify-and-Forward Channels
Authors:	**Gulzaib Rafiq** and Matthias Pätzold
Affiliation:	University of Agder, Faculty of Engineering and Science, P. O. Box 509, NO-4898 Grimstad, Norway
Journal:	*Wireless Sensor Networks (WSN), Invited Paper*, vol. 1, no. 1, Apr. 2009, pp. 7 – 14.

The Influence of LOS Components on the Statistical Properties of the Capacity of Amplify-and-Forward Channels

Gulzaib Rafiq and Matthias Pätzold
Department of Information and Communication Technology
Faculty of Engineering and Science, University of Agder
Servicebox 509, NO-4898 Grimstad, Norway
E-mails: {gulzaib.rafiq, matthias.paetzold}@uia.no

***Abstract* — Amplify-and-forward channels in cooperative networks provide a promising improvement in the network coverage and system throughput. Under line-of-sight (LOS) propagation conditions in such cooperative networks, the overall fading channel can be modeled by a double Rice process. In this article[1], we have studied the statistical properties of the capacity of double Rice fading channels. We have derived the analytical expressions for the probability density function (PDF), cumulative distribution function (CDF), level-crossing rate (LCR), and average duration of fades (ADF) of the channel capacity. The obtained results are studied for different values of the amplitudes of the LOS components in the two links of double Rice fading channels. It has been observed that the statistics of the capacity of double Rice fading channels are quite different from those of double Rayleigh and classical Rice fading channels. Moreover, the presence of an LOS component in any of the two links increases the mean channel capacity and the LCR of the channel capacity. The validity of the theoretical results is confirmed by simulations. The results presented in this article can be very useful for communication system designers to optimize the performance of cooperative networks in wireless communication systems.**

Keywords—Amplify-and-forward channels, channel capacity, cooperative networks, line-of-sight component, double Rice process, double Rayleigh process, level-crossing rate, average duration of fades.

[1]The material in this paper is based on "On the Statistical Properties of the Capacity of Amplify-and-Forward Channels Under LOS Conditions", by Gulzaib Rafiq and Matthias Pätzold which appeared in the proceedings of 11th IEEE International Conference on Communications Systems, ICCS 2008, Guangzhou, China, November 2008.

I. INTRODUCTION

Increased network coverage, improved link quality, and provision of new applications with increased mobility support are the basic demands imposed on future wireless communication systems. One promising solution to fulfil these requirements is the use of cooperative diversity techniques [20, 21, 12]. Single-antenna mobile stations in cooperative networks assist each other to relay the transmitted signal from the source mobile station (SMS) to the destination mobile station (DMS). The cooperation of single-antenna mobile stations in such networks to share their antennas for transmission of the signal makes it possible to form the so-called virtual multiple-input multiple-output (MIMO) system [3], thus, achieving the diversity gain. Moreover, such a cooperation between mobile stations results in an increased network coverage with enhanced mobility support.

For the development and analysis of wireless communication systems that exploit cooperative diversity, a solid knowledge of the multipath fading channel characteristics is required. Recent studies illustrate that mobile-to-mobile (M2M) fading channels associated with relay-based cooperative networks under non-line-of-sight (NLOS) propagation conditions in different propagation scenarios can be modeled either as a double Rayleigh process [2, 11, 4, 14] or an NLOS second-order scattering (NLSS) process [19]. On the other hand, different scenarios under LOS propagation conditions lead to modeling the overall M2M fading channel either by a double Rice process [22], a single-LOS double-scattering (SLDS) process [23], a single-LOS second-order scattering (SLSS) process [19], or a multiple-LOS second-order scattering (MLSS) process [25, 24]. These studies provide results for the statistical characterization of M2M fading channels in cooperative networks under different propagation conditions. The impact of double Rayleigh fading on the performance of a communication system is investigated in [18]. Even with all this research going on, the important question regarding the maximum possible information transfer rate in such fading channels is still unanswered. Thus, the purpose of this paper is to fill in this gap in information regarding the capacity of amplify-and-forward channels in cooperative networks.

Studies pertaining to the analysis of the outage capacity of double Rayleigh channels can be found in [1, 6]. However, to the best of the authors' knowledge, the statistical properties of the capacity of double Rice channels have never been investigated. The analysis of the statistical properties of the channel capacity can be very helpful to study the dynamic behavior of the channel capacity. Here, the statistical properties of interest include the PDF, CDF, LCR, and ADF of the channel capacity. The PDF and CDF of the channel capacity provide the information regarding

mean value and variance of the channel capacity. The LCR and ADF of the channel capacity, on the other hand, give a deep insight into the temporal variations of the channel capacity [7]. The LCR of the channel capacity is a measure of the rate at which the channel capacity crosses a certain threshold level from up to down or vice versa. However, the ADF of the channel capacity is defined as the average duration of time over which the channel capacity is below a certain threshold level [9, 10].

In this paper, we have investigated the statistical properties of the capacity of amplify-and-forward channels in cooperative networks. The transmitted signal from the SMS is received at the DMS via a mobile relay (MR). The MR amplifies the received signal and forwards it to the DMS. We have assumed that there is no direct transmission link between the SMS and the DMS. Moreover, it is also assumed that the LOS components exist in both of the transmission links, i.e., the SMS-MR and MR-DMS links. Hence, the overall fading channel is modeled by a double Rice process[22]. We have derived exact analytical expressions for the PDF, CDF, LCR, and ADF of the channel capacity of double Rice channels. The results are studied for different values of the amplitudes of the LOS components in the two transmission links of double Rice channels. It has been observed that the statistics of the capacity of double Rice channels are quite different from those of double Rayleigh and classical Rice/Rayleigh channels. Specifically, for medium and high signal levels, the presence of LOS components in the two cascaded transmission links increases the mean channel capacity and the LCR of the channel capacity. However, it results in a decrease in the ADF of the channel capacity.

The rest of the paper is organized as follows. In Section II, we describe briefly the double Rice channel model and some of its statistical properties. The statistical properties of the capacity of double Rice channels are studied in Section III. Section IV presents the statistical properties of the capacity of double Rayleigh channels. Numerical results are discussed in Section V. Finally, the concluding remarks are given in Section VI.

II. The Double Rice Channel Model

In cooperative networks employing amplify-and-forward relay, the channel between the SMS and the DMS via an MR can be represented as a concatenation of the SMS-MR and MR-DMS channels [22, 14]. Figure E.1 depicts an example of the transmission link from the SMS to the DMS via the MR in such amplify-and-forward relay-based networks. For the case when an LOS component is present in both of the transmission links, i.e., the SMS-MR link and the MR-DMS link, the overall fading channel can be modeled as a product of two non-zero-mean complex Gaus-

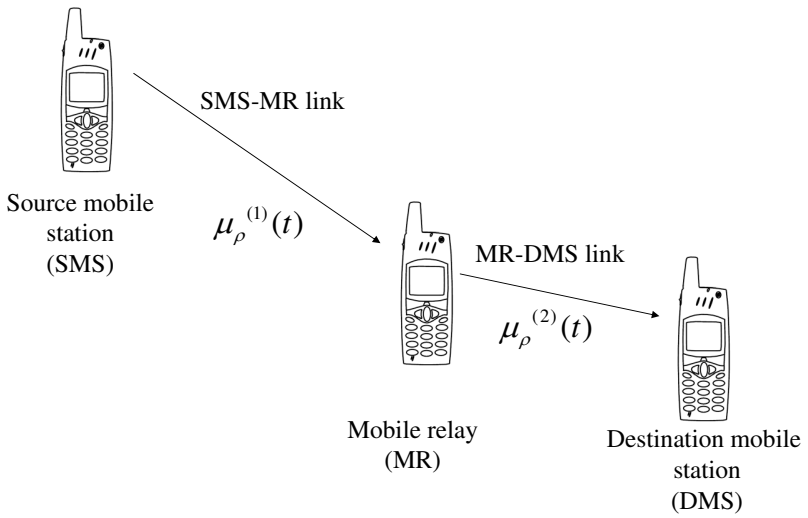

Figure E.1: The propagation scenario describing double Rice fading channels.

sian processes given by [22]

$$\chi(t) = A_{\text{MR}}\,\mu_\rho^{(2)}(t)\mu_\rho^{(1)}(t) \tag{1}$$

where A_{MR} is a real positive constant representing the relay gain and $\mu_\rho^{(i)}(t) = \mu^{(i)}(t) + m^{(i)}(t)$ $(i = 1,2)$ models the fading in the ith link. Here, $\mu^{(i)}(t)$ denotes the scattered component and $m^{(i)}(t)$ is the LOS component. The scattered component $\mu^{(i)}(t)$ can be modeled in the complex baseband as a complex Gaussian process with zero mean and variance $2\sigma_i^2$, i.e., $\mu^{(i)}(t) = \mu_1^{(i)}(t) + j\mu_2^{(i)}(t)$ where, $\mu_1^{(i)}(t)$ and $\mu_2^{(i)}(t)$ are the underlying zero-mean real-valued Gaussian processes. The LOS component $m^{(i)}(t)$ having amplitude ρ_i, Doppler frequency f_{ρ_i}, and phase θ_{ρ_i} can be expressed as $m^{(i)}(t) = \rho_i e^{j(2\pi f_{\rho i}t + \theta_{\rho i})}$. Let $f_{\rho_{\text{SMS}}}$, $f_{\rho_{\text{MR}}}$, and $f_{\rho_{\text{DMS}}}$ represent the respective Doppler frequencies of the SMS, MR, and DMS, then it can be easily observed from Fig. E.1 that $f_{\rho_1} = f_{\rho_{\text{SMS}}} + f_{\rho_{\text{MR}}}$ and $f_{\rho_2} = f_{\rho_{\text{MR}}} + f_{\rho_{\text{DMS}}}$. The envelope of the process $\chi(t)$ in (1) results in a double Rice process given by [22]

$$\begin{aligned} \Xi(t) &= |\chi(t)| = \left|A_{\text{MR}}\,\mu_\rho^{(1)}(t)\,\mu_\rho^{(2)}(t)\right| \\ &= A_{\text{MR}}\,\xi_1(t)\,\xi_2(t) \end{aligned} \tag{2}$$

where $\xi_i(t)$ $(i = 1,2)$ represents the classical Rice process. The PDF of double Rice processes $\Xi(t)$ is given by [22]

$$p_{\Xi}(z) = \frac{z}{\sigma_1^2 \sigma_{\mathrm{MR}}^2} \int_0^{\infty} \frac{1}{y} e^{-\frac{(z/y)^2+\rho_1^2}{2\sigma_1^2}} e^{-\frac{y^2+\rho_{\mathrm{MR}}^2}{2\sigma_{\mathrm{MR}}^2}} I_0\left(\frac{z\rho_1}{y\sigma_1^2}\right) I_0\left(\frac{y\rho_{\mathrm{MR}}}{\sigma_{\mathrm{MR}}^2}\right) dy, \;\; z \geq 0 \qquad (3)$$

where $I_0(\cdot)$ is the modified Bessel function of the first kind of order zero [8], $\sigma_{\mathrm{MR}}^2 = (A_{\mathrm{MR}}\,\sigma_2)^2$, and $\rho_{\mathrm{MR}} = A_{\mathrm{MR}}\,\rho_2$. In order to derive the expressions for the statistical properties of the capacity of double Rice channels, we need the PDF $p_{\Xi^2}(z)$ of the squared process $\Xi^2(t)$ as well as the joint PDF $p_{\Xi^2\dot{\Xi}^2}(z,\dot{z})$ of $\Xi^2(t)$ and its time derivative $\dot{\Xi}^2(t)$[2]. The joint PDF $p_{\Xi^2\dot{\Xi}^2}(z,\dot{z})$ can be found using the joint PDF $p_{\Xi\dot{\Xi}}(z,\dot{z})$ [22] and by using the concept of transformation of random variables [13] as

$$\begin{aligned} p_{\Xi^2\dot{\Xi}^2}(z,\dot{z}) &= \frac{1}{4z}\, p_{\Xi\dot{\Xi}}(\sqrt{z}, \frac{\dot{z}}{2\sqrt{z}}) \\ &= \frac{1/\sqrt{2\pi z}}{(4\pi\sigma_1\sigma_{\mathrm{MR}})^2} \int_0^{\infty} \frac{1}{\sqrt{\beta_1 y^4 + \beta_2 z}} e^{-\frac{z/y^2+\rho_1^2}{2\sigma_1^2}} e^{-\frac{y^2+\rho_{\mathrm{MR}}^2}{2\sigma_{\mathrm{MR}}^2}} \int_{-\pi}^{\pi} e^{-\frac{y\rho_{\mathrm{MR}}\cos\theta_2}{\sigma_{\mathrm{MR}}^2}} \int_{-\pi}^{\pi} e^{-\frac{\sqrt{z}/y\,\rho_1\cos\theta_1}{\sigma_1^2}} \\ &\quad \times e^{-\frac{1}{2}K^2(\sqrt{z},y,\theta_1,\theta_2)} e^{-\frac{(y\dot{z})^2}{8z(\beta_1 y^4+\beta_2 z)} - \frac{y\dot{z}}{2\sqrt{\beta_1 z y^4+\beta_2 z^2}} K(\sqrt{z},y,\theta_1,\theta_2)} d\theta_1 d\theta_2 dy, \\ &\qquad\qquad z \geq 0, |\dot{z}| < \infty \end{aligned} \qquad (4)$$

where

$$\beta_1 = 2\,(\pi\sigma_1)^2\left(f_{\max 1}^2 + f_{\max 2}^2\right) \qquad (5a)$$

$$\beta_2 = 2\,(\pi\sigma_{\mathrm{MR}})^2\left(f_{\max 2}^2 + f_{\max 3}^2\right) \qquad (5b)$$

and

$$K(z,y,\theta_1,\theta_2) = \frac{2\pi\rho_1 f_{\rho_1} y^2 \sin\theta_1 + 2\pi\rho_{\mathrm{MR}} f_{\rho_2} z \sin\theta_2}{\sqrt{\beta_1 z y^4 + \beta_2 z^2}}. \qquad (5c)$$

Here, $f_{\max 1}$, $f_{\max 2}$, and $f_{\max 3}$ denote the maximum Doppler frequencies of the SMS, MR and DMS, respectively. The expression for the PDF $p_{\Xi^2}(z)$ can be obtained by integrating the joint PDF $p_{\Xi^2\dot{\Xi}^2}(z,\dot{z})$ over $\dot{z}$. Alternatively, in our case the PDF $p_{\Xi^2}(z)$ can also be found from the PDF $p_{\Xi}(z)$ in (3) using the concept of transformation of random variables [13] as

$$p_{\Xi^2}(z) = \frac{1}{2\sqrt{z}}\, p_{\Xi}(\sqrt{z})$$

[2] Throughout this paper, we will represent the time derivative of a process by an overdot.

$$= \frac{1}{2\sigma_1^2\sigma_{\text{MR}}^2}\int_0^\infty \frac{1}{y} e^{-\frac{z/y^2+\rho_1^2}{2\sigma_1^2}} e^{-\frac{y^2+\rho_{\text{MR}}^2}{2\sigma_{\text{MR}}^2}} I_0\left(\frac{\sqrt{z}\rho_1}{y\sigma_1^2}\right) I_0\left(\frac{y\rho_{\text{MR}}}{\sigma_{\text{MR}}^2}\right) dy, \;\; z \geq 0. \quad (6)$$

In the next section, we will derive the statistical properties of the capacity of double Rice channels using the results found in this section.

III. Statistical Properties of the Capacity of Double Rice Channels

The instantaneous capacity $C(t)$ of double Rice channels can be expressed using a similar formula found in [5] as

$$\begin{aligned} C(t) &= \log_2\left(1+\gamma_s|\Xi(t)|^2\right) \\ &= \log_2\left(1+\gamma_s\Xi^2(t)\right) \text{ (bits/sec/Hz)} \end{aligned} \quad (7)$$

where γ_s denotes the average received signal-to-noise ratio (SNR) at the DMS. Equation (7) can be considered as a mapping of a random process $\Xi(t)$ to another random process $C(t)$. Hence, the expressions for the statistical properties of the channel capacity $C(t)$ can be derived by using the results for the statistical properties of the process $\Xi(t)$ obtained in the previous section. The PDF $p_C(r)$ of the channel capacity $C(t)$ can be found using (6), (7), and by applying the concept of transformation of random variables as

$$\begin{aligned} p_C(r) &= \frac{2^r\ln(2)}{\gamma_s} p_{\Xi^2}\left(\frac{2^r-1}{\gamma_s}\right) \\ &= \frac{2^r\ln(2)}{2\gamma_s\sigma_1^2\sigma_{\text{MR}}^2}\int_0^\infty \frac{1}{y} e^{-\frac{2^r-1/\gamma_s y^2+\rho_1^2}{2\sigma_1^2}} e^{-\frac{y^2+\rho_{\text{MR}}^2}{2\sigma_{\text{MR}}^2}} I_0\left(\frac{\sqrt{2^r-1}\rho_1}{y\sqrt{\gamma_s}\sigma_1^2}\right) I_0\left(\frac{y\rho_{\text{MR}}}{\sigma_{\text{MR}}^2}\right) dy, \end{aligned} \quad (8)$$

for $r \geq 0$. The CDF $F_C(r)$ of the channel capacity $C(t)$ can now be obtained by solving the integral given by

$$F_C(r) = \int_0^r p_C(z)dz. \quad (9)$$

By substituting (8) in (9) and doing some mathematical manipulations, the CDF of the channel capacity can be expressed as follows

$$F_C(r) = 1 - \frac{1}{\sigma_{\text{MR}}^2}\int_0^\infty y e^{-\frac{y^2+\rho_{\text{MR}}^2}{2\sigma_{\text{MR}}^2}} I_0\left(\frac{y\rho_{\text{MR}}}{\sigma_{\text{MR}}^2}\right) Q_1\left(\frac{\rho_1}{\sigma_1}, \frac{\sqrt{2^r-1}}{y\sqrt{\gamma_s}\sigma_1}\right) dy, \;\; r \geq 0 \quad (10)$$

where $Q_1(\cdot,\cdot)$ is the generalized Marcum Q-function [8]. The LCR $N_C(r)$ of the channel capacity $C(t)$ is defined as [10]

$$N_C(r) = \int_0^\infty \dot{z}\, p_{C\dot{C}}(r,\dot{z})d\dot{z}, \;\; r \geq 0 \tag{11}$$

where $p_{C\dot{C}}(z,\dot{z})$ represents the joint PDF of $C(t)$ and its time derivative $\dot{C}(t)$. The joint PDF $p_{C\dot{C}}(z,\dot{z})$ can be obtained from the joint PDF $p_{\Xi^2\dot{\Xi}^2}(z,\dot{z})$ by applying again the concept of transformation of random variables as

$$\begin{aligned} p_{C\dot{C}}(z,\dot{z}) &= \left(\frac{2^z\ln(2)}{\gamma_s}\right)^2 p_{\Xi^2\dot{\Xi}^2}\left(\frac{2^z-1}{\gamma_s}, \frac{2^z\dot{z}\ln(2)}{\gamma_s}\right) \\ &= \frac{(2^z\ln(2))^2\,(2^z-1)^{-1/2}}{(4\pi)^2\sqrt{2\pi}\gamma_s^{3/2}\sigma_1^2\sigma_{\text{MR}}^2} \int_0^\infty \frac{e^{-\frac{2^z-1\big/\gamma_s y^2+\rho_1^2}{2\sigma_1^2}}}{\sqrt{\beta_1 y^4+\beta_2\left(2^z-1\big/\gamma_s\right)}} e^{-\frac{y^2+\rho_{\text{MR}}^2}{2\sigma_{\text{MR}}^2}} \int_{-\pi}^{\pi} e^{-\frac{y\rho_{\text{MR}}\cos\theta_2}{\sigma_{\text{MR}}^2}} \\ &\quad \times \int_{-\pi}^{\pi} e^{-\frac{\sqrt{2^z-1\big/\gamma_s y^2}\,\rho_1\cos\theta_1}{\sigma_1^2}} e^{-\frac{(y\dot{z}\ln(2)2^z)^2(2^z-1)^{-1}}{8\left(\gamma_s\beta_1 y^4+\beta_2(2^z-1)\right)}} e^{-\frac{y\dot{z}\ln(2)2^z(2^z-1)^{-1/2}}{2\sqrt{\gamma_s\beta_1 y^4+\beta_2(2^z-1)}}} K\left(\sqrt{\tfrac{2^z-1}{\gamma_s}}, y, \theta_1, \theta_2\right) \\ &\quad \times e^{-\frac{1}{2}K^2\left(\sqrt{(2^z-1/\gamma_s)}, y, \theta_1, \theta_2\right)} d\theta_1 d\theta_2 dy, \;\; z \geq 0, |\dot{z}| < \infty \end{aligned} \tag{12}$$

where $K(\cdot,\cdot,\cdot,\cdot)$ is defined in (5c). After substituting (12) in (11) and carrying out some algebraic calculations, we obtain

$$\begin{aligned} N_C(r) &= \frac{\sqrt{2^r-1}}{(2\pi)^{5/2}\sqrt{\gamma_s}\sigma_1^2\sigma_{\text{MR}}^2} \int_0^\infty \sqrt{\beta_1+\beta_2\left(\frac{2^r-1}{y^4\gamma_s}\right)} e^{-\frac{2^r-1\big/\gamma_s y^2+\rho_1^2}{2\sigma_1^2}} e^{-\frac{y\rho_{\text{MR}}\cos\theta_2}{\sigma_{\text{MR}}^2}} \\ &\quad \times \int_{-\pi}^{\pi} e^{-\frac{\sqrt{2^r-1}\rho_1\cos\theta_1}{\sigma_1^2\gamma_s^2 y^4}} \int_{-\pi}^{\pi} e^{-\frac{y^2+\rho_{\text{MR}}^2}{2\sigma_{\text{MR}}^2}} e^{-\frac{1}{2}K^2\left(\sqrt{\frac{2^r-1}{\gamma_s}}, y, \theta_1, \theta_2\right)} \left[1+\sqrt{\frac{\pi}{2}} e^{\frac{1}{2}K^2\left(\sqrt{\frac{2^r-1}{\gamma_s}}, y, \theta_1, \theta_2\right)}\right. \\ &\quad \left. \times K\left(\sqrt{\frac{2^r-1}{\gamma_s}}, y, \theta_1, \theta_2\right)\left\{1+\Phi\left(\frac{K\left(\sqrt{\frac{2^r-1}{\gamma_s}}, y, \theta_1, \theta_2\right)}{\sqrt{2}}\right)\right\}\right] d\theta_1 d\theta_2 dy, \end{aligned} \tag{13}$$

for $r \geq 0$, where $\Phi(\cdot)$ denotes the error function [8]. Finally, from (13) and (10), the ADF $T_C(r)$ of the channel capacity $C(t)$ can be obtained using [10]

$$T_C(r) = \frac{F_C(r)}{N_C(r)}. \tag{14}$$

The results found in this section will be used in the following section to derive the statistical properties of the capacity of double Rayleigh channels.

IV. Statistical Properties of the Capacity of Double Rayleigh Channels

The double Rayleigh channel follows as a special case of the double Rice channel when $\rho_i \to 0$ $(i = 1,2)$. Hence, by letting $\rho_i \to 0$ $(i = 1,2)$ in (8), (10), and (13), the PDF, CDF, and LCR of the channel capacity of double Rayleigh channel can be expressed as

$$p_C(r)\big|_{\rho_i \to 0} = \frac{2^r \ln(2)}{2\gamma_s \sigma_1^2 \sigma_{\text{MR}}^2} \int_0^\infty \frac{1}{y} e^{-\frac{2^r-1}{2\sigma_1^2 \gamma_s y^2}} e^{-\frac{y^2}{2\sigma_{\text{MR}}^2}} dy, \;\; r \geq 0 \tag{15}$$

$$F_C(r)\big|_{\rho_i \to 0} = 1 - \frac{1}{\sigma_{\text{MR}}^2} \int_0^\infty y e^{-\frac{y^2}{2\sigma_{\text{MR}}^2}} e^{-\frac{2^r-1}{2\sigma_1^2 \gamma_s y^2}} dy, \;\; r \geq 0 \tag{16}$$

and

$$N_C(r)\big|_{\rho_i \to 0} = \frac{\sqrt{2^r-1}}{\sqrt{2\pi\gamma_s}\sigma_1^2 \sigma_{\text{MR}}^2} \int_0^\infty \sqrt{\beta_1 + \beta_2 \left(\frac{2^r-1}{y^4 \gamma_s}\right)} e^{-\frac{2^r-1}{2\sigma_1^2 \gamma_s y^2}} e^{-\frac{y^2}{2\sigma_{\text{MR}}^2}} dy, \;\; r \geq 0 \tag{17}$$

respectively. The ADF of the channel capacity $C(t)$ of double Rayleigh channel can be found using (14), (16), and (17).

V. Statistical Properties of the Capacity of Rayleigh and Rice Channels

In this section, we will present the PDF, CDF, and LCR of the capacity of Rayleigh and Rice channels. We will study these results along with the statistical properties of the capacity of double Rice channels in the next section for comparison purposes. The PDF $p_C(r)$ of the capacity $C(t)$ of Rice channels can be found using the PDF $p_{\xi^2}(r)$ of the squared Rice process $\xi^2(t)$ and by employing the expression presented in (7) corresponding to Rice processes $\xi(t)$ as

$$\begin{aligned} p_C(r) &= \frac{2^r \ln(2)}{\gamma_s} p_{\xi^2}\left(\frac{2^r-1}{\gamma_s}\right) \\ &= \frac{2^r \ln(2)}{2\gamma_s \sigma_0^2} e^{-\frac{2^r-1+\gamma_s \rho^2}{2\sigma_0^2 \gamma_s}} I_0\left(\sqrt{\frac{(2^r-1)\rho^2}{\sigma_0^4 \gamma_s}}\right), \;\; r \geq 0 \end{aligned} \tag{18}$$

where ρ represent the amplitude of the LOS component and σ_0^2 denotes the variance of the underlying Gaussian processes. By substituting (18) in $F_C(r) = \int_0^r p_C(x)dx$,

the CDF $F_C(r)$ of the capacity of $C(t)$ of Rice channels can be written as

$$F_C(r) = 1 - Q_1\left(\frac{\rho}{\sigma_0}, \sqrt{\frac{(2^r-1)}{\sigma_0^2\gamma_s}}\right), \ r \geq 0. \tag{19}$$

By solving $N_C(r) = \int_0^\infty p_{C\dot{C}}(r,\dot{z})d\dot{z}$, the LCR $N_C(r)$ of the capacity of $C(t)$ of Rice channels can be represented by

$$N_C(r) = \sqrt{\frac{(2^r-1)\,\beta}{\pi 2\sigma_0^4\gamma_s}} e^{-\frac{2^r-1+\gamma_s\rho^2}{2\sigma_0^2\gamma_s}} I_0\left(\sqrt{\frac{(2^r-1)}{\sigma_0^4\gamma_s/\rho^2}}\right), \ r \geq 0 \tag{20}$$

where β under isotropic scattering conditions is given by $\beta = 2\left(\pi f_{\max}\sigma_0\right)^2$. Here, $p_{C\dot{C}}(z,\dot{z})$ represents the joint PDF of the capacity $C(t)$ and its time derivative $\dot{C}(t)$ and $f_{\max}$ denotes the maximum Doppler frequency.

The results for the PDF, CDF, and LCR of the capacity $C(t)$ of Rayleigh channels can be obtained from (18)–(20), respectively, by letting $\rho \to 0$ as follows:

$$p_C(r)\big|_{\rho\to 0} = \frac{2^r \ln(2)}{2\gamma_s\sigma_0^2} e^{-\left(\frac{2^r-1}{2\gamma_s\sigma_0^2}\right)}, \ r \geq 0 \tag{21}$$

$$F_C(r)\big|_{\rho\to 0} = 1 - e^{-\left(\frac{2^r-1}{2\gamma_s\sigma_0^2}\right)}, \ r \geq 0 \tag{22}$$

$$N_C(r)\big|_{\rho\to 0} = \frac{1}{\sigma_0^2}\sqrt{\frac{\beta\,(2^r-1)}{2\pi\gamma_s}} e^{-\left(\frac{2^r-1}{2\gamma_s\sigma_0^2}\right)}, \ r \geq 0. \tag{23}$$

The expressions (21)–(23) have already been presented in [17, Eqs. (23–25)]. However, we have presented these equations here for the sake of completeness.

VI. Numerical Results

This section aims at the validation and analysis of the analytical results presented in the previous section, using simulations. We have also included the results for double Rayleigh, classical Rayleigh [10], and classical Rice channels in our study for comparison purposes. For the case of classical Rice channels, we denote the amplitude of the LOS component as ρ. The Rice processes $\mu_\rho^{(i)}(t) = \mu^{(i)}(t) + m^{(i)}(t)$ $(i = 1,2)$ were simulated using the sum-of-sinusoids model [15]. The model parameters were computed using the generalized method of exact Doppler spread (GMEDS_1) [16]. The number of sinusoids ($N_1^{(i)}$ and $N_2^{(i)}$) for the resulting deterministic processes $\tilde{\mu}_1^{(i)}(t)$ and $\tilde{\mu}_2^{(i)}(t)$ in GMEDS_1 were chosen to be $N_1^{(i)} = N_2^{(i)} = 20$ for $i = 1,2$, respectively. The maximum Doppler frequencies $f_{\max_2}$ and $f_{\max_3}$ were taken to be 91 and 125 Hz, respectively. We have assumed that the Doppler frequency

$f_{\rho_{\text{SMS}}}$ equals 0. Unless stated otherwise, the values of the Doppler frequencies $f_{\rho_{\text{MR}}}$ and $f_{\rho_{\text{DMS}}}$ were set to be equal to $f_{\max_2}$ and $f_{\max_3}$, respectively. The SNR γ_s was set to 20 dB. The parameters A_{MR} and σ_i $(i = 1, 2)$ were chosen to be unity. Finally, using (2) and (7) the simulation results for the statistical properties of the channel capacity were found.

The PDF $p_\Xi(z)$ of double Rice processes $\Xi(t)$ are shown in Fig. E.2 for different values of the amplitudes of the LOS components ρ_i $(i = 1, 2)$. In Fig. E.3, the PDF of the double Rayleigh process is also shown, which represents a special case of the double Rice process when $\rho_1 = \rho_2 = 0$. It is observed that the presence of the LOS components has a dominant effect on the mean value and spread of the PDF of double Rice processes. It can also be seen that the PDF of double Rice processes is identical for the cases $\rho_2 = 0$; $\rho_1 = 2$ and $\rho_2 = 2$; $\rho_1 = 0$.

Figures E.3 and E.4 present the PDF and CDF of the capacity of double Rice channels, respectively. It is observed that the amplitude of the LOS component has a significant influence on the PDF and CDF of the channel capacity. Specifically, the presence of an LOS component in one or both of the links (i.e., the SMS-MR and MR-DMS links) increases the mean channel capacity. Hence, double Rayleigh channels have a lower mean channel capacity compared to double Rice channels (e.g., when $\rho_2 = \rho_1 = 2$). It is also observed that the capacity of classical Rice channels has a lower mean value compared to that of double Rice channels. These facts are specifically studied in Fig. E.5, where the mean channel capacity of classical Rice as well as double Rice channels is studied for different values of the

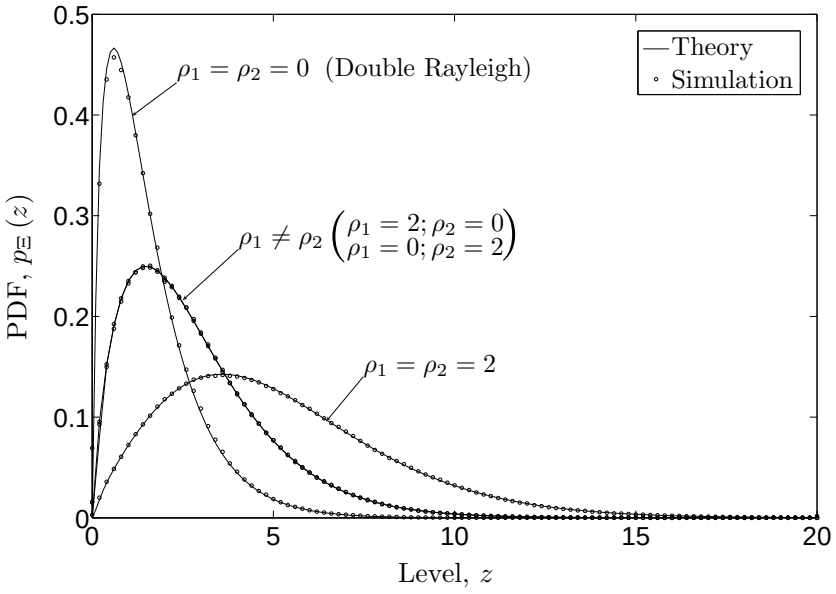

Figure E.2: The PDF $p_\Xi(z)$ of double Rice processes $\Xi(t)$.

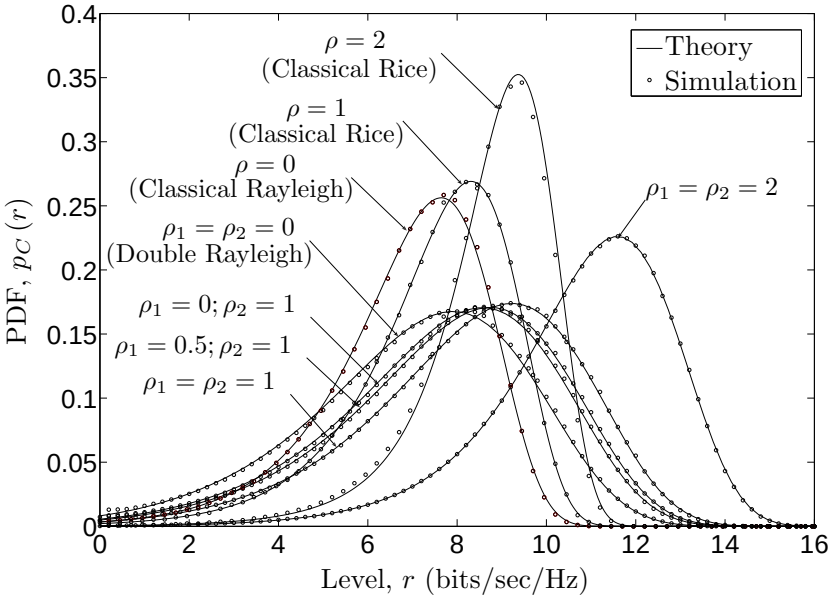

Figure E.3: The PDF $p_C(r)$ of the capacity of double Rice channels.

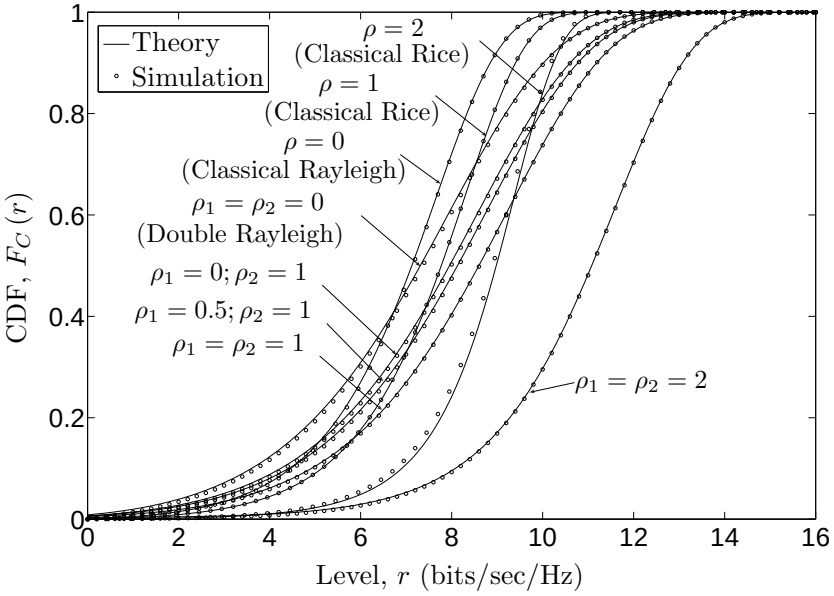

Figure E.4: The CDF $F_C(r)$ of the capacity of double Rice channels.

amplitudes of the LOS component. Figure E.6 shows the influence of the amplitude of LOS component on the variance of the classical Rice and double Rice channels. It is observed that increasing the value of ρ decreases the spread of the channel capacity for medium and large values of ρ, say $\rho \geq 1$. Moreover, the variance of the capacity of double Rice channels is much higher as compared to that of classical Rice channels.

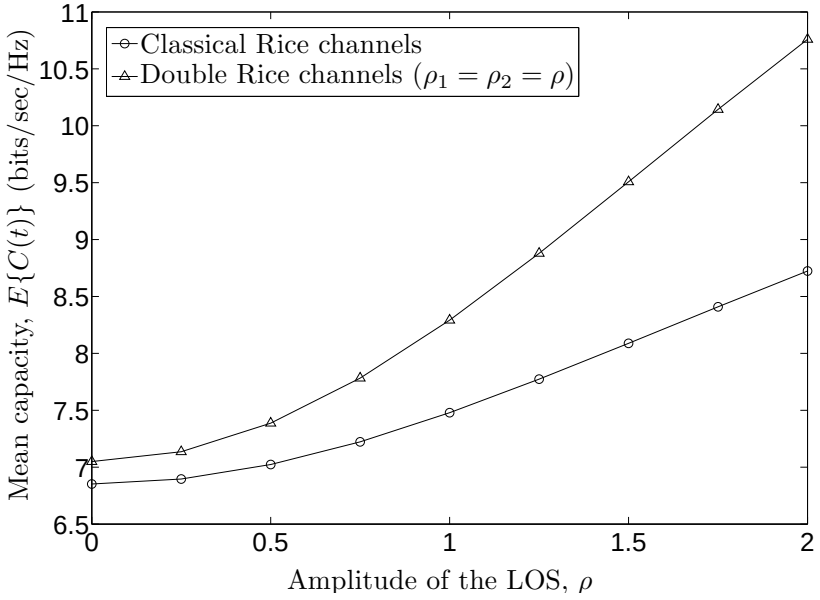

Figure E.5: The mean capacity $E\{C(t)\}$ of classical Rice and double Rice channels.

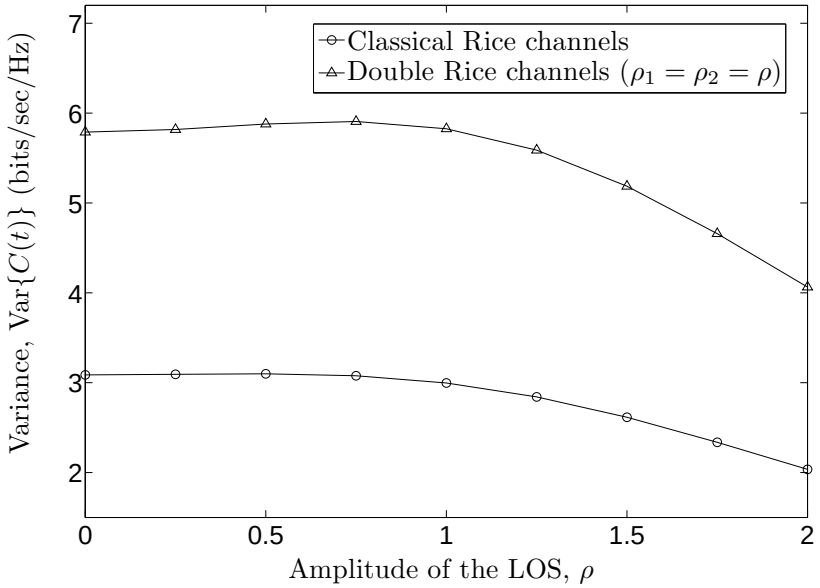

Figure E.6: The variance Var$\{C(t)\}$ of the capacity of classical Rice and double Rice channels.

The LCR and ADF of the channel capacity of double Rice channels are presented in Figs. E.7 and E.8, respectively. It is evident from Fig. E.7 that the maximum value of the LCR of the channel capacity increases with an increase in the value of the amplitude of the LOS component ρ_i $(i = 1, 2)$. It is also observed that the LCR of the capacity of classical Rice channels is much lower compared to that of double Rice channels. The converse statements with respect to the LCR of the

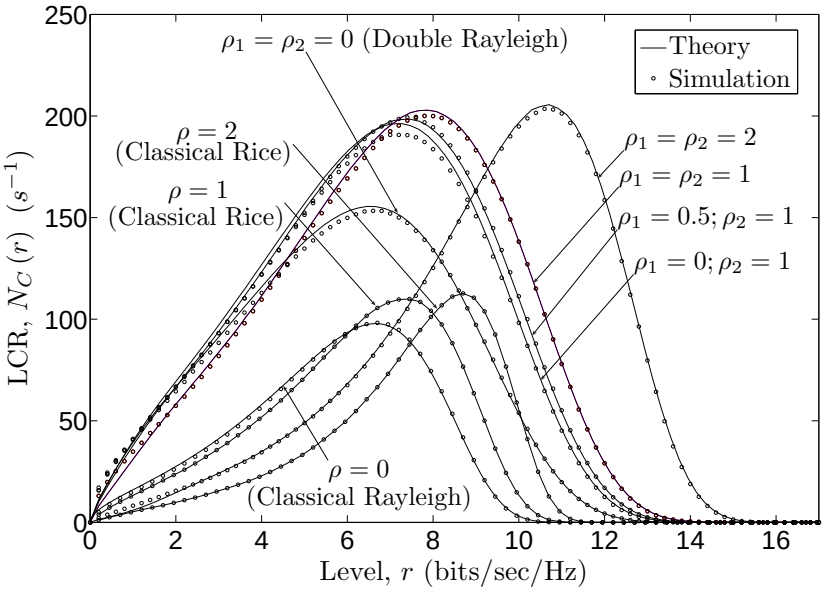

Figure E.7: The LCR $N_C(r)$ of the capacity of double Rice channels.

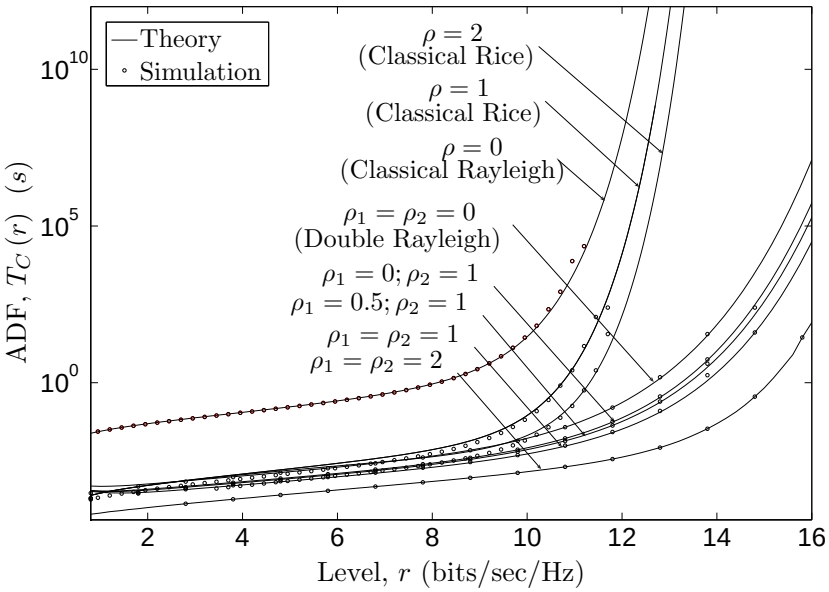

Figure E.8: The ADF $T_C(r)$ of the capacity of double Rice channels.

channel capacity are true for the ADF, as can be seen in Fig. E.8. Figures E.9 and E.10 aim at illustrating the effect of the Doppler frequency on the LCR and ADF of the channel capacity. From Figs. E.9 and E.10, it can clearly be seen that the LCR and ADF are strongly dependent on the Doppler frequencies of the MR and the DMS. It is observed that increasing the Doppler frequencies $f_{\rho_{\text{MR}}}$ and $f_{\rho_{\text{DMS}}}$ from 0 to $f_{\max_2}$ and $f_{\max_3}$, respectively, results in a significant increase in the LCR. However, the ADF decreases by increasing the Doppler frequencies of the MR and the DMS.

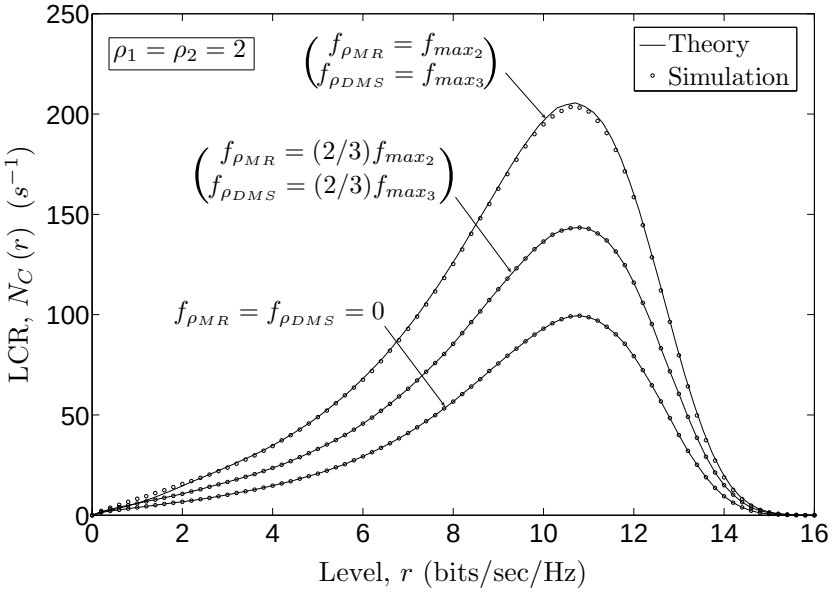

Figure E.9: The LCR $N_C(r)$ of the capacity of double Rice channels.

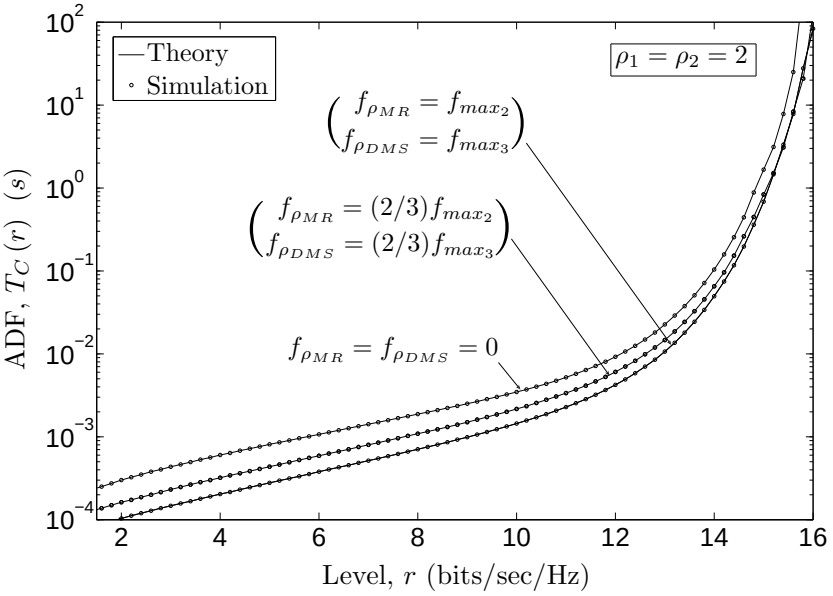

Figure E.10: The ADF $T_C(r)$ of the capacity of double Rice channels.

VI. Conclusion

In this paper, we have studied the statistical properties of the channel capacity of the double Rice channels. We have derived analytical expressions for the PDF, CDF, LCR, and ADF of the channel capacity. The findings of this paper give a deep insight into the influence of the LOS components, corresponding to the two links of amplify-and-forward channels, on the statistical properties of the channel

capacity. It has been observed that for medium and high signal levels, the presence of the LOS components in one or both of the links of the double Rice channel model increases the mean channel capacity and the LCR of the channel capacity. However, it decreases the ADF of the channel capacity. Moreover, the Doppler frequencies of the MR and the DMS have a significant impact on the LCR and ADF of the channel capacity. The validity of all the presented analytical results is confirmed by simulations, whereby a very good fitting between the analytical and simulation results is found.

REFERENCES

[1] P. Almers, F. Tufvesson, and A. F. Molisch. Keyhole effect in MIMO wireless channels: Measurements and theory. *IEEE Trans. Wireless Commun.*, 5(12):3596–3604, December 2006.

[2] J. B. Andersen. Statistical distributions in mobile communications using multiple scattering. In *Proc. 27th URSI General Assembly*. Maastricht, Netherlands, August 2002.

[3] M. Dohler. *Virtual Antenna Arrays*. Ph.D. dissertation, King's College, London, United Kingdom, 2003.

[4] V. Erceg, S. J. Fortune, J. Ling, A. J. Rustako Jr., and R. A. Valenzuela. Comparison of a computer-based propagation prediction tool with experimental data collected in urban microcellular environment. *IEEE J. Select. Areas Commun.*, 15(4):677–684, May 1997.

[5] G. J. Foschini and M. J. Gans. On limits of wireless communications in a fading environment when using multiple antennas. *Wireless Pers. Commun.*, 6:311–335, March 1998.

[6] D. Gesbert, H. Bölcskei, D. A. Gore, and A. J. Paulraj. Outdoor MIMO wireless channels: Models and performance prediction. *IEEE Trans. Wireless Commun.*, 50(12):1926–1934, December 2002.

[7] A. Giorgetti, P. J. Smith, M. Shafi, and M. Chiani. MIMO capacity, level crossing rates and fades: The impact of spatial/temporal channel correlation. *J. Commun. Net.*, 5(2):104–115, June 2003.

[8] I. S. Gradshteyn and I. M. Ryzhik. *Table of Integrals, Series, and Products*. New York: Academic Press, 6th edition, 2000.

[9] B. O. Hogstad and M. Pätzold. Capacity studies of MIMO models based on the geometrical one-ring scattering model. In *Proc. 15th IEEE Int. Symp. on Personal, Indoor and Mobile Radio Communications, PIMRC 2004*, volume 3, pages 1613–1617. Barcelona, Spain, September 2004.

[10] B. O. Hogstad and M. Pätzold. Exact closed-form expressions for the distribution, level-crossing rate, and average duration of fades of the capacity of MIMO channels. In *Proc. 65th Semiannual Vehicular Technology Conference, IEEE VTC 2007-Spring*, pages 455–460. Dublin, Ireland, April 2007.

[11] I. Z. Kovacs, P. C. F. Eggers, K. Olesen, and L. G. Petersen. Investigations of outdoor-to-indoor mobile-to-mobile radio communication channels. In *Proc. IEEE 56th Veh. Technol. Conf., VTC'02-Fall*, pages 430–434. Vancouver BC, Canada, September 2002.

[12] J. N. Laneman, D. N. C. Tse, and G. W. Wornell. Cooperative diversity in wireless networks: Efficient protocols and outage behavior. *IEEE Trans. Inform. Theory*, 50(12):3062–3080, December 2004.

[13] A. Papoulis and S. U. Pillai. *Probability, Random Variables and Stochastic Processes*. New York: McGraw-Hill, 4th edition, 2002.

[14] C. S. Patel, G. L. Stüber, and T. G. Pratt. Statistical properties of amplify and forward relay fading channels. *IEEE Trans. Veh. Technol.*, 55(1):1–9, January 2006.

[15] M. Pätzold. *Mobile Fading Channels*. Chichester: John Wiley & Sons, 2002.

[16] M. Pätzold, C. X. Wang, and B. O. Hogstad. Two new sum-of-sinusoids-based methods for the efficient generation of multiple uncorrelated Rayleigh fading waveforms. *IEEE Trans. Wireless Commun.*, 8(6):3122–3131, June 2009.

[17] G. Rafiq and M. Pätzold. A study of the influence of shadowing on the statistical properties of the capacity of mobile radio channels. *Wireless Personal Communications (WPC)*, 50(1):5–18, July 2009.

[18] J. Salo, H. M. El-Sallabi, and P. Vainikainen. Impact of double-Rayleigh fading on system performance. In *Proc. 1st IEEE Int. Symp. on Wireless Pervasive Computing, ISWPC 2006*. Phuket, Thailand, January 2006.

[19] J. Salo, H. M. El-Sallabi, and P. Vainikainen. Statistical analysis of the multiple scattering radio channel. *IEEE Trans. Antennas Propagat.*, 54(11):3114–3124, November 2006.

[20] A. Sendonaris, E. Erkip, and B. Aazhang. User cooperation diversity—Part I: System description. *IEEE Trans. Commun.*, 51(11):1927–1938, November 2003.

[21] A. Sendonaris, E. Erkip, and B. Aazhang. User cooperation diversity—Part II: Implementation aspects and performance analysis. *IEEE Trans. Commun.*, 51(11):1939–1948, November 2003.

[22] B. Talha and M. Pätzold. On the statistical properties of double Rice channels. In *Proc. 10th International Symposium on Wireless Personal Multimedia Communications, WPMC 2007*, pages 517–522. Jaipur, India, December 2007.

[23] B. Talha and M. Pätzold. On the statistical properties of mobile-to-mobile fading channels in cooperative networks under line-of-sight conditions. In *Proc. 10th International Symposium on Wireless Personal Multimedia Communications, WPMC 2007*, pages 388–393. Jaipur, India, December 2007.

[24] B. Talha and M. Pätzold. Level-crossing rate and average duration of fades of the envelope of mobile-to-mobile fading channels in cooperative networks under line-of-sight conditions. In *Proc. 51st IEEE Global Telecommunications Conference, GLOBECOM 2008*, pages 1–6. New Orleans, US, November 2008.

[25] B. Talha and M. Pätzold. A novel amplify-and-forward relay channel model for mobile-to-mobile fading channels under line-of-sight conditions. In *Proc. 19th IEEE Int. Symp. on Personal, Indoor and Mobile Radio Communications, PIMRC 2008*, pages 1–6. Cannes, France, September 2008.

Appendix F

Paper VI

Title:	Statistical Properties of the Capacity of Double Nakagami-*m* Channels
Authors:	**Gulzaib Rafiq**[1], Bjørn Olav Hogstad[2], and Matthias Pätzold[1]
Affiliations:	[1]University of Agder, Faculty of Engineering and Science, P. O. Box 509, NO-4898 Grimstad, Norway [2]CEIT and Tecnun, University of Navarra, Manuel de Lardizábal 15, 20018, San Sebastián, Spain
Conference:	*5th International Symposium on Wireless Pervasive Computing, ISWPC 2010*, Modena, Italy, May 2010, pp. 39 – 44.

Statistical Properties of the Capacity of Double Nakagami-*m* Channels

Gulzaib Rafiq[1], Bjørn Olav Hogstad[2], and Matthias Pätzold[1]
[1]Department of Information and Communication Technology
Faculty of Engineering and Science, University of Agder
Servicebox 509, NO-4898 Grimstad, Norway
E-mails: {gulzaib.rafiq, matthias.paetzold}@uia.no
[2]CEIT and Tecnun, University of Navarra
Manuel de Lardizábal 15, 20018, San Sebastián, Spain
Email: bohogstad@ceit.es

***Abstract* — In this article, we have presented an extensive statistical analysis of the capacity of double[1] Nakagami-*m* channels. The double Nakagami-*m* channel model has applications in keyhole channels and amplify-and-forward relay based dualhop communication systems in cooperative networks. We have derived exact analytical expressions for the probability density function (PDF), the cumulative distribution function (CDF), the level-crossing rate (LCR), and the average duration of fades (ADF) of the capacity of double Nakagami-*m* channels. Moreover, the influence of severity of fading on the statistical properties of the channel capacity has been studied. It is observed that an increase in the severity of fading in one or both links in dualhop communication systems decreases the mean channel capacity, while it results in an increase in the ADF of the channel capacity. Moreover, this effect decreases the LCR of the channel capacity at lower signal levels. The results presented in this paper also reveal that an increase in the maximum Doppler frequencies of the wireless nodes in a dualhop communication system increases the LCR of the channel capacity, while it has an opposite influence on the ADF of the channel capacity. The results presented in this article are useful for mobile communication system engineers for the design and optimization of dualhop communication systems.**

I. Introduction

The design and analysis of cascaded fading models has been an active area of research in recent years due to its applications in numerous real world scenarios such as keyhole channels [20, 26], and multihop communication systems [2, 10, 24, 23].

[1]Throughout this paper, we will refer to a double process as the product of two independent but may not necessarily identical processes.

It is shown in [4, 3] that in the presence of a keyhole, the fading between each transmit and receive antenna pair in a multi-input multi-output (MIMO) system can be characterized using a double Rayleigh process. Afterwards, this model has been extended to the double Nakagami-*m* fading model in [22]. In [20], authors have listed a few real world scenarios which give rise to the keyhole effect. Two such scenarios include diffraction through the street edges in urban microcellular environments [4] and traversal of the propagation paths through a narrow space for the case when the distance between the rings of scatterers around the transmitter and receiver is large [5].

Multihop communication systems on the other hand fall under the category of cooperative diversity techniques [21, 12]. In such systems, the wireless nodes (in a cooperative network) assist each other by relaying the information from the source mobile station (SMS) to the destination mobile station (DMS), hence improving the network coverage quite significantly. The statistical analysis of the received signal envelope under non-line-of-sight (NLOS) propagation conditions in an amplify-and-forward based dualhop communication system can be found in [16], where the overall channel between the transmitter and the receiver is modeled using a double Rayleigh process. This model is then extended to the double Rice channel model in [23], by taking the line-of-sight propagation conditions into account. The statistical properties of the capacity of double Rice channels have been analyzed in [19]. However, the Nakagami-*m* process is considered to be a more general channel model as compared to the Rice and Rayleigh channel models. Hence, to generalize all the aforementioned works in the regime of multihop communication, the authors of [10] have presented the statistical analysis of the $N*$Nakagami-*m* model (i.e., a product of N Nakagami-*m* processes). Moreover, second order statistics for the double Nakagami-*m* process can be found in [26]. Though a lot of papers have been published in the literature employing the cascaded fading channel model, the statistical properties of the capacity of double Nakagami-*m* channels have not been investigated so far, which finds applications both in keyhole channels and dualhop communication systems [26].

In this article, we present the statistical properties of the capacity of double Nakagami-*m* channels. Specifically, the influence of the severity of fading on the statistical properties of the capacity of double Nakagami-*m* channels is analyzed. We have derived exact analytical expressions for the PDF, CDF, LCR, and ADF of the channel capacity. Here, the LCR and ADF of the channel capacity are important characteristic quantities which provide insight into the temporal behavior of the channel capacity [6], [8]. Our analysis has revealed that if the fading severity in one

or both links of double Nakagami-*m* channels decreases (i.e., increasing the value of the severity parameter *m* in one or both of the cascaded Nakagami-*m* processes), the mean channel capacity increases, while the ADF of the channel capacity decreases. Moreover, this effect results in an increase in the LCR of the channel capacity at lower signal levels.

The rest of the paper is organized as follows. Section II briefly describes the double Nakagami-*m* channel model and some of its statistical properties. In Section III, the statistical properties of the capacity of double Nakagami-*m* channels are presented. Numerical results are analyzed in Section IV. Finally, the concluding remarks are given in Section V.

II. The Double Nakagami-*m* Channel Model

A typical example of the transmission link from the SMS to the DMS via a mobile relay (MR) in an amplify-and-forward relay-based dualhop communication system is depicted in Fig. F.1. In such a scenario, the channel between the SMS and the DMS via an MR can be represented as a concatenation of the SMS-MR and MR-DMS channels [23, 16]. In this article, we have assumed that the fading in the SMS-MR link and the MR-DMS link is characterized by Nakagami-*m* processes denoted by $\chi_1(t)$ and $\chi_2(t)$, respectively. Hence, the overall fading channel describing the SMS-DMS link can be modeled as a double Nakagami-*m* process given by [11, 26]

$$\Xi(t) = A_{\text{MR}}\,\chi_1(t)\chi_2(t) \tag{1}$$

where A_{MR} is a real positive constant representing the relay gain. For the case of keyhole channels, A_{MR} equals unity. The PDF $p_{\chi_i}(z)$ of the Nakagami-*m* process $\chi_i(t)$ $(i = 1,2)$ is given by [14]

$$p_{\chi_i}(z) = \frac{2m_i^{m_i} z^{2m_i-1}}{\Gamma(m_i)\Omega_i^{m_i}} e^{-\frac{m_i z^2}{\Omega_i}},\ z \geq 0 \tag{2}$$

where $\Omega_i = E\left\{\chi_i^2(t)\right\}$, $m_i = \Omega_i^2 \left/ \text{Var}\left\{\chi_i^2(t)\right\}\right.$, and $\Gamma(\cdot)$ represents the gamma function [7]. The parameter m_i controls the severity of the fading. Increasing the value of m_i, decreases the severity of fading and vice versa.

The PDF of double Nakagami-*m* processes $\Xi(t)$ is given by [10]

$$p_{\Xi}(z) = \frac{4z^{m_1+m_2-1}}{\prod_{i=1}^{2}\Gamma(m_i)\left(\acute{\Omega}_i \left/ m_i\right.\right)^{(m_1+m_2)/2}} K_{m_1-m_2}\left(2z\prod_{i=1}^{2}\sqrt{\frac{m_i}{\acute{\Omega}_i}}\right),\ z \geq 0 \tag{3}$$

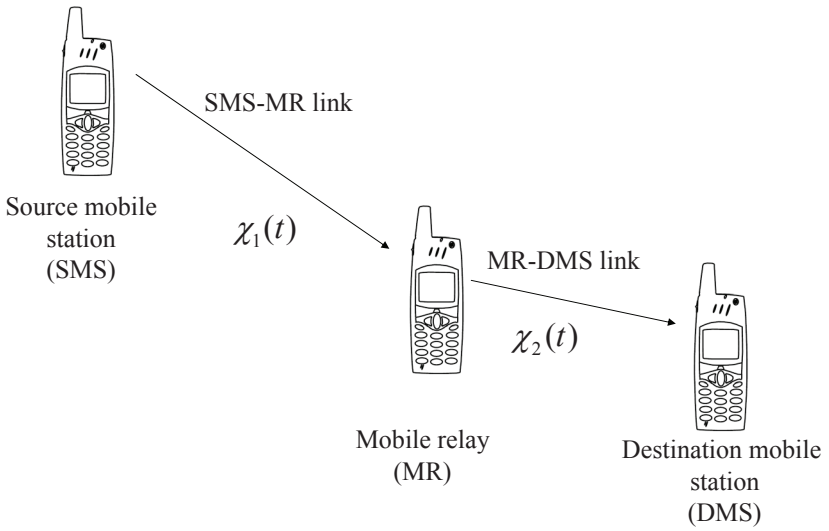

Figure F.1: The propagation scenario describing double Nakagami-*m* fading channels.

where $\acute{\Omega}_1 = A_{\text{MR}}^2 \Omega_1$, $\acute{\Omega}_2 = \Omega_2$, and $K_n(\cdot)$ denotes the modified Bessel function of the second kind of order n [7, Eq. (8.432/1)]. In order to derive the expressions for the PDF, CDF, LCR, and ADF of the capacity of double Nakagami-*m* channels, we need the joint PDF $p_{\Xi^2\dot{\Xi}^2}(z,\dot{z})$ of the squared process $\Xi^2(t)$ and its time derivative $\dot{\Xi}^2(t)$, as well as the PDF $p_{\Xi^2}(z)$ of $\Xi^2(t)$. The joint PDF $p_{\Xi^2\dot{\Xi}^2}(z,\dot{z})$ can be found by following the procedure presented in [26] for the joint PDF $p_{\Xi\dot{\Xi}}(z,\dot{z})$ and then by using the concept of transformation of random variables [15, Eq. (7-8)], which results in

$$\begin{aligned} p_{\Xi^2\dot{\Xi}^2}(z,\dot{z}) &= \frac{1}{4z}\, p_{\Xi\dot{\Xi}}(\sqrt{z}, \frac{\dot{z}}{2\sqrt{z}}) \\ &= \frac{z^{m_2-3/2}}{\sqrt{2\pi}} \left[\prod_{i=1}^{2} \frac{m_i^{m_i}}{\acute{\Omega}_i^{m_i}\Gamma(m_i)}\right] \int_0^\infty \frac{x^{2m_1-2m_2-1}}{\sqrt{\frac{z\beta_1}{x^2}+x^2\beta_2}}\, e^{-\frac{zm_2}{x^2\Omega_2}}\, e^{-\left(\frac{\dot{z}^2}{8z\left(\frac{z\beta_1}{x^2}+x^2\beta_2\right)}+\frac{x^2 m_1}{\Omega_1}\right)} dx, \\ & \qquad\qquad z \geq 0, |\dot{z}| < \infty \end{aligned} \tag{4}$$

where

$$\beta_1 = \frac{\acute{\Omega}_1 \pi^2}{m_1}\left(f_{\max_1}^2 + f_{\max_2}^2\right) \tag{5a}$$

and

$$\beta_2 = \frac{\acute{\Omega}_2 \pi^2}{m_2}\left(f_{\max_2}^2 + f_{\max_3}^2\right). \tag{5b}$$

Here, $f_{\max_1}$, $f_{\max_2}$, and $f_{\max_3}$ represent the maximum Doppler frequencies of the SMS, MR, and DMS, respectively. The expression for the PDF $p_{\Xi^2}(z)$ can be obtained by integrating the joint PDF $p_{\Xi^2\dot{\Xi}^2}(z,\dot{z})$ over $\dot{z}$. Alternatively, the PDF $p_{\Xi^2}(z)$ can also be found from the PDF $p_{\Xi}(z)$ in (3) using the relationship $p_{\Xi^2}(z) = \left(1\big/2\sqrt{z}\right) p_{\Xi}(\sqrt{z})$.

III. Statistical Properties of the Capacity of Double Nakagami-*m* Channels

The instantaneous capacity $C(t)$ of double Nakagami-*m* channels is defined as [13]

$$\begin{aligned} C(t) &= \frac{1}{2}\log_2\left(1+\gamma_s\left|\Xi(t)\right|^2\right) \\ &= \frac{1}{2}\log_2\left(1+\gamma_s\,\Xi^2(t)\right) \text{ (bits/sec/Hz)} \end{aligned} \tag{6}$$

where γ_s denotes the average received signal-to-noise ratio (SNR) at the DMS. The factor $1\big/2$ in (6) is due to the fact that the MR in Fig. F.1 operates in a half-duplex mode, and hence the signal transmitted from the SMS is received at the DMS in two time slots. Equation (6) can be considered as a mapping of a random process $\Xi(t)$ to another random process $C(t)$. Hence, the expressions for the statistical properties of the channel capacity $C(t)$ can be found by using the results for the statistical properties of the process $\Xi(t)$ obtained in the previous section. The PDF $p_C(r)$ of the channel capacity $C(t)$ can be found in closed form with the help of the PDF $p_{\Xi^2}(z)$ and by applying the concept of transformation of random variables [15, Eq. (7-8)] as

$$\begin{aligned} p_C(r) &= \left(\frac{2^{2r+1}\ln(2)}{\gamma_s}\right) p_{\Xi^2}\left(\frac{2^{2r}-1}{\gamma_s}\right) \\ &= \frac{2^{2r+2}\ln(2)\left(\left(2^{2r}-1\right)\big/\gamma_s\right)^{(m_1+m_2)/2}}{\left(2^r-1\right)\prod_{i=1}^{2}\Gamma(m_i)\left(\acute{\Omega}_i\big/m_i\right)^{(m_1+m_2)/2}} K_{m_1-m_2}\left(2\sqrt{\frac{2^{2r}-1}{\gamma_s}}\prod_{i=1}^{2}\sqrt{\frac{m_i}{\acute{\Omega}_i}}\right) \end{aligned} \tag{7}$$

for $r \geq 0$. The CDF $F_C(r)$ of the channel capacity $C(t)$ can now be derived by integrating the PDF $p_C(r)$ and by making the use of relationships in [7, Eq. (9.34/3)] and [1, Eq. (26)] as

$$\begin{aligned} F_C(r) &= \int_0^r p_C(x)dx \\ &= \frac{1}{\prod_{i=1}^{2}\Gamma(m_i)} G_{1,3}^{2,1}\left[\frac{2^{2r}-1}{\gamma_s}\prod_{i=1}^{2}\left(\frac{m_i}{\acute{\Omega}_i}\right)\,\middle|\,\begin{matrix}1\\ m_1,m_2,0\end{matrix}\right],\ r\geq 0 \end{aligned} \tag{8}$$

where $G[\cdot]$ denotes the Meijer's G-function [7, Eq. (9.301)]. The LCR $N_C(r)$ of the channel capacity describes the average rate of up-crossings (or down-crossings) of the capacity through a certain threshold level r. In order to find the LCR $N_C(r)$, we first need to find the joint PDF $p_{C\dot{C}}(z,\dot{z})$ of $C(t)$ and its time derivative $\dot{C}(t)$. The joint PDF $p_{C\dot{C}}(z,\dot{z})$ can be obtained by using the joint PDF $p_{\Xi^2\dot{\Xi}^2}(z,\dot{z})$ given in (4) as

$$\begin{aligned} p_{C\dot{C}}(z,\dot{z}) &= \left(\frac{2^{2z+1}\ln(2)}{\gamma_s}\right)^2 p_{\Xi^2\dot{\Xi}^2}\left(\frac{2^{2z}-1}{\gamma_s},\frac{2\dot{z}\ln(2)}{\gamma_s/2^{2z}}\right) \\ &= \frac{\left(2^{2z+1}\ln(2)\right)^2\left(2^{2z}-1\right)^{m_2-\frac{3}{2}}}{\sqrt{2\pi\gamma_s}\,\gamma_s^{m_2}\left[\prod_{i=1}^{2}\left(\frac{\acute{\Omega}_i}{m_i}\right)^{m_i}\Gamma(m_i)\right]}\int_0^\infty \frac{x^{2m_1-2m_2-1}}{\sqrt{\frac{\left(2^{2z}-1\right)\beta_1}{\gamma_s x^2}+x^2\beta_2}} e^{-\left(\frac{x^2 m_1}{\acute{\Omega}_1}+\frac{\left(2^{2z}-1\right)m_2}{\gamma_s x^2\acute{\Omega}_2}\right)} \\ &\qquad \times e^{-\left(\frac{\left(2^{2z+1}\ln(2)\dot{z}\right)^2}{8\gamma_s\left(2^{2z}-1\right)\left(\frac{\left(2^{2z}-1\right)\beta_1}{\gamma_s x^2}+x^2\beta_2\right)}\right)} dx,\ \ z\geq 0, |\dot{z}|<\infty. \end{aligned} \tag{9}$$

Finally, the LCR $N_C(r)$ can be found as follows

$$\begin{aligned} N_C(r) &= \int_0^\infty \dot{z}\, p_{C\dot{C}}(r,\dot{z})d\dot{z} \\ &= \sqrt{\frac{8}{\pi}}\left(\frac{2^{2r}-1}{\gamma_s}\right)^{m_2-\frac{1}{2}}\left[\prod_{i=1}^{2}\frac{m_i^{m_i}}{\acute{\Omega}_i^{m_i}\Gamma(m_i)}\right]\int_0^\infty \frac{e^{-\frac{\left(2^{2r}-1\right)m_2}{\gamma_s x^2\acute{\Omega}_2}}e^{-\frac{x^2 m_1}{\acute{\Omega}_1}}}{x^{1+2m_2-2m_1}} \\ &\qquad \times\sqrt{\frac{\left(2^{2r}-1\right)\beta_1}{\gamma_s x^2}+x^2\beta_2}\, dx,\ \ r\geq 0. \end{aligned} \tag{10}$$

The ADF $T_C(r)$ of the channel capacity $C(t)$ denotes the average duration of time over which the capacity is below a given level r [8, 9]. The ADF $T_C(r)$ of the channel capacity can be expressed as [9]

$$T_C(r) = \frac{F_C(r)}{N_C(r)} \tag{11}$$

where $F_C(r)$ and $N_C(r)$ are given by (8) and (10), respectively.

IV. Numerical Results

In this section, we will discuss the analytical results obtained in the previous section. The validity of the theoretical results is confirmed with the help of simulations. For comparison purposes, we have also shown the results for double Rayleigh channels,

which represent a special case of double Nakagami-*m* channels. In order to generate Nakagami-*m* processes $\chi_i(t)$, we have used the following relationship [25]

$$\chi_i(t) = \sqrt{\sum_{l=1}^{2\times m_i} \mu_{i,l}^2(t)} \tag{12}$$

where $\mu_{i,l}(t)$ $(l = 1,2,...,2m_i;\, i = 1,2)$ are the underlying independent and identically distributed (i.i.d.) Gaussian processes, and m_i is the parameter of the Nakagami-*m* distribution associated with the *i*th link of the dualhop communication systems. The Gaussian processes $\mu_{i,l}(t)$, each with zero mean and variances σ_0^2, were simulated using the sum-of-sinusoids model [17]. The model parameters were computed using the generalized method of exact Doppler spread (GMEDS_1) [18]. The number of sinusoids for the generation of Gaussian processes $\mu_{i,l}(t)$ was chosen to be $N = 29$. The parameter Ω_i was chosen to be equal to $2m_i\sigma_0^2$. Unless stated otherwise, the values of the maximum Doppler frequencies $f_{\max_1}$, $f_{\max_2}$, and $f_{\max_3}$ were taken to be 0, 91, and 125 Hz, respectively. The SNR γ_s was set to 15 dB. The parameters A_{MR} and σ_0 were chosen to be unity. Finally, using (12), (1), and (6), the simulation results for the statistical properties of the channel capacity were found.

The PDF and CDF of the channel capacity of double Nakagami-*m* channels are presented in Figs. F.2 and F.3, respectively. Both figures illustrate the fact that increasing the value of the severity parameter m_i (i.e., a decrease in the level of the severity of fading) in one or both links of the double Nakagami-*m* channels results in an increase in the mean channel capacity. This result is specifically presented in Fig. F.4, where the mean channel capacity is studied for different values of the severity parameter m_i $(i = 1,2)$. It can also be seen that double Rayleigh channels $(m_i = 1;\, i = 1,2)$ have a lower mean channel capacity as compared to the mean channel capacity of double Nakagami-*m* channels $(m_i = 2;\, i = 1,2)$. Moreover, it can also be observed from Figs. F.2 and F.3 that increasing the value of the severity parameter m_i decreases the variance of the channel capacity.

Figure F.5 presents the LCR $N_C(r)$ of the capacity $C(t)$ of double Nakagami-*m* channels. It is observed that an increase in the level of severity of fading in one or both links of double Nakagami-*m* channels increases the LCR $N_C(r)$ of the channel capacity at low levels r. Hence, at low levels r, the LCR $N_C(r)$ of the capacity of double Rayleigh channels $(m_i = 1;\, i = 1,2)$ is higher as compared to that of double Nakagami-*m* channels $(m_i = 2;\, i = 1,2)$. However, the converse statement is true for higher levels r. The ADF of the capacity of double Nakagami-*m* channels is shown in Fig. F.6. It is evident from this figure that the ADF of the capacity decreases with

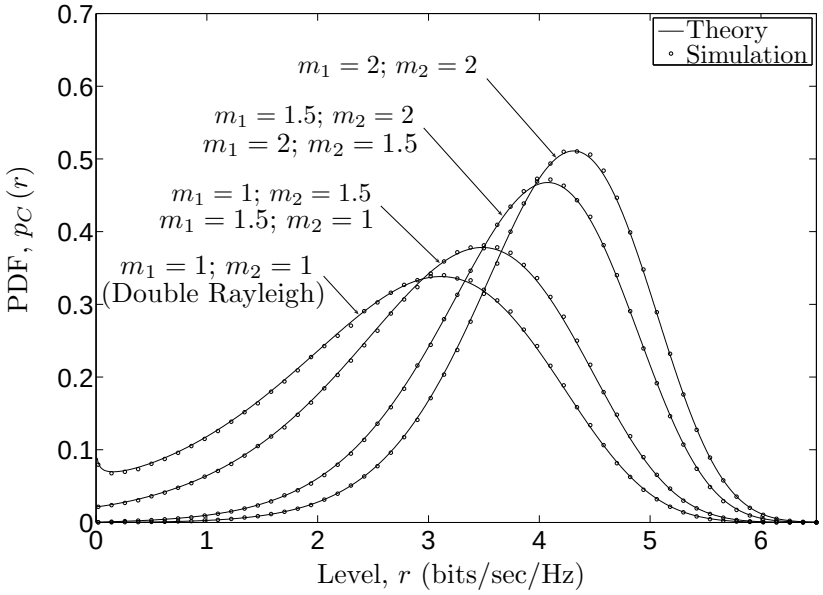

Figure F.2: The PDF $p_C(r)$ of the capacity of double Nakagami-*m* channels.

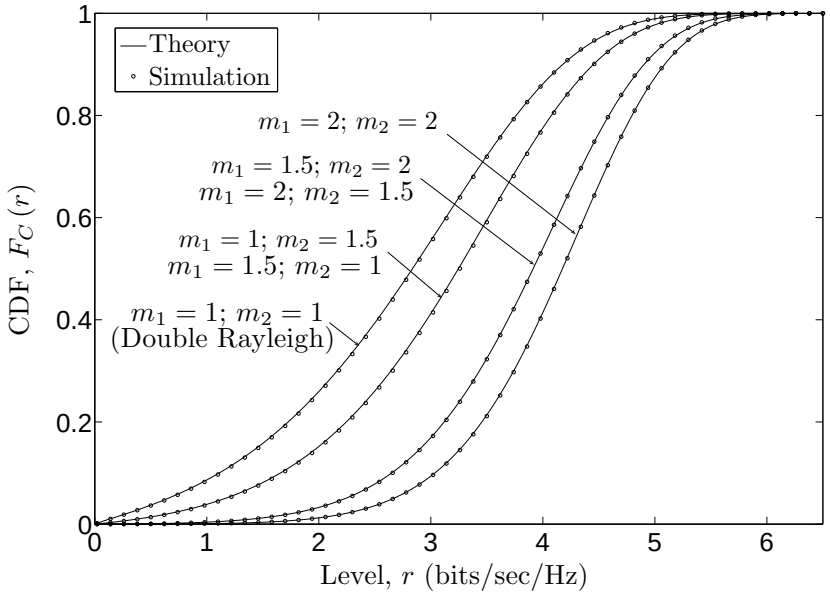

Figure F.3: The CDF $F_C(r)$ of the capacity of double Nakagami-*m* channels.

an increase in the value of the severity parameter m_i $(i = 1, 2)$.

Figures F.7 and F.8 study the influence of the maximum Doppler frequencies of the MR and the DMS on the LCR and ADF of the channel capacity. It can clearly be observed in Figs. F.7 and F.8 that the LCR and ADF are strongly dependent on the Doppler frequencies of the MR and the DMS. This means that the mobility of the MR and the DMS has a significant influence on the LCR and ADF of the channel capacity. It is observed that increasing the maximum Doppler frequencies $f_{\max_2}$ and

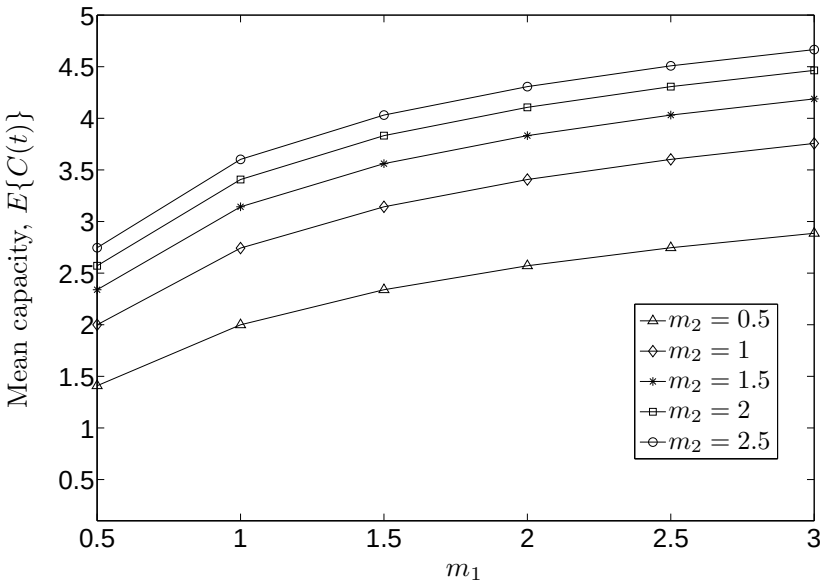

Figure F.4: The mean channel capacity of double Nakagami-*m* channels for different levels of fading severity.

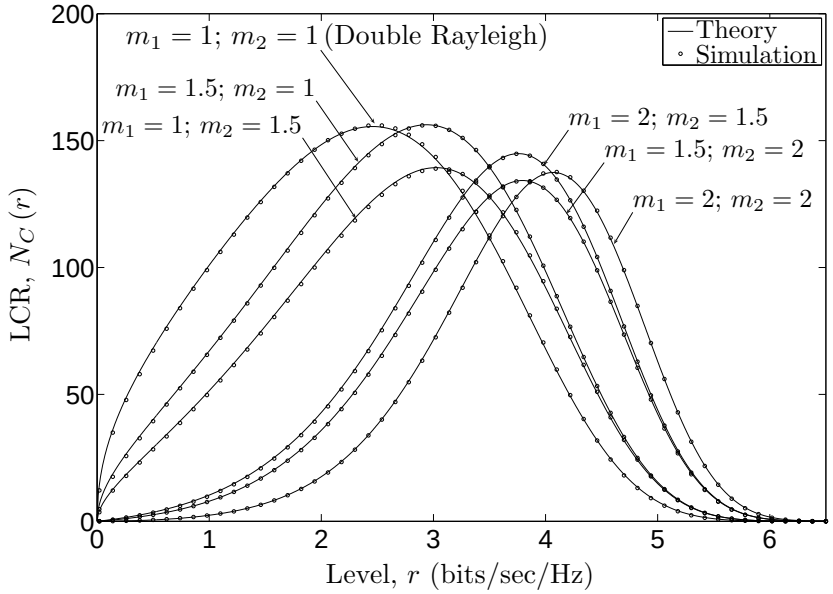

Figure F.5: The LCR $N_C(r)$ of the capacity of double Nakagami-*m* channels.

$f_{\max_3}$ results in a significant increase in the LCR. However, the ADF decreases by increasing the maximum Doppler frequencies of the MR and the DMS.

V. Conclusion

This article presents the derivation of exact analytical expressions for the statistical properties of the capacity of double Nakagami-*m* channels, which finds applications

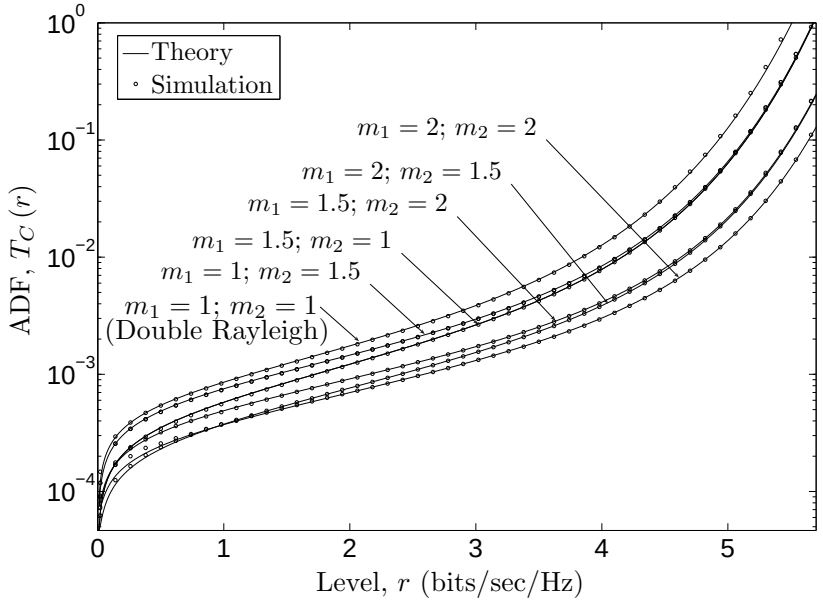

Figure F.6: The ADF $T_C(r)$ of the capacity of double Nakagami-*m* channels.

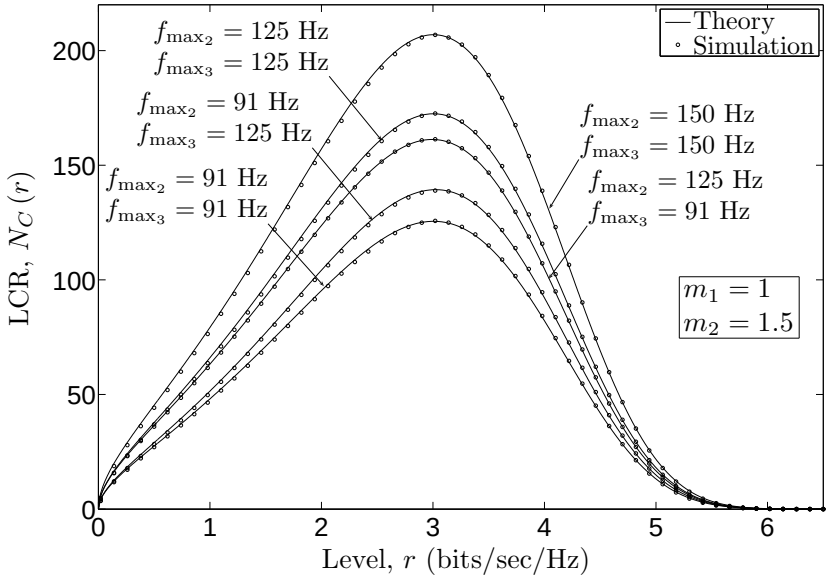

Figure F.7: The LCR $N_C(r)$ of the capacity of double Nakagami-*m* channels.

in cooperative networks and keyhole channels. We have studied the influence of the severity of fading on the PDF, CDF, LCR, and ADF of the channel capacity. It is observed that an increase in the severity of fading in one or both links of double Nakagami-*m* channels decreases the mean channel capacity, while it results in an increase in the ADF of the channel capacity. Moreover, at lower signal levels, this effects increases the LCR of the channel capacity. Results also show that the mobility of the MR and DMS has a significant influence on the LCR and ADF of the

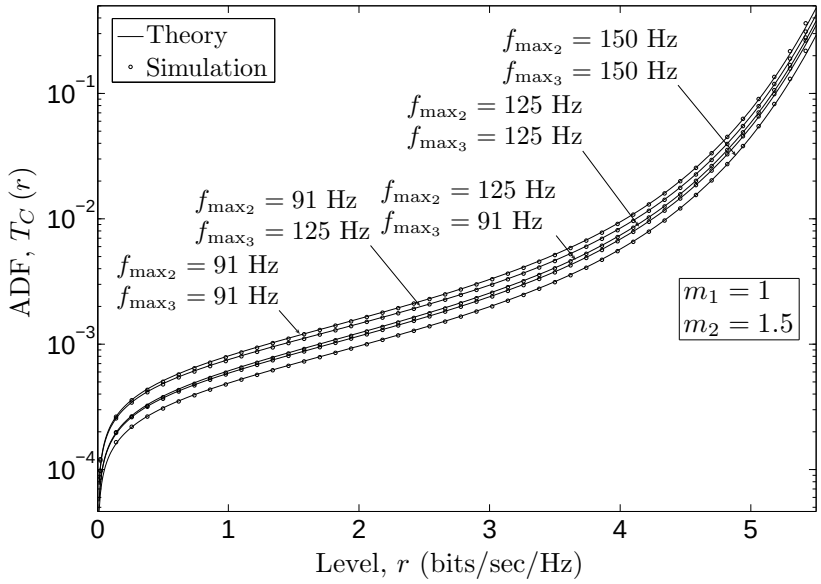

Figure F.8: The ADF $T_C(r)$ of the capacity of double Nakagami-*m* channels.

channel capacity. Specifically, an increase in the maximum Doppler frequencies of the MR and DMS increases the LCR, while it has an opposite influence on the ADF of the channel capacity. The presented exact results are validated with the help of simulations, whereby a very good fitting is observed.

VI. Acknowledgment

The contribution of G. Rafiq and Prof. M. Pätzold in this paper was partially supported by the Research Council of Norway (NFR) through the project 176773/S10 entitled “Optimized Heterogeneous Multiuser MIMO Networks – OptiMO”.

The contribution of Dr. B. O. Hogstad was partially supported by the Spanish Ministry of Education and Science as well as by the European Regional Development Fund through the program CONSOLIDER-INGENIO 2010 CSD2008-00010 COMONSES.

References

[1] V. S. Adamchik and O. I. Marichev. The algorithm for calculating integrals of hypergeometric type functions and its realization in REDUCE system. In *Proc. Int. Symp. Symbolic and Algebraic Computation, ISSAC ’90*, pages 212–224. Tokyo, Japan, 1990.

[2] J. B. Andersen. Statistical distributions in mobile communications using multiple scattering. In *Proc. 27th URSI General Assembly*. Maastricht, Netherlands, August 2002.

[3] D. Chizhik, G. J. Foschini, M. J. Gans, and R. A. Valenzuela. Keyholes, correlations, and capacities of multielement transmit and receive antennas. *IEEE Trans. Wireless Commun.*, 1(2):361–368, April 2002.

[4] V. Ercerg, S. J. Fortune, J. Ling, A. J. Rustako Jr., and R. A. Valenzuela. Comparison of a computer-based propagation prediction tool with experimental data collected in urban microcellular environment. *IEEE J. Select. Areas Commun.*, 15(4):677–684, May 1997.

[5] D. Gesbert, H. Bölcskei, D. A. Gore, and A. J. Paulraj. Outdoor MIMO wireless channels: Models and performance prediction. *IEEE Trans. Wireless Commun.*, 50(12):1926–1934, December 2002.

[6] A. Giorgetti, P. J. Smith, M. Shafi, and M. Chiani. MIMO capacity, level crossing rates and fades: The impact of spatial/temporal channel correlation. *J. Commun. Net.*, 5(2):104–115, June 2003.

[7] I. S. Gradshteyn and I. M. Ryzhik. *Table of Integrals, Series, and Products*. New York: Academic Press, 6th edition, 2000.

[8] B. O. Hogstad and M. Pätzold. Capacity studies of MIMO models based on the geometrical one-ring scattering model. In *Proc. 15th IEEE Int. Symp. on Personal, Indoor and Mobile Radio Communications, PIMRC 2004*, volume 3, pages 1613–1617. Barcelona, Spain, September 2004.

[9] B. O. Hogstad and M. Pätzold. Exact closed-form expressions for the distribution, level-crossing rate, and average duration of fades of the capacity of MIMO channels. In *Proc. 65th Semiannual Vehicular Technology Conference, IEEE VTC 2007-Spring*, pages 455–460. Dublin, Ireland, April 2007.

[10] G. K. Karagiannidis, N. C. Sagias, and P. T. Mathiopoulos. $N*$Nakagami: A novel stochastic model for cascaded fading channels. *IEEE Trans. Commun.*, 55(8):1453–1458, August 2007.

[11] I. Z. Kovacs, P. C. F. Eggers, K. Olesen, and L. G. Petersen. Investigations of outdoor-to-indoor mobile-to-mobile radio communication channels. In *Proc. IEEE 56th Veh. Technol. Conf., VTC'02-Fall*, pages 430–434. Vancouver BC, Canada, September 2002.

[12] J. N. Laneman, D. N. C. Tse, and G. W. Wornell. Cooperative diversity in wireless networks: Efficient protocols and outage behavior. *IEEE Trans. Inform. Theory*, 50(12):3062–3080, December 2004.

[13] R. U. Nabar, H. Bölcskei, and F. W. Kneubühler. Fading relay channels: Performance limits and space-time signal design. *IEEE J. Select. Areas Commun.*, 22:1099–1109, August 2004.

[14] M. Nakagami. The *m*-distribution: A general formula of intensity distribution of rapid fading. In W. G. Hoffman, editor, *Statistical Methods in Radio Wave Propagation*. Oxford, UK: Pergamon Press, 1960.

[15] A. Papoulis and S. U. Pillai. *Probability, Random Variables and Stochastic Processes*. New York: McGraw-Hill, 4th edition, 2002.

[16] C. S. Patel, G. L. Stüber, and T. G. Pratt. Statistical properties of amplify and forward relay fading channels. *IEEE Trans. Veh. Technol.*, 55(1):1–9, January 2006.

[17] M. Pätzold. *Mobile Fading Channels*. Chichester: John Wiley & Sons, 2002.

[18] M. Pätzold, C. X. Wang, and B. O. Hogstad. Two new sum-of-sinusoids-based methods for the efficient generation of multiple uncorrelated Rayleigh fading waveforms. *IEEE Trans. Wireless Commun.*, 8(6):3122–3131, June 2009.

[19] G. Rafiq and M. Pätzold. On the statistical properties of the capacity of amplify-and-forward channels under LOS conditions. In *Proc. IEEE 11th Int. Conf. Communication Systems, IEEE ICCS 2008*, pages 1614–1619. Guangzhou, China, November 2008.

[20] J. Salo, H. M. El-Sallabi, and P. Vainikainen. Impact of double-Rayleigh fading on system performance. In *Proc. 1st IEEE Int. Symp. on Wireless Pervasive Computing, ISWPC 2006*. Phuket, Thailand, January 2006.

[21] A. Sendonaris, E. Erkip, and B. Aazhang. User cooperation diversity—Part I: System description. *IEEE Trans. Commun.*, 51(11):1927–1938, November 2003.

[22] H. Shin and J. H. Lee. Performance analysis of space-time block codes over keyhole Nakagami-*m* fading channels. *IEEE Trans. Veh. Technol.*, 53(2):351–362, March 2004.

[23] B. Talha and M. Pätzold. On the statistical properties of double Rice channels. In *Proc. 10th International Symposium on Wireless Personal Multimedia Communications, WPMC 2007*, pages 517–522. Jaipur, India, December 2007.

[24] Z. H. Velkov, N. Zlatanov, and G. K. Karagiannidis. On the second order statistics of the multihop Rayleigh fading channel. *IEEE Trans. Commun.*, 57(6):1815–1823, June 2009.

[25] M. D. Yacoub, J. E. V. Bautista, and L. G. de Rezende Guedes. On higher order statistics of the Nakagami-*m* distribution. *IEEE Trans. Veh. Technol.*, 48(3):790–794, May 1999.

[26] N. Zlatanov, Z. H. Velkov, and G. K. Karagiannidis. Level crossing rate and average fade duration of the double Nakagami-*m* random process and application in MIMO keyhole fading channels. *IEEE Communications Letters*, 12(11):822–824, November 2008.

Appendix G

Paper VII

Title:	On the First and Second Order Statistics of the Capacity of $N*$Nakagami-m Channels
Authors:	**Gulzaib Rafiq**[1], Bjørn Olav Hogstad[2], and Matthias Pätzold[1]
Affiliations:	[1]University of Agder, Faculty of Engineering and Science, P. O. Box 509, NO-4898 Grimstad, Norway [2]CEIT and Tecnun, University of Navarra, Manuel de Lardizábal 15, 20018, San Sebastián, Spain
Journal:	to be submitted for publication.

On the First and Second Order Statistics of the Capacity of *N*∗Nakagami-*m* Channels

Gulzaib Rafiq[1], Bjørn Olav Hogstad[2], and Matthias Pätzold[1]
[1]Department of Information and Communication Technology
Faculty of Engineering and Science, University of Agder
Servicebox 509, NO-4898 Grimstad, Norway
E-mails: {gulzaib.rafiq, matthias.paetzold}@uia.no
[2]CEIT and Tecnun, University of Navarra
Manuel de Lardizábal 15, 20018, San Sebastián, Spain
Email: bohogstad@ceit.es

***Abstract* — This article deals with the derivation and analysis of the statistical properties of the capacity of *N*∗Nakagami-*m* channels, which has been recently introduced as a suitable stochastic model for multihop fading channels. We have derived exact analytical expressions for the probability density function (PDF), cumulative distribution function (CDF), level-crossing rate (LCR), and average duration of fades (ADF) of the capacity of *N*∗Nakagami-*m* channels. For large number of multihops, we have studied the first order statistics of the capacity by assuming that the fading amplitude of the channel can be modeled as a lognormal process. Furthermore, an accurate closed-form approximation has been derived for the LCR of the capacity. The results are studied for different values of the number of hops as well as for different values of the Nakagami parameters, controlling the severity of fading in different links of the multihop communication system. The results show that an increase in the number of hops or the severity of fading decreases the mean channel capacity, while the ADF of the channel capacity increases. Moreover, an increase in the severity of fading or the number of hops decreases the LCR of the capacity of Nakagami-*m* channels at higher levels. The converse statement is true for lower levels. The presented results provide an insight into the influence of the number of hops and the severity of fading on the channel capacity, and hence they are very useful for the design and performance analysis of the multihop communication systems.**

Index Terms—Multihop communication systems, channel capacity, probability density function, cumulative distribution function, level-crossing rate, average duration of fades.

I. INTRODUCTION

Multihop communication systems fall under the category of cooperative diversity systems, in which the intermediate wireless network nodes assist each other by relaying the information from the source mobile station (SMS) to the destination mobile station (DMS) [26, 30, 18]. This kind of communication scheme promises an increased network coverage, enhanced mobility, and improved system performance. It has applications in wireless local area networks (WLANs) [10], cellular networks [27], ad-hoc networks [1, 2], and hybrid networks [6]. Based on the amount of signal processing used for relaying the received signal, the relays can generally be classified into two types, namely amplify-and-forward (or non-regenerative) relays [11, 12] and decode-and-forward (or regenerative) relays [8]. The relay nodes in multihop communication systems can further be categorized into channel state information (CSI) assisted relays [4], which employ the CSI to calculate the relay gains and blind relays with fixed relay gains [16].

In order to characterize the fading in the end-to-end link between the SMS and the DMS in a multihop communication system with N hops, the authors in [17] have proposed the $N*$Nakagami-m channel model, assuming that the fading in each link between the wireless nodes can be modeled by a Nakagami-m process. The second order statistical properties of multihop Rayleigh fading channels have been studied in[28], while for dualhop Nakagami-m channels, the second order statistics of the received signal envelope has been analyzed in [32]. Moreover, the performance analysis of multihop communication systems for different kinds of relaying can be found in [5, 16, 11, 12] and the multiple references therein. In [25], the authors analyzed the statistical properties of the capacity of dualhop Rice channels employing amplify-and-forward based blind relays. An extension of the work in [25] to the case of dualhop Nakagami-m channels has been presented in [24]. The ergodic capacity of multihop Rayleigh fading channels has been studied in [7, 8]. Though a lot of papers have been published in the literature dealing with the performance and analysis of multihop communication systems, the statistical properties of the capacity of $N*$Nakagami-m channels have not been investigated so far. The aim of this article is to fill in this gap of information.

In this paper, the statistical properties of the capacity of $N*$Nakagami-m channels are analyzed. The mean and the variance of the channel capacity are studied with the help of the PDF of the channel capacity. To provide an insight into the temporal behavior of the channel capacity, we also investigate the LCR and the ADF of the channel capacity. The LCR of the channel capacity describes the average rate of up-crossings (or down-crossings) of the capacity through a certain threshold

level. The ADF of the channel capacity denotes the average duration of time over which the capacity is below a given level [13, 14]. By using a feedback channel, the statistical properties of the channel capacity can be useful for the transmitter to determine the right modulation, coding, and power to maximize the amount of information that can be transmitted over the wireless channel [19].

The rest of the paper is organized as follows. In Section II, we briefly describe the *N*∗Nakagami-*m* channel model and some of its statistical properties. Section III presents the statistical properties of the capacity of *N*∗Nakagami-*m* channels. A study on the first order statical properties of the channel capacity for large number of hops *N* is presented in Section IV. The analysis of the obtained results is carried out in Section V. The concluding remarks are finally stated in Section VI.

II. The *N*∗Nakagami-*m* Channel Model

Amplify-and-forward relay-based multihop communication systems consist of an SMS, a DMS, and $N-1$ blind mobile relays MR_n $(n = 1,2,\ldots,N-1)$, as depicted in Fig. G.1. In this article, we have assumed that the fading in the SMS–MR_1 link, MR_n–MR_{n+1} $(n = 1,2,\ldots,N-2)$ links, and the MR_{N-1}–DMS link is characterized by independent but not necessarily identical Nakagami-*m* processes denoted by $\chi_1(t)$, $\chi_{n+1}(t)$ $(n = 1,2,\ldots,N-2)$, and $\chi_N(t)$, respectively. The received signal $r_n(t)$ at the *n*th mobile relay MR_n $(n = 1,2,\ldots,N-1)$ or the DMS $(n = N)$ can be expressed as [31]

$$r_n(t) = G_{n-1}\,\chi_n(t)\,r_{n-1}(t) + n_n(t) \tag{1}$$

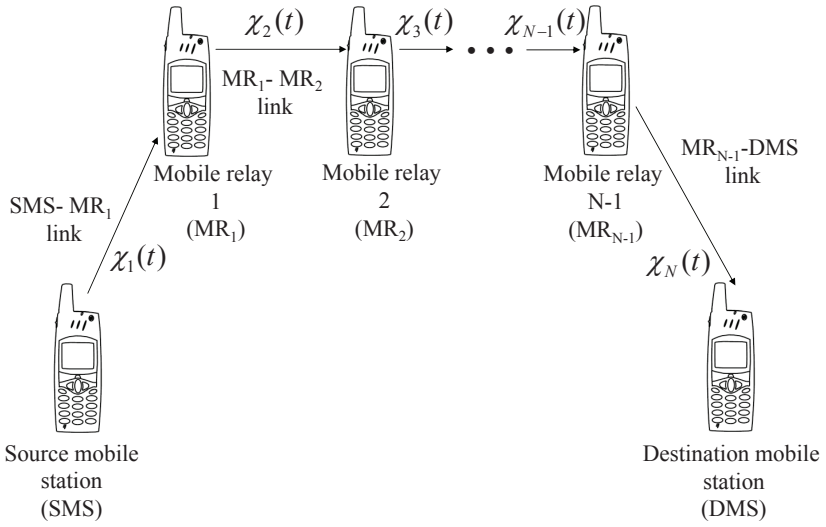

Figure G.1: The propagation scenario describing *N*∗Nakagami-*m* fading channels.

where $n_n(t)$ is the additive white Gaussian noise at the nth relay or the DMS with zero mean and variance $N_{0,n}$, G_{n-1} denotes the gain of the $(n-1)$th $(n=2,3,\ldots,N)$ relay, $r_0(t)$ represents the signal transmitted from the SMS, and G_0 equals unity. The PDF $p_{\chi_n}(z)$ of the Nakagami-m process $\chi_n(t)$ $(n=1,2,\ldots,N)$ is given by [20]

$$p_{\chi_n}(z) = \frac{2m_n^{m_n} z^{2m_n-1}}{\Gamma(m_n)\Omega_n^{m_n}} e^{-\frac{m_n z^2}{\Omega_n}}, \quad z \geq 0 \tag{2}$$

where $\Omega_n = E\left\{\chi_n^2(t)\right\}$, $m_n = \Omega_n^2 / \mathrm{Var}\left\{\chi_n^2(t)\right\}$, and $\Gamma(\cdot)$ represents the gamma function [9]. The expectation and the variance operators are denoted by $E\{\cdot\}$ and $\mathrm{Var}\{\cdot\}$, respectively. The parameter m_n controls the severity of the fading, associated with the nth link of the multihop communication system. Increasing the value of m_n, decreases the severity of fading and vice versa. The overall fading channel describing the SMS–DMS link can be modeled as a $N*$Nakagami-m process given by [17, 28]

$$\Xi(t) = \prod_{n=1}^{N} G_{n-1}\,\chi_n(t) = \prod_{n=1}^{N} \acute{\chi}_n(t) \tag{3}$$

where each of the processes $\acute{\chi}_n(t)$ $(n=1,2,\ldots,N)$ follows the Nakagami-m distribution $p_{\acute{\chi}_n}(z)$ with parameters m_n and $\acute{\Omega}_n = G_{n-1}^2\,\Omega_n$. In order to derive an expression for the received instantaneous signal-to-noise ratio (SNR) $\gamma(t)$ at the DMS, we continue as follows. The overall instantaneous signal power $S(t)$ at the DMS can be expressed as

$$S(t) = \prod_{n=1}^{N} G_{n-1}^2 \left|\chi_n(t)\right|^2. \tag{4}$$

Similarly, the instantaneous noise power $N(t)$ at the DMS can be written as

$$\begin{aligned} N(t) &= N_{0,1}\left(G_1^2 G_2^2 \cdots G_{N-1}^2\right)\left(\left|\chi_2(t)\right|^2 \left|\chi_3(t)\right|^2 \cdots \left|\chi_N(t)\right|^2\right) \\ &\quad + N_{0,2}\left(G_2^2 G_3^2 \cdots G_{N-1}^2\right)\left(\left|\chi_3(t)\right|^2 \left|\chi_4(t)\right|^2 \cdots \left|\chi_N(t)\right|^2\right) + \cdots + N_{0,N} \\ &= \sum_{n=1}^{N} N_{0,n}\left(\prod_{k=n+1}^{N} G_{k-1}^2 \left|\chi_k(t)\right|^2\right). \end{aligned} \tag{5}$$

The instantaneous SNR $\gamma(t)$ at the DMS can now be expressed as

$$\gamma(t) = \frac{S(t)}{N(t)} = \frac{\prod_{n=1}^{N} G_{n-1}^2 \left|\chi_n(t)\right|^2}{\sum_{n=1}^{N} N_{0,n}\left(\prod_{k=n+1}^{N} G_{k-1}^2 \left|\chi_k(t)\right|^2\right)}. \tag{6}$$

Dividing the numerator and the denominator in (6) by $\prod_{n=1}^{N} N_{0,n} G_{n-1}^2$ allows us to write $\gamma(t)$ as [12, Eqs. (12)–(14)]

$$\gamma(t) = \frac{\prod\limits_{n=1}^{N} \gamma_n(t)}{\sum\limits_{n=1}^{N} \left(\prod\limits_{k=n+1}^{N} \gamma_k(t) \Big/ \prod\limits_{k=1}^{n-1} N_{0,k} G_k^2 \right)} \tag{7}$$

where $\gamma_n(t) = |\chi_n(t)|^2 / N_{0,n}$ represents the instantaneous SNR at the nth relay MR_n. By expanding the denominator in (7), it can be observed that, for fixed values of the noise variance $N_{0,n}$, increasing the relay gain G_n increases the instantaneous SNR at the DMS. However, for any values of t, the value of $\gamma(t)$ is always less than or equal to $\gamma_1(t)$, representing the instantaneous SNR at the first mobile relay. This fact can easily be confirmed by choosing the value of the relay gains G_n according to $G_n = 1/\sqrt{C_n N_{0,n}}$ $(n = 1, 2, \ldots, N-1)$ [28, Eq. (35)], where C_n is a real valued constant. By substituting $G_n^2 = 1/(C_n N_{0,n})$ in (7), the resulting expression for the instantaneous SNR $\gamma(t)$ can be written in accordance with [16, Eq. (3)] as

$$\gamma(t) = \left(\frac{1}{\gamma_1(t)} + \frac{C_1}{\gamma_1(t)\gamma_2(t)} + \frac{C_1 C_2}{\gamma_1(t)\gamma_2(t)\gamma_3(t)} + \cdots + \frac{C_1 C_2 \cdots C_{N-1}}{\gamma_1(t)\gamma_2(t)\cdots\gamma_N(t)} \right)^{-1}. \tag{8}$$

Hence, as the value of G_n increases, the value of C_n decreases and thus the value of $\gamma(t)$ approaches $\gamma_1(t)$ for any values of t. In the following, for the sake of simplicity, we will assume a fixed noise power N_0 at the DMS. Hence, the instantaneous SNR at the DMS is given by

$$\gamma(t) = \frac{S(t)}{N_0}. \tag{9}$$

For the calculation of the PDF of the capacity of $N*$Nakagami-m channels, we need to find the PDF $p_{\Xi^2}(z)$ of the squared $N*$Nakagami-m process $\Xi^2(t)$. Furthermore, for the calculation of the LCR and the ADF of the capacity, we need to find an expression for the joint PDF $p_{\Xi^2\dot{\Xi}^2}(z, \dot{z})$ of the squared process $\Xi^2(t)$ and its time derivative $\dot{\Xi}^2(t)$ at the same time t. By employing the relationship $p_{\Xi^2}(z) = p_{\Xi}(\sqrt{z})/(2\sqrt{z})$ [21, Eq. (5-22)], the PDF $p_{\Xi^2}(z)$ can be expressed in terms of the PDF $p_{\Xi}(z)$ of the $N*$Nakagami-m process $\Xi(t)$ in [17, Eq. (4)] as

$$p_{\Xi^2}(z) = \frac{1}{z \prod\limits_{n=1}^{N} \Gamma(m_i)} G_{0,N}^{N,0} \left[z \prod_{n=1}^{N} \left(\frac{m_n}{\acute{\Omega}_n} \right) \middle| \begin{matrix} - \\ m_1, m_2, \ldots, m_N \end{matrix} \right], \quad z \geq 0. \tag{10}$$

In (10), $G[\cdot]$ denotes the Meijer's G-function [9, Eq. (9.301)]. By following a similar procedure presented in [28, Eqs. (12)–(15)] and by applying the concept of transformation of random variables [21, Eq. (7-8)], it can be shown that the expression for the joint PDF $p_{\Xi^2\dot{\Xi}^2}(z,\dot{z})$ under isotropic scattering conditions can be written as

$$p_{\Xi^2\dot{\Xi}^2}(z,\dot{z}) = \frac{1}{4z}\int_{x_1=0}^{\infty}\cdots\int_{x_{N-1}=0}^{\infty}\frac{p_{\frac{\dot{\Xi}}{2\sqrt{\Xi}}\left|\sqrt{\Xi}\acute{\chi}_1\cdots\acute{\chi}_{N-1}\right.}\left(\frac{\dot{z}}{2\sqrt{z}}\middle|\sqrt{z},x_1,\ldots,x_{N-1}\right)}{\prod_{n=1}^{N-1}x_n} \times p_{\acute{\chi}_N}\left(\frac{\sqrt{z}}{\prod_{n=1}^{N-1}x_n}\right)p_{\acute{\chi}_1}(x_1)\cdots p_{\acute{\chi}_{N-1}}(x_{N-1})\,dx_1\cdots dx_{N-1} \quad (11)$$

for $z \geq 0$ and $|\dot{z}| < \infty$, where

$$p_{\frac{\dot{\Xi}}{2\sqrt{\Xi}}\left|\sqrt{\Xi}\acute{\chi}_1\cdots\acute{\chi}_{N-1}\right.}\left(\frac{\dot{z}}{2\sqrt{z}}\middle|\sqrt{z},x_1,\ldots,x_{N-1}\right) = \frac{1}{\sqrt{2\pi}}\frac{e^{-\frac{\dot{z}}{8zK^2(z,x_1,\ldots,x_{N-1})}}}{K(z,x_1,\ldots,x_{N-1})} \quad (12)$$

and

$$K^2(z,x_1,\ldots,x_{N-1}) = \beta_N\left[1+\frac{z\sum_{n=1}^{N-1}\frac{\beta_n}{\beta_N x_n^2}}{\left(\prod_{n=1}^{N-1}x_n^2\right)}\right]\prod_{n=1}^{N-1}x_n^2, \quad (13a)$$

$$\beta_n = \frac{\acute{\Omega}_n\pi^2}{m_n}\left(f_{\max_n}^2+f_{\max_{n+1}}^2\right), \quad n=1,2,\ldots,N. \quad (13b)$$

Here, $f_{\max_1}$ and $f_{\max_{N+1}}$ represent the maximum Doppler frequencies of the SMS and DMS, respectively, while $f_{\max_{n+1}}$ denotes the maximum Doppler frequency of the nth mobile relay MR_n $(n=1,2,\ldots,N-1)$.

III. Statistical Properties of the Capacity of $N*$Nakagami-m Channels

The instantaneous capacity $C(t)$ of $N*$Nakagami-m channels is defined as

$$C(t) = \frac{1}{N}\log_2\left(1+\gamma_s|\Xi(t)|^2\right) = \frac{1}{N}\log_2\left(1+\gamma_s\Xi^2(t)\right) \text{ (bits/s/Hz)} \quad (14)$$

where $\gamma_s = 1/N_0$. The factor $1/N$ in (14) is due to the reason that the relays MR_n $(n=1,2,\ldots,N-1)$ in Fig. G.1 operate in a half-duplex mode, and therefore the signal transmitted from the SMS is received at the DMS in N time slots. We can consider (14) as a mapping of a random process $\Xi(t)$ to another random process

$C(t)$. Therefore, the results for the statistical properties of the process $\Xi(t)$ can be used to obtain the expressions for the statistical properties of the channel capacity $C(t)$. Again, by applying the concept of transformation of random variables, the PDF $p_C(r)$ of the channel capacity $C(t)$ can be expressed in terms of the PDF $p_{\Xi^2}(z)$ as

$$\begin{aligned} p_C(r) &= \left(\frac{N2^{Nr}\ln(2)}{\gamma_s}\right) p_{\Xi^2}\left(\frac{2^{Nr}-1}{\gamma_s}\right) \\ &= \frac{N2^{Nr}\ln(2)}{(2^{Nr}-1)\prod_{n=1}^{N}\Gamma(m_i)} G_{0,N}^{N,0}\left[\frac{2^{Nr}-1}{\gamma_s}\prod_{n=1}^{N}\left(\frac{m_n}{\acute{\Omega}_n}\right)\middle| \begin{matrix} - \\ m_1,m_2,\ldots,m_N \end{matrix}\right] \end{aligned} \quad (15)$$

for $r \geq 0$. By integrating the PDF $p_C(r)$, the CDF $F_C(r)$ of the channel capacity $C(t)$ can be obtained by making use of the relationships in [9, Eq. (9.34/3)] and [3, Eq. (26)] as

$$\begin{aligned} F_C(r) &= \int_0^r p_C(z)dz \\ &= \frac{1}{\prod_{n=1}^{N}\Gamma(m_i)} G_{1,N+1}^{N,1}\left[\frac{2^{Nr}-1}{\gamma_s}\prod_{N=1}^{N}\left(\frac{m_n}{\acute{\Omega}_n}\right)\middle| \begin{matrix} 1 \\ m_1,m_2,\ldots,m_N,0 \end{matrix}\right], \quad r \geq 0. \end{aligned} \quad (16)$$

To find the LCR, denoted by $N_C(r)$, of the capacity $C(t)$, we first need to find the joint PDF $p_{C\dot{C}}(z,\dot{z})$ of $C(t)$ and its time derivative $\dot{C}(t)$. The joint PDF $p_{C\dot{C}}(z,\dot{z})$ can be found by using the joint PDF $p_{\Xi^2\dot{\Xi}^2}(z,\dot{z})$ given in (11) and by employing the relationship $p_{C\dot{C}}(z,\dot{z}) = \left(N2^{Nz}\ln(2)/\gamma_s\right)^2 p_{\Xi^2\dot{\Xi}^2}\left((2^{Nz}-1)/\gamma_s, N2^{Nz}\dot{z}\ln(2)/\gamma_s\right)$. Finally, the LCR $N_C(r)$ can be found as follows

$$\begin{aligned} N_C(r) &= \int_0^\infty \dot{z}\, p_{C\dot{C}}(r,\dot{z})d\dot{z} \\ &= \frac{2^N\Phi}{\sqrt{2\pi}}\left(\frac{2^{Nr}-1}{\gamma_s}\right)^{m_N-\frac{1}{2}} \int_{x_1=0}^{\infty}\cdots\int_{x_{N-1}=0}^{\infty} e^{-\sum_{n=1}^{N-1}\frac{m_n x_n^2}{\acute{\Omega}_n}}\left(\prod_{n=1}^{N-1} x_n^{2(m_n-m_N)-1}\right) \\ &\quad \times K\left(\frac{2^{Nr}-1}{\gamma_s}, x_1,\ldots,x_{N-1}\right) e^{-\frac{m_N\left(2^{Nr}-1\right)}{\gamma_s\acute{\Omega}_N\prod_{n=1}^{N-1}x_n^2}} dx_1\cdots dx_{N-1}, \quad r \geq 0 \end{aligned} \quad (17)$$

where $\Phi = \prod_{n=1}^{N} m_n^{m_n} \Big/ \left(\Gamma(m_n)\acute{\Omega}_n^{m_n}\right)$. The expression for the LCR $N_C(r)$ in (25) is mathematically very complex due to multiple integrals. However, by using the

multivariate Laplace approximation theorem [15], it is shown in the Appendix that the LCR $N_C(r)$ of the channel capacity $C(t)$ can be approximated in a closed form as

$$N_C(r) \approx \frac{(2\pi)^{\frac{N}{2}}\Phi}{\pi\sqrt{N}}\left(\frac{2^{Nr}-1}{\gamma_s}\right)^{m_N-\frac{1}{2}} e^{-N\left(\frac{m_N\left(2^{Nr}-1\right)}{\widetilde{\Phi}}\right)^{\frac{1}{N}}}\left(\prod_{n=1}^{N-1}\frac{\widetilde{x}_n^{2(m_n-m_N)-1}}{\sqrt{m_n/\acute{\Omega}_n}}\right) \times K\left(\frac{2^{Nr}-1}{\gamma_s},\widetilde{x}_1,\ldots,\widetilde{x}_{N-1}\right), \quad r\geq 0 \tag{18}$$

where

$$\widetilde{\Phi} = \gamma_s\acute{\Omega}_N\prod_{n=1}^{N-1}\frac{\acute{\Omega}_n}{m_n} \tag{19a}$$

and

$$\widetilde{x}_n = \left(\frac{m_N\left(2^{Nr}-1\right)}{\widetilde{\Phi}\left(m_n/\acute{\Omega}_n\right)^N}\right)^{\frac{1}{2N}}, \quad n=1,\ldots,N-1\,. \tag{19b}$$

The ADF, denoted by $T_C(r)$, of the channel capacity can be expressed as [14]

$$T_C(r) = \frac{F_C(r)}{N_C(r)} \tag{20}$$

where $F_C(r)$ and $N_C(r)$ are given by (10) and (14), respectively.

IV. Asymptotic Analysis

In this section, we will study the PDF, CDF, mean, and variance of the capacity when the number of hops N is large. Similarly to [17], we will apply the central limit theorem of products [21] to obtain an accurate approximation for the PDF of the $N*$Nakagami-m process in (3). In the case when $N\to\infty$, we will denote the $N*$Nakagami-m process $\Xi(t)$ by $\Xi_\infty(t)$. From [17], it follows that the PDF of $\Xi_\infty(t)$ is lognormal distributed

$$p_{\Xi_\infty}(z) = \frac{1}{\sqrt{2\pi}\sigma_\infty z}e^{-\frac{1}{2\sigma_\infty^2}(\ln z-\mu_\infty)^2}, \quad z\geq 0 \tag{21}$$

where

$$\mu_\infty = \lim_{N\to\infty}\frac{1}{2}\sum_{n=1}^{N}\left[\Psi(m_n)-\ln\left(\frac{m_n}{\acute{\Omega}_n}\right)\right] \tag{22}$$

and

$$\sigma_\infty^2 = \lim_{N\to\infty}\frac{1}{4}\sum_{n=1}^{N}\Psi^{(1)}(m_n)\,. \tag{23}$$

Here, $\Psi^{(1)}(\cdot)$ is the first derivative of the Digamma function $\Psi(\cdot)$ [9, Eq. (8.360)].

In order to derive the PDF of the capacity of $N*$Nakagami-m channels, we need to find the PDF $p_{\Xi_\infty^2}(z)$ of the squared $N*$Nakagami-m process $\Xi_\infty^2(t)$. Again, by employing the relationship $p_{\Xi_\infty^2}(z) = p_{\Xi_\infty}(\sqrt{z})/(2\sqrt{z})$, the PDF $p_{\Xi_\infty^2}(z)$ can be obtained as

$$p_{\Xi_\infty^2}(z) = \frac{1}{2\sqrt{2\pi}\sigma_\infty z} e^{-\frac{1}{2\sigma_\infty^2}(\ln\sqrt{z}-\mu_\infty)^2}, \quad z \geq 0\,. \tag{24}$$

Hence, by using (24) and applying the same transformation technique presented in Section III, the PDF $p_C(t)$ of the capacity $C(t)$ can be approximated as

$$p_C(r) \approx \frac{N2^{Nr}\ln 2}{2\sqrt{2\pi}(2^{Nr}-1)\sigma_N} e^{-\frac{1}{2\sigma_N^2}\left(\ln\sqrt{\frac{2^{Nr}-1}{\gamma_s}}-\mu_N\right)^2}, \quad r \geq 0 \tag{25}$$

where μ_N and σ_N^2 are obtained from (22) and (23), respectively, by using a finite number of hops N. Furthermore, by integrating the PDF $p_C(r)$ in (25), the CDF $F_C(r)$ can be expressed as

$$\begin{aligned} F_C(r) &= \int_0^r p_C(z)dz \\ &\approx \frac{N\ln 2}{2\sqrt{2\pi}\sigma_N}\int_0^r \frac{2^{Nz}}{(2^{Nz}-1)} e^{-\frac{1}{2\sigma_N^2}\left(\ln\sqrt{\frac{2^{Nz}-1}{\gamma_s}}-\mu_N\right)^2} dz\,. \end{aligned} \tag{26}$$

Finally, the mean μ_C and the variance σ_C^2 of $C(t)$ can now be easily obtained as

$$\begin{aligned} \mu_C &= \int_0^\infty z p_C(z)\,dz \\ &\approx \frac{N\ln 2}{2\sqrt{2\pi}\sigma_N}\int_0^\infty \frac{2^{Nz}z}{2^{Nz}-1} e^{-\frac{1}{2\sigma_N^2}\left(\ln\sqrt{\frac{2^{Nz}-1}{\gamma_s}}-\mu_N\right)^2} dz \end{aligned} \tag{27}$$

and

$$\begin{aligned} \sigma_C^2 &= \int_0^\infty (z-\mu_C)^2 p_C(z)\,dz \\ &\approx \frac{N\ln 2}{2\sqrt{2\pi}\sigma_N}\int_0^\infty \frac{2^{Nz}z(z-\mu_C)^2}{2^{Nz}-1} e^{-\frac{1}{2\sigma_N^2}\left(\ln\sqrt{\frac{2^{Nz}-1}{\gamma_s}}-\mu_N\right)^2} dz \end{aligned} \tag{28}$$

respectively. In the next section, it will be shown by simulations that the approximations obtained in (25)–(28) performs well for small numbers of hops N.

V. Numerical Results

In this section, we will discuss the analytical results obtained in the previous sections. The validity of the theoretical results is confirmed with the help of simulations. For comparison purposes, we have also shown the results for Rayleigh channels ($m_n = 1$; $n = 1, 2, \ldots, N$). In order to generate Nakagami-m processes $\chi_n(t)$ for natural values of $2m_n$, the following relationship can be used [29]

$$\chi_n(t) = \sqrt{\sum_{l=1}^{2\times m_n} \mu_{n,l}^2(t)} \tag{29}$$

where $\mu_{n,l}(t)$ $(l = 1, 2, \ldots, 2m_n;\ n = 1, 2, \ldots, N)$ are the underlying independent and identically distributed (i.i.d.) Gaussian processes, and m_n is the parameter of the Nakagami-m distribution associated with the nth link of the multihop communication systems. The Gaussian processes $\mu_{n,l}(t)$, each with zero mean and variances $m_n\sigma_0^2$, were simulated using the sum-of-sinusoids model [22]. The model parameters were computed using the generalized method of exact Doppler spread (GMEDS_1) [23]. The number of sinusoids for the generation of Gaussian processes $\mu_{n,l}(t)$ was chosen to be 20. The parameter Ω_n was chosen to be equal to $2(m_n\sigma_0)^2$, the values of the maximum Doppler frequencies $f_{\max_n}$ were set to be equal to 125 Hz, and the quantity γ_s was equal to 15 dB. The parameters G_{n-1} $(n = 1, 2, \ldots, N)$ and σ_0 were chosen to be unity. Finally, using (3), (14), and (29), the simulation results for the statistical properties of the channel capacity were found.

The PDF $p_C(r)$ and the CDF $F_C(r)$ of the capacity $C(t)$ of $N*$Nakagami-m channels are presented in Figs. G.2 and G.3, respectively. Also, the approximation results obtained in (25) and (26) are shown in Figs. G.2 and G.3, respectively. Specifically, for $N = 6$ and $N = 8$, the approximation results are in a reasonable fitting with the exact results. Furthermore, it can be observed in both figures that an increase in the severity of fading (i.e., decreasing the value of the fading parameter m_n) decreases the mean channel capacity. Similarly, as the number of hops N in $N*$Nakagami-m channels increases, the mean channel capacity decreases. The influence of severity of fading and the number of hops N in a $N*$Nakagami-m channels on the mean channel capacity is specifically studied in Fig. G.4. It can also be observed that the mean capacity of multihop Rayleigh channels ($m_n = 1$; $n = 1, 2, \ldots, N$) is lower as compared to that of $N*$Nakagami-m channels ($m_n = 2$;

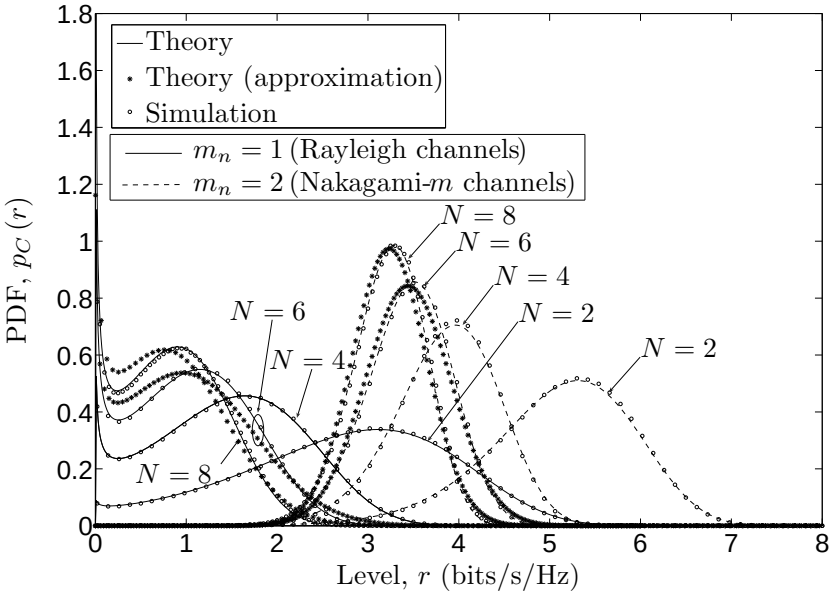

Figure G.2: The PDF of the capacity of *N*∗Nakagami-*m* channels.

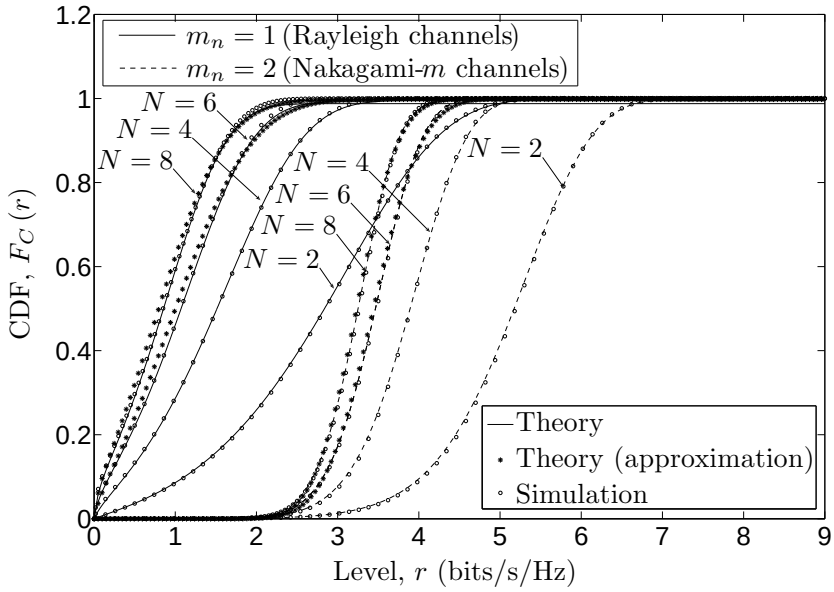

Figure G.3: The CDF of the capacity of *N*∗Nakagami-*m* channels.

$n = 1, 2, \ldots, N$). Moreover, it can also be observed from Figs. G.2 and G.3 that an increase in the value of the fading parameter m_n or the number of hops N in *N*∗Nakagami-*m* channels results in a decrease in the variance of the channel capacity. This result can easily be observed in Fig. G.5, where the variance of the capacity of *N*∗Nakagami-*m* channels is studied for different values of the fading parameter m_n and the number of hops N in *N*∗Nakagami-*m* channels. In Figs. G.4 and G.5, we have also include the approximations obtained in (27) and (28), respectively.

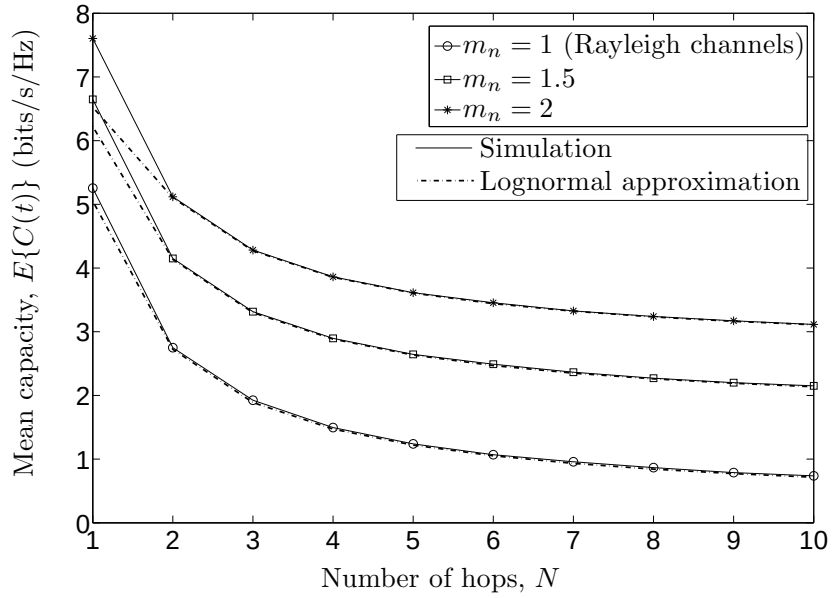

Figure G.4: The mean channel capacity of $N*$Nakagami-m channels.

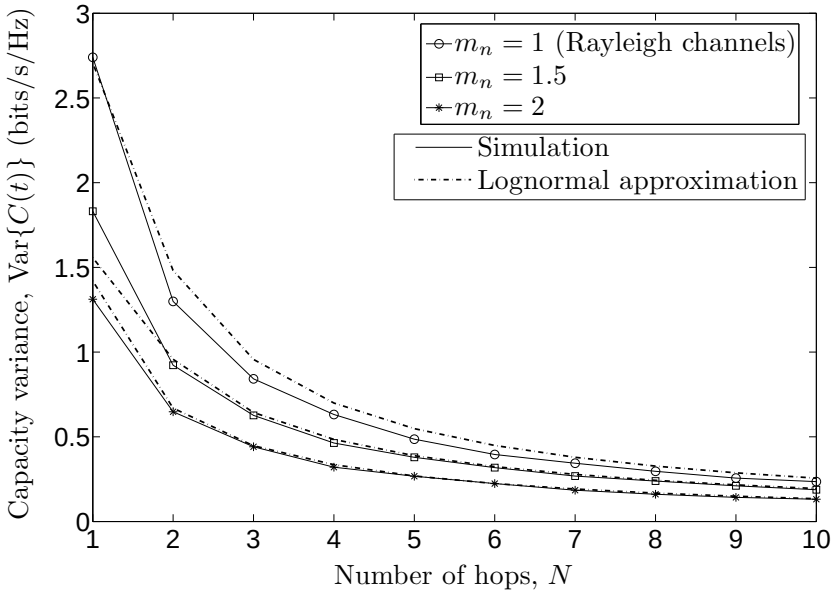

Figure G.5: The variance of the capacity of $N*$Nakagami-m channels.

The results show that as the number of hops N increase the approximation results get in a close correspondence with the exact results. In addition, a carefully study of Figs. G.2–G.5 also reveal that the approximations results given by Eqs. (25)–(28) are more closely fitted to the exact results for larger values of m_n, e.g., $m_n = 2$ $(n = 1, 2, \ldots, N)$.

Figure G.6 presents the LCR $N_C(r)$ of the capacity $C(t)$ of $N*$Nakagami-m channels. It can be observed that at lower levels r, the LCR $N_C(r)$ of the capacity of

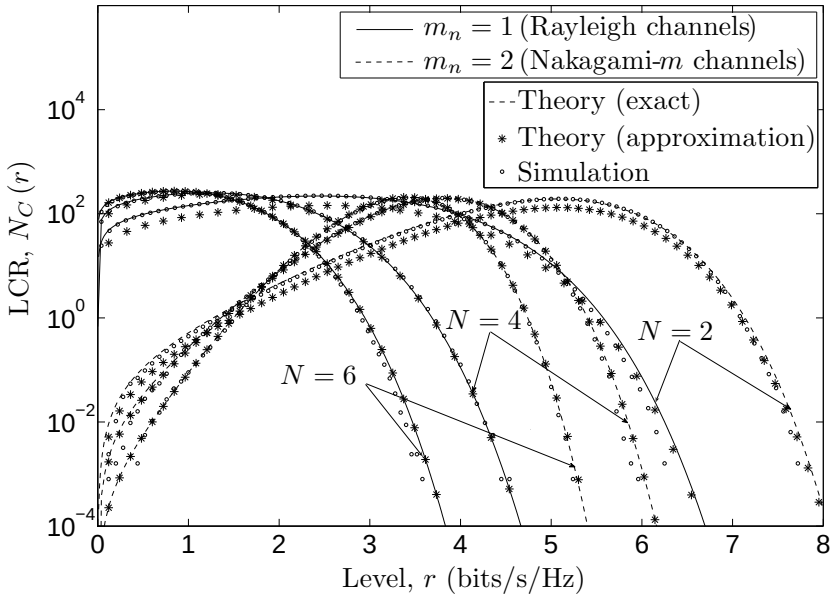

Figure G.6: The LCR of the capacity of *N*∗Nakagami-*m* channels.

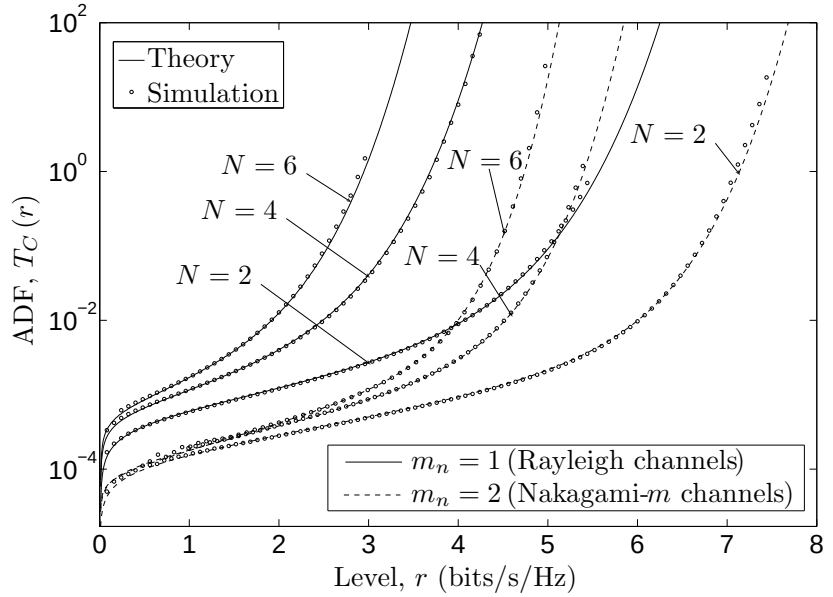

Figure G.7: The ADF of the capacity of *N*∗Nakagami-*m* channels.

N∗Nakagami-*m* channels with lower values of the fading parameter m_n is lower as compared to that of the channels with higher values of fading parameter m_n. However, the converse statement is true for lower levels r. On the other hand, increase in the number of hops N has an opposite influence on the LCR of the channel capacity as compared to the fading parameter m_n. Furthermore, Fig. G.6 illustrates the approximated LCR $N_C(r)$ of the capacity $C(t)$ given by (18). It is observed that as the number of hops N increases, the approximated LCR fits quite closely

to the exact results. Specifically for $N \geq 4$, a very good fitting between the exact and the approximation results is observed. The ADF $T_C(r)$ of the capacity $C(t)$ of $N*$Nakagami-m channels is studied in Fig. G.7 for different values of the number of hops N and the fading parameter m_n. It is observed that an increase in the severity of fading or the number of hops N in $N*$Nakagami-m channels increases the ADF $T_C(r)$ of the channel capacity.

VI. Conclusion

In this article, we have presented a statistical analysis of the capacity of $N*$Nakagami-m channels. Specifically, we have studied the influence of the severity of fading and the number of hops on the PDF, CDF, LCR, and ADF of the channel capacity. We have derived an accurate closed-form approximation for the LCR of the capacity. For large number of hops N, we have investigate the suitability of the assumption that the $N*$Nakagami fading distribution can be approximated by the lognormal distribution. The findings of this paper show that an increase in the number of hops N or the severity of fading decreases the mean channel capacity, while it results in an increase in the ADF of the channel capacity. Moreover, at higher levels r, the LCR $N_C(r)$ of the capacity of $N*$Nakagami-m channels decreases with an increase in severity of fading or the number of hops N. However, the converse statement is true for lower levels r. Furthermore, the variance of the channel capacity decreases by increasing the number of hops, while increase in the severity of fading has an opposite influence on the variance of the channel capacity. It is also observed that increasing the relay gains increases the received SNR at the DMS, however the received SNR at the DMS is always less than or equal to the SNR at the first mobile relay MR_1. The analytical results are verified by simulations, whereby a very good fitting is observed.

G. A Proof of (18)

We can obtain an approximate closed-form expression for (25) by applying a similar technique as presented in [28]. By employing the result given by [28, eq. (A.3)], the LCR $N_C(r)$ can be approximated as

$$N_C(r) \approx \frac{2^N \Phi}{\sqrt{2\pi}} \left(\frac{2^{Nr}-1}{\gamma_s} \right)^{m_N - \frac{1}{2}} (2\pi)^{(N-1)/2} \frac{u(\tilde{\mathbf{x}})}{\sqrt{\alpha}} e^{-h(\tilde{\mathbf{x}})}, \quad r \geq 0, \tag{A.1}$$

where

$$u(\tilde{\mathbf{x}}) = \left(\prod_{n=1}^{N-1} \tilde{x}_n^{2(m_n-m_N)-1}\right) K\left(\frac{2^{Nr}-1}{\gamma_s}, \tilde{x}_1, \ldots, \tilde{x}_{N-1}\right), \tag{A.2}$$

$$h(\tilde{\mathbf{x}}) = \sum_{n=1}^{N-1} \frac{m_n \tilde{x}_n^2}{\acute{\Omega}_n} + \frac{m_N\left(2^{Nr}-1\right)}{\gamma_s \acute{\Omega}_N \prod_{n=1}^{N-1} \tilde{x}_n^2}, \tag{A.3}$$

and $\tilde{\mathbf{x}} = [\tilde{x}_1, \ldots, \tilde{x}_{N-1}]$. Moreover, the values of the parameters $\tilde{x}_1, \ldots, \tilde{x}_{N-1}$ presented in (19b) can be obtained by using [28, eq. (25)]. Furthermore, with the help of [28, eq. (30)], we can easily show that the quantity α in (A.1) is given by

$$\alpha = N 2^{2(N-1)} \prod_{n=1}^{N-1} \frac{m_n}{\acute{\Omega}_n}. \tag{A.4}$$

Finally, by substituting (A.2), (A.3), (A.4), and (19b) in (A.1), we obtain the approximate closed-form expression for the LCR $N_C(r)$ of the channel capacity $C(t)$ given by (18).

REFERENCES

[1] *IEEE J. Select. Areas Commun.: Issue on Wireless ad hoc Networks*, 17, August 1999.

[2] *IEEE Pers. Commun. Mag.: Special Issue on Advances in Mobile ad hoc Networking*, 8, January 2001.

[3] V. S. Adamchik and O. I. Marichev. The algorithm for calculating integrals of hypergeometric type functions and its realization in REDUCE system. In *Proc. Int. Symp. Symbolic and Algebraic Computation, ISSAC '90*, pages 212–224. Tokyo, Japan, 1990.

[4] P. A. Anghel and M. Kaveh. Exact symbol error probability of a cooperative network in a Rayleigh-fading environment. *IEEE Trans. Wireless Commun.*, 3(5):1416–1421, September 2004.

[5] J. Boyer, D. D. Falconer, and H. Yanikomeröglu. Multihop diversity in wireless relaying channels. *IEEE Trans. Commun.*, 52(10):1820–1830, October 2004.

[6] O. Dousse, P. Thiran, and M. Hasler. Connectivity in ad-hoc and hybrid networks. In *Proc. 21st Annual Joint Conf. of the IEEE Computer and Communications Societies, INFOCOM 2002*, volume 2, pages 1079–1088, June 2002.

[7] G. Farhadi and N. C. Beaulieu. On the ergodic capacity of wireless relaying systems over rayleigh fading channels. *IEEE Trans. Wireless Commun.*, 7(11):4462–4467, November 2008.

[8] G. Farhadi and N. C. Beaulieu. On the ergodic capacity of multi-hop wireless relaying systems. *IEEE Trans. Wireless Commun.*, 8(5):2286–2291, May 2009.

[9] I. S. Gradshteyn and I. M. Ryzhik. *Table of Integrals, Series, and Products*. New York: Academic Press, 6th edition, 2000.

[10] T. J. Harrold and A. R. Nix. Intelligent relaying for future personal communication systems. In *Proc. IEE Colloq. Capacity and Range Enhancement Techniques for the Third Generation Mobile Communications and Beyond*, pages 9/1–9/5. London, UK, February 2000.

[11] M. O. Hasna and M. S. Alouini. End-to-end performance of transmission systems with relays over Rayleigh-fading channels. *IEEE Trans. Wireless Commun.*, 2(6):1126–1131, November 2003.

[12] M. O. Hasna and M. S. Alouini. Outage probability of multihop transmission over Nakagami fading channels. *IEEE Commun. Letters*, 7(5):216–218, May 2003.

[13] B. O. Hogstad and M. Pätzold. Capacity studies of MIMO models based on the geometrical one-ring scattering model. In *Proc. 15th IEEE Int. Symp. on Personal, Indoor and Mobile Radio Communications, PIMRC 2004*, volume 3, pages 1613–1617. Barcelona, Spain, September 2004.

[14] B. O. Hogstad, M. Pätzold, N. Youssef, and V. Kontorovitch. Exact closed-form expressions for the distribution, level-crossing rate, and average duration of fades of the capacity of OSTBC-MIMO channels. *IEEE Trans. Veh. Technol.*, 58(2):1011–1016, February 2009.

[15] L. C. Hsu. A theorem on the asymptotic behavior of a multiple integral. *Duke Math. J.*, 15(3):623–632, 1948.

[16] G. K. Karagiannidis. Performance bounds of mltihop wireless communications with blind relays over generalized fading channels. *IEEE Trans. Wireless Commun.*, 5(3):498–502, March 2006.

[17] G. K. Karagiannidis, N. C. Sagias, and P. T. Mathiopoulos. *N∗*Nakagami: A novel stochastic model for cascaded fading channels. *IEEE Trans. Commun.*, 55(8):1453–1458, August 2007.

[18] J. N. Laneman, D. N. C. Tse, and G. W. Wornell. Cooperative diversity in wireless networks: Efficient protocols and outage behavior. *IEEE Trans. Inform. Theory*, 50(12):3062–3080, December 2004.

[19] M. Luccini, A. Shami, and S. Primak. Cross-layer optimization of network performance over multiple-input multiple-output wireless mobile channels. *IET Communications*, 4(6):683–696, April 2010.

[20] M. Nakagami. The *m*-distribution: A general formula of intensity distribution of rapid fading. In W. G. Hoffman, editor, *Statistical Methods in Radio Wave Propagation*. Oxford, UK: Pergamon Press, 1960.

[21] A. Papoulis and S. U. Pillai. *Probability, Random Variables and Stochastic Processes*. New York: McGraw-Hill, 4th edition, 2002.

[22] M. Pätzold. *Mobile Fading Channels*. Chichester: John Wiley & Sons, 2002.

[23] M. Pätzold, C. X. Wang, and B. O. Hogstad. Two new sum-of-sinusoids-based methods for the efficient generation of multiple uncorrelated Rayleigh fading waveforms. *IEEE Trans. Wireless Commun.*, 8(6):3122–3131, June 2009.

[24] G. Rafiq, B. O. Hogstad, and M. Pätzold. Statistical properties of the capacity of double Nakagami-*m* channels. In *Proc. IEEE 5th Int. Symposium on Wireless Pervasive Computing, IEEE ISWPC 2010*, pages 39–44. Modena, Italy, April 2010. DOI 10.1109/ISWPC.2010.5483776.

[25] G. Rafiq and M. Pätzold. The influence of the severity of fading and shadowing on the statistical properties of the capacity of Nakagami-lognormal channels. In *Proc. IEEE Global Telecommunications Conference IEEE GLOBECOM 2008*, pages 1–6, November 2008. DOI 10.1109/GLOCOM.2008.ECP.824.

[26] A. Sendonaris, E. Erkip, and B. Aazhang. User cooperation diversity—Part I: System description. *IEEE Trans. Commun.*, 51(11):1927–1938, November 2003.

[27] V. Sreng, H. Yanikomeroglu, and D. Falconer. Coverage enhancement through two-hop relaying in cellular radio systems. In *Proc. IEEE Wireless Communications and Networking Conference, WCNC 1999*, volume 2, pages 881–885, March 2002.

[28] Z. H. Velkov, N. Zlatanov, and G. K. Karagiannidis. On the second order statistics of the multihop Rayleigh fading channel. *IEEE Trans. Commun.*, 57(6):1815–1823, June 2009.

[29] M. D. Yacoub, J. E. V. Bautista, and L. G. de Rezende Guedes. On higher order statistics of the Nakagami-*m* distribution. *IEEE Trans. Veh. Technol.*, 48(3):790–794, May 1999.

[30] H. Yanikomeröglu. Fixed and mobile relaying technologies for cellular networks. pages 75–81, July 2002.

[31] S. Yeh and O. Leveque. Asymptotic capacity of multi-level amplify-and-forward relay networks. In *IEEE International Symposium on Information Theory, ISIT 2007*, pages 1436–1440. Nice, France, June 2007.

[32] N. Zlatanov, Z. H. Velkov, and G. K. Karagiannidis. Level crossing rate and average fade duration of the double Nakagami-*m* random process and application in MIMO keyhole fading channels. *IEEE Communications Letters*, 12(11):822–824, November 2008.

Appendix H

Paper VIII

Title:	Statistical Properties of the Capacity of Rice Channels with MRC and EGC
Authors:	**Gulzaib Rafiq** and Matthias Pätzold
Affiliation:	University of Agder, Faculty of Engineering and Science, P. O. Box 509, NO-4898 Grimstad, Norway
Book:	*International Conference on Wireless Communications and Signal Processing, WCSP 2009*, Nanjing, China, Nov. 2009, pp. 1 – 5.

Statistical Properties of the Capacity of Rice Channels with MRC and EGC

Gulzaib Rafiq and Matthias Pätzold
Department of Information and Communication Technology
Faculty of Engineering and Science, University of Agder
Servicebox 509, NO-4898 Grimstad, Norway
E-mails: {gulzaib.rafiq, matthias.paetzold}@uia.no

***Abstract* — In this paper, we have studied the statistical properties of the capacity of Rice channels for both maximal ratio combining (MRC) and equal gain combining (EGC) schemes. We have analyzed the effect of the number of diversity branches and the amplitude of the line-of-sight (LOS) components in the diversity branches on the statistics of the channel capacity. Specifically, we have derived analytical expressions for the probability density function (PDF), cumulative distribution function (CDF), level-crossing rate (LCR), and average duration of fades (ADF) of the capacity of Rice channels when using MRC and EGC. It is observed that if the number of diversity branches or the amplitude of the LOS components increases, then the mean channel capacity increases, while the spread and the ADF of the channel capacity decreases. The presented results are very helpful for wireless communication system designers to optimize the receiver design for the case when spatial diversity combining is employed.**

I. Introduction

Diversity combining is widely accepted as an effective method to mitigate the effects of fading in wireless propagation environments [13]. If, for example, spatial diversity techniques are used, the received signals of all diversity branches are combined in an intelligent way which results in an increase in the average received signal-to-noise ratio (SNR) [26, 13, 15, 2] and hence the system throughput increases. Spatial diversity combining techniques have gained considerable attention in the past few decades due to their potential to improve the overall system performance. Two of such combining techniques include MRC and EGC [13, 15]. The performance analysis of EGC in Rayleigh channels can be found in [6, 3, 24]. For Rice channels, the performance analysis of MRC and EGC is presented in [1, 21]. Moreover, the capacity analysis of Rice and Rayleigh channels with MRC can be found in [2, 14, 11]. Furthermore, results for the bit error rate analysis for EGC

in Nakagami and Weibull channels can also be found in the literature (see, e.g., [26, 25, 21] and the references therein). However, to the best of the authors' knowledge, the statistical properties of the capacity of mobile fading channels with MRC or EGC have not been investigated so far.

This article deals with the derivation and analysis of the statistical properties of the capacity of Rice channels with MRC and EGC. We have derived exact analytical expressions for the PDF, CDF, LCR and ADF of the capacity of Rice channels for the case when MRC is employed. Moreover, when EGC is used, the analytical expressions for the PDF, CDF, LCR, and ADF of the channel capacity are derived using an approximation for the PDF of a sum of Rice processes. The PDF and CDF of the channel capacity are very helpful to obtain the mean and the variance of the channel capacity. On the other hand, the LCR and ADF of the channel capacity provide an insight into the temporal variations of the channel capacity [9]. The LCR of the channel capacity represents the average rate of up-crossings (or down-crossings) of the channel capacity through a certain threshold level, while the ADF is the average duration of time over which the channel capacity is below a certain threshold level [12].

We have studied the results for different values of the number of diversity branches, L, and the amplitude of the LOS components, ρ, in different Rice branches. Moreover, the results for the statistical properties of the capacity of Rayleigh and Rice channels are also presented for comparison purposes. It is observed that an increase in the value of L or ρ increases the mean channel capacity for both MRC and EGC. However, it results in a decrease in the variance of the channel capacity. We have also observed that for any of the two aforementioned combining methods, the capacity of Rice channels with a lower value of L or ρ has a higher LCR at low and medium signal levels. The ADF of the channel capacity, on the other hand, decreases with an increase in the value of the parameters L or ρ. The analytical findings are verified with the help of simulations revealing a very good fitting between the theoretical and simulation results.

The rest of the paper is organized as follows. In Section II and III, we will briefly describe the MRC and EGC scheme in Rice channels, respectively. Section IV deals with the derivation of the statistical properties of the capacity of Rice channels with MRC. Section V presents the statistical properties of the capacity of Rice channels with EGC. The analysis of the theoretical and simulation results is carried out in Section VI. Finally, the conclusions are presented in Section VII.

II. Rice Channels with MRC

Let $\chi_l(t)$ denote a Rice process, which characterizes the received signal envelope in the lth fading branch in an L-branch diversity system. Then, the instantaneous SNR $\gamma(t)$ at the combiner output in an MRC diversity scheme is given by [13]

$$\gamma(t) = \frac{P_s}{N_0} \sum_{l=1}^{L} \chi_l^2(t) = \gamma_s \Xi(t) \tag{1}$$

where $\gamma_s = P_s / N_0$ denotes the average SNR of each branch, P_s is the total transmitted power per symbol, N_0 represents the variance of the additive white Gaussian noise (AWGN) in the channel, and $\Xi(t) = \sum_{l=1}^{L} \chi_l^2(t)$. The PDF of the process $\Xi(t)$ is given by [23]

$$p_{\Xi}(z) = \frac{\left(z/s^2\right)^{\frac{L-1}{2}}}{2\sigma_0^2} e^{-\frac{z+s^2}{2\sigma_0^2}} I_{L-1}\left(\frac{\sqrt{z}s}{\sigma_0^2}\right), \ z \geq 0 \tag{2}$$

where σ_0^2 denotes the variance of the underlying Gaussian processes in $\chi_l(t)$, $I_n(\cdot)$ is the modified Bessel function of the first kind of order n [10], $s^2 = \sum_{l=1}^{L} \rho_l^2$, and ρ_l represents the amplitude of the LOS component in the lth diversity branch. Henceforth, without the loss of generality, we assume that $\rho_l = \rho$ holds $\forall l = 1, 2, \ldots, L$, and thus $s = \sqrt{L}\rho$. Under the assumption of isotropic scattering, the joint PDF $p_{\Xi\dot{\Xi}}(z, \dot{z})$ of $\Xi(t)$ and its time derivative $\dot{\Xi}(t)$ can be written as [5]

$$p_{\Xi\dot{\Xi}}(z, \dot{z}) = \frac{z^{\frac{L-1}{2}} e^{-\frac{z+s^2}{2\sigma_0^2} - \frac{\dot{z}^2}{8\beta z}}}{2\sigma_0^2 \sqrt{8\pi\beta z} s^{L-1}} I_{L-1}\left(\frac{\sqrt{z}s}{\sigma_0^2}\right) \tag{3}$$

for $z \geq 0$ and $|\dot{z}| < \infty$. Here, $\beta = 2\left(\pi f_{\max} \sigma_0\right)^2$ for isotropic scattering conditions and $f_{\max}$ denotes the maximum Doppler frequency. Equations (2) and (3) will be used in Section IV for the derivation of the statistical properties of the capacity of Rice channels with MRC.

III. Rice Channels with EGC

For the case when EGC is employed at the receiver in an L-branch diversity system, the instantaneous SNR $\gamma(t)$ at the combiner output is given by

$$\gamma(t) = \frac{P_s}{LN_0} \left(\sum_{l=1}^{L} \chi_l(t) \right)^2 = \frac{\gamma_s}{L} \Xi(t) \tag{4}$$

where $\chi_l(t)$ denotes the received signal envelope in the lth Ricean branch and $\Xi(t) = \left(\sum_{l=1}^{L} \chi_l(t)\right)^2$. To derive the statistical properties of the capacity $C(t)$ of Rice

channels with EGC, we require the PDF $p_\Xi(z)$ of the process $\Xi(t)$ and the joint PDF $p_{\Xi\dot{\Xi}}(z,\dot{z})$ of the process $\Xi(t)$ and its time derivative $\dot{\Xi}(t)$. However, the exact solution for the PDF of a sum of Rice processes and hence the PDF $p_\Xi(z)$ of $\Xi(t)$ are still unknown. For overcoming this problem, different approximations have been proposed in the literature [16, 4]. By using the approximation suggested in [16] for the PDF of a sum of Rice processes and applying the concept of transformation of random variables [17], the PDF $p_\Xi(z)$ of the squared sum of Rice processes $\Xi(t)$ can be expressed as

$$p_\Xi(z) \approx \frac{1}{\sqrt{8\pi z L\sigma_{\chi_l}^2}} e^{-\frac{\left(\sqrt{z}-L\mu_{\chi_l}\right)^2}{2L\sigma_{\chi_l}^2}} + K_{a_1,a_2}(z)\left(\frac{a_0}{2\sqrt{z}a_1}\right) e^{K_{a_1,a_2}^2(z)/2}\left[K_{a_1,a_2}^2(z)-3\right], \quad z \geq 0. \tag{5}$$

Here, $K_{a_1,a_2}(z) = \left(\sqrt{z/L} - a_2 \Big/ a_1\right)$, μ_{χ_l} denotes the mean, and $\sigma_{\chi_l}^2$ represents the variance of the Rice process $\chi_l(t)$ [20, Eq. (2.3-58)]. In this article, we have assumed that all the Rice processes $\chi_l(t)$ have identical means μ_{χ_l} and variances σ_{χ_l}. The constants a_0, a_1, and a_2 can be found using nonlinear least squares fitting with the exact PDF, based on the interior-reflective Newton method [7]. The values of these constants are given in Table H.1 for different numbers L of diversity branches and for different values of the amplitude ρ of the LOS components.

Table H.1: Coefficients for the approximation

	$\rho = 0$			$\rho = 2$		
L	a_0	a_1	a_2	a_0	a_1	a_2
2	0.0225	0.6474	1.7022	0.0071	0.9245	3.0028
3	0.0146	0.6498	2.1154	0.0047	0.9237	3.7713
4	0.0108	0.6513	2.4594	0.0035	0.9236	4.4058
5	0.0086	0.6529	2.7615	0.0028	0.9267	4.9539
6	0.0071	0.653	3.0319	0.0024	0.9276	5.449
7	0.0061	0.6542	3.282	0.002	0.928	5.904
8	0.0053	0.6541	3.5121	0.0018	0.9285	6.3303
9	0.0047	0.6539	3.7301	0.0016	0.9287	6.7264
10	0.0042	0.6538	3.9348	0.0014	0.9286	7.1009

The joint PDF $p_{\Xi\dot{\Xi}}(z,\dot{z})$ can be expressed with the help of [22, Eq. (19)], [5, Eq. (20)] and by using the concept of transformation or random variables [17] as

$$p_{\Xi\dot{\Xi}}(z,\dot{z}) = \frac{e^{-\frac{\dot{z}^2}{8Lz\beta}}}{\sqrt{8\pi zL\beta}}\, p_{\Xi}(z),\ \ z \geq 0, |\dot{z}| < \infty. \tag{6}$$

In (6), $\beta = 2(\pi f_{\max}\sigma_0)^2$ for isotropic scattering conditions. In Section VI, the statistical properties of the capacity of Rice channels with EGC will be derived using (5) and (6).

IV. Statistical Properties of the Capacity of Rice Channels with MRC

The instantaneous capacity $C(t)$ of Rice channels with MRC can be expressed as [8]

$$C(t) = \log_2(1+\gamma(t)) \text{ (bits/s/Hz)}. \tag{7}$$

It can be observed that the expression in (7) represents a mapping of the random process $\gamma(t)$ to another random process $C(t)$. Therefore, the statistical properties of the channel capacity can be found with the help of the statistical properties of the instantaneous SNR $\gamma(t)$. To derive the expression for the PDF of the channel capacity, we first need to find the PDF $p_\gamma(z)$ of the instantaneous SNR $\gamma(t)$ using the relation $p_\gamma(z) = \left(1/\gamma_s\right) p_\Xi\left(z/\gamma_s\right)$. Thereafter, applying the concept of transformation of random variables, the PDF $p_C(r)$ of the channel capacity $C(t)$ is obtained using $p_C(r) = 2^r \ln(2)\, p_\gamma(2^r-1)$ as follows

$$p_C(r) = \frac{2^r \ln(2) e^{-\frac{2^r-1/\gamma_s+s^2}{2\sigma_0^2}} s^{1-L}}{2\gamma_s\sigma_0^2\left(2^r-1/\gamma_s\right)^{\frac{1-L}{2}}} I_{L-1}\left(\frac{\sqrt{2^r-1}s}{\sqrt{\gamma_s}\sigma_0^2}\right),\ \ r \geq 0. \tag{8}$$

To find the CDF $F_C(r)$ of the channel capacity $C(t)$, we will make use of the relationship $F_C(r) = \int_0^r p_C(x)dx$ [17]. After solving the integral, the CDF $F_C(r)$ of $C(t)$ can be expressed as

$$F_C(r) = 1 - Q_L\left(\frac{s}{\sigma_0}, \frac{\sqrt{2^r-1/\gamma_s}s}{\sigma_0^2}\right),\ \ r \geq 0 \tag{9}$$

where $Q_L(\cdot,\cdot)$ represents the generalized Marcum Q-function [20, Eq. (2.3-36)].

The LCR $N_C(r)$ of the channel capacity $C(t)$ is defined as $N_C(r) = \int_0^\infty \dot{z}\, p_{C\dot{C}}(r,\dot{z})d\dot{z}$ [12], where $p_{C\dot{C}}(z,\dot{z})$ denotes the joint PDF of the channel capacity $C(t)$ and its time derivative $\dot{C}(t)$. The joint PDF $p_{C\dot{C}}(z,\dot{z})$ can be obtained using $p_{C\dot{C}}(z,\dot{z}) = (2^z\ln(2))^2\, p_{\gamma\dot{\gamma}}(2^z-1, 2^z\dot{z}\ln(2))$ and $p_{\gamma\dot{\gamma}}(z,\dot{z}) = \left(1/\gamma_s^2\right) p_{\Xi\dot{\Xi}}\left(z/\gamma_s, \dot{z}/\gamma_s\right)$ as

$$p_{C\dot{C}}(z,\dot{z}) = \frac{2^z \ln(2)}{\sqrt{(2^r-1)\,8\pi\beta\gamma_s}} e^{-\frac{(2^z \ln(2)\dot{z})^2}{8\gamma_s\beta(2^z-1)}}\, p_C(z) \tag{10}$$

for $z \geq 0$ and $|\dot{z}| < \infty$. The LCR $N_C(r)$ can now be obtained by substituting (10) in $N_C(r) = \int_0^\infty \dot{z}\, p_{C\dot{C}}(r,\dot{z})d\dot{z}$. After some algebraic manipulations, the LCR $N_C(r)$ can finally be expressed in closed form as

$$N_C(r) = \frac{\sqrt{2\beta\,(2^r-1)\,\gamma_s}}{\sqrt{\pi}2^r \ln(2)}\, p_C(r), \;\; r \geq 0. \tag{11}$$

In order to find the ADF $T_C(r)$ of the channel capacity $C(t)$, we will use the formula $T_C(r) = F_C(r) \big/ N_C(r)$ [13], where $F_C(r)$ and $N_C(r)$ are given by (9) and (11), respectively.

V. Statistical Properties of the Capacity of Rice Channels with EGC

For the case of EGC, the PDF $p_C(r)$ of the channel capacity $C(t)$ is obtained using (4), (7), and by applying the concept of transformation of random variables. Analogous to the MRC case, we will first find the PDF $p_\gamma(z)$ of the instantaneous SNR $\gamma(t)$ by substituting the approximation in (5) in the relationship $p_\gamma(z) = \left(1 \big/ \acute{\gamma}_s\right) p_\Xi\left(z \big/ \acute{\gamma}_s\right)$, where $\acute{\gamma}_s = \gamma_s \big/ L$. Afterwards, the PDF $p_C(r)$ can be obtained using $p_C(r) = 2^r \ln(2)\, p_\gamma(2^r-1)$ as

$$p_C(r) \approx \frac{2^r \ln(2)}{\acute{\gamma}_s} \left\{ \frac{e^{-\frac{\left(\sqrt{2^r-1/\acute{\gamma}_s} - L\mu_{\chi_l}\right)^2}{2L\sigma_{\chi_l}^2}}}{\sqrt{8\pi L\sigma_{\chi_l}^2\left(\frac{2^r-1}{\acute{\gamma}_s}\right)}} + \frac{e^{-\frac{K_{a_1,a_2}^2\left(\frac{2^r-1}{\acute{\gamma}_s}\right)}{2}}}{2a_1\sqrt{\frac{2^r-1}{\acute{\gamma}_s}}} a_0 \left[K_{a_1,a_2}^2\left(\frac{2^r-1}{\acute{\gamma}_s}\right) - 3\right] \right.$$
$$\left. \times\, K_{a_1,a_2}\left(\frac{2^r-1}{\acute{\gamma}_s}\right) \right\} \tag{12}$$

for $r \geq 0$. The CDF $F_C(r)$ of the channel capacity $C(t)$ can now be obtained using $F_C(r) = \int_0^r p_C(x)dx$ as

$$F_C(r) = 1 - Q\left(\frac{\sqrt{2^r - 1\big/\acute{\gamma}_s} - L\mu_{\chi_l}}{\sqrt{L}\sigma_{\chi_l}}\right) - a_0\left[K_{a_1,a_2}^2\left(\frac{2^r-1}{\acute{\gamma}_s}\right) - 1\right] e^{-\frac{K_{a_1,a_2}^2\left(\frac{2^r-1}{\acute{\gamma}_s}\right)}{2}} \tag{13}$$

for $r \geq 0$. In (13), $Q(\cdot)$ represents the error function [20, Eq. (2.3-10)].

The LCR $N_C(r)$ of the capacity $C(t)$ of Rice channels with EGC is defined by $N_C(r) = \int_0^\infty \dot{z}\, p_{C\dot{C}}(r,\dot{z})d\dot{z}$. The joint PDF $p_{C\dot{C}}(z,\dot{z})$ in this case is obtained by using

(6) and by employing the relationships $p_{C\dot{C}}(z,\dot{z}) = (2^z \ln(2))^2 \, p_{\gamma\dot{\gamma}}(2^z - 1, 2^z \dot{z} \ln(2))$ and $p_{\gamma\dot{\gamma}}(z,\dot{z}) = \left(1 \Big/ \acute{\gamma}_s{}^2\right) p_{\Xi\dot{\Xi}}\left(z \Big/ \acute{\gamma}_s \, , \dot{z} \Big/ \acute{\gamma}_s\right)$ as

$$p_{C\dot{C}}(z,\dot{z}) = \frac{\sqrt{\acute{\gamma}_s} e^{-\frac{(2^z \ln(2)\dot{z})^2}{8L\beta\acute{\gamma}_s(2^z-1)}}}{\sqrt{8\pi L\beta\,(2^z-1)}} \; p_C(z), \;\; z \geq 0, |\dot{z}| < \infty. \tag{14}$$

By substituting (14) in $\int_0^\infty \dot{z}\, p_{C\dot{C}}(r,\dot{z}) d\dot{z}$, the LCR $N_C(r)$ of the channel capacity $C(t)$ can be expressed in closed form as

$$N_C(r) = \frac{\sqrt{2\,(2^r-1)\,\acute{\gamma}_s L\beta}}{\sqrt{\pi} 2^r \ln(2)} \; p_C(r), \;\; z \geq 0. \tag{15}$$

Similarly, the ADF $T_C(r)$ of the channel capacity $C(t)$ can be obtained using $T_C(r) = F_C(r) \big/ N_C(r)$, while $F_C(r)$ and $N_C(r)$ are given by (13) and (15), respectively.

VI. Numerical Results

In this section, we will discuss the analytical results obtained in the previous sections. The validity of the analytical results will be verified with the help of simulations. For comparison purposes, we have also shown the results for Rayleigh channels ($\rho \to 0$) for both MRC and EGC. Moreover, we have also presented the results for the classical Rayleigh and Rice channels which arise when $L = 1$. In order to generate the Rice distributed waveforms $\chi_l(t)$ $(l = 1, 2, ..., L)$, we have employed the sum-of-sinusoids model [18]. The model parameters were calculated using the generalized method of exact Doppler spread (GMEDS_1) [19]. The number of sinusoids for the generation of Rice distributed waveforms $\chi_l(t)$ was chosen to be $N_l = 29 + l$ for $l = 1, 2, ..., L$. The maximum Doppler frequency $f_{\max}$ was 91 Hz, the SNR γ_s was equal to 15 dB, and the parameter σ_0 was set to unity. Finally, using (1), (4), and (7), the simulation results for the statistical properties of the channel capacity $C(t)$ of Rice channels with MRC and EGC were obtained.

The PDF $p_C(r)$ of the capacity of Rice channels with MRC and EGC is shown in Figs. H.1 and H.2, respectively, for different values of the number of diversity branches L and the parameter ρ. Results show that in both cases an increase in the amplitude of the LOS components ρ or the number of diversity branches L increases the mean channel capacity. This fact is specifically studied in Fig. H.3, where the mean channel capacity is plotted against different values of the number of diversity branches L and for various values of the amplitude of the LOS components ρ. It can also be seen in Figs. H.1 and H.2 that increasing the parameter ρ and/or L decreases the spread of the channel capacity. Figure H.3 also shows that the MRC diversity

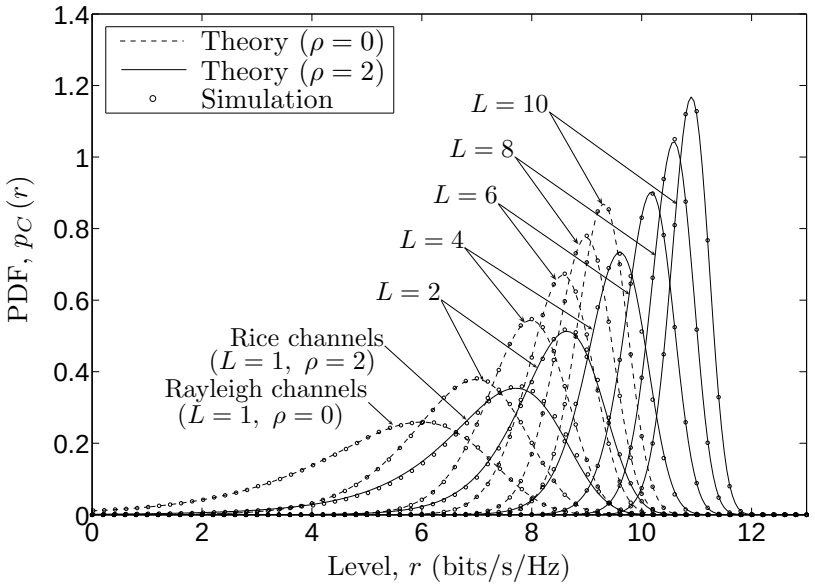

Figure H.1: The PDF $p_C(r)$ of the capacity of Rice channels with MRC.

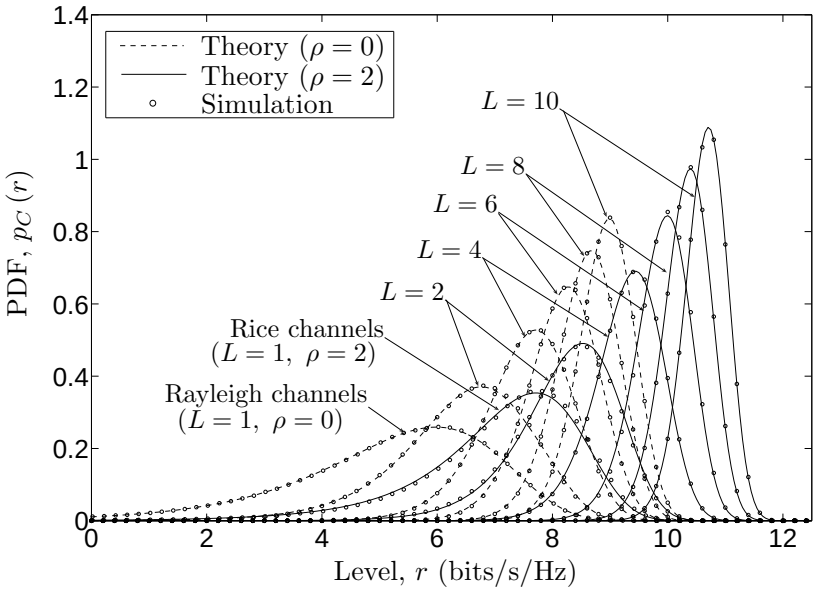

Figure H.2: The PDF $p_C(r)$ of the capacity of Rice channels with EGC.

scheme performs better than the EGC diversity scheme in terms of the mean channel capacity.

The LCR $N_C(r)$ of the capacity of Rice channels with MRC is shown in Fig. H.4 for different values of the number of diversity branches L and the parameter ρ. It is observed that at low signal levels the LCR $N_C(r)$ of the channels with lower values of the amplitude of the LOS component ρ is higher as compared to that of the channels with higher values of ρ. However, the converse statement is true for

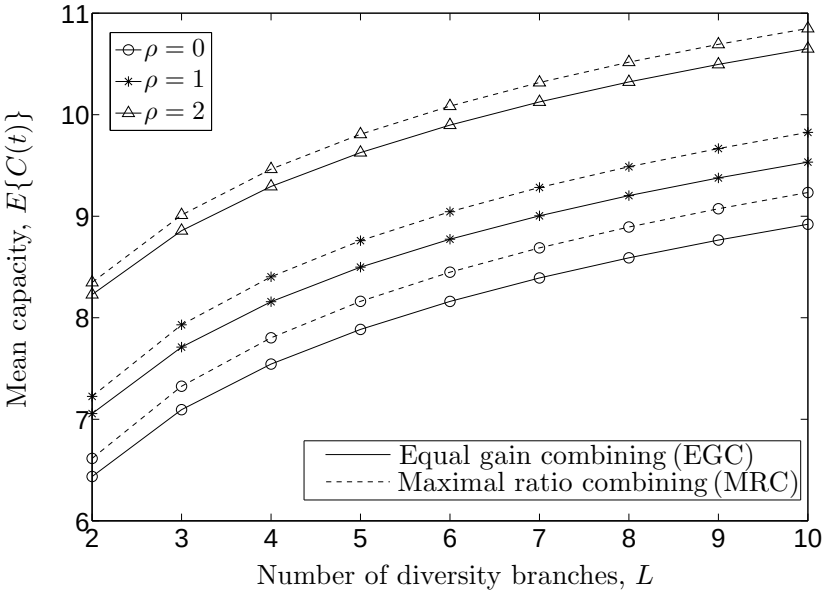

Figure H.3: Comparison of the mean channel capacity of Rice channels with MRC and EGC.

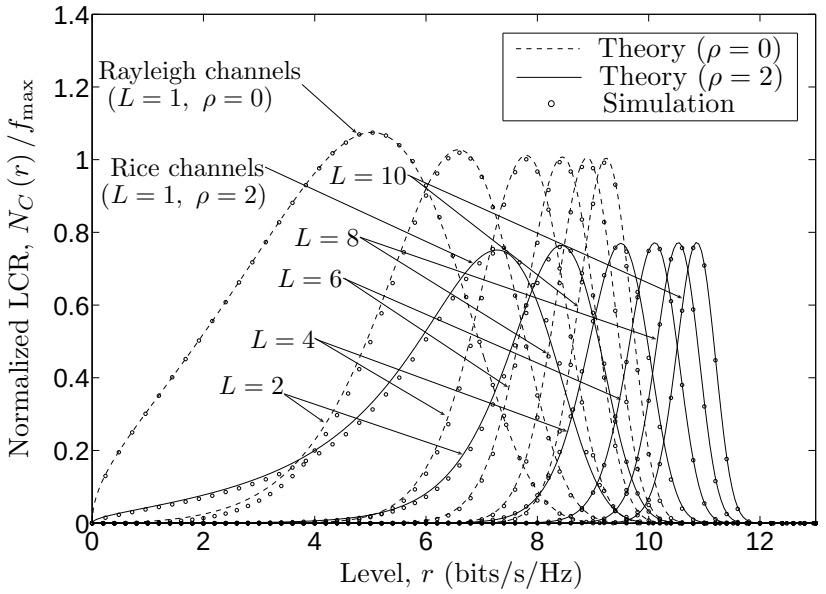

Figure H.4: The LCR $N_C(r)$ of the capacity of Rice channels with MRC.

higher signal levels. Moreover, an increase in the number of diversity branches L has a similar effect on the LCR $N_C(r)$ as the amplitude of the LOS components ρ. For any value of L, it is also observed that the maximum value of the LCR $N_C(r)$ of the channels with lower values of ρ is higher as compared to the channels with higher values of ρ. Figure H.5 depicts the LCR $N_C(r)$ of the capacity of Rice channels with EGC. It can be seen that the parameters L and ρ effect the LCR $N_C(r)$

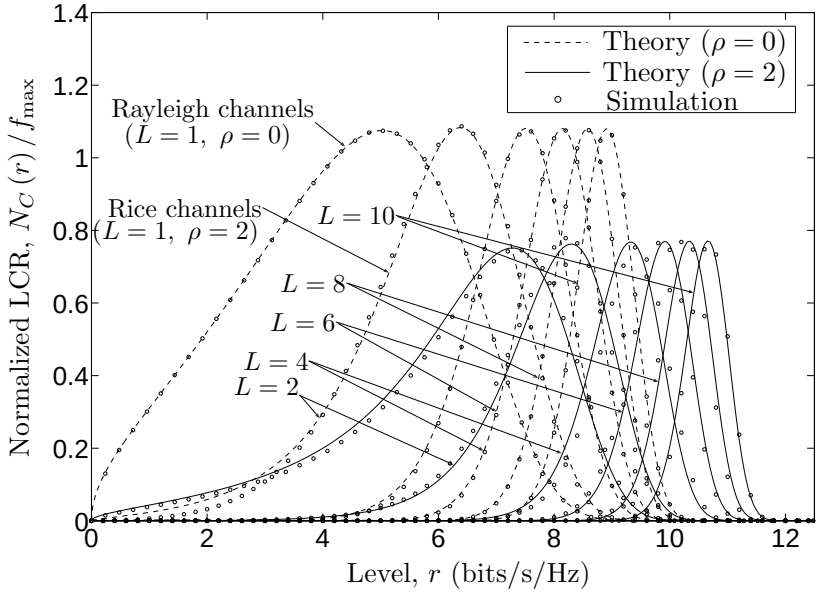

Figure H.5: The LCR $N_C(r)$ of the capacity of Rice channels with EGC.

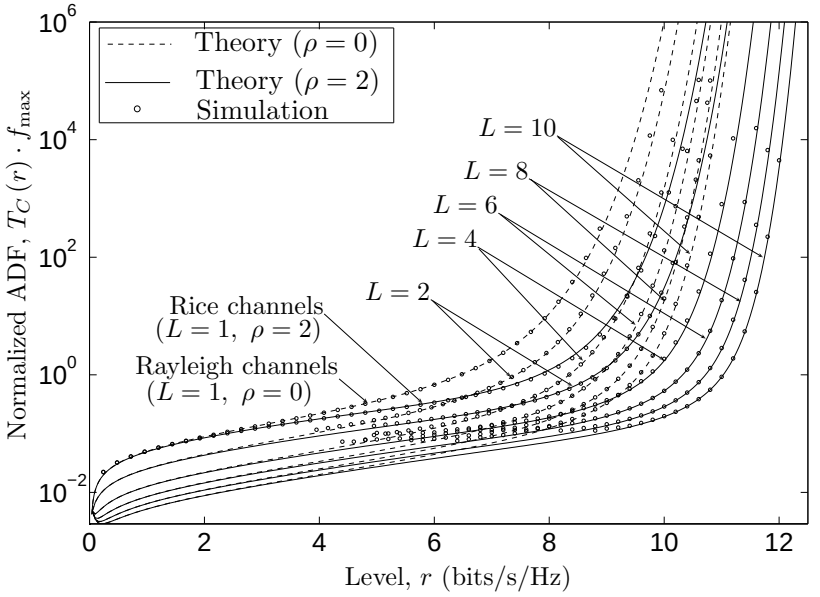

Figure H.6: The ADF $T_C(r)$ of the capacity of Rice channels with MRC.

of the capacity of Rice channels with EGC in a similar fashion as for the case when MRC is employed.

The ADF $T_C(r)$ of the capacity of Rice channels with MRC and EGC is shown in Figs. H.6 and H.7, respectively. Apparently in both cases, an increase in the amplitude of the LOS components or the number of diversity branches decreases the ADF of the channel capacity. For all the presented results, the analytical expressions are verified using simulations, whereby an excellent fitting is observed.

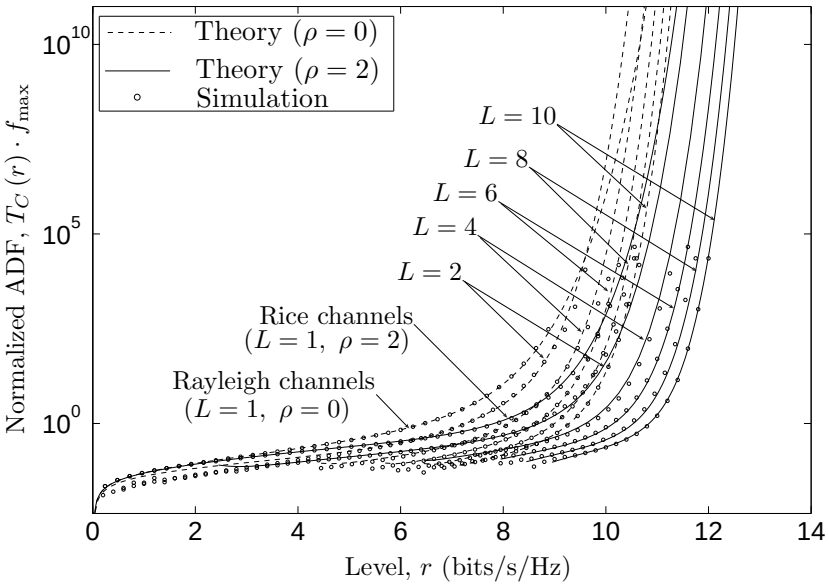

Figure H.7: The ADF $T_C(r)$ of the capacity of Rice channels with EGC.

VII. Conclusion

This article deals with the statistical analysis of the capacity of Rice channels for both MRC and EGC diversity schemes. We have presented analytical closed-form expressions for the PDF, CDF, LCR, and ADF of the channel capacity. The presented results are studied for different values of the amplitude of the LOS components in the diversity branches and the number of diversity branches at the receiver. We have observed that the amplitude of the LOS components and the number of diversity branches have a significant effect on the statistics of the channel capacity. Specifically, an increase in the amplitude of the LOS components and/or the number of diversity branches increase the mean channel capacity. However, it results in a decrease in the ADF of the channel capacity. The findings of this paper also show that the MRC diversity scheme outperforms the EGC diversity scheme w.r.t. the mean channel capacity. Moreover, at low signal levels, the LCR of the channel capacity of channels with lower values of the amplitude of the LOS components ρ or the number of diversity branches L is higher as compared to that of the channels with higher values of ρ. While, the converse statement is true for higher signal levels. The validity of the theoretical results is confirmed by simulations.

References

[1] A. A. Abu-Dayya and N. C. Beaulieu. Microdiversity on Rician fading channels. *IEEE Trans. Commun.*, 42(6):2258–2267, June 1994.

[2] M. S. Alouini and A. J. Goldsmith. Capacity of Rayleigh fading channels under different adaptive transmission and diversity-combining techniques. *IEEE Trans. Veh. Technol.*, 48(4):1165–1181, July 1999.

[3] A. Annamalai, C. Tellambura, and V. K. Bhargava. Equal-gain diversity receiver performance in wireless channels. *IEEE Trans. Commun.*, 48(10):1732–1745, October 2000.

[4] N. C. Beaulieu. An infinite series for the computation of the complementary probability distribution function of a sum of independent random variables and its application to the sum of Rayleigh random variables. *IEEE Trans. Commun.*, 38(9):1463–1474, September 1990.

[5] N. C. Beaulieu and X. Dong. Level crossing rate and average fade duration of MRC and EGC diversity in Ricean fading. 51(5):722–726, May 2003.

[6] Y. Chen and C. Tellambura. Performance analysis of L-branch equal gain combiners in equally correlated Rayleigh fading channels. *IEEE Communications Letters*, 8(3):150–152, March 2004.

[7] T. F. Coleman and Y. Li. An interior trust region approach for nonlinear minimization subject to bounds. *SIAM J. Optimization,*, 6:418–445, May 1996.

[8] G. J. Foschini and M. J. Gans. On limits of wireless communications in a fading environment when using multiple antennas. *Wireless Pers. Commun.*, 6:311–335, March 1998.

[9] A. Giorgetti, P. J. Smith, M. Shafi, and M. Chiani. MIMO capacity, level crossing rates and fades: The impact of spatial/temporal channel correlation. *J. Commun. Net.*, 5(2):104–115, June 2003.

[10] I. S. Gradshteyn and I. M. Ryzhik. *Table of Integrals, Series, and Products*. New York: Academic Press, 6th edition, 2000.

[11] K. A. Hamdi. Capacity of MRC on correlated Rician fading channels. *IEEE Trans. Commun.*, 56(5):708–711, May 2008.

[12] B. O. Hogstad and M. Pätzold. Exact closed-form expressions for the distribution, level-crossing rate, and average duration of fades of the capacity of MIMO channels. In *Proc. 65th Semiannual Vehicular Technology Conference, IEEE VTC 2007-Spring*, pages 455–460. Dublin, Ireland, April 2007.

[13] W. C. Jakes, editor. *Microwave Mobile Communications*. Piscataway, NJ: IEEE Press, 1994.

[14] S. Khatalin and J. P. Fonseka. On the channel capacity in Rician and Hoyt fading environments with MRC diversity. *IEEE Trans. Veh. Technol.*, 55(1):137–141, January 2006.

[15] W. C. Y. Lee. *Mobile Communications Engineering*. New York: McGraw-Hill, 2nd edition, 1998.

[16] J. A. López-Salcedo. Simple closed-form approximation to Ricean sum distributions. *IEEE Signal Processing Letters*, 16(3):153–155, June 2009.

[17] A. Papoulis and S. U. Pillai. *Probability, Random Variables and Stochastic Processes*. New York: McGraw-Hill, 4th edition, 2002.

[18] M. Pätzold. *Mobile Fading Channels*. Chichester: John Wiley & Sons, 2002.

[19] M. Pätzold, C. X. Wang, and B. O. Hogstad. Two new sum-of-sinusoids-based methods for the efficient generation of multiple uncorrelated Rayleigh fading waveforms. *IEEE Trans. Wireless Commun.*, 8(6):3122–3131, June 2009.

[20] J. Proakis and M. Salehi. *Digital Communications*. New York: McGraw-Hill, 5th edition, 2008.

[21] H. Samimi and P. Azmi. An approximate analytical framework for performance analysis of equal gain combining technique over independent Nakagami, Rician and Weibull fading channels. *Wireless Personal Communications (WPC)*, 43(4):1399–1408, December 2007. DOI 10.1007/s11277-007-9314-z.

[22] J. C. S. Santos Filho and M. D. Yacoub. Second-order statistics for equal gain combining with arbitrary channels. In *Proc. International Microwave and Optoelectronics Conference, IMOC 2003*, volume 1, pages 55–60, September 2003.

[23] M. K. Simon. *Probability Distributions Involving Gaussian Random Variables: A Handbook for Engineers and Scientists*. Dordrecht: Kluwer Academic Publishers, 2002.

[24] Q. T. Zhang. Probability of error for equal-gain combiners over Rayleigh channels: Some closed-form solutions. *IEEE Trans. Commun.*, 45(3):270–273, March 1997.

[25] D. A. Zogas, G. K. Karagiannidis, and S. A. Kotsopoulos. Equal-gain and maximal-ratio combining over nonidentical Weibull fading channels. *IEEE Trans. Wireless Commun.*, 4(3):841–846, May 2005.

[26] D. A. Zogas, G. K. Karagiannidis, and S. A. Kotsopoulos. Equal gain combining over Nakagami-*n* (Rice) and Nakagami-*q* (Hoyt) generalized fading channels. *IEEE Trans. Wireless Commun.*, 4(2):374–379, March 2005.

Appendix I

Paper IX

Title:	The Influence of Severity of Fading on the Statistical Properties of the Capacity of Nakagami-*m* Channels with MRC and EGC
Authors:	**Gulzaib Rafiq**[1], Valeri Kontorovich[2], and Matthias Pätzold[1]
Affiliations:	[1]University of Agder, Faculty of Engineering and Science, P. O. Box 509, NO-4898 Grimstad, Norway [2]Centro de Investigación y de Estudios Avanzados, CINVESTAV, 07360 Mexico City, Mexico
Conference:	*16th European Wireless Conference, EW 2010*, Lucca, Italy, Apr. 2010, pp. 406 – 410.

The Influence of Severity of Fading on the Statistical Properties of the Capacity of Nakagami-*m* Channels with MRC and EGC

Gulzaib Rafiq[1], Valeri Kontorovich[2], and Matthias Pätzold[1]
[1]Department of Information and Communication Technology
Faculty of Engineering and Science, University of Agder
Servicebox 509, NO-4898 Grimstad, Norway
E-mails: {gulzaib.rafiq, matthias.paetzold}@uia.no
[2]Centro de Investigación y de Estudios Avanzados, CINVESTAV
07360 Mexico City, Mexico
Email: valeri@cinvestav.mx

***Abstract* — In this article, we have studied the statistical properties of the capacity of Nakagami-*m* channels when spatial diversity combining, such as maximal ratio combining (MRC) and equal gain combining (EGC), is employed at the receiver. The presented results provide insight into the statistical properties of the channel capacity under a wide range of fading conditions in wireless links using *L*-branch diversity combining techniques. We have derived closed-form analytical expressions for the probability density function (PDF), cumulative distribution function (CDF), level-crossing rate (LCR), and average duration of fades (ADF) of the channel capacity. The statistical properties of the capacity are studied for different values of the number of diversity branches and for different severity levels of fading. The analytical results are verified with the help of simulations. It is observed that increasing the number of diversity branches increases the mean channel capacity, while the variance and ADF of the channel capacity decreases. Moreover, systems in which the fading in diversity branches is less severe (as compared to Rayleigh fading) have a higher mean channel capacity. The presented results are very helpful to optimize the design of the receiver of wireless communication systems that employ spatial diversity combining.**

I. Introduction

The received signal impairments, caused by multipath fading in wireless communication systems, can be reduced by diversity combining methods, such as MRC and EGC [9, 11]. In diversity combining schemes, the received signals in different

diversity branches are combined in a way that results in an increased signal-to-noise ratio (SNR) [9, 11]. Hence, such methods increase the system throughput and therefore enhance the overall system performance. Due to these advantages, numerous papers have been published dealing with the system performance and the capacity analysis of Rayleigh and Rice channels (see, e.g., [2, 4, 1, 10] and the references therein). On the other hand, the Nakagami-*m* process is considered to be a more general channel model as compared to Rayleigh and Rice models because it can be used to study the scenarios where the fading is more (or less) severe as compared to Rayleigh fading. The generality of this model also derives from the fact that it incorporates Rayleigh and Rice models as special cases. Results pertaining to the statistical analysis of the signal envelope and the system performance analysis for MRC and EGC in Nakagami-*m* channels can be found in [16, 18]. However, to the best of the authors' knowledge, there is still a gap of information regarding the statistical analysis of the capacity of Nakagami-*m* channels with MRC and EGC. The aim of this paper is to fill in this gap.

This paper deals with the derivation and analysis of the PDF, CDF, LCR, and ADF of the channel capacity of Nakagami-*m* channels for both MRC and EGC. The PDF can be helpful to analyze the mean channel capacity and the variance of the channel capacity, while the LCR and ADF of the channel capacity give an insight into the temporal behavior of the channel capacity. We have studied the statistical properties of the channel capacity for different values of the number of diversity branches L and for different values of m controlling the severity of fading in Nakagami-*m* channels. We have also included the results for Rayleigh channels (which arise for the case when $m = 1$) for comparison purposes. It is observed that for both MRC and EGC, an increase in the number of diversity branches L increases the mean channel capacity, while the variance and the ADF of the channel capacity decrease. Moreover, an increase in the severity of fading results in a decrease in the mean channel capacity, however the variance and ADF of the channel capacity increase. It is also observed that at lower signal levels, the LCR is higher for channels with smaller values of the number of diversity branches L or higher severity levels of fading than for channels with higher values of L or lower severity levels of fading.

The rest of the paper is organized as follows. The MRC and EGC schemes in Nakagami-*m* channels are briefly reviewed in Section II and III, respectively. In Section IV, we present the derivation of the statistical properties of the capacity of Nakagami-*m* channels with MRC. The statistical properties of the capacity of Nakagami-*m* channels with EGC are discussed in Section V. The theoretical and

simulation results are analyzed and illustrated in Section VI. Finally, the conclusions are presented in Section VII.

II. NAKAGAMI-*m* CHANNELS WITH MRC

The signal envelope in the lth branch of an L-branch diversity system can be characterized by a Nakagami-m process $\zeta_l(t)$. The PDF $p_{\zeta_l}(z)$ of the Nakagami-m process $\zeta_l(t)$ is given by [12]

$$p_{\zeta_l}(z) = \frac{2m_l^{m_l} z^{2m_l-1}}{\Gamma(m)\Omega_l^{m_l}} e^{-\frac{m_l z^2}{\Omega_l}}, \ z \geq 0 \tag{1}$$

for $l = 1, 2, \ldots, L$, where $\Omega_l = E\left\{z^2\right\}$, $m_l = \Omega_l^2 \big/ \mathrm{Var}\left\{z^2\right\}$, and $\Gamma(\cdot)$ represents the gamma function [7]. In order to generate Nakagami-m processes $\zeta_l(t)$, we have used the following relation [17]

$$\zeta_l(t) = \sqrt{\sum_{i=1}^{2\times m_l} \mu_{i,l}^2(t)} \tag{2}$$

where $\mu_{i,l}(t)$ $(i = 1, 2, \ldots, 2 \times m_l)$ are the underlying independent and identically distributed (i.i.d.) Gaussian processes, and m_l is the parameter of the Nakagami-m distribution associated with the lth branch. The parameter m_l controls the severity of the fading. Increasing the value of m_l decreases the severity of fading associated with the lth branch and vice versa. In this article, we have assumed that $\Omega_l = 2m_l\sigma_0^2$ for the sake of simplicity. Here, σ_0^2 denotes the variance of the underlying Gaussian processes $\mu_{i,l}(t)$ in $\zeta_l(t)$. In an MRC diversity system, the instantaneous SNR $\gamma(t)$ at the combiner output can be expressed as [9]

$$\gamma(t) = \frac{P_s}{N_0} \sum_{l=1}^{L} \zeta_l^2(t) = \gamma_s \Lambda(t) \tag{3}$$

where $\gamma_s = P_s \big/ N_0$ can be termed as the average SNR of each branch and $\Lambda(t) = \sum_{l=1}^{L} \zeta_l^2(t)$. Here, P_s represents the total transmitted power per symbol, and N_0 denotes the variance of the additive white Gaussian noise (AWGN). The PDF $p_\Lambda(z)$ of the process $\Lambda(t)$ can be expressed using [3, Eq. (2)] as

$$p_\Lambda(z) = \frac{z^{\sum_{l=1}^{L} m_l - 1} e^{-\frac{z}{2\sigma_0^2}}}{\left(2\sigma_0^2\right)^{\sum_{l=1}^{L} m_l} \Gamma\left(\sum_{l=1}^{L} m_l\right)}, \ z \geq 0. \tag{4}$$

Under the assumption of isotropic scattering, the joint PDF $p_{\Lambda\dot{\Lambda}}(z,\dot{z})$ of $\Lambda(t)$ and its time derivative $\dot{\Lambda}(t)$ at the same time t can be written as [18]

$$p_{\Lambda\dot{\Lambda}}(z,\dot{z}) = p_{\Lambda}(z)\frac{1}{\sqrt{8\pi z\sigma^2_{\dot{\zeta}_l}}}e^{-\frac{\dot{z}^2}{8z\sigma^2_{\dot{\zeta}_l}}},\ z \geq 0, |\dot{z}| < \infty. \tag{5}$$

Here, $\sigma^2_{\dot{\zeta}_l} = (\pi f_{\max})^2 \Omega_l / m_l$ denotes the variance of the process $\dot{\zeta}_l(t)$ [18], where $\dot{\zeta}_l(t)$ represents the time derivative of the process $\zeta_l(t)$, and $f_{\max}$ is the maximum Doppler frequency. In Section IV, we will use the results presented in (4) and (5) to analyze the statistical properties of the capacity of Nakagami-*m* channels with MRC.

III. Nakagami-*m* Channels with EGC

The instantaneous SNR $\gamma(t)$ at the combiner output in an L-branch EGC diversity system is given by [9]

$$\gamma(t) = \frac{P_s}{LN_0}\left(\sum_{l=1}^{L}\zeta_l(t)\right)^2 = \frac{\gamma_s}{L}\Lambda(t) \tag{6}$$

where $\Lambda(t) = \left(\sum_{l=1}^{L}\zeta_l(t)\right)^2$, and $\zeta_l(t)$ represents the received signal envelope in the lth Nakagami-*m* branch. We again proceed by first finding the PDF $p_{\Lambda}(z)$ of the process $\Lambda(t)$ and the joint PDF $p_{\Lambda\dot{\Lambda}}(z,\dot{z})$ of the process $\Lambda(t)$ and its time derivative $\dot{\Lambda}(t)$. However, finding the PDF of a sum of Nakagami-*m* processes $\sum_{l=1}^{L}\zeta_l(t)$ is still an open problem, and hence the PDF $p_{\Lambda}(z)$ of $\Lambda(t)$ is thus unknown. One of the remedies for this problem is to use an appropriate approximation to the sum $\sum_{l=1}^{L}\zeta_l(t)$ to find the PDF $p_{\Lambda}(z)$ (see, e.g., [12, 5] and the references therein). In this article, we have approximated the sum of Nakagami-*m* processes $\sum_{l=1}^{L}\zeta_l(t)$ by another Nakagami-*m* process $S(t)$ with parameters m_S and Ω_S, as suggested in [5]. Hence, the PDF $p_S(z)$ of $S(t)$ can be obtained by replacing m_l and Ω_l in (1) by m_S and Ω_S, respectively, where $\Omega_S = E\left\{S^2(t)\right\}$ and $m_S = \Omega_S^2 \big/ \left(E\left\{S^4(t)\right\} - \Omega_S^2\right)$. The quantity $E\left\{S^n(t)\right\}$ can be calculated using [5]

$$\begin{aligned} E[S^n(t)] \;=\; & \sum_{n_1=0}^{n}\sum_{n_2=0}^{n_1}\cdots\sum_{n_{L-1}=0}^{n_{L-2}}\binom{n}{n_1}\binom{n_1}{n_2}\cdots\binom{n_{L-2}}{n_{L-1}} \\ & \times E[\zeta_1^{n-n_1}(t)]E[\zeta_2^{n_1-n_2}(t)]\cdots E[\zeta_L^{n_{L-1}}(t)] \end{aligned}$$

where

$$E[\zeta_l^n(t)] = \frac{\Gamma(m_l + n/2)}{\Gamma(m_l)} \left(\frac{\Omega_l}{m_l}\right)^{n/2}, \ \ l = 1, 2, \ldots, L. \tag{7}$$

By using this approximation for the PDF of a sum $\sum_{l=1}^{L} \zeta_l(t)$ of Nakagami-*m* processes and applying the concept of transformation of random variables [13, Eq. (7–8)], the PDF $p_\Lambda(z)$ of the squared sum of Nakagami-*m* processes $\Lambda(t)$ can be expressed using $p_\Lambda(z) = 1/(2\sqrt{z})\, p_S(\sqrt{z})$ as

$$p_\Lambda(z) \ \approx \ \frac{m_S^{m_S} z^{m_S - 1}}{\Gamma(m_S)\Omega_S^{m_S}} e^{-\frac{m_S z}{\Omega_S}}, \ \ z \geq 0. \tag{8}$$

The joint PDF $p_{\Lambda\dot{\Lambda}}(z, \dot{z})$ can now be expressed with the help of [17, Eq. (13)], (8), and by using the concept of transformation or random variables [13, Eq. (7–8)] as

$$p_{\Lambda\dot{\Lambda}}(z, \dot{z}) \approx \frac{e^{-\frac{\dot{z}^2}{8Lz\sigma_{\dot{\zeta}_l}^2}}}{\sqrt{8\pi z L \sigma_{\dot{\zeta}_l}^2}}\, p_\Lambda(z), \ \ z \geq 0, |\dot{z}| < \infty. \tag{9}$$

Using (8) and (9), the statistical properties of the capacity of Nakagami-*m* channels with EGC will be analyzed in Section VI.

IV. Statistical Properties of the Capacity of Nakagami-*m* Channels with MRC

The instantaneous channel capacity $C(t)$ for the case when diversity combining is employed at the receiver can be expressed as [6]

$$C(t) = \log_2(1 + \gamma(t)) \ \text{(bits/s/Hz)} \tag{10}$$

where $\gamma(t)$ represents the instantaneous SNR given by (3) and (6) for MRC and EGC, respectively. The expression in (10) can be considered as a mapping of the random process $\gamma(t)$ to another random process $C(t)$. Hence, the statistical properties of the instantaneous SNR $\gamma(t)$ can be used to find the statistical properties of the channel capacity. The PDF $p_\gamma(z)$ of the instantaneous SNR $\gamma(t)$ can be obtained using the relation $p_\gamma(z) = \left(1/\gamma_s\right) p_\Lambda\left(z/\gamma_s\right)$. Thereafter, applying the concept of transformation of random variables, the PDF $p_C(r)$ of the channel capacity $C(t)$ is obtained using $p_C(r) = 2^r \ln(2)\, p_\gamma(2^r - 1)$ as follows

$$p_C(r) = \frac{2^r \ln(2)(2^r - 1)^{\sum_{l=1}^{L} m_l - 1}}{\Gamma\left(\sum_{l=1}^{L} m_l\right)\left(2\sigma_0^2\gamma_s\right)^{\sum_{l=1}^{L} m_l}} e^{-\frac{(2^r - 1)}{2\sigma_0^2\gamma_s}}, \ \ r \geq 0. \tag{11}$$

The CDF $F_C(r)$ of the channel capacity $C(t)$ can be found using the relationship $F_C(r) = \int_0^r p_C(x)dx$ [13]. After solving the integral, the CDF $F_C(r)$ of $C(t)$ can be expressed as

$$F_C(r) = 1 - \frac{1}{\Gamma\left(\sum_{l=1}^{L} m_l\right)} \Gamma\left(\sum_{l=1}^{L} m_l, \frac{(2^r-1)}{2\sigma_0^2 \gamma_s}\right), \quad r \geq 0 \tag{12}$$

where $\Gamma(\cdot,\cdot)$ represents the incomplete gamma function [7, Eq. (8.350-2)].

The LCR of the channel capacity defines the average rate of up-crossings (or down-crossings) of the channel capacity through a certain threshold level [8]. In order to find the LCR $N_C(r)$ of the channel capacity $C(t)$, we first need to find the joint PDF $p_{C\dot{C}}(z,\dot{z})$ of the channel capacity $C(t)$ and its time derivative $\dot{C}(t)$. The joint PDF $p_{C\dot{C}}(z,\dot{z})$ can be obtained using $p_{C\dot{C}}(z,\dot{z}) = (2^z \ln(2))^2 \, p_{\gamma\dot{\gamma}}(2^z - 1, 2^z \dot{z} \ln(2))$, where $p_{\gamma\dot{\gamma}}(z,\dot{z}) = \left(1/\gamma_s^2\right) p_{\Lambda\dot{\Lambda}}\left(z/\gamma_s, \dot{z}/\gamma_s\right)$. The expression for the joint PDF $p_{C\dot{C}}(z,\dot{z})$ can be written as

$$p_{C\dot{C}}(z,\dot{z}) = \frac{2^z \ln(2)}{\sqrt{(2^z-1)\, 8\pi\sigma_{\dot{\zeta}_l}^2 \gamma_s}} e^{-\frac{(2^z \ln(2)\dot{z})^2}{8\gamma_s \sigma_{\dot{\zeta}_l}^2 (2^z-1)}} p_C(z) \tag{13}$$

for $z \geq 0$ and $|\dot{z}| < \infty$. The LCR $N_C(r)$ can now be obtained by solving the integral in $N_C(r) = \int_0^\infty \dot{z}\, p_{C\dot{C}}(r,\dot{z})d\dot{z}$. After some algebraic manipulations, the LCR $N_C(r)$ can finally be expressed in closed form as

$$N_C(r) = \sqrt{\frac{2\sigma_{\dot{\zeta}_l}^2 \gamma_s (2^r-1)}{\pi 2^{2r} (\ln(2))^2}} \, p_C(r), \quad r \geq 0. \tag{14}$$

The ADF of the channel capacity denotes the average duration of time over which the channel capacity is below a certain threshold level [8]. The ADF $T_C(r)$ of the channel capacity $C(t)$ can be obtained using $T_C(r) = F_C(r)/N_C(r)$ [9], where $F_C(r)$ and $N_C(r)$ are given by (12) and (14), respectively.

V. Statistical Properties of the Capacity of Nakagami-m Channels with EGC

For the case of EGC, the PDF $p_\gamma(z)$ of the instantaneous SNR $\gamma(t)$ can be obtained by substituting (8) in $p_\gamma(z) = \left(1/\acute{\gamma}_s\right) p_\Lambda\left(z/\acute{\gamma}_s\right)$, where $\acute{\gamma}_s = \gamma_s/L$. Thereafter, the PDF $p_C(r)$ is obtained by applying the concept of transformation of random vari-

ables on (10) as

$$\begin{aligned} p_C(r) &= 2^r \ln(2)\, p_\gamma(2^r-1) \\ &\approx \frac{2^r \ln(2)(2^r-1)^{m_S-1}}{\Gamma(m_S)\left(\acute{\gamma}_s\, \Omega_S / m_S\right)^{m_S}} e^{-\frac{m_S(2^r-1)}{\acute{\gamma}_s \Omega_S}}, \;\; r \geq 0. \end{aligned} \tag{15}$$

By integrating the PDF $p_C(r)$, the CDF $F_C(r)$ of the channel capacity $C(t)$ can be obtained using $F_C(r) = \int_0^r p_C(x)dx$ as

$$F_C(r) \approx 1 - \frac{1}{\Gamma(m_S)} \Gamma\left(m_S, \frac{m_S(2^r-1)}{\acute{\gamma}_s \Omega_S}\right), \;\; r \geq 0. \tag{16}$$

The joint PDF $p_{C\dot{C}}(z,\dot{z})$ for the case of EGC can be obtained using $p_{C\dot{C}}(z,\dot{z}) = (2^z \ln(2))^2\, p_{\gamma\dot{\gamma}}(2^z-1, 2^z \dot{z} \ln(2))$ and $p_{\gamma\dot{\gamma}}(z,\dot{z}) = \left(1 \Big/ \acute{\gamma}_s{}^2\right) p_{\Lambda\dot{\Lambda}}\left(z/\acute{\gamma}_s\,, \dot{z}/\acute{\gamma}_s\right)$ as

$$p_{C\dot{C}}(z,\dot{z}) \approx \frac{2^z \ln(2)}{\sqrt{(2^z-1)\, 8\pi L \sigma_{\dot{\zeta}_l}^2 \acute{\gamma}_s}} e^{-\frac{(2^z \ln(2)\dot{z})^2}{8L\acute{\gamma}_s \sigma_{\dot{\zeta}_l}^2 (2^z-1)}} p_C(z) \tag{17}$$

for $z \geq 0$ and $|\dot{z}| < \infty$. Now by employing the formula $N_C(r) = \int_0^\infty \dot{z}\, p_{C\dot{C}}(r,\dot{z})d\dot{z}$, the LCR $N_C(r)$ of the channel capacity $C(t)$ can be approximated in closed form as

$$N_C(r) \approx \sqrt{\frac{2\sigma_{\dot{\zeta}_l}^2 \acute{\gamma}_s (2^r-1)}{\pi}} \frac{m^{m_S}(2^r-1)^{m_S}}{\Gamma(m_S)\left(\acute{\gamma}_s \Omega_S\right)^{m_S}} e^{-\frac{m_S(2^r-1)}{\acute{\gamma}_s \Omega_S}} \tag{18}$$

for $z \geq 0$. By using $T_C(r) = F_C(r) \big/ N_C(r)$, the ADF $T_C(r)$ of the channel capacity $C(t)$ can be obtained, while $F_C(r)$ and $N_C(r)$ are given by (16) and (18), respectively.

VI. Numerical Results

This section aims to analyze and to illustrate the analytical findings of the previous sections. The correctness of the analytical results will be confirmed with the help of simulations. For comparison purposes, we have also shown the results for Rayleigh channels (obtained for $m_l = 1, \forall l = 1,2,\ldots,L$). Moreover, we have also presented the results for the classical Rayleigh channels which arise when $L = 1$ and $m_l = 1$. The underlying Gaussian processes $\mu_{i,l}(t)$ $(i = 1,2,\ldots,2 \times m_l)$ are generated using the sum-of-sinusoids method [14]. The model parameters were calculated using the generalized method of exact Doppler spread (GMEDS_1) [15]. The number of sinusoids for the generation of the Gaussian processes $\mu_{i,l}(t)$ was chosen to be $N_i = 29$. The SNR γ_s was set to 15 dB, the maximum Doppler frequency $f_{\max}$ was 91 Hz, and the parameter σ_0 was equal to unity. Finally, using (3), (6), and (10),

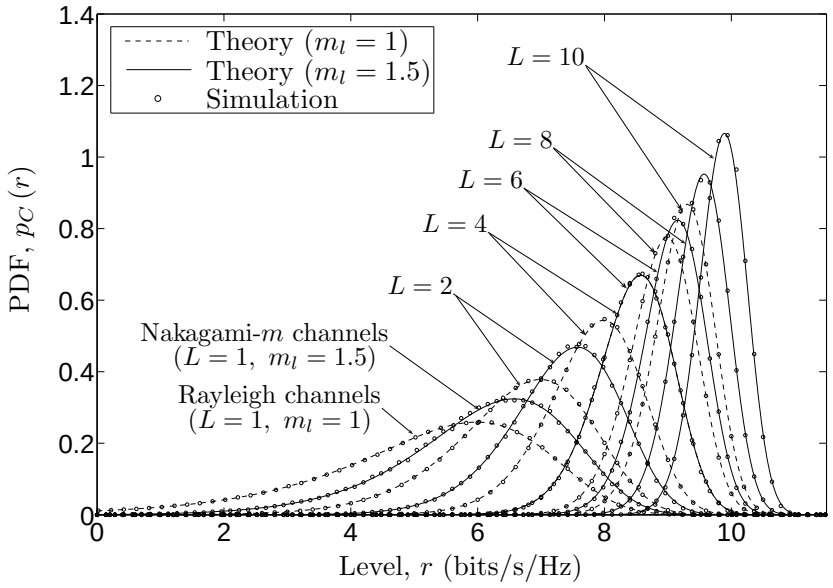

Figure I.1: The PDF $p_C(r)$ of the capacity of Nakagami-*m* channels with MRC.

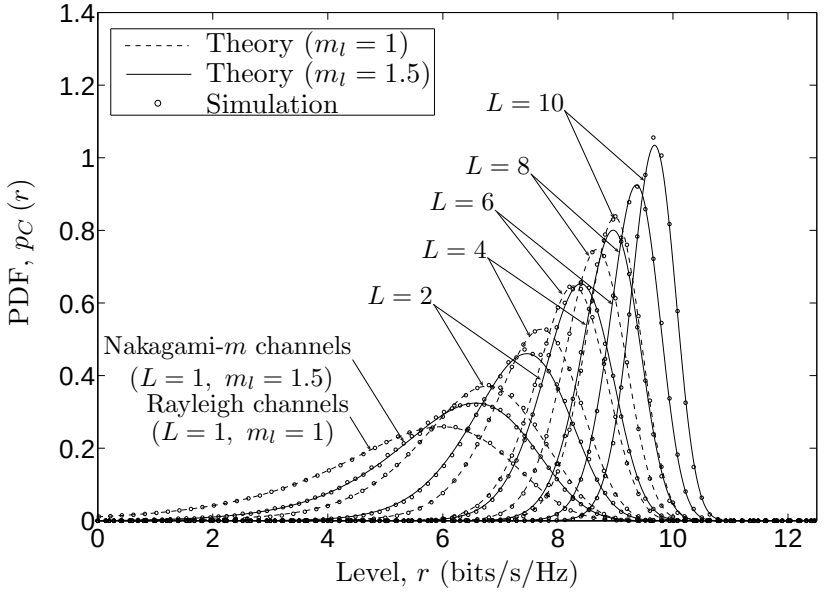

Figure I.2: The PDF $p_C(r)$ of the capacity of Nakagami-*m* channels with EGC.

the simulation results for the statistical properties of the channel capacity $C(t)$ of Nakagami-*m* channels with MRC and EGC were obtained.

Figures I.1 and I.2 present the PDF $p_C(r)$ of the capacity of Nakagami-*m* channels with MRC and EGC, respectively, for different values of the number of diversity branches L and severity parameters m_l. It is observed that in both cases an increase in the number of diversity branches L increases the mean channel capacity. However, the variance of the channel capacity decreases. This fact is specifically

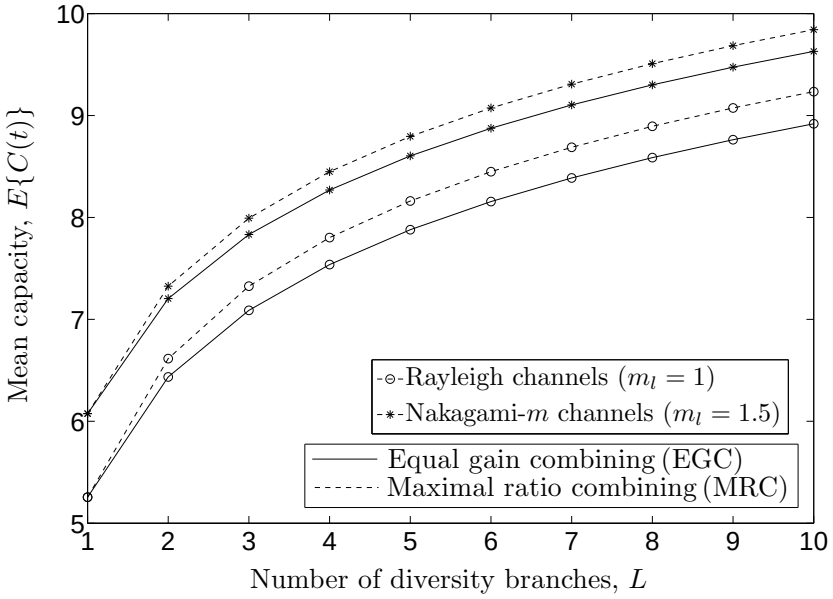

Figure I.3: Comparison of the mean channel capacity of Nakagami-*m* channels with MRC and EGC.

highlighted in Figs. I.3 and I.4, where the mean channel capacity and the variance of the capacity of Nakagami-*m* channels, respectively, is studied for different values of the number of diversity branches L and severity parameters m_l. It can be observed that the mean channel capacity and the variance of the capacity of Nakagami-*m* channels are quite different from those of Rayleigh channels. Specifically for both MRC and EGC, if the branches are less severely faded ($m_l = 1.5$, $\forall l = 1, 2, \ldots, L$) as compared to Rayleigh fading ($m_l = 1$, $\forall l = 1, 2, \ldots, L$), then the mean channel capacity increases, while the variance of the channel capacity decreases.

The LCR $N_C(r)$ of the capacity of Nakagami-*m* channels with MRC and EGC is shown in Figs. I.5 and I.6 for different values of the number of diversity branches L and severity parameters m_l. It can be seen in these two figures that at low signal levels r, the LCR $N_C(r)$ of the channels with lower values of the number of diversity branches L is higher as compared to that of the channels with higher values of L. However, the converse statement is true for high signal levels r.

The ADF $T_C(r)$ of the capacity of Nakagami-*m* channels with MRC and EGC is shown in Figs. I.7 and I.8, respectively. The results show that an increase in the number of diversity branches decreases the ADF of the channel capacity. Moreover, an increase of the severity parameters m_l results in an increase in the ADF of the channel capacity. The analytical expressions are verified using simulations, whereby a very good fitting is found.

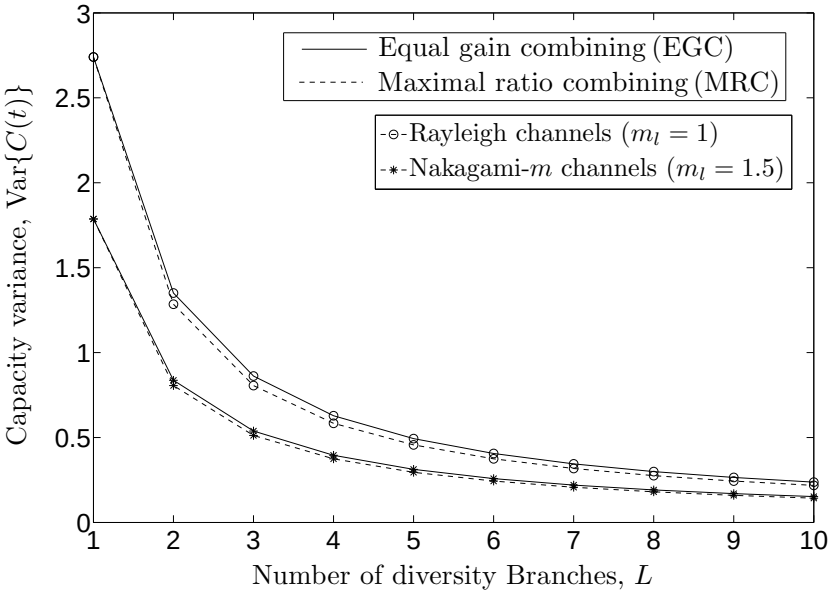

Figure I.4: Comparison of the variance of the channel capacity of Nakagami-*m* channels with MRC and EGC.

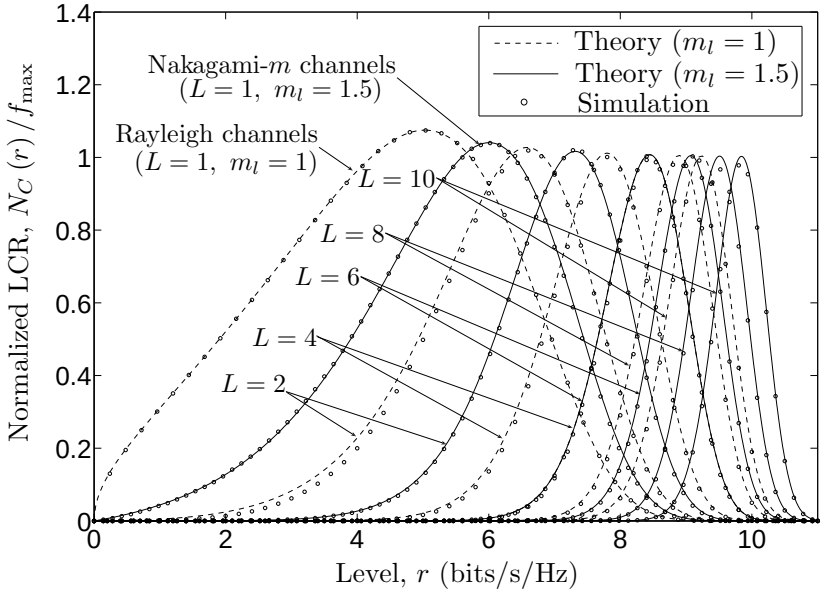

Figure I.5: The normalized LCR $N_C(r)/f_{\max}$ of the capacity of Nakagami-*m* channels with MRC.

VII. Conclusion

This article presents a statistical analysis of the capacity of Nakagami-*m* channels for MRC and EGC diversity schemes. We have derived closed-form analytical expressions for the PDF, CDF, LCR, and ADF of the channel capacity of Nakagami-*m* channels with MRC and EGC. The presented results show that the number of diver-

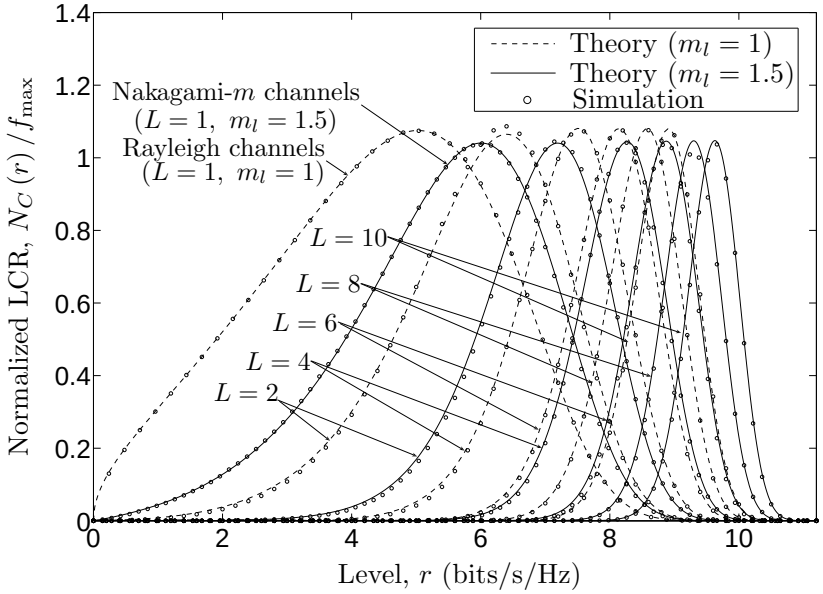

Figure I.6: The normalized LCR $N_C(r)/f_{\max}$ of the capacity of Nakagami-*m* channels with EGC.

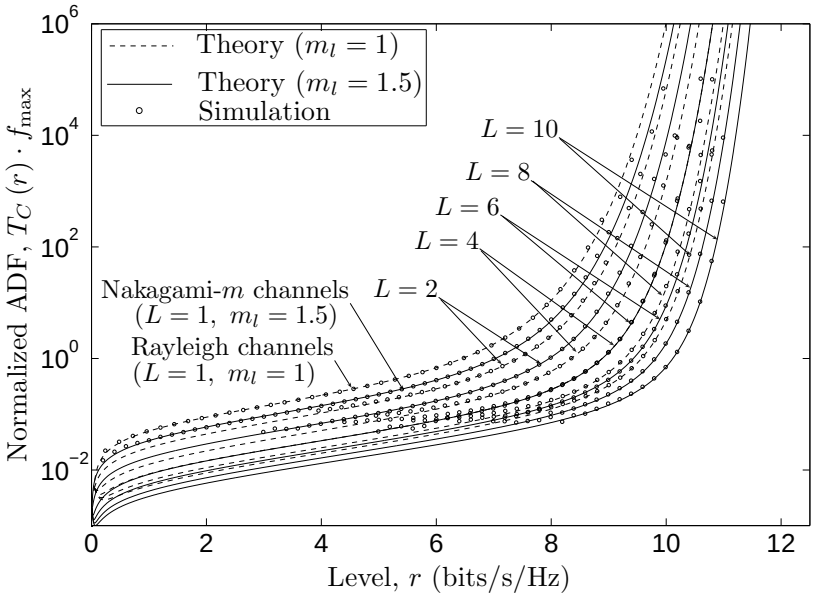

Figure I.7: The normalized ADF $T_C(r) \cdot f_{\max}$ of the capacity of Nakagami-*m* channels with MRC.

sity branches L and the severity of fading have a significant influence on the channel capacity. Specifically, increasing the number of diversity branches increases the mean channel capacity, while the variance and the ADF of the channel capacity decreases. Moreover, an increase in the severity of fading in diversity branches results in a decrease in the mean channel capacity. However, the ADF and the variance of

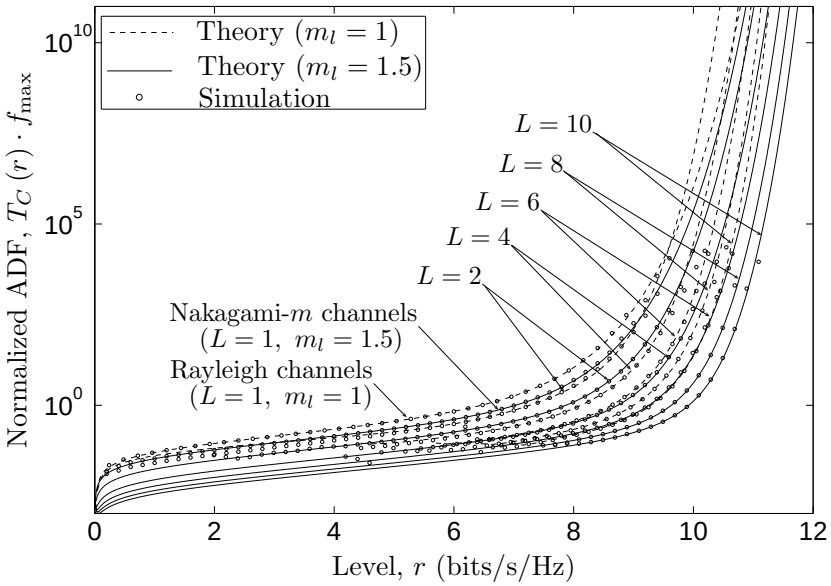

Figure I.8: The normalized ADF $T_C(r) \cdot f_{\max}$ of the capacity of Nakagami-*m* channels with EGC.

the channel capacity increases. It is also observed that at lower signal levels, the LCR is higher for channels with smaller values of the number of diversity branches L or higher severity levels of fading than for channels with higher values of L or lower severity levels of fading. The analytical findings are verified using simulations, where a very good agreement between the theoretical and simulation results was observed.

REFERENCES

[1] A. A. Abu-Dayya and N. C. Beaulieu. Microdiversity on Rician fading channels. *IEEE Trans. Commun.*, 42(6):2258–2267, June 1994.

[2] M. S. Alouini and A. J. Goldsmith. Capacity of Rayleigh fading channels under different adaptive transmission and diversity-combining techniques. *IEEE Trans. Veh. Technol.*, 48(4):1165–1181, July 1999.

[3] Mohamed-Slim. Alouini, A. Abdi, and M. Kaveh. Sum of gamma variates and performance of wireless communication systems over Nakagami-fading channels. *IEEE Trans. Veh. Technol.*, 50(6):1471–1480, November 2001.

[4] Y. Chen and C. Tellambura. Performance analysis of L-branch equal gain combiners in equally correlated Rayleigh fading channels. *IEEE Communications Letters*, 8(3):150–152, March 2004.

[5] D. B. da Costa, M. D. Yacoub, and J. C. S. Santos Filho. An improved closed-form approximation to the sum of arbitrary Nakagami-*m* variates. *IEEE Trans. Veh. Technol.*, 57(6):3854–3858, November 2008.

[6] G. J. Foschini and M. J. Gans. On limits of wireless communications in a fading environment when using multiple antennas. *Wireless Pers. Commun.*, 6:311–335, March 1998.

[7] I. S. Gradshteyn and I. M. Ryzhik. *Table of Integrals, Series, and Products*. New York: Academic Press, 6th edition, 2000.

[8] B. O. Hogstad and M. Pätzold. Exact closed-form expressions for the distribution, level-crossing rate, and average duration of fades of the capacity of MIMO channels. In *Proc. 65th Semiannual Vehicular Technology Conference, IEEE VTC 2007-Spring*, pages 455–460. Dublin, Ireland, April 2007.

[9] W. C. Jakes, editor. *Microwave Mobile Communications*. Piscataway, NJ: IEEE Press, 1994.

[10] S. Khatalin and J. P. Fonseka. On the channel capacity in Rician and Hoyt fading environments with MRC diversity. *IEEE Trans. Veh. Technol.*, 55(1):137–141, January 2006.

[11] W. C. Y. Lee. *Mobile Communications Engineering*. New York: McGraw-Hill, 2nd edition, 1998.

[12] M. Nakagami. The *m*-distribution: A general formula of intensity distribution of rapid fading. In W. G. Hoffman, editor, *Statistical Methods in Radio Wave Propagation*. Oxford, UK: Pergamon Press, 1960.

[13] A. Papoulis and S. U. Pillai. *Probability, Random Variables and Stochastic Processes*. New York: McGraw-Hill, 4th edition, 2002.

[14] M. Pätzold. *Mobile Fading Channels*. Chichester: John Wiley & Sons, 2002.

[15] M. Pätzold, C. X. Wang, and B. O. Hogstad. Two new sum-of-sinusoids-based methods for the efficient generation of multiple uncorrelated Rayleigh fading waveforms. *IEEE Trans. Wireless Commun.*, 8(6):3122–3131, June 2009.

[16] H. Samimi and P. Azmi. An approximate analytical framework for performance analysis of equal gain combining technique over independent Nakagami, Rician and Weibull fading channels. *Wireless Personal Communica-*

tions (WPC), 43(4):1399–1408, December 2007. DOI 10.1007/s11277-007-9314-z.

[17] M. D. Yacoub, J. E. V. Bautista, and L. G. de Rezende Guedes. On higher order statistics of the Nakagami-*m* distribution. *IEEE Trans. Veh. Technol.*, 48(3):790–794, May 1999.

[18] M. D. Yacoub, C. R. C. M. da Silva, and J. E. B. Vargas. Second-order statistics for diversity-combining techniques in Nakagami-fading channels. *IEEE Trans. Veh. Technol.*, 50(6):1464–1470, November 2001.

Appendix J

Paper X

Title:	The Impact of Spatial Correlation on the Statistical Properties of the Capacity of Nakagami-*m* Channels with MRC and EGC
Authors:	**Gulzaib Rafiq**[1], Valeri Kontorovich[2], and Matthias Pätzold[1]
Affiliations:	[1]University of Agder, Faculty of Engineering and Science, P. O. Box 509, NO-4898 Grimstad, Norway [2]Centro de Investigación y de Estudios Avanzados, CINVESTAV, 07360 Mexico City, Mexico
Journal:	to be submitted for publication.

The Impact of Spatial Correlation on the Statistical Properties of the Capacity of Nakagami-*m* Channels with MRC and EGC

Gulzaib Rafiq[1], Valeri Kontorovich[2], and Matthias Pätzold[1]
[1]Department of Information and Communication Technology
Faculty of Engineering and Science, University of Agder
Servicebox 509, NO-4898 Grimstad, Norway
E-mails: {gulzaib.rafiq, matthias.paetzold}@uia.no
[2]Centro de Investigación y de Estudios Avanzados, CINVESTAV
07360 Mexico City, Mexico
Email: valeri@cinvestav.mx

***Abstract* — In this article, we have studied the statistical properties of the capacity of spatially correlated Nakagami-*m* channels for two different diversity combining methods, namely maximal ratio combining (MRC) and equal gain combining (EGC). We have first derived the statistical properties of the signal-to-noise ratio (SNR) at the output of the diversity combiner, for both MRC and EGC. Thereafter, with the help of the statistical properties of the SNR, we have obtained analytical expressions for the probability density function (PDF), cumulative distribution function (CDF), level-crossing rate (LCR), and average duration of fades (ADF) of the channel capacity. The statistical properties of the capacity are studied for different values of the number of diversity branches and for different values of the receiver antennas separation controlling the spatial correlation in the diversity branches. It is observed that an increase in the spatial correlation in the diversity branches of an MRC system increases the variance as well as the LCR of the channel capacity, while the ADF of the channel capacity decreases. Moreover, for the case of EGC, increasing the receiver antennas separation increases the mean channel capacity, while the ADF of the channel capacity decreases. Furthermore, an increase in the spatial correlation increases the LCR of the channel capacity at lower levels. The correctness of the theoretical results is verified by simulations. The presented results are very helpful to optimize the design of the receiver of wireless communication systems that employ spatial diversity combining techniques. Moreover, provided that the feedback channel is available, the transmitter can make use of the information regarding the statistics**

of the channel capacity by choosing the right modulation, coding, and power to achieve the capacity of the wireless channel.

Keywords—Nakagami-*m* channels, spatial correlation, maximal ratio combining, equal gain combining, level-crossing rate, average duration of fades.

I. Introduction

The performance of mobile communication systems is greatly affected by the multipath fading phenomenon. In order to mitigate the effects of fading, spatial diversity combining is widely accepted to be an effective method [16, 20]. In spatial diversity combining, such as MRC and EGC, the received signals in different diversity branches are combined in such a way that results in an increased overall received SNR [16]. Hence, the system throughput increases and therefore the performance of the mobile communication system improves. It is commonly assumed that the received signals in diversity branches are uncorrelated. This assumption is acceptable if the receiver antennas separation is far more than the carrier wavelength of the received signal [29]. However, due to the scarcity of space on small mobile devices, this requirement cannot be always fulfilled. Thus, due to the spatial geometry of the receiver antenna array, the receiver antennas are spatially correlated. It is widely reported in the literature that the spatial correlation has a significant influence on the performance of mobile communication systems employing diversity combining techniques (see, e.g., [17, 21, 8], and the references therein).

There exists a large number of statistical models for describing the statistics of the received radio signal. Among these channel models, the Rayleigh [34], Rice [28] and lognormal [6, 27] models are of prime importance, and are thoroughly investigated in the literature. Numerous papers have been published so far dealing with the performance and the capacity analysis of wireless communication systems employing diversity combining techniques in Rayleigh and Rice channels (e.g., [3, 8, 2, 19]). However, in recent years the Nakagami-*m* channel model [23] has gained considerable attention due to its good fitness to experimental data and mathematically tractable form [9, 32]. Moreover, the Nakagami-*m* channel model can be used to study scenarios where the fading is more (or less) severe than the Rayleigh fading. The generality of this model can also be observed from the fact that it inherently incorporates the Rayleigh and one sided Gaussian models as special cases. For Nakagami-*m* channels, results pertaining to the statistical analysis of the signal envelope at the combiner output in a diversity combining system, assuming spatially uncorrelated diversity branches, can be found in [33]. Moreover, when using EGC, the system performance analysis is reported in [30]. In addition, a large number of articles can also be found in the literature that study Nakagami-*m* channels

in systems with spatially correlated diversity branches [1, 35, 36, 22, 31, 21, 18]. However, to the best of the authors' knowledge, there is still a gap of information regarding the statistical analysis of the capacity of spatially correlated Nakagami-*m* channels with MRC and EGC. Specifically, second order statistical properties, such as the LCR and the ADF, of the capacity of spatially correlated Nakagami-*m* channels with MRC or EGC have not been investigated in the literature. The aim of this paper is to fill this gap.

This paper presents the derivation and analysis of the PDF, CDF, LCR, and ADF of the capacity of spatially correlated Nakagami-*m* channels, for both MRC and EGC. The PDF is helpful to study the mean channel capacity and the variance of the channel capacity, while the temporal behavior of the channel capacity can be investigated with the help of the LCR and ADF of the channel capacity. We have analyzed the statistical properties of the channel capacity for different values of the number of diversity branches L and for different values of the receiver antennas separation δ_R controlling the spatial correlation in diversity branches. For comparison purposes, we have also included the results for the mean and variance of the capacity of spatially correlated Rayleigh channels with MRC and EGC (which arise for the case when $m = 1$). It is observed that for both MRC and EGC, an increase in the number of diversity branches L increases the mean channel capacity, while the variance and the ADF of the channel capacity decrease. Moreover, an increase in the severity of fading results in a decrease in the mean channel capacity, however the variance and ADF of the channel capacity increase. It is also observed that at lower levels, the LCR is higher for channels with smaller values of the number of diversity branches L or higher severity levels of fading than for channels with larger values of L or lower severity levels of fading. We have also studied the influence of spatial correlation in the diversity branches on the statistical properties of the channel capacity. Results show that an increase in the spatial correlation in diversity branches of an MRC system increases the variance as well as the LCR of the channel capacity, while the ADF of the channel capacity decreases. On the other hand, for the case of EGC, increasing the receiver antennas separation increases the mean channel capacity, whereas the ADF of the channel capacity decreases. Moreover, an increase in the spatial correlation increases the LCR of the channel capacity at lower levels r. We have confirmed the correctness of the theoretical results by simulations, whereby a very good fitting is observed.

The rest of the paper is organized as follows. Section II gives a brief overview of the MRC and EGC schemes in Nakagami-*m* channels with spatially correlated diversity branches. In Section III, we present the statistical properties of the ca-

pacity of Nakagami-*m* channels with MRC and EGC. Section IV deals with the analysis and illustration of the theoretical as well as the simulation results. Finally, the conclusions are drawn in Section V.

II. Spatial Diversity Combining in Correlated Nakagami-*m* Channels

We consider the L-branch spatial diversity combining system shown in Fig. J.1, in which it is assumed that the received signals $x_l(t)$ $(l = 1, 2, \ldots, L)$ at the combiner input experience flat fading in all branches. The transmitted signal is represented by $s(t)$, while the total transmitted power per symbol is denoted by P_s. The complex random channel gain of the lth diversity branch is denoted by $\hat{h}_l(t)$ and $n_l(t)$ designates the corresponding additive white Gaussian noise (AWGN) component with variance N_0. The relationship between the transmitted signal $s(t)$ and the received signals $x_l(t)$ at the combiner input can be expressed as

$$\mathbf{x}(t) = \hat{\mathbf{h}}(t)s(t) + \mathbf{n}(t) \tag{1}$$

where $\mathbf{x}(t)$, $\hat{\mathbf{h}}(t)$, and $\mathbf{n}(t)$ are $L \times 1$ vectors with entries corresponding to the lth $(l = 1, 2, \ldots, L)$ diversity branch denoted by $x_l(t)$, $\hat{h}_l(t)$, and $n_l(t)$, respectively. The spatial correlation between the diversity branches arises due to the spatial correlation between closely located receiver antennas in the antenna array. The correlation matrix $\mathbf{R}$, describing the correlation between diversity branches, is given by $\mathbf{R} = E[\hat{\mathbf{h}}(t)\hat{\mathbf{h}}^H(t)]$, where $(\cdot)^H$ represents the Hermitian operator. Using the Kronecker model, the channel vector $\hat{\mathbf{h}}(t)$ can be expressed as $\hat{\mathbf{h}}(t) = \mathbf{R}^{\frac{1}{2}}\mathbf{h}(t)$ [13]. Here, the entries of the $L \times 1$ vector $\mathbf{h}(t)$ are mutually uncorrelated with amplitudes and phases given by $|h_l(t)|$ and ϕ_l, respectively. We have assumed that the phases ϕ_l $(l = 1, 2, \ldots, L)$ are uniformly distributed over $(0, 2\pi]$, while the envelopes

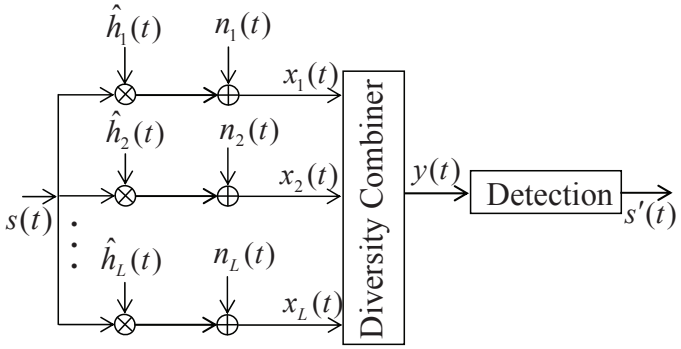

Figure J.1: The block diagram representation of a diversity combining system.

$\zeta_l(t) = |h_l(t)|$ $(l = 1,2,\ldots,L)$ follow the Nakagami-*m* distribution $p_{\zeta_l}(z)$ given by [23]

$$p_{\zeta_l}(z) = \frac{2m_l^{m_l} z^{2m_l-1}}{\Gamma(m_l)\Omega_l^{m_l}} e^{-\frac{m_l z^2}{\Omega_l}}, \; z \geq 0 \tag{2}$$

where $\Omega_l = E\left\{\zeta_l^2(t)\right\}$, $m_l = \Omega_l^2 \big/ \mathrm{Var}\left\{\zeta_l^2(t)\right\}$, and $\Gamma(\cdot)$ represents the gamma function [14]. Here, $E\{\cdot\}$ and $\mathrm{Var}\{\cdot\}$ denote the statistical expectation and variance operators, respectively. The parameter m_l controls the severity of the fading. Increasing the value of m_l decreases the severity of fading associated with the lth branch and vice versa.

The eigenvalue decomposition of the correlation matrix $\mathbf{R}$ can be expressed as $\mathbf{R} = \mathbf{U}\mathbf{\Lambda}\mathbf{U}^H$. Here, $\mathbf{U}$ consists of the eigenbasis vectors at the receiver and the diagonal matrix $\mathbf{\Lambda}$ comprise the eigenvalues λ_l $(l = 1,2,\ldots,L)$ of the correlation matrix $\mathbf{R}$. The receiver antenna correlations $\rho_{p,q}$ $(p,q = 1,2,\ldots,L)$ under isotropic scattering conditions can be expressed as $\rho_{p,q} = J_0\left(b_{pq}\right)$ [7], where $J_0(\cdot)$ is the Bessel function of the first kind of order zero [14] and $b_{pq} = 2\pi\delta_{pq}/\lambda$. Here, λ is the wavelength of the transmitted signal, whereas δ_{pq} represents the spacing between the pth and qth receiver antennas. In this article, we have considered a uniform linear array with adjacent receiver antennas separation represented by δ_R. Increasing the value of δ_R decreases the spatial correlation between the diversity branches and vice versa.

A. Spatially Correlated Nakagami-m Channels with MRC

In MRC, the combiner computes $\mathbf{y}(t) = \hat{\mathbf{h}}^H(t)\mathbf{x}(t)$, hence the instantaneous SNR $\gamma(t)$ at the combiner output in an MRC diversity system with correlated diversity branches can be expressed as [11, 22, 16]

$$\gamma(t) = \frac{P_s}{N_0}\hat{\mathbf{h}}^H(t)\hat{\mathbf{h}}(t) = \frac{P_s}{N_0}\sum_{l=1}^{L}\lambda_l\zeta_l^2(t) = \gamma_s\Xi(t) \tag{3}$$

where $\gamma_s = P_s/N_0$ can be termed as the average SNR of each branch, $\Xi(t) = \sum_{l=1}^{L}\acute{\zeta}_l^2(t)$, and $\acute{\zeta}_l(t) = \sqrt{\lambda_l}\zeta_l(t)$. It is worth mentioning that although we have employed the Kronecker model, it is shown in [22] that (3) holds for any arbitrary correlation model, as long as the correlation matrix $\mathbf{R}$ is non-negative definite. The PDF $p_{\acute{\zeta}_l^2}(z)$ of processes $\acute{\zeta}_l^2(t)$ follows the gamma distribution with parameters $\alpha_l = m_l$ and $\acute{\beta}_l = \lambda_l\,\Omega_l/m_l$ [4, Eq. (1)]. Therefore, the process $\Xi(t)$ can be considered as a sum of weighted gamma variates. The PDF $p_\Xi(z)$ of the process $\Xi(t)$ can

be expressed using [4, Eq. (2)] as

$$p_{\Xi}(z) = \prod_{l=1}^{L} \left(\frac{\acute{\beta}_1}{\acute{\beta}_l} \right)^{\alpha_l} \sum_{k=0}^{\infty} \frac{\delta_k z^{\sum_{l=1}^{L} \alpha_l + k - 1} e^{-z/\acute{\beta}_1}}{\acute{\beta}_1^{\sum_{l=1}^{L} \alpha_l + k} \Gamma\left(\sum_{l=1}^{L} \alpha_l + k \right)}, \ z \geq 0 \tag{4}$$

where

$$\delta_{k+1} \ = \ \frac{1}{k+1} \sum_{i=1}^{k+1} \left[\sum_{l=1}^{L} \alpha_l \left(1 - \frac{\acute{\beta}_1}{\acute{\beta}_l} \right)^{l} \right] \delta_{k+1-l}, \ \ k = 0, 1, 2... \tag{5}$$

$\delta_0 = 1$, and $\beta_1 = \min_l \{\beta_l\}$ $(l = 1, 2, \ldots, L)$. Under the assumption of isotropic scattering, the joint PDF $p_{\Xi\dot{\Xi}}(z, \dot{z})$ of $\Xi(t)$ and its time derivative $\dot{\Xi}(t)$ at the same time t can be written as

$$p_{\Xi\dot{\Xi}}(z, \dot{z}) = p_{\Xi}(z) \frac{1}{\sqrt{2\pi\sigma_{\dot{\Xi}}^2}} e^{-\frac{\dot{z}^2}{2\sigma_{\dot{\Xi}}^2}}, \ z \geq 0, |\dot{z}| < \infty \tag{6}$$

where $\sigma_{\dot{\Xi}}^2 = 4\beta_x z (\pi f_{\max})^2$, $f_{\max}$ is the maximum Doppler frequency, and $\beta_x = \sum_{l=1}^{L} \left(\alpha_l \acute{\beta}_l^2 \right) \Big/ \sum_{l=1}^{L} \left(\alpha_l \acute{\beta}_l \right)$. In Section III, we will use the results presented in (4) and (6) to obtain the statistical properties of the capacity of Nakagami-*m* channels with MRC.

B. Spatially Correlated Nakagami-m Channels with EGC

In EGC, the combiner computes $\mathbf{y}(t) = \phi^H \mathbf{x}(t)$ [17], where $\phi = [\phi_1 \, \phi_2, \cdots, \phi_L]^T$ and $(\cdot)^T$ denotes the vector transpose operator. Therefore, the instantaneous SNR $\gamma(t)$ at the combiner output in an L-branch EGC diversity system with correlated diversity branches can be expressed as [17, 5, 16]

$$\gamma(t) = \frac{P_s}{LN_0} \left(\sum_{l=1}^{L} \sqrt{\lambda_l} \zeta_l(t) \right)^2 = \frac{\gamma_s}{L} \Psi(t) \tag{7}$$

where $\Psi(t) = \left(\sum_{l=1}^{L} \acute{\zeta}_l(t) \right)^2$, while the processes $\acute{\zeta}_l(t)$ follow the Nakagami-*m* distribution with parameters m_l and $\acute{\Omega}_l = \lambda_l \Omega_l$. Again we proceed by first finding the PDF $p_{\Psi}(z)$ of the process $\Psi(t)$ as well as the joint PDF $p_{\Psi\dot{\Psi}}(z, \dot{z})$ of the process $\Psi(t)$ and its time derivative $\dot{\Psi}(t)$. However, the exact solution for the PDF of a sum of Nakagami-*m* processes $\sum_{l=1}^{L} \acute{\zeta}_l(t)$ cannot be obtained. One of the solutions to this problem is to use an appropriate approximation to the sum $\sum_{l=1}^{L} \acute{\zeta}_l(t)$ to find the PDF $p_{\Psi}(z)$ (see, e.g., [23] and [10]). In this article, we have approximated the sum of Nakagami-*m* processes $\sum_{l=1}^{L} \acute{\zeta}_l(t)$ by another Nakagami-*m* process $S(t)$

with parameters m_S and Ω_S, as suggested in [10]. Hence, the PDF $p_S(z)$ of $S(t)$ can be obtained by replacing m_l and Ω_l in (2) by m_S and Ω_S, respectively, where $\Omega_S = E\left\{S^2(t)\right\}$ and $m_S = \Omega_S^2 \big/ \left(E\left\{S^4(t)\right\} - \Omega_S^2\right)$. The nth order moment $E\left\{S^n(t)\right\}$ can be calculated using [10]

$$E\{S^n(t)\} = \sum_{n_1=0}^{n} \sum_{n_2=0}^{n_1} \cdots \sum_{n_{L-1}=0}^{n_{L-2}} \binom{n}{n_1} \binom{n_1}{n_2} \cdots \binom{n_{L-2}}{n_{L-1}} \times E\{\acute{\zeta}_1^{n-n_1}(t)\} E\{\acute{\zeta}_2^{n_1-n_2}(t)\} \cdots E\{\acute{\zeta}_L^{n_{L-1}}(t)\} \tag{8}$$

where $\binom{n_i}{n_j}$, for $n_j \leq n_i$, denotes the binomial coefficient and

$$E\{\acute{\zeta}_l^n(t)\} = \frac{\Gamma(m_l + n/2)}{\Gamma(m_l)} \left(\frac{\acute{\Omega}_l}{m_l}\right)^{n/2}, \quad l = 1, 2, \ldots, L. \tag{9}$$

By using this approximation for the PDF of a sum $\sum_{l=1}^{L} \acute{\zeta}_l(t)$ of Nakagami-m processes and applying the concept of transformation of random variables [24, Eqs. (7–8)], the PDF $p_\Psi(z)$ of the squared sum of Nakagami-m processes $\Psi(t)$ can be expressed using $p_\Psi(z) = 1 \big/ (2\sqrt{z})\, p_S(\sqrt{z})$ as

$$p_\Psi(z) \approx \frac{m_S^{m_S} z^{m_S - 1}}{\Gamma(m_S) \Omega_S^{m_S}} e^{-\frac{m_S z}{\Omega_S}}, \quad z \geq 0. \tag{10}$$

The joint PDF $p_{\Psi\dot{\Psi}}(z, \dot{z})$ can now be expressed with the help of [33, Eq. (19)], (10), and by using the concept of transformation or random variables [24, Eqs. (7–8)] as

$$p_{\Psi\dot{\Psi}}(z, \dot{z}) \approx \frac{e^{-\frac{\dot{z}^2}{2\sigma_{\dot{\Psi}}^2}}}{\sqrt{2\pi\sigma_{\dot{\Psi}}^2}}\, p_\Psi(z), \quad z \geq 0, |\dot{z}| < \infty \tag{11}$$

where $\sigma_{\dot{\Psi}}^2 = 4z(\pi f_{\max})^2 \sum_{l=1}^{L} (\acute{\Omega}_l \big/ m_l)$. Using (10) and (11), the statistical properties of the capacity of Nakagami-m channels with EGC will be obtained in the next section.

III. Statistical Properties of the Capacity of Spatially Correlated Nakagami-m Channels with Diversity Combining

The channel capacity $C(t)$ for the case when diversity combining is employed at the receiver can be expressed as [12]

$$C(t) = \log_2(1 + \gamma(t)) \text{ (bits/s/Hz)} \tag{12}$$

where $\gamma(t)$ represents the instantaneous SNR given by (3) and (7) for MRC and EGC, respectively. The expression in (12) can be considered as a mapping of the random process $\gamma(t)$ to another random process $C(t)$. Hence, the statistical properties of the instantaneous SNR $\gamma(t)$ can be used to find the statistical properties of the channel capacity.

A. Statistical Properties of the Capacity of Spatially Correlated Nakagami-m Channels with MRC

The PDF $p_\gamma(z)$ of the instantaneous SNR $\gamma(t)$ can be found with the help of (4) and by employing the relation $p_\gamma(z) = \left(1/\gamma_s\right) p_\Xi\left(z/\gamma_s\right)$. Thereafter, applying the concept of transformation of random variables, the PDF $p_C(r)$ of the channel capacity $C(t)$ is obtained using $p_C(r) = 2^r \ln(2)\, p_\gamma(2^r-1)$ as follows

$$p_C(r) = \sum_{k=0}^{\infty} \frac{2^r \ln(2) \delta_k (2^r-1)^{\sum_{l=1}^{L}\alpha_l + k - 1} e^{-\frac{2^r-1}{\acute{\beta}_1}\gamma_s}}{\left(\acute{\beta}_1\gamma_s\right)^{\sum_{l=1}^{L}\alpha_l + k} \Gamma\left(\sum_{l=1}^{L}\alpha_l + k\right)} \prod_{l=1}^{L}\left(\frac{\acute{\beta}_1}{\acute{\beta}_l}\right)^{\alpha_l}, \quad r \geq 0. \tag{13}$$

The CDF $F_C(r)$ of the channel capacity $C(t)$ can be found using the relationship $F_C(r) = \int_0^r p_C(x)dx$ [24]. After solving the integral, the CDF $F_C(r)$ of $C(t)$ can be expressed as

$$F_C(r) = 1 - \prod_{l=1}^{L}\left(\frac{\acute{\beta}_1}{\acute{\beta}_l}\right)^{\alpha_l} \sum_{k=0}^{\infty} \frac{\delta_k \Gamma\left(\sum_{l=1}^{L} m_l + k, \frac{(2^r-1)}{\acute{\beta}_1\gamma_s}\right)}{\Gamma\left(\sum_{l=1}^{L} m_l + k\right)} \tag{14}$$

for $r \geq 0$, where $\Gamma(\cdot,\cdot)$ represents the incomplete gamma function [14, Eq. (8.350-2)].

The LCR of the channel capacity defines the average rate of up-crossings (or down-crossings) of the channel capacity through a certain threshold level [15]. In order to find the LCR $N_C(r)$ of the channel capacity $C(t)$, we first need to find the joint PDF $p_{C\dot{C}}(z,\dot{z})$ of the channel capacity $C(t)$ and its time derivative $\dot{C}(t)$. The joint PDF $p_{C\dot{C}}(z,\dot{z})$ can be obtained using $p_{C\dot{C}}(z,\dot{z}) = \left(2^z \ln(2)\right)^2 p_{\gamma\dot{\gamma}}(2^z-1, 2^z\dot{z}\ln(2))$, where $p_{\gamma\dot{\gamma}}(z,\dot{z}) = \left(1/\gamma_s^2\right) p_{\Xi\dot{\Xi}}\left(z/\gamma_s, \dot{z}/\gamma_s\right)$. The expression for the joint PDF $p_{C\dot{C}}(z,\dot{z})$ can be written as

$$p_{C\dot{C}}(z,\dot{z}) = \frac{2^z \ln(2)/\left(\pi f_{\max}\right)}{\sqrt{(2^z-1)\, 8\pi\beta_x\gamma_s}} e^{-\frac{(2^z\ln(2)\dot{z})^2}{8\gamma_s\beta_x(2^z-1)(\pi f_{\max})^2}} p_C(z) \tag{15}$$

for $z \geq 0$ and $|\dot{z}| < \infty$. The LCR $N_C(r)$ can now be obtained by solving the integral in $N_C(r) = \int_0^\infty \dot{z}\, p_{C\dot{C}}(r,\dot{z})d\dot{z}$. After some algebraic manipulations, the LCR $N_C(r)$

can finally be expressed in closed form as

$$N_C(r) = \sqrt{\frac{2\pi\beta_x\gamma_s(2^r-1)}{2^{2r}\left(\ln(2)/\,f_{\max}\right)^2}}\; p_C(r),\;\; r \geq 0. \tag{16}$$

The ADF of the channel capacity denotes the average duration of time over which the channel capacity is below a certain threshold level [15]. The ADF $T_C(r)$ of the channel capacity $C(t)$ can be obtained using $T_C(r) = F_C(r)/\,N_C(r)$ [15], where $F_C(r)$ and $N_C(r)$ are given by (14) and (16), respectively.

B. Statistical Properties of the Capacity of Spatially Correlated Nakagami-m Channels with EGC

For the case of EGC, the PDF $p_\gamma(z)$ of the instantaneous SNR $\gamma(t)$ can be obtained by substituting (10) in $p_\gamma(z) = \left(1/\acute{\gamma}_s\right) p_\Psi\left(z/\acute{\gamma}_s\right)$, where $\acute{\gamma}_s = \gamma_s/L$. Thereafter, the PDF $p_C(r)$ is obtained by applying the concept of transformation of random variables on (7) as

$$\begin{aligned} p_C(r) \;&=\; 2^r \ln(2)\, p_\gamma(2^r-1) \\ &\approx \frac{2^r \ln(2)(2^r-1)^{m_S-1}}{\Gamma(m_S)\left(\acute{\gamma}_s\,\Omega_S/\,m_S\right)^{m_S}} e^{-\frac{m_S(2^r-1)}{\acute{\gamma}_s\Omega_S}},\;\; r \geq 0. \end{aligned} \tag{17}$$

By integrating the PDF $p_C(r)$, the CDF $F_C(r)$ of the channel capacity $C(t)$ can be obtained using $F_C(r) = \int_0^r p_C(x)dx$ as

$$F_C(r) \approx 1 - \frac{1}{\Gamma(m_S)}\Gamma\left(m_S, \frac{m_S(2^r-1)}{\acute{\gamma}_s\Omega_S}\right),\;\; r \geq 0. \tag{18}$$

The joint PDF $p_{C\dot{C}}(z,\dot{z})$, for the case of EGC, can be obtained using $p_{C\dot{C}}(z,\dot{z}) = (2^z\ln(2))^2\, p_{\gamma\dot{\gamma}}(2^z-1, 2^z\dot{z}\ln(2))$ and $p_{\gamma\dot{\gamma}}(z,\dot{z}) = \left(1\Big/\acute{\gamma}_s{}^2\right) p_{\Psi\dot{\Psi}}\left(z/\acute{\gamma}_s\,, \dot{z}/\acute{\gamma}_s\right)$ as

$$p_{C\dot{C}}(z,\dot{z}) \approx \frac{e^{-\frac{\left(2^z\ln(2)\dot{z}/(\pi f_{\max})\right)^2}{8\acute{\gamma}_s(2^z-1)\left(\sum_{l=1}^L \acute{\Omega}_l/m_l\right)}}\; 2^z\ln(2)/\,f_{\max}}{\sqrt{(2^z-1)\,8\pi^3\left(\sum_{l=1}^L \acute{\Omega}_l\Big/ m_l\right)\acute{\gamma}_s}}\; p_C(z) \tag{19}$$

for $z \geq 0$ and $|\dot{z}| < \infty$. Now by employing the formula $N_C(r) = \int_0^\infty \dot{z}\, p_{C\dot{C}}(r,\dot{z})d\dot{z}$, the LCR $N_C(r)$ of the channel capacity $C(t)$ can be approximated in closed form as

$$N_C(r) \approx \sqrt{\frac{2\pi\left(\sum_{l=1}^L \acute{\Omega}_l\Big/ m_l\right)\acute{\gamma}_s(2^r-1)}{2^{2r}\left(\ln(2)/\,f_{\max}\right)^2}}\; p_C(r) \tag{20}$$

for $r \geq 0$. By using $T_C(r) = F_C(r)/N_C(r)$, the ADF $T_C(r)$ of the channel capacity $C(t)$ can be obtained, while $F_C(r)$ and $N_C(r)$ are given by (18) and (20), respectively.

IV. Numerical Results

This section aims to analyze and to illustrate the analytical findings of the previous sections. The correctness of the analytical results will be confirmed with the help of simulations. For comparison purposes, we have shown the results for the mean channel capacity and the variance of the capacity of spatially correlated Rayleigh channels with MRC and EGC (obtained for $m_l = 1, \forall l = 1,2,\ldots,L$). Moreover, we have also presented the results for classical Nakagami-*m* channels, which arise when $L = 1$. In order to generate Nakagami-*m* processes $\zeta_l(t)$, we have used the following relation [32]

$$\zeta_l(t) = \sqrt{\sum_{i=1}^{2\times m_l} \mu_{i,l}^2(t)} \tag{21}$$

where $\mu_{i,l}(t)$ $(i = 1,2,\ldots,2m_l)$ are the underlying independent and identically distributed (i.i.d.) Gaussian processes, and m_l is the parameter of the Nakagami-*m* distribution associated with the lth diversity branch. The Gaussian processes $\mu_{i,l}(t)$, each with zero mean and variances σ_0^2, were generated using the sum-of-sinusoids method [25]. The model parameters were calculated using the generalized method of exact Doppler spread (GMEDS_1) [26]. The number of sinusoids for the generation of the Gaussian processes $\mu_{i,l}(t)$ was chosen to be $N = 20$. The SNR γ_s was set to 15 dB, the parameter Ω_l was assumed to be equal to $2m_l\sigma_0^2$, the maximum Doppler frequency $f_{\max}$ was 91 Hz, and the parameter σ_0^2 was equal to unity. Finally, using (21), (3), (7), and (12), the simulation results for the statistical properties of the capacity $C(t)$ of Nakagami-*m* channels with MRC and EGC were obtained.

Figures J.2 and J.3 present the PDF $p_C(r)$ of the capacity of correlated Nakagami-*m* channels with MRC and EGC, respectively, for different values of the number of diversity branches L and receiver antennas separation δ_R. It is observed that in both MRC and EGC, an increase in the number of diversity branches L increases the mean channel capacity. However, the variance of the channel capacity decreases. This fact is specifically highlighted in Figs. J.4 and J.5, where the mean channel capacity and the variance of the capacity, respectively, of correlated Nakagami-*m* channels is studied for different values of the number of diversity branches L and receiver antennas separation δ_R. The exact closed-form expressions for the mean $E\{C(t)\}$ and variance $\text{Var}\{C(t)\}$ of the channel capacity cannot be obtained. Therefore, results in Figs. J.4 and J.5 are obtained numerically, using (17) and (13).

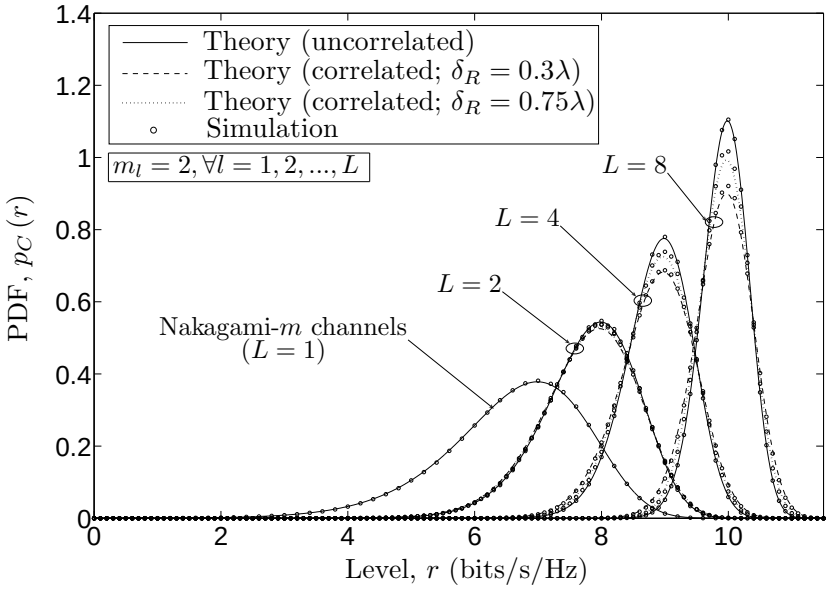

Figure J.2: The PDF $p_C(r)$ of the capacity of correlated Nakagami-*m* channels with MRC.

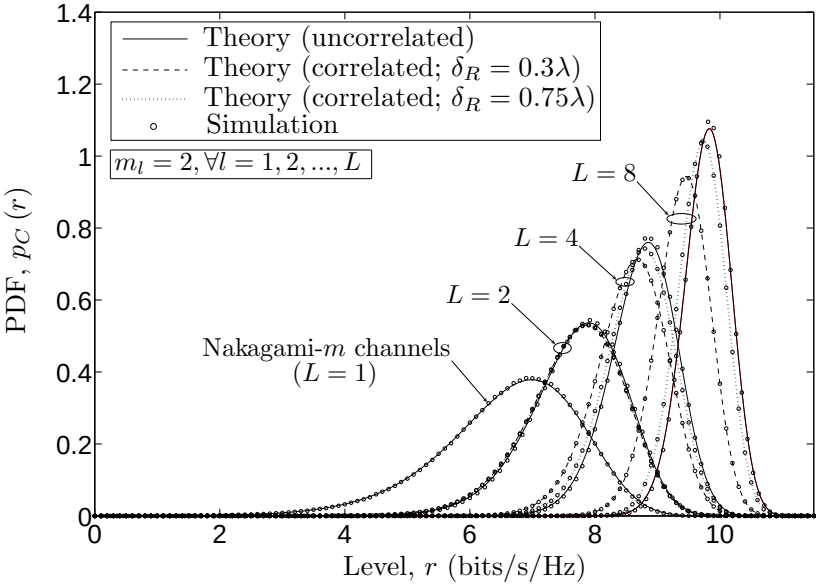

Figure J.3: The PDF $p_C(r)$ of the capacity of correlated Nakagami-*m* channels with EGC.

It can be observed that the mean channel capacity and the variance of the capacity of Nakagami-*m* channels are quite different from those of Rayleigh channels. Specifically, for both MRC and EGC, if the branches are less severely faded ($m_l = 2,\ \forall l = 1, 2, \ldots, L$) as compared to Rayleigh fading ($m_l = 1,\ \forall l = 1, 2, \ldots, L$), then the mean channel capacity increases, while the variance of the channel capacity decreases.

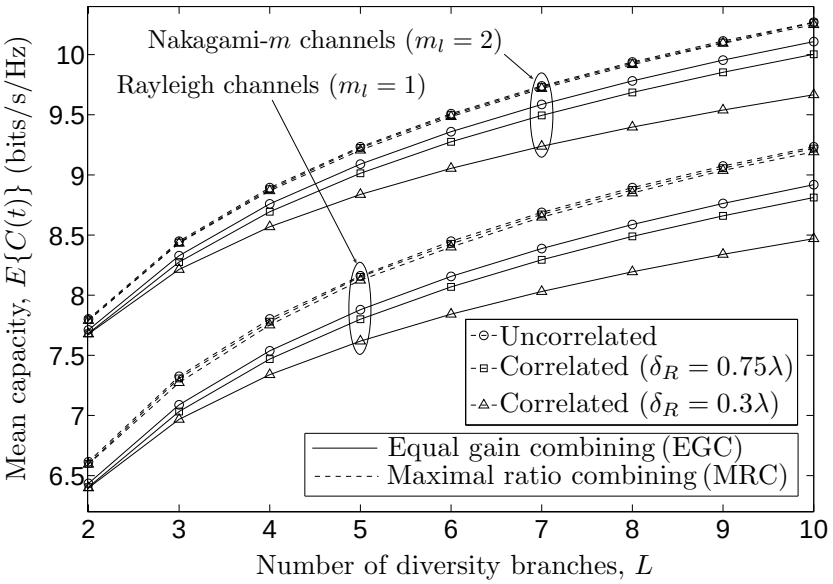

Figure J.4: Comparison of the mean channel capacity of correlated Nakagami-*m* channels with MRC and EGC.

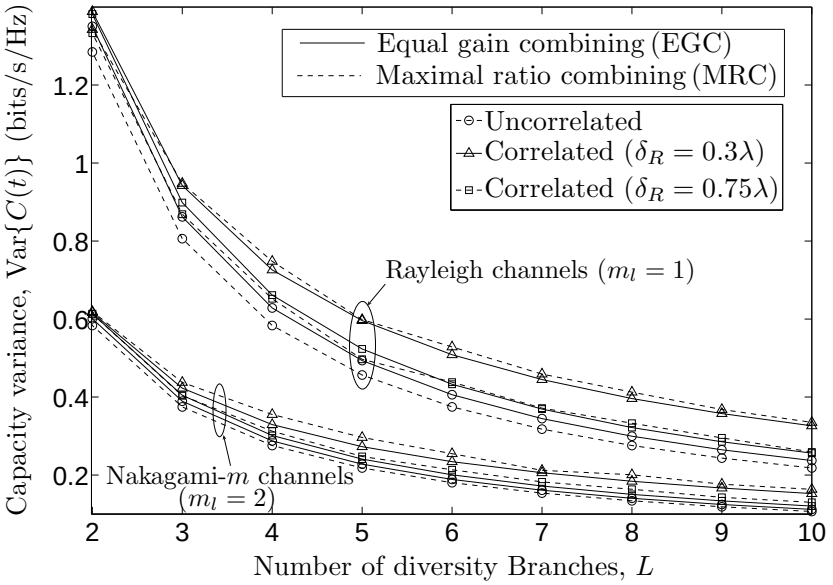

Figure J.5: Comparison of the variance of the channel capacity of correlated Nakagami-*m* channels with MRC and EGC.

The influence of spatial correlation on the PDF of the channel capacity is also studied in Figs. J.2 and J.3. The results show that for Nakagami-*m* channels with MRC, an increase in the spatial correlation in the diversity branches increases the variance of the channel capacity, while the mean channel capacity is almost unaffected. However, for the case of EGC, an increase in the spatial correlation de-

creases the mean channel capacity and has a minor influence on the variance of the channel capacity. Figures J.4 and J.5 also illustrate the effect of spatial correlation on the mean channel capacity and variance of the channel capacity, respectively, of Nakagami-*m* channels with MRC and EGC. For the sake of completeness, we have also presented the results for the CDF of the capacity of correlated Nakagami-*m* channels with MRC and EGC in Figs. J.6 and J.7, respectively. Figures J.6 and J.7 can be studied to draw similar conclusions regarding the influence of diversity branches L as well as the spatial correlation on the mean channel capacity and the variance of the channel capacity as from Figs. J.2 and J.3.

The LCR $N_C(r)$ of the capacity of Nakagami-*m* channels with MRC and EGC is shown in Figs. J.8 and J.9 for different values of the number of diversity branches L and receiver antennas separation δ_R. It can be seen in these two figures that at lower levels r, the LCR $N_C(r)$ of the capacity of Nakagami-*m* channels with smaller values of the number of diversity branches L is higher as compared to that of the channels with larger values of L. However, the converse statement is true for higher levels r. Moreover, an increase in the spatial correlation increases the LCR of the capacity of Nakagami-*m* channels with MRC. On the other hand when EGC is employed, an increase in the spatial correlation increases the LCR of the capacity of Nakagami-*m* channels at only lower levels r, while the LCR decreases at the higher levels r.

The ADF $T_C(r)$ of the capacity of Nakagami-*m* channels with MRC and EGC is studied in Figs. J.10 and J.11, respectively. The results show that the ADF of

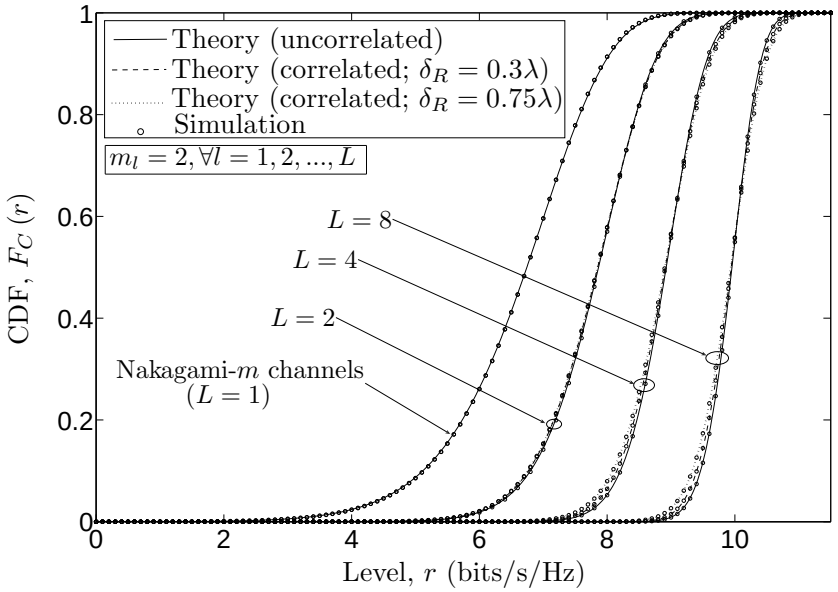

Figure J.6: The CDF $F_C(r)$ of the capacity of correlated Nakagami-*m* channels with MRC.

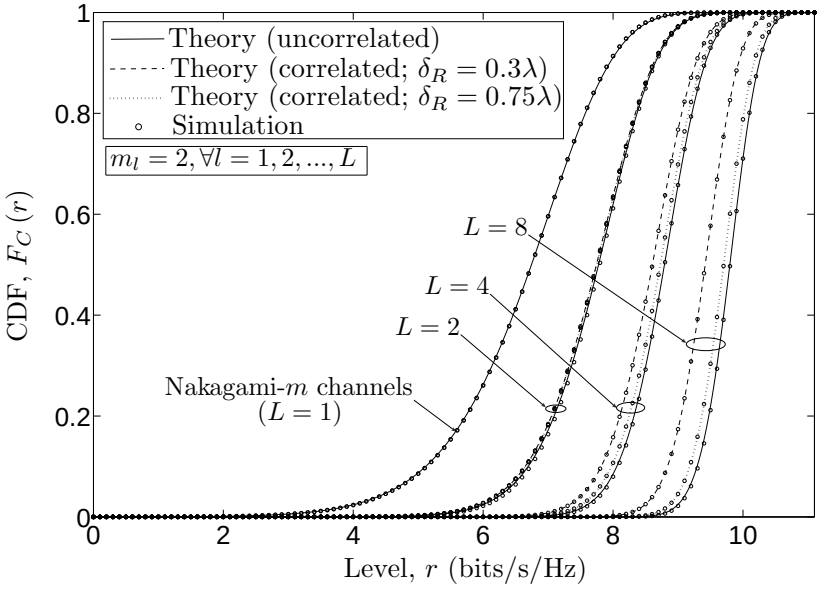

Figure J.7: The CDF $F_C(r)$ of the capacity of correlated Nakagami-*m* channels with EGC.

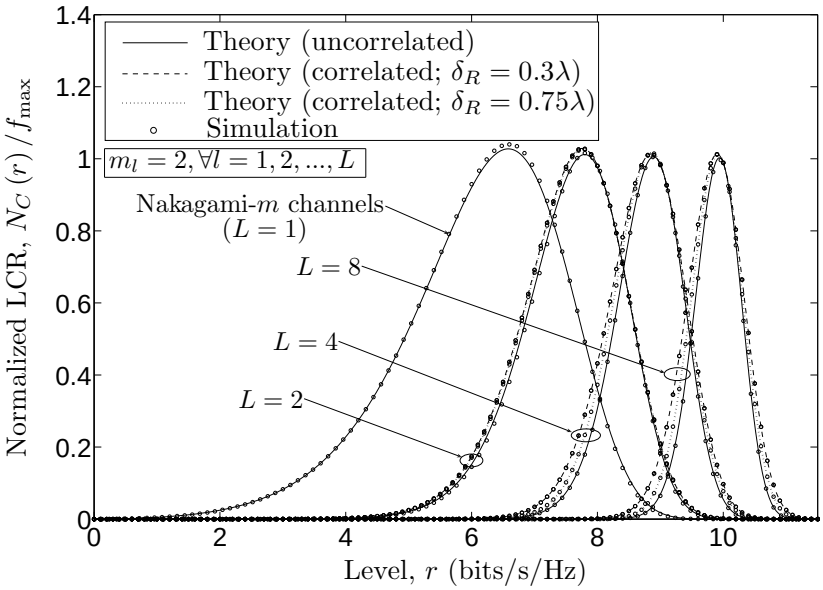

Figure J.8: The normalized LCR $N_C(r)/f_{\max}$ of the capacity of correlated Nakagami-*m* channels with MRC.

the capacity of Nakagami-*m* channels with MRC decreases with an increase in the spatial correlation in the diversity branches. However, this effect is more prominent at higher levels r. While for the case of EGC, an increase in the spatial correlation increases the ADF of the channel capacity. Moreover for both MRC and EGC, an increase in the number of diversity branches decreases the ADF of the channel

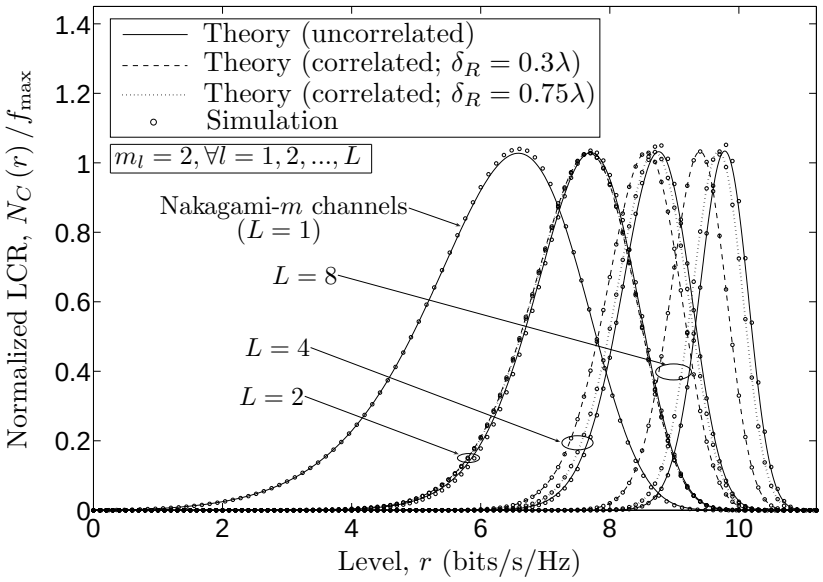

Figure J.9: The normalized LCR $N_C(r)/f_{\max}$ of the capacity of correlated Nakagami-*m* channels with EGC.

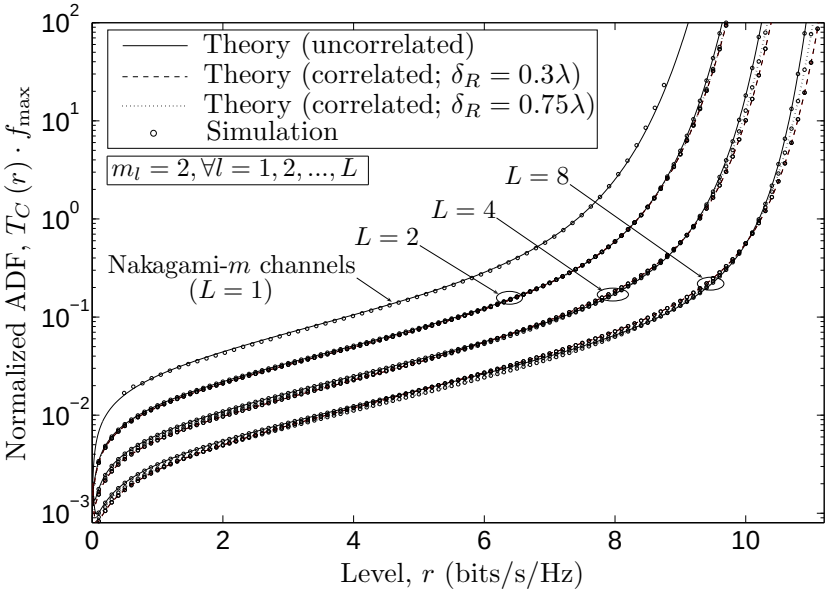

Figure J.10: The normalized ADF $T_C(r) \cdot f_{\max}$ of the capacity of correlated Nakagami-*m* channels with MRC.

capacity. The analytical expressions are verified using simulations, whereby a very good fitting is found.

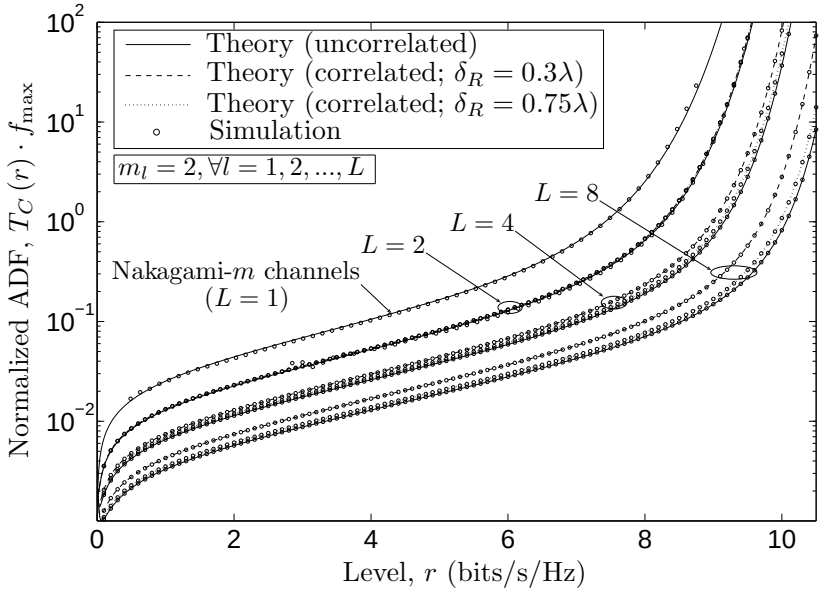

Figure J.11: The normalized ADF $T_C(r) \cdot f_{\max}$ of the capacity of correlated Nakagami-*m* channels with EGC.

VII. Conclusion

This article studies the statistical properties of the capacity of spatially correlated Nakagami-*m* channels with MRC and EGC. We have derived analytical expressions for the PDF, CDF, LCR, and ADF of the capacity of Nakagami-*m* channels with MRC and EGC. The results are studied for different values of the number of diversity branches L and receiver antennas separation δ_R. It is observed that for MRC, an increase in the spatial correlation increases the variance as well as the LCR of the channel capacity, however the ADF of the channel capacity decreases. On the other hand, when using EGC, as the receiver antenna separation increases the mean channel capacity increases, whereas the ADF of the channel capacity decreases. Moreover, an increase in the spatial correlation increases the LCR of the channel capacity at only lower levels r. It is also observed that for both MRC and EGC, an increase in the number of diversity branches increases the mean channel capacity, while the variance and ADF of the channel capacity decreases. The results also show that at lower levels, the LCR is higher for channels with smaller values of the number of diversity branches L than for channels with larger values of L. The analytical findings are verified using simulations, where a very good agreement between the theoretical and simulation results was observed.

REFERENCES

[1] V. A. Aalo. Performance of maximal-ratio diversity systems in a correlated Nakagami-fading environment. *IEEE Trans. Commun.*, 43(8):2360–2369, August 1995.

[2] A. A. Abu-Dayya and N. C. Beaulieu. Microdiversity on Rician fading channels. *IEEE Trans. Commun.*, 42(6):2258–2267, June 1994.

[3] M. S. Alouini and A. J. Goldsmith. Capacity of Rayleigh fading channels under different adaptive transmission and diversity-combining techniques. *IEEE Trans. Veh. Technol.*, 48(4):1165–1181, July 1999.

[4] Mohamed-Slim. Alouini, A. Abdi, and M. Kaveh. Sum of gamma variates and performance of wireless communication systems over Nakagami-fading channels. *IEEE Trans. Veh. Technol.*, 50(6):1471–1480, November 2001.

[5] A. Annamalai, C. Tellambura, and V. K. Bhargava. Equal-gain diversity receiver performance in wireless channels. *IEEE Trans. Commun.*, 48(10):1732–1745, October 2000.

[6] D. M. Black and D. O. Reudink. Some characteristics of mobile radio propagation at 836 MHz in the Philadelphia area. *IEEE Trans. Veh. Technol.*, 21:45–51, February 1972.

[7] G. J. Byers and F. Takawira. Spatially and temporally correlated MIMO channels: modeling and capacity analysis. *IEEE Trans. Veh. Technol.*, 53(3):634–643, May 2004.

[8] Y. Chen and C. Tellambura. Performance analysis of L-branch equal gain combiners in equally correlated Rayleigh fading channels. *IEEE Communications Letters*, 8(3):150–152, March 2004.

[9] S. H. Choi, P. J. Smith, B. Allen, W. Q. Malik, and M. Shafi. Severely fading MIMO channels: Models and mutual information. In *Proc. IEEE International Conference on Communications, ICC 2007*, pages 4628–4633. Glasgow, UK, June 2007.

[10] D. B. da Costa, M. D. Yacoub, and J. C. S. Santos Filho. An improved closed-form approximation to the sum of arbitrary Nakagami-*m* variates. *IEEE Trans. Veh. Technol.*, 57(6):3854–3858, November 2008.

[11] X. Dong and N. C. Beaulieu. Average level crossing rate and fade duration of maximal ratio diversity in unbalanced and correlated channels. In *Proc. IEEE Wireless Communications and Networking 2002, WCNC 2002*, volume 2, pages 762–767, March 2002.

[12] G. J. Foschini and M. J. Gans. On limits of wireless communications in a fading environment when using multiple antennas. *Wireless Pers. Commun.*, 6:311–335, March 1998.

[13] A. Giorgetti, P. J. Smith, M. Shafi, and M. Chiani. MIMO capacity, level crossing rates and fades: The impact of spatial/temporal channel correlation. *J. Commun. Net.*, 5(2):104–115, June 2003.

[14] I. S. Gradshteyn and I. M. Ryzhik. *Table of Integrals, Series, and Products*. New York: Academic Press, 6th edition, 2000.

[15] B. O. Hogstad and M. Pätzold. Exact closed-form expressions for the distribution, level-crossing rate, and average duration of fades of the capacity of MIMO channels. In *Proc. 65th Semiannual Vehicular Technology Conference, IEEE VTC 2007-Spring*, pages 455–460. Dublin, Ireland, April 2007.

[16] W. C. Jakes, editor. *Microwave Mobile Communications*. Piscataway, NJ: IEEE Press, 1994.

[17] E. A. Jorswieck, T. J. Oechtering, and H. Boche. Performance analysis of combining techniques with correlated diversity. In *Proc. IEEE Wireless Communications and Networking Conference, WCNC 2005*, volume 2, pages 849–854, March 2005.

[18] S. Khatalin and J. P. Fonseka. Capacity of correlated Nakagami-*m* fading channels with diversity combining techniques. *IEEE Trans. Veh. Technol.*, 55(1):142–150, January 2006.

[19] S. Khatalin and J. P. Fonseka. On the channel capacity in Rician and Hoyt fading environments with MRC diversity. *IEEE Trans. Veh. Technol.*, 55(1):137–141, January 2006.

[20] W. C. Y. Lee. *Mobile Communications Engineering*. New York: McGraw-Hill, 2nd edition, 1998.

[21] P. Lombardo, G. Fedele, and M. M. Rao. MRC performance for binary signals in Nakagami fading with general branch correlation. *IEEE Trans. Commun.*, 47(1):44–52, January 1999.

[22] C. Mun, C. Kang, and H. Park. Approximation of SNR statistics for MRC diversity systems in arbitrarily correlated Nakagami fading channels. *IEEE Electronics Letters*, 35(4):266–267, February 1999.

[23] M. Nakagami. The *m*-distribution: A general formula of intensity distribution of rapid fading. In W. G. Hoffman, editor, *Statistical Methods in Radio Wave Propagation*. Oxford, UK: Pergamon Press, 1960.

[24] A. Papoulis and S. U. Pillai. *Probability, Random Variables and Stochastic Processes*. New York: McGraw-Hill, 4th edition, 2002.

[25] M. Pätzold. *Mobile Fading Channels*. Chichester: John Wiley & Sons, 2002.

[26] M. Pätzold, C. X. Wang, and B. O. Hogstad. Two new sum-of-sinusoids-based methods for the efficient generation of multiple uncorrelated Rayleigh fading waveforms. *IEEE Trans. Wireless Commun.*, 8(6):3122–3131, June 2009.

[27] D. O. Reudink. Comparison of radio transmission at X-band frequencies in suburban and urban areas. *IEEE Trans. Ant. Prop.*, 20:470–473, July 1972.

[28] S. O. Rice. Mathematical analysis of random noise. *Bell Syst. Tech. J.*, 24:46–156, January 1945.

[29] J. Salz and J. H. Winters. Effect of fading correlation on adaptive arrays in digital mobile radio. *IEEE Trans. Veh. Technol.*, 43(4):1049–1057, November 1994.

[30] H. Samimi and P. Azmi. An approximate analytical framework for performance analysis of equal gain combining technique over independent Nakagami, Rician and Weibull fading channels. *Wireless Personal Communications (WPC)*, 43(4):1399–1408, December 2007. DOI 10.1007/s11277-007-9314-z.

[31] M. Z. Win and J. H. Winters. Exact error probability expressions for MRC in correlated Nakagami channels with unequal fading parameters and branch powers. In *Proc. IEEE Global Telecommunications Conference, GLOBECOM 1999*, volume 5, pages 2331–2335, December 1999.

[32] M. D. Yacoub, J. E. V. Bautista, and L. G. de Rezende Guedes. On higher order statistics of the Nakagami-*m* distribution. *IEEE Trans. Veh. Technol.*, 48(3):790–794, May 1999.

[33] M. D. Yacoub, C. R. C. M. da Silva, and J. E. B. Vargas. Second-order statistics for diversity-combining techniques in Nakagami-fading channels. *IEEE Trans. Veh. Technol.*, 50(6):1464–1470, November 2001.

[34] W. R. Young. Comparison of mobile radio transmission at 150, 450, 900, and 3700 MHz. 31:1068–1085, November 1952.

[35] Q. T. Zhang. Exact analysis of postdetection combining for DPSK and NFSK systems over arbitrarily correlated Nakagami channels. *IEEE Trans. Commun.*, 46(11):1459–1467, November 1998.

[36] Q. T. Zhang. Maximal-ratio combining over Nakagami fading channels with an arbitrary branch covariance matrix. *IEEE Trans. Veh. Technol.*, 48(4):1141–1150, July 1999.

Appendix K

Paper XI

Title:	Capacity Studies of Spatially Correlated MIMO Rice Channels
Authors:	Bjørn Olav Hogstad[1], **Gulzaib Rafiq**[2], Valeri Kontorovich[3], and Matthias Pätzold[2]
Affiliations:	[1]CEIT and Tecnun, University of Navarra, Manuel de Lardizábal 15, 20018, San Sebastián, Spain [2]University of Agder, Faculty of Engineering and Science, P. O. Box 509, NO-4898 Grimstad, Norway [3]Centro de Investigación y de Estudios Avanzados, CINVESTAV, 07360 Mexico City, Mexico
Conference:	*5th International Symposium on Wireless Pervasive Computing, ISWPC 2010*, Modena, Italy, May 2010, pp. 45 – 50.

Capacity Studies of Spatially Correlated MIMO Rice Channels

Bjørn Olav Hogstad[1], Gulzaib Rafiq[2], Valeri Kontorovich[3], and Matthias Pätzold[2]

[1]CEIT and Tecnun, University of Navarra
Manuel de Lardizábal 15, 20018, San Sebastián, Spain
Email: bohogstad@ceit.es

[2]Department of Information and Communication Technology
Faculty of Engineering and Science, University of Agder
Servicebox 509, NO-4898 Grimstad, Norway
E-mails: {gulzaib.rafiq, matthias.paetzold}@uia.no

[3]Centro de Investigación y de Estudios Avanzados, CINVESTAV
07360 Mexico City, Mexico
Email: valeri@cinvestav.mx

***Abstract* — In this paper, we have studied the statistical properties of the capacity of spatially correlated multiple-input multiple-output (MIMO) Rice channels. We have derived an exact closed-form expression for the probability density function (PDF) and an exact expression for the cumulative distribution function (CDF) of the channel capacity for single-input multiple-output (SIMO) and multiple-input single-output (MISO) systems. Furthermore, an accurate closed-form expression has been derived for the level-crossing rate (LCR) and an accurate expression has been obtained for the average duration of fades (ADF) of the SIMO and MISO channel capacities. For the MIMO case, we have investigated the PDF, CDF, LCR, and ADF based on a lower bound on the channel capacity. The results are studied for a different number of transmit and receive antennas, but the proposed method can also be used to investigate the influence of some key parameters on the channel capacity, such as the antenna spacings of the transmitter and the receiver antenna arrays, and the amplitude of the time-invariant line-of-sight (LOS) component. The analytical expressions are valid for the well-known Kronecker model and an LOS component orthogonal to the direction of motion of the receiver. The correctness of the derived expressions is confirmed by simulations.**

I. Introduction

It is well known that the employment of multiple antennas at both the transmitter and the receiver greatly improves the link reliability and increases the overall system

capacity [6, 22]. Therein, it is shown that under idealized propagation conditions, i.e., when the channel matrix has independent and identically distributed (i.i.d.) entries, the channel capacity increases linearly with the minimum of the number of transmitter and receiver antennas. However, it is also well known that the gains in the MIMO channel capacity are sensitive to the presence of temporal and spatial correlations introduced by the propagation environment [21, 3]. Therefore, it is of great importance to study the MIMO channel capacity under non-idealized propagation conditions, i.e., when the elements of the channel matrix are correlated.

In the literature, different MIMO channel models have been proposed, which take the correlations between the sub-channels into account. An overview of the most commonly used MIMO channel models can be found in [1]. In this paper, we have employed a popular separable correlation model known as the Kronecker model [21, 5, 11]. Although it has been observed that the Kronecker model underestimates the channel capacity in some environments [15], it remains a cornerstone of a large number of analyses [23].

Rice processes have intensively been used to model the random fluctuations of the signal amplitude at the receiver. In case there is no LOS component between the transmitter and the receiver, Rayleigh processes are commonly been used for the modeling of fading in strongly dispersive urban environments. A Rice process is a generalization of a Rayleigh process. Also, under a certain condition a Rice process can approximate a Nakagami process. Hence, Rice processes are useful to model the random signal fluctuations in various propagation environments.

The statistical properties of the MIMO channel capacity have been intensively studied in the literature. For example, exact closed-form expressions for the ergodic capacity and the complementary CDF of the capacity are derived in [25] for correlated SIMO Rayleigh channels. Also in [25], accurate and closed-form capacity expressions are derived for correlated SIMO Rice channels. In this paper, we have studied the statistical properties of the capacity of correlated MIMO Rice channels. By using the lower bound on the capacity of correlated MIMO Rice channels presented in [20], we have derived exact analytical expressions for the PDF, CDF, LCR, and ADF of the capacity. In contrast to the PDF and CDF, the LCR and ADF provide useful information on the dynamic behavior of the capacity. The LCR of the channel capacity describes the average number of up-crossings (or down-crossings) of the capacity through a fixed level within a time interval of one second. Analogously, the ADF of the channel capacity is the expected value of the length of the time intervals in which the capacity is below a given level [9].

The remainder of this paper is organized as follows. In Section II, we describe briefly the MIMO channel model. A detailed study of the statistical properties of the MIMO channel capacity is the topic of Section III. The analytical results obtained in Section III will be compared with simulation results in Section IV. Finally, the conclusions are drawn in Section V.

II. The MIMO Channel Model

Throughout the paper, we are dealing with MIMO frequency-nonselective mobile channel models. The number of transmit and receive antennas will be denoted by N_T and N_R, respectively. The input-output relation for such a MIMO system can be expressed as

$$\mathbf{y}(t) = \hat{\mathbf{H}}(t)\mathbf{x}(t) + \mathbf{n}(t)\,. \tag{1}$$

In this equation, $\mathbf{x}(t)$ is an $N_T \times 1$ transmit signal vector, $\mathbf{y}(t)$ is an $N_R \times 1$ received signal vector, $\hat{\mathbf{H}}(t)$ is the so-called $N_R \times N_T$ MIMO channel matrix, and $\mathbf{n}(t)$ is an $N_R \times 1$ additive white Gaussian noise (AWGN) vector. We assume that the components of the AWGN vector $\mathbf{n}(t)$ are uncorrelated and that each element has zero mean and variance (noise power) equal to N_0. In this paper, we will apply the well-known Kronecker model to describe the correlation between the elements. According to the Kronecker model, the channel matrix $\hat{\mathbf{H}}(t)$ can be expressed as

$$\hat{\mathbf{H}}(t) = \mathbf{R}_{R_\mathbf{x}}^{1/2}\mathbf{H}(t)\mathbf{R}_{T_\mathbf{x}}^{1/2} \tag{2}$$

where $\mathbf{R}_{R_\mathbf{x}} = E\{\hat{\mathbf{H}}(t)\hat{\mathbf{H}}(t)^H\}$ and $\mathbf{R}_{T_\mathbf{x}} = E\{\hat{\mathbf{H}}(t)^H\hat{\mathbf{H}}(t)\}$ denote the transmit and the receive correlation matrices, respectively, with $E\{\cdot\}$ as the expectation operator and $(\cdot)^H$ represents the Hermitian operator. In (2), the notation $(\cdot)^{1/2}$ denotes the matrix square root. Furthermore, $\mathbf{H}(t) = [h_{i,j}(t)]$ is an $N_R \times N_T$ complex random matrix with i.i.d. entries. The complex entries $h_{i,j}(t)$ can be expressed as

$$h_{i,j}(t) = h_{i,j}^I(t) + jh_{i,j}^Q(t) \tag{3}$$

where the inphase and quadratic components of $h_{i,j}(t)$ are denoted by $h_{i,j}^I(t)$ and $h_{i,j}^Q(t)$, respectively. In this article, $h_{i,j}^I(t)$ and $h_{i,j}^Q(t)$ are real-valued Gaussian noise processes with identical variances $\sigma^2_{h_{i,j}^I} = \sigma^2_{h_{i,j}^Q} = \sigma^2$. The mean of $h_{i,j}^I(t)$ is denoted by ρ, while the mean of $h_{i,j}^Q(t)$ is equal to zero. It should be mentioned that ρ denotes the amplitude of the LOS component of the received signal [17]. Since, $h_{i,j}(t)$ is a complex Gaussian process with mean ρ and variance $2\sigma^2$, the absolute

value of $h_{i,j}(t)$ (also denoted as envelope)

$$\xi(t) = |h_{i,j}(t)| = \sqrt{[h^I_{i,j}(t)]^2 + [h^Q_{i,j}(t)]^2} \tag{4}$$

follows the Rice distribution.

To express the MIMO channel matrix $\hat{\mathbf{H}}(t)$ using the unitary-independent-unitary (UIU) formulation [24, 14, 8, 23], we continue as follows. Let the eigenvalue decomposition of the correlation matrices $\mathbf{R}_{R_\mathbf{x}}$ and $\mathbf{R}_{T_\mathbf{x}}$ be expressed as

$$\mathbf{R}_{R_\mathbf{x}} = \mathbf{U}_{R_\mathbf{x}} \mathbf{\Lambda}_{R_\mathbf{x}} \mathbf{U}^H_{R_\mathbf{x}} \tag{5}$$

$$\mathbf{R}_{T_\mathbf{x}} = \mathbf{U}_{T_\mathbf{x}} \mathbf{\Lambda}_{T_\mathbf{x}} \mathbf{U}^H_{T_\mathbf{x}} \tag{6}$$

where the unitary matrix $\mathbf{U}_{R_\mathbf{x}}$ $(\mathbf{U}_{T_\mathbf{x}})$ consists of the eigenvectors of the correlation matrix $\mathbf{R}_{R_\mathbf{x}}$ $(\mathbf{R}_{T_\mathbf{x}})$. The diagonal matrix $\mathbf{\Lambda}_{R_\mathbf{x}}$ $(\mathbf{\Lambda}_{T_\mathbf{x}})$ contains the eigenvalues of $\mathbf{R}_{R_\mathbf{x}}$ $(\mathbf{R}_{T_\mathbf{x}})$. After substituting (5) and (6) in (2), we can express the MIMO channel matrix $\hat{\mathbf{H}}(t)$ using the UIU formulation as

$$\hat{\mathbf{H}}(t) = \mathbf{U}_{R_\mathbf{x}} (\mathbf{G} \odot \mathbf{H}(t)) \mathbf{U}^H_{T_\mathbf{x}} \tag{7}$$

where $\mathbf{G}$ is a given deterministic coupling matrix, and the operator $\odot$ denotes the element-wise Schur-Hadamard multiplication, i.e., the element-wise product of two matrices. For the Kronecker model defined in (2), the coupling matrix $\mathbf{G}$ can be expressed as

$$\mathbf{G} = \boldsymbol{\lambda}^{1/2}_{R_\mathbf{x}} (\boldsymbol{\lambda}^{1/2}_{T_\mathbf{x}})^T \tag{8}$$

where the vectors $\boldsymbol{\lambda}^{1/2}_{R_\mathbf{x}}$ and $\boldsymbol{\lambda}^{1/2}_{T_\mathbf{x}}$ contain the square roots of the eigenvalues of $\mathbf{R}_{R_\mathbf{x}}$ and $\mathbf{R}_{T_\mathbf{x}}$, respectively. In (8), the transpose operator is denoted by $(\cdot)^T$. Closed-form expressions for the elements of the transmit and receive correlation matrices, denoted by ρ^T_{pq} and ρ^R_{mn}, respectively, can be found by using Lee's spatio-temporal correlation model [12] under isotropic scattering conditions. From [4], we obtain

$$\rho^T_{pq} = J_0(b_{pq}) \tag{9}$$

$$\rho^R_{mn} = J_0(c_{mn}) \tag{10}$$

where $J_0(\cdot)$ is the zeroth-order Bessel function of the first kind, $b_{pq} = 2\pi\delta_{pq}/\lambda$, and $c_{mn} = 2\pi d_{mn}/\lambda$. Here, λ denotes the wavelength of the transmitted signal. The antenna spacing between the pth and qth transmit antenna is given by δ_{pq}, while d_{mn} represents the antenna spacing between the mth and nth receive antenna. It should be mentioned that (9) and (10) are only valid when the temporal correlation

is neglected.

III. The MIMO Channel Capacity

In this section, we study the capacity of the proposed MIMO channel model in Section II. In case that the transmitter has no knowledge about the channel, whereas the receiver has the perfect channel state information, the capacity $C(t)$, in bits/s/Hz, is defined as

$$C(t) = \log_2 \left[\det \left(\mathbf{I}_{N_R} + \frac{\gamma_s}{N_T} \hat{\mathbf{H}}(t) \hat{\mathbf{H}}(t)^H \right) \right] \tag{11}$$

where $\det(\cdot)$ designates the determinant, $\mathbf{I}_{N_R}$ is the identity matrix of order N_R, and the quantity $\gamma_s = P/N_0$ is the average signal-to-noise ratio (SNR). Here, P is the total transmitted power allocated uniformly to all the transmit antenna elements, and again N_0 represents the noise power. By substituting the UIU formulation (7) in (11), and using the matrix determinant identity $\det(\mathbf{I} + \mathbf{AB}) = \det(\mathbf{I} + \mathbf{BA})$, the MIMO channel capacity $C(t)$ can be expressed as

$$C(t) = \log_2 \left[\det \left(\mathbf{I}_{N_R} + \frac{\gamma_s}{N_T} (\mathbf{G} \odot \mathbf{H}(t)) (\mathbf{G} \odot \mathbf{H}(t))^H \right) \right]. \tag{12}$$

In [20], it is shown that a lower bound on the channel capacity $C(t)$ can be expressed as

$$C_{lb}(t) = \log_2 \left(1 + \frac{\gamma_s}{N_T} \sum_{i=1}^{N_R} \sum_{j=1}^{N_T} \lambda_{R_{\mathbf{x}} i} \lambda_{T_{\mathbf{x}} j} |h_{i,j}(t)|^2 \right) \tag{13}$$

where $\lambda_{R_{\mathbf{x}} i}$ and $\lambda_{T_{\mathbf{x}} j}$ denote the ith and jth eigenvalues of the correlation matrices $\mathbf{R}_{R_{\mathbf{x}}}$ and $\mathbf{R}_{T_{\mathbf{x}}}$, respectively. For the SIMO and MISO case, it is important to mention that the lower bound $C_{lb}(t)$ is equal to the capacity $C(t)$ defined in (11) (or (12)). Furthermore, it should be mentioned that (13) holds only for the coupling matrix $\mathbf{G}$ defined in (8) and when the i.i.d. nature of the entries of the MIMO channel matrix $\mathbf{H}(t)$ can be exploited [20].

In order to study the statistical properties of the channel capacity $C_{lb}(t)$, we continue as follows. Let us define $Y(t) = \sum_{i=1}^{N_R} \sum_{j=1}^{N_T} \lambda_{R_{\mathbf{x}} i} \lambda_{T_{\mathbf{x}} j} |h_{i,j}(t)|^2$. To obtain the PDF and CDF of the channel capacity $C_{lb}(t)$, we need to find the PDF of $Y(t)$. Moreover, to obtain the LCR and ADF of $C_{lb}(t)$, we need to find the joint PDF $p_{Y\dot{Y}}(r, \dot{r})$ of the process $Y(t)$ and its time derivative $\dot{Y}(t)$ at the same time instant. Throughout the paper, we let the overdot of a process denote the time derivative. For completeness, we mentioned that the PDF of the squared envelope $|h_{i,j}(t)|^2$ follows

the non-central chi-square distribution given by [19]

$$p_{|h_{i,j}(t)|^2}(r) = \frac{1}{2\sigma^2} e^{-(\rho^2+r)/2\sigma^2} I_0\left(\sqrt{r}\frac{\rho}{\sigma^2}\right), \quad r \geq 0 \tag{14}$$

where $I_0(\cdot)$ is the zeroth-order modified Bessel function of the first kind. The parameter ρ^2 is the so-called non-centrality parameter of the distribution. From [13, p. 116], the PDF $p_Y(r)$ of $Y(t)$ can be written as

$$p_Y(r) = \sum_{k=0}^{\infty} c_k f(p+2k;r), \quad r \geq 0 \tag{15}$$

where

$$f(p+2k;r) = \frac{r^{p/2+k-1} e^{-r/2}}{2^{p/2+k}\Gamma(p/2+k)}. \tag{16}$$

Here, $p = 2N_R N_T$ and $\Gamma(\cdot)$ is the gamma function [7, Eq. (8.310)]. The coefficients c_k can be calculated from the formulas

$$c_0 = e^{-p\rho^2/4\sigma^2} \prod_{j=1}^{p} (1/\lambda_j)^{1/2} \tag{17}$$

$$c_k = (2k)^{-1} \sum_{r=0}^{k-1} d_{k-r} c_r, \quad k \geq 1 \tag{18}$$

with

$$d_k = \sum_{j=1}^{p} (1-1/\lambda_j)^k + k\rho^2/\sigma^2 \sum_{j=1}^{p/2} (1/\lambda_j)(1-1/\lambda_j)^{k-1}. \tag{19}$$

To determine the vector $\mathbf{\Lambda} = (\lambda_1, \ldots, \lambda_p)^T$, we define an $N_R \times N_T$ matrix $\mathbf{A}$ with elements $A_{ij} = \lambda_{R_{\mathbf{x}}i}\lambda_{T_{\mathbf{x}}j}$. Hence, $\mathbf{\Lambda} = \sigma^2 \mathrm{vec}([\mathbf{A}, \mathbf{A}])$, where $\mathrm{vec}(\mathbf{A})$ represents a vector formed by stacking all the columns of $\mathbf{A}$ into a column vector. Note that $f(p+2k;r)$ represents the central chi-square distribution with $n = p+2k$ degrees of freedom.

By defining $p_X^{(k)}(r) = f(p+2k;r)$, the PDF $p_Y(r)$ of $Y(t)$ can be expressed as

$$p_Y(r) = \sum_{k=0}^{\infty} c_k p_X^{(k)}(r). \tag{20}$$

In [20], it is shown that the joint PDF $p_{Y\dot{Y}}(r,\dot{r})$ of $Y(t)$ and $\dot{Y}(t)$ can be approximated as

$$p_{Y\dot{Y}}(r,\dot{r}) \approx \sum_{k=0}^{\infty} c_k p_{X\dot{X}}^{(k)}(r,\dot{r}). \tag{21}$$

Here, $p^{(k)}_{X\dot{X}}(r,\dot{r})$ is defined in analogy to (20) as the joint PDF of $X(t)$ and $\dot{X}(t)$, where $X(t)$ follows the central chi-square distribution with $n = p+2k$ degrees of freedom. Analogously to the central chi-square case [2], an expression for the joint PDF $p^{(k)}_{X\dot{X}}(r,\dot{r})$ can be found. The calculation of the joint PDF $p^{(k)}_{X\dot{X}}(r,\dot{r})$ is omitted for brevity. The joint PDF $p_{Y\dot{Y}}(r,\dot{r})$ can now be written as

$$p_{Y\dot{Y}}(r,\dot{r}) \approx \sum_{k=0}^{\infty} \frac{c_k r^{p/2+k-3/2} e^{-r/(2\sigma^2)-\dot{r}^2/(16\beta\pi^2 f_{\max}^2\sigma^2 r)}}{2^{p/2+k+2}\pi\sqrt{\beta\pi} f_{\max}\sigma^{p+2k+1}\Gamma(p/2+k)}, \quad r \geq 0, |\dot{r}| < \infty \tag{22}$$

where $\beta = \sum_{i=1}^{N_R}\sum_{j=1}^{N_T}(\lambda_{R_{\mathbf{x}}i}\lambda_{T_{\mathbf{x}}j})^2/(N_R N_T)$. It should be noted that (22) holds only for isotropic scattering conditions.

A. PDF and CDF of the MIMO Channel Capacity

The PDF of $C_{lb}(t)$, denoted by $p_{C_{lb}}(r)$, can be found by using (15) and by applying the concept of transformation of random variables [16] as

$$\begin{aligned} p_{C_{lb}}(r) &= \frac{2^r \ln(2)}{\gamma_s'} p_Y\left(\frac{2^r-1}{\gamma_s'}\right) \\ &= \sum_{k=0}^{\infty} \frac{c_k 2^r \ln(2)}{\gamma_s'} f(p+2k;(2^r-1)/\gamma_s'), \ r \geq 0 \end{aligned} \tag{23}$$

where $\gamma_s' = \gamma_s/N_T$. Furthermore, the CDF $F_{C_{lb}}(r)$ of $C_{lb}(t)$ can be expressed as

$$\begin{aligned} F_{C_{lb}}(r) &= \int_0^r p_{C_{lb}}(x)\,dx \\ &= \sum_{k=0}^{\infty} \frac{c_k \ln(2)}{\gamma_s'} \int_0^r 2^x f(p+2k;(2^x-1)/\gamma_s')\,dx, \ r \geq 0. \end{aligned} \tag{24}$$

B. LCR and ADF of the MIMO Channel Capacity

The LCR $N_{C_{lb}}(r)$ of the channel capacity $C_{lb}(t)$ is defined as

$$N_{C_{lb}}(r) = \int_0^{\infty} \dot{z} p_{C_{lb}\dot{C}_{lb}}(r,\dot{z})\,d\dot{z}, \quad r \geq 0\,. \tag{25}$$

Hence, to find the LCR of the channel capacity $C_{lb}(t)$, the joint PDF $p_{C_{lb}\dot{C}_{lb}}(r,\dot{r})$ of $C_{lb}(t)$ and $\dot{C}_{lb}(t)$ is required. Thus, by applying the concept of transformation of random variables, we obtain

$$p_{C_{lb}\dot{C}_{lb}}(r,\dot{r}) = \left(\frac{2^r \ln(2)}{\gamma_s'}\right)^2 p_{Y\dot{Y}}\left(\frac{2^r-1}{\gamma_s'}, \frac{2^r \dot{r} \ln(2)}{\gamma_s'}\right)$$

$$\approx \sum_{k=0}^{\infty} \frac{c_k (2^r \ln(2))^2 e^{-\frac{(2^r \dot{r} \ln(2))^2}{\gamma_s' 16\beta\pi^2 f_{\max}^2 \sigma^2 (2^r-1)}}}{\gamma_s'^2 2^{p/2+k+2} \pi\sqrt{\pi} f_{\max} \sigma^{p+2k+1} \Gamma(p/2+k)} \left(\frac{2^r-1}{\gamma_s'}\right)^{p/2+k-3/2} \times e^{-\frac{2^r-1}{\gamma_s' 2\sigma^2}}, \quad r \geq 0, |\dot{r}| < \infty. \tag{26}$$

After substituting (26) in (25) and carrying out some algebraic computations, we obtain the following closed-form solution

$$N_{C_{lb}}(r) \approx \sum_{k=0}^{\infty} \frac{c_k \sqrt{\beta\pi} f_{\max} \left(\frac{2^r-1}{\gamma_s'}\right)^{p/2+k-1/2} e^{-\frac{2^r-1}{\gamma_s' 2\sigma^2}}}{2^{p/2+k-1} \sigma^{p+2k-1} \Gamma(p/2+k)}, \quad r \geq 0. \tag{27}$$

Note that $N_{C_{lb}}(r)$ is proportional to $f_{\max}$, and hence, the normalization of $N_{C_{lb}}(r)$ onto $f_{\max}$ removes the influence of the vehicle speed.

Finally, by means of [10], the ADF $T_{C_{lb}}(r)$ of the channel capacity $C_{lb}(t)$ is obtained as

$$T_{C_{lb}}(r) = \frac{F_{C_{lb}}(r)}{N_{C_{lb}}(r)}. \tag{28}$$

An expression can directly be obtained for $T_{C_{lb}}(r)$ by using the results in (24) and (27).

IV. Simulation results

In this section, we present analytical and simulation results for the statistical properties of the capacity of various MIMO Rice channels. In order to generate mutually uncorrelated Rice fading waveforms, we have used the sum-of-sinusoids principle. For the computation of the model parameters, we have applied the generalized method of exact Doppler spread ($GMEDS_1$) [18]. In the designed Rice fading channel simulator, the number of sinusoids were $N_1 = 35$ and $N_2 = 36$. The variance of the two real-valued uncorrelated Gaussian noise processes was chosen to be $\sigma^2 = 1$. The maximum Doppler frequency $f_{\max}$ was 91, the SNR γ_s was chosen to be 17 dB, and the amplitude of the time-invariant LOS component was $\rho = 1$. Unless otherwise stated, both the transmitter and the receiver antenna spacings are taken to be $\lambda/2$, i.e., $\delta_{pq} = |p-q|\lambda/2$ and $d_{mn} = |m-n|\lambda/2$. Firstly, we consider the PDF of the capacity for a different number of receive and transmit antennas in Figs. K.1–K.3. By comparing Figs. K.1 and K.2, we gather that it is more important for increasing the channel capacity to have a high number of receive antennas rather than a high number of transmit antennas. In Figs. K.4–K.6, we have presented the normalized LCR of the capacity. In the SIMO and MISO cases, the spread of the LCR of the capacity decreases with increasing the number of antennas. Similar

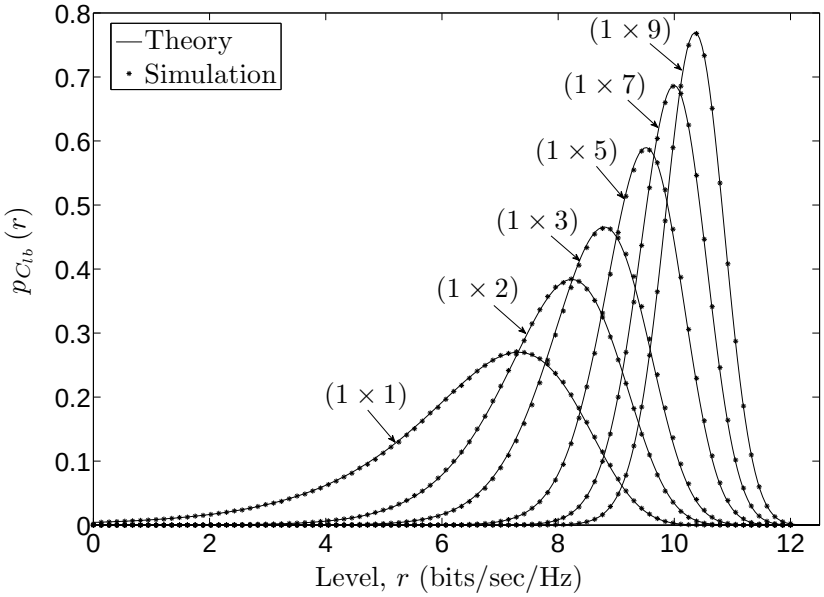

Figure K.1: The PDF of the $(1 \times N_R)$ SIMO channel capacity.

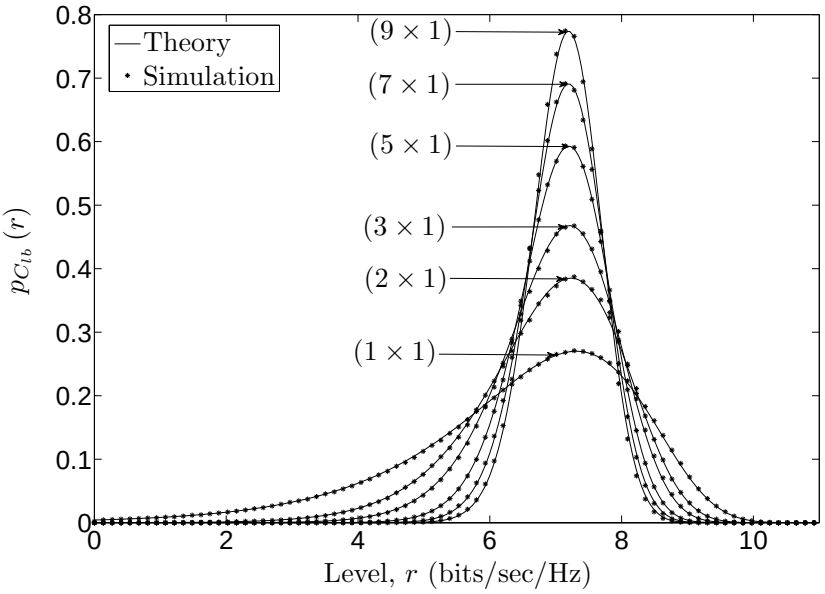

Figure K.2: The PDF of the $(N_T \times 1)$ MISO channel capacity.

to the simulation results presented in [9] for the capacity of uncorrelated Rayleigh SIMO (MISO) channels, the maximum LCR is nearly independent on the number of receive (transmit) antennas. Finally, in Fig. K.7, we present the normalized ADF of the MIMO channel capacity. This figure shows that the mean value for the length of the time intervals in which the capacity $C_{lb}(t)$ is below a given length r, is decreasing with the number of transmit and receive antennas. In all figures, a good fitting between the analytical and the simulation results can be observed.

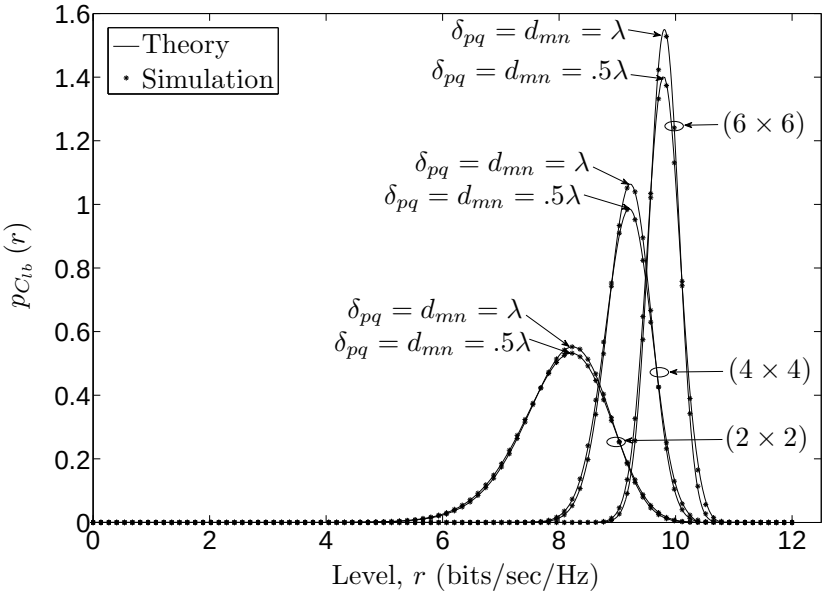

Figure K.3: The PDF of the $(N_T \times N_R)$ MIMO channel capacity.

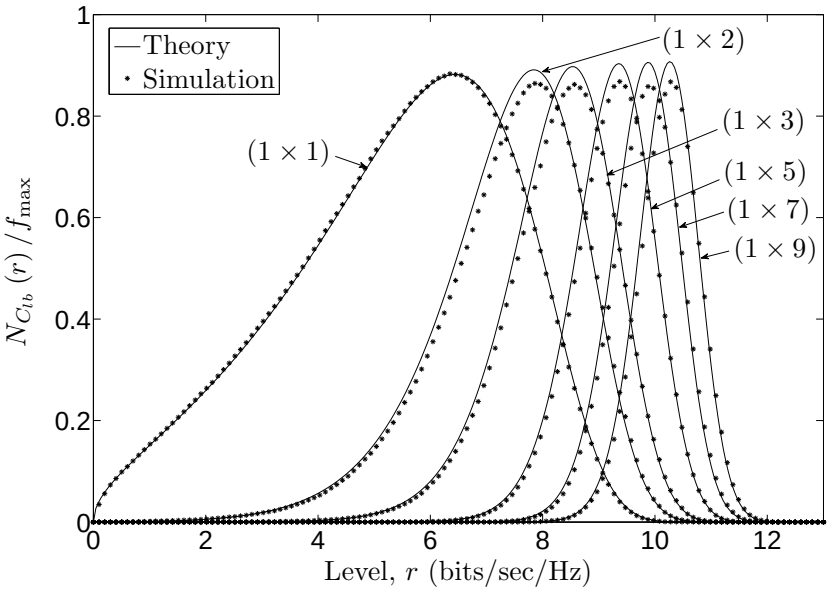

Figure K.4: The LCR of the $(1 \times N_R)$ SIMO channel capacity.

V. Conclusions

In this paper, we have studied the statistical properties of the capacity of spatially correlated MIMO Rice channels. For the SIMO and MISO case, exact expressions for the PDF and CDF are derived. In order to obtain a high mean value for the channel capacity, it is more important to have a high number of receive antennas rather than a high number of transmit antennas. Furthermore, accurate expressions for the

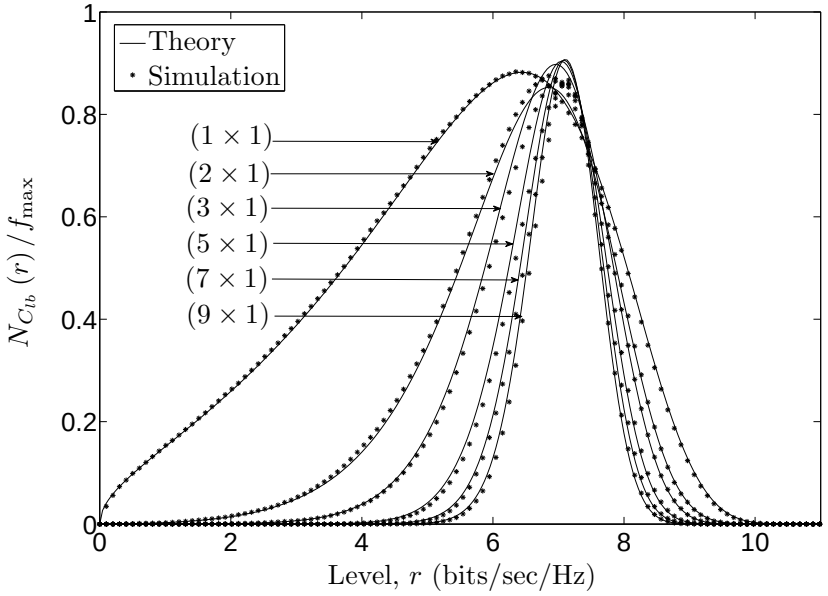

Figure K.5: The LCR of the $(N_T \times 1)$ MISO channel capacity.

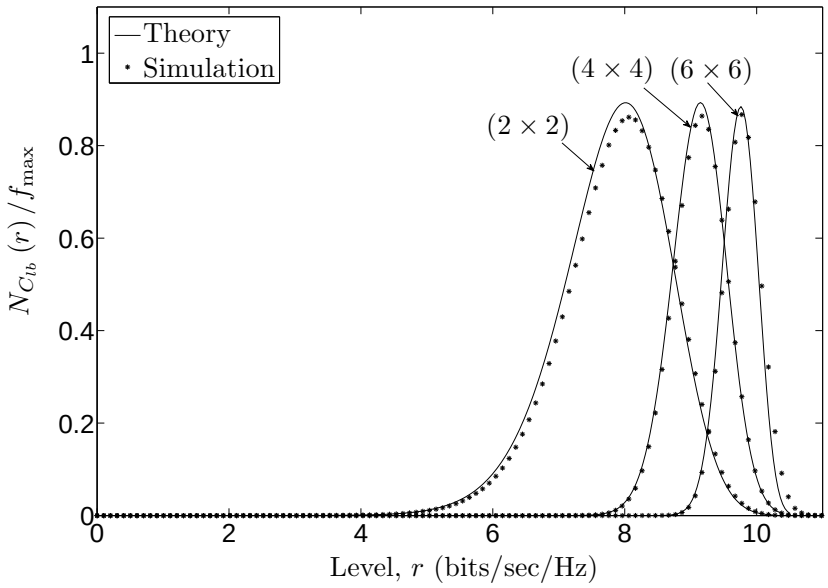

Figure K.6: The LCR of the $(N_T \times N_R)$ MIMO channel capacity.

LCR and ADF of the capacity are also obtained. For the MIMO case, we have derived the PDF, CDF, LCR, and ADF of a lower bound on the channel capacity. The analytical expressions are valid for any number of transmit and receive antennas under isotropic scattering conditions, and a time-invariant LOS component. The analytical results are verified by simulations.

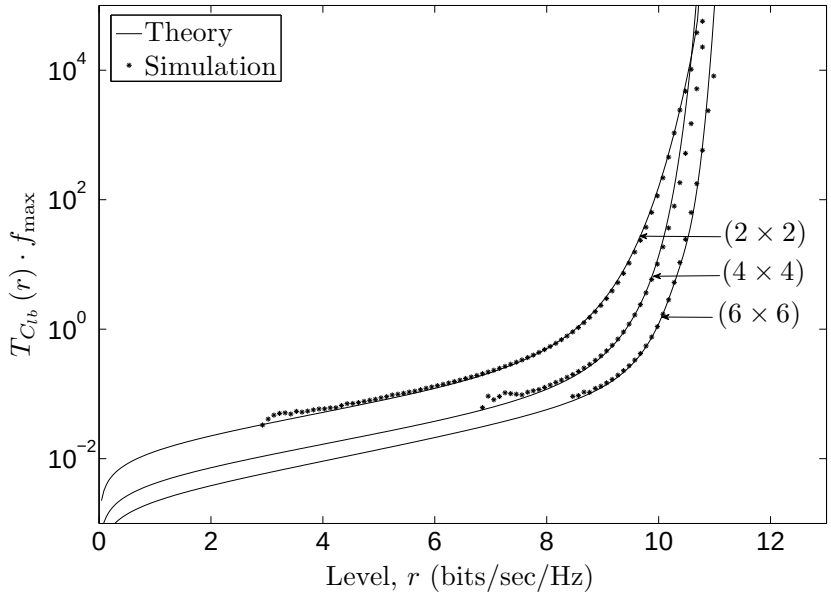

Figure K.7: The ADF of the $(N_T \times N_R)$ MIMO channel capacity.

VI. Acknowledgment

The contribution of Dr. B. O. Hogstad in this paper was partially supported by the Spanish Ministry of Education and Science as well as by the European Regional Development Fund through the program CONSOLIDER-INGENIO 2010 CSD2008-00010 COMONSES.

The contribution of G. Rafiq and Prof. M. Pätzold was partially supported by the Research Council of Norway (NFR) through the project 176773/S10 entitled "Optimized Heterogeneous Multiuser MIMO Networks – OptiMO".

References

[1] P. Almers, E. Bonek, A. Burr, N. Czink, M. Debbah, V. Degli-Esposti, H. Hofstetter, P. Kyösti, D. Laurenson, G. Matz, A. F. Molisch, C. Oestges, and H. Özcelik. Survey of channel and radio propagation models for wireless MIMO systems. *EURASIP J. Wirel. Commun. Netw.*, 2007(1):56–56, January 2007. DOI 10.1155/2007/19070.

[2] N. C. Beaulieu and X. Dong. Level crossing rate and average fade duration of MRC and EGC diversity in Ricean fading. 51(5):722–726, May 2003.

[3] G. J. Byers and F. Takawira. The influence of spatial and temporal correlation on the capacity of MIMO channels. In *Proc. IEEE Wireless Communications and Networking 2003, WCNC 2003*, pages 359–364, March 2003.

[4] G. J. Byers and F. Takawira. Spatially and temporally correlated MIMO channels: modeling and capacity analysis. *IEEE Trans. Veh. Technol.*, 53(3):634–643, May 2004.

[5] C. N. Chuah, J. M. Kahn, and D. Tse. Capacity of multiantenna array systems in indoor wireless environment. In *Proc. 50th IEEE Global Telecommunications Conference, GLOBECOM 2007*, volume 4, pages 1894–1899. Sydney, Australia, November 1998.

[6] G. J. Foschini and M. J. Gans. On limits of wireless communications in a fading environment when using multiple antennas. *Wireless Pers. Commun.*, 6:311–335, March 1998.

[7] I. S. Gradstein and I. M. Ryshik. *Tables of Series, Products, and Integrals*, volume I and II. Frankfurt: Harri Deutsch, 5th edition, 1981.

[8] M. Herdin, G. Gritsch, B. Badic, and E. Bonek. The influence of channel models on simulated MIMO performance. In *Proc. IEEE 59th Vehicular Technology Conference, IEEE VTC 2004-Spring*, pages 304–307. Milan, Italy, May 2004.

[9] B. O. Hogstad, M. Pätzold, N. Youssef, and V. Kontorovitch. Exact closed-form expressions for the distribution, level-crossing rate, and average duration of fades of the capacity of OSTBC-MIMO channels. *IEEE Trans. Veh. Technol.*, 58(2):1011–1016, February 2009.

[10] W. C. Jakes, editor. *Microwave Mobile Communications*. Piscataway, NJ: IEEE Press, 1994.

[11] J. P. Kermoal, L. Schumacher, K. I. Pedersen, P. E. Mogensen, and F. Fredriksen. A stochastic MIMO radio channel model with experimental validation. *IEEE Journal on Selected Areas in Communications*, 20(6):1211–1226, August 2002.

[12] W. C. Y. Lee. Level crossing rates of an equal-gain predection diversity combiner. *IEEE Trans. Commun. Technol.*, 18(4):417–426, August 1970.

[13] A. M. Mathai and S. B. Provost. *Quadratic Forms in Random Variables*. New York: Marcel Dekker, 1992.

[14] H. Özcelik, N. Czink, and E. Bonek. What makes a good MIMO channel model? In *Proc. IEEE 61st Vehicular Technology Conference, IEEE VTC 2005-Spring*, volume 1, pages 156–160. Stockholm, Sweden, May 2005.

[15] H. Özcelik, M. Herdin, W. Weichselberger, J. Wallace, and E. Bonek. Deficiencies of 'Kronecker' MIMO radio channel model. *IEEE Electronics Letters*, 39(16):1209–1210, August 2003.

[16] A. Papoulis and S. U. Pillai. *Probability, Random Variables and Stochastic Processes*. New York: McGraw-Hill, 4th edition, 2002.

[17] M. Pätzold. *Mobile Fading Channels*. Chichester: John Wiley & Sons, 2002.

[18] M. Pätzold and B. O. Hogstad. Two new methods for the generation of multiple uncorrelated Rayleigh fading waveforms. In *Proc. 63rd IEEE Semi-annual Vehicular Technology Conference, IEEE VTC 2006-Spring*, volume 6, pages 2782–2786. Melbourne, Australia, May 2006.

[19] J. Proakis. *Digital Communications*. New York: McGraw-Hill, 4th edition, 2001.

[20] G. Rafiq, V. Kontorovich, and M. Pätzold. On the statistical properties of the capacity of the spatially correlated Nakagami-*m* MIMO channels. In *Proc. IEEE 67th Vehicular Technology Conference, IEEE VTC 2008-Spring*, pages 500–506. Marina Bay, Singapore, May 2008.

[21] D.-S. Shiu, G. J. Foschini, M. J. Gans, and J. M. Kahn. Fading correlation and its effect on the capacity of multielement antenna systems. *IEEE Trans. Commun.*, 48(3):502–513, March 2000.

[22] I. E. Telatar. Capacity of multi-antenna Gaussian channels. *European Trans. Telecommun. Related Technol.*, 10(6):585–595, November/December 1999.

[23] A. Tulino, A. Lozano, and S. Verdu. Impact of antenna correlation on the capacity of multiantenna channels. *IEEE Trans. Inform. Theory*, 51(7):2491–2509, July 2005.

[24] W. Weichselberger, M. Herdin, H. Özcelik, and E. Bonek. A stochastic MIMO channel model with joint correlation of both link ends. *IEEE Trans. Wireless Commun.*, 5(1):90–100, January 2006.

[25] Y. Zhao, M. Zhao, S. Zhou, and J. Wang. Closed-form capacity expressions for SIMO channels with correlated fading. In *Proc. 62th IEEE Vehicular Technology Conference, VTC2005-Spring*, volume 2, pages 982–985. Dallas, USA, September 2005.

Appendix L

Paper XII

Title:	On the Statistical Properties of the Capacity of Spatially Correlated Nakagami-*m* MIMO Channels
Authors:	**Gulzaib Rafiq**[1], Valeri Kontorovich[2], and Matthias Pätzold[1]
Affiliations:	[1]University of Agder, Faculty of Engineering and Science, P. O. Box 509, NO-4898 Grimstad, Norway [2]Centro de Investigación y de Estudios Avanzados, CINVESTAV, 07360 Mexico City, Mexico
Conference:	*67th IEEE Vehicular Technology Conference, VTC2008-Spring*, Singapore, May. 2008, pp. 500 – 506.

On the Statistical Properties of the Capacity of Spatially Correlated Nakagami-*m* MIMO Channels

Gulzaib Rafiq[1], Valeri Kontorovich[2], and Matthias Pätzold[1]
[1]Department of Information and Communication Technology
Faculty of Engineering and Science, University of Agder
Servicebox 509, NO-4898 Grimstad, Norway
E-mails: {gulzaib.rafiq, matthias.paetzold}@uia.no
[2]Centro de Investigación y de Estudios Avanzados, CINVESTAV
07360 Mexico City, Mexico
Email: valeri@cinvestav.mx

***Abstract* — This paper studies the statistical properties of the channel capacity of spatially correlated Nakagami-*m* multiple-input multiple-output (MIMO) channels. We have derived closed-form expressions for the probability density function (PDF), the cumulative distribution function (CDF), the level-crossing rate (LCR), and the average duration of fades (ADF) of the lower bound on the channel capacity. In order to study the impact of the spatial correlation on the channel capacity, the analysis of the statistical properties of the channel capacity is carried out for different receiver antenna spacings. It is observed that the antenna spacing has a significant influence on the spread and maximum value of the PDF and LCR. The proposed method can be employed to study the statistical properties of the capacity of MIMO channels in different fading environments. The correctness of the analytical expressions is confirmed by simulations.**

I. Introduction

MIMO systems have gained considerable attention in recent years due to their potential to provide remarkable gain in the channel capacity [21, 7]. One of the reasons for the gain in capacity is the assumption that the channel matrix has independent and identically distributed (i.i.d.) entries. Under such ideal conditions, a linear increase in the channel capacity w.r.t. the increase in the minimum of the number of receiver and transmitter antennas is observed [21, 7]. However, such idealized propagation conditions can rarely be found in real practice. It is shown in [24] and multiple references therein that due to the spatial correlation between the MIMO channel coefficients, realistic MIMO channels show a reduced channel capacity as compared to the results found in [21] and [7]. It is therefore of great practical and

theoretical interest to study the capacity of MIMO systems when the elements of the channel matrix are correlated.

In recent years, different channel models have been proposed in order to address the problem of correlated fading in MIMO channels, e.g., [24, 25, 14, 10, 5, 8, 19, 23]. An overview encapsulating all the available channel models can be found in [1]. In this paper, we have employed one of the most commonly used channel models known as the Kronecker model [5, 8, 22]. This model, though restrictive to some cases, provides an adequate framework for the information theoretic analysis of MIMO channels.

In order to model the random fluctuations of the signal amplitude at the receiver, several distributions have been proposed in the literature. The most commonly used distributions include the Rayleigh and Ricean distribution for the modeling of fading in strongly dispersive urban environments. Results for the channel capacity and its statistical properties for Rayleigh-faded MIMO channels can be found in [24, 8, 13]. However, in wireless communication systems it is common to come across such scenarios where fading is more (or less) severe than Rayleigh fading. For such cases, the Nakagami-*m* distribution has been widely accepted as an appropriate statistical model to characterize fading in MIMO channels due to its wide range of applications, tractable analytical form, and having good fitness with experimental results [4, 6, 26, 2]. Moreover, the Nakagami-*m* distribution inherently includes the Gaussian and the Rayleigh distributions as special cases, i.e., for $m = 0.5$ and $m = 1$, respectively. Similarly, for $m > 1$, the Nakagami-*m* distribution can be used as a statistical model for MIMO channels where fading is less severe as compared to Rayleigh fading [26]. Hence, the Nakagami-*m* distribution can be considered as an appropriate generalized statistical model for MIMO channels for different fading conditions.

In this paper, we have studied the impact of the spatial correlation on the capacity of Nakagami-*m* MIMO channels. Studies pertaining to unveil the dynamics of the channel capacity can be very helpful to achieve higher data rates while keeping the probability of error as low as possible. In mobile communication systems, the LCR and ADF of the channel capacity are important characteristic quantities which provide insight into the dynamic behavior of the channel capacity [8, 12]. The LCR of the channel capacity describes the average number of up-crossings (or down-crossings) of the capacity through a fixed level within a time interval of one second. Analogously, the ADF of the channel capacity is the expected value of the length of the time intervals in which the capacity is below a given level [12, 11]. We have presented a lower bound on the capacity of Nakagami-*m* MIMO channels. Based on

this, we have derived closed-form expressions for the PDF, CDF, LCR, and ADF of the capacity of spatially correlated Nakagami-*m* MIMO channels. Our analysis has revealed that the spatial correlation of the antenna elements has a dominant effect on the MIMO channel capacity.

The rest of the paper is organized as follows. In Section II, we describe briefly the Kronecker model for MIMO channels. In Section III, we have defined the MIMO channel capacity and its lower bound. Furthermore, some important results are derived which are then used in Section IV, where the focus is on the analysis of the statistical properties of the channel capacity. The theoretical and the simulation results are discussed in Section V. Finally, the conclusions are given in Section VI.

II. The Channel Model

We consider a flat fading MIMO channel with N_T transmit and N_R receive antennas. The input-output relation for such a system is given by

$$\mathbf{y}(t)=\hat{\mathbf{H}}(t)\mathbf{x}(t)+\mathbf{n}(t) \tag{1}$$

where $\mathbf{x}(t)$ is an $N_T \times 1$ transmit signal vector, $\mathbf{y}(t)$ is an $N_R \times 1$ received signal vector, $\hat{\mathbf{H}}(t)$ is the $N_R \times N_T$ channel matrix, and $\mathbf{n}(t)$ is an $N_R \times 1$ additive white Gaussian noise (AWGN) vector. The channel matrix $\hat{\mathbf{H}}(t)$ is modeled using a separable correlation model referred to as the Kronecker model given in [5, 8, 22], i.e.,

$$\hat{\mathbf{H}}(t)=\mathbf{R}_{R_\mathbf{x}}^{1/2}\mathbf{H}(t)\left(\mathbf{R}_{T_\mathbf{x}}^{1/2}\right)^H \tag{2}$$

where $\mathbf{R}_{R_\mathbf{x}}$ is the $N_R \times N_R$ receive correlation matrix, $\mathbf{R}_{T_\mathbf{x}}$ is the $N_T \times N_T$ transmit correlation matrix, $(\cdot)^H$ represents the Hermitian operator, and $(\cdot)^{1/2}$ here represents the matrix square root. In (2), $\mathbf{H}(t)$ is the $N_R \times N_T$ matrix with complex random i.i.d. entries $h_{i,j}(t)$. In this article, we have assumed that the envelope $\left|h_{i,j}(t)\right|$ of the complex entries $h_{i,j}(t)$ follows a Nakagami-*m* distribution given by

$$p_{\left|h_{i,j}(t)\right|}(r)=\frac{2m^m r^{2m-1}}{\Gamma(m)\,\Omega m}e^{-\frac{mr^2}{\Omega}}, \quad r \geq 0 \tag{3}$$

where $\Omega = E\left\{r^2\right\}$, $m=\Omega^2/\mathrm{Var}\left\{r^2\right\}$, and $\Gamma(\cdot)$ represents the gamma function [9]. Here, $E\{\cdot\}$ and $\mathrm{Var}\{\cdot\}$ denote the expectation and the variance operator, respectively. Moreover, the phase of the complex entries $h_{i,j}(t)$ is considered to be uniformly distributed between $[-\pi,\pi]$. The eigenvalue decomposition of the correlation matrices $\mathbf{R}_{R_\mathbf{x}}$ and $\mathbf{R}_{T_\mathbf{x}}$ can be expressed as

$$\mathbf{R}_{R_\mathbf{x}} = \mathbf{U}_{R_\mathbf{x}} \mathbf{\Lambda}_{R_\mathbf{x}} \mathbf{U}_{R_\mathbf{x}}^H \tag{4a}$$

$$\mathbf{R}_{T_\mathbf{x}} = \mathbf{U}_{T_\mathbf{x}} \mathbf{\Lambda}_{T_\mathbf{x}} \mathbf{U}_{T_\mathbf{x}}^H \tag{4b}$$

where $\mathbf{U}_{R_\mathbf{x}}$ ($\mathbf{U}_{T_\mathbf{x}}$) represents the eigenbasis vector at the receiver (transmitter) and the diagonal matrix $\mathbf{\Lambda}_{R_\mathbf{x}}$ ($\mathbf{\Lambda}_{T_\mathbf{x}}$) comprise the eigenvalues of the correlation matrix $\mathbf{R}_{R_\mathbf{x}}$ ($\mathbf{R}_{T_\mathbf{x}}$). Substituting (4a) and (4b) in (2), we can express the MIMO channel matrix $\hat{\mathbf{H}}(t)$ using the unitary-independent-unitary (UIU) formulation as [24, 25, 14, 10, 22]

$$\hat{\mathbf{H}}(t) = \mathbf{U}_{R_\mathbf{x}}^{1/2} \left(\mathbf{G} \odot \mathbf{H}(t)\right) \mathbf{U}_{T_\mathbf{x}}^{1/2^H} \tag{5}$$

where the matrix $\mathbf{G}$ is the element-wise square root of the eigenmode coupling matrix $\mathbf{G}_2$ and $\odot$ denotes the element-wise product of two matrices. For the Kronecker model defined in (2), the matrices $\mathbf{G}$ and $\mathbf{G}_2$ can be expressed as

$$\mathbf{G} = \boldsymbol{\lambda}_{R_\mathbf{x}}^{1/2} \boldsymbol{\lambda}_{T_\mathbf{x}}^{1/2^H}, \ \mathbf{G}_2 = \boldsymbol{\lambda}_{R_\mathbf{x}} \boldsymbol{\lambda}_{T_\mathbf{x}}^H \tag{6}$$

where $\boldsymbol{\lambda}_{R_\mathbf{x}}^{1/2}$ and $\boldsymbol{\lambda}_{T_\mathbf{x}}^{1/2}$ are the vectors containing the diagonal entries of the matrices $\mathbf{\Lambda}_{R_\mathbf{x}}^{1/2}$ and $\mathbf{\Lambda}_{T_\mathbf{x}}^{1/2}$, respectively. The closed-form expressions for the transmit and receive antenna correlations under isotropic scattering conditions can be found in [3] as

$$\rho_{p,q}^T = J_0\left(b_{pq}\right) \tag{7a}$$

$$\rho_{m,n}^R = J_0\left(c_{mn}\right). \tag{7b}$$

where $\rho_{p,q}^T$ ($\rho_{m,n}^R$) represent the transmit (receive) antenna correlation. In (7), $J_0(\cdot)$ is the Bessel function of the first kind of order zero, $b_{pq} = 2\pi\delta_{pq}/\lambda$, and $c_{mn} = 2\pi d_{mn}/\lambda$. Here, λ is the wavelength of the transmitted signal, whereas d_{mn} and δ_{mn} represent the spacing between the transmit and receive antenna elements, respectively. It should be noted from (7) that, for the sake of simplicity, we have only considered the spatial transmit and receive antenna correlations, while the temporal correlation has been omitted.

III. The MIMO Channel Capacity

In this section, we define the capacity of a MIMO channel represented by the channel matrix in (5). It is assumed that the total transmitted power is constrained to P. Furthermore, it is also assumed that the transmitter has no knowledge about the channel, whereas the receiver has the perfect channel state information (CSI). For such a scenario, the capacity of the MIMO system is given by [21, 7, 8, 8, 20]

$$C(t) = \log_2 \left[\det \left(\mathbf{I}_{N_R} + \frac{\gamma_s}{N_T} \hat{\mathbf{H}}(t) \hat{\mathbf{H}}^H(t) \right) \right] \text{ (bits/sec/Hz)} \tag{8}$$

where $\mathbf{I}_{N_R}$ is the identity matrix of order N_R, and $\gamma_s = P/N_0$ is the received signal-to-noise ratio (SNR). Here, N_0 represents the power spectral density (PSD) of the AWGN vector $\mathbf{n}(t)$, defined in (1) at the receiver. Substituting (5) in (8) and using the matrix determinant identity $\det(\mathbf{I}+\mathbf{AB}) = \det(\mathbf{I}+\mathbf{BA})$, the MIMO channel capacity $C(t)$ can be expressed as

$$C(t) = \log_2 \left[\det \left(\mathbf{I}_{N_R} + \frac{\gamma_s}{N_T} (\mathbf{G} \odot \mathbf{H}(t)) (\mathbf{G} \odot \mathbf{H}(t))^H \right) \right] \tag{9}$$

After substituting (6) in (9) and carrying out some algebraic manipulations, a lower bound on the channel capacity $C(t)$ can be expressed as (the proof is included in Appendix L. A)

$$C_{lb}(t) = \log_2 \left(1 + \frac{\gamma_s}{N_T} \sum_{i=1}^{N_R} \sum_{j=1}^{N_T} \lambda_{R_{\mathbf{x}} i} \lambda_{T_{\mathbf{x}} j} \left| h_{i,j}(t) \right|^2 \right). \tag{10}$$

Here, $\lambda_{R_{\mathbf{x}} i}$ and $\lambda_{T_{\mathbf{x}} j}$ are the i^{th} and j^{th} entries of the vectors $\boldsymbol{\lambda}_{R_{\mathbf{x}}}$ and $\boldsymbol{\lambda}_{T_{\mathbf{x}}}$ in (6), respectively. Moreover, $h_{i,j}(t)$ are the i.i.d. entries of the matrix $\mathbf{H}(t)$. However, it should be noted that (10) holds only for the eigenmode coupling matrix $\mathbf{G}_2$ defined in (6) and when the i.i.d. nature of the entries of the matrix $\mathbf{H}(t)$ is exploited. The mean channel capacity for a 4×4 MIMO system given by (9) and the mean channel capacity of the lower bound represented by (10) are shown in Fig. L.1. The parameters used for the simulation of (9) and (10) are discussed in detail in Section V. Here, $E\{\cdot\}$ represents the expected value operator.

Let $X_{ij}(t) = \lambda_{R_{\mathbf{x}} i} \lambda_{T_{\mathbf{x}} j} \left| h_{i,j}(t) \right|^2$ and $Y(t) = \sum_{i=1}^{N_R} \sum_{j=1}^{N_T} X_{ij}(t)$. In order to investigate the statistical properties of the channel capacity $C_{lb}(t)$, we need to find the PDF $p_Y(r)$ of $Y(t)$ and the joint PDF $p_{Y\dot{Y}}(r,\dot{r})$ of the process $Y(t)$ and its time derivative $\dot{Y}(t)$ at the same time instant.[1] By using the transformation of random variables and (3), the PDF of the squared envelope $\left| h_{i,j}(t) \right|^2$ can be written as [15]

$$p_{|h_{i,j}|^2}(r) = \frac{r^{\alpha_\Gamma - 1}}{\Gamma(\alpha_\Gamma) \beta_\Gamma^{\alpha_\Gamma}} e^{-r/\beta_\Gamma} = G_r(\alpha_\Gamma, \beta_\Gamma), \;\; r \geq 0 \tag{11}$$

where $\alpha_\Gamma = m$, $\beta_\Gamma = \Omega/m$, and $G_r(\alpha_\Gamma, \beta_\Gamma)$ represents the gamma distribution with parameters α_Γ and β_Γ. The parameters m and Ω are defined below (3). Using (11),

[1] Throughout this paper, we will represent the time derivative of a process by an overdot.

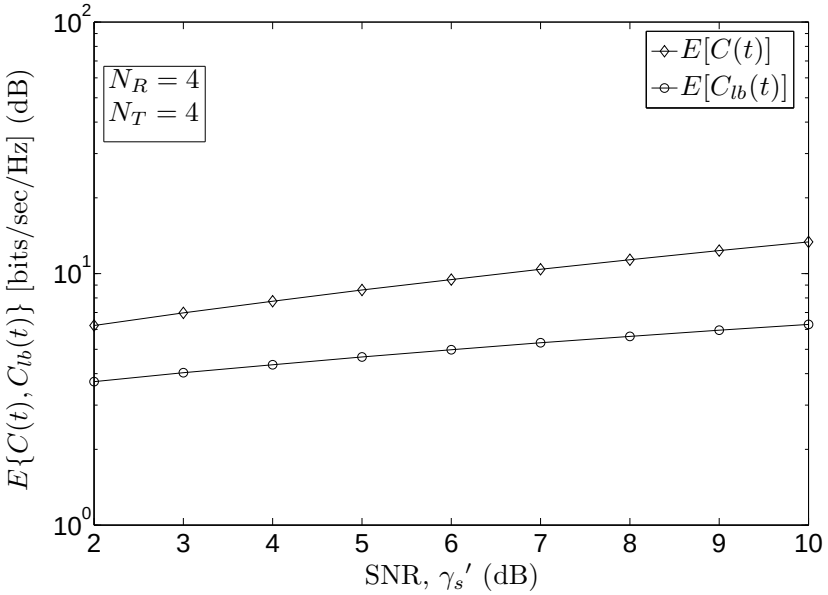

Figure L.1: Mean channel capacity of a 4×4 MIMO system and the lower bound on the capacity.

we can write the PDF $p_{X_{ij}}(r)$ of $X_{ij}(t)$ as follows [15]

$$p_{X_{ij}}(r) = G_r(\alpha_\Gamma, \beta_{\Gamma ij}) \tag{12}$$

where $\beta_{\Gamma ij} = \beta_\Gamma \lambda_{R_{\mathbf{x}} i} \lambda_{T_{\mathbf{x}} j}$. Note that the process $Y(t)$ can be considered as a sum of weighted gamma variates. Hence, the PDF $p_Y(r)$ of $Y(t)$ is given by [2]

$$p_Y(r) = \prod_{i=1}^{N_R} \prod_{j=1}^{N_T} \left(\frac{\beta_{\Gamma 1}}{\beta_{\Gamma ij}} \right)^{\alpha_\Gamma} \sum_{k=0}^{\infty} \frac{\delta_k r^{\alpha_\Gamma{}' + k - 1} e^{-r/\beta_{\Gamma 1}}}{\beta_{\Gamma 1}^{\alpha_\Gamma{}' + k} \Gamma(\alpha_\Gamma{}' + k)} = \sum_{k=0}^{\infty} c_k G_r(\alpha_\Gamma{}' + k, \beta_{\Gamma 1}), \;\; r \geq 0 \tag{13}$$

where

$$c_k = \prod_{i=1}^{N_R} \prod_{j=1}^{N_T} \left(\frac{\beta_{\Gamma 1}}{\beta_{\Gamma ij}} \right) \delta_k \tag{14a}$$

$$\beta_{\Gamma 1} = \min_{ij}(\beta_{\Gamma ij}) \tag{14b}$$

$$\alpha_\Gamma{}' = N_R N_T \alpha_\Gamma \tag{14c}$$

$$\delta_{k+1} = \frac{\alpha_\Gamma}{k+1} \sum_{l=1}^{k+1} \left[\sum_{i=1}^{N_R} \sum_{j=1}^{N_T} \left(1 - \frac{\beta_{\Gamma 1}}{\beta_{\Gamma ij}} \right)^{\alpha_\Gamma} \right] \delta_{k+1-l}, \quad k = 0, 1, 2... \tag{14d}$$

and $\delta_0 = 1$.

By defining $W_G^{(k)}(r) = G_r(\alpha_\Gamma{}' + k, \beta_{\Gamma 1})$, the PDF $p_Y(r)$ of $Y(t)$ can be written as

$$p_Y(r) = \sum_{k=0}^{\infty} c_k W_G^{(k)}(r) \tag{15}$$

where $W_G^{(k)}(r)$ represents the gamma distribution with parameters $\alpha_\Gamma{}' + k$ and $\beta_{\Gamma 1}$. It is shown in Appendix L. B that the joint PDF $p_{Y\dot{Y}}(r,\dot{r})$ of $Y(t)$ and $\dot{Y}(t)$ can be approximated as

$$p_{Y\dot{Y}}(r,\dot{r}) \approx \sum_{k=0}^{\infty} c_k W_{G\dot{G}}^{(k)}(r,\dot{r}). \tag{16}$$

Here, $W_{G\dot{G}}^{(k)}(r,\dot{r})$ is defined in analogy to (15) as the joint PDF of $X(t)$ and $\dot{X}(t)$, where $X(t)$ follows the gamma distribution given by (11) with parameters $\alpha_\Gamma{}' + k$ and $\beta_{\Gamma 1}$. The expression for $W_{G\dot{G}}^{(k)}(r,\dot{r})$ can be found using $p_{h_{i,j}\dot{h}_{i,j}}(r,\dot{r})$ in [26, Eq. 13]. After substituting the expression for $W_{G\dot{G}}^{(k)}(r,\dot{r})$ in (16), the PDF $p_{Y\dot{Y}}(r,\dot{r})$ can be written as

$$p_{Y\dot{Y}}(r,\dot{r}) = \sum_{k=0}^{\infty} \frac{c_k r^{\alpha_\Gamma{}'+k-1} e^{-r/\beta_{\Gamma 1}} e^{-\left(\frac{\dot{r}^2}{8\dot{\sigma}^2 r}\right)}}{2\sqrt{2\pi r}\dot{\sigma}\beta_{\Gamma 1}^{\alpha_\Gamma{}'+k}\Gamma(\alpha_\Gamma{}'+k)},\ r \geq 0 \tag{17}$$

where c_k is defined in (14a) and $\dot{\sigma}$ is defined in [26, Eq. 11]. In the next section, we will present the statistical properties of the channel capacity $C_{lb}(t)$ using the results presented above.

IV. The Statistical Properties of the MIMO Channel Capacity

The PDF $p_{C_{lb}}(r)$ of the channel capacity $C_{lb}(t)$ can be found using (13) and by applying the concept of transformation of random variables as [15]

$$\begin{aligned} p_{C_{lb}}(r) &= \frac{2^r \ln(2)}{\gamma_s'} p_Y\left(\frac{2^r-1}{\gamma_s'}\right) \\ &= \sum_{k=0}^{\infty} \frac{c_k 2^r \ln(2)\left(\frac{2^r-1}{\gamma_s'}\right)^{\alpha_\Gamma{}'+k-1} e^{-\left(\frac{2^r-1}{\gamma_s'\beta_{\Gamma 1}}\right)}}{\gamma_s'\beta_{\Gamma 1}^{\alpha_\Gamma{}'+k}\Gamma(\alpha_\Gamma{}'+k)},\ r \geq 0 \end{aligned} \tag{18}$$

where $\gamma_s' = \gamma_s / N_T$. The CDF $F_{C_{lb}}(r)$ of the channel capacity $C_{lb}(t)$ can now be expressed using $F_{C_{lb}}(r) = \int_0^r p_{C_{lb}}(x)dx$ as

$$\begin{aligned} F_{C_{lb}}(r) &= \sum_{k=0}^{\infty} \frac{c_k \ln(2)}{\gamma_s'^{\alpha_\Gamma{}'+k}\beta_{\Gamma 1}^{\alpha_\Gamma{}'+k}\Gamma(\alpha_\Gamma{}'+k)} \int_0^r 2^x (2^x-1)^{\alpha_\Gamma{}'+k-1} e^{-\left(\frac{2^x-1}{\gamma_s'\beta_{\Gamma 1}}\right)} dx, \\ &\qquad r \geq 0. \end{aligned} \tag{19}$$

The LCR $N_{C_{lb}}(r)$ of the channel capacity $C_{lb}(t)$ is defined as [12]

$$N_{C_{lb}}(r) = \int_0^\infty \dot{z} p_{C_{lb}\dot{C}_{lb}}(r,\dot{z}) d\dot{z}, \ r \geq 0. \tag{20}$$

Thus, in order to find the LCR of the channel capacity, the joint PDF $p_{C_{lb}\dot{C}_{lb}}(r,\dot{r})$ of $C_{lb}(t)$ and $\dot{C}_{lb}(t)$ is required. Again by applying the concept of transformation of random variables [15], the joint PDF $p_{C_{lb}\dot{C}_{lb}}(r,\dot{r})$ can be obtained using (17) as follows

$$\begin{aligned} p_{C_{lb}\dot{C}_{lb}}(r,\dot{r}) &= \left(\frac{2^r \ln(2)}{\gamma_s'}\right)^2 p_{Y\dot{Y}}\left(\frac{2^r-1}{\gamma_s'}, \frac{2^r \dot{r} \ln(2)}{\gamma_s'}\right) \\ &= \sum_{k=0}^{\infty} \frac{c_k \left(\frac{2^r \ln(2)}{\gamma_s'}\right)^2 \left(\frac{2^r-1}{\gamma_s'}\right)^{\alpha_\Gamma'+k-1} e^{-\left(\frac{2^r-1}{\gamma_s' \beta_{\Gamma 1}}\right)}}{2\sqrt{2\pi r}\dot{\sigma}\beta_{\Gamma 1}^{\alpha_\Gamma'+k}\Gamma(\alpha_\Gamma'+k)} e^{-\left(\frac{(2^r \dot{r} \ln(2))^2}{8\gamma_s' \dot{\sigma}^2 (2^r-1)}\right)} \end{aligned} \tag{21}$$

for $r \geq 0$, $|\dot{r}| < \infty$. After substituting (21) in (20) and carrying out some algebraic calculations, we obtain

$$N_{C_{lb}}(r) = \sqrt{\frac{2}{\pi}} \sum_{k=0}^{\infty} \frac{c_k \left(\frac{2^r-1}{\gamma_s'}\right)^{\alpha_\Gamma'+k-1/2} e^{-\left(\frac{2^r-1}{\gamma_s' \beta_{\Gamma 1}}\right)} \dot{\sigma}}{\beta_{\Gamma 1}^{\alpha_\Gamma'+k}\Gamma(\alpha_\Gamma'+k)}, \ r \geq 0. \tag{22}$$

Finally, from (19) and (22), the ADF $T_{C_{lb}}(r)$ of the channel capacity $C_{lb}(t)$ can easily be calculated using [12]

$$T_{C_{lb}}(r) = \frac{F_{C_{lb}}(r)}{N_{C_{lb}}(r)}. \tag{23}$$

In the next section, we will compare our analytical findings with simulation results.

V. Simulation Results

In this section, we will present the analytical and simulation results for the statistical properties of the capacity of various Nakagami-*m* MIMO channels. In order to generate different Nakagami-*m* fading waveforms $h_{i,j}(t)$, we have used the following model [26]

$$h_{i,j}(t) = \sqrt{\sum_{k=1}^{2\times m} r_k^2(t)} \tag{24}$$

where $r_k(t)$ $(k = 1,2,...,2m)$ are real-valued uncorrelated Gaussian distributed random processes and m is the parameter of the Nakagami-*m* distribution. In order to

generate these Gaussian distributed waveforms $r_k(t)$, we have employed the sum-of-sinusoids principle [16]. For the computation of model parameters, we have used the generalized method of exact Doppler spread (GMEDS_1) [17]. The number of sinusoids for the generation of Gaussian distributed waveforms $r_k(t)$ were chosen to be $N_k = 29 + k$. The maximum Doppler frequency $f_{\max}$ was 91 Hz, the SNR γ_s was chosen to be 15 dB, and the parameter Ω for the Nakagami-*m* distribution was set to be $2 \times m$. Since our results are based on the isotropic scattering assumption, therefore $\dot{\sigma} = \sqrt{2}\pi f_{\max}\sigma_0$ and $\sigma_0 = 1$. Unless otherwise stated, the transmitter and the receiver antenna spacings are taken to be 0.75λ. Using (24) in conjunction with (10), the channel capacity $C_{lb}(t)$ of Nakagami-*m* MIMO channel can be simulated. Thereafter, the simulation results for the PDF, CDF, LCR, and ADF of the channel capacity can be found.

The PDF, CDF, LCR, and ADF of the channel capacity for 2×2, 4×4, and 6×6 Nakagami-*m* MIMO channels are shown in Figs. L.2–L.5, respectively. The value of *m* for these results was set to 2. It can be observed from Figs. L.2 and L.3 that as the number of antennas increases, the capacity of the system increases, whereas the spread of the PDF of capacity decreases. On the other hand, with the increase of the number of antennas, a decrease in the maximum value of the LCR was observed as shown in Fig. L.4. Analogously, the converse statement is true for the ADF of the channel capacity presented in Fig. L.5. The PDF, CDF, LCR, and ADF of the channel capacity for different values of receiver antenna spacings d_{mn}

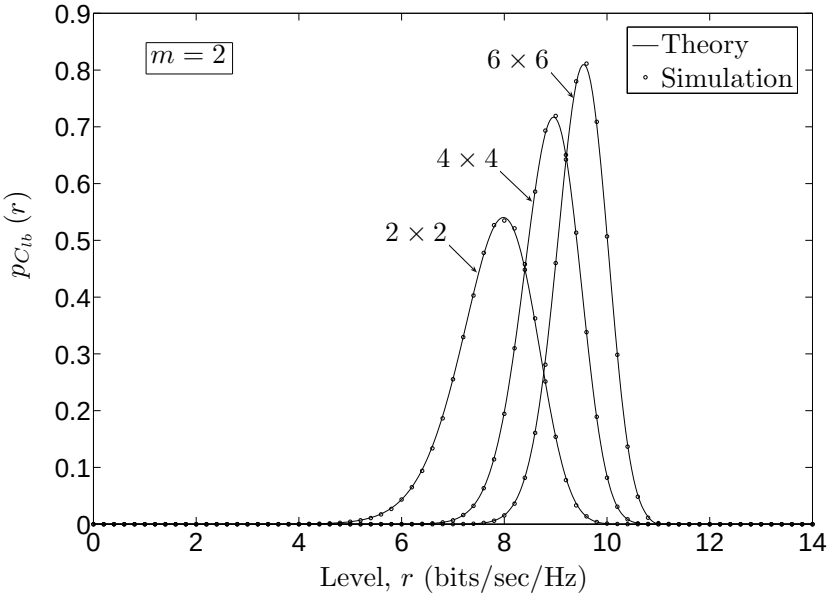

Figure L.2: The PDF of the capacity of Nakagami-*m* 2×2, 4×4, and 6×6 MIMO channels.

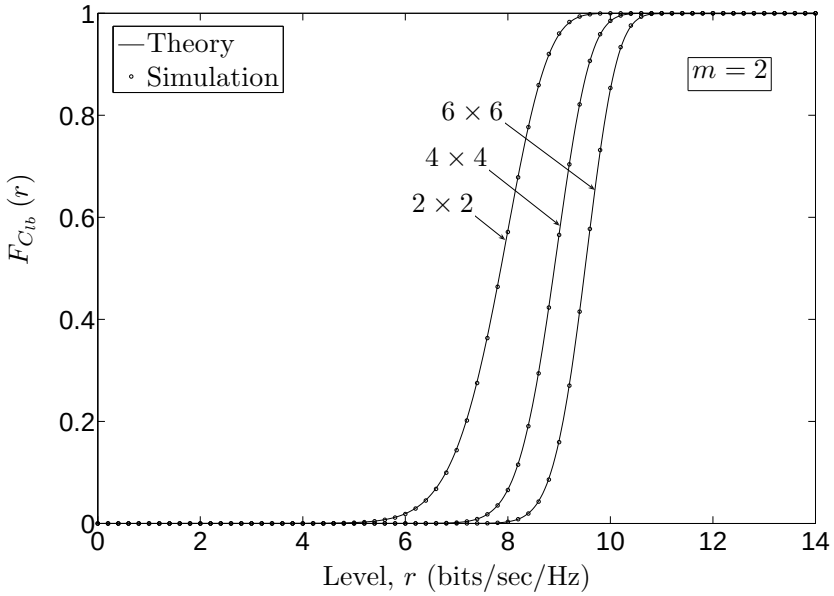

Figure L.3: The CDF of the capacity of Nakagami-*m* 2×2, 4×4, and 6×6 MIMO channels.

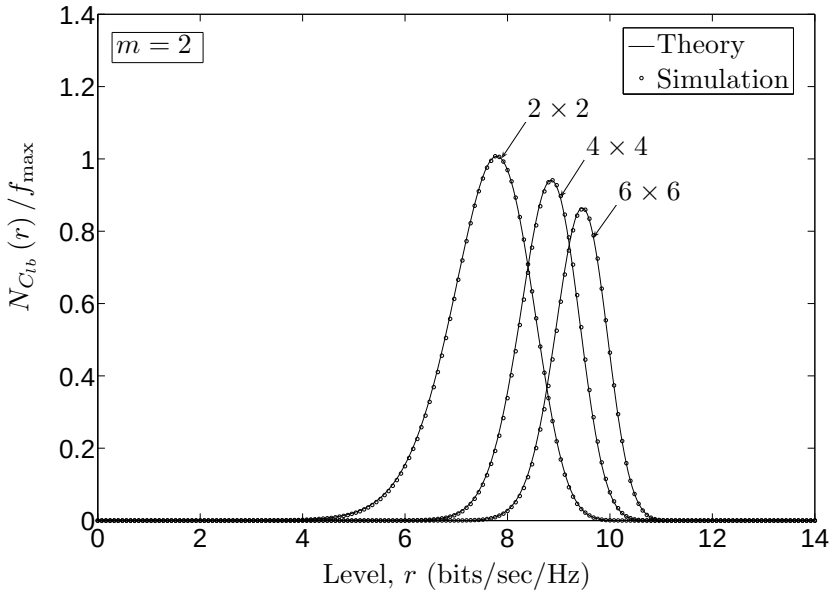

Figure L.4: The LCR of the capacity of Nakagami-*m* 2×2, 4×4, and 6×6 MIMO channels.

for 2×2, 4×4, and 6×6 Nakagami-*m* MIMO channels are presented in Figs. L.6–L.9, respectively. From these results it is obvious that the increase in the receiver antenna spacing results in the decrease in the variance of the PDF of channel capacity, while the mean channel capacity remains unaffected. However, increasing the receiver antenna spacing results in the increase in the maximum value of the

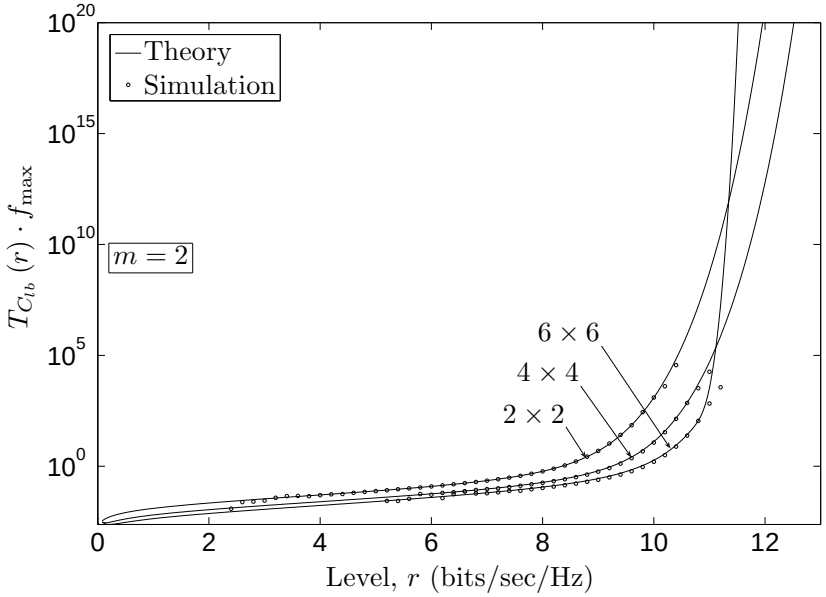

Figure L.5: The ADF of the capacity of Nakagami-*m* 2×2, 4×4, and 6×6 MIMO channels.

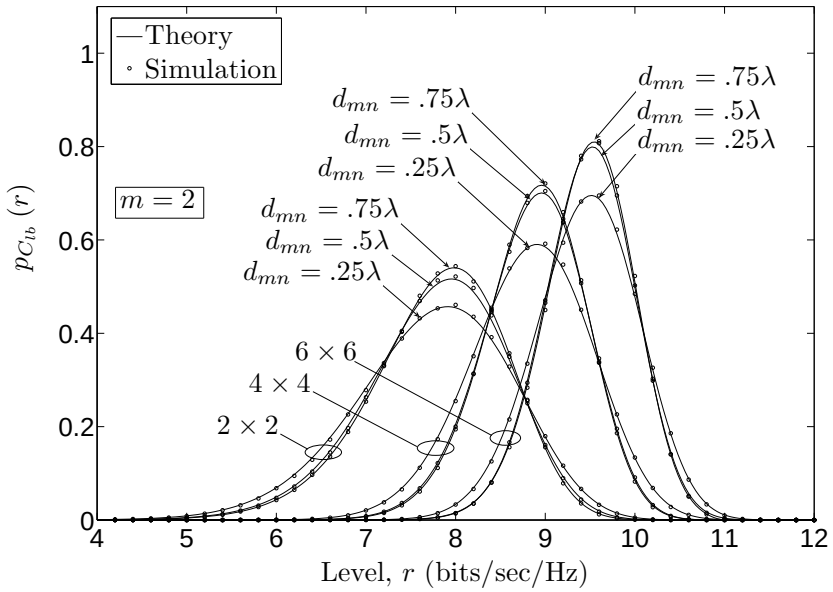

Figure L.6: The PDF of the capacity of Nakagami-*m* MIMO channels for different receiver antenna spacings.

LCR. Moreover, as the receiver antenna spacing increase the ADF of the channel capacity remains unchanged for low levels *r*, whereas for high levels *r*, it results in an increase of the ADF of the channel capacity. In all results presented here, the simulation results are found to be in very good correspondence with analytical results.

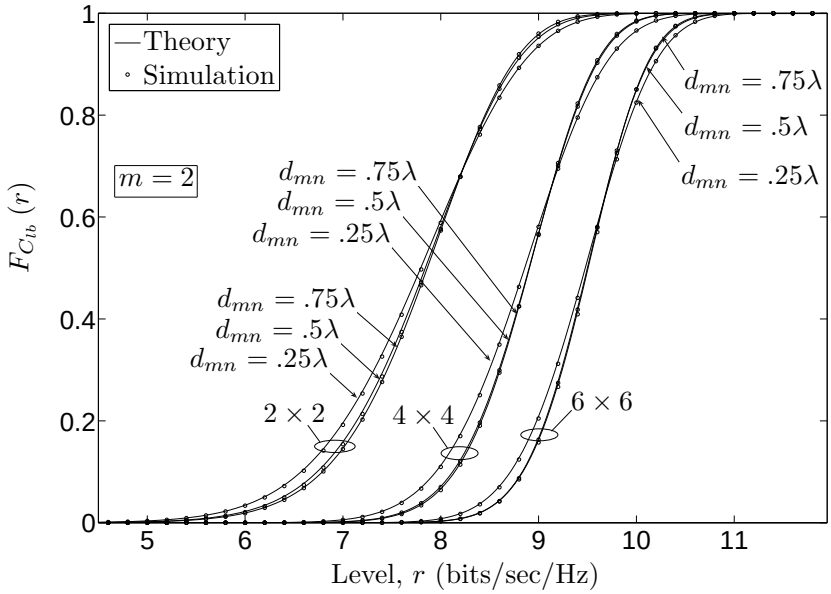

Figure L.7: The CDF of the capacity of Nakagami-*m* MIMO channels for different receiver antenna spacings.

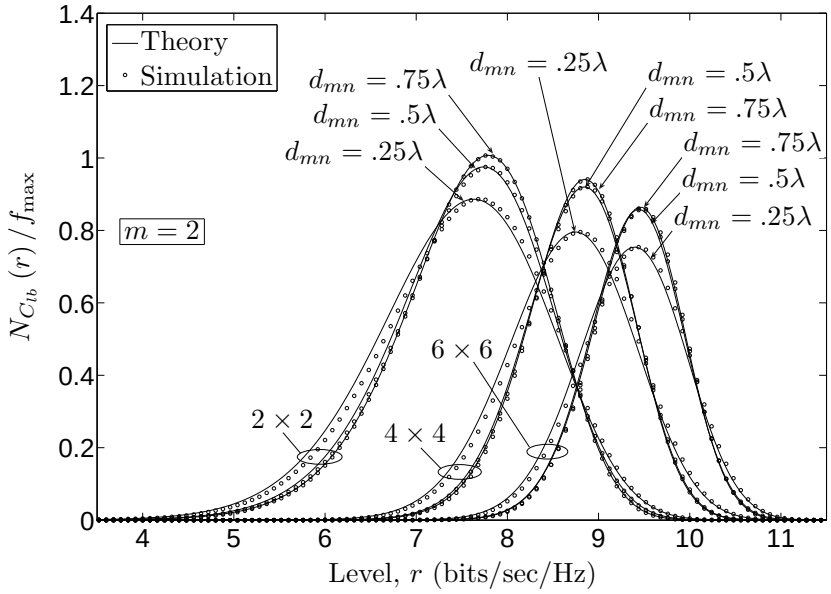

Figure L.8: The LCR of the capacity of Nakagami-*m* MIMO channels for different receiver antenna spacings.

VI. Conclusions

In this paper, we have studied the statistical properties of the capacity of spatially correlated Nakagami-m MIMO channels. We have derived the expressions for the PDF, CDF, LCR, and ADF of the lower bound on the channel capacity. Moreover, the influence of the spatial correlation on the capacity of the MIMO channels has

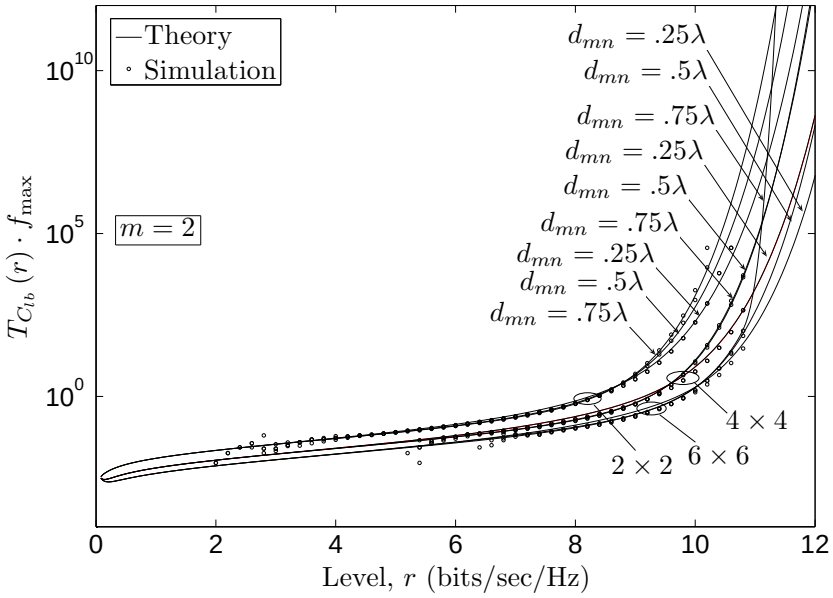

Figure L.9: The ADF of the capacity of Nakagami-*m* MIMO channels for different receiver antenna spacings.

been investigated. It has been observed that the increase in the spatial correlation increases the variance of the PDF of the channel capacity, but it has no effect on the mean channel capacity. Moreover, increasing the spatial correlation results in a decrease of the LCR of the channel capacity. Furthermore, as the receiver antenna spacing increases the ADF of the channel capacity remains unchanged for low levels *r*, whereas for high levels *r*, it results in the increase in the ADF of the channel capacity. The theoretical results are verified using simulations and a very good fitting of the analytical expressions and the simulation results is found.

L. A Proof of (10)

Consider the expression for MIMO channel capacity in (9)

$$C(t) = \log_2 \left[\det \left(\mathbf{I}_{N_R} + \frac{\gamma_s}{N_T} \left(\mathbf{G} \odot \mathbf{H}(t) \right) \left(\mathbf{G} \odot \mathbf{H}(t) \right)^H \right) \right] \tag{A.1}$$

where the matrix **G** is given by

$$\begin{aligned}\mathbf{G} &= \boldsymbol{\lambda}_{R_\mathbf{x}}^{1/2}\boldsymbol{\lambda}_{T_\mathbf{x}}^{1/2^H} \\ &= \begin{bmatrix} \lambda_{R_\mathbf{x}1}^{1/2}\lambda_{T_\mathbf{x}1}^{1/2} & \lambda_{R_\mathbf{x}1}^{1/2}\lambda_{T_\mathbf{x}2}^{1/2} & \cdots & \lambda_{R_\mathbf{x}1}^{1/2}\lambda_{T_\mathbf{x}N_T}^{1/2} \\ \lambda_{R_\mathbf{x}2}^{1/2}\lambda_{T_\mathbf{x}1}^{1/2} & \lambda_{R_\mathbf{x}2}^{1/2}\lambda_{T_\mathbf{x}2}^{1/2} & \cdots & \lambda_{R_\mathbf{x}2}^{1/2}\lambda_{T_\mathbf{x}N_T}^{1/2} \\ \vdots & \vdots & \ddots & \vdots \\ \lambda_{R_\mathbf{x}N_R}^{1/2}\lambda_{T_\mathbf{x}1}^{1/2} & \lambda_{R_\mathbf{x}N_R}^{1/2}\lambda_{T_\mathbf{x}2}^{1/2} & \cdots & \lambda_{R_\mathbf{x}N_R}^{1/2}\lambda_{T_\mathbf{x}N_T}^{1/2} \end{bmatrix}\end{aligned} \tag{A.2}$$

where

$$\boldsymbol{\lambda}_{R_\mathbf{x}}^{1/2} = \left[\lambda_{R_\mathbf{x}1}^{1/2}\ \lambda_{R_\mathbf{x}2}^{1/2}\cdots\lambda_{R_\mathbf{x}N_R}^{1/2}\right]^T \tag{A.3a}$$

$$\boldsymbol{\lambda}_{T_\mathbf{x}}^{1/2^H} = \left[\lambda_{T_\mathbf{x}1}^{1/2}\ \lambda_{T_\mathbf{x}2}^{1/2}\cdots\lambda_{T_\mathbf{x}N_T}^{1/2}\right] \tag{A.3b}$$

and $(\cdot)^T$ denotes the matrix transpose operator. Using (A.2), the expression for $(\mathbf{G}\odot\mathbf{H}(t))(\mathbf{G}\odot\mathbf{H}(t))^H$ can be written as

$$(\mathbf{G}\odot\mathbf{H}(t))(\mathbf{G}\odot\mathbf{H}(t))^H = \begin{bmatrix} \sum_{i=1}^{N_T}\lambda_{R_\mathbf{x}1}\lambda_{T_\mathbf{x}i}h_{1,i}(t)h_{1,i}^H(t) & \sum_{i=1}^{N_T}\lambda_{R_\mathbf{x}1}^{1/2}\lambda_{R_\mathbf{x}2}^{1/2}\lambda_{T_\mathbf{x}i}h_{1,i}(t)h_{2,i}^H(t) & \cdots & \sum_{i=1}^{N_T}\lambda_{R_\mathbf{x}1}^{1/2}\lambda_{R_\mathbf{x}N_R}^{1/2}\lambda_{T_\mathbf{x}i}h_{1,i}(t)h_{N_R,i}^H(t) \\ \sum_{i=1}^{N_T}\lambda_{R_\mathbf{x}2}^{1/2}\lambda_{R_\mathbf{x}1}^{1/2}\lambda_{T_\mathbf{x}i}h_{2,i}(t)h_{1,i}^H(t) & \sum_{i=1}^{N_T}\lambda_{R_\mathbf{x}2}\lambda_{T_\mathbf{x}i}h_{2,i}(t)h_{2,i}^H(t) & \cdots & \sum_{i=1}^{N_T}\lambda_{R_\mathbf{x}2}^{1/2}\lambda_{R_\mathbf{x}N_R}^{1/2}\lambda_{T_\mathbf{x}i}h_{2,i}(t)h_{N_R,i}^H(t) \\ \vdots & \vdots & \ddots & \vdots \\ \sum_{i=1}^{N_T}\lambda_{R_\mathbf{x}N_R}^{1/2}\lambda_{R_\mathbf{x}1}^{1/2}\lambda_{T_\mathbf{x}i}h_{N_R,i}(t)h_{1,i}^H(t) & \sum_{i=1}^{N_T}\lambda_{R_\mathbf{x}N_R}^{1/2}\lambda_{R_\mathbf{x}2}^{1/2}\lambda_{T_\mathbf{x}i}h_{N_R,i}(t)h_{2,i}^H(t) & \cdots & \sum_{i=1}^{N_T}\lambda_{R_\mathbf{x}N_R}\lambda_{T_\mathbf{x}i}h_{N_R,i}(t)h_{N_R,i}^H(t) \end{bmatrix} \cdot \tag{A.4}$$

Substituting (A.4) in (A.1) allows us to write the channel capacity $C(t)$ as follows

$$C(t) \;=\; \log_2 \left\{ \det \begin{bmatrix} 1+\frac{\gamma_s}{N_T}\sum_{i=1}^{N_T}\lambda_{R_{\mathbf{x}}1}\lambda_{T_{\mathbf{x}}i}h_{1,i}(t)h_{1,i}^H(t) & \frac{\gamma_s}{N_T}\sum_{i=1}^{N_T}\lambda_{R_{\mathbf{x}}1}^{1/2}\lambda_{R_{\mathbf{x}}2}^{1/2}\lambda_{T_{\mathbf{x}}i}h_{1,i}(t)h_{2,i}^H(t) & \cdots & \frac{\gamma_s}{N_T}\sum_{i=1}^{N_T}\lambda_{R_{\mathbf{x}}1}^{1/2}\lambda_{R_{\mathbf{x}}N_R}^{1/2}\lambda_{T_{\mathbf{x}}i}h_{1,i}(t)h_{N_R,i}^H(t) \\ \frac{\gamma_s}{N_T}\sum_{i=1}^{N_T}\lambda_{R_{\mathbf{x}}2}^{1/2}\lambda_{R_{\mathbf{x}}1}^{1/2}\lambda_{T_{\mathbf{x}}i}h_{2,i}(t)h_{1,i}^H(t) & 1+\frac{\gamma_s}{N_T}\sum_{i=1}^{N_T}\lambda_{R_{\mathbf{x}}2}\lambda_{T_{\mathbf{x}}i}h_{2,i}(t)h_{2,i}^H(t) & \cdots & \frac{\gamma_s}{N_T}\sum_{i=1}^{N_T}\lambda_{R_{\mathbf{x}}2}^{1/2}\lambda_{R_{\mathbf{x}}N_R}^{1/2}\lambda_{T_{\mathbf{x}}i}h_{2,i}(t)h_{N_R,i}^H(t) \\ \vdots & \vdots & \ddots & \vdots \\ \frac{\gamma_s}{N_T}\sum_{i=1}^{N_T}\lambda_{R_{\mathbf{x}}N_R}^{1/2}\lambda_{R_{\mathbf{x}}1}^{1/2}\lambda_{T_{\mathbf{x}}i}h_{N_R,i}(t)h_{1,i}^H(t) & \frac{\gamma_s}{N_T}\sum_{i=1}^{N_T}\lambda_{R_{\mathbf{x}}N_R}^{1/2}\lambda_{R_{\mathbf{x}}2}^{1/2}\lambda_{T_{\mathbf{x}}i}h_{N_R,i}(t)h_{2,i}^H(t) & \cdots & 1+\frac{\gamma_s}{N_T}\sum_{i=1}^{N_T}\lambda_{R_{\mathbf{x}}N_R}\lambda_{T_{\mathbf{x}}i}h_{N_R,i}(t)h_{N_R,i}^H(t) \end{bmatrix} \right\}. \tag{A.5}$$

By solving the determinant in (A.5), it can be shown that the expression for the lower bound on the channel capacity $C(t)$ in (A.5) can be written as

$$C_{lb}(t) = \log_2\left(1+\frac{\gamma_s}{N_T}\sum_{i=1}^{N_R}\sum_{j=1}^{N_T}\lambda_{R_{\mathbf{x}}i}\lambda_{T_{\mathbf{x}}j}h_{i,j}(t)h_{i,j}^H(t)\right). \tag{A.6}$$

It can be observed that (A.6) only represents an approximation of (A.5), where the entries with maximum contribution (i.e., entries with the terms $h_{i,j}(t)h_{i,j}^H(t)$) are kept and the cross product terms are omitted.

L. B Proof of (16)

Consider a stationary random process $\xi(t)$. The self-joint distribution of the process $\xi(t)$ at two different time instants t and $t+\tau$ is denoted by $p_{\xi\xi}(x,x_\tau;\tau)$. Here, τ represents the time difference between x and x_τ. The orthogonal expansion of the joint PDF $p_{\xi\xi}(x,x_\tau;\tau)$ can be expressed as [18]

$$p_{\xi\xi}(x,x_\tau;\tau) = p_\xi(x)p_\xi(x_\tau)\sum_{n=0}^{\infty}\varepsilon_n(\tau)Q_n(x)Q_n(x_\tau) \tag{B.1}$$

where $\{Q_n(x)\}_1^\infty$ is the set of orthogonal polynomials generated by the PDF $p_\xi(x)$ and the coefficients $\varepsilon_n(\tau)$ are defined in [18, Eq. (4.88)]. For the case when $\lim_{\tau\to 0}$

$\varepsilon_n(\tau) \to 1$, and by using the orthogonality condition of $Q_n(x)$ given by

$$\sum_{n=0}^{\infty} Q_n(x)Q_n(x_\tau) = \delta(x_\tau - x) \tag{B.2}$$

the joint PDF $p_{\xi\xi}(x, x_\tau; \tau)$ can be expressed as

$$\lim_{\tau\to 0} p_{\xi\xi}(x, x_\tau) = p_\xi(x)p_\xi(x_\tau)\delta(x_\tau - x). \tag{B.3}$$

In (B.2), $\delta(\cdot)$ represents the Dirac's delta function. Moreover, the joint PDF $p_{\xi\dot{\xi}}(x, \dot{x}; \tau)$ of the a stationary random process $\xi(t)$ and $\dot{\xi}(t)$ can be expressed as [18]

$$p_{\xi\dot{\xi}}(x, \dot{x}; \tau) = \lim_{\tau\to 0} \tau p_{\xi\xi}(x - \frac{\tau}{2}\dot{x}, x + \frac{\tau}{2}\dot{x}; \tau). \tag{B.4}$$

By the analysis of the results presented in (B.1) to (B.4), the joint PDF $p_{Y\dot{Y}}(r, \dot{r})$ of Y and $\dot{Y}$ under the limit when $\tau \to 0$ can be approximated as

$$p_{Y\dot{Y}}(r, \dot{r}) \approx \sum_{k=0}^{\infty} c_k W_{G\dot{G}}^{(k)}(r, \dot{r}). \tag{B.5}$$

REFERENCES

[1] P. Almers, E. Bonek, A. Burr, N. Czink, M. Debbah, V. Degli-Esposti, H. Hofstetter, P. Kyösti, D. Laurenson, G. Matz, A. F. Molisch, C. Oestges, and H. Özcelik. Survey of channel and radio propagation models for wireless MIMO systems. *EURASIP J. Wirel. Commun. Netw.*, 2007(1):56–56, January 2007. DOI 10.1155/2007/19070.

[2] Mohamed-Slim. Alouini, A. Abdi, and M. Kaveh. Sum of gamma variates and performance of wireless communication systems over Nakagami-fading channels. *IEEE Trans. Veh. Technol.*, 50(6):1471–1480, November 2001.

[3] G. J. Byers and F. Takawira. Spatially and temporally correlated MIMO channels: modeling and capacity analysis. *IEEE Trans. Veh. Technol.*, 53(3):634–643, May 2004.

[4] S. H. Choi, P. J. Smith, B. Allen, W. Q. Malik, and M. Shafi. Severely fading MIMO channels: Models and mutual information. In *Proc. IEEE International Conference on Communications, ICC 2007*, pages 4628–4633. Glasgow, UK, June 2007.

[5] C. N. Chuah, J. M. Kahn, and D. Tse. Capacity of multiantenna array systems in indoor wireless environment. In *Proc. 50th IEEE Global Telecommunications Conference, GLOBECOM 2007*, volume 4, pages 1894–1899. Sydney, Australia, November 1998.

[6] S. Elnoubi, S. A. Chahine, and H. Abdallah. BER performance of GMSK in Nakagami fading channels. In *Proc. 21st National Radio Science Conference, NRSC 2004*, pages C13–1–8, March 2004.

[7] G. J. Foschini and M. J. Gans. On limits of wireless communications in a fading environment when using multiple antennas. *Wireless Pers. Commun.*, 6:311–335, March 1998.

[8] A. Giorgetti, P. J. Smith, M. Shafi, and M. Chiani. MIMO capacity, level crossing rates and fades: The impact of spatial/temporal channel correlation. *J. Commun. Net.*, 5(2):104–115, June 2003.

[9] I. S. Gradshteyn and I. M. Ryzhik. *Table of Integrals, Series, and Products*. New York: Academic Press, 6th edition, 2000.

[10] M. Herdin, G. Gritsch, B. Badic, and E. Bonek. The influence of channel models on simulated MIMO performance. In *Proc. IEEE 59th Vehicular Technology Conference, IEEE VTC 2004-Spring*, pages 304–307. Milan, Italy, May 2004.

[11] B. O. Hogstad and M. Pätzold. Capacity studies of MIMO models based on the geometrical one-ring scattering model. In *Proc. 15th IEEE Int. Symp. on Personal, Indoor and Mobile Radio Communications, PIMRC 2004*, volume 3, pages 1613–1617. Barcelona, Spain, September 2004.

[12] B. O. Hogstad and M. Pätzold. Exact closed-form expressions for the distribution, level-crossing rate, and average duration of fades of the capacity of MIMO channels. In *Proc. 65th Semiannual Vehicular Technology Conference, IEEE VTC 2007-Spring*, pages 455–460. Dublin, Ireland, April 2007.

[13] A. Müller and J. Speidel. Characterization of mutual information of spatially correlated MIMO channels with keyhole. In *Proc. IEEE Int. Conf. Commun., ICC 2007*, pages 750–755. Glasgow, UK, June 2007.

[14] H. Özcelik, N. Czink, and E. Bonek. What makes a good MIMO channel model? In *Proc. IEEE 61st Vehicular Technology Conference, IEEE VTC 2005-Spring*, volume 1, pages 156–160. Stockholm, Sweden, May 2005.

[15] A. Papoulis and S. U. Pillai. *Probability, Random Variables and Stochastic Processes*. New York: McGraw-Hill, 4th edition, 2002.

[16] M. Pätzold. *Mobile Fading Channels*. Chichester: John Wiley & Sons, 2002.

[17] M. Pätzold and B. O. Hogstad. Two new methods for the generation of multiple uncorrelated Rayleigh fading waveforms. In *Proc. 63rd IEEE Semi-annual Vehicular Technology Conference, IEEE VTC 2006-Spring*, volume 6, pages 2782–2786. Melbourne, Australia, May 2006.

[18] S. Primak, V. Kontorovich, and V. Lyandres. *Stochastic Methods and their Applications to Communications*. Chichester: John Wiley & Sons, 2004.

[19] A. M. Sayeed. Deconstructing multiantenna fading channels. *IEEE Trans. Signal Processing*, 50(10):2563–2579, October 2002.

[20] P. J. Smith and M. Shafi. Characterization of mutual information of spatially correlated MIMO channels with keyhole. In *Proc. IEEE Int. Conf. Commun., ICC 2004*, volume 5, pages 2924–2928. Paris, France, June 2004.

[21] I. E. Telatar. Capacity of multi-antenna Gaussian channels. *European Trans. Telecommun. Related Technol.*, 10(6):585–595, November/December 1999.

[22] A. Tulino, A. Lozano, and S. Verdu. Impact of antenna correlation on the capacity of multiantenna channels. *IEEE Trans. Inform. Theory*, 51(7):2491–2509, July 2005.

[23] V. Veeravalli, Y. Liang, and A. M. Sayeed. Correlated wireless MIMO channels: capacity, optimal signaling, and asymptotics. *IEEE Trans. Inform. Theory*, 51(6):2058–2072, June 2005.

[24] W. Weichselberger, M. Herdin, H. Özcelik, and E. Bonek. A stochastic MIMO channel model with joint correlation of both link ends. *IEEE Trans. Wireless Commun.*, 5(1):90–100, January 2006.

[25] W. Weichselberger and H. Özcelik. A novel stochastic MIMO channel model and its physical interpretation. In *Proc. 7th COST-273 Meeting and Workshop*. Paris, France, May 2003. TD(03)144, CD-ROM.

[26] M. D. Yacoub, J. E. V. Bautista, and L. G. de Rezende Guedes. On higher order statistics of the Nakagami-*m* distribution. *IEEE Trans. Veh. Technol.*, 48(3):790–794, May 1999.

Appendix M

Paper XIII

Title:	The Influence of Spatial Correlation and Severity of Fading on the Statistical Properties of the Capacity of OSTBC Nakagami-*m* MIMO channels
Authors:	**Gulzaib Rafiq**[1], Matthias Pätzold[1], and Valeri Kontorovich[2]
Affiliations:	[1]University of Agder, Faculty of Engineering and Science, P. O. Box 509, NO-4898 Grimstad, Norway [2]Centro de Investigación y de Estudios Avanzados, CINVESTAV, 07360 Mexico City, Mexico
Conference:	*69th IEEE Vehicular Technology Conference, VTC2009-Spring*, Barcelona, Spain, Apr. 2009, pp. 1 – 5.

The Influence of Spatial Correlation and Severity of Fading on the Statistical Properties of the Capacity of OSTBC Nakagami-*m* MIMO channels

Gulzaib Rafiq[1], Matthias Pätzold[1], and Valeri Kontorovich[2]
[1]Department of Information and Communication Technology
Faculty of Engineering and Science, University of Agder
Servicebox 509, NO-4898 Grimstad, Norway
E-mails: {gulzaib.rafiq, matthias.paetzold}@uia.no
[2]Centro de Investigación y de Estudios Avanzados, CINVESTAV
07360 Mexico City, Mexico
Email: valeri@cinvestav.mx

***Abstract* — This paper deals with the analysis of statistical properties of the capacity of spatially uncorrelated orthogonal space-time block coded (OSTBC) Nakagami-*m* multiple-input multiple-output (MIMO) channels. We have derived exact closed-form expressions for the probability density function (PDF), cumulative distribution function (CDF), level-crossing rate (LCR), and average duration of fades (ADF) of the channel capacity. We have also investigated the statistical properties of the approximated capacity of spatially correlated OSTBC Nakagami-*m* MIMO channels. The results are studied for different values of the fading parameter *m*, corresponding to different fading conditions. It is observed that an increase in the MIMO dimension[1] or a decrease in the severity of fading increases the mean channel capacity. While, a significant decrease in the mean channel capacity is observed with an increase in the spatial correlation. The correctness of theoretical results is confirmed by simulations.**

I. Introduction

Provision of multiple antennas at the receiver and transmitter allows the design of multiple-input multiple-output (MIMO) systems to exploit spatial diversity in order to increase the spectral efficiency and to acquire a diversity gain [23]. One promising method to achieve the desired capacity is to use space-time coding techniques, such as space-time trellis codes (STTC) [18] or space-time block codes (STBC)

[1]Throughout this paper, we will refer to the MIMO dimension as $N_R \times N_T$, where N_R is the number of receive antennas and N_T denotes the number of transmit antennas.

[1, 17]. One of the advantages of using OSTBC is that it transforms MIMO fading channels into equivalent single-input single-output (SISO) channels [9]. Moreover, being orthogonal in structure, maximum likelihood decoding can be applied at the receiver that results in a significant decrease in the complexity of the receiver structure, compared to the prevailing coding techniques (e.g., STTC) [17]. Studies pertaining to the analysis of the capacity of OSTBC MIMO channels can be found in [4, 11]. The outage performance and the error probability analysis of OSTBC MIMO systems have been studied in [21, 22, 10].

In this paper, we have extended the analysis of the statistical properties of the capacity of uncorrelated OSTBC Rayleigh MIMO channels presented in [8] to uncorrelated OSTBC Nakagami-m MIMO channels. The Nakagami-m distribution can be considered as a more general channel model compared to a Rayleigh channel as it incorporates scenarios where the fading can be more (or less) severe than Rayleigh fading. Moreover, the one-sided Gaussian and the Rayleigh distribution are inherently included in the Nakagami-m distribution as special cases, i.e., for $m = 0.5$ and $m = 1$, respectively.

We have derived analytical expressions for the PDF, CDF, LCR, and ADF of the channel capacity of uncorrelated OSTBC Nakagami-m MIMO channels. The mean value and spread of the channel capacity has been analyzed with the help of the PDF of the channel capacity. On the other hand, the analysis of the LCR and ADF of the channel capacity is very helpful to study the temporal behavior of the channel capacity. The LCR of the channel capacity provides the information regarding the expected number of up-crossings (or down-crossings) of the channel capacity through a certain threshold level in a time interval of one second. While, the ADF of the channel capacity describes the average duration of the time intervals over which the channel capacity is below a given level [6, 7]. We have studied the above mentioned statistical quantities for different values of the fading parameter m and for different MIMO dimensions. It is observed that an increase in the MIMO dimension or a decrease in the severity of fading results in an increase in the mean channel capacity. The results for the PDF, CDF, LCR, and ADF of the capacity of Rayleigh channels can be readily obtained as a special case from the findings in [8] by setting $m = 1$. We have also investigated the capacity of spatially correlated OSTBC Nakagami-m MIMO channels. For such channels, we have derived an approximate expression for the channel capacity. Thereafter, the expressions for the PDF, CDF, LCR, and ADF of the channel capacity are found. It is observed that the spatial correlation significantly reduces the mean channel capacity. We have verified the theoretical results by simulations, whereby a very good fitting is

observed.

The rest of the paper is organized as follows. In Section II, we define briefly the capacity of OSTBC Nakagami-*m* MIMO channels. Section III deals with the derivation of the statistical properties of the capacity of uncorrelated OSTBC Nakagami-*m* MIMO channels. In Section IV, the statistical properties of the approximate capacity of spatially correlated OSTBC Nakagami-*m* MIMO channels are investigated. Section V aims at the validation and analysis of the obtained results with the help of simulations. Finally, the conclusions are given in Section VI.

II. The Capacity of Spatially Uncorrelated OSTBC Nakagami-*m* MIMO Channels

In this article, we have considered a MIMO system with N_T transmit and N_R receive antennas. The complex random channel gains are represented by $h_i(t)$ $(i = 1,2,...,N_R N_T)$. Moreover, we have assumed that the stochastic processes $h_i(t)$ are mutually uncorrelated and the envelope $|h_i(t)|$ follows a Nakagami-*m* distribution

$$p_{|h_i|}(z) = \frac{2m^m z^{2m-1}}{\Gamma(m)\Omega^m} e^{-\frac{mz^2}{\Omega}},\ z \geq 0 \tag{1}$$

for $i = 1,2,...,N_R N_T$, where $\Omega = E\left\{|h_i(t)|^2\right\}$, $m = \Omega^2 \big/ \mathrm{Var}\left\{|h_i(t)|^2\right\}$, and $\Gamma(\cdot)$ represents the gamma function [5]. The capacity of OSTBC MIMO systems can be expressed as [15]

$$C(t) = \log_2\left(1 + \frac{\gamma_s}{N_T}\mathbf{h}^H(t)\mathbf{h}(t)\right) \text{ (bits/sec/Hz)} \tag{2}$$

where $\mathbf{h}(t)$ represents the $N_R N_T \times 1$ complex channel gain vector with entries $h_i(t)$ $(i = 1,2,...,N_R N_T)$, $(\cdot)^H$ denotes the Hermitian operator, and γ_s is the signal-to-noise ratio (SNR). The channel capacity $C(t)$ given by (2) can be written as

$$C(t) = \log_2\left(1 + \gamma_s' \sum_{i=1}^{N_R N_T} \chi_i^2(t)\right) \text{ (bits/sec/Hz)} \tag{3}$$

where $\gamma_s' = \gamma_s \big/ N_T$ and $\chi_i^2(t) = |h_i(t)|^2$ $(i = 1,2,...,N_R N_T)$. Due to the assumption that the envelope $|h_i(t)|$ is Nakagami-*m* distributed, the squared envelope $\chi_i^2(t)$ follows the gamma distribution. Let $\Xi(t) = \sum_{i=1}^{N_R N_T} \chi_i^2(t)$, then the PDF $p_\Xi(z)$ of $\Xi(t)$ can be expressed as [2]

$$p_\Xi(z) = \frac{z^{N_R N_T m-1} e^{-\frac{z}{\beta}}}{\beta^{N_R N_T m}\Gamma(N_R N_T m)},\ z \geq 0 \tag{4}$$

where $\beta = \Omega/m$ is a parameter of the Nakagami-*m* distribution. In order to derive the expressions for the LCR of the OSTBC Nakagami-*m* MIMO channel capacity, we require the joint PDF $p_{\Xi\dot{\Xi}}(z,\dot{z})$ of $\Xi(t)$ and $\dot{\Xi}(t)$ at the same time t. In this article, the time derivative of a process is denoted by a raised dot. The joint PDF $p_{\Xi\dot{\Xi}}(z,\dot{z})$ can be expressed as [16]

$$p_{\Xi\dot{\Xi}}(z,\dot{z}) = \frac{z^{N_R N_T m - 3/2} e^{-\frac{z}{\beta}} e^{-\frac{\dot{z}^2}{8\beta_N z}}}{2\beta^{N_R N_T m}\Gamma(N_R N_T m)\sqrt{2\beta_N \pi}} \tag{5}$$

for $z \geq 0$ and $|\dot{z}| < \infty$, where under isotropic scattering conditions β_N is given by [19]

$$\beta_N = 2(\pi f_{\max})^2. \tag{6}$$

In the next section, we will derive the expressions for the PDF, CDF, LCR, and ADF of the OSTBC Nakagami-*m* MIMO channel capacity.

III. Statistical Properties of the Capacity of Spatially Uncorrelated OSTBC Nakagami-*m* MIMO Channels

The channel capacity $C(t)$ presented in (2) can be considered as a mapping of a random vector process $\mathbf{h}(t)$ to another random process, namely $C(t)$. Hence, the PDF $p_C(z)$ of the channel capacity $C(t)$ can be found using the PDF $p_\Xi(z)$ in (4) and by applying the concept of transformation of random variables [12] as follows

$$\begin{aligned} p_C(r) &= \frac{2^r \ln(2)}{\gamma_s'} p_\Xi\left(\frac{2^r - 1}{\gamma_s'}\right) \\ &= \frac{2^r (2^r-1)^{N_R N_T m - 1} \ln(2) e^{-\frac{2^r-1}{\beta\gamma_s'}}}{(\beta\,\gamma_s')^{N_R N_T m}\Gamma(N_R N_T m)}, \quad r \geq 0. \end{aligned} \tag{7}$$

The CDF $F_C(r)$ of the channel capacity can be found using

$$F_C(r) = \int_0^r p_C(x)dx. \tag{8}$$

By substituting (7) in (8) and doing some algebraic manipulations, the CDF of the channel capacity can be expressed as

$$F_C(r) = 1 - \frac{\Gamma(N_R N_T m, \frac{1}{\beta\gamma_s'})}{\Gamma(N_R N_T m)}, \quad r \geq 0 \tag{9}$$

where $\Gamma(\cdot,\cdot)$ denotes the generalized gamma function [5]. The LCR $N_C(r)$ of the channel capacity can be obtained by solving the following integral [7]

$$N_C(r) = \int_0^\infty \dot{z} p_{C\dot{C}}(r,\dot{z}) d\dot{z}, \;\; r \geq 0 \tag{10}$$

where $p_{C\dot{C}}(z,\dot{z})$ is the joint PDF of $C(t)$ and $\dot{C}(t)$. The joint PDF $p_{C\dot{C}}(z,\dot{z})$ can be obtained using (5) and by applying the concept of transformation of random variables [12] as follows

$$\begin{aligned} p_{C\dot{C}}(z,\dot{z}) &= \left(\frac{2^z \ln(2)}{\gamma_s'}\right)^2 p_{\Xi\dot{\Xi}}\left(\frac{2^z-1}{\gamma_s'}, \frac{2^z \dot{z} \ln(2)}{\gamma_s'}\right) \\ &= \left(\frac{2^z \ln(2)}{\gamma_s'}\right)^2 \frac{\left(2^z - 1/\gamma_s'\right)^{N_R N_T m - 3/2} e^{-\frac{(\dot{z}2^z \ln(2))^2}{8\beta_N \gamma_s' (2^z-1)}}}{2\beta^{N_R N_T m}\Gamma(N_R N_T m)\sqrt{2\beta_N \pi}} e^{-\frac{2^z-1}{\beta\gamma_s'}}, \\ & \qquad z \geq 0, |\dot{z}| < \infty. \end{aligned} \tag{11}$$

By inserting (11) in (10), the final expression for the LCR of the channel capacity can be written as

$$N_C(r) = \sqrt{\frac{2\beta_N}{\pi}} \frac{\left(2^r - 1/\gamma_s'\right)^{N_R N_T m - 1/2} e^{-\frac{2^r-1}{\beta\gamma_s'}}}{\beta^{N_R N_T m}\Gamma(N_R N_T m)}, \;\; r \geq 0. \tag{12}$$

The ADF $T_C(r)$ of the channel capacity can now be obtained using [7]

$$T_C(r) = \frac{F_C(r)}{N_C(r)} \tag{13}$$

where $F_C(r)$ and $N_C(r)$ are given by (9) and (12), respectively.

IV. High SNR approximation of the Channel Capacity of Spatially Correlated OSTBC Nakagami-*m* MIMO Channels

It is widely reported in the literature that a spatial correlation between the sub-channels of a MIMO channel has a significant influence on the channel capacity. At high SNR, the channel capacity $C_{app}(t)$ of spatially correlated OSTBC MIMO channels can be approximated as [15]

$$C_{app}(t) \approx \log_2 \det\left(\gamma_s' \mathbf{h}^H(t)\mathbf{h}(t)\right) + \alpha_R \tag{14}$$

where

$$\begin{aligned}\alpha_R &= \log_2 \det(R_{Rx}) + \log_2 \det(R_{Tx}) \\ &= \log_2\left(\prod_{i=1}^{N_R} \lambda_{R_{Rx}}^{(i)}\right) + \log_2\left(\prod_{i=1}^{N_R} \lambda_{R_{Tx}}^{(i)}\right). \end{aligned} \tag{15}$$

Here R_{Rx} (R_{Tx}) is the full rank $N_R \times N_R$ ($N_T \times N_T$) receiver (transmitter) correlation matrix, $\det(\cdot)$ denotes the matrix determinant, and $\lambda_{R_{Rx}}^{(i)}$ $\left(\lambda_{R_{Tx}}^{(i)}\right)$ represent the eigenvalues of the receiver (transmitter) correlation matrix. In (14), $\log_2 \det\left(\gamma_s' \mathbf{h}^H(t)\mathbf{h}(t)\right)$ denotes the high SNR approximation of the channel capacity $C(t)$ of OSTBC MIMO channels and α_R can be considered as a correction term added to the high SNR approximation due to the spatial correlation. The receive and transmit antenna correlations under isotropic scattering conditions can be expressed in closed form as [3]

$$\rho_{p,q}^T\left(\delta_{pq}\right) = J_0\left(2\pi\delta_{pq}/\lambda_s\right) \tag{16a}$$

$$\rho_{m,n}^R\left(d_{mn}\right) = J_0\left(2\pi d_{mn}/\lambda_s\right) \tag{16b}$$

where $\rho_{p,q}^T\left(\delta_{pq}\right)$ $\left(\rho_{m,n}^R\left(d_{mn}\right)\right)$ represents the transmit (receive) antenna correlation and $J_0(\cdot)$ is the Bessel function of the first kind of order zero. In (16a) and (16b), δ_{pq} (d_{mn}) represents the spacing between the receive (transmit) antenna elements and λ_s is the wavelength of the transmitted signal. The statistical properties of the approximated channel capacity $C_{app}(t)$ of spatially correlated OSTBC Nakagami-m MIMO channels presented in (14) can be found by following a similar procedure as developed in the previous section for the channel capacity $C(t)$ of spatially uncorrelated OSTBC Nakagami-m MIMO channels. The PDF, CDF, and LCR of the channel capacity $C_{app}(t)$ can be approximated as

$$p_{C_{app}}(r) \approx \frac{2^{r-\alpha_R}\left(2^{r-\alpha_R}\right)^{N_R N_T m-1}\ln(2) e^{-\frac{2^{r-\alpha_R}}{\beta\gamma_s'}}}{\left(\beta\,\gamma_s'\right)^{N_R N_T m}\Gamma(N_R N_T m)}, \;\; r \geq 0 \tag{17}$$

$$F_{C_{app}}(r) \approx \frac{\ln(2)}{\left(\beta\,\gamma_s'\right)^{N_R N_T m}\Gamma(N_R N_T m)} \int_0^r 2^{x-\alpha_R} e^{-\frac{2^{x-\alpha_R}}{\beta\gamma_s'}} \left(2^{x-\alpha_R}\right)^{N_R N_T m-1} dx, \;\; r \geq 0 \tag{18}$$

$$N_{C_{app}}(r) \approx \frac{\left(2^{r-\alpha_R}/\gamma_s'\right)^{N_R N_T m-1/2} e^{-\frac{2^{r-\alpha_R}}{\beta\gamma_s'}}}{\sqrt{\pi/2\beta_N}\,\beta^{N_R N_T m}\Gamma(N_R N_T m)}, \;\; r \geq 0, \tag{19}$$

respectively. The ADF of the channel capacity $C_{app}(t)$ can be found by substituting (18) and (19) in (13).

V. Numerical Results

In this section, we will discuss the analytical results found in the previous section and their validity will be tested by simulations. For the natural values of $2 \times m$, the Nakagami-*m* distributed waveforms are generated by employing the following model [20]

$$|h_i(t)| = \sqrt{\sum_{k=1}^{2\times m} r_{i,k}^2(t)} \tag{20}$$

where $r_{i,k}(t)$ $(i = 1,2,...,N_R N_T$ and $k = 1,2,...,2m)$ are zero-mean real-valued uncorrelated Gaussian distributed random processes with variance σ_0^2, and m is the parameter of the Nakagami-*m* distribution. In order to generate these Gaussian distributed waveforms $r_k(t)$, we have applied the sum-of-sinusoids model [13]. The model parameters are calculated from the generalized method of exact Doppler spread (GMEDS_1) [14]. The number of sinusoids used for the generation of the Gaussian distributed waveforms $r_k(t)$ was selected to be $N_k = 29 + k$. The maximum Doppler frequency $f_{\max}$ was 91 Hz, the SNR γ_s was chosen to be 15 dB, $\sigma_0^2 = 1$, and the parameter Ω for the Nakagami-*m* distribution was set to be $2 \times m$. The transmit and the receive antenna spacings are taken to be $0.4\lambda_s$. Finally, using (3) and (14), the simulation results for the statistical properties of the channel capacity $C(t)$ and $C_{app}(t)$ of OSTBC Nakagami-*m* MIMO channels are found.

The PDF and CDF of the channel capacity $C(t)$ for 2×2, 4×4, and 6×6 MIMO channels are shown in Figs. M.1 and M.2, respectively for different values of the fading parameter m. It is observed that as the severity of fading decreases (i.e., increasing the value of m), the mean channel capacity increases for all MIMO dimensions. However, the spread of the PDF decreases. Moreover, it can also clearly be seen that increasing the MIMO dimension results in a prominent increase in the channel capacity. The LCR and ADF of the channel capacity $C(t)$ for 2×2, 4×4, and 6×6 MIMO channels are shown in Figs. M.3 and M.4, respectively for different values of the fading parameter m. Figure M.3 shows that as the MIMO dimension or the value of the fading parameter m increases, the spread of the LCR curve gets narrower. Moreover, for low MIMO dimensions (e.g., 2×2) with small values of m, high LCR is observed at lower signal levels. However, for large MIMO dimensions (e.g., 6×6) with large values of m, a high LCR is observed at high signal levels. The ADF of the channel capacity, on the other hand, decreases with an increase in the MIMO dimension or the fading parameter m at low and medium

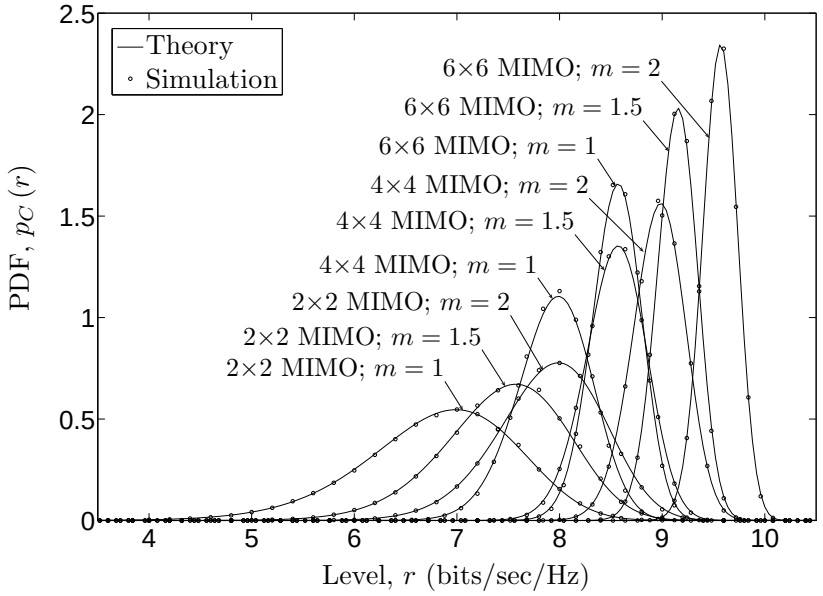

Figure M.1: The PDF $p_C(r)$ of the capacity of OSTBC Nakagami-*m* MIMO channels.

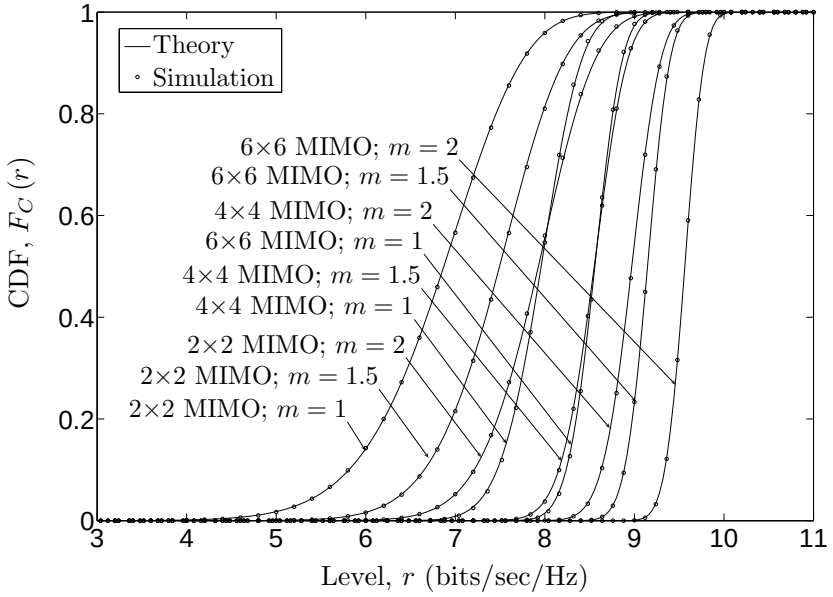

Figure M.2: The CDF $F_C(r)$ of the capacity of OSTBC Nakagami-*m* MIMO channels.

signal levels.

Figures M.5–M.8 aim at the comparative analysis of the statistical properties of the channel capacity of the uncorrelated OSTBC Nakagami-*m* MIMO channels and the approximated channel capacity of the correlated OSTBC Nakagami-*m* MIMO channels. The PDF and CDF of the channel capacity of 4×4 MIMO channels are

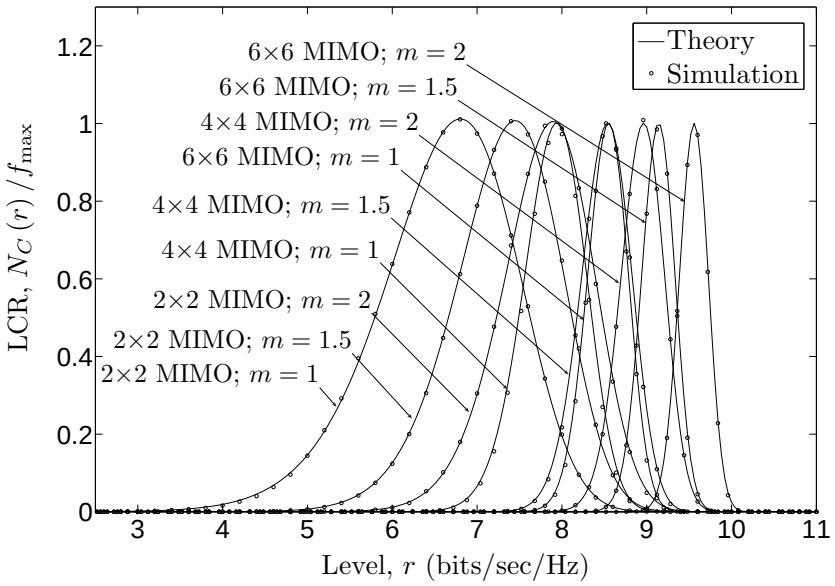

Figure M.3: The normalized LCR $N_C(r)/f_{\max}$ of the capacity of OSTBC Nakagami-*m* MIMO channels.

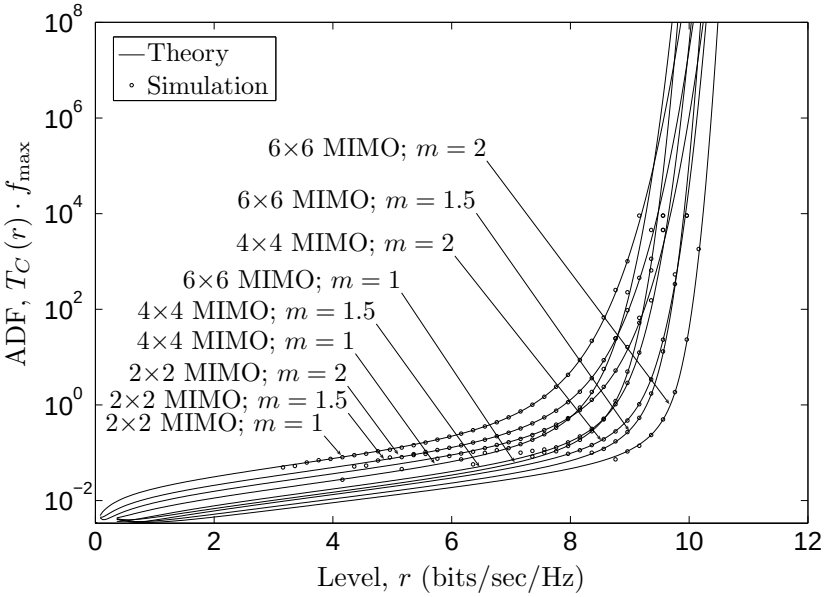

Figure M.4: The normalized ADF $T_C(r) \cdot f_{\max}$ of the capacity of OSTBC Nakagami-*m* MIMO channels.

shown in Figs. M.5 and M.6, respectively, for different values of the fading parameter *m*. It can clearly be observed that the spatial correlation has a noticeable influence on the mean channel capacity. The LCR and ADF of the channel capacity are presented in Figs. M.7 and M.8, respectively. It is apparent that the spatial correlation shifts the maximum value of the LCR to lower signal levels. Hence, for

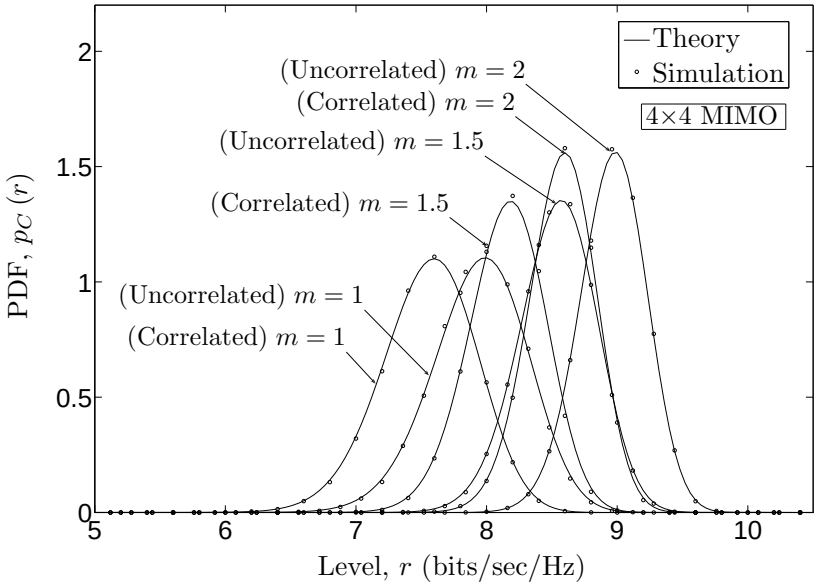

Figure M.5: The PDF $p_C(r)$ of the capacity of spatially correlated OSTBC Nakagami-*m* MIMO channels.

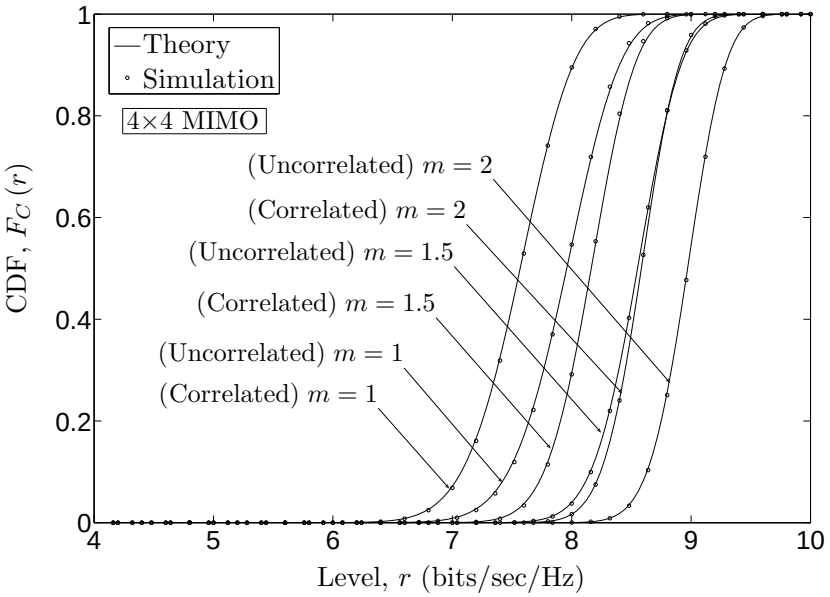

Figure M.6: The CDF $F_C(r)$ of the capacity of spatially correlated OSTBC Nakagami-*m* MIMO channels.

correlated systems the LCR of the capacity is higher for low signal levels compared to uncorrelated systems. On the other hand, the ADF of the channel capacity of correlated systems is higher for all the signal levels compared to uncorrelated systems. For all the cases studied in this paper, the analytical results are found to be in very good correspondence with the simulation results.

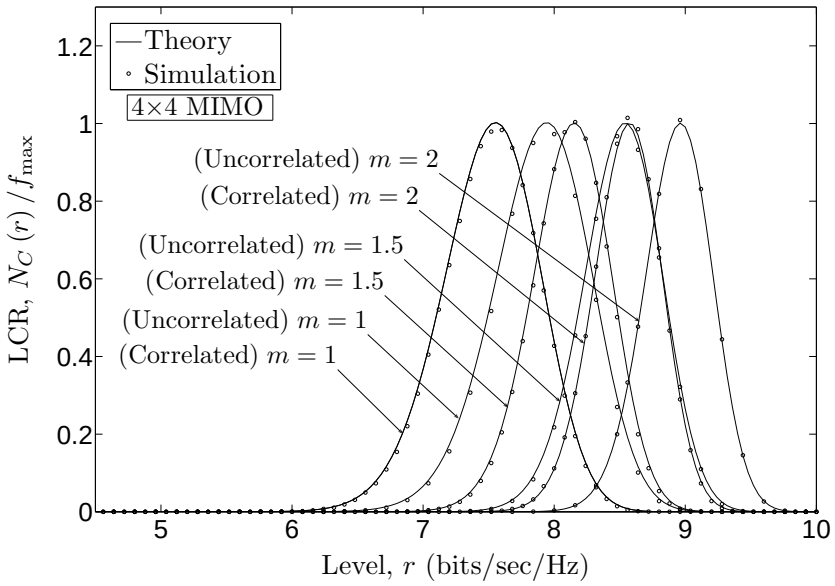

Figure M.7: The normalized LCR $N_C(r)/f_{\max}$ of the capacity of spatially correlated OSTBC Nakagami-*m* MIMO channels.

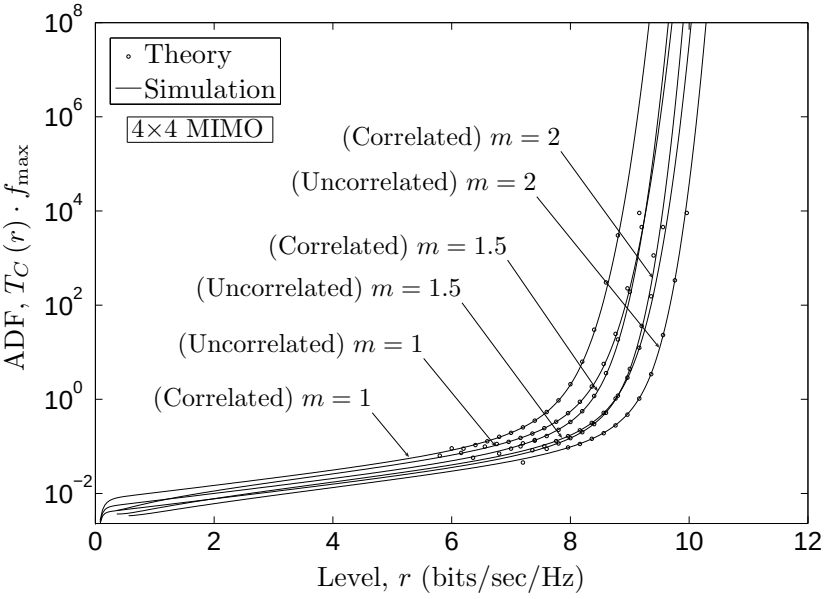

Figure M.8: The normalized ADF $T_C(r) \cdot f_{\max}$ of the capacity of spatially correlated OSTBC Nakagami-*m* MIMO channels.

VI. Conclusions

In this article, we have studied the statistical properties of the capacity of uncorrelated OSTBC Nakagami-*m* MIMO channels. It is observed that the severity of fading has a significant influence on the capacity of OSTBC systems. Specifically, an increase in the MIMO dimension or a decrease in the severity of fading results

in an increase in the mean channel capacity. However, it results in a decrease in the ADF of the channel capacity at low and medium signal levels. We have also investigated the statistical properties of the approximated channel capacity of spatially correlated OSTBC Nakagami-*m* MIMO channels. It is observed that the spatial correlation reduces the mean channel capacity of OSTBC Nakagami-*m* MIMO channels. The validity of all analytical results has been verified by simulations.

REFERENCES

[1] S. M. Alamouti. A simple transmit diversity technique for wireless communications. *IEEE J. Select. Areas Commun.*, 16(8):1451–1458, October 1998.

[2] Mohamed-Slim. Alouini, A. Abdi, and M. Kaveh. Sum of gamma variates and performance of wireless communication systems over Nakagami-fading channels. *IEEE Trans. Veh. Technol.*, 50(6):1471–1480, November 2001.

[3] G. J. Byers and F. Takawira. Spatially and temporally correlated MIMO channels: modeling and capacity analysis. *IEEE Trans. Veh. Technol.*, 53(3):634–643, May 2004.

[4] J. Chen, Z. Du, and X. Gao. Approximate capacity of OSTBC-OFDM in spatially correlated MIMO Nakagami-*m* fading channels. *IEEE Electronics Letters*, 44(8):534–535, April 2008.

[5] I. S. Gradshteyn and I. M. Ryzhik. *Table of Integrals, Series, and Products*. New York: Academic Press, 6th edition, 2000.

[6] B. O. Hogstad and M. Pätzold. Capacity studies of MIMO models based on the geometrical one-ring scattering model. In *Proc. 15th IEEE Int. Symp. on Personal, Indoor and Mobile Radio Communications, PIMRC 2004*, volume 3, pages 1613–1617. Barcelona, Spain, September 2004.

[7] B. O. Hogstad and M. Pätzold. Exact closed-form expressions for the distribution, level-crossing rate, and average duration of fades of the capacity of MIMO channels. In *Proc. 65th Semiannual Vehicular Technology Conference, IEEE VTC 2007-Spring*, pages 455–460. Dublin, Ireland, April 2007.

[8] B. O. Hogstad, M. Pätzold, N. Youssef, and V. Kontorovitch. Exact closed-form expressions for the distribution, level-crossing rate, and average duration of fades of the capacity of OSTBC-MIMO channels. *IEEE Trans. Veh. Technol.*, 58(2):1011–1016, February 2009.

[9] E. G. Larsson and P. Stoica. *Space-Time Block Coding for Wireless Communications*. Cambridge Univ. Press, 1st edition, 2003.

[10] A. Maaref and S. Aïssa. Performance analysis of orthogonal space-time block codes in spatially correlated MIMO Nakagami fading channels. *IEEE Trans. Wireless Commun.*, 5(4):807–817, April 2006.

[11] L. Musavian, M. Dohler, M. R. Nakhai, and M. H. Aghvami. Closed-form capacity expressions of orthogonalized correlated MIMO channels. *IEEE Commun. Letter*, 8(6):365–367, June 2004.

[12] A. Papoulis and S. U. Pillai. *Probability, Random Variables and Stochastic Processes*. New York: McGraw-Hill, 4th edition, 2002.

[13] M. Pätzold. *Mobile Fading Channels*. Chichester: John Wiley & Sons, 2002.

[14] M. Pätzold, C. X. Wang, and B. O. Hogstad. Two new sum-of-sinusoids-based methods for the efficient generation of multiple uncorrelated Rayleigh fading waveforms. *IEEE Trans. Wireless Commun.*, 8(6):3122–3131, June 2009.

[15] A. J. Paulraj, R. U. Nabar, and D. A. Gore. *Introduction to Space-Time Wireless Communications*. Cambridge, UK: Cambridge University Press, 2003.

[16] G. Rafiq, V. Kontorovich, and M. Pätzold. On the statistical properties of the capacity of the spatially correlated Nakagami-*m* MIMO channels. In *Proc. IEEE 67th Vehicular Technology Conference, IEEE VTC 2008-Spring*, pages 500–506. Marina Bay, Singapore, May 2008.

[17] V. Tarokh, H. Jafarkhani, and A. R. Calderbank. Space-time block codes from orthogonal designs. *IEEE Trans. on Inform. Theory*, 45(5):1456–1467, July 1999.

[18] V. Tarokh, N. Seshadri, and A. R. Calderbank. Space-time codes for high data rate wireless communication: performance criterion and code construction. *IEEE Trans. Inform. Theory*, 44(2):744–765, March 1998.

[19] T. T. Tjhung and C. C. Chai. Fade statistics in Nakagami-lognormal channels. *IEEE Trans. on Communications*, 47(12):1769–1772, December 1999.

[20] M. D. Yacoub, J. E. V. Bautista, and L. G. de Rezende Guedes. On higher order statistics of the Nakagami-*m* distribution. *IEEE Trans. Veh. Technol.*, 48(3):790–794, May 1999.

[21] L. Yang. Outage performance of OSTBC in double scattering MIMO channels. *Wireless Personal Communications (WPC)*, 45(2):225–230, April 2008.

[22] H. Zhang and T. A. Gulliver. Capacity and error probability analysis for orthogonal space-time block codes over fading channels. *IEEE Trans. Wireless Commun.*, 4(2):808–819, March 2005.

[23] L. Zheng and D. N. C. Tse. Diversity and multiplexing: A fundamental tradeoff in multiple antenna channels. *IEEE Trans. Inform. Theory*, 49:1073–1096, May 2003.

Appendix N

Paper XIV

Title:	The Impact of Shadowing and the Severity of Fading on the First and Second Order Statistics of the Capacity of OSTBC Nakagami-Lognormal MIMO Channels
Authors:	**Gulzaib Rafiq** and Matthias Pätzold
Affiliation:	University of Agder, Faculty of Engineering and Science, P. O. Box 509, NO-4898 Grimstad, Norway
Journal:	*Wireless Personal Communications*, 2010, submitted for publication.

The Impact of Shadowing and the Severity of Fading on the First and Second Order Statistics of the Capacity of OSTBC Nakagami-Lognormal MIMO Channels

Gulzaib Rafiq and Matthias Pätzold
Department of Information and Communication Technology
Faculty of Engineering and Science, University of Agder
Servicebox 509, NO-4898 Grimstad, Norway
E-mails: {gulzaib.rafiq, matthias.paetzold}@uia.no

***Abstract* — This article[1] presents a thorough statistical analysis of the capacity of orthogonal space-time block coded (OSTBC) Nakagami-lognormal (NLN) multiple-input multiple-output (MIMO) channels. The NLN channel model allows to study the joint effects of fast fading and shadowing on the statistical properties of the channel capacity. We have derived exact analytical expressions for the probability density function (PDF), cumulative distribution function (CDF), level-crossing rate (LCR), and average duration of fades (ADF) of the capacity of NLN MIMO channels. It is observed that an increase in the MIMO dimension[2] or a decrease in the severity of fading results in an increase in the mean channel capacity, while the variance of the channel capacity decreases. On the other hand, an increase in the shadowing standard deviation increases the spread of the channel capacity, however the shadowing effect has no influence on the mean channel capacity. We have also presented approximation results for the statistical properties of the channel capacity, obtained using the Gauss-Hermite integration method. It is observed that approximation results not only reduce the complexity, but also have a very good fitting with the exact results. The presented results are very useful and general because they provide the flexibility to study the impact of shadowing on the channel capacity under different fading conditions. Moreover, the effects of severity of fading on**

[1]The material in this paper is based on "On the Statistical Properties of the Capacity of OSTBC Nakagami-Lognormal MIMO Channels", by Gulzaib Rafiq and Matthias Pätzold which will appear in the proceedings of 4th IEEE International Conference on Signal Processing and Communication Systems, ICSPCS 2010, Gold Coast, Australia, December 2010.

[2]Throughout this paper, we will refer to the MIMO dimension as $N_R \times N_T$, where N_R is the number of receive antennas and N_T denotes the number of transmit antennas.

the channel capacity can also be studied. The correctness of theoretical results is confirmed by simulations.

Keywords—Nakagami-lognormal channels, MIMO, Land mobile terrestrial channels, channel capacity, shadowing effects, level-crossing rate, average duration of fades.

I. Introduction

Multiple-input multiple-output (MIMO) systems exploit spatial diversity by utilizing multiple antennas at the receiver and transmitter in order to increase the spectral efficiency and to acquire a diversity gain [37]. To achieve the desired capacity in MIMO channels, space-time coding techniques, such as space-time trellis codes (STTC) [28] or space-time block codes (STBC) [2, 27] are considered to be an effective method. Among different space-time coding techniques, OSTBC has gained much attention in recent years due to its orthogonal structure, which allows to use maximum likelihood decoding at the receiver [27]. Hence, it results in a decrease in the complexity of the receiver structure. Another advantage of using OSTBC is that it transforms MIMO fading channels into equivalent single-input single-output (SISO) channels, which significantly simplifies the mathematical formulation of MIMO channels [12]. Studies pertaining to the analysis of the capacity of OSTBC MIMO channels can be found in [4, 14]. The outage performance and the error probability analysis of OSTBC MIMO systems have been studied in [35, 36, 13]. Moreover, the statistical properties of the capacity of OSTBC Nakagami-m MIMO channels have been analyzed in [22].

The analysis presented in the aforementioned articles only considers fast fading in MIMO channels due to multipath propagation, where the local mean of the received signal envelope is assumed to be constant [9]. While for land mobile terrestrial channels, the local mean fluctuates due to shadowing effects [26]. Moreover, shadowing can adequately be modeled by a lognormal process and can be incorporated in the channel model as a multiplicative process [26, 18, 29, 23]. Hence, to study the joint effects of fast fading and shadowing in land mobile terrestrial channels, the Suzuki process is considered to be a more appropriate channel model [18]. A Suzuki process can be expressed as a product of a Rayleigh process and a lognormal process. However, by employing a Nakagami-m process instead of the Rayleigh process in a Suzuki process, we obtain a more general channel model referred to as the NLN channel model [29, 23], which contains the Suzuki process as a special case when $m = 1$. The generality of this model derives from the fact that the one-sided Gaussian and Rayleigh processes are inherently included in the Nakagami-m process as special cases, i.e., for $m = 0.5$ and $m = 1$, respectively.

Moreover, it can be used to study the scenarios where the fading is more (or less) severe as compared to Rayleigh fading [15, 32].

For MIMO channels, the authors in [25] have proposed a channel model that takes into account the joint effects of shadowing and fast fading. This model is then employed in [34] to study the outage performance in OSTBC MIMO channels. The analysis in [25] and [34] is however restricted only to Rayleigh MIMO channels. While in this article, we have considered a more general channel model referred to as NLN MIMO channel model, where the fast fading in the MIMO channel is modeled by a Nakagami-*m* process as compared to the Rayleigh process in [25]. Thereafter, we have analyzed the statistical properties of the capacity of NLN MIMO channels for the case when OSTBC is employed. To the best of the authors' knowledge, the statistical properties of the capacity of OSTBC NLN MIMO channels have not been investigated so far. The NLN MIMO channel model provides the flexibility to study the impact of shadowing on the channel capacity under different fading conditions. Moreover, the effects of severity of fading on the channel capacity can also be studied.

This paper analyzes the statistical properties of the capacity of OSTBC NLN MIMO channels for various levels of shadowing and for different MIMO dimensions. We have derived exact analytical expressions for the PDF, CDF, LCR, and ADF of the capacity of NLN MIMO channels. The mean value and spread of the channel capacity has been analyzed with the help of the PDF of the channel capacity. On the other hand, the analysis of the LCR and ADF of the channel capacity is very helpful to study the temporal behavior of the channel capacity. It is observed that an increase in the MIMO dimension or a decrease in the severity of fading results in an increase in the mean channel capacity, while the variance of the channel capacity decreases. Moreover, the shadowing effect has no influence on the mean channel capacity, whereas an increase in the shadowing standard deviation increases the spread of the channel capacity. It is also observed that an increase in either the shadow standard deviation or the MIMO dimension decreases the maximum value of the LCR of the channel capacity. Whereas, this effect decreases the ADF of the channel capacity only at higher signal levels. We have also presented approximation results for the statistical properties of the channel capacity using the Gauss-Hermite integration method [24]. It is observed that the approximation results not only reduce the complexity, but also have a very good fitting with the exact results.

The remainder of this paper is organized as follows. In Section II, we first give a brief description of the NLN MIMO channel model. Thereafter, the capacity

of NLN MIMO channels is formulated for the case when OSTBC is employed. Section III presents the statistical properties of the capacity of OSTBC NLN MIMO channels. Section IV deals with the analysis and illustration of the theoretical as well as the simulation results. Finally, the conclusions are drawn in Section V.

II. The Capacity of OSTBC NLN MIMO Channels

In this article, we have considered a MIMO system with N_T transmit and N_R receive antennas. The input-output relation for such a system is given by

$$\mathbf{y}(t)=\hat{\mathbf{H}}(t)\mathbf{x}(t)+\mathbf{n}(t) \tag{1}$$

where $\mathbf{x}(t)$ is an $N_T \times 1$ transmit signal vector, $\mathbf{y}(t)$ is an $N_R \times 1$ received signal vector, $\hat{\mathbf{H}}(t)$ is the $N_R \times N_T$ channel matrix, and $\mathbf{n}(t)$ is an $N_R \times 1$ additive white Gaussian noise (AWGN) vector. In order to study the joint effects of fast fading and shadowing in MIMO channels, the authors in [25] have proposed the following MIMO channel model

$$\hat{\mathbf{H}}(t) = \lambda(t)\mathbf{H}(t) \tag{2}$$

where $\mathbf{H}(t)$ is the $N_R \times N_T$ matrix with complex random independent and identically distributed (i.i.d.) entries $h_{i,j}(t)$, which model the fast fading in the channel between the ith receive and jth transmit antenna. In addition to fast fading, it is assumed that the local mean of the signal envelope fluctuates due to shadowing. Moreover, shadowing can adequately be modeled by a lognormal process $\lambda(t)$ and can be incorporated in the channel model as a multiplicative process. Hence, the lognormal process $\lambda(t)$ is multiplied to $\mathbf{H}(t)$ in (2). Furthermore, shadowing influences the signal envelope on large spatial scales as compared to the fast fading, thus it is assumed that a single lognormal process $\lambda(t)$ equally effects all the elements of the matrix $\mathbf{H}(t)$ and is independent of $\mathbf{H}(t)$. In [25], the authors have restricted the analysis to Rayleigh channels, where the envelope $\left|h_{i,j}(t)\right|$ is Rayleigh distributed. However in this article, we have assumed that the envelope $\left|h_{i,j}(t)\right|$ of the complex entries $h_{i,j}(t)$ follows a Nakagami-m distribution given by

$$p_{\left|h_{i,j}(t)\right|}(r) = \frac{2m_{i,j}^{m_{i,j}} r^{2m_{i,j}-1}}{\Gamma\left(m_{i,j}\right)\Omega_{i,j}^{m_{i,j}}} e^{-\frac{m_{i,j}r^2}{\Omega_{i,j}}}, \quad r \geq 0 \tag{3}$$

where $\Omega_{i,j} = E\left\{|h_{i,j}(t)|^2\right\}$, $m_{i,j} = \Omega_{i,j}^2 \big/ \mathrm{Var}\left\{|h_{i,j}(t)|^2\right\}$, and $\Gamma(\cdot)$ represents the gamma function [6]. Here, $E\{\cdot\}$ and $\mathrm{Var}\{\cdot\}$ denote the expectation and the variance operators, respectively. Moreover, the phase of the complex entries $h_{i,j}(t)$ is

considered to be uniformly distributed between $[0, 2\pi)$. The lognormal process $\lambda(t)$ in (1) can be expressed as

$$\lambda(t) = 10^{[\sigma_L \nu(t) + m_L]/20} \tag{4}$$

where σ_L represents the shadowing standard deviation, m_L denotes the area mean, and $\nu(t)$ is a zero-mean real-valued Gaussian process with unit variance. The PDF $p_\lambda(z)$ of the lognormal process $\lambda(t)$ can be written as

$$p_\lambda(z) = \frac{20}{z\sigma_L\sqrt{2\pi}\ln(10)} e^{-\frac{(10\log(z)-m_L)^2}{2\sigma_L^2}}, \; z \geq 0. \tag{5}$$

There exist numerous models in the literature for the spectral shape of the Gaussian process $\nu(t)$ in (4). In this article, we have assumed a Gaussian power spectral density (PSD) for the Gaussian process $\nu(t)$ given by [18], [20]

$$S_{\nu\nu}(f) = \frac{1}{\sqrt{2\pi}\sigma_c} e^{-\frac{f^2}{2\sigma_c^2}} \tag{6}$$

where the parameter σ_c controls the spread of the PSD $S_{\nu\nu}(f)$ and can be expressed in terms of the 3 dB cutoff frequency f_c as $\sigma_c = f_c/\sqrt{2\ln(2)}$. We have assumed that the value of f_c is much smaller than the maximum Doppler frequency $f_{\max}$, i.e., $f_{\max}/f_c \gg 1$. By taking the inverse Fourier transform of $S_{\nu\nu}(f)$, the ACF $r_{\nu\nu}(\tau)$ of the process $\nu(t)$ can be expressed as

$$r_{\nu\nu}(\tau) = e^{-2(\pi\sigma_c\tau)^2}. \tag{7}$$

The capacity of OSTBC MIMO systems can be expressed as [21]

$$C(t) = \log_2\left(1 + \frac{\gamma_s}{N_T}\lambda^2(t)\mathbf{h}^H(t)\mathbf{h}(t)\right) \text{ (bits/s/Hz)} \tag{8}$$

where $\mathbf{h}(t)$ represents the $N_R N_T \times 1$ vector formed by stacking the columns of the $N_R \times N_T$ matrix $\mathbf{H}(t)$ one below the other. For simplicity, we will represent the entries of the vector $\mathbf{h}(t)$ as $h_i(t)$ $(i = 1, 2, ..., N_R N_T)$. It can clearly be seen that the envelopes $|h_i(t)|$ are i.i.d. following the Nakagami-*m* distribution with the parameters m_i and Ω_i. In (8), $(\cdot)^H$ denotes the Hermitian operator, and γ_s is the signal-to-noise ratio (SNR). In order to generate Nakagami-*m* processes $|h_i(t)|$, the following

relation can be employed [32]

$$|h_i(t)| = \sqrt{\sum_{n=1}^{2m_i} \mu_{n,i}^2(t)} \tag{9}$$

where $\mu_{n,i}(t)$ $(n = 1,2,\ldots,2m_i)$ are the underlying i.i.d. Gaussian processes, and m_i is the parameter of the Nakagami-*m* distribution associated with the *i*th channel $h_i(t)$. The parameter m_i controls the severity of the fading. Increasing the value of m_i decreases the severity of fading associated with the *i*th channel $h_i(t)$ and vice versa. In this article, we have assumed that $\Omega_i = 2m_i\sigma_0^2$ for the sake of simplicity. Here, σ_0^2 denotes the variance of the underlying Gaussian processes $\mu_{n,i}(t)$ in $|h_i(t)|$. The channel capacity $C(t)$ given by (8) can be written as

$$C(t) = \log_2\left(1+\gamma_s'\lambda^2(t)\sum_{i=1}^{N_RN_T}\chi_i^2(t)\right) = \log_2\left(1+\gamma_s'\Xi(t)\right) \text{ (bits/s/Hz)} \tag{10}$$

where $\gamma_s' = \gamma_s/N_T$, $\Xi(t) = \lambda(t)\sum_{i=1}^{N_RN_T}\chi_i^2(t)$, and $\chi_i^2(t) = |h_i(t)|^2$ $(i = 1,2,...,N_RN_T)$. Due to the assumption that the envelope $|h_i(t)|$ is Nakagami-*m* distributed, the squared envelope $\chi_i^2(t)$ follows the gamma distribution. Let $Y(t) = \sum_{i=1}^{N_RN_T}\chi_i^2(t)$, then the PDF $p_\Xi(z)$ of $\Xi(t)$ can be expressed using [3, Eq. (2)], (5), and by employing the relationship $p_\Xi(z) = \int_{-\infty}^{\infty} 1/|y|\ p_Y(z/y)p_\lambda(y)dy$ [16] as

$$p_\Xi(z) = \frac{10z^{\acute{\alpha}-1}\beta^{-\acute{\alpha}}}{\sqrt{2\pi}\ln(10)\sigma_L\Gamma(\acute{\alpha})}\int_0^\infty\left(\frac{1}{y}\right)^{\acute{\alpha}+1} e^{-\frac{(10\log y-m_L)^2}{2\sigma_L^2}} e^{-\frac{z}{y\beta}},\ z\geq 0 \tag{11}$$

where $\acute{\alpha} = \sum_{i=1}^{N_RN_T}\alpha_i$ and $\beta = \Omega_i/m_i = 2\sigma_0^2$. In order to derive the expressions for the LCR of the OSTBC NLN MIMO channel capacity, we require the joint PDF $p_{\Xi\dot{\Xi}}(z,\dot{z})$ of $\Xi(t)$ and $\dot{\Xi}(t)$ at the same time t. In this article, the time derivative of a process is denoted by a dot notation. The joint PDF $p_{\Xi\dot{\Xi}}(z,\dot{z})$ can be expressed using [33, Eq. (35)], [18, Eq. (40)], and with the help of the relationship $p_{\Xi\dot{\Xi}}(z,\dot{z}) = \int_0^\infty\int_{-\infty}^\infty 1/y^2\ p_{Y\dot{Y}}(z/y,\dot{z}/y-\dot{y}z/y^2)p_{\lambda^2\dot{\lambda^2}}(y,\dot{y})d\dot{y}dy$ [10] as

$$p_{\Xi\dot{\Xi}}(z,\dot{z}) = \frac{10z^{\acute{\alpha}-3/2}\beta^{-\acute{\alpha}}}{4\pi\sqrt{\beta_N}\ln(10)\sigma_L\Gamma(\acute{\alpha})}\int_0^\infty y^{-\acute{\alpha}-3/2}\frac{e^{-\frac{z}{y\beta}}}{K(z,y)}e^{-\frac{(10\log y-m_L)^2}{2\sigma_L^2}} e^{-\frac{\dot{z}^2}{8\beta_N zyK^2(z,y)}},$$
$$z\geq 0, |\dot{z}|<\infty \tag{12}$$

where

$$K(z,y)=\sqrt{1+\frac{z\gamma\sigma_L^2}{y\beta_N(20/\ln(10))^2}} \quad \text{and} \quad \gamma=-\ddot{r}_{vv}(\tau)|_{\tau=0}=(2\pi\sigma_c)^2. \quad \text{(12b, c)}$$

In (12), $\beta_N=2(\pi\sigma_0 f_{\max})^2$ for isotropic scattering conditions [33]. In the next section, we will derive the expressions for the PDF, CDF, LCR, and ADF of the capacity of OSTBC NLN MIMO channels.

III. Statistical Properties of the Capacity of OSTBC NLN MIMO Channels

The expression in (10) can be considered as a mapping of the random process $\Xi(t)$ to another random process $C(t)$. Hence, the statistical properties of the process $\Xi(t)$ can be used to find the statistical properties of the channel capacity. By applying the concept of transformation of random variables [16, Eq. (7–8)], the PDF $p_C(r)$ of the channel capacity $C(t)$ is obtained as follows

$$\begin{aligned} p_C(r) &= \frac{2^r\ln(2)}{\gamma_s'}p_\Xi\left(\frac{2^r-1}{\gamma_s'}\right) \\ &= \frac{10\ln(2)2^r(2^r-1)^{\acute{\alpha}-1}}{(\gamma_s'\beta)^{\acute{\alpha}}\sqrt{2\pi}\ln(10)\sigma_L\Gamma(\acute{\alpha})}\int_0^\infty\left(\frac{1}{y}\right)^{\acute{\alpha}+1}e^{-\frac{2^r-1}{\gamma_s' y\beta}}e^{-\frac{(10\log y-m_L)^2}{2\sigma_L^2}}, \quad r\geq 0. \end{aligned} \tag{13}$$

The CDF $F_C(r)$ of the channel capacity $C(t)$ can be found using the relationship $F_C(r)=\int_0^r p_C(x)dx$ [16]. After solving the integral, the CDF $F_C(r)$ of $C(t)$ can be expressed as

$$F_C(r) = 1-\frac{10/\ln(10)}{\sqrt{2\pi}\sigma_L\beta^{\acute{\alpha}}\Gamma(\acute{\alpha})}\int_0^\infty\left(\frac{1}{y}\right)^{\acute{\alpha}+1}e^{-\frac{(10\log y-m_L)^2}{2\sigma_L^2}}\Gamma\left(\acute{\alpha},\frac{2^r-1}{y\gamma_s'\beta}\right), \quad r\geq 0 \tag{14}$$

where $\Gamma(\cdot,\cdot)$ represents the incomplete gamma function [6, Eq. (8.350-2)].

The LCR of the channel capacity defines the average rate of up-crossings (or down-crossings) of the channel capacity through a certain threshold level [8]. In the literature, there exist numerous articles dealing with the analysis of the LCR of the received signal envelope and the channel capacity (see, e.g., [17, 26, 8, 5], and the references therein). The analysis pertaining to the LCR of the received signal envelope has applications in the finite-state Markov modeling (FSMM) of fading channels [31], the analysis of handoff algorithms [30], and estimation of packet error rates [11]. In a similar fashion, using FSMM for the instantaneous capacity evolv-

ing process $C(t)$ and feeding the predicted capacity to the transmitter allows the transmitter that adapts the transmission rate according to the instantaneous channel capacity to minimize the probability of errors. For single-input single-output (SISO) channels, the LCR $N_C(r)$ of the channel capacity $C(t)$ can be expressed in terms of the LCR $N_X(r)$ of the received signal envelop $X(t)$ as $N_C(r) = N_X\left(\sqrt{(2^r-1)/\gamma_s'}\right)$ (see Section N. A for the proof). However in order to find the LCR $N_C(r)$ of the capacity $C(t)$ of MIMO channels, we first need to find the joint PDF $p_{C\dot{C}}(z,\dot{z})$ of the channel capacity $C(t)$ and its time derivative $\dot{C}(t)$. The joint PDF $p_{C\dot{C}}(z,\dot{z})$ can be obtained as

$$\begin{aligned} p_{C\dot{C}}(z,\dot{z}) &= \left(\frac{2^z\ln(2)}{\gamma_s'}\right)^2 p_{\Xi\dot{\Xi}}\left(\frac{2^z-1}{\gamma_s'},\frac{2^z\dot{z}\ln(2)}{\gamma_s'}\right) \\ &= \frac{10\left(2^z\ln(2)\right)^2\left(2^z-1\right)^{\dot{\alpha}-3/2}}{\sqrt{\gamma_s'\beta_N}4\pi\sigma_L\beta^{-\dot{\alpha}}\Gamma(\dot{\alpha})}\int_0^\infty y^{-\dot{\alpha}-3/2}\frac{e^{-\frac{2^z-1}{\gamma_s' y\beta}}}{K\left(\frac{2^z-1}{\gamma_s'},y\right)}e^{-\frac{(10\log y-m_L)^2}{2\sigma_L^2}} \\ &\quad\times e^{-\frac{(2^z\ln(2)\dot{z})^2}{8\beta_N(2^z-1)\gamma_s' y K^2\left(\frac{2^z-1}{\gamma_s'},y\right)}}dy,\ \ z\geq 0,|\dot{z}|<\infty. \end{aligned} \tag{15}$$

The LCR $N_C(r)$ can now be obtained by solving the integral in $N_C(r)=\int_0^\infty \dot{z}\,p_{C\dot{C}}(r,\dot{z})d\dot{z}$. After some algebraic manipulations, the LCR $N_C(r)$ can finally be expressed as

$$\begin{aligned} N_C(r) &= \frac{10\left(2^r-1\right)^{\dot{\alpha}-1/2}\sqrt{\gamma_s'\beta_N}}{(\gamma_s'\beta)^{\dot{\alpha}}\pi\ln(10)\sigma_L\Gamma(\dot{\alpha})}\int_0^\infty\left(\frac{1}{y}\right)^{\dot{\alpha}+1/2}e^{-\frac{2^r-1}{\gamma_s' y\beta}}K\left(\frac{2^z-1}{\gamma_s'},y\right) \\ &\quad\times e^{-\frac{(10\log y-m_L)^2}{2\sigma_L^2}},\ \ r\geq 0. \end{aligned} \tag{16}$$

The ADF of the channel capacity denotes the average duration of time over which the channel capacity is below a certain threshold level [8]. The ADF $T_C(r)$ of the channel capacity $C(t)$ can be obtained using [9]

$$T_C(r)=\frac{F_C(r)}{N_C(r)} \tag{17}$$

where $F_C(r)$ and $N_C(r)$ are given by (10) and (13), respectively.

A. Approximation of the statistical properties of the channel capacity using Gauss-Hermite integration method

By letting $(10\log y-m_L)^2=2\sigma_L^2x^2$, we can express the equations (13), (14), and (16) as

$$p_C(r) = \frac{2^r \ln(2)\,(2^r-1)^{\acute{\alpha}-1}}{(\gamma_s'\beta)^{\acute{\alpha}}\sqrt{\pi}\Gamma(\acute{\alpha})} \int_{-\infty}^{\infty} e^{-x^2} f_1(r,x)dx, \;\; r \geq 0 \tag{18}$$

$$F_C(r) = \frac{1}{\sqrt{\pi}\beta^{\acute{\alpha}}\Gamma(\acute{\alpha})} \int_{-\infty}^{\infty} e^{-x^2} f_2(r,x)dx, \;\; r \geq 0 \tag{19}$$

$$N_C(r) = \frac{(2^r-1)^{\acute{\alpha}-\frac{1}{2}}\sqrt{2\gamma_s'}}{(\gamma_s'\beta)^{\acute{\alpha}}\pi\Gamma(\acute{\alpha})/\sqrt{\beta_N}} \int_{-\infty}^{\infty} e^{-x^2} f_2(r,x)dx, \;\; r \geq 0 \tag{20}$$

respectively, where $f_1(r,x)$, $f_2(r,x)$, and $f_3(r,x)$ are given by

$$f_1(r,x) = e^{\left(-\frac{2^r-1}{\gamma_s'\beta}\right)10^{-\frac{\sqrt{2}\sigma_L x+m_L}{10}}} 10^{-\acute{\alpha}\left(\frac{\sqrt{2}\sigma_L x+m_L}{10}\right)} \tag{21}$$

$$f_2(r,x) = \Gamma\left(\acute{\alpha}, \frac{(2^r-1)/\gamma_s'\beta}{10^{\frac{\sqrt{2}\sigma_L x+m_L}{10}}}\right) 10^{-\acute{\alpha}\left(\frac{\sqrt{2}\sigma_L x+m_L}{10}\right)} \tag{22}$$

$$f_3(r,x) = e^{\left(-\frac{2^r-1}{\gamma_s'\beta}\right)10^{-\frac{\sqrt{2}\sigma_L x+m_L}{10}}} 10^{-\left(\acute{\alpha}-\frac{1}{2}\right)\left(\frac{\sqrt{2}\sigma_L x+m_L}{10}\right)} K\left(\frac{2^r-1}{\gamma_s'}, 10^{\frac{\sqrt{2}\sigma_L x+m_L}{10}}\right) \tag{23}$$

respectively. The integrals $I_i = \int_{-\infty}^{\infty} e^{-x^2} f_i(r,x)dx$ $(i = 1,2, \text{ and } 3)$ in (18)–(20) can now be approximated using the Gauss-Hermite integration method [24] as

$$I_i = \int_{-\infty}^{\infty} e^{-x^2} f_i(r,x)dx \approx \sum_{m=1}^{M} W_m f_i(r,\omega_m) \tag{24}$$

where ω_m, W_m, and M are the roots, weighting factors , and the order, respectively, of the Hermite polynomials $H_M(x) = (-1)^N e^{x^2}\, d^M/dx^M \left(e^{-x^2}\right)$. Here d^M/dx^M represents the Mth order differentiation of the exponential function e^{-x^2} with respect to x. The approximation in (24) yields many advantages. Firstly, it allows to get rid of the cumbersome integrals in (18)–(20), which reduces the complexity of the results. Secondly, it is observed that using only a small number of the terms M in (24) provides a very good fitting with the exact results, specifically for Rayleigh-lognormal MIMO channels (i.e., for $m_i = 1$) with smaller dimensions (e.g., 2x2). Moreover, the values of the roots (ω_m) and weighting factors (W_m) for a given M are constant irrespective of the integrand $e^{-x^2} f_i(r,x)$ $(i = 1,2, \text{ and } 3)$. The tables containing the values of ω_m and W_m can easily be found in literature (see, e.g., [1]), or can be obtained numerically using numerical computation softwares, such as MATLAB and MATHEMATICA.

IV. Numerical Results

In this section, we will discuss the analytical results obtained in the previous section and their validity will be tested by simulations. In order to investigate the influence of shadowing on the capacity of OSTBC NLN MIMO channels, we have studied the results for different values of the shadowing standard deviation σ_L, ranging from 1 dB to 10 dB. Specifically, the results for $\sigma_L = 4.3$ dB (urban environment [7]) and $\sigma_L = 7.5$ dB (suburban environment [7]) are shown. For comparison purposes, we have included a special case, namely the OSTBC Nakagami-*m* MIMO channels $(\sigma_L \to 0 \text{ dB})$. Moreover, we have also presented the approximation results for the statistical properties of the channel capacity given by (18)–(20) and (24). It is observed in all cases that the approximation results match the exact theoretical results very closely. Furthermore, we have also studied the impact of the MIMO dimension on the statistical properties of the channel capacity for both $\sigma_L = 4.3$ dB and $\sigma_L = 7.5$ dB.

The Nakagami-*m* distributed waveforms $|h_i(t)|$ $(i = 1, 2, ..., N_R N_T)$ are generated using (9). In order to simulate Gaussian processes $\mu_{n,i}(t)$ $(n = 1, 2, \ldots, 2m_i)$ and $v(t)$ in (9) and (4), respectively, we have applied the sum-of-sinusoids model [17]. The model parameters are calculated from the generalized method of exact Doppler spread (GMEDS_1) [19]. The number of sinusoids used for the generation of the Gaussian distributed waveforms was selected to be $N = 21$. The maximum Doppler frequency $f_{\max}$ was 91 Hz, the SNR γ_s was chosen to be 15 dB, and $\sigma_0^2 = 1$. Finally, using (2), (4) and (8), the simulation results for the statistical properties of the capacity $C(t)$ of OSTBC NLN MIMO channels were obtained.

Figures N.1 and N.2 present the PDF of the capacity of OSTBC NLN MIMO channels for different values of the shadowing standard deviation σ_L and for different MIMO dimensions, respectively. It is observed that an increase in the shadowing standard deviation σ_L increases the spread of the channel capacity, while it has no influence on the mean channel capacity. Moreover, an increase in the MIMO dimension results in an increase in the mean channel capacity, whereas the spread of the channel capacity decreases. This fact is specifically highlighted in Figs. N.3 and N.4, where the mean channel capacity and the variance of the channel capacity, respectively, are studied for different values of the shadowing standard deviation σ_L and for different MIMO dimensions. We have also analyzed the influence of severity of fading on the mean channel capacity and the variance of the channel capacity. The results show that as the fading severity increases, the mean channel capacity decreases. However, this effect has an opposite influence on the variance of the channel capacity. For the sake of completeness, we have also illustrated the CDF

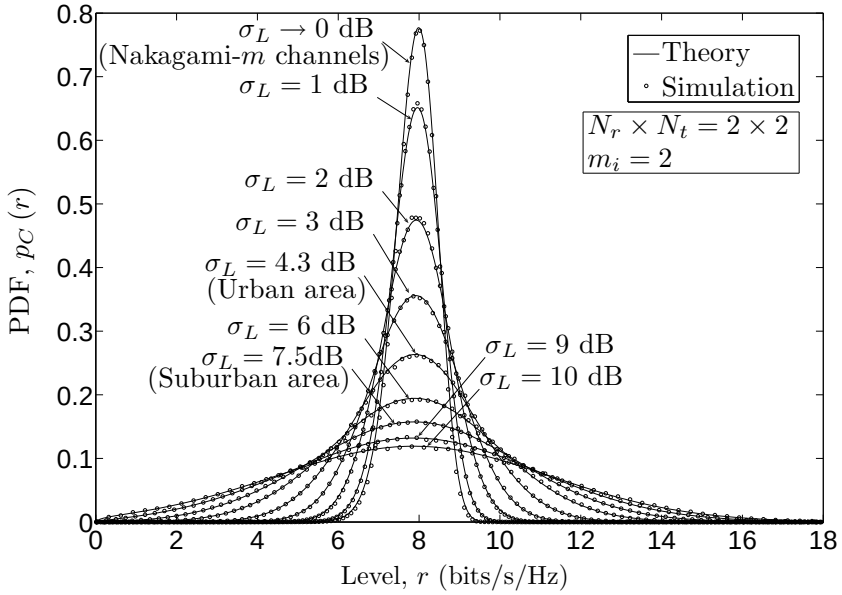

Figure N.1: The PDF $p_C(r)$ of the capacity $C(t)$ of OSTBC NLN MIMO channels for different values of the shadowing standard deviation σ_L.

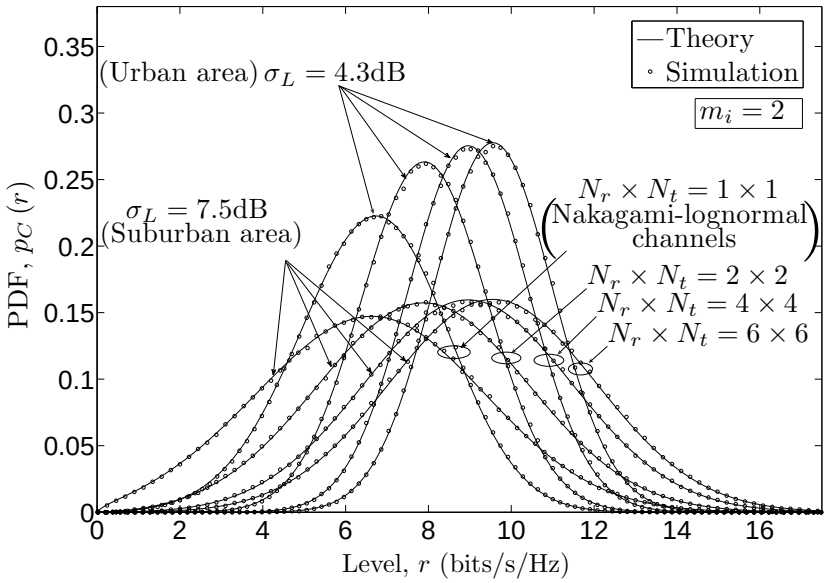

Figure N.2: The PDF $p_C(r)$ of the capacity $C(t)$ of OSTBC NLN MIMO channels for different MIMO dimensions.

of the capacity of OSTBC NLN MIMO channels for different values of the shadowing standard deviation σ_L and for different MIMO dimensions in Figs. N.5 and N.6, respectively. The results presented in Figs. N.5 and N.6 can be studied to draw similar conclusions regarding the influence of shadowing standard deviation σ_L as well as the MIMO dimensions on the mean channel capacity and the variance of the

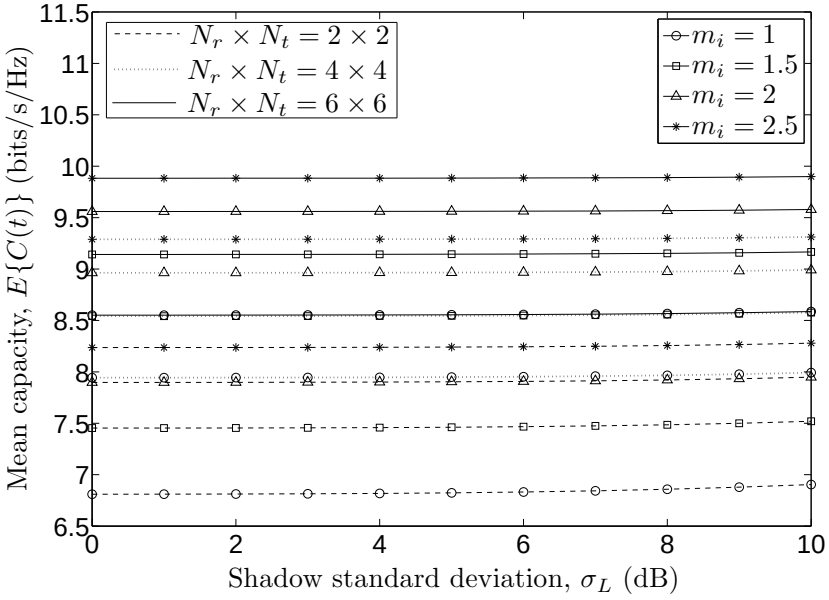

Figure N.3: The mean channel capacity $E\{C(t)\}$ of OSTBC NLN MIMO channels.

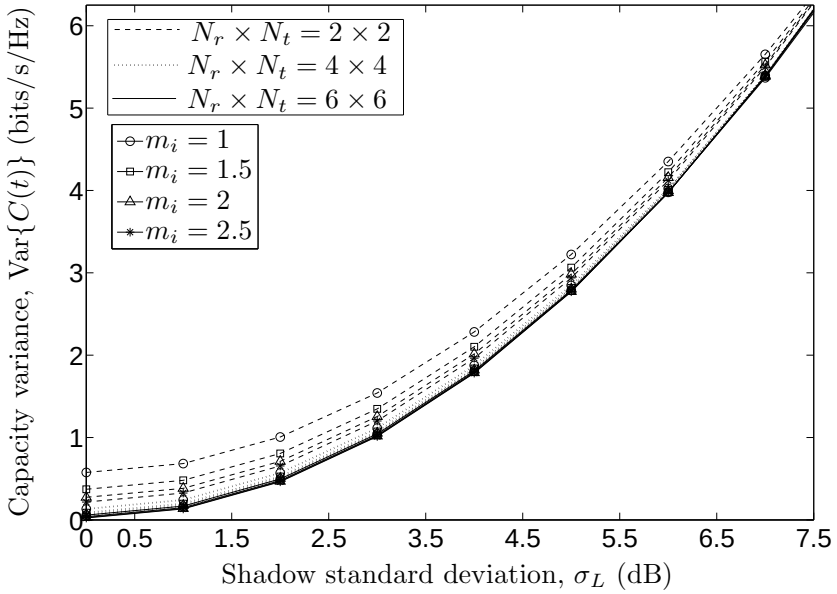

Figure N.4: The variance Var$\{C(t)\}$ of the capacity of OSTBC NLN MIMO channels.

channel capacity as from Figs. N.1 and N.2.

Figures N.7 and N.8 highlight the influence of shadowing and MIMO dimensions on the LCR of the channel capacity. It is observed that an increase in the shadowing standard deviation σ_L or the MIMO dimension results in a decrease in the maximum value of the LCR of the channel capacity, while the spread of the LCR increases. Moreover, at low and medium signal levels r, the channel capacity

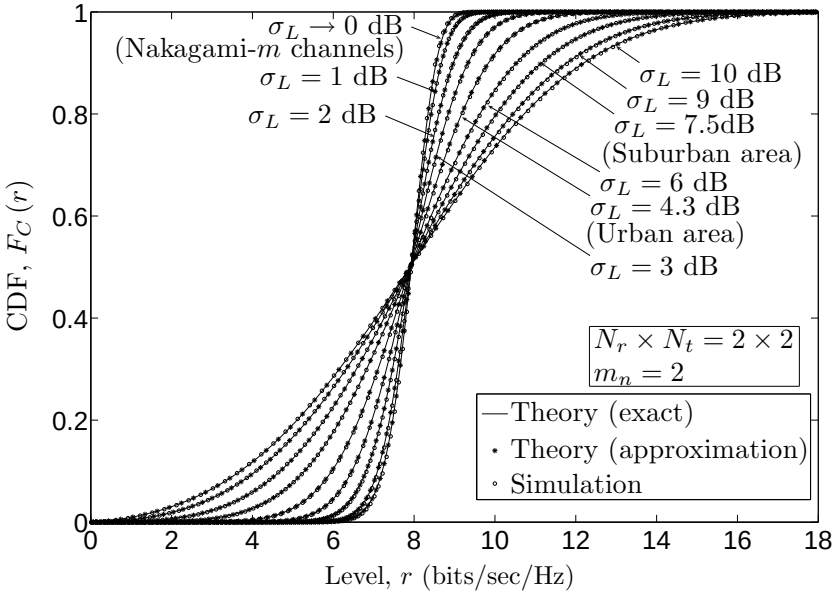

Figure N.5: The CDF $F_C(r)$ of the capacity $C(t)$ of OSTBC NLN MIMO channels for different values of the shadowing standard deviation σ_L.

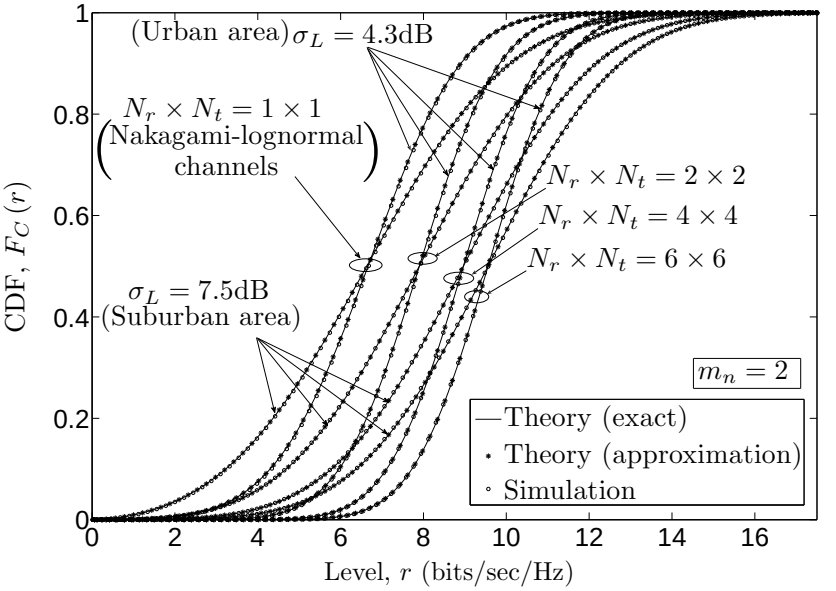

Figure N.6: The CDF $F_C(r)$ of the capacity $C(t)$ of OSTBC NLN MIMO channels for different MIMO dimensions.

of systems with smaller MIMO dimensions has a higher LCR as compared to the ones with larger MIMO dimensions. The ADF of the channel capacity for different values of the shadowing standard deviation σ_L and for different MIMO dimensions is presented in Figs. N.9 and N.10, respectively. It is observed that at higher signal levels r, an increase in the shadowing standard deviation σ_L decreases the ADF

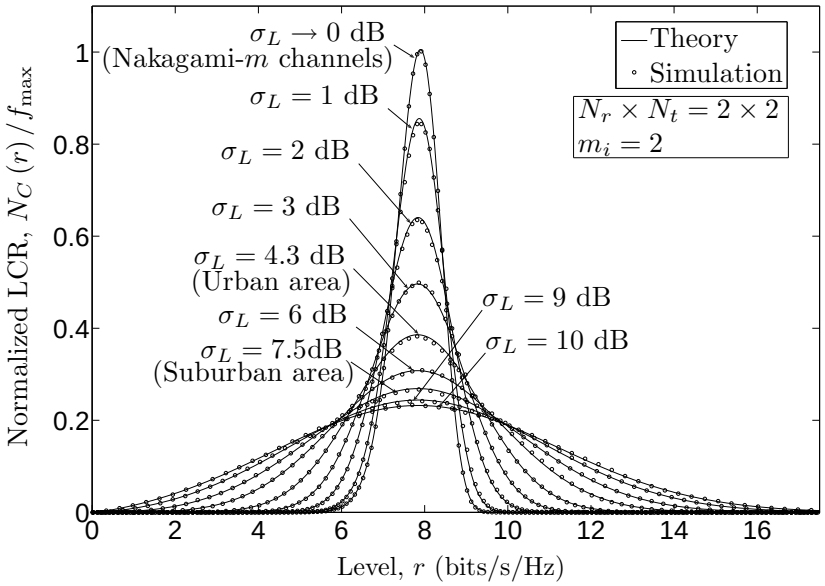

Figure N.7: The normalized LCR $N_C(r)/f_{\max}$ of the capacity $C(t)$ of OSTBC NLN MIMO channels for different values of the shadowing standard deviation σ_L.

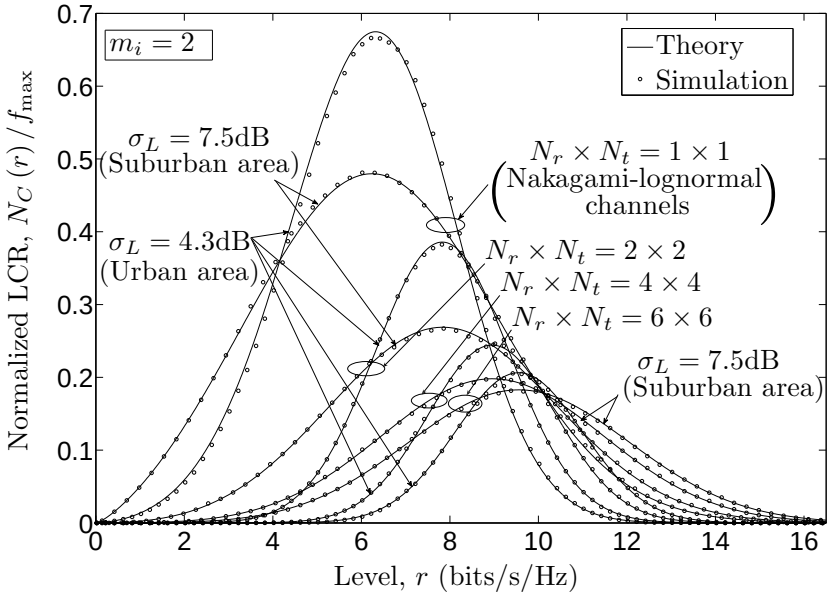

Figure N.8: The normalized LCR $N_C(r)/f_{\max}$ of the capacity $C(t)$ of OSTBC NLN MIMO channels for different MIMO dimensions.

of the channel capacity. However, the converse statement is true for lower signal levels. Moreover, an increase in the MIMO dimension has a similar influence on the ADF of the channel capacity as the shadowing standard deviation σ_L. The analytical expressions are verified using simulations, whereby an excellent fitting is observed.

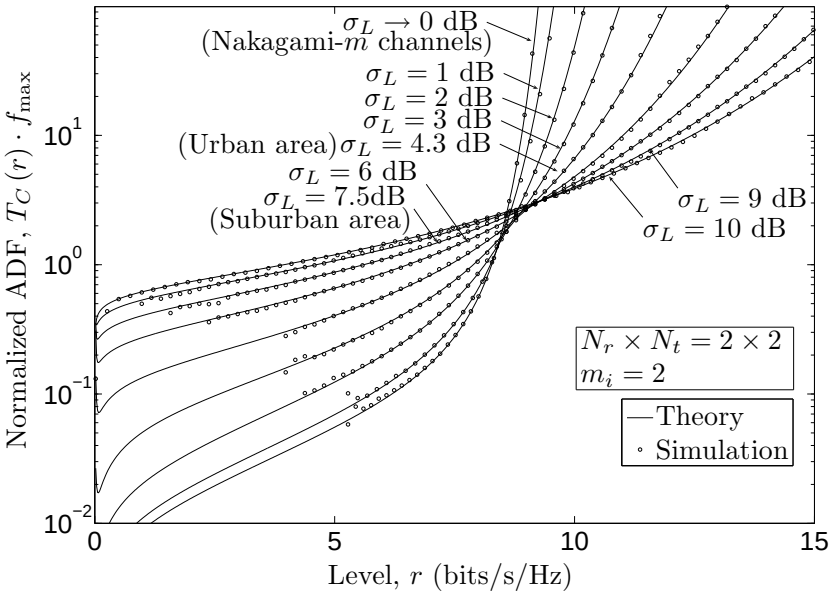

Figure N.9: The normalized ADF $T_C(r) \cdot f_{\max}$ of the capacity $C(t)$ of OSTBC NLN MIMO channels for different values of the shadowing standard deviation σ_L.

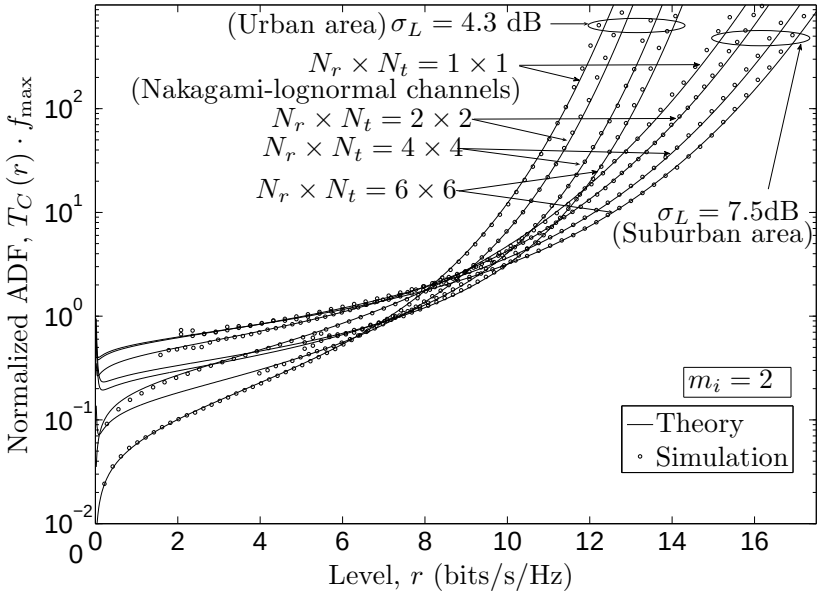

Figure N.10: The normalized ADF $T_C(r) \cdot f_{\max}$ of the capacity $C(t)$ of OSTBC NLN MIMO channels for different MIMO dimensions.

V. Conclusion

This paper studies the statistical properties of the capacity of OSTBC NLN MIMO channels for various levels of shadowing and for different MIMO dimensions. We have derived exact analytical expressions for the PDF, CDF, LCR, and ADF of the capacity of NLN MIMO channels. It is observed that an increase in the MIMO

dimension or a decrease in the severity of fading results in an increase in the mean channel capacity, while the variance of the channel capacity decreases. On the other hand, the shadowing effect has no influence on the mean channel capacity; however an increase in the shadowing standard deviation increases the spread of the channel capacity. It is also observed that an increase in either the shadow standard deviation or the MIMO dimension decreases the maximum value of the LCR of the channel capacity. Whereas, this effect decreases the ADF of the channel capacity only at higher signal levels. We have also presented approximation results for the statistical properties of the channel capacity obtained using the Gauss-Hermite integration method. It is observed that the approximation results reduce the complexity as well as fit very closely to the exact results. The correctness of the analytical results is confirmed by simulations.

N. A Relationship between the LCR of the Received Signal Envelop in SISO Channels and the LCR of the Channel Capacity

Consider the received signal envelop in a SISO system denoted by $X(t)$. The corresponding channel capacity can be expressed as $C(t) = \log_2\left(1+\gamma_s X^2(t)\right)$, where γ_s denotes the average received SNR. The LCR $N_C(r)$ of the channel capacity $C(t)$ is defined as [8]

$$N_C(r) = \int_0^\infty \dot{z}\, p_{C\dot{C}}(r,\dot{z})\, d\dot{z},\ r \geq 0 \tag{A.1}$$

where $p_{C\dot{C}}(z,\dot{z})$ denotes the joint PDF of $C(t)$ and $\dot{C}(t)$. By applying the concept of transformation of random variables [16, Eq. (7–8)], the joint PDF $p_{C\dot{C}}(z,\dot{z})$ can be obtained using $p_{C\dot{C}}(z,\dot{z}) = \left(2^z \ln(2)/\gamma_s\right)^2 p_{X^2\dot{X}^2}\left((2^z-1)/\gamma_s, (2^z \dot{z}\ln(2))/\gamma_s\right)$, where $p_{X^2\dot{X}^2}(z,\dot{z}) = \left(1/(4z)\right) p_{X\dot{X}}\left(\sqrt{z}, \dot{z}/(2\sqrt{z})\right)$. By substituting $p_{C\dot{C}}(z,\dot{z})$ in (A.1) and letting $\dot{w} = (2^z \dot{z}\ln(2)\sqrt{\gamma_s})/(2\sqrt{2^z-1})$, the LCR $N_C(r)$ can be finally expressed as

$$N_C(r) = \int_0^\infty \dot{w}\, p_{X\dot{X}}\left(\sqrt{\frac{2^r-1}{\gamma_s}}, \dot{w}\right) d\dot{w} = N_X\left(\sqrt{\frac{2^r-1}{\gamma_s}}\right) \tag{A.2}$$

where $N_X(r)$ is the LCR of the received signal envelope $X(t)$.

REFERENCES

[1] M. Abramowitz and I. A. Stegun. *Handbook of Mathematical Functions with Formulas, Graphs, and Mathematical Tables*. Washington: National Bureau of Standards, 1984.

[2] S. M. Alamouti. A simple transmit diversity technique for wireless communications. *IEEE J. Select. Areas Commun.*, 16(8):1451–1458, October 1998.

[3] Mohamed-Slim. Alouini, A. Abdi, and M. Kaveh. Sum of gamma variates and performance of wireless communication systems over Nakagami-fading channels. *IEEE Trans. Veh. Technol.*, 50(6):1471–1480, November 2001.

[4] J. Chen, Z. Du, and X. Gao. Approximate capacity of OSTBC-OFDM in spatially correlated MIMO Nakagami-*m* fading channels. *IEEE Electronics Letters*, 44(8):534–535, April 2008.

[5] A. Giorgetti, P. J. Smith, M. Shafi, and M. Chiani. MIMO capacity, level crossing rates and fades: The impact of spatial/temporal channel correlation. *J. Commun. Net.*, 5(2):104–115, June 2003.

[6] I. S. Gradshteyn and I. M. Ryzhik. *Table of Integrals, Series, and Products*. New York: Academic Press, 6th edition, 2000.

[7] M. Gudmundson. Correlation model for shadow fading in mobile radio systems. *Electron. Lett.*, 27(23):2145–2146, November 1991.

[8] B. O. Hogstad and M. Pätzold. Exact closed-form expressions for the distribution, level-crossing rate, and average duration of fades of the capacity of MIMO channels. In *Proc. 65th Semiannual Vehicular Technology Conference, IEEE VTC 2007-Spring*, pages 455–460. Dublin, Ireland, April 2007.

[9] W. C. Jakes, editor. *Microwave Mobile Communications*. Piscataway, NJ: IEEE Press, 1994.

[10] A. Krantzik and D. Wolf. Distribution of the fading-intervals of modified Suzuki processes. In L. Torres, E. Masgrau, and M. A. Lagunas, editors, *Signal Processing V: Theories and Applications*, pages 361–364. Amsterdam, The Netherlands: Elsevier Science Publishers, B.V, 1990.

[11] J. Lai and N. B. Mandayam. Packet error rate for burst-error-correcting codes in rayleigh fading channels. In *Proc. IEEE 48th Veh. Technol. Conf., VTC'98*. Ottawa, Ont. , Canada, May 1998.

[12] E. G. Larsson and P. Stoica. *Space-Time Block Coding for Wireless Communications*. Cambridge Univ. Press, 1st edition, 2003.

[13] A. Maaref and S. Aïssa. Performance analysis of orthogonal space-time block codes in spatially correlated MIMO Nakagami fading channels. *IEEE Trans. Wireless Commun.*, 5(4):807–817, April 2006.

[14] L. Musavian, M. Dohler, M. R. Nakhai, and M. H. Aghvami. Closed-form capacity expressions of orthogonalized correlated MIMO channels. *IEEE Commun. Letter*, 8(6):365–367, June 2004.

[15] M. Nakagami. The *m*-distribution: A general formula of intensity distribution of rapid fading. In W. G. Hoffman, editor, *Statistical Methods in Radio Wave Propagation*. Oxford, UK: Pergamon Press, 1960.

[16] A. Papoulis and S. U. Pillai. *Probability, Random Variables and Stochastic Processes*. New York: McGraw-Hill, 4th edition, 2002.

[17] M. Pätzold. *Mobile Fading Channels*. Chichester: John Wiley & Sons, 2002.

[18] M. Pätzold, U. Killat, and F. Laue. An extended Suzuki model for land mobile satellite channels and its statistical properties. *IEEE Trans. Veh. Technol.*, 47(2):617–630, May 1998.

[19] M. Pätzold, C. X. Wang, and B. O. Hogstad. Two new sum-of-sinusoids-based methods for the efficient generation of multiple uncorrelated Rayleigh fading waveforms. *IEEE Trans. Wireless Commun.*, 8(6):3122–3131, June 2009.

[20] M. Pätzold and K. Yang. An exact solution for the level-crossing rate of shadow fading processes modelled by using the sum-of-sinusoids principle. In *Proc. 9th International Symposium on Wireless Personal Multimedia Communications, WPMC 2006*, pages 188–193. San Diego, USA, September 2006.

[21] A. J. Paulraj, R. U. Nabar, and D. A. Gore. *Introduction to Space-Time Wireless Communications*. Cambridge, UK: Cambridge University Press, 2003.

[22] G. Rafiq, M. Pätzold, and V. Kontorovich. The influence of spatial correlation and severity of fading on the statistical properties of the capacity of OSTBC Nakagami-*m* MIMO channels. In *Proc. IEEE 69th Vehicular Technology Conference, IEEE VTC 2009-Spring*, pages 1–5. Barcelona, Spain, April 2009.

[23] F. Ramos, V. Ya. Kontorovitch, and M. Lara. Generalization of Suzuki model for analog communication channels. In *Proc. IEEE Antennas and Propagation for Wireless Communication, IEEE APS 2000*, pages 107–110, November 2000.

[24] H. E. Salzer, R. Zucker, and R. Capuano. Table of the zeros and weight factors of the first twenty hermite polynomials. *J. Res. Nat. Bu. Standards*, 48:111–116, February 1952.

[25] Z. Shen, R. W. Heath Jr., J. G. Andrews, and B. L. Evans. Space-time water-filling for composite MIMO fading channels. *EURASIP J. Wirel. Commun. Netw.*, 2006(2):48–48, 2006.

[26] G. L. Stüber. *Principles of Mobile Communications*. Boston, MA: Kluwer Academic Publishers, 2nd edition, 2001.

[27] V. Tarokh, H. Jafarkhani, and A. R. Calderbank. Space-time block codes from orthogonal designs. *IEEE Trans. on Inform. Theory*, 45(5):1456–1467, July 1999.

[28] V. Tarokh, N. Seshadri, and A. R. Calderbank. Space-time codes for high data rate wireless communication: performance criterion and code construction. *IEEE Trans. Inform. Theory*, 44(2):744–765, March 1998.

[29] T. T. Tjhung and C. C. Chai. Fade statistics in Nakagami-lognormal channels. *IEEE Trans. on Communications*, 47(12):1769–1772, December 1999.

[30] R. Vijayan and J. M. Holtzman. Foundations for level crossing analysis of handoff algorithms. In *Proc. IEEE Int. Conf. on Communications, ICC 1993*, pages 935–939. Geneva ,Switzerland, May 1993.

[31] H. S. Wang and N. Moayeri. Finite-state markov channel a useful model for radio communication channels. *IEEE Trans. Veh. Technol.*, 44(1):163–171, February 1995.

[32] M. D. Yacoub, J. E. V. Bautista, and L. G. de Rezende Guedes. On higher order statistics of the Nakagami-*m* distribution. *IEEE Trans. Veh. Technol.*, 48(3):790–794, May 1999.

[33] M. D. Yacoub, C. R. C. M. da Silva, and J. E. B. Vargas. Second-order statistics for diversity-combining techniques in Nakagami-fading channels. *IEEE Trans. Veh. Technol.*, 50(6):1464–1470, November 2001.

[34] L. Yang. Outage performance of OSTBC in MIMO channels with shadowing. *Wireless Personal Communications (WPC)*, 43(4):1751–1754, December 2007.

[35] L. Yang. Outage performance of OSTBC in double scattering MIMO channels. *Wireless Personal Communications (WPC)*, 45(2):225–230, April 2008.

[36] H. Zhang and T. A. Gulliver. Capacity and error probability analysis for orthogonal space-time block codes over fading channels. *IEEE Trans. Wireless Commun.*, 4(2):808–819, March 2005.

[37] L. Zheng and D. N. C. Tse. Diversity and multiplexing: A fundamental tradeoff in multiple antenna channels. *IEEE Trans. Inform. Theory*, 49:1073–1096, May 2003.